Ocular Adnexal Lesions

A Clinical, Radiological and Pathological Correlation

Shantha Amrith
Gangadhara Sundar
Stephanie Ming Young
Editors

Springer

Ocular Adnexal Lesions

Shantha Amrith
Gangadhara Sundar • Stephanie Ming Young
Editors

Ocular Adnexal Lesions

A Clinical, Radiological and Pathological Correlation

Springer

Editors
Shantha Amrith
National University Hospital
National University of Singapore
Singapore

Gangadhara Sundar
National University Hospital
National University of Singapore
Singapore

Stephanie Ming Young
National University Hospital
National University of Singapore
Singapore

ISBN 978-981-13-3797-0 ISBN 978-981-13-3798-7 (eBook)
https://doi.org/10.1007/978-981-13-3798-7

This Springer imprint is published by the registered company Springer Nature Singapore Pte Ltd.
The registered company address is: 152 Beach Road, #21-01/04 Gateway East, Singapore 189721, Singapore

Foreword

One of the great privileges and obligations in the practice of medicine is the opportunity to engage in lifelong learning. This is particularly significant for the analysis and elucidation of complex disorders. An important vehicle for this is a multidisciplinary approach to the diagnosis and management of orbital and adnexal disorders. I learned this early in my career devoted to pathology, orbital disease, and ocular oncology. In each of these disciplines, one had to interact with colleagues in related disciplines and collate the clinical observations, imaging, and pathology to arrive at a diagnosis and treatment plan in the context of evolving knowledge and techniques. In addition, since the gamut of possible diagnoses may also include such disciplines as rheumatology, infectious disease, immunology, and oncology, it is frequently necessary to involve specialist in these disciplines. From my experience of collating disorders clinically, for diagnosis, management, teaching, presentation, and publication, I found it useful to analyze diverse findings in a disciplined order. This led to the development of the "CLOSE" technique, which has been used as a framework in this book by Professor Shantha Amrith, her coeditors Gangadhara Sundar and Stephanie Ming Young, and colleagues at NUH.

An important and valuable feature of this book is a commitment to organization and documentation of personal experience in developing knowledge and diagnostic tools. This is also a patient-centric book, which focuses on a multidisciplinary approach to diagnosis and management. Too often in our time, students and practitioners are distracted by using digital devices while trying to make a diagnosis in the presence of a patient when they should be focused on what the patient is remembering, describing, feeling, and demonstrating. Direct personal interaction is the framework for the multidisciplinary analysis elucidated in this book.

In an era where we have been increasingly dissociated from personal shared medical knowledge and memory in the interest of the patient with complex problems, it is a delight to share and benefit from their interactive experience and discipline. I am particularly impressed by the quality of discourse and illustrations provided from the clinical, imaging, pathology, and laboratory contributed by the authors. This provides and illustrates a pathway to develop engrams that are so important to the diagnosis of the wide range of disorders presented. It will surely be useful to developing your own visual and experiential memory bank.

The chapters include basic anatomy, contemporary imaging, and pathology. In addition, the authors cover the essential gamut of orbital disorders that we are likely to encounter in clinical practice including structural lesions, inflammations, vascular anomalies and lesions, benign and malignant neoplasms both regional and metastatic, and lymphoproliferative disorders. All are presented with their own case examples, in the context of interdisciplinary rounds. In addition, they provide a review of the literature pertinent to the diagnosis as well as treatment plans and outcomes. The reviews of the disorders also include recent literature as well as regional differences.

Overall, this is a readable handbook for students and clinicians who may encounter similar patients in practice. The authors are to be congratulated for sharing their practical and useful experience for those in the field as well as our students.

Jack Rootman, FRCS
Emeritus Professor Ophthalmology and
Vision Science and Pathology,
University of British Columbia,
Vancouver, BC, Canada

Preface

The Orbit and Oculofacial Service of the Department of Ophthalmology, National University Hospital, Singapore, has been conducting monthly clinical, pathological, and radiological conferences on ocular and ocular adnexal lesions with our colleagues from the Departments of Diagnostic Imaging and Pathology since 2004. The spectrum of diseases covered in these rounds typically included immunological, oncological, and other diseases with multidisciplinary inputs, not only from the radiologist and pathologist but also from specialties such as rheumatology/immunology, endocrinology, adult and pediatric oncology, neurology, and surgical specialties like facial plastic surgery, otorhinolaryngology, neurosurgery, etc. These multidisciplinary sessions contributed immensely to the knowledge and understanding of common disorders, especially for the residents, fellows, and consultants, and aided in the compilation of recent advances in diagnosis and management of rare ocular adnexal disorders.

The cases discussed in the book were carefully chosen from our archives to educate not only the ophthalmology residents and general ophthalmologists but also the residents from the diagnostic imaging and pathology departments.

The term, ocular adnexa, is used in the wider sense in this book, encompassing the eyelids, lacrimal system, and orbit including conditions of the globe with orbital extension. The book begins with a brief description of applied anatomy relevant to clinical diagnosis and surgical principles.

The sections on imaging and pathology were contributed by experts in the field. The coauthors from the Department of Diagnostic Imaging, Poh Sun Goh and Eric Ting, have written a section each on imaging with some basic principles and concepts of computed tomography (CT) and magnetic resonance imaging (MRI), special imaging techniques, and their applications, highlighting some of the indications, contraindications, advantages, and disadvantages of the different forms of imaging. In addition, they have diligently worked to choose representative images for each case with radiologic description of the images.

Similarly, insights into the basic understanding of histopathologic techniques have been provided by Drs. Min En Nga and Bingcheng Wu from the Department of Pathology, National University Hospital. The chapter also provides useful advice regarding the importance of discussing the case with the pathologist, prior to incisional or excisional tissue biopsy. The pathologists have expertly chosen the histopathological figures, along with relevant immunohistochemical stains for each condition, and provided the descriptions and figure legends.

The clinical conditions are classified by pathology rather than the anatomical structures to avoid repetitions. Common eyelid conditions, such as chalazion, papillomas, nevi, and sweat gland cysts, are not included in this book, as most ophthalmic residents and general ophthalmologists are quite conversant with these conditions. Nevertheless, warning signs have been highlighted under different conditions, so that unusual signs of benign-looking lesions could be identified for prompt and early diagnosis.

Each part is divided into chapters representing the anatomical part. All cases are discussed systematically starting with an introduction, clinical scenario, differential diagnoses, imaging features, histopathology including immunohistochemical features, molecular features (where relevant), final diagnosis, outline of management, and a brief discussion and latest evidence-based update of that condition.

After the description of the clinical scenario, there is a CLOSE summary for each case (introduced by Professor Jack Rootman), which is a mnemonic for *C*linical process, *L*ocation, *O*nset, *S*igns and symptoms, and *E*pidemiology. At the end of clinical examination, the summary helps to formulate a differential diagnosis, which in turn guides additional imaging, incisional or excisional biopsy. CLOSE is described in great detail in the introductory chapter of the book, "Orbital Surgery: A Conceptual Approach" (Rootman J, Stewart B, Goldberg RA. Orbital surgery: a conceptual approach. 2nd ed. Philadelphia: Wolters Kluwer Lippincott Williams & Wilkins; 2014). Each case write-up concludes with some learning points and a list of references for further reading.

Our sincere thanks and acknowledgments are due to our neuro-ophthalmology colleagues, Drs. Hazel Lin and Clement Tan for the neuro-ophthalmology section and our hematologist-oncologist Dr. Michelle Poon for the overview of lymphoproliferative disorders. Our sincere thanks also go to all our past fellows and residents, who had researched and presented with fervor in our monthly teaching rounds, most of which has been shared in the book with recent updates.

The uniqueness of this book lies in the contribution of not only the orbital surgeons/clinicians in conventional knowledge and recent advances in diagnosis and management but also the radiologists and pathologists to each case. We sincerely hope that this book will be a good teaching tool for all the aspiring and practicing orbit and oculoplastic surgeons and serve as a reference tool for residents and fellows in training institutions worldwide.

Singapore

Shantha Amrith
Gangadhara Sundar
Stephanie Ming Young

The original version of this book was revised. The correction to this book can be found at DOI https://doi.org/10.1007/978-981-13-3798-7_67.

Acknowledgments

Other special thanks to our past fellows, who put in hard work to make stellar presentations during the teaching rounds: Mike Munoz (the Philippines), Passorn Preechawai (Thailand), Cheng Jin Fong (Singapore), Radwan Al Mousa (Syria), Naseem Mansurali (Malaysia), Rosniza Abdul Razak (Malaysia), Shruthi Tara (India), Tricia Morada (the Philippines), Ko Ko Lin (Myanmar), Sharifah Intan (Malaysia), Joy Chan (Singapore), Raghuraj Suresh Hegde (India), Stephanie Ming Young (Singapore), Zin May Htoon (Myanmar), Mariel Angelou Parulan (the Philippines), and Prerana Kansakar (Nepal).

Thanks also to Bay Song Lin, medical illustrator from the Department of Anatomy, National University of Singapore, who made anatomical illustrations for this book.

Contents

Part VII Benign Neoplasms: Orbit

Part VIII Benign Neoplasms: Lacrimal System

Part IX Lymphoproliferative Disorders

About the Editors

Shantha Amrith is a Senior Consultant Eye Surgeon/Oculoplastic Surgeon at the Department of Ophthalmology, National University Hospital, Singapore, and a Clinical Associate Professor with the Yong Loo Lin School of Medicine, National University of Singapore (NUS). She completed two brief fellowships in ophthalmic plastic and reconstructive surgery at Sydney Eye Hospital, Australia, and the University of Cincinnati Hospitals, USA. She has vast experience in managing patients with various eyelid, lacrimal, and orbital pathologies including tumors and injuries, in addition to cosmetic surgeries on eyebrows, and upper and lower eyelid blepharoplasties. She has published several articles in notable journals and reviewed several articles for international ophthalmology journals. Her landmark study was on tear outflow physiology.

Her main areas of interest are thyroid eye disease, Asian perspective in eyelid and lacrimal and orbital diseases, and trauma reconstruction. She is a Founding Member and Former Treasurer of the Asia Pacific Society of Ophthalmic Plastic and Reconstructive Surgery (ASOPRS) and Founding Member of the Singapore Society of Ophthalmic Plastic and Reconstructive Surgery (SSOPRS). In recognition of her contributions, she has received the "APAO Achievement Award."

Gangadhara Sundar is the Head and Senior Consultant of the Division of Orbit and Oculofacial Surgery, Department of Ophthalmology, National University Hospital, Singapore, with affiliate positions as an Assistant Professor at the same institution and an Adjunct Faculty at the Department of Pediatrics, National University Hospital. He obtained his degrees from Madras Medical College and the Government Ophthalmic Hospital, Chennai, India, and advanced subspecialty training at the Henry Ford Hospital, Detroit, USA, under the preceptorship of Murray D. Christianson MD FACS (who had trained under John Wright, UK, and Richard Tenzel, USA). Apart from specializing in diseases and surgery of the eyelid, lacrimal, and orbital disorders, his interests include orbitofacial trauma, ophthalmic oncology, and thyroid eye disease. Committed to clinical, surgical, and academic excellence with numerous international awards and orations, he is a Regional and International Expert in his field and serves in leadership roles in various national and international educational and professional oculoplastic societies. His contributions include numerous scientific papers, textbook chapters, and a major treatise on *Orbital Fractures: Principles, Concepts and Techniques*. He has been instrumental in starting various multidisciplinary services, including the NUH retinoblastoma service (with pediatric oncologists, neuro-interventional radiologists, pathologists, and ocularists), NUH thyroid eye disease service (with endocrinologists and immunologists), and the NUH lacrimal service (with rhinologists).

Stephanie Ming Young is a Consultant at the Department of Ophthalmology, National University Hospital (NUH), and Assistant Professor at the Yong Loo Lin School of Medicine, National University of Singapore (NUS). She has a special interest in ophthalmic plastic and reconstructive surgery of the eyelid, lacrimal system, and orbit and has completed two surgically intensive fellowships at the National University Hospital, Singapore, and Samsung Medical Center, Seoul. She has received several grants and published numerous papers on the subject in peer-reviewed journals, as well as two book chapters. A graduate of the National

University of Singapore (NUS), she won the Gold Medal and Book Prize in Ophthalmology and received a Distinction Award for ophthalmology-related research for her undergraduate research opportunity program. As a House Officer at NUH Medicine, she was awarded the Best House Officer Award in 2008. Since joining the Ophthalmology Department at NUH, she has won several ophthalmology-related awards, including Asia Pacific Academy of Ophthalmology Best Free Paper Award, American Academy of Ophthalmology Best Poster Award, Eye Foundation Award, and Best Paper Award – NUHS Residents Research Day. She teaches medical students as well as residents in ophthalmology. She has received the Wong Hock Boon Society Outstanding Mentor Award for her efforts in mentoring medical students.

Contributors

Shantha Amrith Department of Ophthalmology, National University Hospital, Singapore
Department of Ophthalmology, Yong Loo Lin School of Medicine, National University of Singapore, Singapore

Yun Song Choo Department of Diagnostic Imaging, National University Hospital, Singapore

Poh Sun Goh Department of Diagnostic Imaging, National University Hospital, Singapore
Department of Diagnostic Imaging, Yong Loo Lin School of Medicine, National University of Singapore, Singapore

Hazel Anne Lin Department of Ophthalmology, National University Hospital, Singapore

Min En Nga Department of Pathology, National University Hospital, Singapore
Department of Pathology, Yong Loo Lin School of Medicine, National University of Singapore, Singapore

Mariel Angelou Parulan Department of Ophthalmology, National University Hospital, Singapore

Limei Michelle Poon Department of Haematology-Oncology, National Cancer Institute, Singapore
Department of Haematology-Oncology, Yong Loo Lin School of Medicine, National University of Singapore, Singapore

Gangadhara Sundar Department of Ophthalmology, National University Hospital, Singapore
Department of Ophthalmology, Yong Loo Lin School of Medicine, National University of Singapore, Singapore

Clement Tan Department of Ophthalmology, National University Hospital, Singapore
Department of Ophthalmology, Yong Loo Lin School of Medicine, National University of Singapore, Singapore

Eric Ting Department of Diagnostic Imaging, National University Hospital, Singapore
Department of Diagnostic Imaging, Yong Loo Lin School of Medicine, National University of Singapore, Singapore
Advanced Medicine Imaging, Singapore

Bingcheng Wu Department of Pathology, National University Hospital, Singapore

Stephanie Ming Young Department of Ophthalmology, National University Hospital, Singapore
Department of Ophthalmology, Yong Loo Lin School of Medicine, National University of Singapore, Singapore

Abbreviations

AJCC	*A*merican *J*oint *C*ommittee on *C*ancer
ANA	Antinuclear antibody
ANCA	Antineutrophil cytoplasmic antibody
AVM	Arteriovenous malformation
CCF	Carotid cavernous fistula
cGY	Centigray (unit of radiation)
CRP	Cryo-reactive protein
CT	Computerized tomography or Computed tomography
CTA	Computed tomography angiography or CT angiography
DWI	Diffusion-weighted MRI
EMA	Epithelial membrane antigen
ENA	Extractable nuclear antigen
ENMZL	Extranodal marginal zone lymphoma
EOM	Extraocular muscles
ESR	Erythrocyte sedimentation rate
FBC	Full blood count
FDG	Fluorine-18 (F-18) fludeoxyglucose
FISH	Fluorescence in situ hybridization
FNAC	Fine-needle aspiration biopsy
GY	Gray (Unit of radiation)
H&E	Hematoxylin and eosin
HVF	Humphrey visual field
ICA	Internal carotid artery
IgG	Immunoglobulin G
IOP	Intraocular pressure
ISSVA	*I*nternational *S*ociety for the *S*tudy of *V*ascular *A*nomalies
LCH	Langerhans cell histiocytosis
LDH	Lactate dehydrogenase
MALT	Mucosa-associated lymphoid tissue
MRA	Magnetic resonance angiography
MRI	Magnetic resonance imaging
NF-1	Neurofibromatosis 1
NF-2	Neurofibromatosis 2
NHL	Non-Hodgkin lymphoma
NLD	Nasolacrimal duct
NPL	No perception of light
NSOID	Non-specific orbital inflammatory disease
OAL	Ocular adnexal lymphoma
OID	Orbital inflammatory disease
PCR	Polymerase chain reaction
PET	Positron emission tomography
RAPD	Relative afferent pupillary defect

R-CHOP	*R*ituximab in combination with *C*yclophosphamide, *H*ydroxydaunorubicin (Doxorubicin), *O*ncovin (Vincristine), *P*rednisolone
SLE	Systemic lupus erythematosus
T1w FS + C	T1-weighted MRI with fat suppression and contrast
T1w FS	T1-weighted MRI with fat suppression
T1w	T1-weighted MRI
T2w FS	T2-weighted MRI with fat suppression
T2w	T2-weighted MRI
T4	Free thyroxine
TNM classification	*T*umor, *N*ode, *M*etastasis classification
TRab	TSH receptor antibody
TSH	Thyroid-stimulating hormone

Part I

Basic Anatomy, Imaging and Pathology

Anatomy

1

Shantha Amrith and Stephanie Ming Young

Eyelids

The eyelid can be divided into two lamellae, namely, the anterior and the posterior. The anterior lamella consists of the skin and orbicularis, while the posterior lamella is formed by tarsus and conjunctiva. The transition zone between the two lamellae at the lid margin is marked by the mucocutaneous junction called the grey line. The meibomian gland orifices are visible just posterior to the grey line. The anterior lid margin is where the eyelashes are, and the posterior lid margin is in apposition with the globe. The architecture of the lid margin may be lost along with the loss of eyelashes in malignant neoplasms of the eyelid.

Fig. 1.1 shows the cross section of the eye lids.

In the upper eyelid, the layers below the lid crease include the skin, orbicularis, levator aponeurosis, and tarsoconjunctiva. The crease is formed by the attachment of slips of levator aponeurosis to the skin, and this may be shallow, absent or low in normal healthy East Asians, resulting in more distal insertion of the orbital septum and inferior extension of the preaponeurotic fat. Sometimes there are changes to the lid crease in East Asians when they develop a proptosis due to a space-occupying lesion in the orbit.

The orbicularis oculi is a complex striated muscle sheet lying just beneath the eyelid skin, and is innervated by the temporal and zygomatic branches of the facial nerve, with variable contribution from the buccal branch. It is divided anatomically into (1) the orbital portion, which overlies the bony orbital rims, and (2) the palpebral portion, which lies within the mobile portion of the eyelid, and is further divided into the preseptal (overlying orbital septum) and pretarsal (overlying tarsus) portions. The Horner's muscle is a medial slip of the pretarsal orbicularis extending behind the lacrimal sac and contributes to the pump function of the lacrimal drainage system.

The orbital septum separates the eyelid from orbital structures and is considered as the middle lamella of the eyelid. The septum extends from the orbital rim (arcus marginalis) to the levator aponeurosis separating the preaponeurotic fat from the orbicularis. There are two major fat pads in the upper eyelid, namely, the medial and the central (Fig. 1.1 inset). The levator aponeurosis attaches to the anterior surface of the tarsal plate and fans out to form medial and lateral horns. The lateral horn is attached to Whitnall's tubercle (a protuberance in the anterior lateral orbital wall), and it separates the orbital from the palpebral portions of the lacrimal gland. The medial horn is attached to the posterior lacrimal crest. The smooth sympathetic muscle (Muller's muscle) arises from the posterior aspect of the levator aponeurosis and is attached to the upper border of the tarsal plate.

The blood supply to the upper eyelid is through two vascular arcades derived from the branches of external and internal carotid arteries. The lymphatic drainage is into the submandibular and preauricular lymph nodes before draining into the deep cervical lymph nodes. The sensory nerve supply is from the first division of the V cranial nerve (V1).

The lower eye lid structures are very similar to the upper lid except that the tarsal height is less than half of the upper eyelid tarsus. In place of the levator, there is an inferior retractor muscle called the capsulopalpebral fascia which is an extension of the sheaths of the inferior rectus and inferior oblique muscles (Fig. 1.1). There is also a smooth muscle akin to the Muller's muscle called the inferior tarsal muscle on the posterior aspect of the inferior retractor, however, this is not as well developed as the Muller's muscle. There are three preaponeurotic fat pads: medial, central and lateral (Fig. 1.1 inset). The blood supply is through a single vascular arcade formed by the branches of external and internal carotid arteries. The lymphatic drainage is to the submandibular and preauricular lymph nodes.

S. Amrith (✉) · S. M. Young
Department of Ophthalmology, National University Hospital, Singapore

Department of Ophthalmology, Yong Loo Lin School of Medicine, National University of Singapore, Singapore
e-mail: shantha_amrith@nuhs.edu.sg; stephanie.young@nuhs.edu.sg

S. Amrith et al. (eds.), *Ocular Adnexal Lesions*, https://doi.org/10.1007/978-981-13-3798-7_1

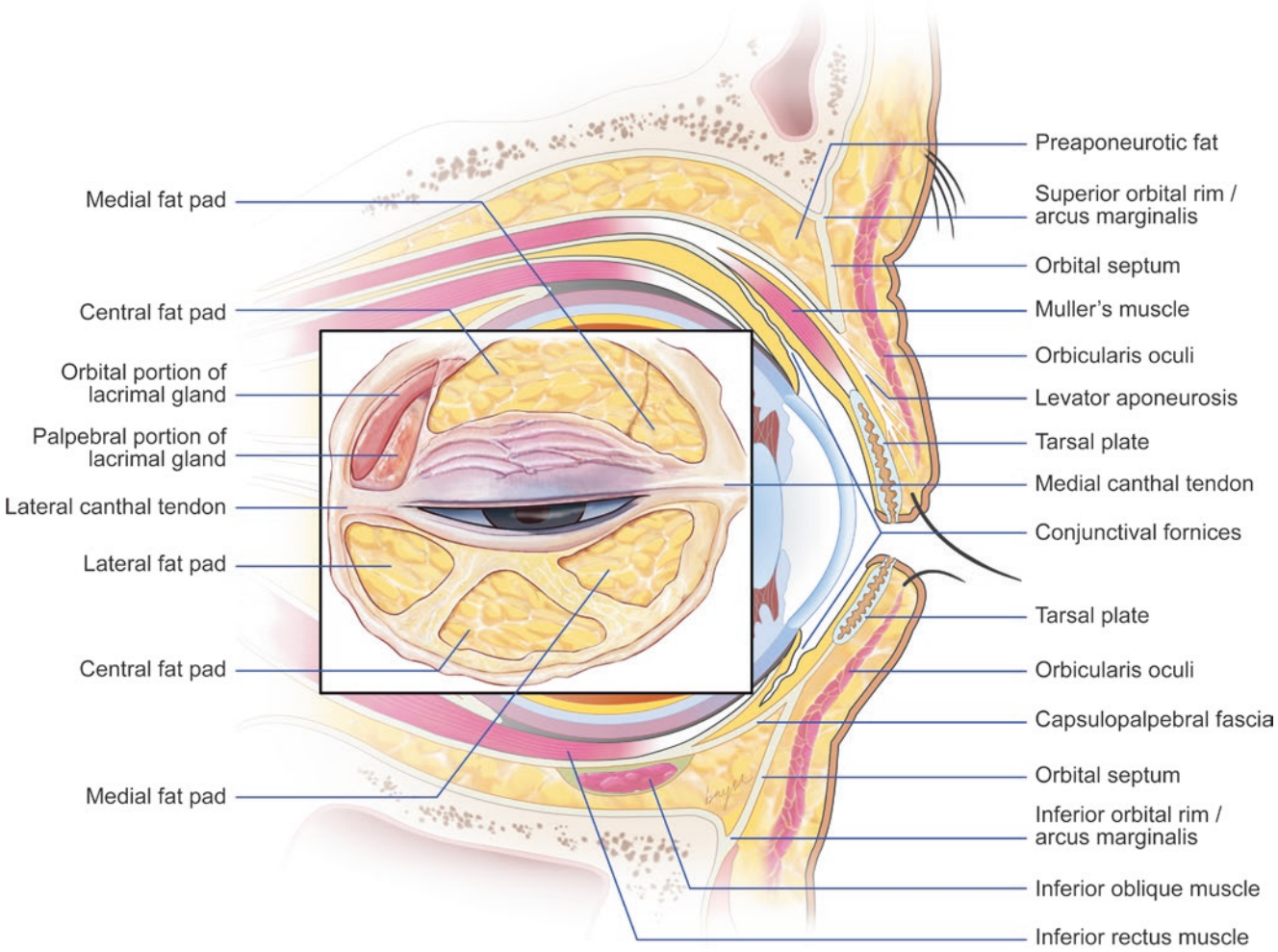

Fig. 1.1 A sagittal cross section of the upper and lower lids. Inset: An anteroposterior view of the eyelids showing the preaponeurotic fat pads

Lacrimal Drainage System

Tears are produced by accessory lacrimal glands and the main lacrimal gland. The tears are held in a layer between the lid margins on the ocular surface, and renewed with each blink. There are two puncta in the medial ends of the eyelids which draw the tears from the medial part of the conjunctival sac (lacus lacrimalis) into the canaliculi, before draining into the lacrimal sac and the duct (Fig. 1.2). The puncta and the lacrimal canaliculi may be involved in medial lid margin tumours, in which case they may need to be removed.

The lacrimal sac is situated in the lacrimal sac fossa between the anterior and posterior lacrimal crests in the frontal process of the maxilla and the lacrimal bones, respectively. The lacrimal sac drains into nasolacrimal duct which is in a bony canal in the medial wall of the maxillary sinus. The nasolacrimal duct is directed inferiorly, posteriorly and slightly laterally to open into the inferior meatus of the nasal cavity (Fig. 1.3). This may act as a conduit for spread of tumours between the lacrimal apparatus and the nose and/or sinuses. Intrinsic sac tumours will require removal of the tear sac, and the entire lacrimal drainage system along with a medial maxillectomy or total maxillectomy depending on the extent of the tumour.

Orbit

The orbit is a pyramidal structure with four bony walls, namely, medial, floor, lateral, and roof with orifices that connect it to other spaces (Fig. 1.4) such as the nasal cavity, paranasal sinuses, intracranial cavity, temporal and infratemporal fossa and pterygopalatine fossa.

The roof of the orbit (Fig. 1.5) separates the frontal sinus and frontal lobe of the brain from the orbital contents. It is formed by the orbital plate of the frontal bone and the lesser wing of sphenoid. The frontal sinus occupies the medial aspect of the roof anteriorly. At the apex of the roof is the oval optic foramen that transmits the optic nerve and the ophthalmic artery (Fig. 1.4). It is formed by the lesser wing and body of the sphenoid. In the anterolateral aspect of the roof is a fossa that accommodates the lacrimal gland. In the anteromedial aspect, there is a depression which accommodates the

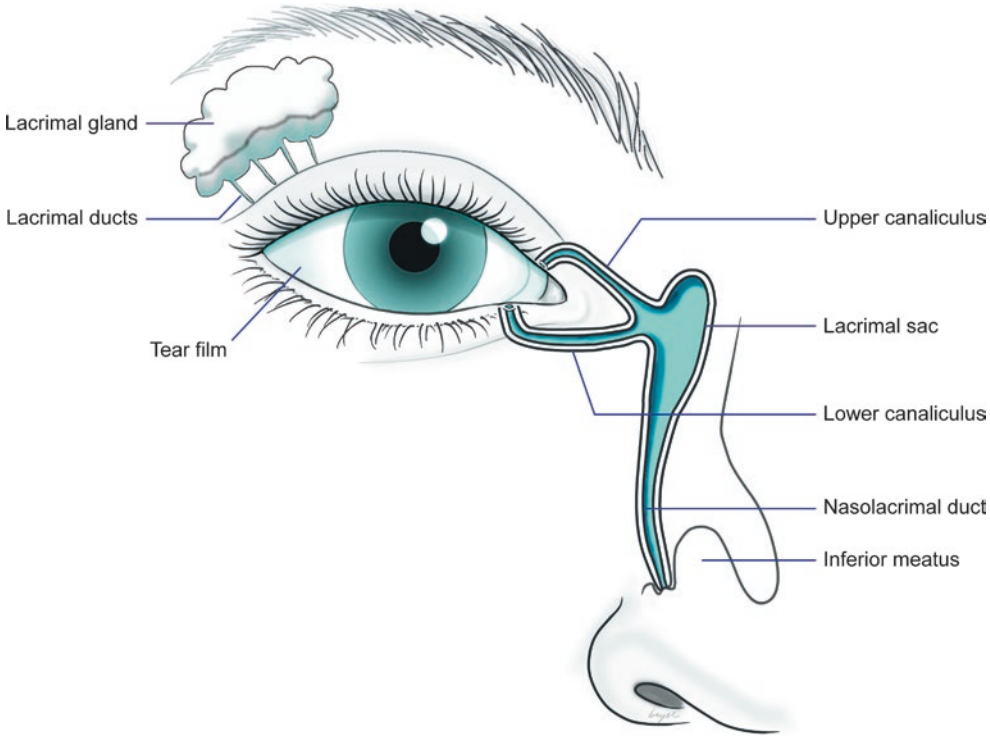

Fig. 1.2 Lacrimal drainage system

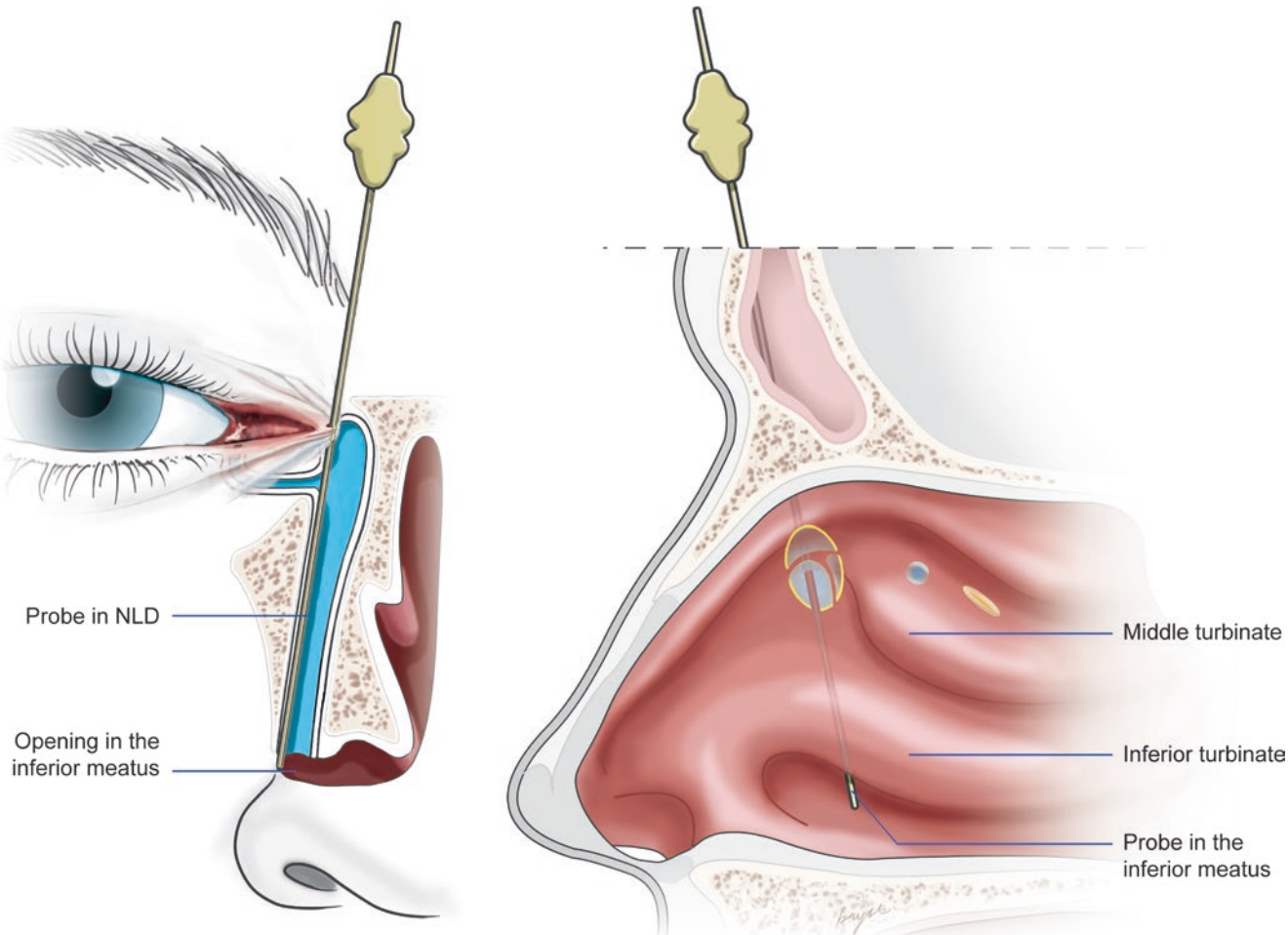

Fig. 1.3 Left: The probe in the nasolacrimal duct (NLD) shows the direction of NLD and the inferior meatus in relation to the exterior. Right: View of the lateral nasal wall with blue-grey area showing the area corresponding to the lacrimal fossa and its relationship to the middle turbinate

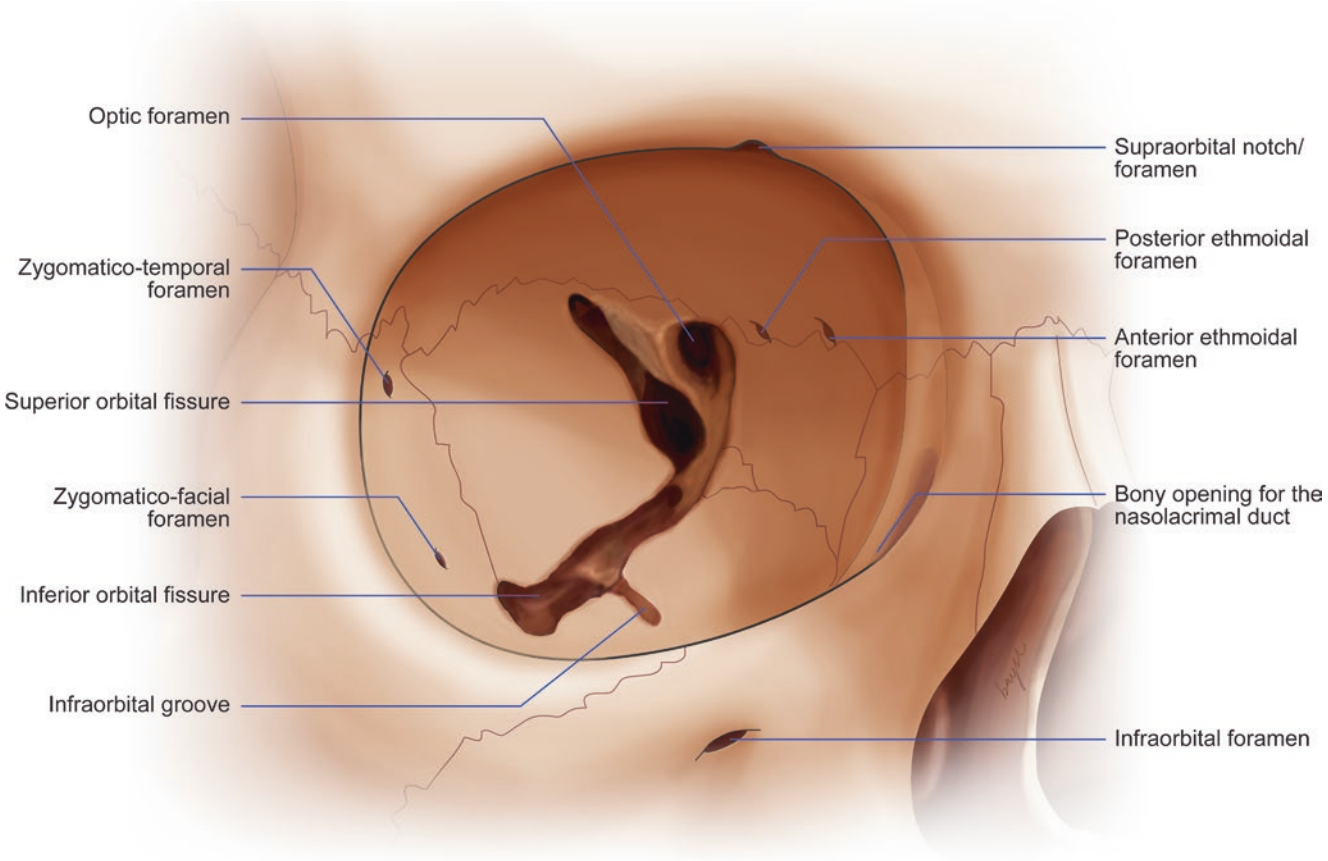

Fig. 1.4 Bony fissures and orifices in the orbit

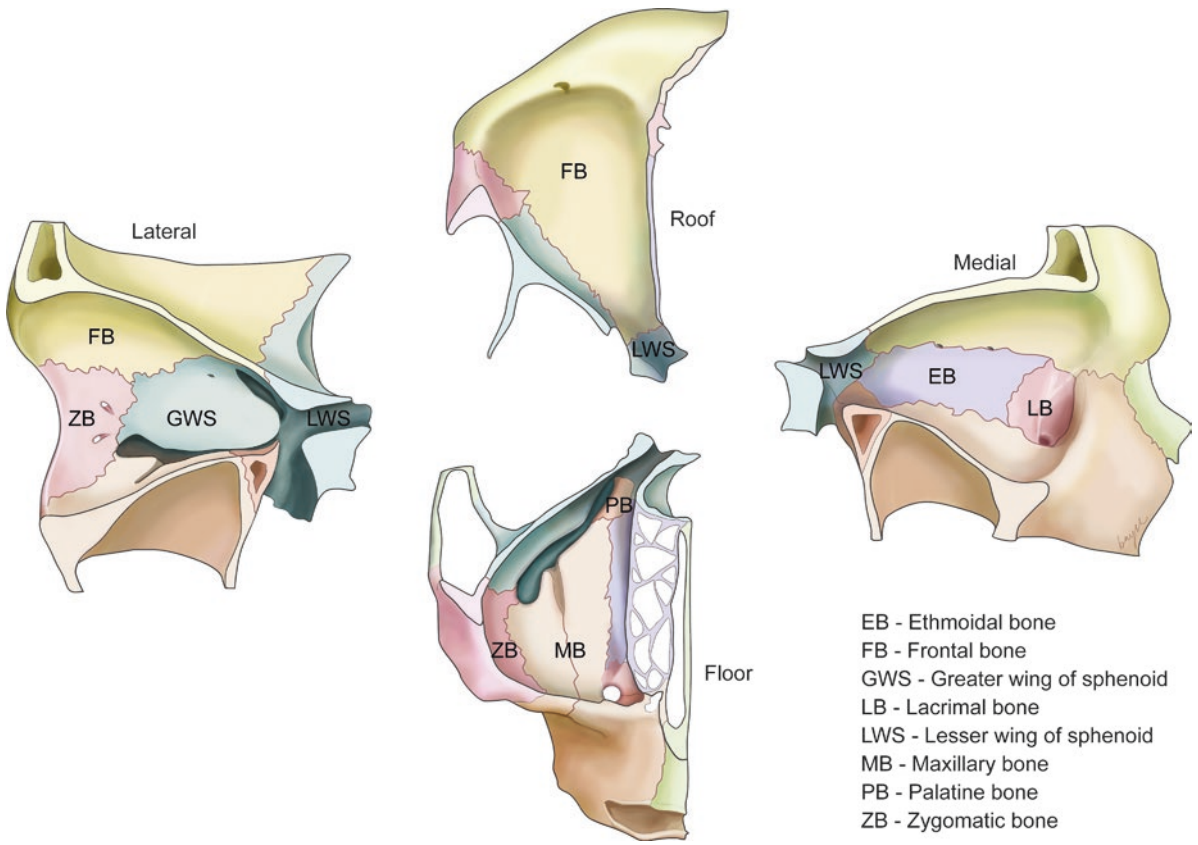

Fig. 1.5 Composition of the four bony orbital walls

trochlea. At the superior orbital rim, the supraorbital and supratrochlear nerves (branches of frontal nerve) emerge from the orbit to supply sensation to the forehead (Fig. 1.4).

The lateral wall (Fig. 1.5) is made of the zygomatic bone and greater wing of sphenoid connected with a sphenozygomatic suture, which is utilised in lateral orbitotomies. There are two foramina in the lateral wall (Fig. 1.4) that transmit the zygomaticofacial and zygomaticotemporal nerves (branches of V2) which are responsible for the sensation over the cheek and the temporal aspect of the face, respectively.

The orbital floor (Fig. 1.5) is formed by orbital plates of the maxillary and zygomatic bones anteriorly, and the orbital plate of the palatine bone posteriorly. The infraorbital groove and canal pass through the floor (Fig. 1.4) and transmit the infraorbital neurovascular bundle which emerges on the anterior maxillary wall. The infraorbital nerve is a branch from the second division of V cranial nerve (V2). The floor medial to the infraorbital canal is very thin and breaks easily during trauma.

The medial orbital wall (Fig. 1.5), from anterior to posterior, consists of the frontal process of the maxilla including anterior lacrimal crest, lacrimal bone including the posterior lacrimal crest, and lamina papyracea of the ethmoid (a thin bone separating the orbit from the ethmoidal sinus) and lesser wing of the sphenoid. It has two important foramina (Fig. 1.4) at its superior border, which transmit the anterior and posterior ethmoidal neurovascular bundle. Injury to these vessels is an important cause of orbital haemorrhage during surgery or trauma to the medial wall, and these vessels mark the upper limit for medial maxillectomy and medial orbital wall decompression. These communicating channels may serve as conduits for the spread of infection from the ethmoid sinuses to the orbit usually in the form of thrombophlebitis. The posterior ethmoidal foramen is 6 mm from the optic canal and therefore acts as an important surgical landmark for the optic canal.

Separating the floor from lateral wall is the inferior orbital fissure (Fig. 1.4). This communicates with the infratemporal fossa. Closely associated with the fissure are V2 and its branches as well as branches from sphenopalatine ganglion. The secretomotor fibres from superior salivatory nucleus are relayed in the sphenopalatine ganglion and through the zygomaticotemporal nerve and lacrimal nerve reach the lacrimal gland.

Similarly, separating the roof from lateral wall is the superior orbital fissure (SOF) (Fig. 1.4). The superior orbital fissure is bordered by the greater and the lesser wings of sphenoid bone. The annulus of Zinn divides the fissure into three compartments. The SOF transmits superior and inferior divisions of III, IV, branches of V1 and VI cranial nerves, as well as the superior ophthalmic vein (Fig. 1.6). The deep

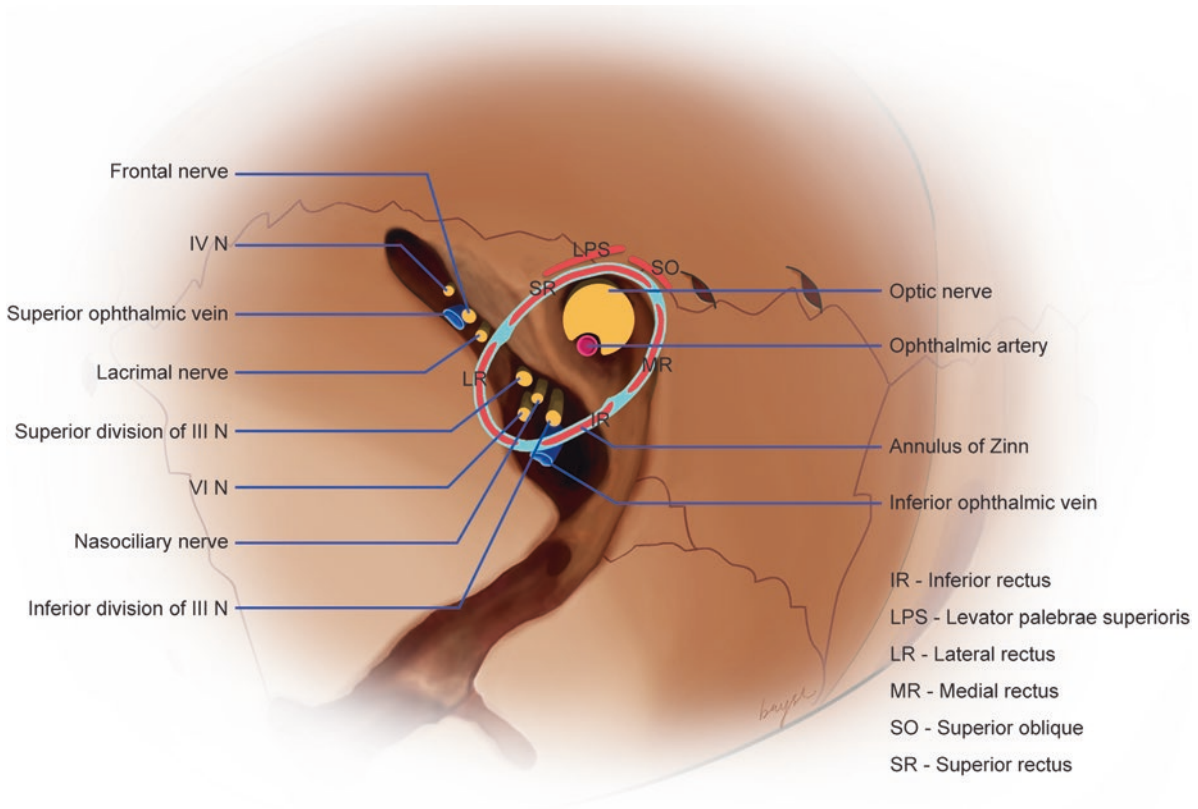

Fig. 1.6 Structures passing through the superior orbital fissure

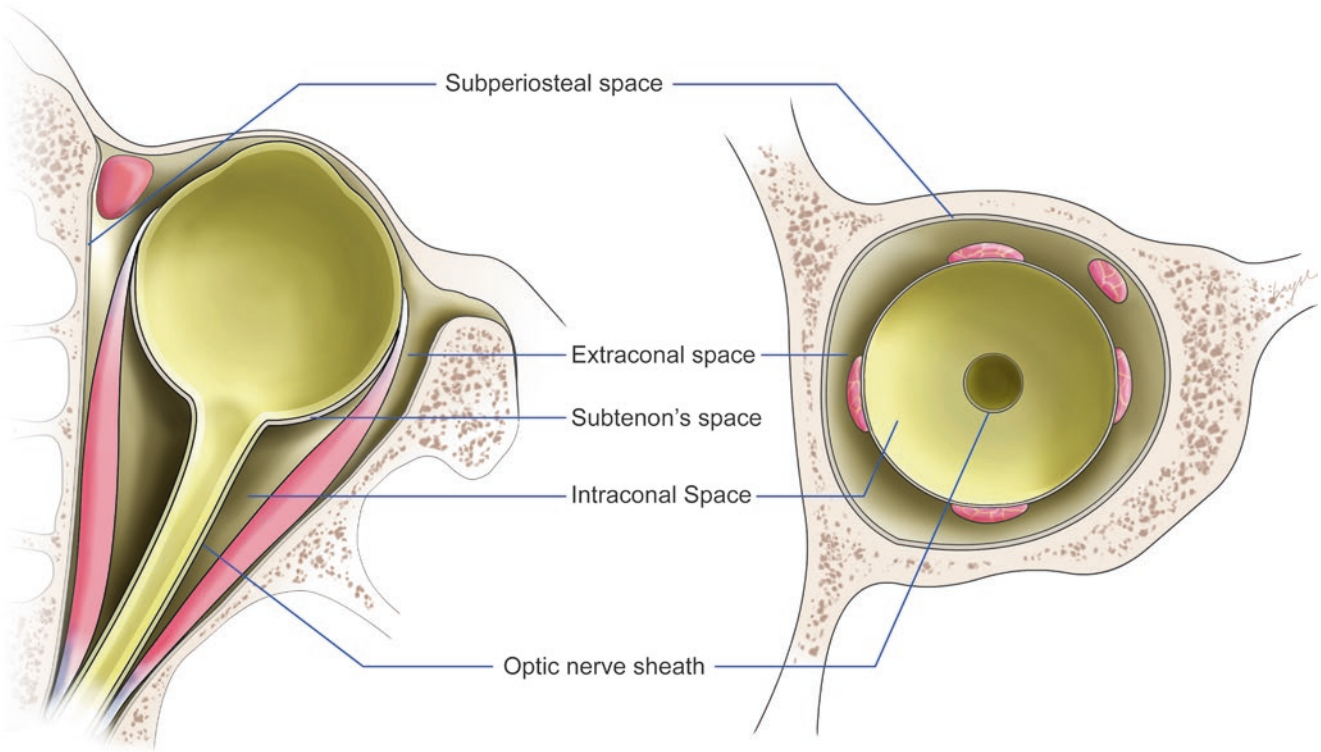

Fig. 1.7 Different spaces of the orbit, axial and coronal views

lateral wall that is removed during orbital decompression lies between the superior and inferior orbital fissures.

Among the soft tissues within the orbit, the globe forms the most important unit. The total volume of the orbit is about 30 ml and that of the globe is about 7 ml. The optic nerve connects the globe to the optic chiasma through the optic canal. The intraorbital portion of the optic nerve is about 25 mm long in the orbit, and has an undulating course so there is room for stretching without loss of function in cases of progressive proptosis due to tumours or inflammation.

The orbit itself is divided into four spaces (Fig. 1.7), an intraconal space, an extraconal space, a subperiosteal space, and a lacrimal space. The extraocular muscles and the intermuscular septae separate the intraconal from the extraconal space. The intraconal space is occupied by the optic nerve and the intraconal fat. The extraconal space is bounded by the periorbita externally, and contains the extraconal fat. The nerves (sensory and motor) and vessels travel in both intra- and extraconal spaces. The subperiosteal space is a potential space, and it expands only when fluid, blood or pus accumulate. The periorbita serves as a barrier for the spread of tumours; therefore the spreading tumour from adjacent sinuses occupies the subperiosteal space initially before breaking into the orbit. The lacrimal gland fossa may be considered a separate compartment and accommodates the orbital lobe of the lacrimal gland. The neurovascular bundle enters the gland from the posterior aspect. In addition to the above spaces, there is optic nerve sheath and the subtenon's space around the eye. These various spaces can be accessed surgically from various aspects, anteriorly through the eyelid and conjunctiva, medially through an endoscopic nasal and retro-caruncular approaches, inferiorly through the oral cavity and inferior conjunctiva, superiorly through transcranial/coronal approach, and temporally through lateral canthus, lateral orbital wall and/or the temporal fossa.

The vascular supply to the orbit is primarily from the ophthalmic artery, branch of internal carotid artery, which enters the orbit through the optic canal. The main branches of the artery include the central retinal artery, the short and long ciliary arteries, anterior and posterior ethmoidal arteries, muscular arteries, the lacrimal, supraorbital, and the supratrochlear and dorsal nasal arteries (Fig. 1.8). The venous drainage is through superior and inferior ophthalmic veins, the latter usually joins the superior and also communicates with the pterygoid plexus. The superior ophthalmic vein then passes through the SOF and drains into the cavernous sinus. It is enlarged in cavernous sinus thrombosis as well as in carotid-cavernous fistula. The orbital veins are valveless, and this is one of the reasons for spreading infective thrombi from sinuses as well as from the orbit to the cavernous sinus.

Apart from the optic nerve, the nerve supply comes from the cranial nerves III, IV, and VI for the extraocular muscles constituting the motor supply (Fig. 1.9), and the V1 and V2 providing the sensory supply to the superior and inferior orbits, respectively (Fig. 1.10). There are no lymphatics in the orbit.

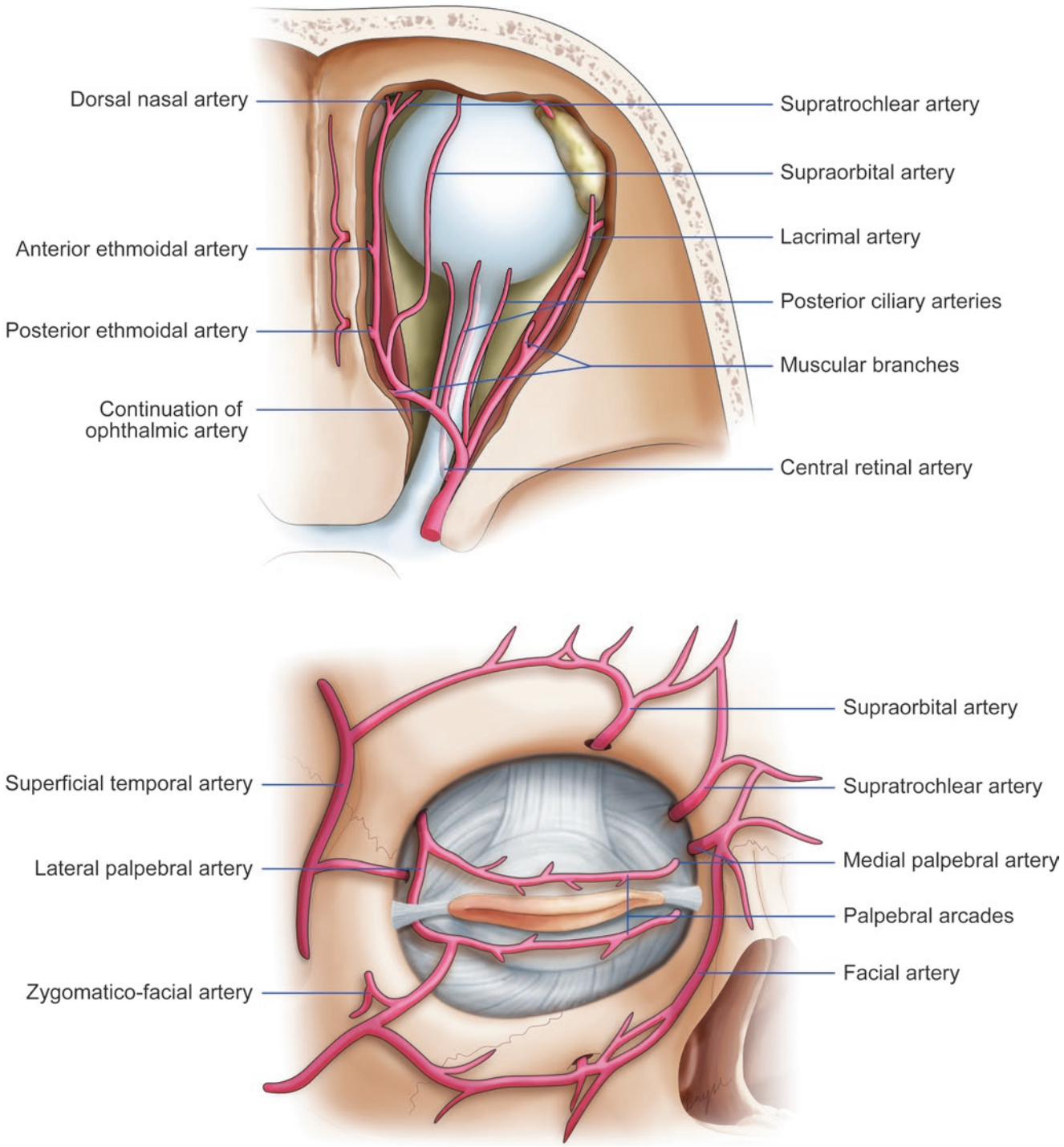

Fig. 1.8 Arterial supply of the orbital structures (above) and arterial supply of the eyelids showing anastomosis between external and internal carotid circulations (below)

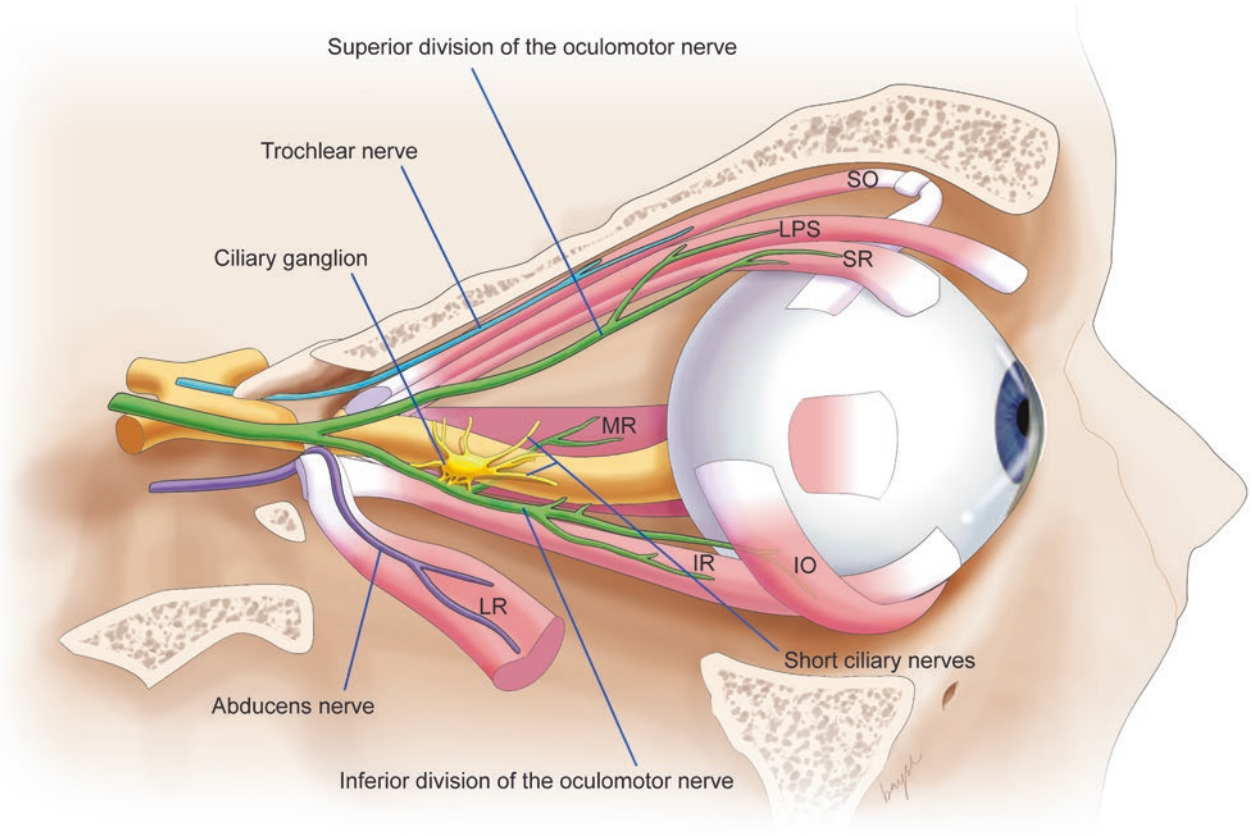

Fig. 1.9 Motor nerve supply to orbital structures. IO, inferior oblique muscle; IR, inferior rectus muscle; LPS, levator palpebrae superioris; LR, lateral rectus muscle; MR, medial rectus muscle; SO, superior oblique muscle; SR, superior rectus muscle

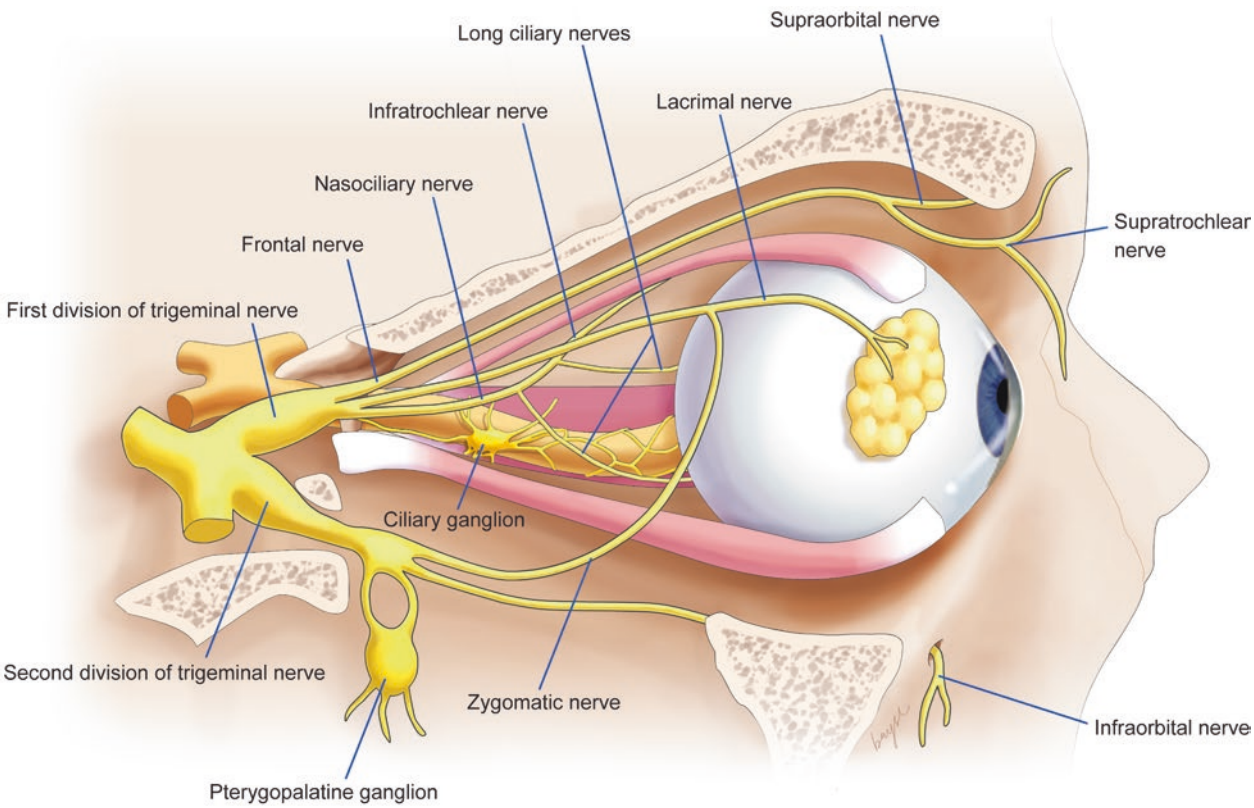

Fig. 1.10 Sensory nerves of the orbit

Further Reading

1. Dutton J. The lacrimal systems. In: Dutton J, editor. Atlas of clinical and surgical orbital anatomy. Philadelphia: WB Saunders; 1994.
2. Ezra DG, Beaconsfield M, Collin R. Surgical anatomy of the upper eyelid: old controversies, new concepts. Expert Rev Ophthalmol. 2014;4(1):47–57. https://doi.org/10.1586/17469899.4.1.47.
3. Jordan DR, Mawn L, Anderson RL. Surgical anatomy of the ocular adnexa. In: Parrish R, editor. Sponsored by American Academy of Ophthalmology. 2nd ed. New York: Oxford University Press; 2012.
4. Lemke B, Della Rocca R. Surgery of the eyelids and orbit: an anatomical approach. East Norwalk: Appleton & Lange; 1990.
5. Lemke BN. Lucarelli M.J. Anatomy of the ocular adnexa, orbit, and related facial structures. In: Black E, Nesi F, Calvano C, Gladstone G, Levine M, editors. Smith and Nesi's ophthalmic plastic and reconstructive surgery. New York: Springer; 2012.
6. Rootman J. Diseases of the orbit, a multidisciplinary approach. 2nd ed. Philadelphia: Wolters Kluwer Lippincott Williams & Wilkins; 2003.
7. Rootman J, Stewart B, Goldberg RA. Orbital surgery – a conceptual approach. 2nd ed. Philadelphia: Wolters Kluwer Lippincott Williams & Wilkins; 2013. p. 79–146.
8. Rose JG Jr, Lucarelli MJ, Lemke BN. Lacrimal, orbital, and sinus anatomy. In: Woog J, editor. Manual of endoscopic lacrimal and orbital surgery. New York: Elsevier; 2003.
9. Zide BM, Jelks GW. Surgical anatomy of the orbit. New York: Raven Press; 1985.

Imaging: Computerised Tomography

2

Poh Sun Goh

Introduction

Computerised tomography (CT) scan was introduced in clinical practice in 1971 with single axial slice at a time scanning capability. This has progressively evolved into current modern CT scanners which perform volumetric imaging, with retrospectively reconstructing images in different planes and thicknesses providing high-resolution soft tissue and bone images in short scan durations.

Indications of CT Scan

Computed tomography (CT) scan is the modality of choice for most orbital pathology especially for orbital and orbitofacial trauma. In the evaluation of orbital space-occupying lesions, apart from soft tissue characteristics, CT offers additional information regarding osseous involvement such as bony erosions (Fig. 2.1a, b), bony tumours (Fig. 2.1c), calcification (Fig. 2.1d), and radio-opaque foreign bodies (FB) (Fig. 2.2a) that may be difficult to detect on MRI. It also delineates bony remodelling in long-standing tumours, such as pleomorphic adenoma, and bony erosions in adenoid cystic carcinoma of the lacrimal gland. It shows a typical ground glass appearance in fibrous dysplasia, densely calcified nidus in osteoma, hyperostosis in sphenoidal wing meningioma, and osteoclastic lesions in Langerhans histiocytosis, metastatic prostate carcinoma (sunburst appearance), and neuroblastoma. It is useful in localizing air in the orbit (Fig. 2.2b) as a result of trauma and cellulitis caused by gas-forming anaerobic infections. It can show clinically useful details for orbital infection such as fat stranding and subperiosteal abscess with sinusitis (Fig. 2.3).

Multiplanar imaging not only displays images in coronal and sagittal planes to add to axial planes, but it can also produce reconstructed images in curved planes. Three-dimensional (3D) reconstructions, as well as CT angiography, with and without 3D visualization of the main neck and intracranial vessels using bone subtraction, can be done quickly and rapidly with modern CT scanners. In cases of suspected orbital vascular malformations, a dedicated dynamic arterial phase CT angiogram and Valsalva-augmented venous phase CT protocol have been used. They have the advantage of assessing arterial anatomy, lesion morphology, enhancement kinetics, and distensibility of orbital masses, all in one examination.

CT with 3D reconstructions are beneficial not only in treatment planning but also in preoperative patient education and counselling in cases of orbital fractures and deformities. Image-guided surgery (IGS) utilizes DICOM (Digital Imaging and Communications in Medicine) compatible data from sub-mm imaging of CT scans, not only to perform virtual treatment planning but also for stereolithographic (STL) modelling which aids in post-traumatic and tumour deformity management.

The detailed osseous anatomy available on CT (especially on bone windows) is also helpful in assessing the thickness of cortical and cancellous bone when planning orbital decompression surgery.

Cone beam CT (CBCT) is a more recent application used in radiology facilities as well as in the clinic and intraoperative spaces. It has low radiation compared to standard CT and gives clinically useful images of the bony anatomy and is therefore used to guide treatment preoperatively and intraoperatively to ensure good reduction in fractures and correction of deformities.

P. S. Goh (✉)
Department of Diagnostic Imaging, National University Hospital, Singapore

Department of Diagnostic Imaging, Yong Loo Lin School of Medicine, National University of Singapore, Singapore
e-mail: dnrgohps@nus.edu.sg

S. Amrith et al. (eds.), *Ocular Adnexal Lesions*, https://doi.org/10.1007/978-981-13-3798-7_2

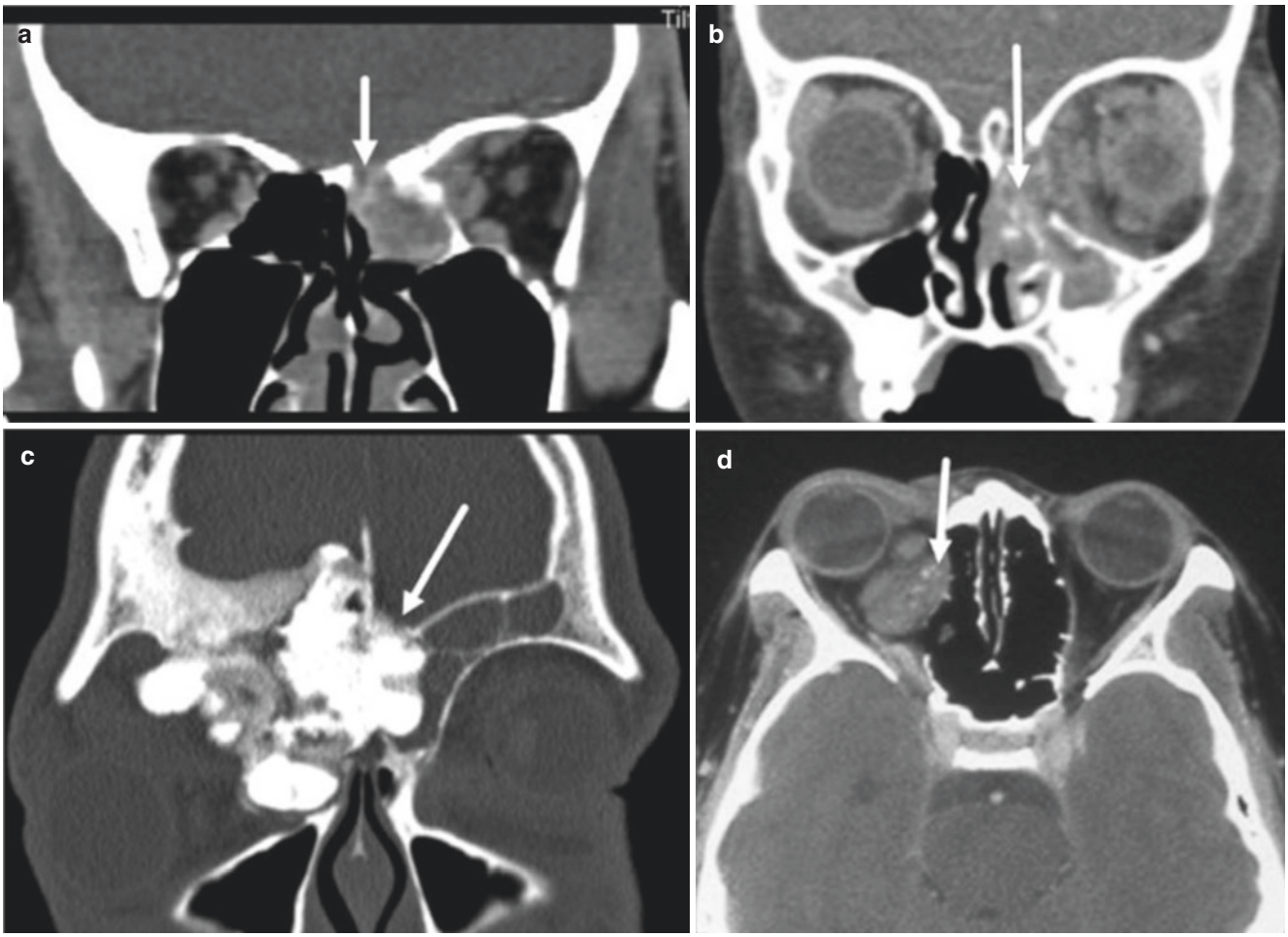

Fig. 2.1 (**a**) Coronal CT scan showing sinus tumour eroding the base of the skull (arrow). (**b**) Note the bony erosion of the medial orbital wall in a sinus tumour (arrow). (**c**) Bony lesion of the orbit. (**d**) Calcification in a vascular malformation

Intravenous iodine-containing contrast can be used to evaluate tumour enhancement and vascularity. Neural tumours show avid contrast enhancement, and the vascular malformations such as cavernous hemangioma show progressive enhancement. The contrast can be used in CT angiogram to evaluate the feeding and draining vessels in arteriovenous malformations (AVMs) and large carotid-cavernous (CC) fistulae.

Positron emission tomography combined with CT (PET-CT) is a form of isotope imaging using a tracer fluorine-18 (F-18) fludeoxyglucose (FDG), an analogue of glucose, that is taken up by glucose-using cells such as rapidly growing malignant tumours (Fig. 2.4). This is used to screen disease during systemic workup (e.g. in lymphomas), to evaluate for active disease versus scar during follow-up, and to monitor disease activity after treatment. PET-CT has been found to be extremely useful for the latter.

Contraindications for CT Scan

As with any ionizing radiation including X-rays, CT scan is generally avoided in pregnancy, especially during the early stages, and when indicated employed with radiation-minimizing strategies such as lead apron shielding, etc. Iodine contrast is taken up by the foetal thyroid with resultant hypothyroidism, and hence should not be used during pregnancy. For patients with iodine allergy, CT scan can be obtained without contrast (as is done for suspected fractures) where sufficient details can be seen; however MRI is prefer-

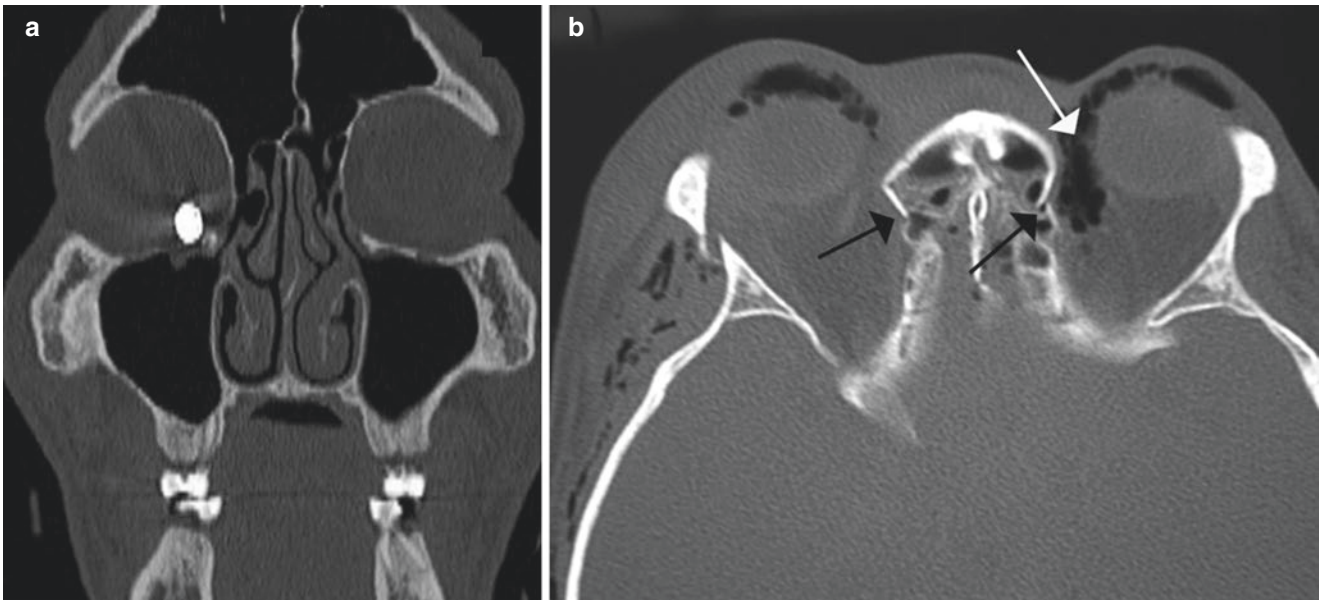

Fig. 2.2 (**a**) Coronal CT showing an intraorbital foreign body. (**b**) An axial CT scan with the black arrows showing the naso-ethmoidal fracture and the white arrows showing air in the orbit

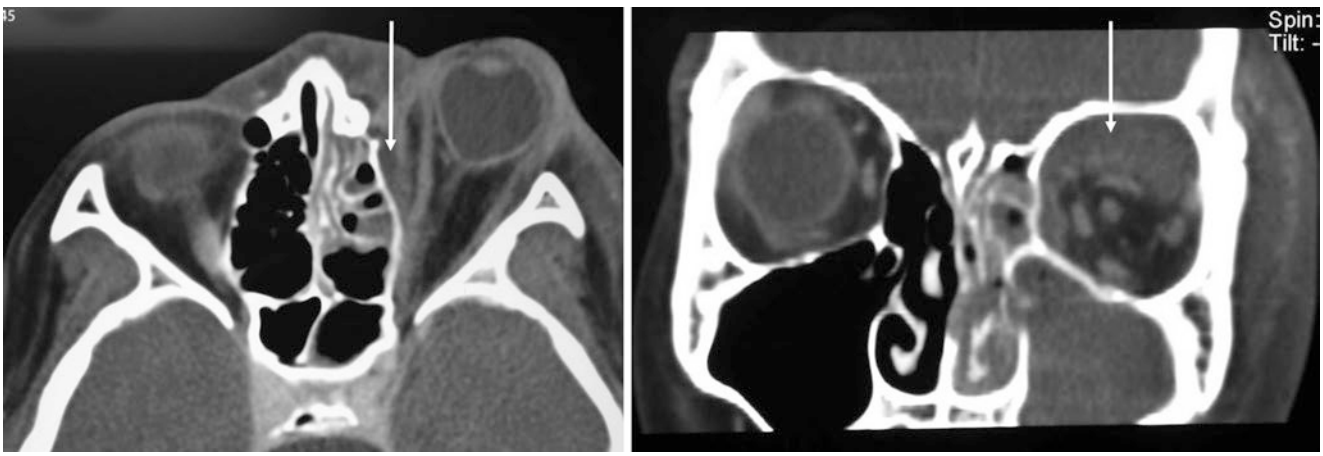

Fig. 2.3 Axial scan on the left orbit shows the arrow pointing to the medial subperiosteal abscess. Note the tenting of the globe showing extreme proptosis. The coronal scan on the right shows superior subperiosteal abscess (white arrow)

able for studying tumours and vascular conditions where CT scan does not give sufficient details without contrast.

Some patients who receive intravenous contrast may experience a deterioration of renal function (contrast-induced nephropathy). Patients whose eGFR (estimated glomerular filtration rate) is less than 60 ml/minute and who are on metformin for their type 2 diabetes are at particular risk. Thus it is advised that metformin should be stopped 48 hours before the scan to minimize the risk of renal failure. Although not an absolute contraindication, contrast use and increased radiation exposure limit the use of CT scan in paediatric population and also for those requiring serial imaging for monitoring disease progression.

Advantages of CT Scan

Modern-day CT scanners are widely available and significantly less expensive than MRI. CT scan is preferable in patients who have difficulty keeping still, as the scan is com-

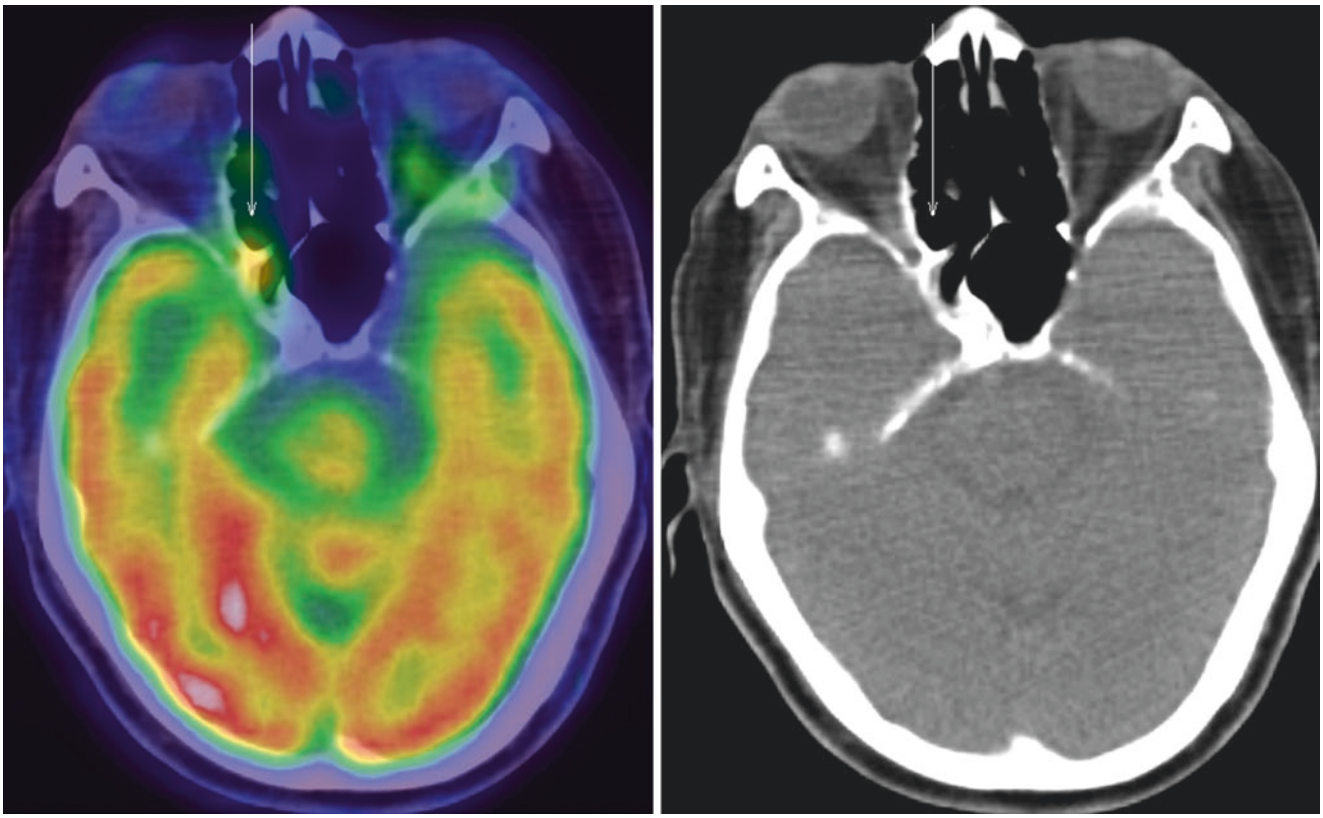

Fig. 2.4 A PET-CT (left) and a CT scan (right), with the arrow pointing to avid uptake of FDG in a tumour at the right orbital apex

pleted relatively quickly (in seconds), compared with 20 minutes to an hour for comprehensive MR imaging of the orbits and brain, and MR angiography. In addition, motion artefacts are minimized because of fast acquisition of data by the new-generation volumetric CT scanners. Hence, it is also useful in patients who are claustrophobic, are medically unstable, and require a rapid scan in conditions such as head trauma, facial trauma, suspected intracranial haemorrhage, orbital and globe trauma (including penetrating injuries), evaluation of aneurysms, and CC fistulas.

Disadvantages of CT Scan

Although CT scan can be used to detect intraocular tumours (such as retinoblastoma and melanoma) and optic nerve and sheath tumours, soft tissue resolution may be better in MRI scan. Moreover, tissue characteristics including paramagnetic properties of tumours (uveal melanoma) are better studied with MRI. Ionizing radiation is a potential risk especially in children and those with germline mutations with tumour diathesis, particularly with repeated follow-up CTs. US Food and Drug Administration (FDA) has provided estimates about the effective radiation doses from diagnostic CT procedures, and they are typically in the range of 1–10 mSv (millisievert). The radiation received in a head CT is estimated to be 2 mSv. However, studies have shown that the risk of developing cancer is quite low compared to the natural risk of cancer. There is a substantial increase in dose efficiency with modern CT scanners and hence may be of negligible significance in clinical practice.

Conclusion

Computed tomography (CT) is still the mainstay in the investigation of orbital trauma and disease. It has wide-ranging applications in the diagnosis, treatment planning, and reconstruction of the orbit. The advantages/disadvantages of CT are highlighted in this chapter, and when safety issues are a concern, the clinician should discuss with the radiologist to vary CT protocols as necessary.

Further Reading

1. Ben Simon GJ, Annunziata CC, Fink J, Villablanca P, McCann JD, Goldberg RA. Rethinking orbital imaging. Establishing guidelines for interpreting orbital imaging studies and evaluating their predictive value in patients with orbital tumors. Ophthalmology. 2005;112(12):2196–22.

2. Goh PS, Gi MT, Charlton A, Tan C, Gangadhara Sundar JK, Amrith S. Review of orbital imaging. Eur J Radiol. 2008;66(3):387–95.
3. Naik MN, Tourani KL, Sekhar GC, Honavar SG. Interpretation of computed tomography imaging of the eye and orbit. A systematic approach. Indian J Ophthalmol. 2002;50:339–53.
4. Prokop M. Multislice CT: technical principles and future trends. Eur Radiol. 2003;13(Suppl 5):3–13.
5. Smith-Bindman R, Lipson J, Marcus R, Kim KP, Mahesh M, Gould R, Miglioretti DL. Radiation dose associated with common computed tomography examinations and the associated lifetime attributable risk of cancer. Arch Intern Med. 2009;169(22): 2078–86.
6. Stacul F, van der Molen AJ, Reimer P, et al. Contrast Media Safety Committee of European Society of Urogenital Radiology (ESUR). Contrast induced nephropathy: updated ESUR Contrast Media Safety Committee guidelines. Eur Radiol. 2011;21(12):2527–41.
7. Tawfik HA, Abdelhalim A, Elkafrawy MH. Computed tomography of the orbit – a review and an update. Saudi J Ophthalmol. 2012;26(4):409–18.

Imaging: Magnetic Resonance Imaging

3

Yun Song Choo and Eric Ting

The use of magnetic resonance imaging (MRI) for the investigation of orbital pathology was first reported in 1983 [1]. There have been many developments since, including technological advances and wider availability of MRI resulting in its increasing use in ophthalmological practices. MRI is now widely accepted as complementary to physical examination and other investigative tools for the diagnosis, staging, prognostication, and ongoing monitoring of many orbital pathologies. This article aims to inform the reader of the basic principles and imaging protocols used in MRI of the orbits.

Basic MRI Physics

MRI provides high-resolution imaging of soft tissue in the body, which contains abundant hydrogen atoms. The patient is placed within a strong magnetic field, where radiofrequency pulses are used to excite the hydrogen (^{1}H) protons to produce signals which are detected and processed to produce images. The magnetic field is created by a large magnet within the scanner apparatus (commonly 1.5 T [Tesla] or 3.0 T in clinical orbital MRI). The protons in the patient's tissues act as tiny dipoles and are aligned along the direction of the magnetic field (longitudinal magnetisation) with rotation around their own axes (precession) according to the strength of the magnetic field. The protons usually precess in different phases, but the application of a radiofrequency pulse (transmitted by coils) during MRI results in them precessing in phase with one another. With the cessation of the radiofrequency pulse, the protons will revert back to their resting state: the longitudinal magnetisation along the axis of the main magnet is regained with time (T1-relaxation), and the protons will also begin to precess out of phase (T2-relaxation). The T1- and T2-relaxation times depend on the composition of the tissue and also the environment in which the tissue is situated (i.e. tissue-specific property).

As the longitudinal magnetisation is regained, the protons emit the extra energy that they have gained during the radiofrequency pulse application in the form of weak radiofrequency signals (also known as echo). These echoes are received by receiver coils and processed with the computer to generate the images. Variable tissue contrast can be obtained by using different pulse sequences and by changing the imaging parameters, thereby conferring MRI the distinct advantage of soft tissue contrast [2].

The head coil is used to image both the orbits and brain. Smaller surface coils may be used in combination with the head coil when imaging ocular tumours to improve signal-to-noise ratio (SNR) within superficial structure, particularly at 1.5 T. The main advantage of higher magnetic field strength (3.0 T) is greater SNR, which can be used to achieve higher-resolution images and/or faster image acquisition times.

Common Sequences Used in MRI of the Orbits and the Visual Pathway

A systematic review of the included anatomical structures on the various sequences, including comparison with the contralateral orbit and with previous imaging studies of the orbits, should be performed when reading a MRI study of the orbits [3]. This section aims to describe the conventional MRI sequences used in routine clinical practice.

Y. S. Choo (✉)
Department of Diagnostic Imaging, National University Hospital, Singapore

E. Ting (✉)
Department of Diagnostic Imaging, National University Hospital, Singapore

Department of Diagnostic Imaging, Yong Loo Lin School of Medicine, National University of Singapore, Singapore

Advanced Medicine Imaging, Singapore
e-mail: eric.ting@proton.sg

S. Amrith et al. (eds.), *Ocular Adnexal Lesions*, https://doi.org/10.1007/978-981-13-3798-7_3

Planes of Acquisition

A three-plane localiser is performed at the beginning to allow localisation of the structures and enable planning of the sequences. Routine orbital imaging should include both axial and coronal thin sections (mm). Oblique imaging of the orbits can aid in visualisation of the optic nerve and chiasm, as well as the extraocular muscles and orbital apex [4]. While oblique imaging may be performed in any plane, only oblique sagittal sequences of each orbit are performed routinely in the author's institution. As oblique sagittal and coronal sequences have to be performed individually for each orbit, they may result in considerable increase in scan acquisition times.

T1-weighted (T1w)

Tissues with shorter T1-relaxation times such as fat are of higher signal intensity (brighter) than those with longer T1-relaxation times such as vitreous humour or cerebrospinal fluid (CSF). This sequence also forms the basis of comparison when establishing enhancement characteristics on the contrast-enhanced sequences.

T2-weighted (T2w)

Tissues with longer T2-relaxation times such as vitreous humour or CSF are of higher signal intensity than those with shorter T2-relaxation times such as blood products. Pathological areas are commonly T2w hyperintense.

Diffusion-Weighted Imaging (DWI)

Diffusion-weighted imaging is a technique that measures the motion of water molecules in the extracellular, extravascular space [5]. This sequence is usually performed in the transaxial plane and must be interpreted in conjunction with the accompanying apparent diffusion coefficient (ADC) maps. DWI is useful in both benign (such as abscesses [6], epidermoid inclusion cyst [7]) and malignant pathologies of the orbit. Generally, malignant orbital tumours demonstrate lower ADC values due to the enlarged nuclei, hypercellularity, and resultant limited extracellular space, with recent attempts at deriving an ADC threshold value for the differentiation between benign and malignant orbital tumours [8, 9].

Three-Dimensional (3D) Steady-State Free Precession (SSFP) Sequences

3D SSFP sequences are a type of gradient-echo sequence in which the image contrast is determined by the T2/T1 ratio of the tissue [10]. The various MRI vendors have different names for these sequences, but they are similarly valued for the excellent contrast between CSF or vitreous humour and other structures, particularly useful for the interrogation of the cisternal segments of the cranial nerves and in resolving small intraocular tumours. However there is poor contrast resolution of the surrounding soft tissue and brain parenchyma. The advantages of the 3D SSFP sequences are their high signal-to-noise ratio, high contrast-to-noise ratio [11], as well as intrinsic insensitivity to motion.

Fluid Attenuation Inversion Recovery (FLAIR)

FLAIR is a special pulse sequence that effectively nulls the high signal from CSF and vitreous humour [12]. While it is commonplace in neuroimaging for demyelinating diseases such as multiple sclerosis, there are now increasing reports of its potential utility in the characterisation of intraocular masses [13] and detection of optic neuritis [14].

Fat-Suppressed Sequences

The suppression of the high signal of fat may be achieved by several techniques [15] – fat saturation, short T1 inversion recovery (STIR), and opposed phase imaging – amongst which, the first two are more commonly employed in imaging of the orbits. Fat saturation is lipid-specific (excluding the water within adipose tissue) and hence reliable for contrast-enhanced T1w imaging and tissue characterisation in areas with large amounts of fat. However, it is susceptible to local magnetic field inhomogeneities such as those found at the air-bone interfaces in the lower portion of the orbit, leading to incomplete fat signal suppression and artifacts. STIR suppresses the signal of whole adipose tissue (including the water fraction) and is insensitive to magnetic field inhomogeneities. Both T1 and T2 differences contribute additively to image contrast in STIR, enhancing tissue contrast and aiding tumour detection. However, the signal suppression is non-specific, and signal from tissue with similar T1 to that of fat will also be suppressed (e.g. mucoid tissue, haemorrhage, gadolinium); on the other hand, fat-containing lesions may not have the same T1 as white fat, resulting in incomplete fat suppression.

Contrast-Enhanced Sequences

Gadolinium-based contrast agents (GBCAs) are administered intravenously prior to the acquisition of the contrast-enhanced sequences in multiple planes. It is essential to compare with the accompanying pre-contrast sequence when evaluating a contrast-enhanced image. Concomitant fat saturation has previously been advocated to accentuate the enhancement seen in optic nerve pathologies; however, the

technique has been associated with disease-mimicking artifacts [16] alluded to above, such that it is no longer recommended in the imaging of certain pathologies such as retinoblastoma [17]. Dynamic contrast enhancement (DCE) MRI can also be performed with plotting of time-intensity curves using regions of interest over an orbital mass. Washout-type curves have been shown to have high sensitivity and specificity for malignant orbital masses [18].

MR Angiography (MRA)

MRA is commonly performed using time-of-flight or phase-contrast techniques and may be performed with or without the administration of intravenous GBCAs [19]. MRA is commonly performed to evaluate the intracranial vasculature, for example, in excluding a posterior communicating artery aneurysm in a pupil-involving third nerve palsy or in evaluating the posterior circulation in homonymous hemianopia. MRA may also be employed to interrogate intra-orbital vascular pathologies such as malformations or carotid-cavernous fistula. However, conventional MRA techniques may have limitations in the evaluation of intra-orbital vascular lesions – phase-contrast techniques are limited by high-velocity phase-related artifacts and are susceptible to motion artifacts, while time-of-flight techniques may not visualise smaller vessels and only provide indirect flow information of larger arteries [19]. Newer dynamic contrast-enhanced MRA techniques such as time-resolved imaging of contrast kinetics (TRICKS) seek to bypass the above limitations and offer non-invasive evaluation of intralesional flow assessment with high-resolution soft tissue imaging without ionising radiation [20].

Indications for MRI of the Orbits

The indications for MRI of the orbits are varied and described in guidelines such as the American College of Radiology Appropriateness Criteria [21], with additional MRI techniques recommended depending on the clinical findings or for problem-solving if there are incidental findings on the routine sequences. Contrast-enhanced MRI of the orbits is the imaging modality of choice in the evaluation of intraocular masses and pre-chiasmal visual loss. Time-resolved MRA may be included if there is suspicion of a vascular lesion. A heavily T2-weighted sequence covering the cisternal segments of the cranial nerves and cavernous sinuses may be included when evaluating ophthalmoplegia. Contrast-enhanced MRI of the brain should also be performed in conjunction when evaluating possible optic neuritis. Contrast-enhanced computed tomography (CT) and MRI of the orbits are both appropriate in the context of suspected orbital infection, although availability is dependent on institution. In the evaluation of post-traumatic visual defects or suspected orbital trauma, CT is the initial modality of choice for evaluating orbital fractures as well as foreign bodies, while MRI occasionally plays a complementary role, being more sensitive in detecting optic nerve oedema and avulsion. MRI is rarely indicated in the evaluation of non-neoplastic intraocular processes such as glaucoma, vitreous haemorrhage, and retinal detachment.

Given the many MRI protocols in use, it is advisable to communicate the suspected pathology and anatomical localisation clearly on the requisition form such that the most appropriate imaging protocol may be recommended to optimise the diagnostic yield of the study.

Contraindications and Disadvantages of MRI

The following is a non-exhaustive list of common contraindications to MRI:

- Implantable cardiac devices: MRI has been discouraged in patients with implantable cardiac devices due to the potential for device failure and fatal arrhythmia. In cases where MRI is essential, informed consent and close monitoring of the patient must be in place [22]. A recent prospective study however suggests that with the use of a prespecified safety protocol, no long-term clinically significant adverse event is associated with MRI scans in patients with implantable cardiac devices of unknown MRI safety status [23]. In patients with MR-compatible pacemakers, studies have reported favourable outcomes.
- Intra-orbital metallic foreign bodies and intracranial aneurysm clips may dislodge.
- Otologic implants require special measures prior to MRI scans with caution especially for implantable hearing devices in MRI environments due to their direct attachment to the ossicles and use of magnets [24].

There are booklets listing the MR compatibility of implants or devises which are available in the MR rooms. These implants must have undergone safety testing within MR magnetic fields.

There is currently no conclusive evidence of any deleterious effects of MRI on the developing foetus [21]. However, recommendations for pregnant patients are institution-dependent; for example, MRI is strongly discouraged in the first trimester in the author's institution. Gadolinium-based contrast agents (GBCAs) can cross the placenta and should also not be routinely administered to pregnant patients given the unknown risks posed to the foetus [25].

In lactating mothers, some centres advise informed consent and to stop breastfeeding (to express and discard the breastmilk) for 24 hours following intravenous contrast administration. However the amount of contrast excreted in breastmilk and subsequently absorbed by the infant's digestive system is believed to be negligible.

GBCAs are also contraindicated in patients with severe renal dysfunction (estimated glomerular filtration rate of <30 mL/min/1.73 m^2) because of the association with potentially fatal nephrogenic systemic fibrosis [25].

There is now strong evidence for the deposition of GBCAs in the deep nuclei of the brain. The observation of high signal intensity in the dentate nucleus and globus pallidus on unenhanced T1w MR images of patients who had received repeated doses GBCAs was first reported in 2014 by Kanda et al. [26] GBCAs are commonly classified as non-ionic or ionic and linear or macrocyclic, based on the structure of the chelating agent bound to the gadolinium ion. Emerging evidence suggests differences in deposition amongst different agents and classes of agents (e.g. macrocyclic vs linear agents). To date, there are no known risks associated with gadolinium deposition in the brain. However, it is advisable to discuss the need for GBCAs with a radiologist and to consider the latest evidence regarding the choice of the individual GBCA.

Allergy or anaphylaxis due to gadolinium-based contrast agents is very rare and occurs less frequently compared with iodinated contrast in CT.

In addition to the technical artifacts described above, MRI of the orbits is also susceptible to motion artifacts commonly caused by blinking [27] or globe motion [4, 28] (whether involuntary or otherwise), which is also contributed by the long acquisition time of certain sequences. Significant susceptibility artifacts may also be generated by orthodontic implants, eye make-up/tattoos, or aneurysm clips, obscuring the structures of interest – newer scanners may have metal artifact reduction capabilities that can bypass this limitation [29]. The relatively long scan time may also necessitate sedation or general anaesthesia in paediatric or claustrophobic patients [30].

Summary

This chapter provides a short introduction of the basic principles and protocols utilised in MR imaging of the orbits for clinicians. It is important for clinicians to communicate their key clinical findings and preliminary diagnostic suspicions so that the correct imaging protocols may be recommended and to allow correct image interpretation by the radiologist. In addition, important safety features and contraindications to MRI are also highlighted in this chapter.

Further Reading

1. Moseley I, Brant-Zawadski M, Mills C. Nuclear magnetic resonance imaging of the orbit. Br J Ophthalmol. 1983;67(6):333–42.
2. Arathi S, Aparna I, Sarada D. Magnetic resonance imaging for the ophthalmologist: a primer. Indian J Ophthalmol. 2012;60(4):301–10.
3. Kruger JM, Cestari DM, Cunnane MB. Systematic approaches for reviewing neuro-imaging scans in ophthalmology. Digit J Ophthalmol. 2017;23(3):50–9.
4. Herrick RC, Hayman LA, Taber KH, et al. Artifacts and pitfalls in MR imaging of the orbit: a clinical review. Radiographics. 1997;17:707–24.
5. Koh DM, Collins DJ. Diffusion-weighted MRI in the body: applications and challenges in oncology. Am J Roentgenol. 2007;188(6):1622–35.
6. Sepahdari AR, Aakalu VK, Kapur R, et al. MRI of orbital cellulitis and orbital abscess: the role of diffusion-weighted imaging. Am J Roentgenol. 2009;193(3):W244–50.
7. Rao AA, Naheedy JH, Chen JYY, et al. A clinical update and radiologic review of paediatric orbital and ocular tumours. J Oncol. 2013;2013:975908.
8. Sepahdari AR, Politi LS, Aakalu VK, et al. Diffusion-weighted imaging of orbital masses: multi-institutional data support a 2-ADC threshold model to categorize lesions as benign, malignant, or indeterminate. Am J Neuroradiol. 2014;35(1):170–5.
9. Xu XQ, Hu H, Su GY, et al. Diffusion-weighted imaging for differentiating benign from malignant orbital tumours: diagnostic performance of the apparent diffusion coefficient based on region of interest selection method. Korean J Radiol. 2016;17(5):650–6.
10. Chavhan GB, Babyn PS, Jankharia BG, et al. Steady-state MR imaging sequences: physics, classification, and clinical applications. Radiographics. 2008;28(4):1147–60.
11. Roser F, Ebner FH, Danz S, et al. Three-dimensional constructive interference in steady-state magnetic resonance imaging in syringomyelia: advantages over conventional neuroimaging. J Neurosurg Spine. 2008;8(5):429–35.
12. De Coene B, Hajnal JV, Gatehouse P, et al. MR of the brain using fluid-attenuated inversion recovery (FLAIR) pulse sequences. Am J Neuroradiol. 1992;13(6):1555–64.
13. Damento GM, Koeller KK, Salomao DR, Pulido JS. T2 fluid-attenuated inversion recovery imaging of uveal melanomas and other ocular pathology. Ocul Oncol Pathol. 2016;2(4):251–61.
14. Boegel KH, Tyan AE, Iyer VR, et al. Utility of contrast-enhanced fat-suppressed FLAIR in the evaluation of optic neuropathy and atrophy. Eur J Radiol Open. 2017;4:13–8.
15. Delfaut EM, Beltran J, Johnson G, et al. Fat suppression in MR imaging: techniques and pitfalls. Radiographics. 1999;19(2):373–82.
16. Borges AR, Lufkin RB, Huang AY, et al. Frequency-selective fat suppression MR imaging: localised asymmetric failure of fat suppression mimicking orbital disease. J Neuroophthalmol. 1997;17(1):12–7.
17. de Graaf P, Goricke S, Rodjan F, et al. Guidelines for imaging retinoblastoma: imaging principles and MRI standardization. Pediatr Radiol. 2012;42(1):2–14.
18. Xian JF, Zhang ZY, Wang ZC, et al. Value of MR imaging in the differentiation of benign and malignant orbital tumours in adults. Eur Radiol. 2010;20(7):1692–702.
19. Ozsariak O, van Goethem JW, Maes M, Parizel PM. MR angiography of the intracranial vessels: technical aspects and clinical applications. Neuroradiology. 2004;46:955–72.
20. Kahana A, Lucarelli MJ, Grayev AM. Noninvasive dynamic magnetic resonance angiography with time-resolved imaging of contrast kinetics (TRICKS) in the evaluation of orbital vascular lesions. Arch Ophthalmol. 2007;125(12):1635–42.
21. Orbits, vision and visual loss. American College of Radiology. Appropriateness Criteria; 2017.
22. Kanal E, Barkovich AK, Bell C, et al. ACR guidance document on MR safe practices: 2013. J Magn Reson Imaging. 2013;13:501–30.
23. Nazarian S, Hansford R, Rahsepar AA, et al. Safety of magnetic resonance imaging in patients with cardiac devices. N Engl J Med. 2017;377:2555–64.

24. Fritsch MH, Mosier KM. MRI compatibility issues in otology. Curr Opin Otolaryngol Head Neck Surg. 2007;15:335–40.
25. ACR Committee on Drugs and Contrast Media. ACR manual on contrast media, version 10.3. American College of Radiology; 2017.
26. Kanda T, Ishii K, Kawaguchi H, Kitajima K, Takenaka D. High signal intensity in the dentate nucleus and globus pallidus on unenhanced T1-weighted MR images: relationship with increasing cumulative dose of a gadolinium-based contrast material. Radiology. 2014;270(3):834–41.
27. Berkowitz BA, McDonald C, Ito Y, et al. Measuring the human retinal oxygenation response to a hyperoxic challenge using MRI: eliminating blinking artifacts and demonstrating proof of concept. J Magn Reson Med. 2001;46(2):412–6.
28. Fanea L, Fagan AJ. Review: magnetic resonance imaging techniques in ophthalmology. Mol Vis. 2012;18:2538–60.
29. Gach HM, Mackey SL, Rehman S, et al. Magnetic resonance imaging metal artifact reduction for eye plaque patient with dental braces. J Contemp Brachytherapy. 2017;9(5): 490–5.
30. Kennedy TA, Corey AS, Policeni B, et al. ACR Appropriateness Criteria Â® Orbits Vision and Visual Loss. J Am Coll of Radiol. 2018;15(5):S116–31.

Pathology: Principles of Basic Histopathology

4

Bingcheng Wu and Min En Nga

Introduction

The diagnostic pathology service aims to provide an accurate and timely diagnosis on examination of tissue biopsies in order to facilitate prompt and appropriate management.

Close communication between the clinical team and pathologist is of key importance. The salient clinical information should be provided to the pathologist, starting with an accurate description of the location and nature of the tissue and the type of tissue biopsy. Important information also includes the relevant clinical findings, the clinical impression and any relevant current or previous investigations. This information can be clearly stated in the pathology request form and further supplemented by direct interaction with the pathologist.

Here, we provide a brief outline of the main types of specimens received by the pathology laboratory and how they are handled. We will also highlight ways in which clinicians can assist in the diagnostic process by providing concise and relevant information to the pathology laboratory.

Types of Biopsy Specimens

Specimens for pathology can be divided into two main types: *histology* (solid tissue pieces ranging from small punch biopsies to excision biopsies) and *cytology* (material from fine needle aspiration (FNA) or fluid samples). Most of the specimens from the ocular adnexa are solid tissue biopsies for histologic examination.

Here we describe the range of specimens received in the pathology laboratory from ocular adnexal lesions.

Cytology: Fine Needle Aspiration (FNA) of Ocular Adnexal Masses

Orbital masses that are relatively superficial and palpable can be accessed by FNA cytology. A fine bore needle (often 23 or 25 gauge) can be used to sample such lesions for cytologic examination. Lesions may be cystic (e.g. dermoid cyst, adnexal cystic lesions) or solid (e.g. lymphoid proliferations, inflammatory lesions, lacrimal gland neoplasms or intracranial neoplasms extending into the orbit). Most of the time, samples yield a small amount of material which is directly smeared onto glass slides and stained for microscopic evaluation.

The smears are best performed with on-site evaluation by a trained laboratory technologist (e.g. cytotechnologist), who can evaluate specimen adequacy immediately and can optimise tissue handling for ancillary testing.

For FNAs, here are the steps taken in smear preparation:

For each pass, two types of smears are prepared so as to provide complementary information:

1. An air-dried smear for immediate staining and on-site review (air-dried smears allow for evaluation of the cytoplasm, stroma and background material)
2. An alcohol-fixed smear for later review (these allow for evaluation of nuclear and cytoplasmic detail)

It is important that material is fixed *immediately* – whether by air-drying or alcohol. Delayed fixation causes artefacts that may result in a non-diagnostic or inaccurate cytologic interpretation.

B. Wu
Department of Pathology, National University Hospital, Singapore

M. E. Nga (✉)
Department of Pathology, National University Hospital, Singapore

Department of Pathology, Yong Loo Lin School of Medicine, National University of Singapore, Singapore
e-mail: patngame@nus.edu.sg

S. Amrith et al. (eds.), *Ocular Adnexal Lesions*, https://doi.org/10.1007/978-981-13-3798-7_4

Cytotechnologists are able to evaluate for sample adequacy and provide useful information for sample triage, e.g. to obtain more for microbiologic assessment, or more material for ancillary testing.

Cell blocks are solid tissue pieces processed from cytology specimens (FNAs or fluids), which are fixed in formalin, and are useful for performing ancillary tests. They are similar to very small histology biopsies. Often, a dedicated needle pass is required for a good cell block. Cytotechnologists, during on-site evaluation, may suggest that a cell block is necessary, whereupon the clinician should perform an additional needle pass.

Vitreous fluid specimens may also be obtained for examination for the exclusion of malignancy; however, these are not within the scope of this book.

Practical Points

1. Proper smear preparation, fixation and staining are essential to an accurate diagnosis. Hence the pathology department should be contacted where possible for on-site specimen evaluation for all FNAs.
2. In some instances, additional ancillary tests (e.g. immunocytochemistry) may be helpful; hence cytotechnologists may prompt clinicians to perform additional passes to obtain more tissue.

Histology

Histological tissue samples are solid tissue pieces that can range in size from minute pieces to entire organ resection specimens. Unless fresh tissue is required, these are usually immersed in 10% neutral buffered formalin and sent in sealed containers.

Here are the specimen processing steps following receipt in the pathology lab. Aside from the actual description and trimming of the specimens, most of the processing work is handled by qualified laboratory technologists.

From Specimen to Slide

1. Specimens are checked for correct identification and matched with the description given by the requesting clinician. An accession number (unique specimen number) is assigned to each specimen. Specimen details are entered into the laboratory information system, the electronic laboratory database which interfaces with the hospital medical record system.
2. Following adequate tissue fixation in formalin, the laboratory technologist/duty pathologist or resident then examines the specimen, providing a detailed gross description highlighting clinically relevant information.

Note: Poorly fixed tissue results in ultimately poor slide quality. Tissues should thus be immersed in sufficient quantities of formalin solution as soon as possible after biopsy and transported to the lab without delay. Formalin penetrates tissue at a rate of approximately 1 mm per hour.

3. The pathologist then cuts up the specimen, sampling areas that provide the most optimal diagnostic and prognostic information. This is known as grossing, trimming or specimen cut-up. The tissue pieces are approximately 3–4 mm thick and have flat surfaces which are readily cut into thin tissue sections on glass slides.

Note: Only the tissue pieces specifically sampled by the pathologist will be processed into glass slides. Hence, appropriate sampling is crucial for rendering an accurate diagnosis.

4. The trimmed tissue pieces are placed into labelled fenestrated plastic cassettes (Fig. 4.1a) and then reimmersed in formalin. For small biopsies, the entire biopsy tissue is usually sampled.
5. The cassettes are then placed into an automated tissue processor, which usually has an overnight 12-hour run. The steps involved in tissue processing include fixation, dehydration, clearing and infiltration with paraffin wax.
   The following day, the processed tissue is manually embedded into melted paraffin wax within a rectangular metal mould (Fig. 4.1b). The tissue piece is placed flat within the mould, and the mould then placed on a cold plate to allow the paraffin wax to solidify. The resultant product is known as the tissue block (Fig. 4.1c).

Note: The tissue has to be embedded with the correct orientation, such that the surface of interest is the first to be sectioned for microscopic examination.

6. The tissue block is then placed onto a microtome machine, on which thin sections (4um thick) are cut from the surface of interest (Fig. 4.1d).
7. Tissue sections are floated in a water bath and then "fished" out using pre-labelled glass slide (Fig. 4.1e). The slides are now ready for staining.
8. Slides are stained with haematoxylin and eosin and coverslipped. The appropriate specimen label is placed into each glass slide, containing the specimen accession number and the designation of the specific tissue block the section is cut from. The slides are now ready to be examined by the pathologist.

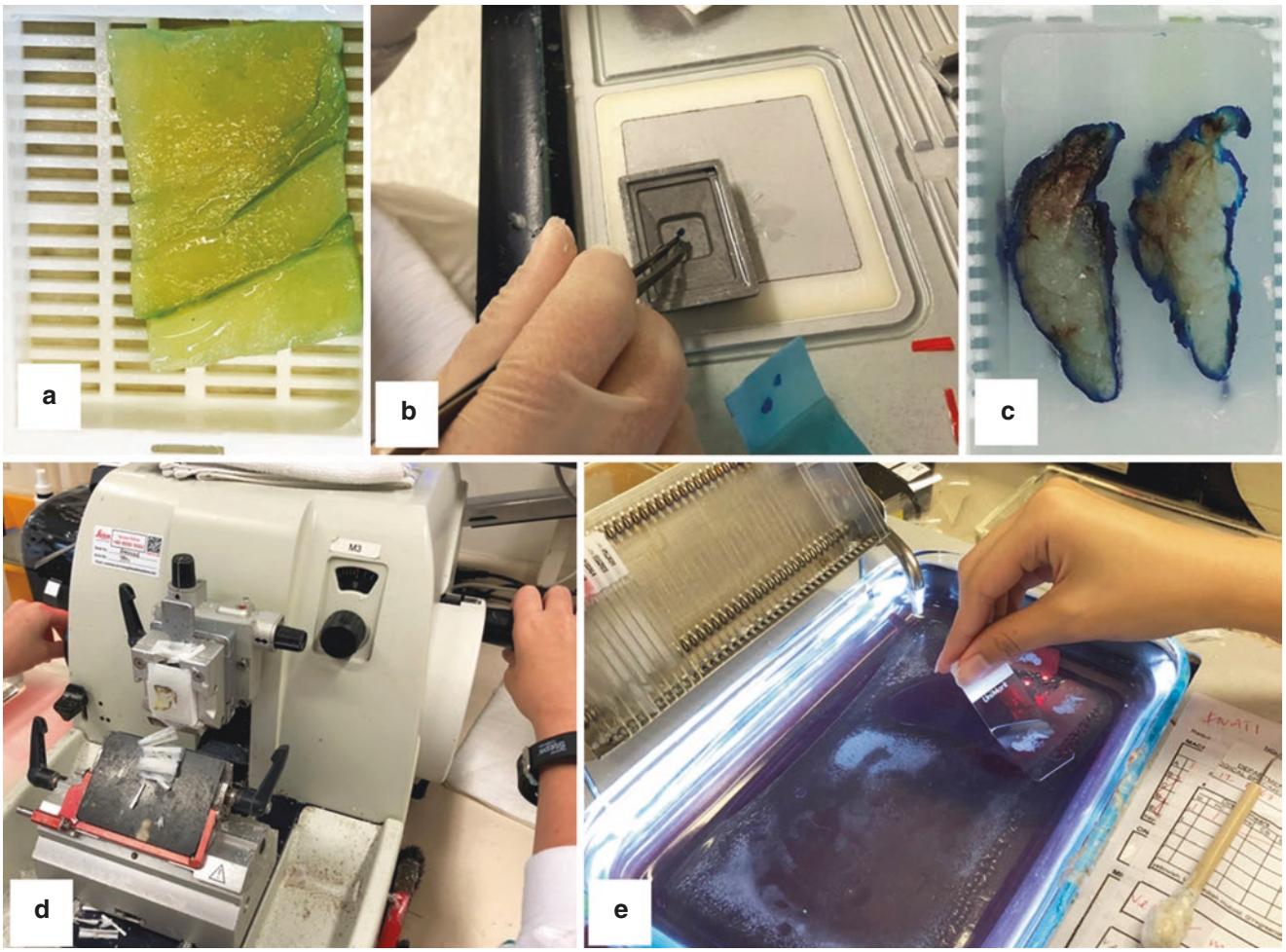

Fig. 4.1 Handling the histology specimen – from specimen to slide: (**a**) Trimmed tissue from a specimen, within fenestrated tissue cassette. (**b**) Embedding – placing the tissue within the metal mould that is filled with melted paraffin wax, to create a tissue block. (**c**) A tissue block with two pieces of embedded tissue within a flat block of paraffin wax. (**d**) The microtome machine showing the tissue block (rectangular white block in centre). The flat blade is below the tissue block. (**e**) The tissue sections are being fished onto the labelled glass slide from the water bath

Types of Biopsies

Biopsies can range in size from minute to large. Here are several types of biopsies one commonly encounters in the pathology laboratory.

Small Biopsies

Biopsies can sometimes be very small, as small as under 1 mm in maximal dimension. In practice, extremely small tissue biopsies are wrapped in filter paper in the pathology lab before being placed into the cassette in order to minimise the risk of tissue loss, as they might otherwise escape through the fenestrations in the tissue cassettes.

For clinicians, after biopsy, very small fragments of tissue should be placed onto filter paper before placing into the formalin-filled specimen bottle to ensure that they are not free floating or lost within the specimen bottle.

If feasible, the number of pieces of tissue within the specimen bottle should be properly documented in the clinical request form.

There is usually some tissue shrinkage during processing; hence if biopsies are too small, this might impact microscopic examination.

Small pieces of tissue have a high surface area to volume ratio and hence undergo rapid specimen fixation. Poor

specimen fixation is usually not a problem with small biopsies.

Excision Biopsies

Excision specimens should be accompanied by a clinical request form documenting the precise location (side and site) of the lesion. For example, "left upper eyelid lesion" is far more informative than "eyelid lesion". The specimen should be handled gently to avoid inadvertent disruption to its anatomy.

Excision biopsy specimens should be well oriented by means of suture(s), annotated drawings, and/or in person by the surgeon. This is to ensure that all relevant anatomical structures and excision margins are properly communicated to the pathologist and properly assessed microscopically.

In some instances, the surgeon may choose to make an incision into the specimen prior to sending the specimen to the pathology laboratory. If this is done, the incision made should be described and documented in the clinical request form, so as to avoid confusion for the pathologist.

Frozen Sections

Intraoperative histologic evaluation using frozen sections is often performed when information is required in order to decide on further management in the immediate setting:

1. *Excision margins*

   The evaluation of surgical margins for completeness of excision of lesional tissue. In these instances, it is preferred that margins be sampled separately and sent in separate specimen bottles so that they can be examined individually.

   An accurate and concise history should also be provided as to the nature of the tumour and the previous diagnostic biopsy results if available.
2. *To confirm lesional tissue*

   Sometimes biopsies are performed with frozen-section support so that quick histological examination can confirm the presence of lesional tissue that is sufficient for later diagnostic workup.

An acceptable frozen-section turnaround time is generally 20 minutes from the time of specimen receipt in the laboratory. A longer time is acceptable in multipart specimens, e.g. multiple margins.

Practical Points

1. Specimens should be sent fresh in a properly labelled, sealed bottle without delay. Very small specimens can be placed onto moistened gauze. Specimens should not be sent in saline or fixative.
2. It is important to provide the duty pathologist with an accurate and concise history, especially, with the specific reason for the frozen section.
3. In potentially infectious specimens, frozen sections should be avoided as far as possible due to health and safety risks, as well as the need to shut down laboratory equipment for decontamination. If absolutely necessary still, the laboratory should be properly informed and the specimen properly labelled.

Fixation

As mentioned above, specimens are usually put into a bottle containing 10% buffered formalin as a fixative before they are sent to the pathology laboratory. Fixation stops the process of decomposition and hence maintains tissue morphology. Fixed tissues (i.e. tissues put into formalin solution) are not suitable for microbiologic investigation or flow cytometry.

In scenarios where there is a clinical suspicion of lymphoma, the specimen should be sent fresh to the pathology laboratory, where imprints or smears can be made to determine if flow cytometry or cytogenetic tests are required. In general, if the smear findings are in keeping with a diagnosis of non-Hodgkin lymphoma, then a portion of the specimen may be sent by the pathology laboratory for flow cytometry, which is helpful in demonstrating a clonal population of neoplastic lymphoid cells. The rest of the specimen will be fixed in formalin by the pathology laboratory. The exact practice varies from institution to institution.

If there is a suspicion of infection, a separate specimen sample should be sent fresh in a sterile container directly to the microbiology laboratory for tissue culture and sensitivity.

If there is a clinical suspicion of sebaceous neoplasm (such as sebaceous carcinoma), the specimen may be sent fresh to the pathology laboratory, where frozen section can be performed with Oil Red O stain to demonstrate the presence of intra-cytoplasmic lipid, which is a fairly specific feature in distinguishing poorly differentiated sebaceous carcinoma from squamous cell carcinoma and basal cell carcinoma. The Oil Red O stain cannot be performed on fixed tissue. Following frozen section with Oil Red O stain, the frozen tissue will be thawed by the pathology laboratory for further processing. This practice also varies between institutions.

An immunohistochemical antibody, adipophilin, is now available and is a fairly specific marker for sebaceous neoplasms. Adipophilin immunostaining can be performed on formalin-fixed tissue, hence negating the need for performing Oil Red O staining on fresh tissue. However, not all pathology laboratories have access to the adipophilin stain. Surgeons are advised to check with their pathology laboratory with regard to the tissue protocol for suspected sebaceous neoplasms.

Practical Points

1. For formalin fixation, immerse the tissue in formalin without delay, and fill the specimen container with sufficient formalin. A general rule of thumb is a formalin to tissue volume ratio of at least 10:1.
2. In general, formalin-immersed tissue undergoes fixation at a rate of 1 mm/hour from the formalin-exposed surface. The outer surface of the tissue is often better fixed than the inner aspect. This may be an issue with large specimens. This is why all specimens should be sent to the *pathology* laboratory without delay, so that the pathologist can slice the large specimen for better penetration of formalin.
3. Examples of specimens that may be sent fresh (during laboratory operating hours):
   - Suspected lymphoma
   - Suspected sebaceous carcinoma (depending on laboratory protocol)
   - Specimens for frozen section (always sent fresh)

   It is prudent to communicate closely with the duty pathologist or laboratory staff if a specimen is to be sent fresh to ensure that there is someone to receive and handle it.

Ancillary Tests

Histologic biopsies are routinely stained using haematoxylin and eosin (H + E) stain. Haematoxylin is blue and binds to DNA/RNA; hence nuclei stain blue. Eosin is reddish or pink and binds to amino acids from proteins, which are primarily in the cytoplasm. Much of the time, a diagnosis can be reached after examining the H + E stained slides alone.

Sometimes, additional tests are required to fine-tune the diagnosis or to subtype a certain tumour, e.g. lymphoma.

Ancillary tests usually can be performed on fixed tissues (e.g. histology biopsy specimens, cell blocks from cytology specimens).

In the pathology laboratory, common types of ancillary tests include histochemical stains, immunohistochemical stains and an increasing incidence of molecular tests. Immunohistochemistry is based on applying specific antibodies to antigens on the lesional or tumour cells, which helps confirm the cell type/differentiation. Molecular tests can also be helpful, especially in the diagnosis of neoplastic conditions, e.g. amplifications or translocations in specific lymphomas.

Flow cytometry is an ancillary test performed by the haematology laboratory, and this is for the evaluation of suspected haematolymphoid malignancies. Material must be sent fresh for this test, in a specific collecting solution.

Microbiologic tests may also be helpful, and the tissue is best submitted fresh at the time of biopsy and sent directly to the microbiologic laboratory in a sterile container.

Table 4.1 shows some examples of some types of ancillary tests.

Turnaround Time

Most routine cases have a turnaround time of approximately 2–4 working days from the time of specimen receipt by the pathology laboratory. Usually, small biopsies can be reported within 1 working day, while larger biopsies take more time. Cases that require ancillary testing (e.g. immunohistochemical or special stains) will require a longer turnaround time.

Important Information to Provide

In most laboratories, a formal written request for pathological examination accompanies the sample to the pathology laboratory. This request form should contain a *concise* account of the *relevant clinical findings* that will optimise the pathologist's evaluation of the tissue. Essentially, the *reason for biopsy* must be clearly conveyed to the pathologist, so that he/she can answer the clinical question at hand.

Table 4.2 summarises useful information to provide in the pathology request form.

In conclusion, adequate representative biopsy samples should be provided to the pathologist with a good clinical history, relevant clinical findings, site of biopsy, and a specific question. In order to provide the optimal sample, prior discussion with the pathologist is essential. The pathologist will choose the immunochemical or special stains depending on the histology findings and the clinical question.

Table 4.1 Ancillary tests and suitable tissue

Test type (laboratory service)	Specimen type/fixation	Sample diagnosis	Sample test
Histochemical stains (pathology laboratory)	Histologic biopsies Cell block from cytology	Suspected tuberculous infection (necrotising granulomatous inflammation seen)	Ziehl-Neelsen stain
Immunohistochemical stains (pathology laboratory)		Suspected lymphoma	CD3, CD20; various lymphocytic cell markers and proliferation markers
		Various markers, depending on primary site	Diagnosis
Molecular tests (diagnostic molecular laboratory)		Lymphoma for subtyping	c-myc amplification for B-cell lymphomas; translocations in specific B-cell lymphomas
Flow cytometry (haematology laboratory)	Fresh tissue (fresh biopsy tissue in specific fixative; FNA needle wash in fixative)	Suspected haematolymphoid malignancy	Various cell surface markers for B and T lymphocytes, sometimes myeloid cells; antibody light chains to evaluate B-cell clonality

Table 4.2 Useful clinical information to provide to pathologist

Information	Example
Nature and location of sample	"Left lower eyelid medial canthus lump"
Type of procedure for sample acquisition	Excision biopsy; incisional biopsy; punch biopsy; fine needle aspiration biopsy
Clinical or intraoperative findings	"Indurated enlarged lacrimal gland"
If applicable, a diagram or clear statement regarding orientation sutures	"Long suture, lateral; medium suture, medial; short suture, superior"
The clinical impression	Chalazion; sebaceous carcinoma; lymphoma; IgG4-related disease; recurrent or metastatic malignancy
Any relevant clinical history	"Immunocompromised patient due to leukaemia treatment; history of malignancy (specify type and grade)"
Any specific requests	"Kindly stain for fungal organisms"
Any other relevant current or past investigations	Imaging findings Results of previous biopsies, etc.

Further Reading

1. Eagle RC Jr. Eye pathology: an atlas and text. 3rd ed. Philadelphia: Wolters Kluwer; 2016.
2. Ford AL, Mudhar HS, Farr R, Parsons MA. The ophthalmic pathology cut-up—Part 1: the enucleation and exenteration specimen. Curr Diagn Pathol. 2005;11:284–90.
3. Ford AL, Mudhar HS, Farr R, Parsons MA. The ophthalmic pathology cut-up—Part 2. Curr Diagn Pathol. 2005;11:340–8.
4. Roberts F, Chee KT. Lee's ophthalmic histopathology. 3rd ed. London: Springer-Verlag London Ltd; 2014.

Part II

Structural Lesions

Dermoid

5

Shantha Amrith, Stephanie Ming Young, Eric Ting, Bingcheng Wu, Min En Nga, and Gangadhara Sundar

Introduction

Periorbital and orbital dermoid cysts are congenital choristomas (benign tumours consisting of histologically normal cells occurring in an abnormal location) presenting themselves either superficially in the eyelid, periorbit or deep in the orbit.

Superficial or periorbital cysts, also known as angular dermoids, are one of the most common lesions of childhood, which present congenitally, and enlarge progressively with age. Deeper ones may only be evident in adulthood. Histologically, the cysts are lined by keratinizing stratified squamous epithelium and contain dermal appendages such as hair follicles, sweat glands, sebaceous glands, smooth muscle, and fibroadipose tissue. There is an admixture of oil and keratin in the lumen. In epidermoid cysts, the cysts are lined with epithelium without adnexal elements. The cysts occur most commonly in the area of the lateral brow, adjacent to the fronto-zygomatic suture and less commonly in the medial upper eyelid adjacent to the fronto-ethmoidal suture. Imaging is useful to confirm the diagnosis and rule out any extension beyond the suture in a dumbbell form.

Periorbital Dermoid

Case 1

A 10-month-old healthy Chinese boy was brought to the clinic by his mother with a history of left medial sub-brow lump since birth (Fig 5.1a). It was not increasing in size and did not change with crying.

On examination, the visual assessment using Cardiff visual acuity cards by the orthoptist revealed a visual acuity of 6/24 in both eyes. A firm lump, not tethered to the skin, was palpated along the superomedial orbit, and it was difficult to reach the posterior limit of the lesion. There was no discolouration of the skin over the mass. The ocular motility was full.

CLOSE summary is given in Table 5.1.

Table 5.1 CLOSE summary: Case 1 – periorbital dermoid

*C*linical process: nonprogressive
*L*ocation: superomedial along the orbital rim
*O*nset: congenital
*S*igns and symptoms: mass lesion
*E*pidemiology: 10-month-old Chinese infant

S. Amrith (✉) · S. M. Young · G. Sundar
Department of Ophthalmology, National University Hospital, Singapore

Department of Ophthalmology, Yong Loo Lin School of Medicine, National University of Singapore, Singapore
e-mail: shantha_amrith@nuhs.edu.sg; stephanie.young@nuhs.edu.sg; gangadhara_sundar@nuhs.edu.sg

E. Ting
Department of Diagnostic Imaging, National University Hospital, Singapore

Department of Diagnostic Imaging, Yong Loo Lin School of Medicine, National University of Singapore, Singapore

Advanced Medicine Imaging, Singapore

B. Wu
Department of Pathology, National University Hospital, Singapore

M. E. Nga
Department of Pathology, National University Hospital, Singapore

Department of Pathology, Yong Loo Lin School of Medicine, National University of Singapore, Singapore

S. Amrith et al. (eds.), *Ocular Adnexal Lesions*, https://doi.org/10.1007/978-981-13-3798-7_5

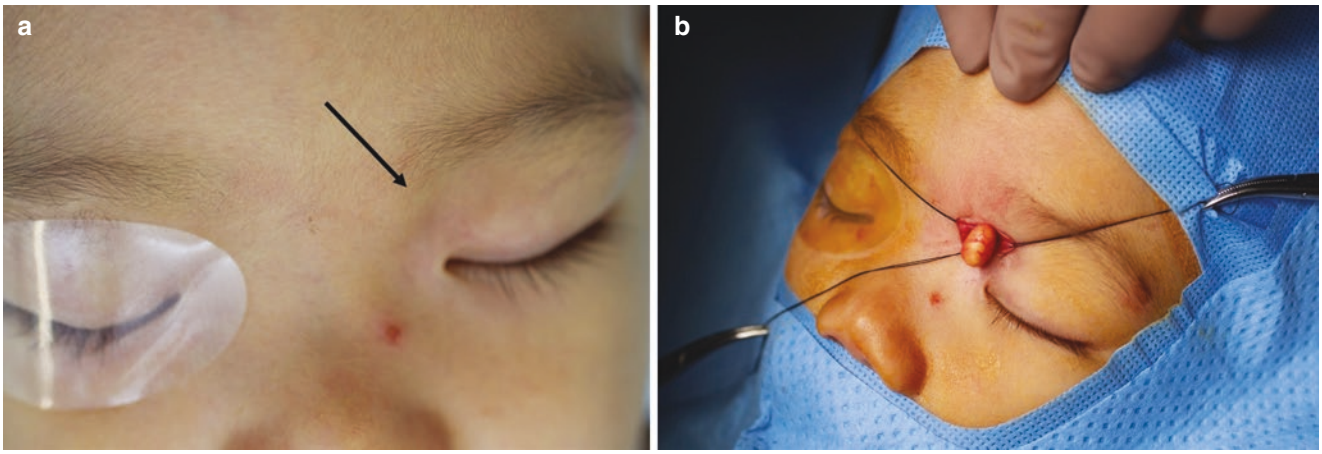

Fig. 5.1 (**a**) Clinical picture of case 1 with periorbital dermoid showing the lump in the medial part of left upper lid. (**b**) Intact cyst being surgically removed

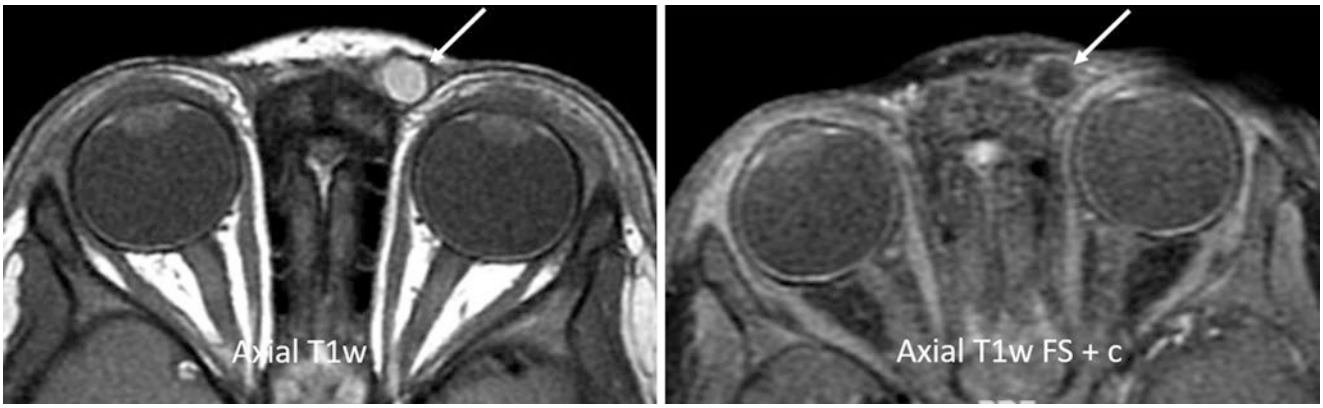

Fig. 5.2 Axial T1w and T1w FS + C sequences show a well-circumscribed lesion (white arrows) in the medial canthal region which is uniformly T1w hyperintense and shows loss of signal on FS, indicating a fat containing lesion

Differential Diagnosis

- Periorbital dermoid
- Meningoencephalocele
- Implantation cyst
- Hematic cyst
- Vascular malformation/tumour

MRI of the orbits was carried out under sedation.

Imaging

MRI showed a well-circumscribed superficial thin-walled left medial canthal/sub-brow focal nodular mass measuring around 8 mm in axial diameter, showing high T1 and T2-weighted signals, low signal on fat suppression (Fig. 5.2), and no enhancement with contrast. Appearance was suggestive of an internal angular dermoid cyst.

Intervention

The parents were keen on surgical removal.

Under general anaesthesia, an incision was made in the superomedial orbit, and the cyst was removed intact. No hairs were seen on the external surface. The cyst measured 9 mm × 6 mm (Fig 5.1b).

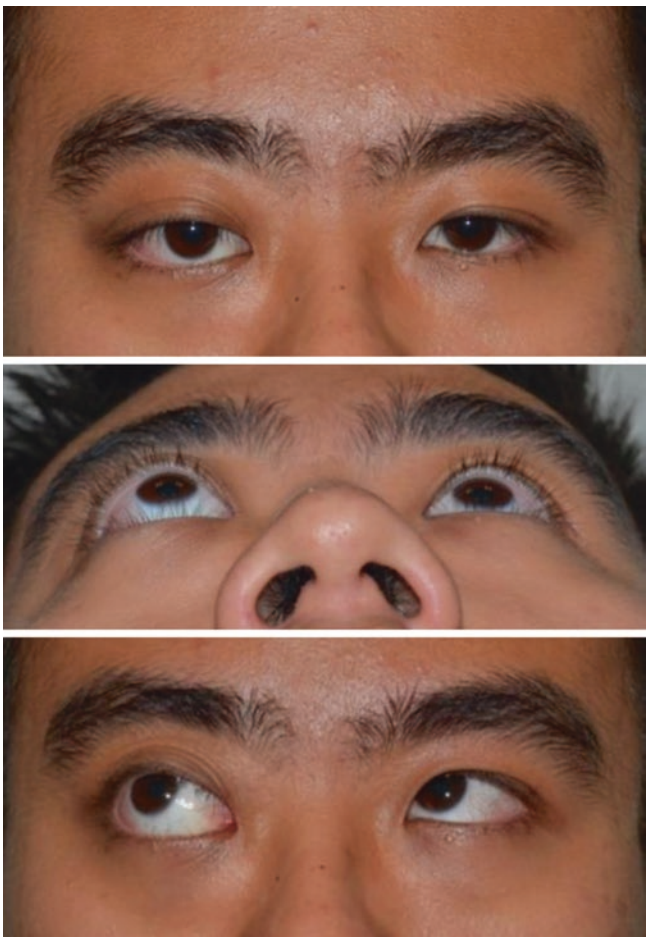

Fig. 5.3 Clinical picture of the patient with orbital dermoid, from top to bottom: frontal view, worm's-eye view showing proptosis of the right eye, and patient looking up and to the right showing restriction of right eye movement

Orbital Dermoid

Case 2

A 23-year-old Chinese male noticed a few weeks before consult that his right eye was more prominent than the left. He denied any discomfort, pain, or worsening with cold. There was no history of trauma.

Examination of the right eye revealed normal visual acuity, normal pupillary reaction, and restriction of ocular movements on supraduction and abduction with diplopia. The exophthalmometry showed a right proptosis of 8 mm (Fig. 5.3), which was non-pulsatile and non-reducible. There was no worsening with Valsalva manoeuvre. The fundus examination was normal with no choroidal striae.

Table 5.2 CLOSE summary: case 2 – orbital dermoid

*C*linical process: mass effect
*L*ocation: orbit possibly superior/intraconal
*O*nset: chronic
*S*igns and symptoms: proptosis with limitation of eye movements
*E*pidemiology: young Chinese adult male

CLOSE summary is given in Table 5.2.

Differential Diagnosis

- Cavernous haemangioma
- Schwannoma
- Dermoid cyst
- Lymphatic-venous malformation
- Thyroid eye disease

The patient underwent CT and MRI scans.

Imaging

Computed tomography (CT) scan: A cystic lesion was identified in the right orbit. There were no solid tissues identified. The contents had a density of fat. It was located in the extraconal space displacing the lateral rectus muscle medially. The eyeball was displaced anteromedially. The cystic lesion measured 33 mm at the maximal diameter. This lesion was associated with remodeling of the underlying bone, indicating a long-standing abnormality (Fig. 5.4). Possibilities such as a dermoid cyst or a lymphatic malformation were considered for diagnosis.

MRI: A large, multilobulated mass was noted in the right orbit corresponding to the lesion seen in the CT (Fig. 5.5). The mass was located in the superolateral aspect of the right orbit. It was predominantly extraconal but bulged medially into the conus, distorting the lateral rectus and displacing it into an inferior plane. The optic nerve was also displaced medially but retained normal signal. Laterally, there was smooth remodeling of the lateral orbital wall. There was associated proptosis.

The dominant lobule was heterogeneously hypointense in T1 and hyperintense in T2, interspersed with tiny foci of fat signal intensity, which resulted in loss of signal on the fat-suppressed sequences. There was a globule of fat signal intensity seen along the anterolateral aspect of the mass. A small cyst-like lobule was also seen at its anteroinferior aspect, indicative of a possible rupture. The lesion demonstrated thin rim enhancement on post-contrast images.

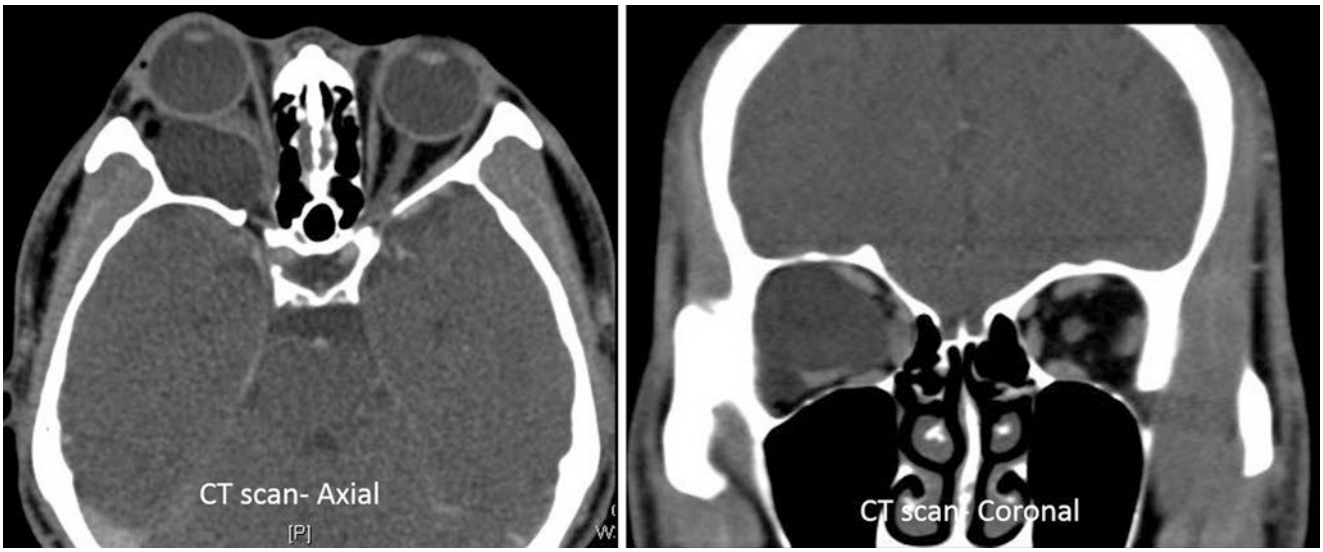

Fig. 5.4 Axial and coronal CT of the orbits show a well-circumscribed cystic appearing mass in the right orbit displacing the optic nerve medially. Anteriorly, there is a locule of fat and inferiorly a smaller cystic locule (axial scan). Note the smooth remodeling of the adjacent lateral orbital wall

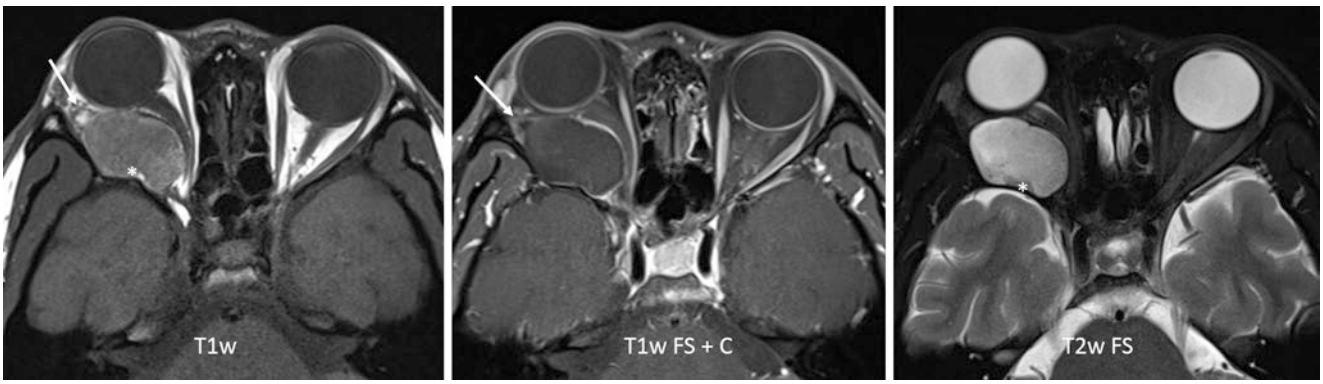

Fig. 5.5 Axial T1w, T1w-FS + contrast, T2w-FS images show heterogeneous T1w signal with subtle T1w hyperintense foci (white arrow and asterisk). These areas show loss of signal on the T1w-FS + contrast image and low signal intensity on the T2w-FS image, indicating the presence of fat

Management

Through a lateral orbitotomy, the cyst was completely removed and sent for histopathology.

Histopathology

Histology was similar in both cases. There was a cyst lined by keratinizing stratified squamous epithelium. The cyst wall contained pilosebaceous units (hair follicles and sebaceous glands) (Fig. 5.6). The features were those of a dermoid cyst.

Discussion

Dermoid cysts show no gender or racial predilection, and they are considered the most frequent periorbital tumour.

Clinically, periorbital dermoid cysts present as palpable, smooth, painless, oval masses that enlarge slowly. They occur most commonly in the superotemporal quadrant. They are either freely mobile or fixed to the periosteum at the underlying suture. The globe and adnexa may be displaced if they grow posteriorly (deep or orbital dermoid cysts) causing progressive proptosis, diplopia, erosion or remodeling of the bone (long standing cysts). As the dermoid cysts enlarge, they can leak oil and keratin from the cyst causing inflamma-

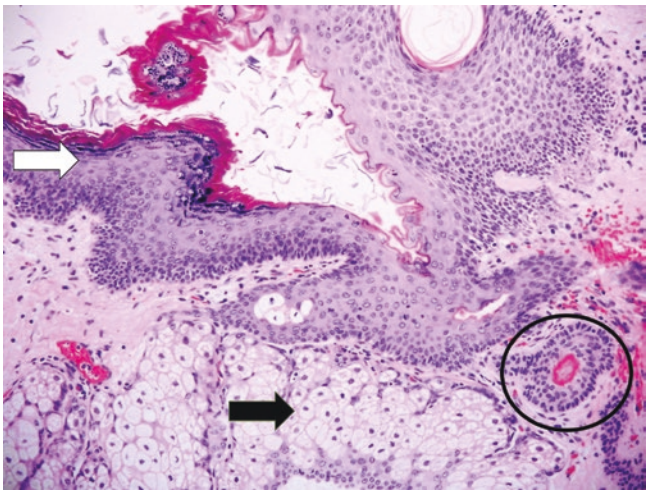

Fig. 5.6 There is a cyst lined by keratinizing stratified squamous epithelium (white arrow). The cyst wall contains pilosebaceous units (black arrow). A hair follicle is circled. HE stain; 100× magnification

tory reaction in the surrounding tissues and can therefore present as inflammatory lesions.

Pathogenesis: During embryogenesis, foetal suture lines close, and embryonic epithelial nests (dermal or epidermal) may become entrapped to form a cyst. The most commonly involved suture is the fronto-zygomatic suture, others such as fronto-ethmoidal (as in the case 1 above), and fronto-maxillary suture may also be involved.

Role of Imaging

If present in the temporal fossa, imaging will help to rule out dumbbell expansion through a bony defect in the suture line into the underlying orbit. They may present as pulsating proptosis with mastication (highly specific feature). Imaging will also help to evaluate medial lesions and distinguish them from congenital encephalocoeles, dacryocoeles, mucocoeles and other vascular lesions, and lateral lesions from lacrimal gland tumours.

Common features on CT scan: Dermoid cysts appear as well-defined and well-circumscribed lesions with an enhancing (hyperdense) wall and non-enhancing (hypodense) lumen. It can show partially calcified margin or rim. MRI is best evaluated on FSE (fat suppression) sequence. The dermoid cyst appears as a well-defined round to ovoid structure, variable in size, hypointense with respect to orbital fat on T1-weighted images and hyperintense on T2-weighted images.

Treatment

Conservative management in the form of observation may be appropriate if the lesion is small and asymptomatic.

The mainstay of treatment is surgical excision. It is sometimes carried out early to avoid the risk of traumatic rupture. The primary goal of excision is removal of dermoid cyst with the wall intact without causing an iatrogenic rupture. The approach will depend upon the location of the lesion. If anteriorly located, an anterior orbitotomy through eyelid crease incision can be used. If orbital, a lateral orbitotomy may be necessary. Intracranial extension requires working with neurosurgeons for complete excision. Incomplete removal can lead to recurrence or abscess formation, whereas lesions removed in entirety rarely recur. An acute inflammatory process (lipogranulomatous inflammation) may occur, if part of the cyst wall or any of the contents remain within the eyelid/orbit, which may lead to an orbitocutaneous fistula. There is excellent prognosis following successful early surgical intervention.

Learning Points

Dermoid cysts are congenital choristomas. They commonly occur at the fronto-zygomatic suture or fronto-ethmoidal suture. Anterior lesions are mobile and subcutaneous. Posterior lesions present as proptosis. Treatment is excision in all cases. Goal is to remove the cyst intact for the best prognosis.

Further Reading

1. Ahuja R, Azar NF. Orbital dermoids in children. Semin Ophthalmol. 2006;21:207–11.
2. Eldesouky MA, Elbakary MA. Orbital dermoid cyst: classification and its impact on surgical management. Semin Ophthalmol. 2018;33(2):170–4.
3. Lane CM, Ehrlich WW, Wright JE. Orbital dermoid cyst. Eye. 1987;1:504–11.

Fibro-osseous Lesions: Fibrous Dysplasia

6

Gangadhara Sundar, Stephanie Ming Young, Poh Sun Goh, Bingcheng Wu, Min En Nga, and Shantha Amrith

Introduction

The orbit is composed of bone and soft tissue structures of mesenchymal origin. The bones are formed from membranous and endochondral ossification. The spectrum of mesenchymal tumors includes fibro-osseous lesions, cartilaginous lesions, reactive bone lesions, and vascular lesions. The fibro-osseous lesions are a poorly defined group of lesions that affect the jaw and the craniofacial bones. The World Health Organization (WHO) classified these lesions in 2005, which include ossifying fibroma, fibrous dysplasia, and osseous dysplasia (Paget's disease), in addition to reactive bone lesions. The diagnosis is sometimes challenging, and so is the management of these lesions, because of the systemic involvement in some cases and the need for long-term follow-up.

Case Scenario

A 17-year-old Chinese female presented with progressive and persistent headaches accompanied by fullness of the left upper eyelid, pressure sensation, and facial disfiguration for over 5 years. She complained of visual blurring without diplopia. Ophthalmic examination revealed a Snellen visual acuity of 6/6 in each eye. She had fullness of the left forehead and a marked left hypoglobus, with a 6 mm left non-pulsatile proptosis (Fig. 6.1), with full range of ocular movements. Pupils were unremarkable without RAPD, and visual fields, color vision, and fundus examination were within normal limits.

CLOSE summary is given in Table 6.1.

Differential Diagnosis

Orbital and periorbital soft tissue tumor
- Fibrous dysplasia
- Ossifying fibroma
- Osteoma
- Paget's disease

She underwent a CT scan of the orbit and facial skeleton.

Radiology

Non-contrast-enhanced axial CT of the face was acquired, along with sagittal and coronal reconstructions. Bony expansion with ground-glass matrix was seen, involving the left

G. Sundar · S. M. Young · S. Amrith (✉)
Department of Ophthalmology, National University Hospital, Singapore

Department of Ophthalmology, Yong Loo Lin School of Medicine, National University of Singapore, Singapore
e-mail: gangadhara_sundar@nuhs.edu.sg; stephanie.young@nuhs.edu.sg; shantha_amrith@nuhs.edu.sg

P. S. Goh
Department of Diagnostic Imaging, National University Hospital, Singapore

Department of Diagnostic Imaging, Yong Loo Lin School of Medicine, National University of Singapore, Singapore

B. Wu
Department of Pathology, National University Hospital, Singapore

M. E. Nga
Department of Pathology, National University Hospital, Singapore

Department of Pathology, Yong Loo Lin School of Medicine, National University of Singapore, Singapore

S. Amrith et al. (eds.), *Ocular Adnexal Lesions*, https://doi.org/10.1007/978-981-13-3798-7_6

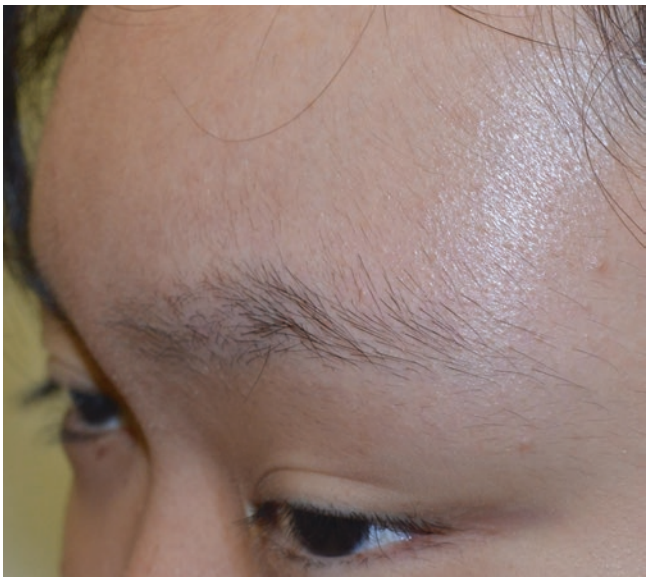

Fig. 6.1 Clinical picture showing left non-axial proptosis with hypoglobus and fullness of lateral part of the left upper lid and forehead

Table 6.1 CLOSE summary

*Cl*inical process: mass effect
*L*ocation: superior orbit and frontal region on the left side
*O*nset: chronic and progressive
*S*ymptoms and signs: headaches, visual blurring, and disfiguration with proptosis and hypoglobus
*E*pidemiology: adolescent Chinese female

frontal cranial vault as well as the anterior and central skull base, predominantly on the left. Multiple lucent foci were seen within the affected osseous structures. Severe bony expansion of the left orbital walls (predominantly the superior and lateral walls) resulted in distortion and narrowing of the left orbit (Fig. 6.2). Crowding of the intra-orbital contents was observed. There was also mild narrowing of the left optic canal. The Vidian canals and foramen ovale remained patent. Mild expansion of the left pterygoid process caused slight narrowing of the pterygomaxillary fissure. Obliteration of the bifrontal sinuses and bilateral anterior ethmoidal air cells was observed. The left middle and anterior cranial fossae also demonstrated reduction in volume due to the severe osseous expansion. Mass effect upon the left temporal and frontal lobes was noted.

Management

Options of observation vs conservative excision vs maximal debulking were discussed. The patient subsequently underwent a near total complete excision of frontal, nasal, and zygomatic bones sparing the sphenoid with reconstruction by a multidisciplinary team of surgeons, including the orbital surgeon, facial plastic surgeon, and neurosurgeon under intraoperative navigation guidance. Postoperatively, she recovered well with resolution of proptosis, improvement of the hypoglobus, and resolution of the headaches with preservation of visual function.

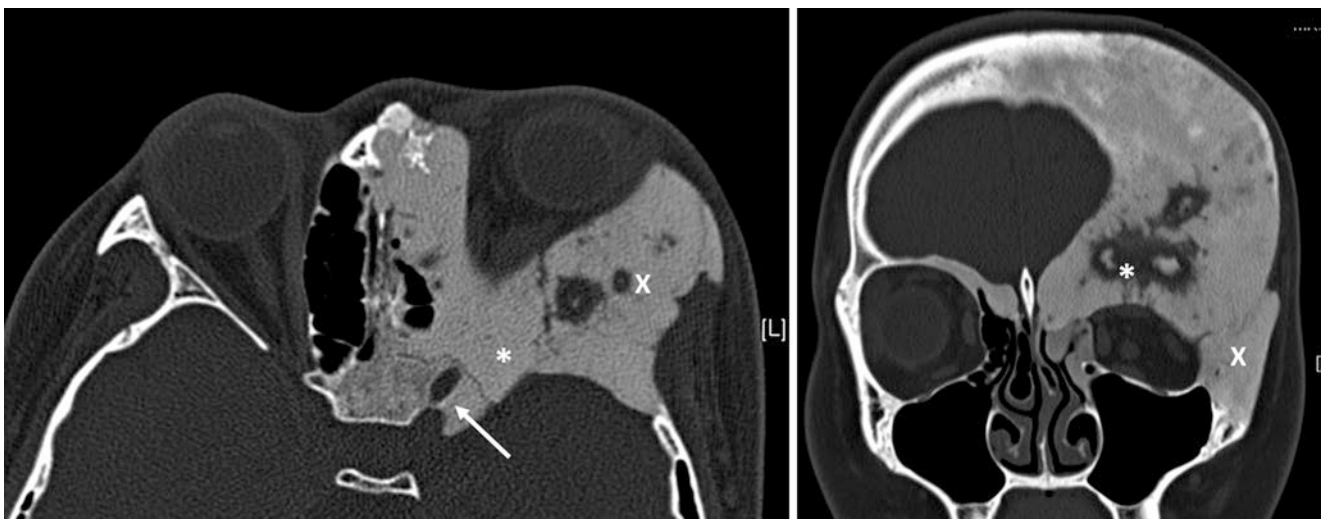

Fig. 6.2 Non-contrast, bone window CT showing ground-glass appearance of fibrous dysplasia involving left frontal and zygomatic bone constituting roof (*) and lateral wall (**x**) of the left orbit. Note the reduction in volume of the left orbital space. White arrow points to the region of the left optic canal

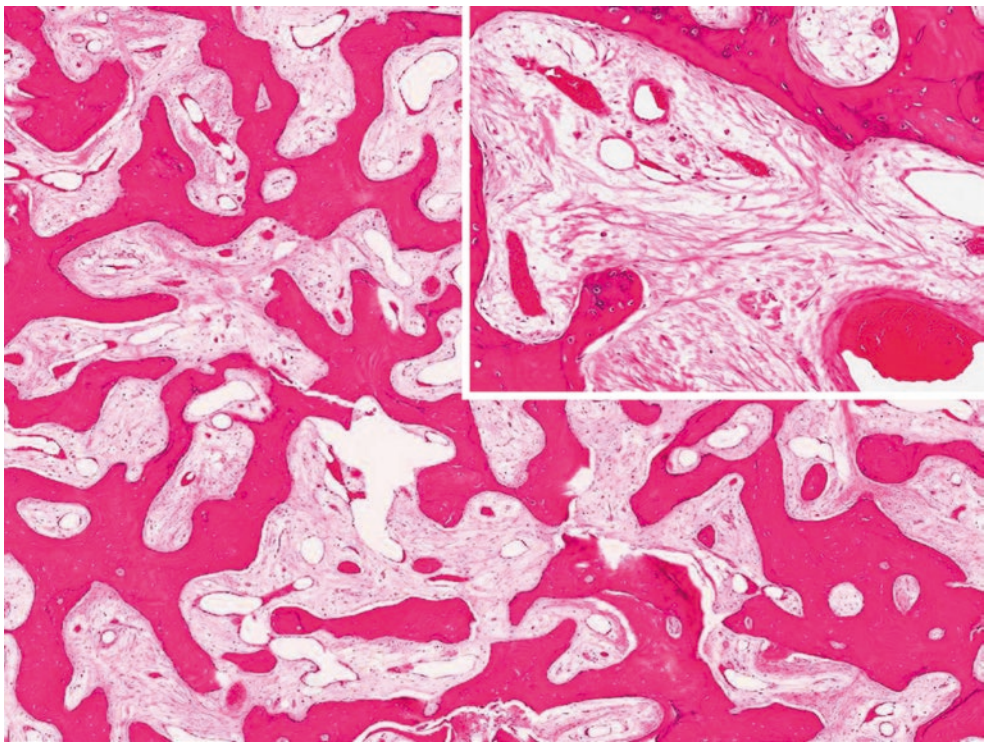

Fig. 6.3 Histopathology shows a fibro-osseous lesion composed of irregular trabeculae of woven bone surrounded by fibrous stroma. There is no significant nuclear atypia. Osteoblastic rimming of the bony trabeculae is not appreciated. Main: HE stain, 40× magnification. Inset: HE stain, 200× magnification

Histopathology

Sections showed a fibro-osseous lesion composed of irregular trabeculae of woven bone surrounded by a fibrous stroma (Fig. 6.3). There was no significant nuclear atypia within the bony or fibrous elements. The bony trabeculae showed no discernible rimming by osteoblastic cells. The features were consistent with fibrous dysplasia.

Discussion

Fibrous dysplasia is a slowly progressive proliferation of benign fibrous tissue of the orbits and midface of membranous origin. They may either be monostotic, polyostotic, or rarely panostotic. McCune-Albright syndrome is a systemic condition characterized by polyostotic fibrous dysplasia, precocious puberty, and café au lait spots. Mazabraud syndrome is the association of intramuscular myxomas with a polyostotic fibrous dysplasia. Most commonly found in the long bones, presentation in the craniomaxillofacial region is not uncommon. Malignant transformation is rarely reported. While lesions often cause disfiguration and globe dystopia, they rarely cause visual loss. On imaging it is seen as a hazy, radiolucent, or ground-glass pattern, affecting multiple bones beyond the suture lines. More recently, mutations affecting the Wnt/β-catenin pathway have been proposed as a possible etiology. Management of this condition is not only challenging but controversial. Conventional management is observation alone. In patients with progressive visual symptoms, severe disfiguration, or headaches, surgical management may be indicated. Often multidisciplinary, the spectrum may include orbital and optic canal decompression alone to conservative debulking to a maximal debulking as considered safe followed by reconstruction.

Learning Points

Fibro-osseous lesions are not uncommon and often pose great challenges in management. A judicious approach with conservative and expectant observation followed by cautious surgical debulking may be indicated in significantly symptomatic patients. A complete ophthalmic and systemic evaluation and multidisciplinary approach remain the mainstay of treatment. Advances in molecular diagnostics and targeted medical therapies may pave the way for nonsurgical management in the future.

Further Reading

1. Goisis M, Biglioli F, Guareschi M, Frigerio A, Mortini P. Fibrous dysplasia of the orbital region: current clinical perspectives in ophthalmology and cranio-maxillofacial surgery. Ophthal Plast Reconstr Surg. 2006;22:383–7.
2. Selva D, White VA, O'Connell JX, Rootman J. Primary bone tumors of the orbit. Surv Ophthalmol. 2004;49(3):328–42.
3. Wenig BM, Mafee MF, Ghosh L. Fibro-osseous, osseous, and cartilaginous lesions of the orbit and paraorbital region. Correlative clinicopathologic and radiographic features, including the diagnostic role of CT and MR imaging. Radiol Clin N Am. 1998;36(6):1241–59. xii

Part III

Infections

Orbital Cellulitis: Bacterial

7

Shantha Amrith, Stephanie Ming Young, Poh Sun Goh, Bingcheng Wu, Min En Nga, and Gangadhara Sundar

Introduction

Acute orbital cellulitis refers to the infection of the soft tissues of the orbit. It is characterized by acute onset of fever and constitutional symptoms associated with lid swelling, conjunctival chemosis, proptosis and limitation of eye movements. In a severe case, it may be associated with visual loss. In the overwhelming majority (90%) of cases, the source of infection is the paranasal sinuses. Occasionally, an infection in the eyelid or lacrimal sac can extend posteriorly, resulting in orbital cellulitis. An external penetrating wound or a retained orbital foreign body may also be responsible for the cellulitis. In a rare event, an endogenous infective embolus can lodge in the orbital tissues causing orbital cellulitis.

Case Scenario

A 13-year-old Malay female presented with a 3-day history of worsening eyelid swelling, redness and pain on the right side. There was no notable trauma or insect bite, but she complained of blocked nose and one episode of fever. On examination, the visual acuities were normal with full colour vision. The left ophthalmic examination was completely normal. On the right side, there was swelling of the right upper lid with erythema (Fig. 7.1), some limitation of eye movements along with a non-axial proptosis and hypoglobus.

CLOSE summary is given in Table 7.1.

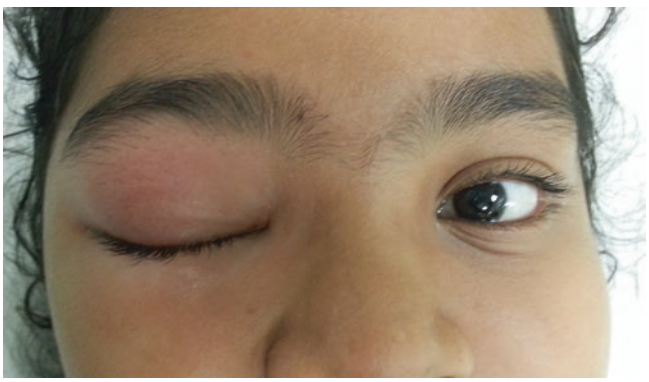

Fig. 7.1 Clinical picture showing lid swelling and proptosis of the right eye

Table 7.1 CLOSE summary

*C*linical process: inflammatory
*L*ocation: right upper lid and orbit
*O*nset: acute
*S*igns and symptoms: swelling, pain and redness
*E*pidemiology: young Malay female

S. Amrith (✉) · S. M. Young · G. Sundar
Department of Ophthalmology, National University Hospital, Singapore

Department of Ophthalmology, Yong Loo Lin School of Medicine, National University of Singapore, Singapore
e-mail: shantha_amrith@nuhs.edu.sg; stephanie.young@nuhs.edu.sg; gangadhara_sundar@nuhs.edu.sg

P. S. Goh
Department of Diagnostic Imaging, National University Hospital, Singapore

Department of Diagnostic Imaging, Yong Loo Lin School of Medicine, National University of Singapore, Singapore

B. Wu
Department of Pathology, National University Hospital, Singapore

M. E. Nga
Department of Pathology, National University Hospital, Singapore

Department of Pathology, Yong Loo Lin School of Medicine, National University of Singapore, Singapore

S. Amrith et al. (eds.), *Ocular Adnexal Lesions*, https://doi.org/10.1007/978-981-13-3798-7_7

The child was admitted to the hospital, and intravenous amoxicillin with clavulanate was started, and a CT scan of the orbits and sinuses was carried out.

Differential Diagnosis

- Preseptal cellulitis
- Orbital cellulitis – bacterial or fungal
- Acute non-specific orbital inflammation
- Dacryoadenitis
- Masquerades: fulminant malignant conditions such as leukaemia, rhabdomyosarcoma, etc.

Radiology

CT scan of the orbits and sinuses (Fig. 7.2) showed opacification of right maxillary, ethmoidal and frontal sinuses. There was streaking of orbital fat with some opacification in the superior orbit above the superior muscle complex, raising the suspicion of a subperiosteal abscess.

Other investigations included the following:

- FBC: Leukocytosis with increase in neutrophils
- Renal functions: Normal
- Blood glucose: Normal
- Blood culture negative for aerobic and anaerobic organisms

Management

The child was referred to the otolaryngology surgeon while being continued on intravenous antibiotics. Endoscopic sinus surgery along with anterior orbitotomy to drain subperiosteal abscess was carried out under general anaesthesia. Multiple fragments of sinus mucosa were sent for histopathological examination. Culture of the pus revealed *Streptococcus anginosus*, sensitive to penicillin and clindamycin.

Histopathology

Fragments of bone and tissue partly lined by respiratory epithelium with underlying hyperplastic glands were seen. There was an acute inflammatory cellular infiltrate composed of polymorphonuclear cells (neutrophils) (Fig. 7.3) and some

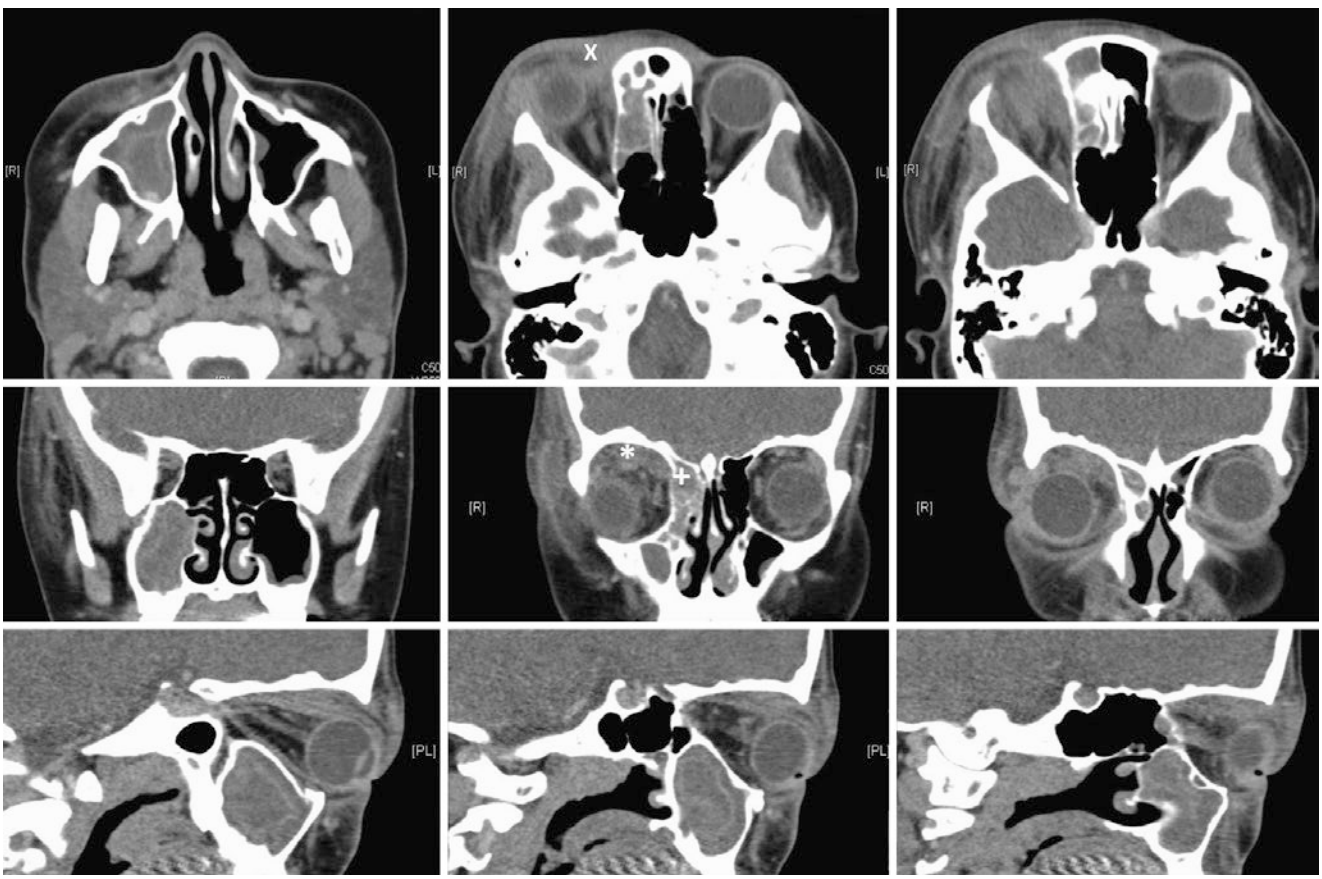

Fig. 7.2 Axial, coronal and sagittal views of the CT scan of the orbits and the sinuses. Note the opacification of the sinuses (+), subperiosteal abscess (*) and preseptal cellulitis and swelling (×)

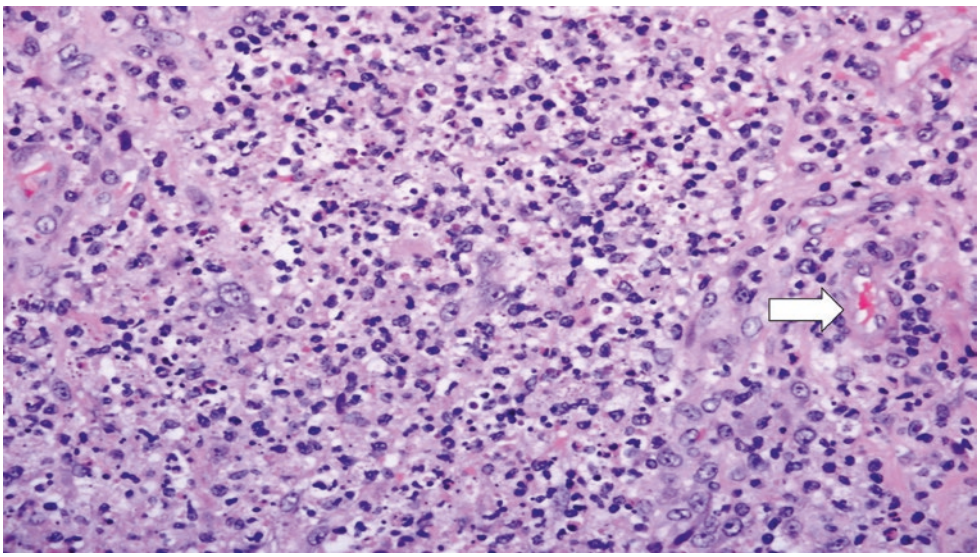

Fig. 7.3 Acute inflammatory cellular infiltrate and some capillaries (white arrow). HE stain; 200× magnification

karyorrhectic debris (blackish, fragmented nuclear material). There was an associated proliferation of capillaries lined by reactive endothelial cells. Admixed fibroblasts were also present. The findings are consistent with orbital cellulitis.

Discussion

A preseptal cellulitis results from a hordeolum, insect bite, trauma, and acute dacryocystitis. In an infant, an upper respiratory tract infection can cause preseptal cellulitis. However, it is important to recognize an orbital cellulitis as it is more serious and vision-threatening. The important signs to note are the presence of proptosis and limitation of ocular movements. Chandler's classification describes different groups, but it is not a continuous scale.

Bacterial sinusitis spreads to the orbits through the valveless venous channels as thrombophlebitis. The common organisms are *Streptococcus* species, *Staphylococcus* aureus, *Pseudomonas*, *Enterococcus*, *Klebsiella* and *Haemophilus influenzae* type B. The infection with the latter has declined in the recent years due to increasing vaccination.

Clinically, the patients present with lid swelling, pain, chemosis, proptosis, and restricted ocular motility. When the optic nerve is threatened, there is RAPD, reduced visual acuity, and colour vision. It is imperative to admit these patients to the hospital for close monitoring, so that aggressive and appropriate treatment can be instituted at the right time.

Systemically, patients may have fever and leukocytosis with elevated neutrophils. In addition to the elevated WBC, the ESR and CRP may also be raised. A culture of the nasal mucosa is advised if no obvious discharge is noted in the eye. Blood cultures are done only if the patient has signs of septicaemia. CT scan of the orbits and paranasal sinuses is mandatory in all patients. The presence of gas in the orbit may suggest an anaerobic infection. The patients are co-managed with the otolaryngologists.

The first sign that the patient is responding to antibiotic therapy is the subsidence of fever, and no further deterioration of signs as the eye signs take time to improve. Deterioration of signs despite the treatment warrants a repeat CT scan to rule out pus collection in the orbit.

Surgical management is less likely in patients under the age of 9, because the infection is caused by a single organism and it responds well to antibiotic therapy. In older children and adults, the infection is usually polymicrobial; hence any deterioration must be followed by surgical intervention.

A rare complication of orbital cellulitis is a posterior spread resulting in cavernous sinus thrombosis, meningitis or even a brain parenchymal infection.

Learning Points

Acute orbital cellulitis is a vision-threatening condition and is distinguished from preseptal cellulitis by the presence of proptosis and ocular motility restriction. In majority of the patients, there is a sinus infection, and it is necessary to co-manage the patients with otolaryngologists. Close monitoring and surgical intervention when necessary are mandatory to prevent visual loss.

Further Reading

1. Garcia GH, et al. Criteria for nonsurgical management of subperiosteal abscess of the orbit. Ophthalmology. 2000;107:1454–8.
2. Harris GJ. Subperiosteal abscess of the orbit: age as a factor in the bacteriology and response to treatment. Ophthalmology. 1994;101:585–95.
3. McKinley SH, et al. Microbiology of pediatric orbital cellulitis. Am J Ophthalmol. 2007;144:497–501.
4. Nageswaran S, et al. Orbital cellulitis in children. Pediatr Infect Dis J. 2006;25:695–9.

Orbital Cellulitis: Invasive Fungal

8

Shantha Amrith, Stephanie Ming Young, Eric Ting, Bingcheng Wu, Min En Nga, and Gangadhara Sundar

Introduction

Invasive fungal infections of the orbit are of two types: acute fulminant and chronic invasive. Orbital fungal infections have intracranial extensions in immunocompromised patients and are rare and difficult to diagnose; they pose challenges in the management and are often fatal. They arise from two types of fungal infections, zygomycosis and aspergillosis.

Given their poor prognoses, early detection becomes one of the key strategies to the management. This gives a better chance of local control of the infection, and along with early restoration of the immunologic or metabolic condition, it significantly influences the patient's treatment outcomes. Here, an example of each type of invasive fungal infection with orbital involvement is discussed.

Case 1: Mucormycosis

A 70-year-old woman who was diagnosed with relapsed angio-immunoblastic T-cell lymphoma had previously completed chemotherapy, and developed cytomegalovirus (CMV) infection and methicillin-resistant *Staphylococcus aureus* (MRSA) septicemia on the days following chemotherapy. While she was on tapering doses of prednisolone, antiviral and antibiotic therapy, she was hospitalized for neutropenia and fever. Prior to hospitalisation, she developed facial numbness and blurring of vision in the left eye. Examination revealed a total ophthalmoplegia with no perception of light in the left eye that progressed rapidly to involve the right side. There was increasing necrosis of the eyelids with conjunctival chemosis and proptosis (Fig. 8.1a, b).

CLOSE summary is given in Table 8.1.

Differential Diagnosis

- Fungal infection
- Non-specific orbital inflammation
- Granulomatosis with polyangiitis
- Primary neoplastic process
- Metastatic tumour
- Secondary tumour from the sinuses
- Cavernous sinus thrombosis

S. Amrith (✉) · S. M. Young · G. Sundar
Department of Ophthalmology, National University Hospital, Singapore

Department of Ophthalmology, Yong Loo Lin School of Medicine, National University of Singapore, Singapore
e-mail: shantha_amrith@nuhs.edu.sg; stephanie.young@nuhs.edu.sg; gangadhara_sundar@nuhs.edu.sg

E. Ting
Department of Diagnostic Imaging, National University Hospital, Singapore

Department of Diagnostic Imaging, Yong Loo Lin School of Medicine, National University of Singapore, Singapore

Advanced Medicine Imaging, Singapore

B. Wu
Department of Pathology, National University Hospital, Singapore

M. E. Nga
Department of Pathology, National University Hospital, Singapore

Department of Pathology, Yong Loo Lin School of Medicine, National University of Singapore, Singapore

S. Amrith et al. (eds.), *Ocular Adnexal Lesions*, https://doi.org/10.1007/978-981-13-3798-7_8

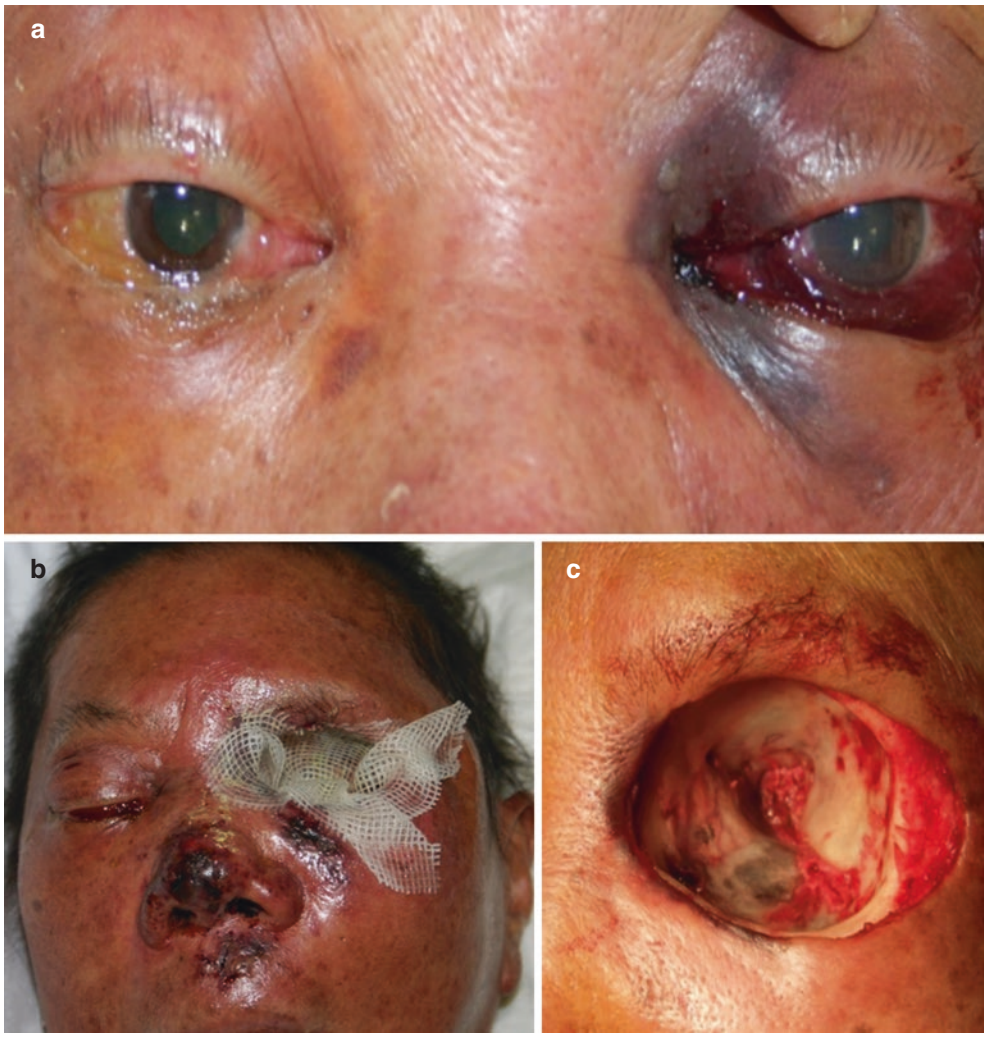

Fig. 8.1 (**a**) Clinical picture of case 1 shows left proptosis with blackening lesions in eyelids, chemosis, lustreless cornea on day 2. (**b**) Note the right-sided proptosis, ischaemic necrosis of the ala of nose and left lower lid on day 7. (**c**) The picture shows the exenterated orbit immediately after surgery. Note blackening of the bone in the floor and the absence of bleeding

Table 8.1 CLOSE summary case 1

*C*linical scenario: infiltrative
*L*ocation: bilateral orbit
*O*nset: acute fulminant
*S*igns and symptoms: loss of vision, eyelid swelling and blackening
*E*pidemiology: an immunocompromised 70-year-old Chinese female

Radiology

CT and MRI (Fig. 8.2) showed mild left-sided proptosis, associated with mucosal thickening of the ipsilateral ethmoid and maxillary sinuses. There was complete opacification of the left nasal cavity associated with septal deviation to the left. No focal mass lesion was noted in the retrobulbar space to account for proptosis. The left optic nerve appeared relatively taut compared to the contralateral side, and there was distension and enhancement of the optic nerve sheath**.** The inflammation was seen to extend to the left cavernous sinus.

Management

Nasal debridement on day 4 showed zygomycosis (mucormycosis) infection, and the patient was started on intravenous liposomal amphotericin B injections. The culture revealed the growth of *Rhizopus* species. The left orbital exenteration was performed on day 7 to reduce fungal load, but the patient progressed with no perception of light in the right eye with right orbital apex syndrome. During exenteration, there was no bleeding, indicating severe ischaemia (Fig. 8.1c). The patient's condition deteriorated when the family decided to withdraw all treatment, and she eventually succumbed to the disease.

Histopathology

The biopsy of the turbinates and the nasal mucosa showed broad hyphal fungal fragments in the blood vessels, within the lumina and vessel walls and surrounding connective tissue stroma and nerves (Fig. 8.3). These hyphae were of variable thickness,

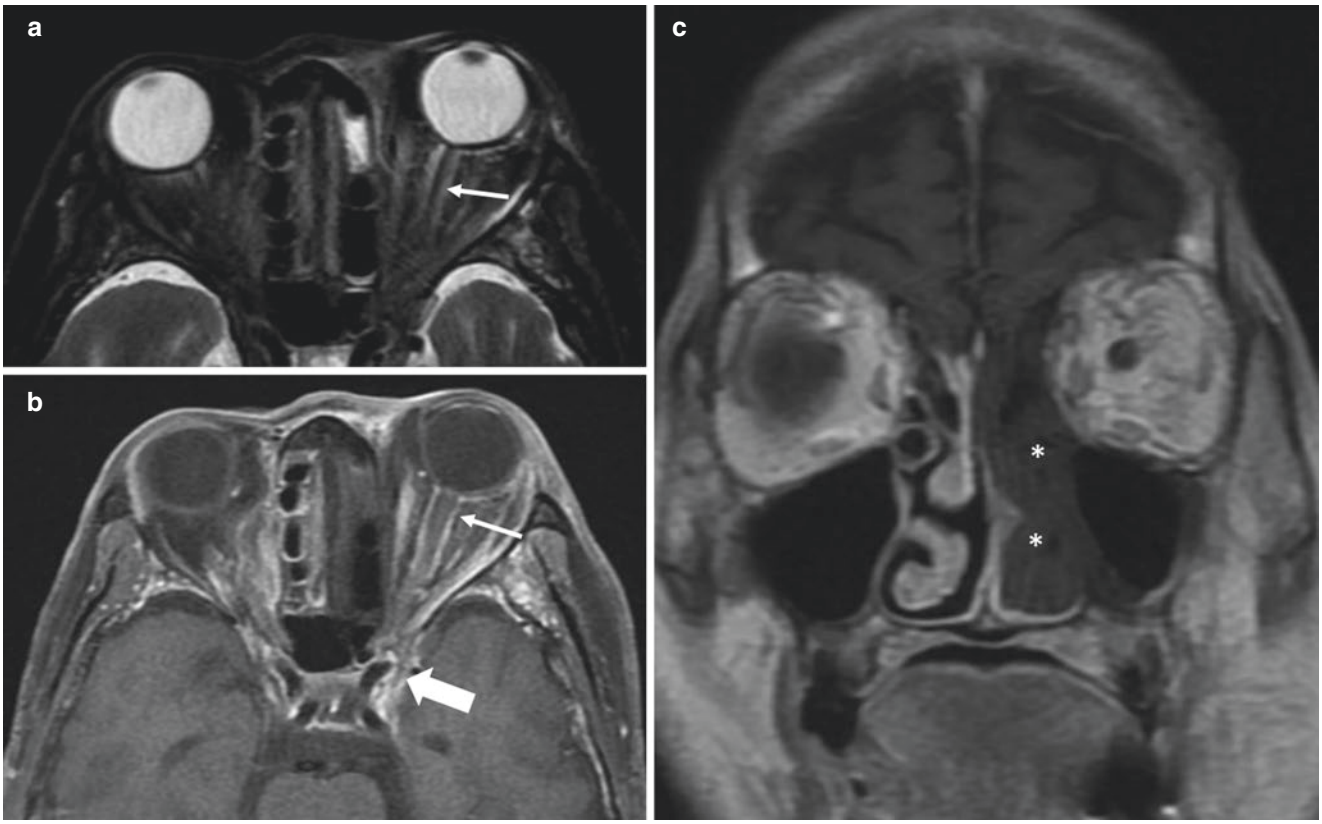

Fig. 8.2 Axial T2w FS (**a**) and axial T1w FS + C (**b**) show distension and enhancement of the optic nerve sheath (white arrow), oedema in Tenon's space and inflammation spreading to the left cavernous sinus (white block arrow) resulting in thrombophlebitis. Coronal T1w + C image (**c**) shows extensive non-enhancement of the left sinonasal mucosa and turbinates (white asterisk), indicating infarction and necrosis

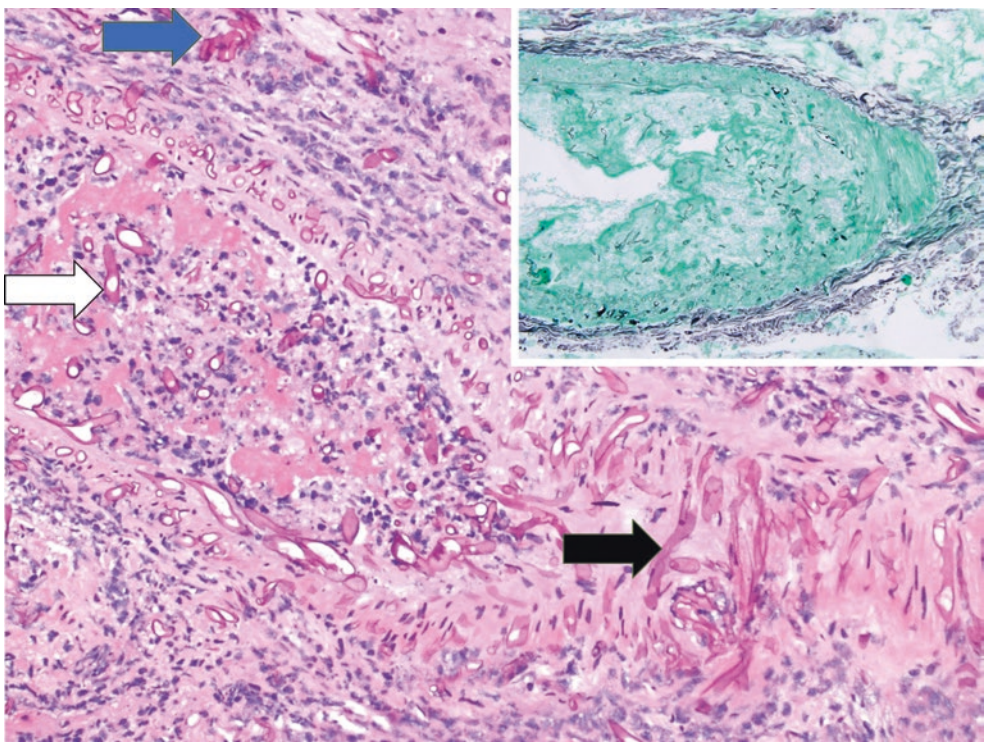

Fig. 8.3 A blood vessel is seen stretching diagonally downwards from the left upper edge of the picture to the bottom right edge. There are broad fungal hyphae within the vessel lumen (white arrow) and invading the vessel wall (black arrow), as well as in the surrounding connective tissue (blue arrow). Septa are not readily seen in this figure. HE stain; 200× magnification. GMS stain highlights the fungal hyphae in the optic nerve (inset; GMS stain; 100× magnification)

ranging from approximately 6 to 9 um in diameter. Rare septa were identified. The organisms were positive for Gomori methenamine silver (GMS) and periodic acid-Schiff (PAS) stains. This was accompanied by areas of infarction and patchy, predominantly chronic inflammation. The findings were consistent with the invasive fungal infection by zygomycosis.

The orbital contents after exenteration showed similar findings with invasive fungal infection, consistent with zygomycosis, with prominent vascular invasion and extensive ischaemic-type of necrosis. Fungal hyphae were present in all tissues including optic nerve and at all resection margins.

Case 2

A 57-year-old Chinese diabetic man with the history of nasopharyngeal carcinoma treated previously with chemoradiotherapy (completed 2 years previously), considered to be in remission, developed headache with vomiting and double vision of acute onset. On examination, his eyes were white with good vision. A right sixth nerve palsy was noted (Fig. 8.4). He was admitted to the hospital for investigations to rule out the possibility of recurrent tumour. MRI scan did not reveal any intracranial lesion but showed a sphenoidal sinusitis. The patient was discharged on systemic antibiotics but returned to the emergency department 2 weeks later with persistent headache and acute loss of vision in the right eye. He was hospitalized again, and an ophthalmic examination revealed a vision of counting fingers in the right eye with total ophthalmoplegia. A repeat MRI revealed orbital apical infiltration and fat stranding with opacification of adjacent sphenoid sinus. The PET-CT scan did not reveal any evidence of tumour recurrence. On suspicion of fungal infection, a biopsy of sphenoid sinus was carried out but was negative for fungus and tumour recurrence. Patient's eye condition worsened to no perception of light and total ophthalmoplegia in the right eye. A repeat biopsy from the apex of the orbit was advised, but the patient declined biopsy and any form of treatment and left the hospital, only to return 8 weeks later with delirium.

CLOSE summary is given in Table 8.2.

Table 8.2 CLOSE summary case 2

*C*linical scenario: infiltrative
*L*ocation: right orbit
*O*nset: subacute to chronic
*S*igns and symptoms: pain, headache, loss of vision, orbital apex syndrome
*E*pidemiology: 57-year-old diabetic Malay male

Differential Diagnosis

- Same as case 1

In addition:

- Optic neuritis
- Cranial nerve palsies

Radiology

Initial MRI showed mucosal thickening and fluid in bilateral sphenoid sinus with a bony defect in the lateral wall with marrow oedema. Persistent soft tissue thickening and enhancement at the right orbital apex and anterior cavernous sinus with suspected cranial nerve involvement and compression were seen (Fig. 8.5). The differentials included tumour recurrence as well as inflammatory/infective causes. The MRI carried out 3 weeks and 3 months later showed worsening mass lesion centred around the right orbital apex, optic nerve and cavernous sinus (Fig. 8.6) with invasion into the right middle cranial fossa, likely temporal lobe abscess formation and invasion/thrombosis of the right internal carotid artery. An invasive fungal infection was most likely from the above findings.

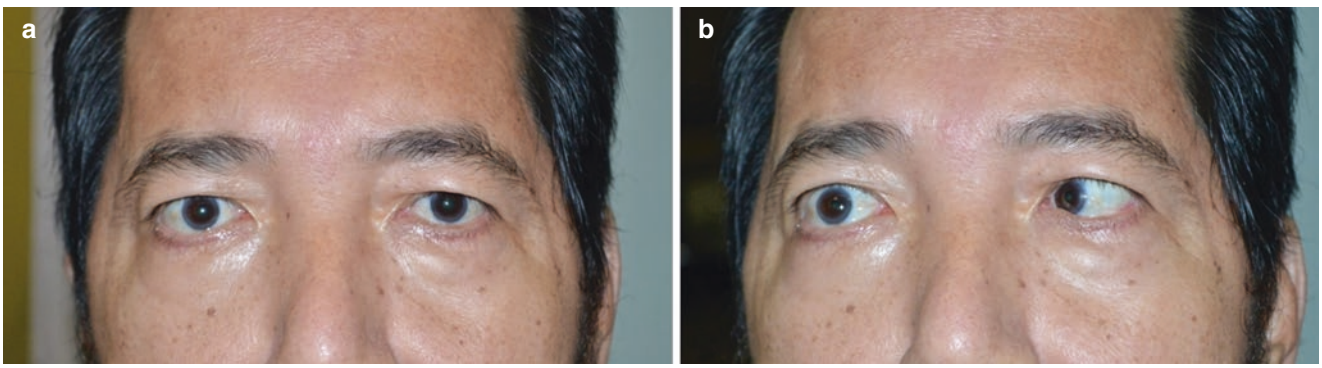

Fig. 8.4 Clinical picture of case 2 at the initial presentation (**a**) in primary position and (**b**) on right gaze. Note the right 6th nerve palsy

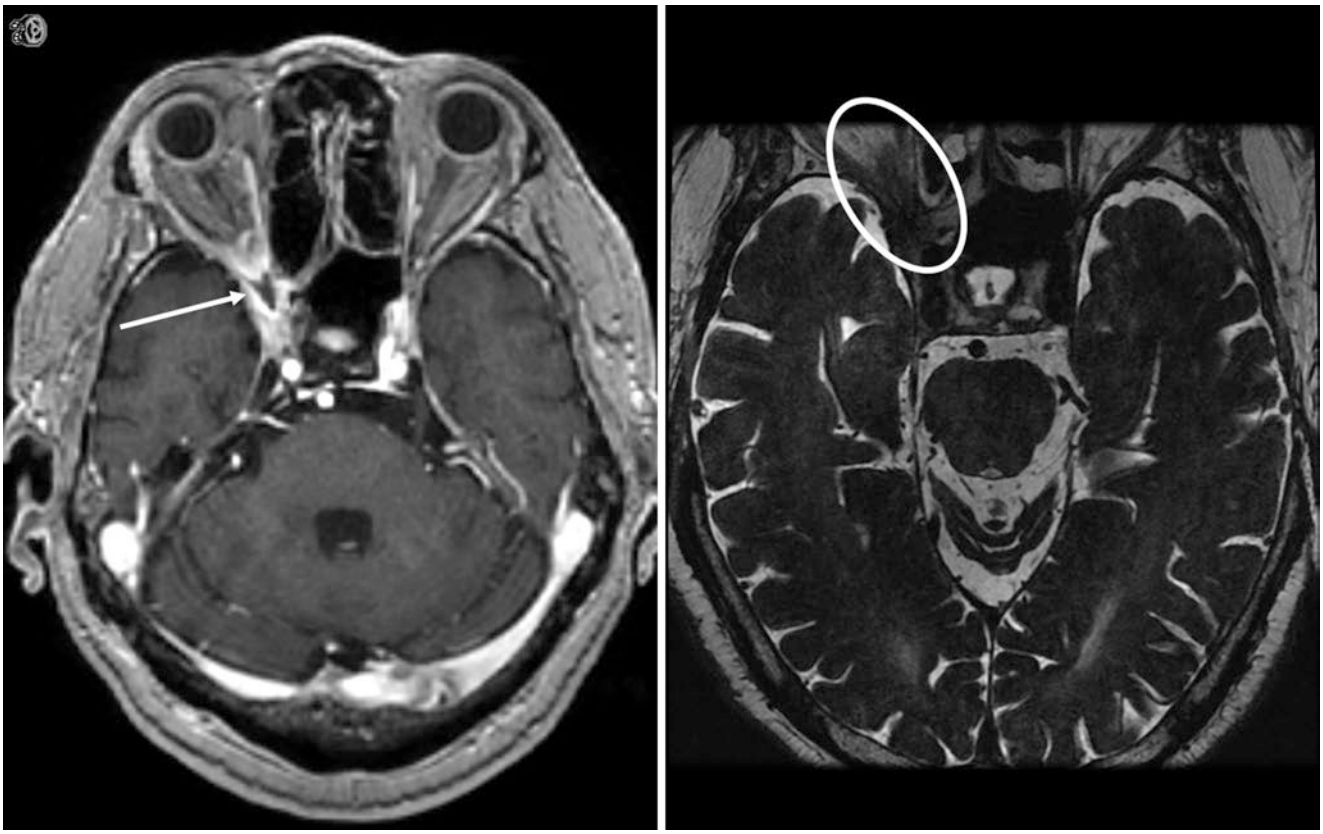

Fig. 8.5 Axial T1w + C (left) and 3D isotropic heavily T2w sequence (right), showing infiltration and enhancement of the fat at the orbital apex, with central necrosis/suppuration (white arrow and circle) at presentation

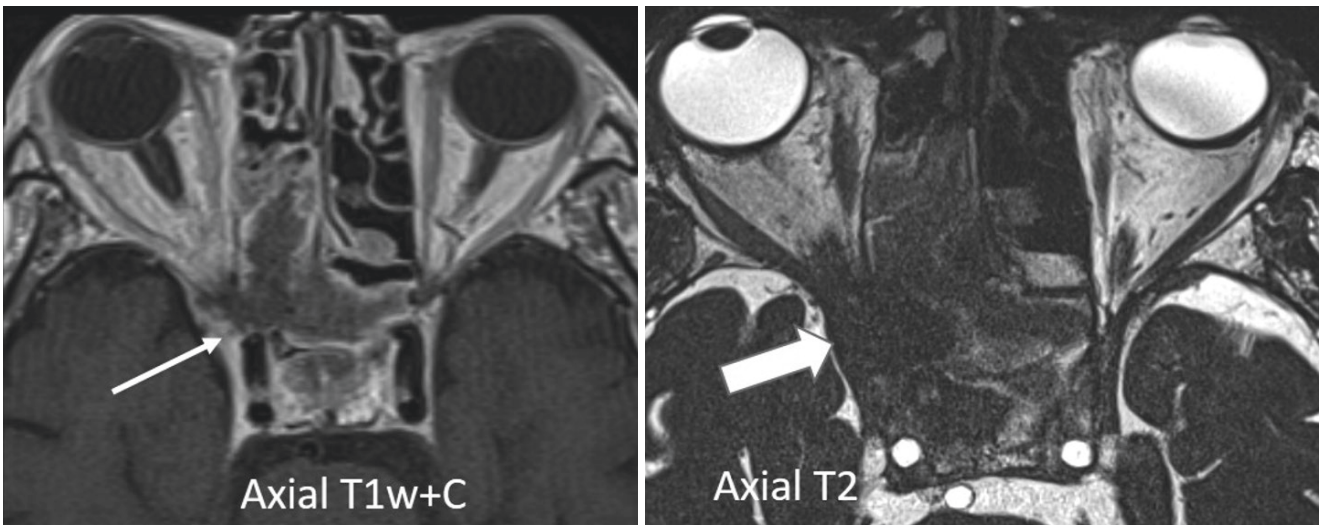

Fig. 8.6 Top: axial T1w + C and 3D isotropic heavily T2w sequences 3 weeks later showing spreading of inflammation to the anterior cavernous sinus (white arrow) and worsening necrosis (Block arrow) and enlargement of the abscess. Bottom: axial T1w FS + C and T2w FS sequences 3 months later showing worsening orbital, cavernous sinus and intracranial involvement (white arrows)

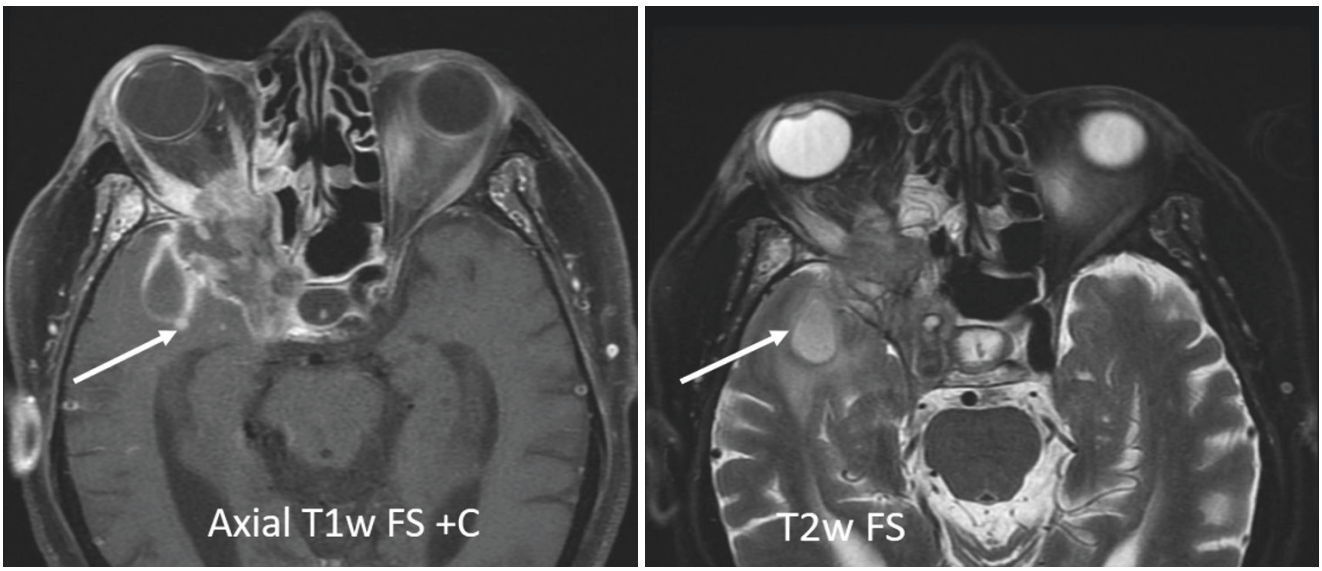

Fig. 8.6 (continued)

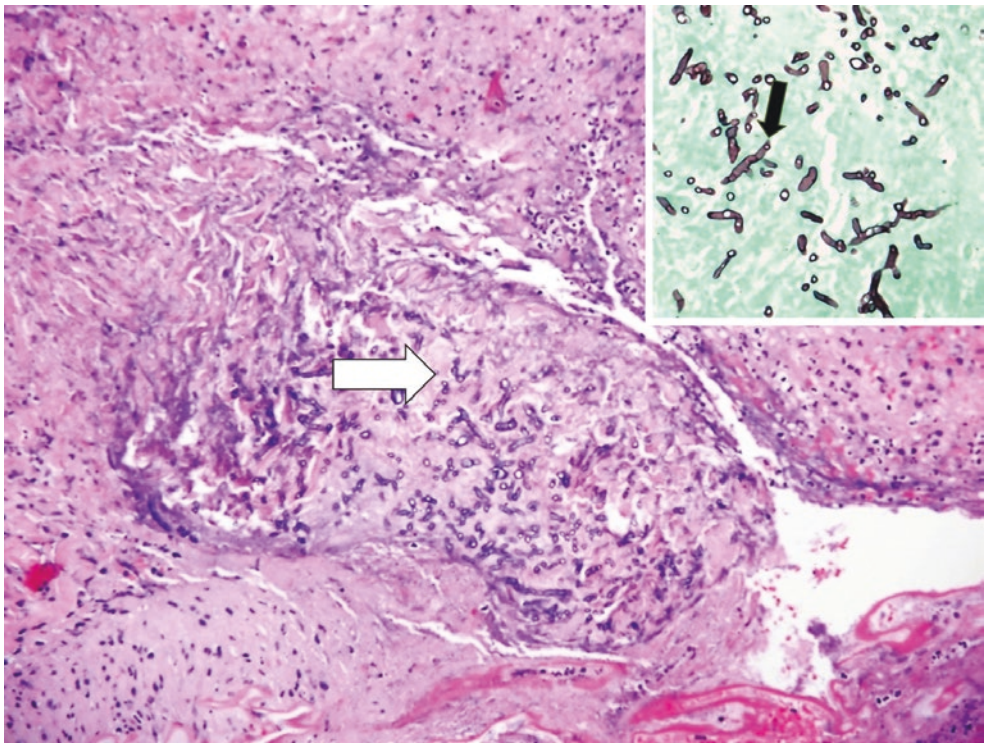

Fig. 8.7 A blood vessel is seen in the centre of the field. There is an organized thrombus within the vessel lumen within which are many fungal hyphae (white arrow). Septa are discernible (black arrow). HE stain; 200× magnification. GMS stain highlights the fungal hyphae (inset; GMS stain; 400× magnification)

Intervention

Biopsy was performed from the orbital apex by an endoscopic approach. Aspergillus PCR was positive in the tissues obtained by biopsy from the orbital apex.

Management

The patient was started on fluconazole and liposomal amphotericin B intravenously, but his condition worsened, and the patient died 5 months after the initial presentation.

Histopathology

The biopsy of the orbital apex showed a blood vessel containing an organized thrombus and adjacent to it, necrotic material. Fungal hyphae (highlighted by GMS stain) were seen within the thrombus in the vessel lumen and in the adjacent dense necrotic fibrous tissue.

Aspergillus could be recognized in histology as relatively thin fungal hyphae (approximately 3–6 um thick) which were septated and exhibited acute angle and dichotomous branching. The organisms were highlighted on special stains such as Gomori methenamine silver (GMS) (Fig. 8.7) and

periodic acid-Schiff (PAS). However, a definite diagnosis required microbiologic investigations, because other organisms could closely resemble *Aspergillus.*

Discussion

Invasive orbital fungal diseases are important causes of mortality and morbidity. Orbital fungal infections like the bacterial orbital cellulitis spread from the neighbouring sinuses, and are generally uncommon, but should be suspected in diabetics and immunocompromised patients with orbital cellulitis. Case 1 is an example of an acute invasive fungal infection that is usually caused by zygomycosis, a member of phycomycetes, in an immunocompromised individual. The condition is usually referred to as cerebro-rhino orbital mucormycosis (CROM).

Zygomycosis, also known as mucormycosis, is caused by fungus in the order Mucorales, of which *Rhizopus* species is the most common. It is an angiotropic fungus, and it is an obligate aerobe with nonseptate hyphae showing right-angled branches. The spores attach themselves to nasal mucosa and proliferate and germinate into hyphae. Patients with diabetes and ketoacidosis, accounting for 80–90%, are more prone to CROM, as the neutrophils are unable to mount a response. Mucor has a predilection for internal elastic lamina of the blood vessels, especially arteries, and forms thrombotic vascular occlusions resulting in gangrene and a haemorrhagic necrosis. The fungus also infiltrates nerves, causing loss of sensation and paralysis of extraocular muscles. There is very little inflammation, and the fungus thrives in dead organic tissue. The nonseptate hyphae are identified in all ocular tissues including the optic nerve.

Other than diabetes, patients with haematological malignancies, neutropenia (as in case 1), renal/bone marrow transplant, chronic renal failure, and iron overload are also predisposed to the development of CROM.

Clinically, there is destruction of the turbinates (seen as black turbinates in MRI), serosanguinous exudate from the nose, necrosis of the eyelids (blackening), and completely frozen orbit with ischaemic necrosis of all orbital tissues.

Diagnosis is difficult, as cultures often fail to grow mucorales. Culture can be taken from necrotic tissue. Rapid diagnosis may be possible using PCR. Early debridement, followed by local irrigation of antifungal agent, and intravenous amphotericin B, should be the treatment of choice. Rapid diagnosis and treatment seem to be the only way of reducing mortality or morbidity.

Case 2 is an example of a chronic invasive fungal infection. The predisposing causes were diabetes and previous radiotherapy with reduced local immunity. In chronic cases, the infection progresses slowly over months and, if untreated, spreads to the brain.

Aspergillus fumigatus often starts in the sphenoid sinus; the predilection for that sinus is poorly understood. As the fungus invades blood vessel walls and bone causing ischaemic necrosis and bony destruction, it spreads through the vessel walls or adjacent bony erosion into the orbit.

Invasive aspergillus infection occurs more commonly in immunocompromised patients with neutrophil deficiency and corticosteroid use. The other risk factors are diabetes, HIV infection and trauma. Rarely, there have been reports of aspergillus infection in immunocompetent patients. Aspergillus has a characteristic microscopic appearance. It has septate hyphae branching at 45°, seen well in PAS stain.

Clinically, persistent pain in the head and retrobulbar area is characteristic. Pain can precede ophthalmic symptoms. Imaging findings are subtle, and MRI may be the best modality, which shows focal enhancing lining in sphenoid sinus. Diagnosis is often delayed by months, as biopsy can yield negative results in about 50% of cases. If clinical suspicion is strong, a repeat biopsy would be necessary to clinch the diagnosis. Histologically, when fungal organisms are seen in the tissues, it is important to look for blood vessel invasion, which predicts a worse prognosis.

If treated early, the prognosis is better with a mortality rate of 25%. Intracranial extension is a significant factor in mortality of chronic invasive fungal infections. Fatality was described as 100% in two different studies. The treatment of choice is surgical debridement followed by local irrigation of amphotericin B, along with intravenous liposomal amphotericin B. The response rate is only 40–60% as the drug doesn't reach the tissues due to ischaemia. Voriconazole has been proven to be effective with less systemic effects than amphotericin B. If diagnosis is not certain, posaconazole can be used which has a wide spectrum of antifungal activity.

Learning Points

Invasive rhino-orbital fungal infections are rare, but must be considered in patients with immunocompromised status and diabetes. The diagnosis can be challenging, and it is important to obtain adequate diagnostic material for microbiological and pathological examination. Treatment should be started early and should include surgical debridement followed by irrigation of antifungal agent along with intravenous amphotericin B.

Mortality and morbidity are high in invasive fungal orbital infections.

Further Reading

1. Baeesa SS, et al. Invasive aspergillus sinusitis with orbitocranial extension. Asian J Neurosurg. 2017;12(2):172–9.
2. Lee DH, Yoon TM, Lee JK, Joo YE, Park KH, Lim SC. Invasive fungal sinusitis of the sphenoid sinus. Clin Exp Otorhinolaryngol. 2014;7(3):181–7.
3. Levin LA, Avery R, Shore JW, Woog JJ, Baker AS. The spectrum of orbital aspergillosis: a clinicopathological review. Sur Ophthalmol. 1996;41(2):142–54.
4. Sivak-Callcott JA, Livesley N, Nugent RA, Rasmussen SL, Saeed P, Rootman J. Localised invasive sino-orbital aspergillosis: characteristic features. Br J Ophthalmol. 2004;88(5):681–7.
5. Thajeb P, Thajeb T, Dai D. Fatal strokes in patients with rhino-orbito-cerebral mucormycosis and associated vasculopathy. Scand J Infect Dis. 2004;36(9):643–8.
6. Wali U, Balkhair A-MAJ. Cerebro-rhino orbital mucormycosis: An update. Infect Public Health. 2012;5:116–26.

Part IV

Inflammations

Granulomatosis with Polyangiitis (GPA)

9

Gangadhara Sundar, Stephanie Ming Young, Eric Ting, Bingcheng Wu, Min En Nga, and Shantha Amrith

Introduction

Granulomatosis with polyangiitis (GPA), formerly known as Wagener's granulomatosis, is one of the less common but often devastating multiorgan systemic diseases presenting as a specific orbital inflammatory syndrome. It is a pauci-immune small vessel, commonly antineutrophil cytoplasmic antibody (ANCA)-associated vasculitic syndrome characterized by the formation of necrotizing granulomas of upper and lower respiratory tracts and the kidneys. Delayed treatment often results in significant ophthalmic and systemic morbidity and when missed, mortality as well.

Case Scenario

A 55-year-old male presented with a chronic intermittent redness, pain, and blurred vision of the left bulgy eye of a few years. He had been treated elsewhere as a chronic conjunctivitis with topical antibiotics and steroids prior to presentation. He did have a history of diabetes and hypertension, and recent onset of weight loss with loss of appetite. There was no history of asthma or tuberculosis.

Ophthalmic examination revealed a best-corrected Snellen visual acuity of 6/6 and 6/24 in the right and left eyes, respectively. While the right eye was normal in all aspects, on the left, he had a mild proptosis with conjunctival injection (Fig. 9.1) and induration. There was evidence of peripheral corneal infiltration with ischaemia of the limbus and sclera. There was no relative afferent pupillary defect. Anterior and posterior segments were quiet except for a suspicion of optic nerve head swelling.

CLOSE summary is given in Table 9.1.

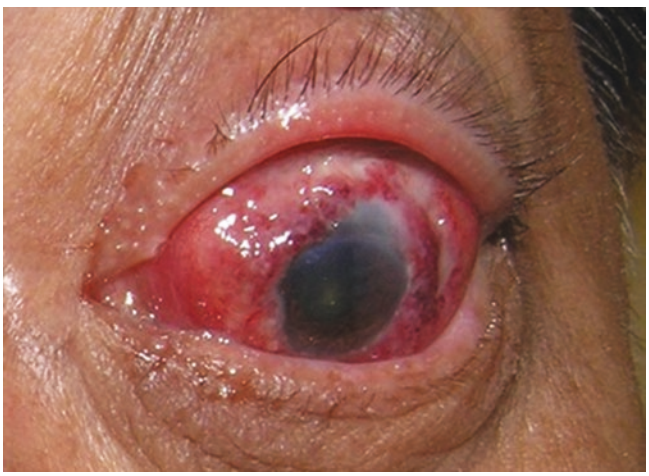

Fig. 9.1 Clinical presentation showing inflammatory signs in the conjunctiva, peripheral corneal infiltration with limbal and scleral ischaemia

G. Sundar · S. M. Young · S. Amrith (✉)
Department of Ophthalmology, National University Hospital, Singapore

Department of Ophthalmology, Yong Loo Lin School of Medicine, National University of Singapore, Singapore
e-mail: gangadhara_sundar@nuhs.edu.sg; shantha_amrith@nuhs.edu.sg

E. Ting
Department of Diagnostic Imaging, National University Hospital, Singapore

Department of Diagnostic Imaging, Yong Loo Lin School of Medicine, National University of Singapore, Singapore

Advanced Medicine Imaging, Singapore

B. Wu
Department of Pathology, National University Hospital, Singapore

M. E. Nga
Department of Pathology, National University Hospital, Singapore

Department of Pathology, Yong Loo Lin School of Medicine, National University of Singapore, Singapore

S. Amrith et al. (eds.), *Ocular Adnexal Lesions*, https://doi.org/10.1007/978-981-13-3798-7_9

Table 9.1 CLOSE summary

*C*linical process: inflammatory, infiltrative lesion
*L*ocation: ocular surface, left orbit
*O*nset: chronic
*S*ymptoms and signs: blurred vision, redness, pain, and proptosis
*E*pidemiology: middle-aged East Asian male

Differential Diagnosis

- Orbital cellulitis (bacterial)
- Orbital inflammatory disorder – specific (including sarcoidal lesion, granulomatosis with polyangiitis, etc.) versus nonspecific
- Lymphoproliferative disorder
- Metastasis/masquerade syndromes

Investigations

Initial investigations included systemic workup which showed the following:

- Full blood count (FBC): Mild leukocytosis
- Erythrocyte sedimentation rate (ESR) and cryo-reactive protein (CRP): Slightly raised
- Serum electrolytes, renal function tests: Normal
- Blood sugar: Raised
- Antineutrophil cytoplasmic antibodies against proteinase-3 (PR-3): Raised
- Urinalysis showed RBCs
- Chest x-ray: Normal
- Additional investigations included orbital imaging (CT scan).

Radiology

CT scan: A mass lesion was seen on the left side, along the posterior superolateral aspect, involving both intraconal and extraconal compartments, adjacent to the superior orbital fissure (Fig. 9.2). It engulfed the superior ophthalmic vein and posterior parts of lateral rectus and superior rectus-levator palpebrae superioris complex which were not seen separately.

Intervention

Serologic testing with documented c-ANCA and multiorgan disease may be sufficient for diagnosis of GPA; however, for limited forms of GPA like above, a diagnostic biopsy of the orbital mass was necessary.

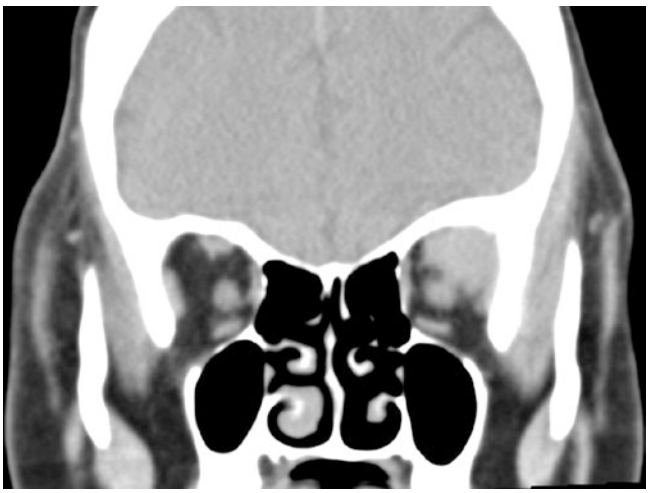

Fig. 9.2 Coronal CT orbit showing a poorly defined, extraconal soft tissue density lesion, which is otherwise nonspecific

Histopathology

There was geographic necrosis and a mixed inflammatory cellular infiltrate composed of many eosinophils, multinucleated giant cells, and poorly formed granulomas (granuloma = an aggregate of epithelioid histiocytes) (Fig. 9.3). There was also an associated destructive vasculitis (Fig. 9.4).

Fungal and acid fast bacilli stains to exclude infections were negative.

Management

Patient was initially treated with oral corticosteroids and later changed to azathioprine.

Discussion

Granulomatosis with polyangiitis may affect the eyelids, ocular surface, orbit, or adjacent ocular adnexal tissues, typically in adult Caucasians, but may affect other ethnic groups and rarely children. A high degree of suspicion should be maintained in progressive suspicious infiltrative and inflammatory disease of these tissues. It may present as either a typical generalized disease (classical clinical features with positive c-ANCA serology) or a limited atypical disease (yellow eyelid sign, orbital inflammation, and negative c-ANCA serology). Classic stages include acute, generalized systemic disease with ophthalmic/paranasal sinus involvement; a subacute, localized form of the disease; and, finally, a chronic indolent or refractory form of the disease.

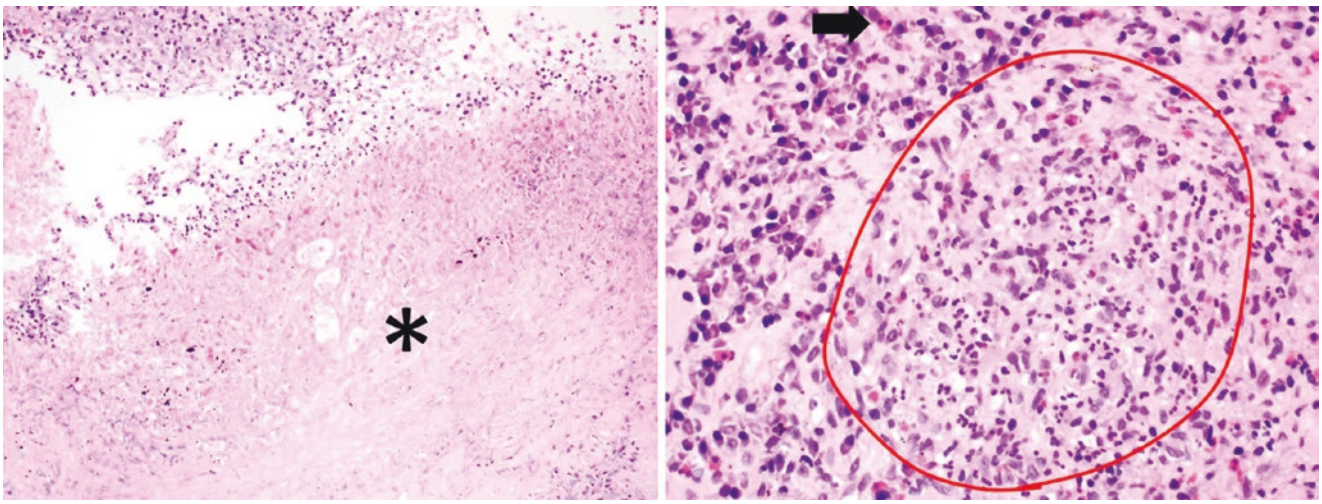

Fig. 9.3 Left – there are areas of geographic necrosis (*). Right – there is a mixed inflammatory cellular infiltrate with poorly formed granulomas (outlined in red), eosinophils (black arrow), lymphocytes, and plasma cells. Left: HE stain, 200× magnification. Right: HE stain, 400× magnification

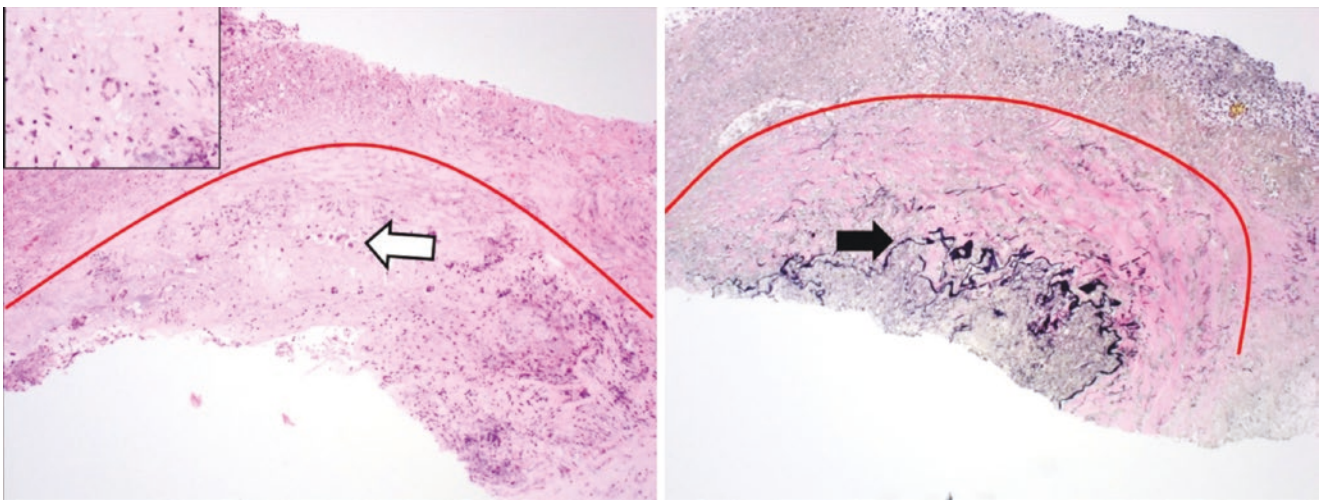

Fig. 9.4 Left – red line outlines a medium-sized blood vessel, seen in the lower half of each picture. There is inflammation within the wall of this vessel. A multinucleated giant cell is seen as a component of the inflammatory cellular infiltrate (white arrow). Left inset: shows a multinucleated giant cell in higher magnification. Right – the elastic layer of the blood vessel has been disrupted (black arrow). Left (main): Left: HE stain, 100× magnification. Left (Inset) HE stain, 400x magnification. Right: elastic van Gieson stain, 100× magnification

Histological features alone are not definitively diagnostic of Wegener granulomatosis; clinical and serological correlation is required.

Management

Almost always fatal prior to the 1960s, the advent of aggressive corticosteroid administration and, more importantly, cyclophosphamide has radically changed outcomes in organ destruction and life expectancy. Treatment is often begun with high doses of steroids supplanted with immunosuppressant therapy, usually in collaboration with an immunologist. This is dependent on the stage of the disease and the activity. Corticosteroids may be administered as oral prednisolone or intravenous methylprednisolone. Cyclophosphamide although very effective has significant and cumulative toxicity. Current steroid-sparing immunosuppressive agents include methotrexate, azathioprine, mycophenolate mofetil, and leflunomide. Trimethoprim/sulfamethoxazole may be considered as an alternative for localized disease. Newer agents include biologics that block B cells and TNF-alpha antagonists.

Learning Points

Granulomatosis with polyangiitis is a vision and life-threatening disease where there has to be a high degree of suspicion and low threshold for tissue diagnosis when serological tests are negative and ideally managed with an immunologist.

Further Reading

1. Cassells-Brown A, Morrell AJ, Davies BR, et al. Wegener's granulomatosis causing lid destruction: a further sight-threatening complication. Eye. 2003;17:652–4.
2. Duffy M. Advances in diagnosis, treatment and management of orbital and periocular Wegener's granulomatosis. Curr Opin Ophthalmol. 1999;10:352–7.
3. Espinoza GM, Desai A, Akduman L. Ocular vasculitis. Curr Rheumatol Rep. 2013;15(9):355. https://doi.org/10.1007/s11926-013-0355-x.
4. Pakalniskis MG, Berg AD, Policeni BA, Gentry LR, Sato Y, Moritani T, Smoker WR. The many faces of granulomatosis with polyangiitis: a review of the head and neck imaging manifestations. AJR Am J Roentgenol. 2015;205(6):W619–29. https://doi.org/10.2214/AJR.14.13864.
5. Shields JA, Shields CL. Eyelid, conjunctival and orbital tumors. An atlas and textbook. 3rd ed. Philadelphia: Wolters Kluwer; 2016. isbn:978-1-4963-2148-0.
6. Sundar G. Antineutrophil cytoplasmic antibody (ANCA)-associated vasculitic orbital syndromes. In: Demirci H, editor. Orbital inflammatory diseases and their differential diagnosis, Essentials in ophthalmology series. Berlin/Heidelberg: Springer; 2015. isbn:978-3-662-46527-1.

Thyroid Eye Disease

10

Shantha Amrith, Stephanie Ming Young, Poh Sun Goh, Bingcheng Wu, Min En Nga, and Gangadhara Sundar

Introduction

Thyroid eye disease (TED), also known as thyroid-associated orbitopathy (TAO), is a chronic inflammation of the orbital tissues. It is an autoimmune process that mostly affects patients with Graves' disease, but it can also affect patients with other autoimmune disorders of the thyroid. Middle-aged women are more prone; the gender ratio between women and men is 4:1. When males develop TED, it tends to be more severe. The disease is also severe in smokers. The diagnosis is often made with clinical signs along with the biochemical changes of thyroid hormone in the blood. Occasionally, imaging is necessary to differentiate it from other causes of muscle enlargement and space-occupying lesions of the orbit. Very rarely, a biopsy of the muscle is necessary to rule out other serious causes of muscle enlargement.

S. Amrith (✉) · S. M. Young · G. Sundar
Department of Ophthalmology, National University Hospital, Singapore

Department of Ophthalmology, Yong Loo Lin School of Medicine, National University of Singapore, Singapore
e-mail: shantha_amrith@nuhs.edu.sg; gangadhara_sundar@nuhs.edu.sg

P. S. Goh
Department of Diagnostic Imaging, National University Hospital, Singapore

Department of Diagnostic Imaging, Yong Loo Lin School of Medicine, National University of Singapore, Singapore

B. Wu
Department of Pathology, National University Hospital, Singapore

M. E. Nga
Department of Pathology, National University Hospital, Singapore

Department of Pathology, Yong Loo Lin School of Medicine, National University of Singapore, Singapore

Case Scenario

A 47-year-old Indonesian male, a passive smoker, presented with the prominence of his right eye for about 1 year. The patient was seen by an ophthalmologist, who treated him with oral prednisolone for non-specific orbital inflammation; however, the improvement after the steroid treatment was only modest. The thyroid function tests at that time were normal.

The patient did not experience any pain either at rest or moving the eyeball. On examination, he had good visual acuities in both eyes with normal pupillary reactions. Examination of the right eye revealed conjunctival injection with a 4–5 mm of proptosis. There was vertical diplopia in primary position with a right hypotropia of 44 prism dioptres. The ocular motility revealed severe limitation of right eye movement in the upgaze. The cranial nerves were normal. A forced duction test revealed restriction of upward movement of the right eye (Fig. 10.1).

CLOSE summary is given in Table 10.1.

Differential Diagnosis

- Non-specific inflammation of the orbit/myositis
- Thyroid eye disease

Table 10.1 CLOSE summary

*C*linical process: inflammatory/infiltrative
*L*ocation: right orbit
*O*nset: subacute to chronic
*S*igns and symptoms: proptosis, deviation of the eye and diplopia with limitation of eye movements
*E*pidemiology: 47-year-old Indonesian male, passive smoker

S. Amrith et al. (eds.), *Ocular Adnexal Lesions*, https://doi.org/10.1007/978-981-13-3798-7_10

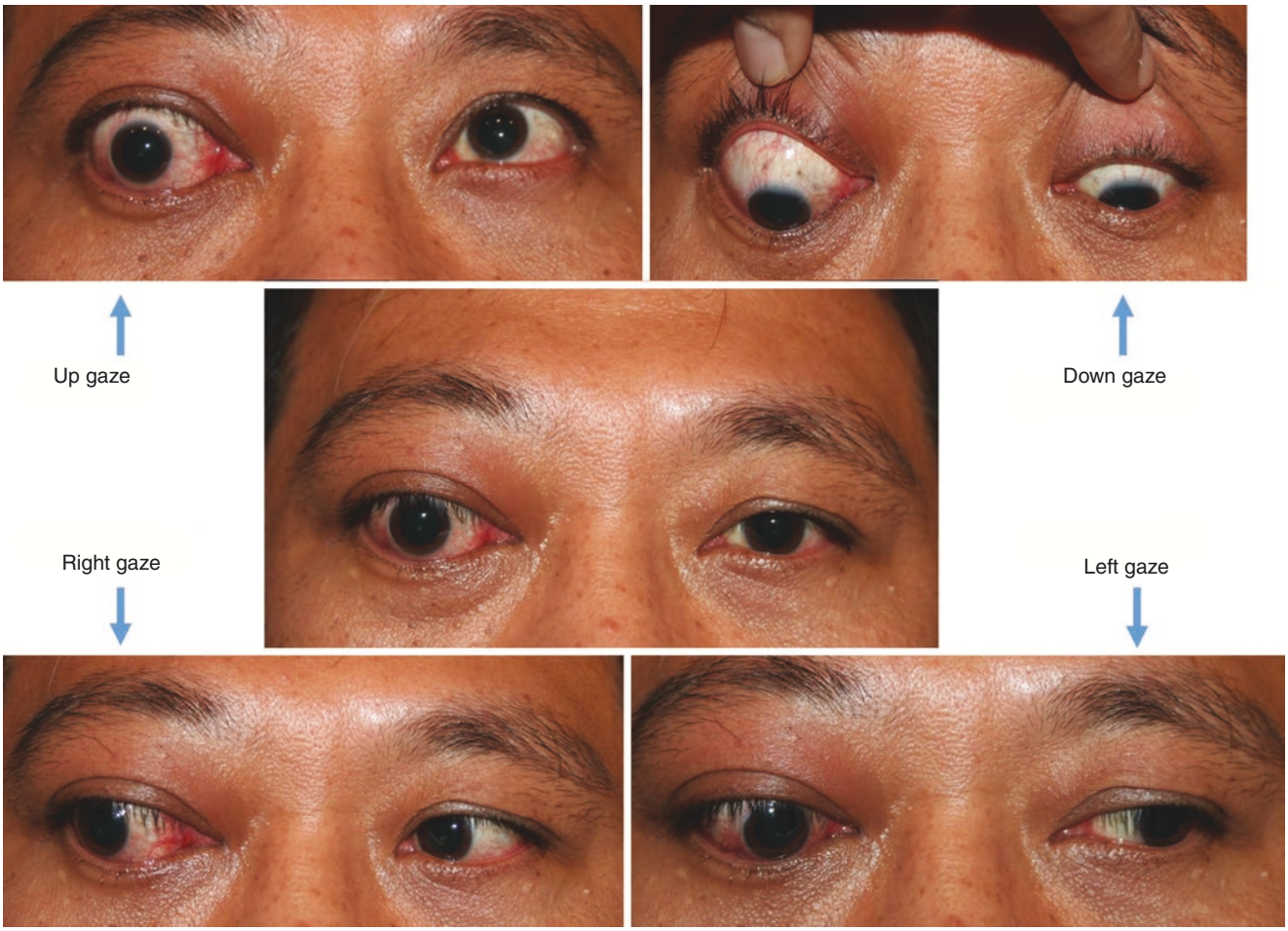

Fig. 10.1 Clinical picture showing right proptosis, soft tissue signs, right hypotropia and limitation of right eye movements in up and left gazes

- Myasthenia gravis
- Granulomatosis with polyangiitis (GPA or Wegener's granulomatosis)
- Lymphoproliferative disease such as lymphoma
- Metastatic disease
- Infectious diseases such as tuberculosis, syphilis, etc.

Other Investigations

Full blood count – Normal
ESR – Normal
ANCA – Negative
Syphilis screen – Negative

Radiology

MRI of the Orbits

Diffuse enlargement of the right inferior rectus muscle was noted with enhancement of periocular tissues (Fig. 10.2). Other extraocular muscles were unremarkable.

Intervention

The patient underwent an inferior rectus muscle biopsy to rule out other causes of muscle enlargement. Intraoperatively, the muscle sheath appeared thickened with increased vascularity. Muscle itself appeared normal, although enlarged.

Histopathology

The muscle fibres were of varying sizes and there was interstitial fibrosis. Patchy chronic inflammatory infiltrate was noted (Fig. 10.3). Some regenerating fibres were also noted. The findings were in keeping with an inflammatory myositis. Correlation with clinical features was recommended.

Management

The patient was advised a course of intravenous methylprednisolone but declined. Six months later, when he returned for a follow-up, he had developed a proptosis of the left eye, with limitation of ocular motility, lid swelling, and conjunctival

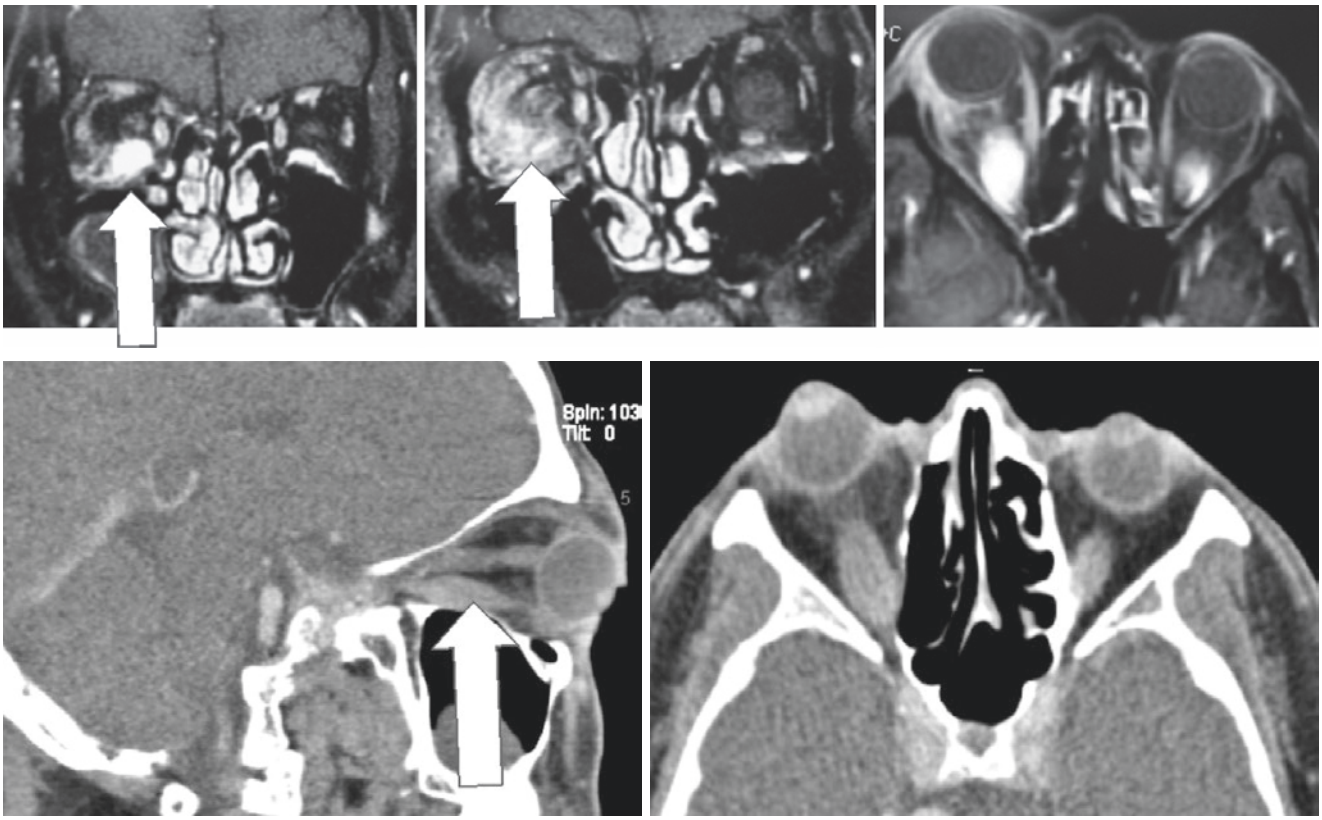

Fig. 10.2 Clockwise from the top left: coronal T1w MRI with contrast shows enlarged enhancing right inferior rectus muscle (arrow). Coronal T1w MRI with contrast showing diffuse enhancement of right intraconal fat (arrow). Axial T1w MRI with contrast shows enlarged right inferior rectus with enhancement in Tenon's capsule indicating inflammation. Axial contrast-enhanced CT showing similar enlargement of right inferior rectus and proptosis of the right eye Sagittal contrast-enhanced CT shows tendon-sparing enlargement of inferior rectus (arrow)

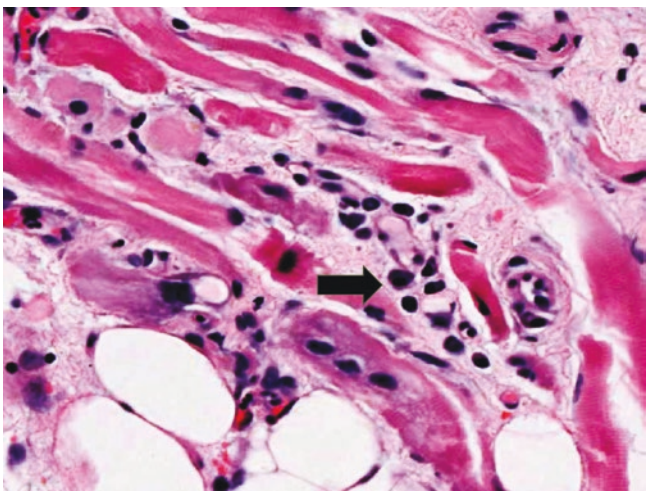

Fig. 10.3 There is a chronic inflammatory cellular infiltrate (black arrow) in between the muscle fibres. Increased pinkish collagen deposition is also seen between the muscle fibres. HE stain; 400× magnification

injection. The thyroid function tests were repeated. The free T4 was raised at 45.5 (normal range 10–23), TSH was decreased at <0.02 (normal range 0.45–4.5), and TSH receptor antibody (TRab) was increased at >23.1 (>2 considered positive). The other thyroid antibodies were normal. The patient was referred to an endocrinologist for the control of hyperthyroidism.

Discussion

Patients with TED have a history of thyrotoxicosis diagnosed concurrently or in the past (90%). Occasionally, TED develops before the onset of hyperthyroidism as in the case described above. Ten percent (10%) of cases have euthyroid eye disease.

Normally, TED has an initial active phase during which the inflammatory signs are predominant. The patients feel pain or retrobulbar ache, redness and puffiness/oedema in and around the eyes along with proptosis of the eyes, made

worse by the lid retraction. They may develop diplopia, and blurring of vision due to dry eyes, exposure keratopathy, and in about 5–10% optic nerve compression.

The inflammatory signs are graded according to Mourits clinical activity score or VISA scoring system.

Pathophysiology

TED is believed to be an autoimmune process affecting the fibroblasts of the orbit which are present in the orbital fat and extraocular muscles (EOM). Fibroblasts express insulin like growth factor-1 (IGF-1) receptors on their surface. Patients with TED are found to have high levels of circulating IGF-1 antibodies that bind to the receptors in orbital fibroblasts and trigger an inflammation. During the inflammatory process, there is stimulation of the T and B lymphocytes, production of pro-inflammatory cytokines and accumulation of glycosaminoglycans (GAG) in the interstitial spaces of EOM, connective tissues of the orbit, and lacrimal gland. The fibroblasts undergo differentiation into adipocytes and myofibroblasts. This gives rise to fat expansion, enlargement of EOM, enlargement of the lacrimal gland, and a proptosis that is seen clinically in TED.

In the chronic phase, the acute inflammation subsides, giving rise to fibrosis of muscles and restrictive myopathy.

MRI is able to show oedema in a STIR sequence (prolonged T2 relaxation time). Enlarged extraocular muscles with sparing of tendons and crowding of orbital apex can be visualized both in CT and MRI.

The histological examination does not help to differentiate between myositis and TED, but it can rule out other causes of muscle enlargement such as those due to lymphoma or metastatic disease.

The poor prognostic factors include smoking, older age group, males and pretreatment with radioiodine.

Management

In early stages of the active disease, patients who are smokers are strongly advised to quit smoking. Co-management of these patients with endocrinologists is essential to keep their thyroid functions under control. Generally, milder cases are managed with tear replacements, head-up position while sleeping to reduce the oedema, and topical steroids for superior limbic keratitis if present. In moderate to severe cases, the patients are given intravenous steroids (found to be superior to oral steroids) to reduce soft tissue swelling, a form of medical decompression, especially if compressive optic neuropathy is present. Steroid-sparing immunomodulatory agents can be added to reduce the side effects of steroids, especially in patients with co-morbidities. Steroids however do not help in restrictive myopathy or in reducing the proptosis in the chronic stage.

The other forms of treatment include radiotherapy and surgical decompression. Radiotherapy is non-specific, and targets the lymphocytes that are highly radiosensitive. Therefore, radiotherapy will work only in acute TED. A dosage of 20 Gy (Gray) is given in ten divided doses. It is contraindicated in patients with diabetic microvascular disease in the retina.

Surgical decompression in acute stage of the disease is performed in patients who do not respond well to intravenous steroids and continue to lose their vision due to compressive optic neuropathy or who have severe proptosis and exposure keratopathy. Decompressive surgery is also performed for rehabilitation of patients who are in the chronic and stable phase. Orbital decompression is followed by EOM surgery in patients who have persistent strabismus after surgery, and finally the patients may need an eyelid surgery for the lid retraction when the condition stabilises after EOM surgery.

Learning Points

- TED is the most common cause of unilateral or bilateral proptosis.
- In a patient with no hormonal change, the proptosis needs to be investigated for other causes, including biopsy if necessary.
- Serial testing of thyroid functions is necessary in a patient who is euthyroid but has strong clinical suspicion of TED.

Further Reading

1. Website for European Group on Grave's Orbitopathy (EUGOGO) Website: http://www.eugogo.eu/
2. International Thyroid Eye Disease Society Website: www.thyroideyedisease.org
3. Bartalena L, Marcocci C, Chiovato L, et al. Orbital cobalt irradiation combined with systemic corticosteroids for Graves' ophthalmopathy: comparison with systemic corticosteroids alone. J Clin Endocrinol Metab. 1983;56(6):1139–44. 28.
4. Dolman PJ, Rootman J. VISA classification for Graves' orbitopathy. Ophthal Plast Reconstr Surg. 2006;22(5):319–24. 23.
5. Kendall-Taylor P, Perros P. Clinical presentation of thyroid associated orbitopathy. Thyroid. 1998;8:427–8. 7.
6. Mourits MP, Prummel MF, Wiersinga WM, et al. Clinical activity score as a guide in the management of patients with Graves' ophthalmopathy. Clin Endocrinol. 1997;47:9. 22.
7. Perros P, Kendall-Taylor P. Natural history of thyroid eye disease. Thyroid. 1998;8:423–5.
8. Rajendram R, Taylor PN, Wilson VJ, et al. Combined immunosuppression and radiotherapy in thyroid eye disease (CIRTED): a multicentre, 2 × 2 factorial, double-blind, randomised controlled trial. Lancet Diabetes Endocrinol. 2018;S2213–8587(18):30021–4.
9. Rao R, MacIntosh PW, Yoon MK, Lefebvre DR. Current trends in the management of thyroid eye disease. Curr Opin Ophthalmol. 2015;26(6):484–90.
10. Rootman J, Dolman PJ. Thyroid orbitopathy (Chapter eight). In: Diseases of the orbit. A multidisciplinary approach. Hagerstown: Lippincott Williams & Wilkins; 2003.
11. Taylor and Francis, Prummel MF, Wiersinga WM. Smoking and risk of Graves' disease. JAMA. 1993;269:479–82.
12. Werner SC. Classification of the eye changes of Graves' disease. Am J Ophthalmol. 1969;68:646–8. 21.

IgG4-Related Ophthalmic Disease

11

Shantha Amrith, Stephanie Ming Young, Eric Ting, Bingcheng Wu, Min En Nga, and Gangadhara Sundar

Introduction

IgG4-related disease (RD) was originally recognized in 2001 in a patient with autoimmune pancreatitis with elevated serum IgG4. Subsequently, a fibro-inflammatory condition, characterized by tumefactive lesions at multiple sites, with dense lymphoplasmacytic infiltrate, rich in IgG4-positive plasma cells, storiform fibrosis, and obliterative phlebitis was found to be associated with autoimmune pancreatitis. The sites include the biliary tree, salivary glands, periorbital tissue, kidneys, lungs, lymph nodes, meninges, aorta, breast, prostate, thyroid, pericardium, and skin. Mikulicz syndrome with lacrimal and salivary gland enlargements is now considered as IgG4-RD. Clinically, the lacrimal gland is the most affected among the ophthalmic tissues, but the others include extraocular muscles, trigeminal nerve, orbital fat, eyelids, and nasolacrimal system. For ophthalmic disease, the term IgG4-related ophthalmic disease (IgG4-ROD) is used.

Clinically, the lacrimal gland is the most affected among the ophthalmic tissues, but the others include extraocular muscles (EOM), trigeminal nerve, orbital fat, eyelids, and nasolacrimal system. For ophthalmic disease, the term IgG4-related ophthalmic disease (IgG4-ROD) is used.

Clinical Scenarios

Case 1: Eyelid

A 55-year-old Eurasian male presented with progressive painless right lower eyelid swelling for 2 months. On examination, there was a well-defined mass occupying the whole width of the right lower eyelid. The mass was non-tender and firm on palpation, and the skin over the mass was slightly erythematous and mobile (Fig. 11.1). The rest of the eye examination was normal.

CLOSE summary is shown in Table 11.1.

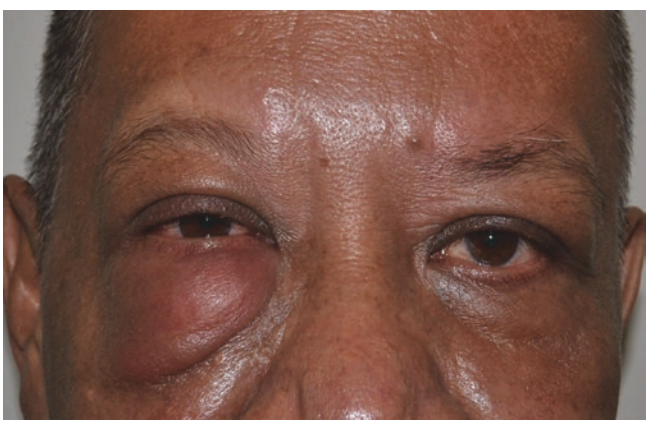

Fig. 11.1 Right lower lid mass in a 55-year-old male patient

S. Amrith (✉) · S. M. Young · G. Sundar
Department of Ophthalmology, National University Hospital, Singapore

Department of Ophthalmology, Yong Loo Lin School of Medicine, National University of Singapore, Singapore
e-mail: shantha_amrith@nuhs.edu.sg; gangadhara_sundar@nuhs.edu.sg

E. Ting
Department of Diagnostic Imaging, National University Hospital, Singapore

Department of Diagnostic Imaging, Yong Loo Lin School of Medicine, National University of Singapore, Singapore

Advanced Medicine Imaging, Singapore

B. Wu
Department of Pathology, National University Hospital, Singapore

M. E. Nga
Department of Pathology, National University Hospital, Singapore

Department of Pathology, Yong Loo Lin School of Medicine, National University of Singapore, Singapore

S. Amrith et al. (eds.), *Ocular Adnexal Lesions*, https://doi.org/10.1007/978-981-13-3798-7_11

Differential Diagnosis

- Lymphoproliferative disease including lymphoma
- Skin carcinomas, especially sebaceous gland carcinoma
- Necrobiotic xanthogranuloma
- Rosai-Dorfman disease
- Schwannoma
- Sarcoidal lesion
- Infective granulomas such as TB/syphilis
- Kaposi's sarcoma
- IgG4-related disease
- Kimura's disease

Radiology

The CT scan showed an enhancing soft tissue lesion inferior to right globe in the lower eyelid (Fig. 11.2). The lesion was seen extending posteriorly and medially into the orbit, abutting the tendinous portion of the inferior rectus (IR) muscle. Equivocal mild enlargement of IR muscle was noted. It was in close proximity to the right lacrimal sac. There was no involvement of the optic nerve. Incidentally, extensive bilateral sinusitis was noted.

Investigations included the following:

- FBC: normal except for eosinophilia
- ESR: raised at 91 mm/h
- CRP: <5 mg/l
- ANA: positive
- SLE, ENA panels, and ANCA: negative
- Myeloma screen: generalized increase in immunoglobulin
- Hepatitis B/C screen: negative
- TB spot: borderline
- IgG subclass: total IgG, subclasses 1, 2, and 3 elevated, IgG4 not elevated

Table 11.1 CLOSE summary for case 1: eyelid

*C*linical process – mass lesion
*L*ocation – right lower eyelid
*O*nset – subacute
*S*igns and symptoms – disfiguring, painless
*E*pidemiology – middle-aged Eurasian male

Intervention

An incisional biopsy of the eyelid lesion was carried out and the specimens sent fresh for histopathology and flow cytometry. The patient also underwent a biopsy of the nasal mucosa.

Case 2: Lacrimal Gland

A 53-year-old Malay female with co-morbidities such as diabetes mellitus, hypertension, and hyperlipidaemia presented with painless right upper lid swelling of 1-month duration. About 6 months earlier, she had undergone biopsy for bilateral breast lumps. The biopsy revealed atypical lymphoid proliferation and negative for malignancy.

The eye examination revealed normal visual acuities and mild ptosis of the right upper eyelid with full ocular motility. There was fullness in the lateral aspect of the right upper eyelid (Fig. 11.3) with the lacrimal gland slipping under the fingers on palpation, it was non-tender, and the conjunctiva was white. There was no proptosis as measured by exophthalmometer.

CLOSE summary is given in Table 11.2.

Differential Diagnosis

- Sarcoidosis
- Ideopathic orbital inflammation
- Autoimmune disease such as Sjogren's syndrome
- IgG4 inflammation
- Lymphoproliferative disorder
- Malignant epithelial tumour/metastasis

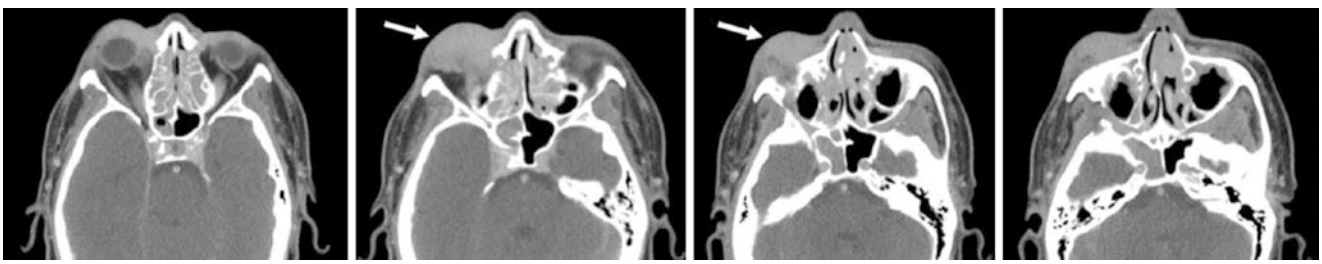

Fig. 11.2 CT scans showing ill-defined, infiltrative soft tissue density involving the preseptal lower lid and premaxillary soft tissue (white arrow). Diffuse sinonasal inflammation with polypoidal soft tissue densities is also present

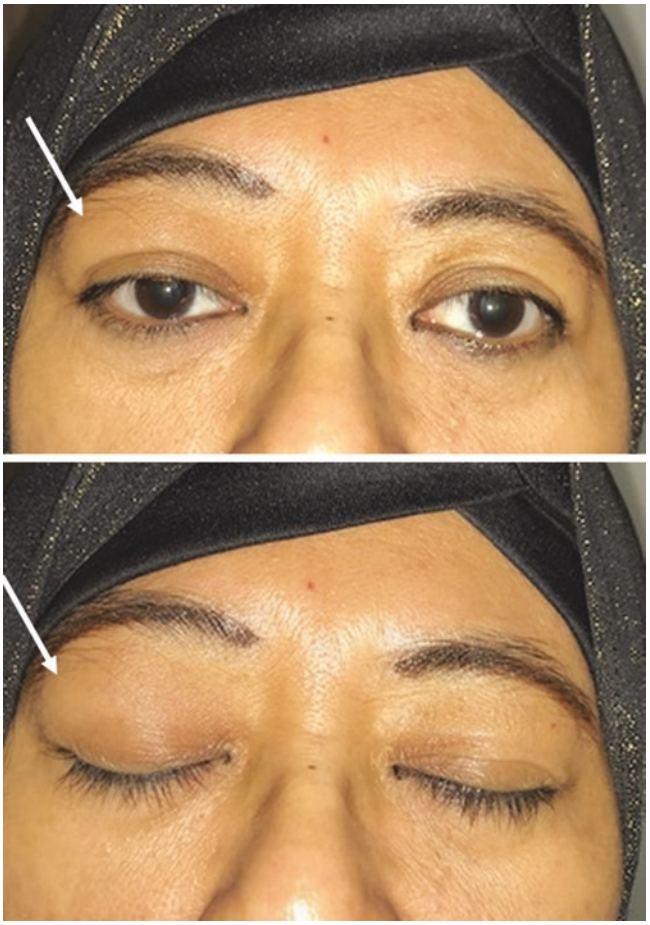

Fig. 11.3 Fullness in the right upper lid (white arrow) with mild ptosis in a 53-year-old Malay woman

Table 11.2 CLOSE summary for case 2: lacrimal gland

*C*linical process: infiltrative mass
*L*ocation: right upper lid
*O*nset: subacute
*S*igns and symptoms: painless upper lid swelling and fullness in the lateral aspect
*E*pidemiology: 53-year-old Malay female

Radiology

CT scan of the orbits showed enlargement of the right lacrimal gland (Fig. 11.4). Soft tissue swelling was noted in the upper eyelid. The left lacrimal gland was also mildly enlarged which was not noted clinically. The rest of the orbits was unremarkable. Possibility of a lymphoma was considered.

Investigations

Serum IgG subclasses

Total IgG	1740 mg/dl (raised)	Normal range: 767–1590
IgG1	993 mg/dl (raised)	Normal range: 341–894
IgG2	1030 mg/dl (raised)	Normal range: 171–632
IgG3	130 mg/dl (raised)	Normal range: 18.4–106
IgG4	590 mg/dl (raised)	Normal range: 2.4–121

FBC, C-reactive protein, renal and liver panels – normal
ESR – slightly raised
Myeloma panel – no abnormal bands or monoclonality detected
Anti-nuclear antibody, anti-SSA, and anti-SSB – negative

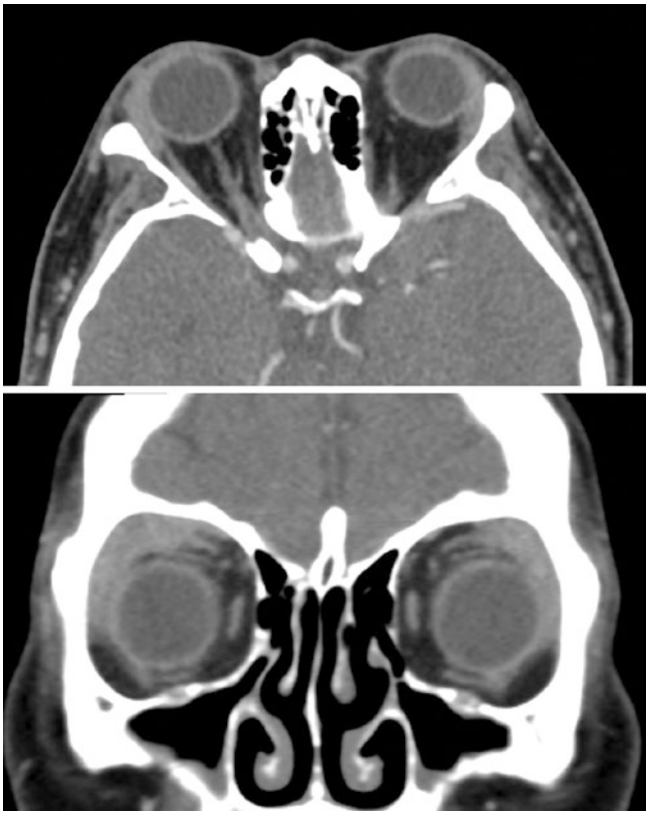

Fig. 11.4 CT scans showing ill-defined, infiltrative soft tissue density involving bilateral lacrimal glands

Intervention

An incisional biopsy of the right lacrimal gland and orbital fat was performed through an anterior orbitotomy and lid crease incision. Tissues were sent fresh for histopathology.

Histopathology

The histopathological features from three biopsies (eyelid, nasal mucosa from case 1, and lacrimal gland in case 2) showed similar features. There was dense fibrosis and prominent aggregates of lymphoid cells admixed with numerous plasma cells (Fig. 11.5). The lymphocytes were composed of a mixture of B cells (CD20 and PAX5 positive), as well as T cells (CD3 positive). There were more than 100 IgG4-positive plasma cells per high-power field. The IgG4/IgG

ratio was more than 40% (Fig. 11.6). The histologic features were consistent with a diagnosis of IgG4-related disease in the appropriate clinical context.

Comment from pathologist: Other features that would be supportive of a diagnosis of IgG4-related disease include storiform fibrosis and obliterative phlebitis. These features were not prominent in these biopsies and are seldom seen in orbital tissues. It should be noted that the quantitative criteria might vary according to the site of the biopsy.

IgVH mutation from paraffin block from case 1 showed polyclonality, thus ruling out MALT lymphoma as a possibility.

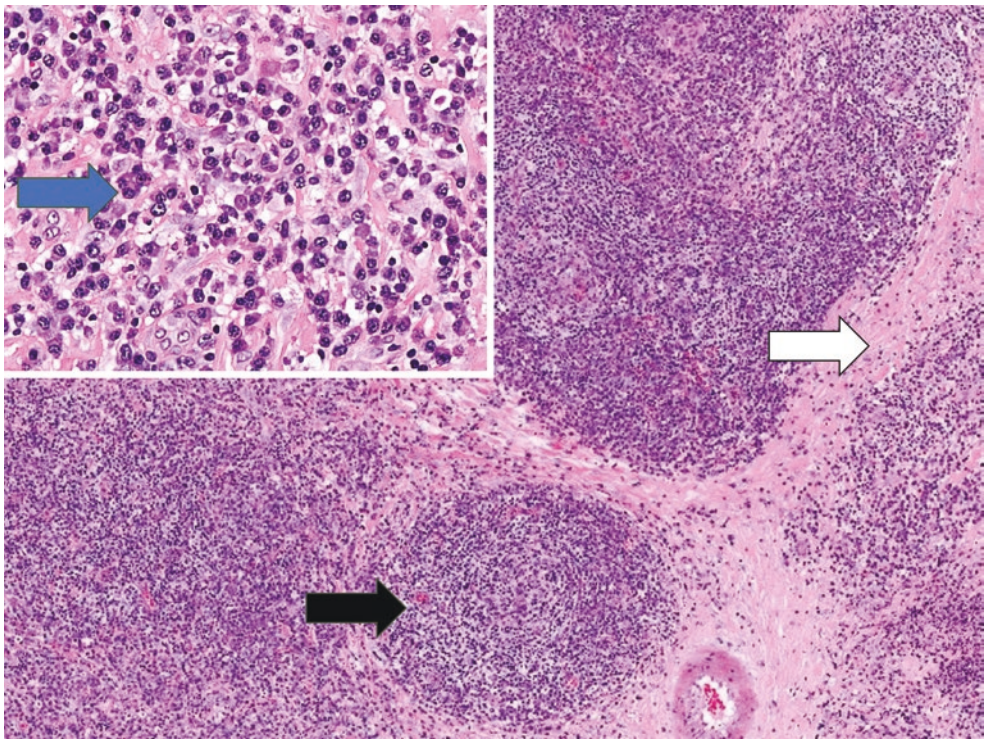

Fig. 11.5 There is dense sclerotic fibrous tissue (white arrow) and prominent aggregates of lymphocytes (black arrow) admixed with numerous plasma cells (inset; blue arrow). HE stain; 400× magnification

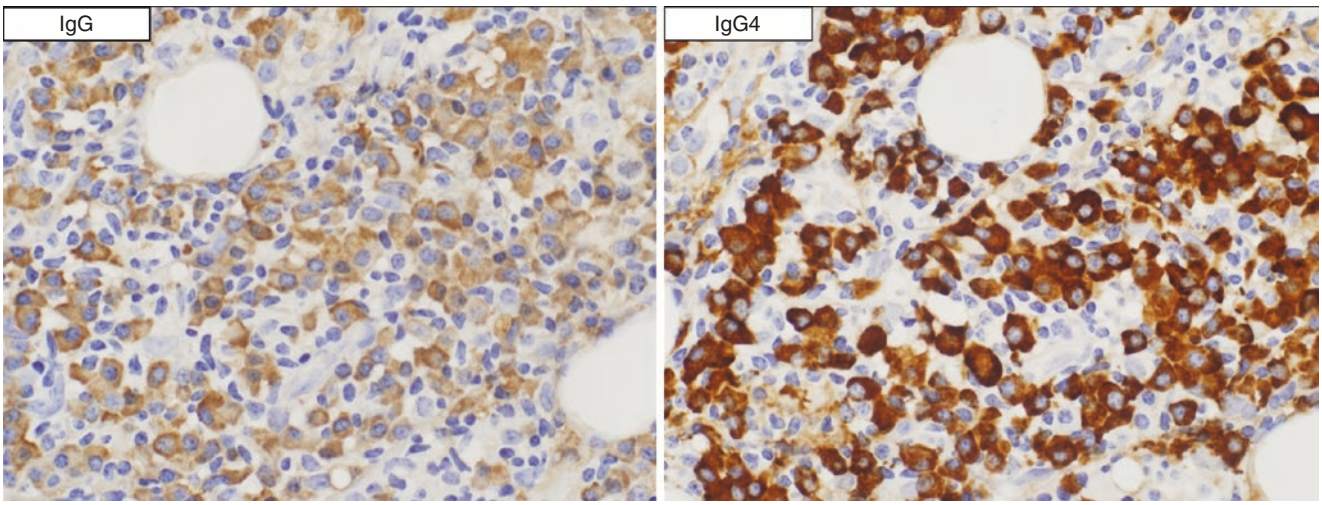

Fig. 11.6 Left: There are an increased number of IgG4-positive plasma cells (more than 100 per high-power field) and an increased IgG4 to IgG ratio (more than 40%). Right: Immunohistochemistry (IgG and IgG4 antibodies); 400× magnification

The breast biopsy from case 2 was reviewed, and in retrospect, similar IgG and IgG4 staining characteristics were noted in the tissues.

Management

Case 1 had sinus involvement and case 2 breast involvement. Patients underwent systemic screening for more organ involvements but were negative. They were treated with oral steroids. The response was good, and eventually steroid-sparing agent azathioprine was started. The eyelid lesion reduced in size in case 1. In case 2, repeat serum IgG subclasses revealed normal levels of total IgG1, IgG2, and IgG3, while IgG4 remained slightly elevated although it was less than the previous reading.

Discussion

IgG4-RD was first described in autoimmune pancreatitis with tumefactive lesions showing classic features of dense lymphoplasmacytic infiltrate rich in IgG4+ plasma cells, storiform fibrosis, and obliterative phlebitis. An elevated serum IgG4 ≥ 135 mg/dl concentrations may or may not be present, and only 40% of patients show raised subclass IgG4 concentrations. Some studies have shown that in the lacrimal glands, there may not be any obliterative phlebitis or storiform fibrosis, but instead a collagenous fibrosis is present.

Imaging in the form of CT or MRI is useful in cases where the soft tissues of the orbit or EOM are affected. The MRI shows isodensity in T1-weighted images and hypodensity on T2-weighted images with homogeneous enhancement with gadolinium. FDG-PET scans can be used for systemic evaluation.

IgG4-ROD is diagnosed with the criteria (Goto et al.) listed in Table 11.3.

Histologic diagnosis of IgG4-ROD is made only if two of the three criteria mentioned in Table 11.3 are present; in which case, it should show a number of IgG4-staining plasma cells on immunostaining to be >50 per high-power field and the ratio of IgG4 plasma cells to IgG plasma cells be at least 40%. Bilateral involvement is likely to have higher IgG4 serum levels.

A subset of patients with IgG4-RD are known to have associated allergic symptoms with raised eosinophilia (as in our first patient) and elevated IgE.

Until discoveries pertaining to the aetiology and pathophysiology of the disease surface, the term IgG4-RD or ROD will be used in the light of the presence of IgG4 (as per the guidelines) within involved organs with elevated serum IgG4 concentrations.

The mainstay of treatment is systemic corticosteroids. In cases where serum IgG concentrations are elevated, it may be used as a marker for monitoring treatment response and for relapse of the disease.

Table 11.3 Criteria for diagnosis of IgG4-ROD

1. Enlargement of the lacrimal gland, extraocular muscles, trigeminal nerve or mass lesions in any of the ophthalmic tissue
2. Histopathological examination showing marked lymphocyte and plasma cell infiltration associated sometimes with fibrosis. Ratio of IgG4+ cells to IgG+ cells is 40% or above or more than 50 IgG4+ cells per high-power field (×400)
3. Blood tests showing serum IgG4 levels of ≥135 mg/dl

Definite IgG4-ROD is diagnosed if all three features are present, probable IgG4-ROD if only 1 and 2 are present, and possible IgG4-ROD if only 1 and 3 are present

Learning Points

IgG4-related ophthalmic disease (ROD) is still evolving. There are some variations in the presentation of ophthalmic disease compared to systemic IgG4-RD.

IgG4 inflammation is rare in the eyelids, but more common in lacrimal glands and extraocular muscles, and should be suspected in all painless lumps in ocular adnexa.

Further Reading

1. Deshpande V, Zen Y, Chan JK, et al. Consensus statement on the pathology of IgG4-related disease. Mod Pathol. 2012;25(9):1181–92.
2. Gervasio KA, Chelnis J, Burkat CN. IgG4-related orbital inflammation.eyewiki.aao.org. 2017.
3. Goto H, Takahira M, Azumi A, et al. Diagnostic criteria for IgG4 related ophthalmic disease. Jpn J Ophthalmol. 2015;59:1–7.
4. Sogabe Y, Miyatani K, Goto R, et al. Pathological findings of infraorbital nerve enlargement in IgG4-related ophthalmic disease. Jpn J Ophthalmol. 2012;56:511–4.
5. Toyoda K, Oba H, Kutomi K, et al. MR imaging of IgG4-related disease in the head and neck and brain. Am J Neuroradiol. 2012;33(11):2136–9.
6. Umehara H, Okazaki K, Masaki Y, et al. Comprehensive diagnostic criteria for IgG4-related disease (IgG-RD), 2011. Mod Rheumatol. 2012;22:21–30.
7. Wallace ZS, Deshpande V, Stone JH. Ophthalmic manifestations of IgG4-related disease: single centre experience and literature review. Semin Arthritis Rheum. 2014;43(6):806–17.

Sarcoidosis

12

Gangadhara Sundar, Stephanie Ming Young, Poh Sun Goh, Bingcheng Wu, Min En Nga, and Shantha Amrith

Introduction

Sarcoidosis is a granulomatous disorder of uncertain aetiology often involving multiple organ systems. Ophthalmic presentation may include intraocular inflammation – anterior or posterior uveitis, which may be granulomatous or non-granulomatous – dacryoadenitis, and extraocular muscle and optic nerve involvement. Presence of conjunctival granulomas, appearing like follicles, enables tissue diagnosis by simple biopsy technique.

Clinical Scenario

A 30-year-old South Asian female presented with a history of recurrent fullness of both upper eyelids of 2–3 years duration. She had been started on oral steroids with repeated taper over that period for a presumed diagnosis of orbital inflammatory disorder – chronic dacryoadenitis. She was reportedly well otherwise and denied visual symptoms. Ophthalmic examination showed normal visual acuity, intraocular pressures, and anterior and posterior segments. She however had prominent firm lesions along the superotemporal quadrant of both upper eyelids (Fig. 12.1), made prominent on globe retropulsion. There was no tenderness or paraesthesia over the left lacrimal nerve distribution. Seemingly prominent 'follicles' were seen in the inferior fornix. Review of systems was unremarkable. Systemic workup performed previously for autoimmune disorders did not yield any positive results (Table 12.1).

Fig. 12.1 Clinical picture showing bilateral fullness in the superolateral quadrants of the upper lids

Table 12.1 CLOSE summary

*C*linical scenario: inflammatory/mass lesion
*L*ocation: bilateral lacrimal glands
*O*nset: chronic
*S*igns and symptoms: bilateral painless recurrent eyelid swelling and palpable enlarged lacrimal glands
*E*pidemiology: young South Asian female

G. Sundar · S. M. Young · S. Amrith (✉)
Department of Ophthalmology, National University Hospital, Singapore

Department of Ophthalmology, Yong Loo Lin School of Medicine, National University of Singapore, Singapore
e-mail: gangadhara_sundar@nuhs.edu.sg; shantha_amrith@nuhs.edu.sg

P. S. Goh
Department of Diagnostic Imaging, National University Hospital, Singapore

Department of Diagnostic Imaging, Yong Loo Lin School of Medicine, National University of Singapore, Singapore

B. Wu
Department of Pathology, National University Hospital, Singapore

M. E. Nga
Department of Pathology, National University Hospital, Singapore

Department of Pathology, Yong Loo Lin School of Medicine, National University of Singapore, Singapore

S. Amrith et al. (eds.), *Ocular Adnexal Lesions*, https://doi.org/10.1007/978-981-13-3798-7_12

Differential Diagnosis

- Infectious: Tuberculosis
- Non-infectious inflammations: Dacryoadenitis (idiopathic [NSOID]), far less likely viral, sarcoidosis, IgG4-related orbital inflammation, and others
- Neoplastic disorders
  - Benign: Reactive lymphoid hyperplasia, atypical lymphoid hyperplasia, pleomorphic adenoma (less likely)
  - Malignant: Lymphoma, adenoid cystic or other carcinomas of the lacrimal gland (less likely)

Radiology

CT scan of the orbits showed prominent orbital lobes of the lacrimal glands bilaterally (Fig. 12.2a, b). They were partly wrapped around the globes and showed enhancement with contrast. There were no overlying bony irregularity, indentation of the globe, and involvement of the extraocular muscles.

Intervention

A conjunctival biopsy of the follicles of the lower fornix was performed under local anaesthesia in the outpatient setting and specimen sent for routine histopathology and immunohistochemistry.

Histopathology

Conjunctival tissue showed chronic inflammation of the superficial stroma, including some prominent lymphoid follicles with germinal centres. There was granulomatous inflammation within the subepithelial stroma. These granulomas were small, tight, well-defined without necrosis or significant acute inflammation. The granulomas were composed of aggregates of epithelioid histiocytes with elongated, slipper-shaped nuclei, and fairly abundant cytoplasm (Fig. 12.3). Multinucleated cells were also seen. No malignancy was identified. No acid-fast bacilli or fungal organisms were detected on the Ziehl-Neelsen and GMS stains, respectively.

A diagnosis of chronic inflammation with focal non-necrotising granulomata suggestive of sarcoidosis was made.

Investigations

- Full blood count including differential count – Mild leukocytosis
- Erythrocyte sedimentation rate (ESR), C-reactive protein (CRP) – Normal
- Rheumatoid factor – Negative
- Antinuclear antibody (ANA), serum angiotensin-converting enzyme (ACE) assay – Normal
- Chest x-ray (Fig. 12.2c) – PA view showed bilateral hilar lymphadenopathy

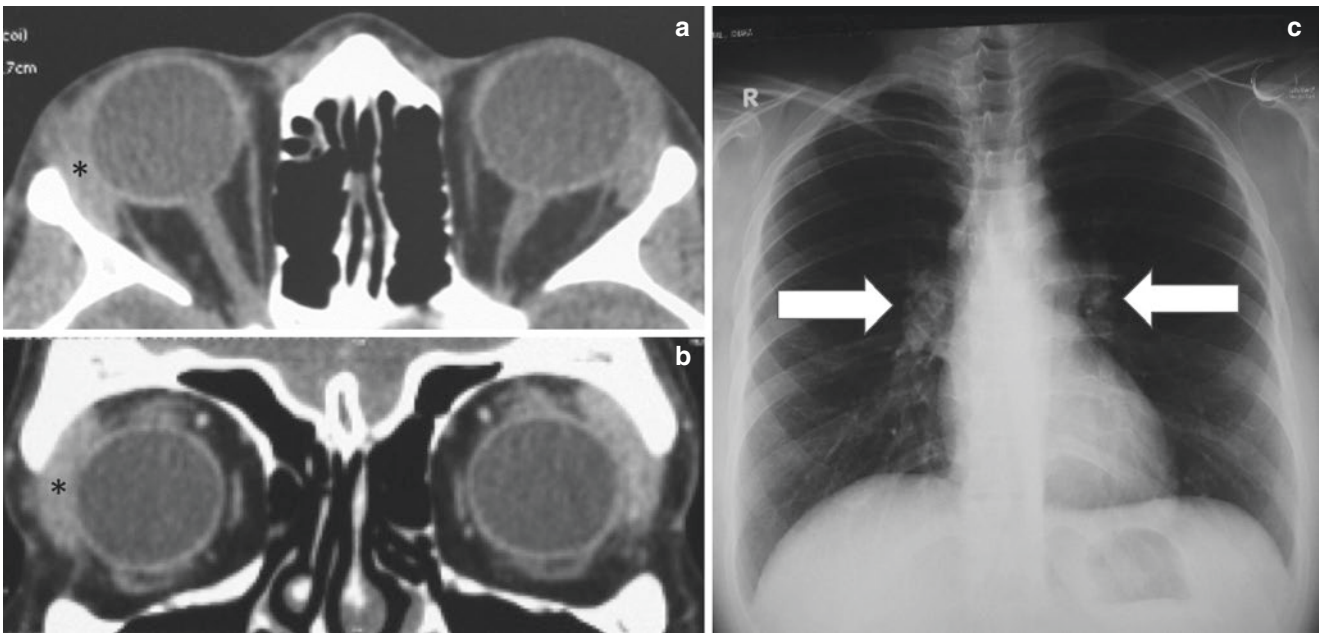

Fig. 12.2 (**a**, **b**) Axial and coronal CT scan of the orbits showing bilateral hyperdense, enhanced, bulky lacrimal glands (*) partly wrapped around the globe. (**c**) Frontal chest x-ray showing bilateral hilar lymphadenopathy (arrows)

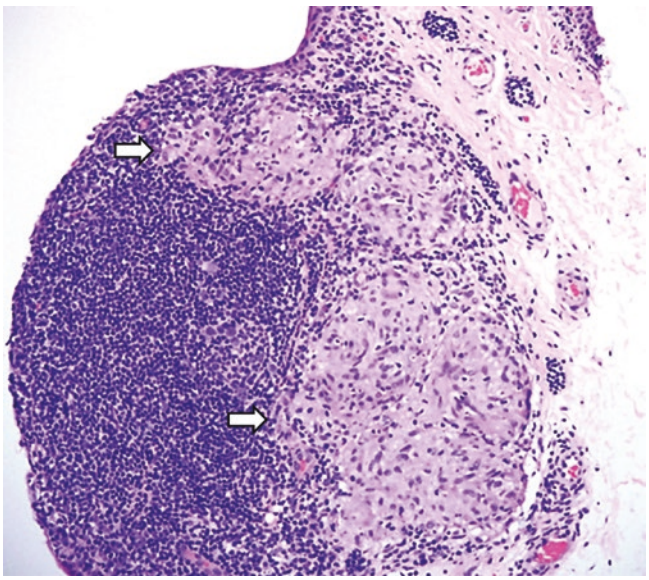

Fig. 12.3 There are tightly cohesive and well-defined granulomas within the subepithelial stroma (white arrows). Lymphoid aggregates are also seen to the left of the granulomas. HE stain; 200× magnification

Management

The patient was seen by the immunologist for systemic screening. Based on the histopathology, response to corticosteroids and chest x-ray findings, she was restarted on oral prednisolone with possible need for immunomodulatory agents as indicated at a later date.

Discussion

Ethnic predisposition for sarcoidosis includes those of African descent, South Asians and the Scandinavians, and it is relatively rare in the East Asian population. Systemic features include bilateral hilar lymphadenopathy with parenchymal changes, peripheral lymphadenopathy, evanescent erythema nodosa-like skin lesions, lacrimal and salivary gland involvement, and hepatosplenomegaly. In about 5% of patients, the optic nerve and intracranial involvement may also occur.

Apart from organ involvement detected on imaging, serological testing may demonstrate hypercalcemia, elevated alkaline phosphatase and more specifically elevated ACE levels. There may also be hypercalciuria.

Diagnosis is typically made on histopathology. When granulomatous inflammation is seen, it is important to exclude fungal and mycobacterial infections with GMS and ZN stains, respectively. This is especially so when there is accompanying necrosis.

Sarcoidosis is a diagnosis of exclusion and often gives rise to small, tightly formed granulomas without evidence of necrosis. Additional features suggestive of sarcoidosis include asteroid bodies and Schaumann bodies within multinucleated giant cells; however, these are not specific.

Principles of management include systemic evaluation, in collaboration with an immunologist, followed by either topical (for anterior uveitis) or systemic corticosteroids. Patients unresponsive to corticosteroids may require a reverification of diagnosis or other steroid-sparing immunological agents.

Learning Points

Sarcoidosis should be considered in the differential diagnosis of unilateral or bilateral lacrimal gland masses especially in those of Scandinavian, African and South Asian descent. Differential diagnosis should include other inflammatory disorders including IgG4 disorders and in the elderly, lymphoproliferative disorders. When skin or conjunctival lesions are absent, a low threshold for lacrimal gland biopsy should be present. Systemic workup and corticosteroid therapy remain the mainstay of treatment of these lesions.

Further Reading

1. Azari AA, Kanavi MR, Lucarelli M, Lee V, Lundin AM, Potter HD, Albert DM. Angiolymphoid hyperplasia with eosinophilia of the orbit and ocular adnexa: report of 5 cases. JAMA Ophthalmol. 2014;32(5):633–6. https://doi.org/10.1001/jamaophthalmol.2013.8243.
2. Espinoza GM, Desai A, Akduman L. Ocular vasculitis. Curr Rheumatol Rep. 2013;15(9):355. https://doi.org/10.1007/s11926-013-0355-x.
3. Lokdarshi G, Pushker N, Bajaj MS. Sclerosing lesions of the orbit: a review. Middle East Afr J Ophthalmol. 2015;22(4):447–51.
4. McNab AA. The 2017 Doyne Lecture: the orbit as a window to systemic disease. Eye (Lond). 2018;32(2):248–61. https://doi.org/10.1038/eye.2017.224. Epub 2017 Nov 10.
5. Pakalniskis MG, Berg AD, Policeni BA, Gentry LR, Sato Y, Moritani T, Smoker WR. The many faces of granulomatosis with polyangiitis: a review of the head and neck imaging manifestations. AJR Am J Roentgenol. 2015;205(6):W619–29. https://doi.org/10.2214/AJR.14.13864.
6. Prabhakaran VC, Saeed P, Esmaeli B, et al. Orbital and adnexal sarcoidosis. Arch Ophthalmol. 2007;125(12):1657–62.
7. Srinivasan A, Kleinberg TT, Murchison AP, Bilyk JR. Laboratory investigations for diagnosis of autoimmune and inflammatory periocular disease: part II. Ophthal Plast Reconstr Surg. 2017;33(1):1–8.
8. Srinivasan A, Kleinberg TT, Murchison AP, Bilyk JR. Laboratory investigations for diagnosis of autoimmune and inflammatory periocular disease: part I. Ophthal Plast Reconstr Surg. 2016;32(5):321–8.

Langerhans Cell Histiocytosis

13

Shantha Amrith, Stephanie Ming Young, Eric Ting, Bingcheng Wu, Min En Nga, and Gangadhara Sundar

Introduction

Langerhans cell histiocytosis (LCH) is one of the three major groups of histiocytic disorders (Fig. 13.1). The most frequent type among the histiocytic lesions in the orbit is LCH, and among those, eosinophilic granuloma is the most frequent, accounting for 70% of cases. Eosinophilic granuloma is a poorly understood disease, and the opinion varies between a neoplasia and reactive inflammation. Orbital disease can be unifocal or part of a multifocal bone disease. It runs a benign course compared to the multisystem disease, known as Hand-Schüller-Christian disease (HSC) which is of intermediate severity. Litterer-Siwe disease is an acute fulminant form with multisystem involvement and associated with a grave prognosis.

S. Amrith (✉) · S. M. Young · G. Sundar
Department of Ophthalmology, National University Hospital, Singapore

Department of Ophthalmology, Yong Loo Lin School of Medicine, National University of Singapore, Singapore
e-mail: shantha_amrith@nuhs.edu.sg; gangadhara_sundar@nuhs.edu.sg

E. Ting
Department of Diagnostic Imaging, National University Hospital, Singapore

Department of Diagnostic Imaging, Yong Loo Lin School of Medicine, National University of Singapore, Singapore

Advanced Medicine Imaging, Singapore

B. Wu
Department of Pathology, National University Hospital, Singapore

M. E. Nga
Department of Pathology, National University Hospital, Singapore

Department of Pathology, Yong Loo Lin School of Medicine, National University of Singapore, Singapore

Case Scenario

A 3-year-old Indonesian female child presented with a history of prominent right eye for about 3–4 months. On examination of the right eye, there was mild erythema in the upper lid and proptosis with downward displacement (Fig. 13.2). The ocular motility appeared to be restricted on upgaze. The anterior and posterior segments of both eyes were normal, and orthoptic examination revealed normal visual acuities.

The child underwent MRI of the orbits.

CLOSE summary is given in Table 13.1.

Differential Diagnosis

- Specific and non-specific orbital inflammation
- Ruptured dermoid cyst
- Rhabdomyosarcoma
- Metastatic disease such as neuroblastoma
- Myelosarcoma (chloroma)
- Langerhans cell histiocytosis
- Lymphoproliferative disorder such as lymphoma

Imaging

MRI with contrast showed a hyperintense extraconal mass in the right superotemporal orbit, replacing right frontal bone, greater wing of sphenoid, and extending along the superior lateral right orbital margin (Fig. 13.3). The mass displaced the globe and extraocular muscles inferiorly and was enhancing with contrast. A resultant proptosis was noted. Abnormal marrow signal and enhancement of the lateral wall, roof, and floor of the left orbit and left maxilla were seen. However, there was no mass effect seen on the left orbital contents.

Typical punched-out lytic skull lesions were seen on plain X-ray (Fig. 13.4) with corresponding extensive foci of calvarial bone replacement by soft tissue masses on MRI showing T2 hyperintensity and contrast enhancement (Fig. 13.4).

S. Amrith et al. (eds.), *Ocular Adnexal Lesions*, https://doi.org/10.1007/978-981-13-3798-7_13

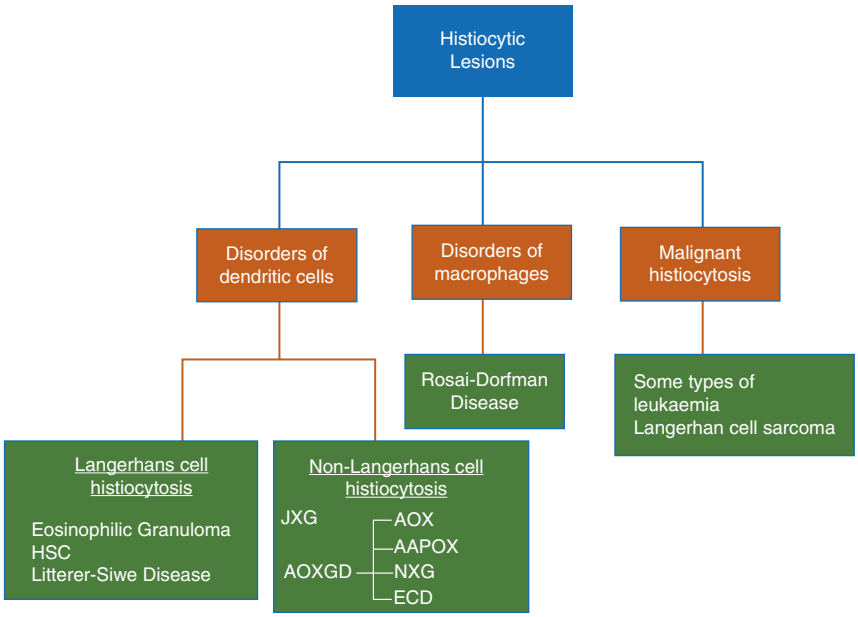

HSC-Hand–Schüller–Christian disease, JXG-Juvenile Xanthogranuloma, AOXD-Adult-onset Xanthogranulomatous disease, AOX-Adult-onset Xanthogranuloma, Adult-onset Asthma with Periocular Xanthogranuloma, NXG-Necrobiotic Xanthogranuloma, ECD-Erdheim-Chester Disease

Fig. 13.1 Classification of histiocytic lesions

Fig. 13.2 Clinical picture showing a right proptosis and downward displacement

Table 13.1 CLOSE summary

*C*linical scenario: mass lesion
*L*ocation: right orbit
*O*nset: subacute
*S*igns and symptoms: proptosis of the right eye
*E*pidemiology: 3-year-old Indonesian female child

Intervention

A biopsy of the orbital mass did not yield useful information (mild chronic inflammation); hence a biopsy of the left temporal bone mass was performed.

Histopathology

Section showed a soft tissue mass composed of numerous Langerhans cells with eosinophilic to clear cytoplasm with reniform nuclei. There was an accompanying mixed inflammatory cellular infiltrate composed predominantly of eosinophils, as well as scattered neutrophils and lymphocytes (Fig. 13.5). The Langerhans cells were positive for S100 and CD1a on immunohistochemistry (Fig. 13.5 inset). The features were those of Langerhans cell histiocytosis.

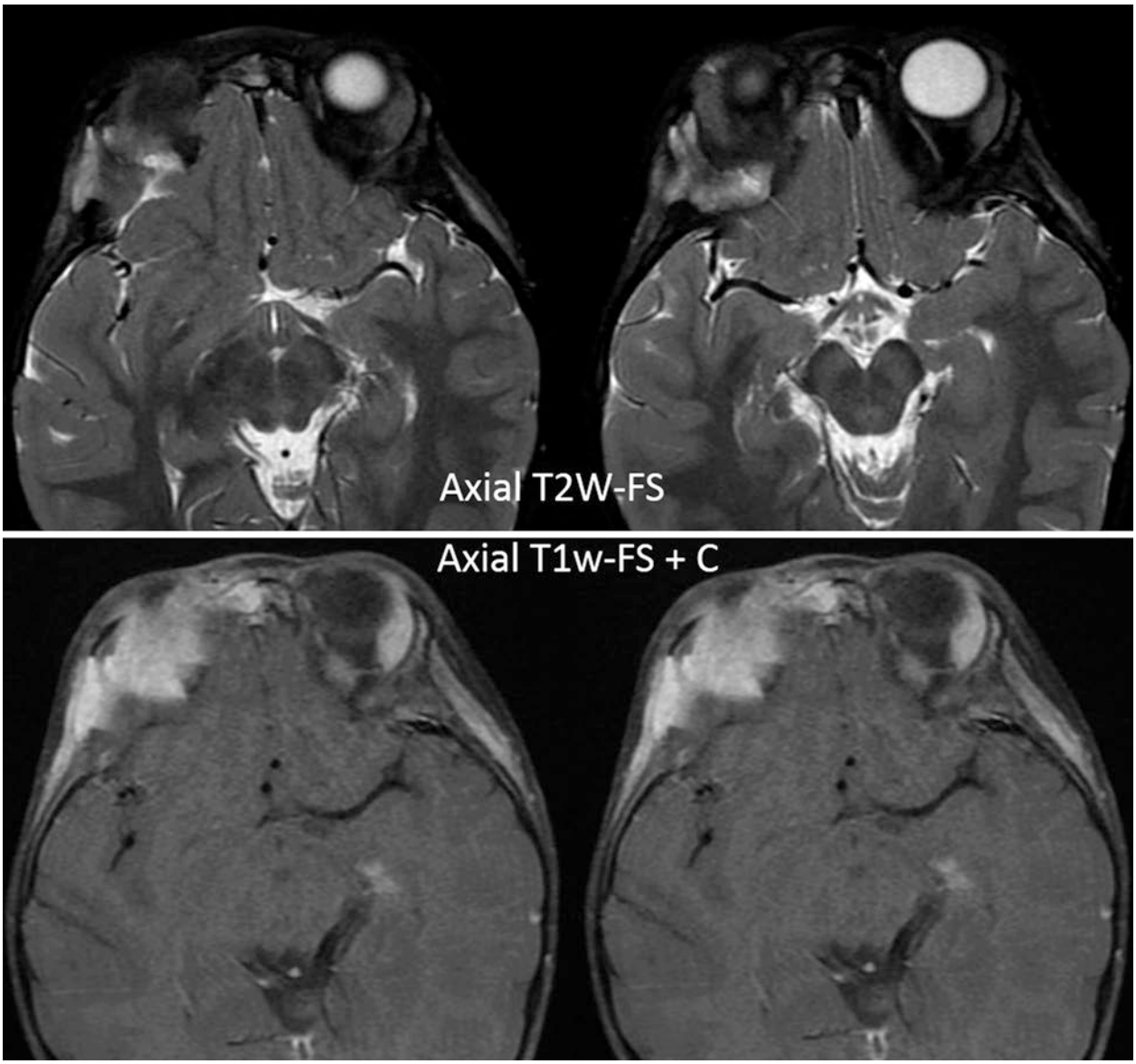

Fig. 13.3 T2w and T1w + C sequences showing a mass centred on the right greater wing of sphenoid with involvement of the orbital walls

Fig. 13.4 Lateral skull radiograph showing punched-out lytic lesions without sclerotic rim (white arrows). Axial T1w + contrast MRI sequence shows the corresponding enhancing skull lesions (white arrows)

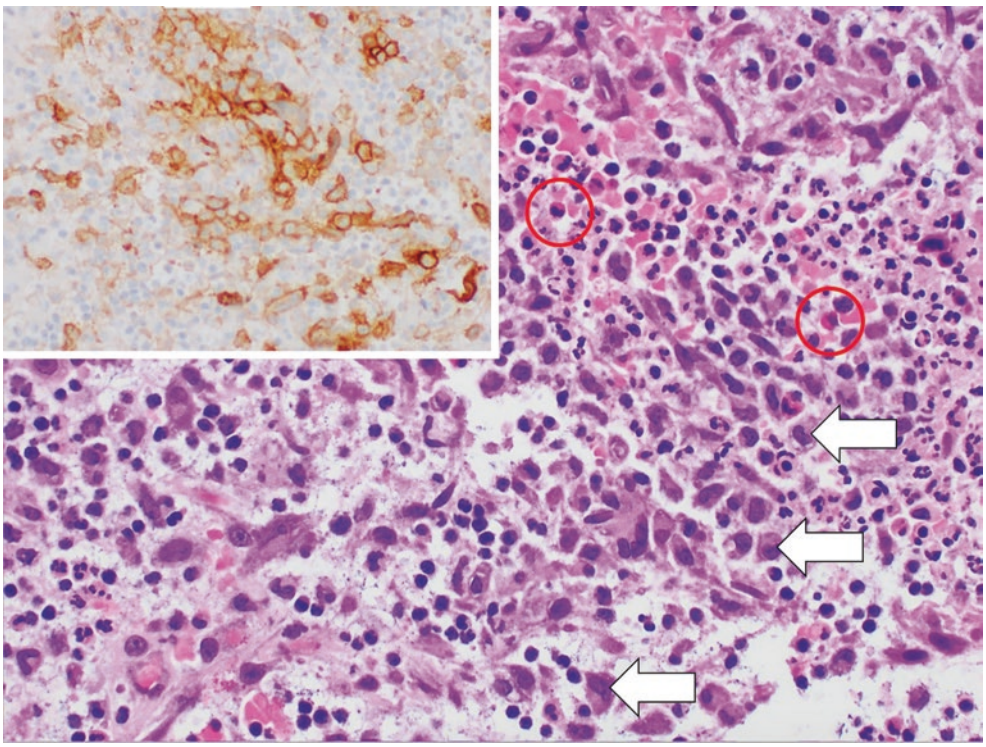

Fig. 13.5 There are numerous Langerhans cells with eosinophilic to clear cytoplasm and reniform nuclei (white arrows). There is an accompanying mixed inflammatory cellular infiltrate composed predominantly of eosinophils (red circles). The Langerhans cells are positive for CD1a on immunohistochemistry. Main: HE stain; 200× magnification. Inset: immunohistochemistry (CD1a antibody); 200× magnification

Other Investigations

The ultrasound of the abdomen did not reveal any hepatosplenomegaly. The urine osmolarity was normal. The child was assessed by the endocrinologist, and there was no evidence of diabetes insipidus.

The bone scan revealed a few photopaenic defects noted at the calvarium, largest at the occipital region. There was no other distinct abnormal decreased or increased osteoblastic activity detected in rest of the axial or appendicular skeleton.

Management

A multifocal Langerhans cell histiocytosis was made by the paediatric oncologists, and the patient was given six cycles of vinblastine and prednisolone.

Discussion

LCH is a clonal proliferation of pathologic Langerhans cells. This, in association with chromosomal instability, such as BRAF mutation indicates the possibility of this being a neoplasm. However, presence of inflammatory cytokines that recruit eosinophils and T lymphocytes may point towards a reactive inflammatory process.

LCH affects children aged 1–4, and affects males more commonly than females. LCH of the orbit presents usually as an isolated unifocal bone involvement associated with a soft tissue mass. It affects predominantly the superior and superolateral orbit. Clinical presentation may be in the form of eyelid swelling, erythema, proptosis, and ptosis. Sometimes, the orbital involvement may be part of mutifocal bone disease as in the case above. When more than two organ systems such as bone and skin or lymph nodes are involved, it is called Hand-Schüller-Christian (HSC) disease.

Plain X-ray shows a typical "punched-out" lytic lesion in the bone. CT and MRI show osteolytic lesions accompanied by soft tissue involvement. In addition to the imaging, a referral to paediatric oncology service for a complete workup to rule out multisystem involvement is necessary.

Histologically, there is clonal proliferation of Langerhans cells. They appear more like macrophages than the dendritic cells of the skin. In addition there are osteoclast-like giant cells, infiltration with lymphocytes, plasma cells, polymorphonuclear leucocytes, and eosinophils (not mandatory). There is immunopositivity for S-100 and CD1a and CD 207. The electron microscope reveals Birbeck granules.

Treatment of unifocal disease is in the form of surgery (biopsy and curettage) along with intralesional steroids. Radiotherapy can be considered in selective cases. Some recommend chemotherapy with vinblastine, prednisone, etoposide, and methotrexate in various combinations for 6 months to prevent a CNS involvement. Chemotherapy should also be used in multifocal bone disease, multisystem disease or

orbital disease with dural involvement. Bone marrow transplantation and immunoglobulin therapy are reserved for uncontrolled recurrent disease.

Further Reading

1. Esmaili N, Harris GJ. Langerhans cell histiocytosis of the orbit: spectrum of disease and risk of central nervous system sequelae in unifocal cases. Ophthal Plast Reconstr Surg. 2016;32:28–34.
2. Gündüz K, Temel E. Histiocytic lesions of the orbit: a study of 9 cases. Saudi J Ophthalmol. 2018;32:40–4.
3. Harris GJ. Langerhans cell histiocytosis of the orbit: a need for interdisciplinary dialogue. Am J Ophthalmol. 2006;141:374–8. 5. Woo KI, Harris KJ.
4. Herwig MC, Wojno T, Zhang Q, Grossniklaus HE. Langerhans cell histiocytosis of the orbit: five clinicopathologic cases and review of the literature. Surv Ophthalmol. 2013;58:330–40. 17
5. Rootman J. Diseases of the orbit, a multidisciplinary approach. 2nd ed. Philadelphia: Wolters Kluwer Lippincott Williams & Wilkins; 2003.

Xanthogranuloma

14

Shantha Amrith, Stephanie Ming Young, Poh Sun Goh, Bingcheng Wu, Min En Nga, and Gangadhara Sundar

Introduction

Adult xanthogranulomatous disease (AOXGD) involving the ocular adnexal tissues is rare and constitutes a group of entities with varying manifestations. These are non-Langerhans cell histiocytic disorders that are diagnosed histopathologically by the presence of foamy histiocytes, Touton giant cells, varying degrees of fibrosis, and necrosis in some entities. Refer to Fig. 13.1 in Chap. 13 for the classification of histiocytic lesions.

Four forms of the disease have been described:

1. Adult-onset xanthogranuloma (AOX) is an isolated condition without systemic involvement.
2. Adult-onset asthma with periocular xanthogranuloma (AAPOX).
3. Necrobiotic xanthogranuloma (NBX) associated with paraproteinemia or multiple myeloma.
4. Erdheim-Chester disease (ECD), the most devastating and fatal form of the disease.

Adult xanthogranulomatous disease, in general, is poorly understood.

Case Scenario

A 31-year-old Chinese male presented with a painful left upper eyelid mass that was gradually increasing in size over several weeks. He was healthy with no known systemic disease, specifically atopy or asthma.

On examination, a left medial canthal lump above the medial canthal tendon was seen with extension to one third of the upper lid. There was some erythema over it, but no punctum or discharge was noted (Fig. 14.1). It was firm to

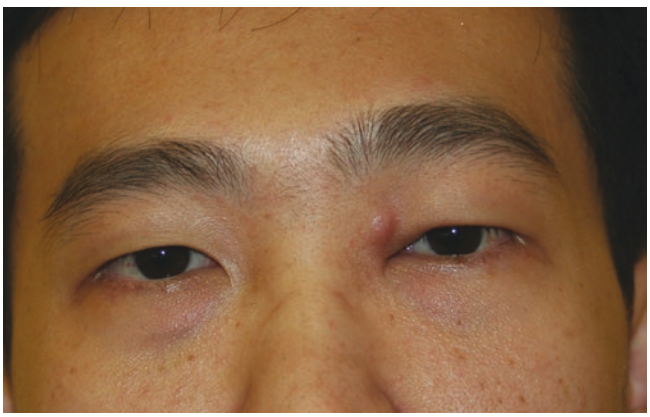

Fig. 14.1 Clinical picture of the patient showing the lump in the upper medial part of the left eyelid. Note the erythema over the lump

S. Amrith (✉) · S. M. Young · G. Sundar
Department of Ophthalmology, National University Hospital, Singapore

Department of Ophthalmology, Yong Loo Lin School of Medicine, National University of Singapore, Singapore
e-mail: shantha_amrith@nuhs.edu.sg; gangadhara_sundar@nuhs.edu.sg

P. S. Goh
Department of Diagnostic Imaging, National University Hospital, Singapore

Department of Diagnostic Imaging, Yong Loo Lin School of Medicine, National University of Singapore, Singapore

B. Wu
Department of Pathology, National University Hospital, Singapore

M. E. Nga
Department of Pathology, National University Hospital, Singapore

Department of Pathology, Yong Loo Lin School of Medicine, National University of Singapore, Singapore

S. Amrith et al. (eds.), *Ocular Adnexal Lesions*, https://doi.org/10.1007/978-981-13-3798-7_14

palpation with smooth margins with no induration around. The rest of the eye examination was normal.

CLOSE summary is in Table 14.1.

Differential Diagnosis

- Infected epidermal cyst and leaking dermoid cyst
- Left frontal mucocoele
- Orbital inflammatory disease
- Neoplasm: local vs. metastasis, e.g., lymphoma

Radiology

CT orbits showed a soft tissue lesion adjacent to the left medial canthus (Fig. 14.2) measuring 1.2 × 1.4 cm. The lesion was seen to erode through the bone into the ethmoid sinus. A rim-enhancing collection was noted. There was some extension into the anterior medial orbit, with no involvement of extraocular muscles.

Intervention

An excision biopsy was performed with clean dissection plane all around. The tissue was subjected to histopathology.

Histopathology

There were sheets of foamy macrophages and histiocytes admixed with chronic inflammatory cellular infiltrate such as lymphocytes and plasma cells (Fig. 14.3). Occasional multinucleated giant cells were also seen. Special stains for microorganisms such as Ziehl-Neelsen (ZN) and Gomori methenamine silver (GMS) stains were negative. The features were consistent with xanthogranuloma.

Table 14.1 CLOSE summary

*C*linical process**:** mass lesion
*L*ocation**:** inner third of left upper eyelid
*O*nset**:** subacute
*S*igns and symptoms**:** pain and erythema with fever at the onset
*E*pidemiology**:** 31-year-old Chinese male

Management

More laboratory tests showed normal full blood count and renal functions. ESR was slightly raised. ANA was negative, and serum protein electrophoresis did not reveal any abnormal bands. The flow cytometry was negative for lymphoproliferative disease. The patient was given a course of antibiotics and steroid nasal spray.

Discussion

Adult-onset xanthogranuloma (AOX) is an isolated xanthogranulomatous lesion without systemic involvement. It is the rarest of the xanthogranulomatous lesions. The age of incidence is 17–85 with no gender predilection. It is often self-limiting and no aggressive treatment is required.

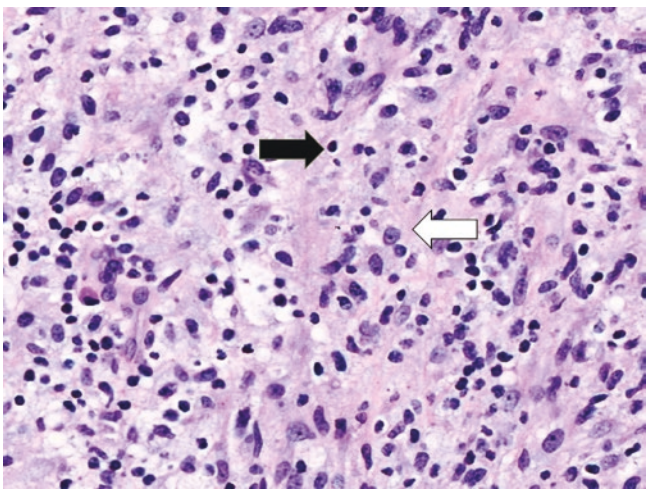

Fig. 14.3 There is an inflammatory cellular infiltrate composed of sheets of foamy histiocytes (white arrow) admixed with lymphocytes (black arrow). HE stain; 400× magnification

Fig. 14.2 Coronal and axial contrast-enhanced CT scan showing a left medial canthal preseptal mass eroding through anterior lamina papyracea (arrow). (*) shows retained sinus secretion in frontal and ethmoidal sinuses

Adult-onset asthma with periocular xanthogranuloma (AAPOX) presents with bilateral elevated xanthomatous, indurated, and non-ulcerated eyelid lesions with extension to anterior orbital fat. Occasionally, it can involve the extraocular muscles and/or the lacrimal gland. The patients have adult-onset asthma within a few months to a few years after the onset of eyelid lesions. They may also have lymphadenopathy, raised IgG levels, and paraproteinaemia. There is some evidence that this might be a variant of IgG4-related disease; however more studies are needed to confirm it.

Necrobiotic xanthogranuloma (NBX) is the most common of all the xanthogranulomatous lesions. It is characterized by the presence of subcutaneous lesions in the eyelids and anterior orbit. The subcutaneous lesions often ulcerate and fibrose. Systemically, the patients are noted to have paraproteinaemia and multiple myeloma. Histologically, it is characterized by the presence of necrosis.

Erdheim-Chester disease (ECD) is the most devastating disease, characterized by dense, progressive, recalcitrant fibrosclerosis of the orbit, mediastinum, pericardium, pleural, perinephric, and retroperitoneal spaces. In the orbit, the infiltration is fairly extensive leading to blindness. Long bones' involvement is common, and the disease is fatal despite aggressive treatment.

Other histiocytic and related lesions that need to be distinguished are Langerhans cell histiocytosis, Rosai-Dorfman disease, myofibroblastic tumour, malignant fibrous histiocytoma, multiple myeloma, and lymphoma.

Histologically, in the context of xanthogranulomatous inflammation, it is important to look for fungal and acid-fast bacilli infections with the GMS and ZN stains, respectively.

Treatment is usually empirical as the mechanisms in xanthogranulomatous disorders are poorly understood, and there is no information on the genetic basis of the disease. Immunosuppression in the form of corticosteroids is the mainstay of treatment. For a limited disease, surgical debulking with intralesional corticosteroids can be considered. For systemic disease, apart from corticosteroids, chemotherapy may be necessary. Radiotherapy has been administered in recurrent cases, but it is considered empirical.

Learning Points

- Adult orbital xanthogranulomatous disease (AOXGD) is an extremely rare group of conditions causing persistent orbital swelling and lid discomfort.
- Treatment of AOXGD is challenging with no general consensus, and prognosis of certain subtypes is poor.
- Our understanding of AOXGD will be advanced by comprehensive assessment for systemic manifestations and histopathological study of tissue specimens.
- Long-term follow-up is necessary to pick up systemic disease manifestation early.

Further Reading

1. Hammond MD, Niemi EW, Ward TP, et al. Adult orbital xanthogranuloma with associated adult-onset asthma. Ophthal Plast Reconstr Surg. 2004;20:329–32.
2. Karcioglu ZA, Sharara N, Boles TL, et al. Orbital xanthogranuloma clinical and morphologic features in eight patients. Ophthalmic Plast Reconstr Surg. 2003;19:373–81.
3. Miszkiel KA, Sohaib SAA, Rose GE, et al. Radiological and clinicopathological features of orbital xanthogranuloma. Br J Ophthalmol. 2000;84:251–8.
4. Netland P, Font RL, Jacobiec FA. Orbital histiocytic disorders. In: Albert DM, Jacobiec FA, editors. Principles and practice of ophthalmology. Philadelphia: WB Saunders; 1996. (CD Rom) Chapter 179.
5. Rootman J. Diseases of the orbit, a multidisciplinary approach. 2nd ed. Philadelphia: Wolters Kluwer Lippincott Williams & Wilkins; 2003.
6. Sivak-Callcott JA, Rootman J, Rasmussen SL, Nugent RA, White VA, Paridaens D, Currie Z, Rose G, Clark B, McNab AA, Buffam FV, Neigel JM, Kazim M. Adult xanthogranulomatous disease of the orbit and ocular adnexa: new immunohistochemical findings and clinical review. Br J Ophthalmol. 2006;90(5):602–8.

Kimura Disease

15

Shantha Amrith, Stephanie Ming Young, Poh Sun Goh, Bingcheng Wu, Min En Nga, and Gangadhara Sundar

Introduction

Kimura disease (KD) is a rare chronic inflammatory disorder of unknown aetiology that is characterized by subcutaneous nodules, predominantly involving the head and neck region of male patients of oriental origin, the common sites being subcutaneous tissue, parotid glands, and submandibular glands. Isolated lesion in the eyelid or orbit is uncommon.

Clinical Scenarios

Case 1

A 50-year-old Indian male presented with a 2-month history of a slow-growing, painless lump in the left upper eyelid. Clinical examination revealed a firm subcutaneous lesion in the left upper lid beneath the eyebrow, with slight erythema of the overlying skin (Fig. 15.1). The lesion was not fixed to underlying structures, and there was no punctum or obvious posterior extension. The patient had Snellen visual acuity of 6/6 on the affected side and a full range of ocular movements. The rest of the eye examination was normal. On systemic examination, no enlargement of the regional lymph nodes was noted.

CLOSE summary is shown in Table 15.1.

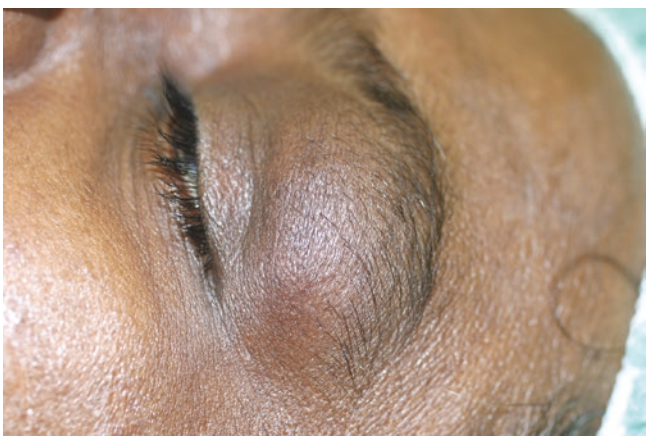

Fig. 15.1 Case 1: Clinical picture showing left upper lid subcutaneous lesion. There is mild erythema but no punctum

Table 15.1 CLOSE summary cases 1 and 2

*C*linical process: mass lesion
*L*ocation: upper eyelid
*O*nset: subacute/acute on chronic
*S*ymptoms and signs: slowly enlarging painless non-tender mass
*E*pidemiology: middle-aged Indian and Chinese males

S. Amrith (✉) · S. M. Young · G. Sundar
Department of Ophthalmology, National University Hospital, Singapore

Department of Ophthalmology, Yong Loo Lin School of Medicine, National University of Singapore, Singapore
e-mail: shantha_amrith@nuhs.edu.sg; gangadhara_sundar@nuhs.edu.sg

P. S. Goh
Department of Diagnostic Imaging, National University Hospital, Singapore

Department of Diagnostic Imaging, Yong Loo Lin School of Medicine, National University of Singapore, Singapore

B. Wu
Department of Pathology, National University Hospital, Singapore

M. E. Nga
Department of Pathology, National University Hospital, Singapore

Department of Pathology, Yong Loo Lin School of Medicine, National University of Singapore, Singapore

S. Amrith et al. (eds.), *Ocular Adnexal Lesions*, https://doi.org/10.1007/978-981-13-3798-7_15

Case 2

A 60-year-old Chinese male, diagnosed 15 years previously as Kimura disease of the parotid and submandibular glands, presented with right upper lid swelling of 2 years' duration with a sudden increase in size after an upper respiratory tract infection. Clinical examination revealed a 4 × 2.5 cm mobile, non-tender firm mass in the right upper lid, with ptosis obscuring the visual axis (Fig. 15.2a). There was also a left parotid swelling (Fig. 15.2b).

CLOSE summary is shown in Table 15.1.

Differential Diagnosis

- Sebaceous cyst
- Lymphoproliferative lesion
- Specific or non-specific inflammatory mass
- Nodular squamous cell carcinoma
- Sebaceous gland carcinoma

Radiology

CT scans were available for case 2. A diffuse radiodense lesion was seen in the upper lid, with infiltration to the surrounding eyelid tissue (Fig. 15.3a, b). Orbit itself was normal. There were similar lesions found in the left parotid and submandibular glands (Fig. 15.3c, d).

Investigations

Full blood count showed eosinophilia in both cases with normal renal functions.

Excisional biopsy was carried out in both cases. The lesions were noted to be infiltrating the orbicularis and subcutaneous tissue. They had no real capsule and no definite excisional plane. The lesions were sent for histopathological assessment.

Histopathology

Cases 1 and 2: Microscopic examination with haematoxylin and eosin staining showed fibroadipose tissue with lymphoid infiltrate and lymphoid follicular hyperplasia, a large number of interfollicular eosinophils, and a proliferation of thin-walled blood vessels (Fig. 15.4). The follicular centres showed infiltration by eosinophils as well as deposition of hyaline material. Some focal eosinophilic microabscesses were seen. The features were those of Kimura disease. Special stains for fungi and mycobacterium were not carried out due to the absence of granulomatous reaction and necrosis.

Histological features of previous biopsies on parotid, submandibular gland, and jaw in case 2 were similar to the eyelid lesion.

Discussion

Kimura disease (KD) has been predominantly described in young oriental males in China and Japan. Presentation is of a single or multiple firm, painless subcutaneous nodule(s) in the head and neck region. The disease was first described by Kimura et al. in 1948 as an unusual granulation combined with hyperplastic changes of lymphatic tissue. In 1969, Wells and Whimster introduced the term subcutaneous angiolymphoid hyperplasia with eosinophilia (ALHE).

Although KD and ALHE were once considered variants of the same disease, more recent studies have shown them to be histopathologically distinct, with a predisposition for different age groups, gender, and race.

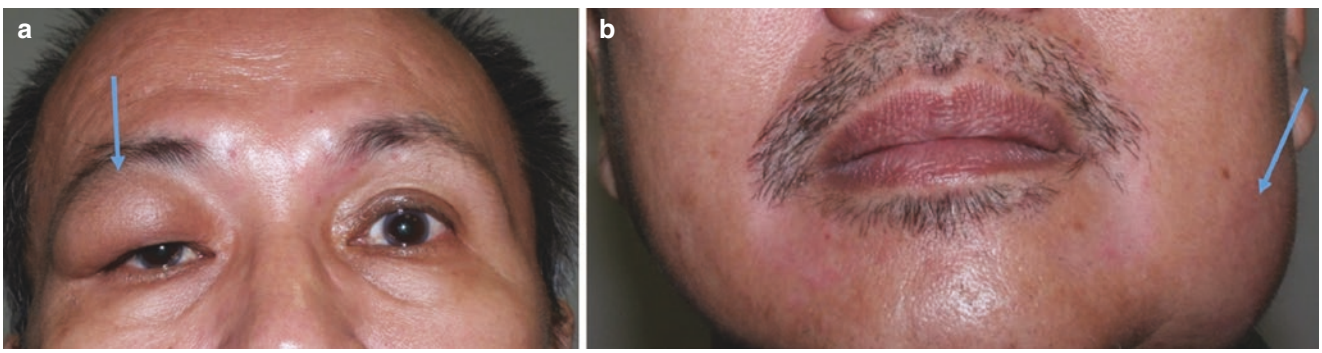

Fig. 15.2 Case 2: (**a**) Clinical picture showing right upper lid swelling (arrow) with ptosis as well as (**b**) the left parotid swelling (arrow)

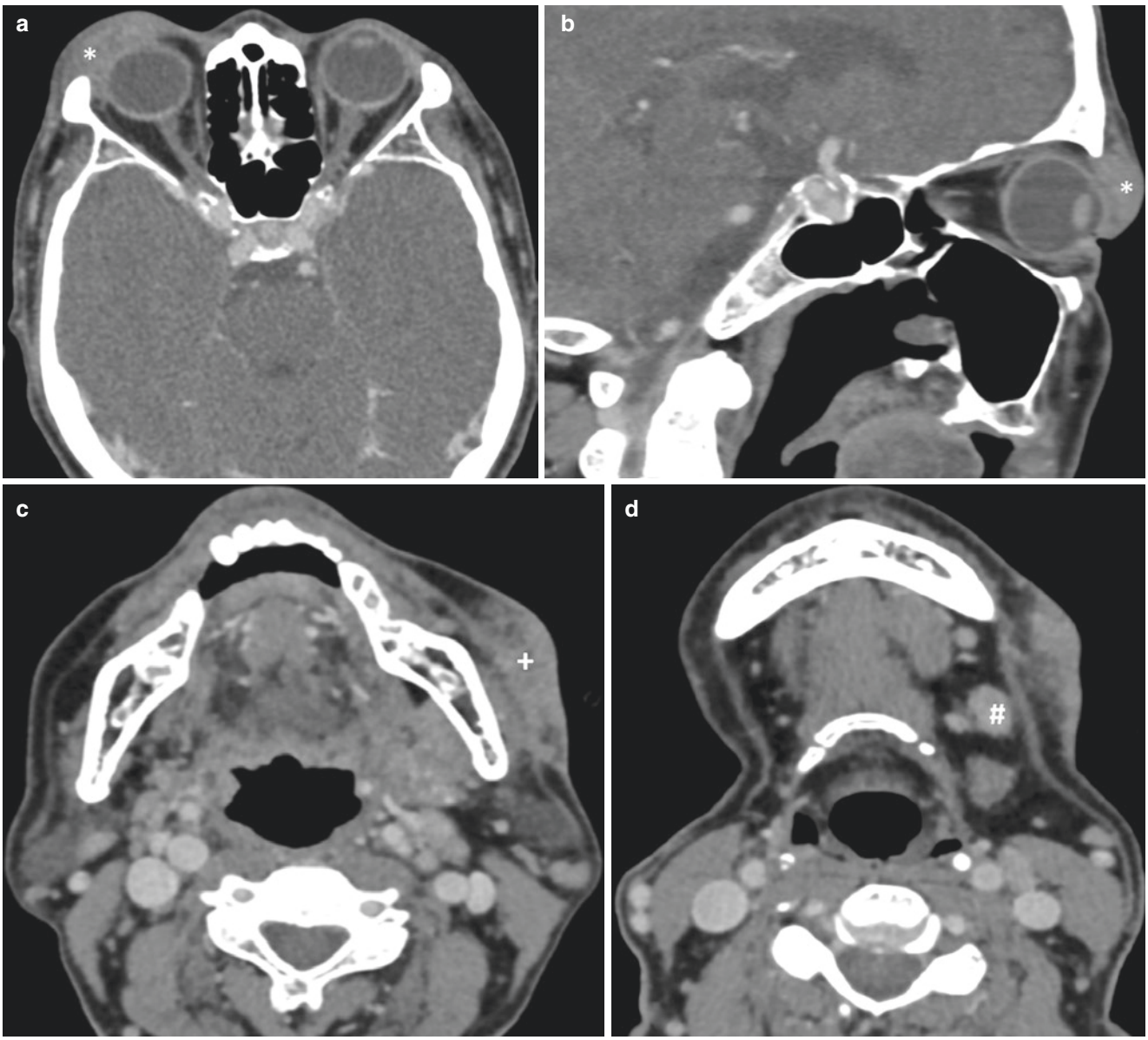

Fig. 15.3 Case 2: (**a**, **b**) CT-axial and sagittal scans showing the preseptal mass in the right upper lid (*). (**c**) Axial CT scan showing left parotid mass (+). (**d**) Axial CT scan showing left enlarged submandibular gland (#)

KD is reported in adolescent Oriental males. It occurs in both superficial and deep tissues and is commonly associated with regional lymphadenopathy. On the contrary, ALHE is more common in middle-aged white females and tends to be situated in the subcutis and dermis, with rare lymph node involvement. On peripheral blood film, eosinophilia is more commonly seen in KD as compared to ALHE. IgE levels have also been described to be elevated in KD but not ALHE. These findings suggest an allergic or autoimmune aetiology for KD. Although KD is usually localized, it has been shown to be associated with renal disease. Histologically, the main difference between KD and ALHE is the presence of vascular proliferation with plump epithelioid endothelial cells in ALHE.

KD is usually associated with male teenagers, but it has been reported in different ages (7–59 years). KD affecting the orbit and ocular adnexa is relatively rare, and the most common location of ophthalmic lesions is the orbit, followed by combined eyelid and orbit, and finally eyelid alone. Eyelid lesions have been described in Afro-Caribbean, Caucasian, in addition to East Asian patients.

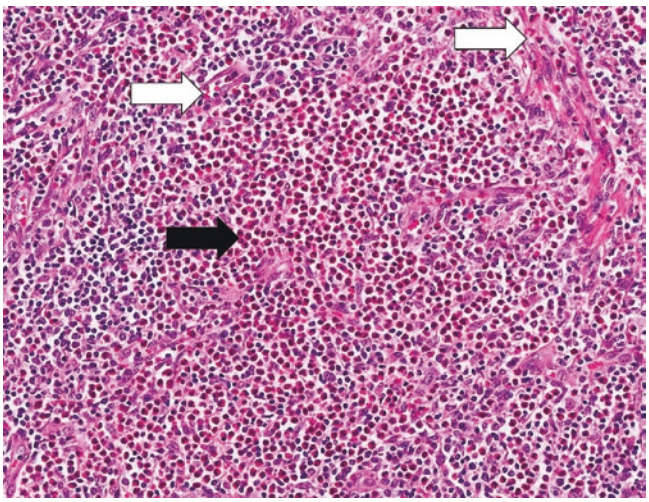

Fig. 15.4 The interfollicular areas show a large number of eosinophils (black arrow) and a proliferation of thin-walled blood vessels (white arrows). HE stain; 100× magnification

The treatment of choice for periorbital KD is surgical excision. Other techniques including oral steroids and intralesional steroid injections have been described. KD is shown to have relatively high relapse rates.

Learning Points

Despite its rarity, it is important to understand that KD can affect people of different races and age groups, and it should be included in the differential diagnosis of an eyelid growth. When Kimura disease is diagnosed, referral to the nephrologist is required to exclude any renal disease.

Further Reading

1. Buggage RR, Spraul CW, Wojno TH, Grossniklaus HE. Kimura disease of the orbit and ocular adnexa. Surv Ophthalmol. 1999;44:79–91.
2. Kanazawa S, Gong H, Kitaoka T, Amemiya T. Eosinophilic granuloma (Kimura's disease) of the orbit: a case report. Graefes Arch Clin Exp Ophthalmol. 1999;237:518–21.
3. Kennedy SM, Pitts JF, Lee WR, Gibbons DC. Bilateral Kimura's disease of the eyelids. Br J Ophthalmol. 1992;76:755–7.
4. Kimura T, Yoshimura S, Ishikawa E. Unusual granulation combined with hyperplastic change of lymphatic tissue. Trans Soc Pathol Jpn. 1948;37:179–80.
5. Prabhakaran VC, Sachdev A, Cheung D, Fletcher A, Brown LJ, Sampath R. Kimura disease of the eyelid: a clinicopathologic study with electron microscopic observations. Ophthal Plast Reconstr Surg. 2006;22:495–8.
6. Wells GC, Whimster IW. Subcutaneous angiolymphoid hyperplasia with eosinophilia. Br J Dermatol. 1969;81:1–14.

Non-specific Orbital Inflammatory Disease

16

Stephanie Ming Young, Shantha Amrith, Poh Sun Goh, Bingcheng Wu, Min En Nga, and Gangadhara Sundar

Introduction

The term orbital pseudotumour was first coined in 1905 to describe an idiopathic condition that produced a mass effect and inflammatory features in the orbit, after exclusion of infection and malignancy. It is now increasingly replaced by the terms "orbital inflammatory disease" (OID) or "idiopathic orbital inflammation", as its wide spectrum of clinical presentation is increasingly recognized.

Orbital inflammatory disease accounts for approximately 5–10% of orbital disorders and can be divided into specific and non-specific orbital inflammations. Specific orbital inflammatory disorders include idiopathic sclerosing inflammation, granulomatous disorders, transitional lesions (e.g. Sjogren's syndrome, Kimura disease), vasculitic disorders (e.g. granulomatosis with polyangiitis [Wegener's granulomatosis]), and others. Non-specific inflammatory cases can be classified according to their location in the orbit: anterior, diffuse, apical, myositic, and lacrimal.

Clinical Scenario

A 32-year-old Malay female presented with left eye redness of 6 months' duration, associated with headache, as well as left progressive proptosis of 2 months' duration.

On examination, she had left conjunctival injection and left proptosis of 4 mm (Fig. 16.1). Dilated fundal exam revealed a hyperaemic disc with dilated and tortuous vessels.

CLOSE summary is given in Table 16.1.

S. M. Young · S. Amrith (✉) · G. Sundar
Department of Ophthalmology, National University Hospital, Singapore

Department of Ophthalmology, Yong Loo Lin School of Medicine, National University of Singapore, Singapore
e-mail: shantha_amrith@nuhs.edu.sg; gangadhara_sundar@nuhs.edu.sg

P. S. Goh
Department of Diagnostic Imaging, National University Hospital, Singapore

Department of Diagnostic Imaging, Yong Loo Lin School of Medicine, National University of Singapore, Singapore

B. Wu
Department of Pathology, National University Hospital, Singapore

M. E. Nga
Department of Pathology, National University Hospital, Singapore

Department of Pathology, Yong Loo Lin School of Medicine, National University of Singapore, Singapore

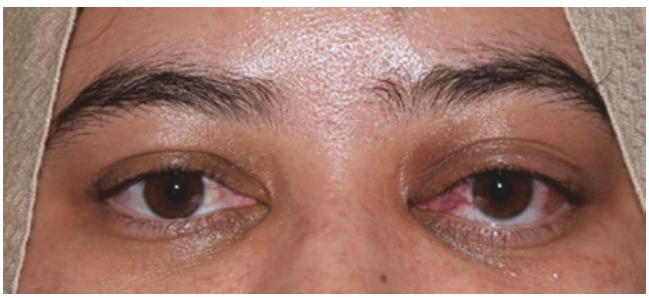

Fig. 16.1 Left conjunctival injection and left proptosis

Table 16.1 CLOSE summary

*C*linical process: infiltrative, mass lesion
*L*ocation: left orbit possibly intra/extraconal
*O*nset: chronic (months)
*S*igns and symptoms: proptosis, conjunctival injection
*E*pidemiology: 32-year-old Malay female

S. Amrith et al. (eds.), *Ocular Adnexal Lesions*, https://doi.org/10.1007/978-981-13-3798-7_16

Differential Diagnosis

- Orbital inflammation
  - Specific, e.g. sclerosing, vasculitis, granulomatous
  - Non-specific, e.g. myositis
- Solitary fibrous tumour
- Vascular malformation (cavernous haemangioma) and other orbital vascular tumours
- Metastatic lesion

Imaging

MRI sequences showed an extensive, poorly defined, contrast-enhancing, infiltrative soft tissue lesion in the inferomedial left orbit, with resultant left proptosis and lateral globe displacement (Fig. 16.2).

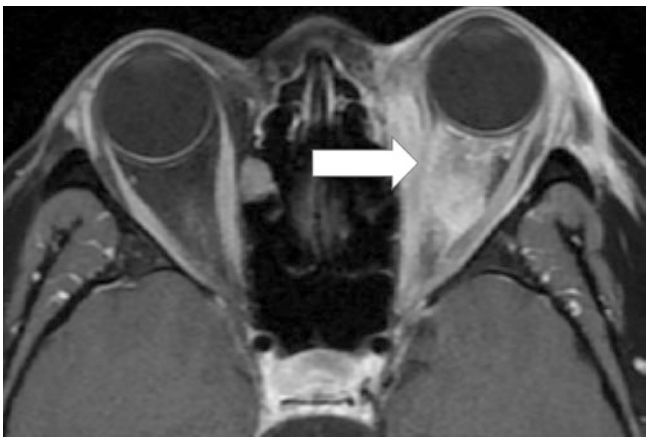

Fig. 16.2 Axial T1 weighted MRI with contrast shows a diffuse enhancing infiltrative lesion in both intra and extraconal compartments of the left orbit involving the medial rectus (arrow) with proptosis

Other Investigations

A full inflammatory workup including chest x-ray, full blood count, erythrocyte sedimentation rate (ESR), C-reactive protein (CRP), antineutrophil cytoplasmic antibodies (ANCA), anti-nuclear Ab, anti-dsDNA, and syphilis screen was negative.

Intervention

The patient underwent left anterior orbitotomy and incision biopsy of orbital fat and medial and inferior recti muscles.

Histopathology

There was stromal fibrosis with patchy lymphoplasmacytic chronic inflammatory cellular infiltrates (Fig. 16.3). The features were non-specific. A diagnostic consideration is IgG4-related disease, in which one would also sometimes find storiform fibrosis and obliterative phlebitis.

IgG and IgG4 immunohistochemistry were performed. Quantitative criteria were used in the histologic evaluation for IgG4-related disease. In this case, the number of IgG4-positive plasma cells per high-power field and the ratio of IgG4-positive plasma cells to IgG-positive plasma cells did not meet the histologic criteria for IgG4-related disease.

To conclude, the features were those of non-specific chronic inflammation.

Management

The patient was treated with tapering doses of oral steroids.

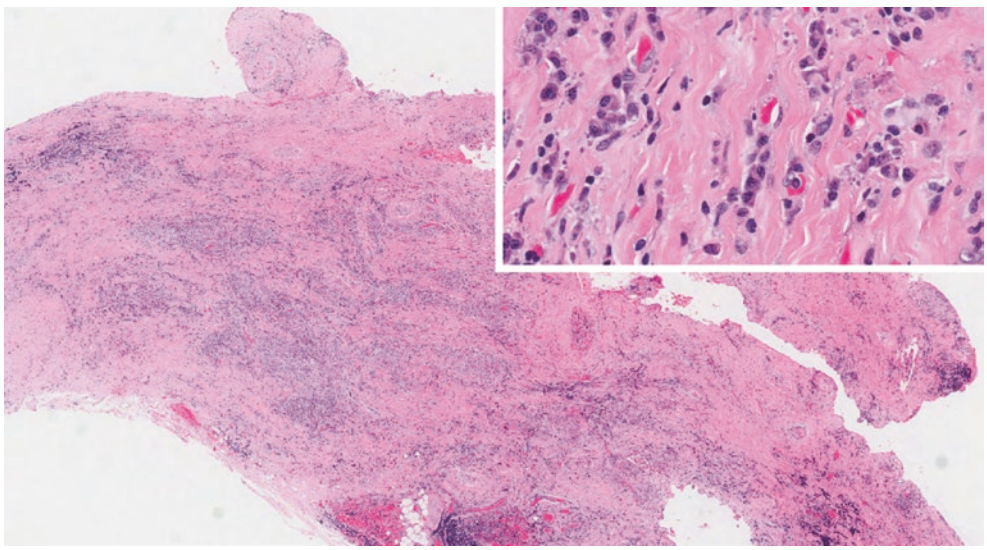

Fig. 16.3 Histopathology shows stromal fibrosis with a patchy lymphoplasmacytic infiltrate. Main: HE stain, 20× magnification; inset: HE stain, 200× magnification

Discussion

Non-specific orbital inflammatory disease (NSOID) can affect any structure in the orbit, and the presentation can range from abrupt to insidious onset. It is a diagnosis that is made following careful investigations to exclude common orbital tumours, thyroid eye disease, and systemic causes of inflammatory mass lesions.

Patients usually present with a mixture of infiltrative and inflammatory signs and symptoms, including swelling, pain, proptosis, extraocular muscle restriction, diplopia, decreased vision, and ptosis. The inflammation can occur either focally or in a diffuse manner, with orbital fat, lacrimal gland, and extraocular muscles being common sites of involvement. Relapses are common during the course of the disease.

While NSOID tends to respond to steroids, this is not diagnostic of the disease. There have been reported steroid-unresponsive cases of NSOID. Furthermore, other orbital conditions such as thyroid eye disease may respond to steroid therapy initially. Hence, a biopsy should be performed to confirm the diagnosis of NSOID with histopathological subtyping, except in cases where surgery is contraindicated (e.g. patient is unfit for surgery) or if there is a significant risk of damage to the optic nerve.

Treatment

A good initial response to high-dose systemic corticosteroids, either oral or intravenous, is observed in most cases of NSOID. However, roughly half of cases relapse on tapering or ceasing. In severe recurrent or recalcitrant cases with a high morbidity, additional therapy includes steroid-sparing agents such as methotrexate or azathioprine, radiotherapy, or biologic drugs such as rituximab or infliximab**.**

Learning Points

Orbital inflammation has a wide spectrum of clinical presentation. Other orbital conditions should be excluded before the diagnosis of NSOID is made. Inflammatory workup is required before starting steroids blindly. In order to know the subtype of OID, histopathologic diagnosis with a tissue biopsy is recommended.

Further Reading

1. Swamy BN, McCluskey P, Nemet A, et al. Idiopathic orbital inflammatory syndrome: clinical features and treatment outcomes. The British Journal of Ophthalmology. 2007;91:1667–70.
2. Young SM, Chan ASY, Jajeh IA, Shen S, Seah LL, Choo CT, Lang SS, Looi ALG. Clinical features and treatment outcomes of orbital inflammatory disease in Singapore: a 10-year clinicopathologic review. Ophthalmic Plastic & Reconstructive Surgery. 2017;33:182–8.
3. Yuen SJ, Rubin PA. Idiopathic orbital inflammation: ocular mechanisms and clinicopathology. Ophthalmology Clinics of North America. 2002;15:121–6.

Nodular Fasciitis

17

Stephanie Ming Young, Shantha Amrith, Eric Ting, Bingcheng Wu, Min En Nga, and Gangadhara Sundar

Introduction

Nodular fasciitis is a rapidly growing non-neoplastic soft tissue lesion frequently located in the deep subcutaneous region or in the fascia. It was first described as subcutaneous pseudosarcomatous fibromatosis. Subsequent reports confirmed its benign nature, and the disease was renamed as pseudosarcomatous fasciitis, and later changed to nodular fasciitis.

It is commonly located on the extremities, occasionally on the trunk, back, chest wall, and upper arm, but very rarely in the head and neck region. It most often occurs in patients between 20 and 40 years of age.

Clinical Scenario

A 31-year-old Indian female with no significant past medical history presented with a swelling in the left medial canthal area of 3 months' duration. According to the patient, the mass had been there for a few months, and occasionally associated with pain. There was no tearing or discharge.

On examination, there was a well-circumscribed, hard mass in the medial canthal region (Fig. 17.1a). It was slightly tender on deep palpation without overlying skin changes. Ocular motility was full, and the rest of the ophthalmic examination did not reveal any abnormalities.

CLOSE summary is given in Table 17.1.

Differential Diagnosis

- Dermoid cyst
- Nodular fasciitis
- Extranasal glioma
- Osteoma
- Neurofibroma
- Fibrous histiocytoma
- Solitary fibrous tumour

Imaging

MRI images showed a nodule with irregular margins in the medial canthus of the right eye. It appeared to be entirely preseptal and there was no extension into the orbit. The tumour was avidly enhancing with gadolinium. A surface marker (vitamin E capsule) was placed over the region of interest (Fig. 17.2).

Intervention

The patient underwent a right anterior orbitotomy, and excision of the right medial canthal region mass. Intraoperatively, a 0.7 cm bossellated pale pink firm mass anterior to medial canthal tendon (Fig. 17.1b) was found.

S. M. Young · S. Amrith (✉) · G. Sundar
Department of Ophthalmology, National University Hospital, Singapore

Department of Ophthalmology, Yong Loo Lin School of Medicine, National University of Singapore, Singapore
e-mail: shantha_amrith@nuhs.edu.sg; gangadhara_sundar@nuhs.edu.sg

E. Ting
Department of Diagnostic Imaging, National University Hospital, Singapore

Department of Diagnostic Imaging, Yong Loo Lin School of Medicine, National University of Singapore, Singapore

Advanced Medicine Imaging, Singapore

B. Wu
Department of Pathology, National University Hospital, Singapore

M. E. Nga
Department of Pathology, National University Hospital, Singapore

Department of Pathology, Yong Loo Lin School of Medicine, National University of Singapore, Singapore

S. Amrith et al. (eds.), *Ocular Adnexal Lesions*, https://doi.org/10.1007/978-981-13-3798-7_17

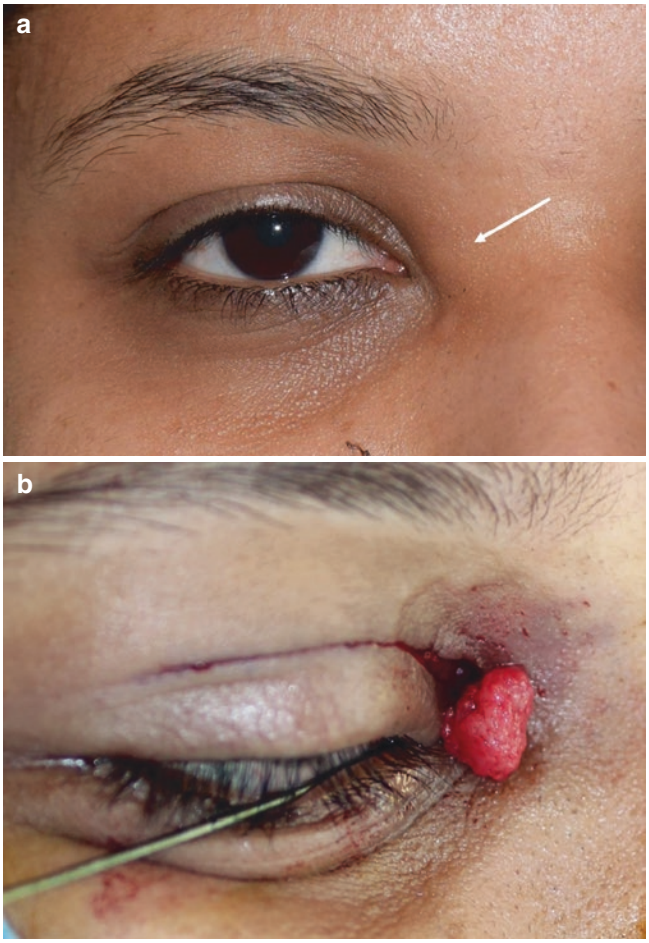

Fig. 17.1 (**a**) Right medial canthal mass, hard and well-circumscribed, without overlying skin changes. (**b**) Excision biopsy of right medial canthal mass via a lid crease incision

Table 17.1 CLOSE summary

*C*linical process: well-defined mass
*L*ocation: right medial canthal region, at junction of anterior orbit and paranasal region
*O*nset: subacute
*S*igns and symptoms: mass lesion with occasional pain
*E*pidemiology: adult Indian female

Histopathology

There was a haphazard proliferation of bland-appearing spindle and stellate cells within a loose oedematous stroma. A tissue culture-like growth pattern was discernible (Fig. 17.3). Extravasated red blood cells (cells that have moved outside the vessels) and a sparse chronic inflammatory cellular infiltrate were present.

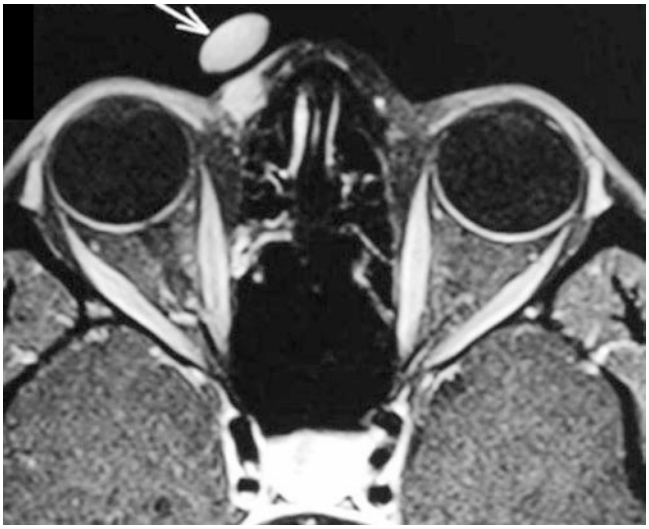

Fig. 17.2 Axial T1w FS + contrast MRI image showing an avidly enhancing nodule at the medial canthus. A surface marker (vitamin E capsule) was placed over the region of interest (white arrow)

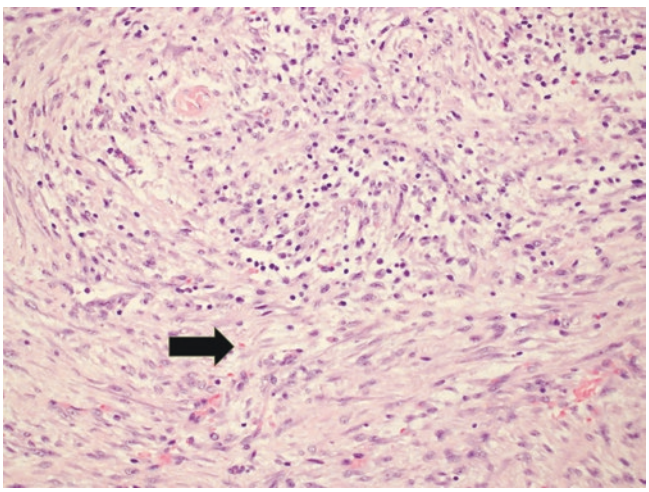

Fig. 17.3 There is a haphazard proliferation of bland-appearing spindle and stellate cells within a loose oedematous stroma. A tissue culture-like growth pattern is present. Extravasated red blood cells (black arrow) and a chronic inflammatory cell infiltrate are present. HE stain; 100× magnification

Discussion

Nodular fasciitis typically manifests as a rapidly growing mass which tends to be somewhat small (<4 cm) in size. Symptoms of tenderness and pain are frequently described. There are three general subtypes of nodular fasciitis on the basis of lesion location: subcutaneous, intramuscular and fascial.

Pathology reveals a benign proliferation of fibroblasts and myofibroblasts and is typically mistaken for a sarco-

matous lesion due to features of rapid growth, abundant spindle-shaped cells, and mitotic activity. Its pathogenesis is poorly understood, and is believed to be a reactive lesion related to trauma, although many cases may not reveal a history of trauma. In some studies, a high proportion of the proliferating cells were found to be in the S and G2 growth phases of cell division, and as a polyclonal cellular expansion using HUMARA-methylation-specific polymerase chain reaction. This suggests a reactive rather than a neoplastic process.

Treatment

Marginal excision of lesion is the treatment of choice. Local recurrences are rare. Observation or intralesional corticosteroid injections are other options, although these cannot confirm the diagnosis.

Learning Points

Nodular fasciitis lesions are well circumscribed and fast growing, and may show clinical signs of inflammation, including pain lasting for a month or less. They present as superficial, palpable masses, and can cause eyelid deformity. Although trauma has been suggested as a trigger, most cases do not include history of trauma.

Further Reading

1. Koizumi H, Mikami M, Doi M, et al. Clonality analysis of nodular fasciitis by HUMARA-methylation-specific PCR. Histopathology. 2005;47:320–34.
2. Shields JA, Shields CL, Scartozzi R. Survey of 1264 patients with orbital tumors and simulating lesions: the 2002 Montgomery Lecture, part 1. Ophthalmology. 2004;111:997–1008.
3. Vestal KP, Bauer TW, Berlin AJ. Nodular fasciitis presenting as an eyelid mass. Ophthal Plast Reconstr Surg. 1990;6:130–2.

Part V

Vascular Lesions

Vascular Tumours: Capillary Haemangioma

18

Shantha Amrith, Stephanie Ming Young, Eric Ting, and Gangadhara Sundar

Introduction

Infantile (capillary) haemangiomas are vascular tumours occurring commonly in the periorbital region. They are also the most common hamartomas (abnormal proliferation of cells in a normal location) in infancy, affecting 1–2% of all births, and 60% of the tumours that occur in the head and neck region. They run a self-limiting clinical course characterized by an early proliferation, followed by spontaneous involution. They can be cutaneous and/or subcutaneous with orbital extension with predilection for the upper eyelids and eyebrows. Combined lesions with both components are often seen. Cutaneous lesions appear as a crimson red maculae or papules surrounded by halo of vascular blanching, whereas the subcutaneous ones present as bluish nodules.

Case Scenario

A 2-month-old Chinese infant presented with a left upper lid lump for a month, which increased in size when she cried. The child had reddish cutaneous lesions on the chin and back. The ophthalmic examination revealed a bluish mass in the inner canthal area of the left upper lid causing a mild ptosis medially. On crying, the lesion enlarged to cover the visual axis. The globe appeared to be pushed laterally, and measurement of proptosis was difficult. The rest of the eye examination was normal. Investigations for systemic involvement revealed a hypo-echoic lesion in the liver, most likely a haemangioma (Fig. 18.1).

CLOSE summary is given in Table 18.1.

Differential Diagnosis

- Infantile (capillary) haemangioma
- Lymphatic-venous malformation
- Malignant tumours such as chloroma, rhabdomyosarcoma, neuroblastoma
- Langerhans histiocytosis or eosinophilic granuloma

Imaging

Targeted ultrasound scans of the left orbit revealed a slightly lobulated and heterogeneous and hypoechoic solid extraconal mass in the medial aspect of the left orbit. Prominent internal mixed arterial and venous flow was demonstrated within the mass (Fig. 18.2).

Sonographic findings were consistent with a left orbital capillary haemangioma.

Management

The child was referred to the paediatric service for co-management and was commenced on oral propranolol for multiple capillary haemangiomas, initially as an inpatient for cardiac monitoring. The dosage of propranolol was gradually titrated up from 0.8 mg to 1.6 mg, and then

S. Amrith (✉) · S. M. Young · G. Sundar
Department of Ophthalmology, National University Hospital, Singapore

Department of Ophthalmology, Yong Loo Lin School of Medicine, National University of Singapore, Singapore
e-mail: shantha_amrith@nuhs.edu.sg; gangadhara_sundar@nuhs.edu.sg

E. Ting
Department of Diagnostic Imaging, National University Hospital, Singapore

Department of Diagnostic Imaging, Yong Loo Lin School of Medicine, National University of Singapore, Singapore

Advanced Medicine Imaging, Singapore

S. Amrith et al. (eds.), *Ocular Adnexal Lesions*, https://doi.org/10.1007/978-981-13-3798-7_18

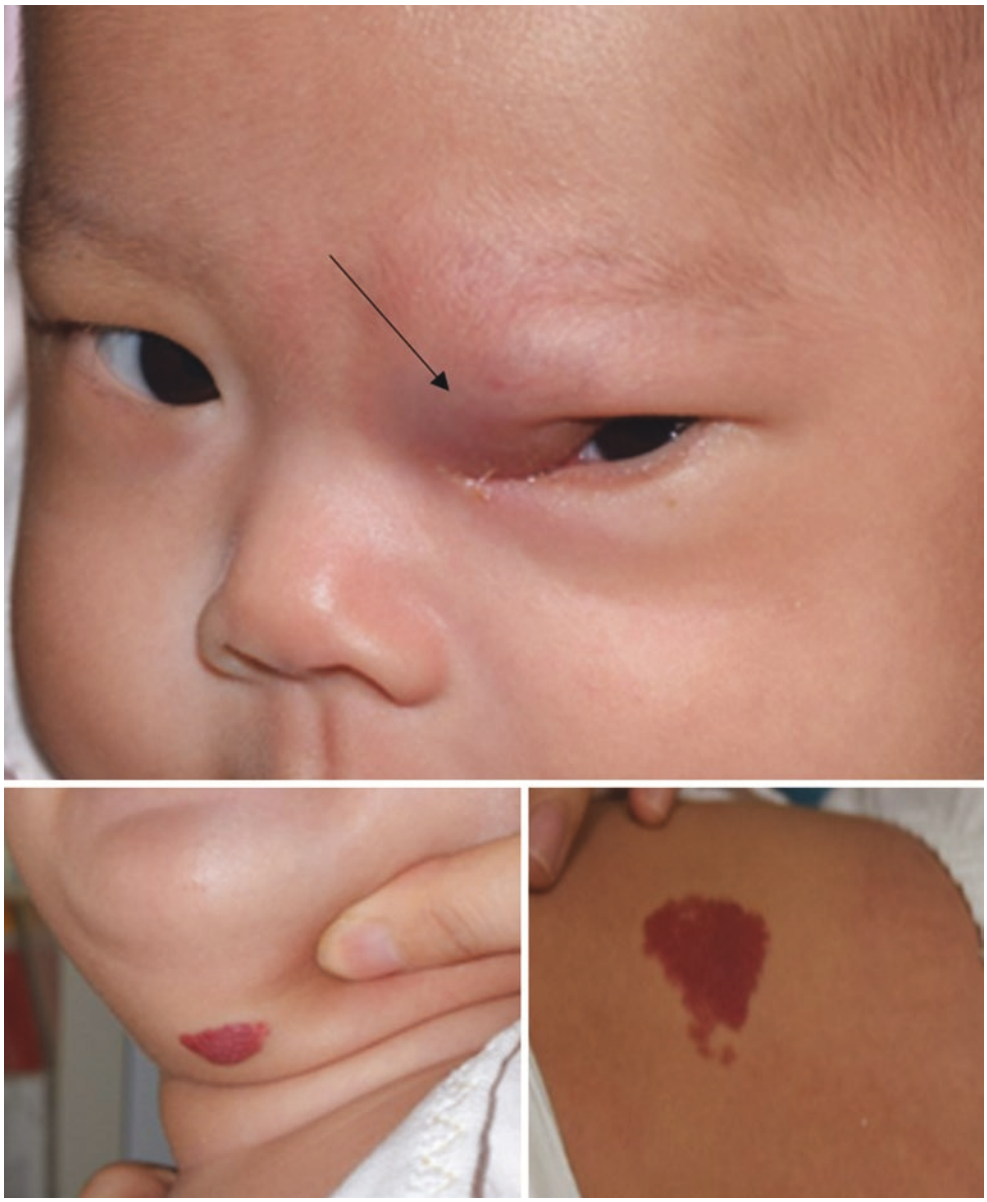

Fig. 18.1 Top: Clinical picture showing the medial canthal bluish lesion extending to the upper lid causing ptosis. Bottom left: Reddish cutaneous lesion under the chin. Bottom right: Similar lesion at the lumbar region

Table 18.1 CLOSE summary

*C*linical process: vascular lesion
*L*ocation: left anterior orbit and eyelid
*O*nset: acute-subacute
*S*igns and symptoms: bluish mass increasing in size on crying, reddish cutaneous lesions on the chin and back
*E*pidemiology: 2-month-old female infant

to 3.2 mg every 8 hours (maximum of 0.67 mg/kg) over 2 days. It was continued for 8 months titrated to the body weight. The eyelid lesion completely involuted and the ptosis improved.

Discussion

Infantile (capillary) haemangioma (IH) usually occurs after birth as against congenital haemangioma (CH) which are fully grown at birth and may be either non-involuting (NICH) or rapidly involuting (RICH). IH appears within a few days to weeks of life, and rapidly grows during infancy, but usually demonstrates spontaneous involution – 40% involute at 4 years, and 80% disappear by the age of 7 or 8. The upper eyelid lesions may cause mechanical ptosis or produce high astigmatism; therefore, the treatment should be initiated early to prevent

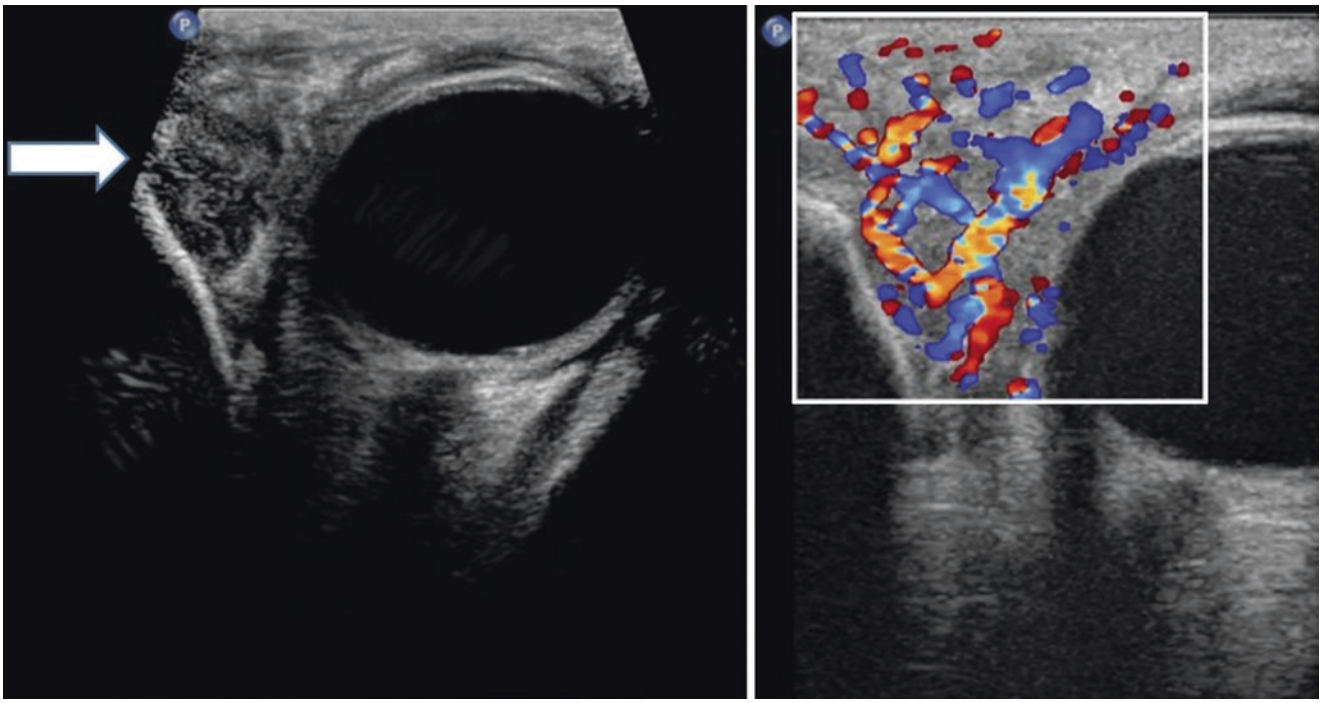

Fig. 18.2 Targeted ultrasound scans of the left orbit showing a slightly lobulated and heterogeneous and hypoechoic solid extraconal mass in the medial aspect of the left orbit (white arrow). Prominent internal mixed arterial and venous flow is demonstrated within the mass in the picture on the right

deprivation or meridional amblyopia. Orbital lesions may cause proptosis.

Systemic association is seen in syndromic conditions such as PHACES (*p*osterior fossa malformations, *h*aemangiomas, *a*rterial anomalies, *c*oarctation of the aorta/cardiac defects, *e*ye abnormalities, *s*ternal clefting and supraumbilical raphe), and Kasabach-Merritt syndrome (consumptive thrombocytopenic coagulopathy where platelets are rapidly sequestered within the vascular lesion).

Ultrasound scans are useful to rule out deeper orbital involvement, as well as to monitor progress during treatment. IH appears as enhancing low-flow lesions without overlying bone destruction. CT scans are best avoided to avert the risk of exposing the child to ionising radiation. MRI shows a lesion hypointense on T1w and hyperintense on T2w with contrast enhancement.

Indications for treatment include systemic involvement, ptosis, amblyopia and significant proptosis. Amblyopia management must be instituted at the same time as the definitive treatment.

Beta-blockers are currently the mainstay of treatment for infantile haemangiomas and can be used systemically, and topically, the latter in the form of ointment for cutaneous lesions.

Intralesional corticosteroids were the mainstay in the treatment of localised lesions before propranolol was introduced for the treatment of IH. The risks of steroid injections in the periocular region include blindness due to central retinal artery occlusion, skin hypopigmentation, atrophy, and skin necrosis. Systemic steroids have side effects and rebound growth after discontinuation.

Immunomodulators such as cyclophosphamide and interferon α2b are rarely indicated, as they have significant adverse events including bone marrow suppression and hepatotoxicity.

Laser photocoagulation with pulsed dye laser is useful as an adjunct therapy for superficial lesions.

Surgical excision of localised haemangiomas can be done with caution, with the use of laser or cautery to avoid blood loss in young babies. This is probably the only option in NICH lesions.

Learning Points

Infantile haemangiomas are common lesions that can be easily diagnosed based on clinical appearance, progression and age at presentation. It is important to rule out more serious malignant conditions during the rapid growth phase, as well as orbital and systemic involvement. Ultrasound or MRI scans are useful to know the extent of deeper involvement. Management should include amblyopia management along

with oral and/or topical propranolol. Other treatment modalities would include oral or intralesional injections of corticosteroids, immunomodulators, pulsed dye laser photocoagulation for cutaneous lesions, and surgical excision in selected cases.

Further Reading

1. Alniemi ST, Griepentrog GJ, Diehl N, Mohney BG. Incidence and clinical characteristics of periocular infantile hemangiomas. Arch Ophthalmol. 2012;130(7):889–93.
2. Callahan AB, Yoon MK. Infantile hemangiomas: a review. Saudi J Ophthalmol. 2012;26(3):283–91.
3. Haik BG, Karcioglu ZA, Gordon RA, Pechous BP. Capillary hemangioma (infantile periocular hemangioma). Surv Ophthalmol. 1994;38(5):399–426.
4. Metry DW. Ten lessons learned from a hemangioma clinic. Semin Plast Surg. 2006;20(3):157–62.
5. Ni N, Guo S, Langer P. Current concepts in the management of periocular infantile (capillary) hemangioma. Curr Opin Ophthalmol. 2011;22(5):419–25.
6. Painter SL, Hildebrand GD. Review of topical beta blockers as treatment for infantile hemangiomas. Surv Ophthalmol. 2016;61(1):51–8.
7. Rizvi SA, Yusuf F, Sharma R, Rizvi SW. Management of superficial infantile capillary hemangiomas with topical timolol maleate solution. Semin Ophthalmol. 2015;30(1):62–4.
8. Tavakoli M, Yadegari S, Mosallaei M, Aletaha M, Salour H, Lee WW. Infantile periocular hemangioma. J Ophthalmic Vis Res. 2017;12(2):205–11.
9. Weiss AH, Kelly JP. Reappraisal of astigmatism induced by periocular capillary hemangioma and treatment with intralesional corticosteroid injection. Ophthalmology. 2008;115:390–7.

Lymphatic and Lymphatic-Venous Malformation

19

Shantha Amrith, Stephanie Ming Young, Eric Ting, Bingcheng Wu, Min En Nga, and Gangadhara Sundar

Introduction

The international society for the study of vascular malformations (ISSVA) has classified lymphatic malformations (LM)/lymphatic-venous malformations (LVM) (Fig. 19.1) as simple and combined. Simple is one end of the spectrum being purely lymphatic and, the combined at the other end with venous dominant LVM. Simple forms, formerly known as lymphangiomas, are hamartomas that are non-distensible due to their hemodynamic isolation. The combined forms with varying lymphatic and venous components, are characterized by onset at early childhood with frequent episodes of haemorrhage. Sometimes, it may be difficult to distinguish LVM from a distensible venous malformation, but the diagnosis should be based on clinical evaluation, haemodynamic behaviour, and radiological and histopathological features. Based on the location, there are four types: superficial, deep, combined, and complex. In the complex form, the orbital lesion is a component of multiple facial, intracranial, or systemic lesions.

Case Scenario

A 43-year-old Malay female presented with a sudden onset of reddish swelling in her left eye of 2 weeks duration. She gave a history of recurrent episodes of bluish swelling and discomfort on the left side of the face for about 20 years, not associated with trauma. Ten months prior to presentation, she had a sudden, spontaneous increase in the swelling. At that time she was noted to have a bluish lump in the inferomedial aspect of the left orbit with 3 mm of proptosis and lateral displacement of the globe.

Examination at presentation revealed a left sided inferior bulbar and palpebral conjunctival ecchymosis (Fig. 19.2a) with a non-axial proptosis and superolateral displacement of the globe. There was no increase in proptosis with Valsalva manoeuvre. There was limitation of infraduction and adduction of the left eye. The rest of the ophthalmic examination including vision, intraocular pressures, pupils, and fundi were normal. Examination of the palate revealed bluish lesions suggestive of a vascular malformation (Fig. 19.2b).

CLOSE summary is given in Table 19.1.

S. Amrith (✉) · S. M. Young · G. Sundar
Department of Ophthalmology, National University Hospital, Singapore

Department of Ophthalmology, Yong Loo Lin School of Medicine, National University of Singapore, Singapore
e-mail: shantha_amrith@nuhs.edu.sg; gangadhara_sundar@nuhs.edu.sg

E. Ting
Department of Diagnostic Imaging, National University Hospital, Singapore

Department of Diagnostic Imaging, Yong Loo Lin School of Medicine, National University of Singapore, Singapore

Advanced Medicine Imaging, Singapore

B. Wu
Department of Pathology, National University Hospital, Singapore

M. E. Nga
Department of Pathology, National University Hospital, Singapore

Department of Pathology, Yong Loo Lin School of Medicine, National University of Singapore, Singapore

S. Amrith et al. (eds.), *Ocular Adnexal Lesions*, https://doi.org/10.1007/978-981-13-3798-7_19

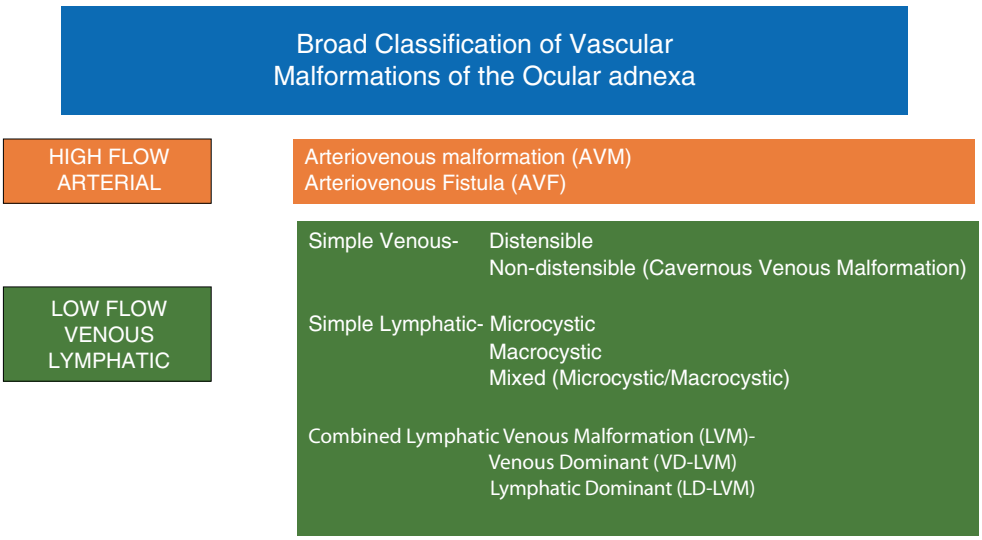

Fig. 19.1 Broad classification of vascular malformations of the ocular adnexa based on ISSVA guidelines

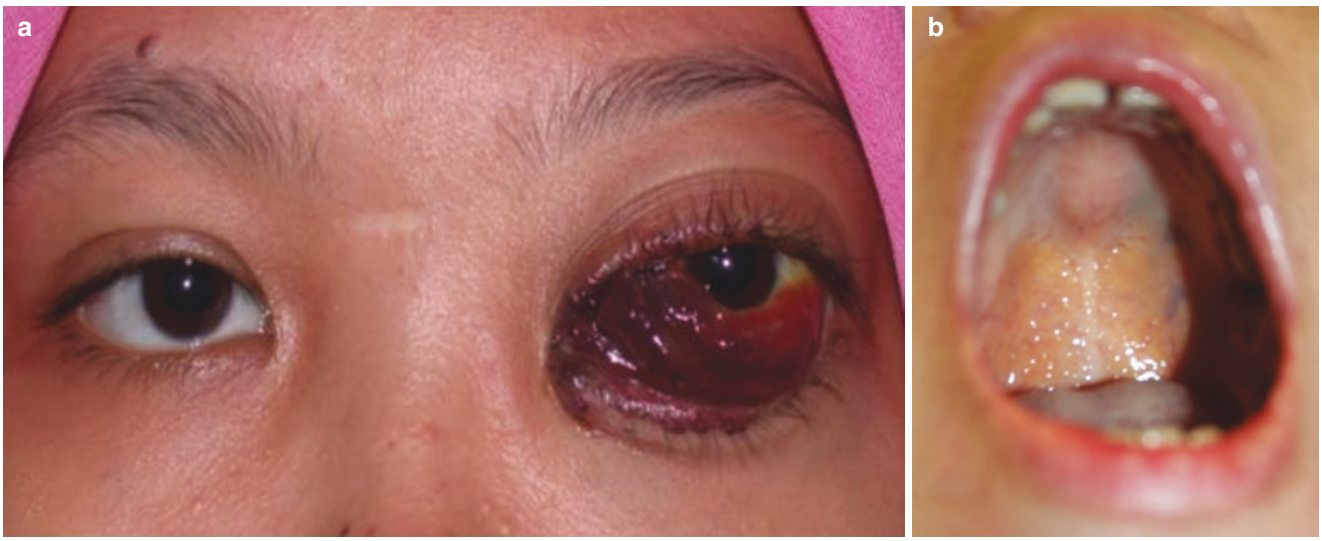

Fig. 19.2 Clinical picture showing left non-resolving conjunctival ecchymosis, and non-axial proptosis (**a**), and palatal venolymphatic malformation (**b**)

Table 19.1 CLOSE summary

*C*linical scenario: acute spontaneous haemorrhagic episodes
*L*ocation: left orbit
*O*nset: acute on chronic
*S*igns and symptoms: frequent episodes of increasing bluish swelling, non-axial proptosis with acute haemorrhage and conjunctival ecchymosis
*E*pidemiology: 43-year-old Malay female

Differential Diagnosis

- Lymphatic/ lymphatic-venous malformation
- Venous malformation
- Arteriovenous malformation

Imaging

Contrast-enhanced CT scan (Fig. 19.3) showed a mildly enhancing extraconal multilobulated mass in the left inferomedial orbit with remodelling of the adjacent medial orbital wall.

Multiplanar MRI with contrast showed a multilobulated mass in the inferomedial left orbit showing a microcystic pattern with fine, enhancing septations giving a spongiform appearance (Fig. 19.4).

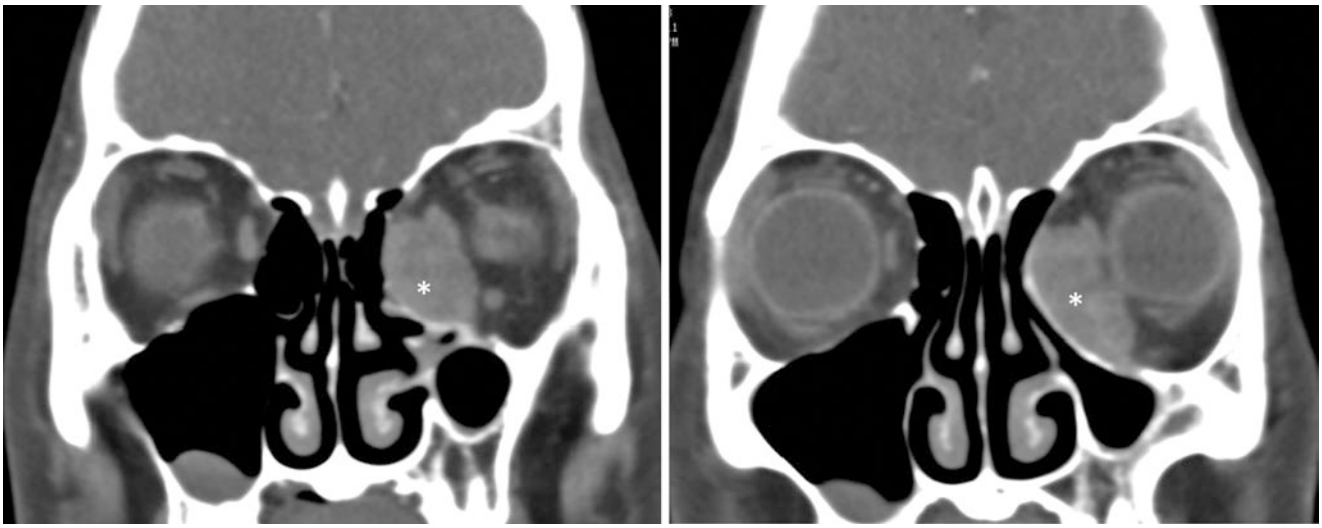

Fig. 19.3 Coronal CT scan showing an extraconal multilobulated mass (asterisk) in the left inferomedial orbit with remodelling of the adjacent medial orbital wall

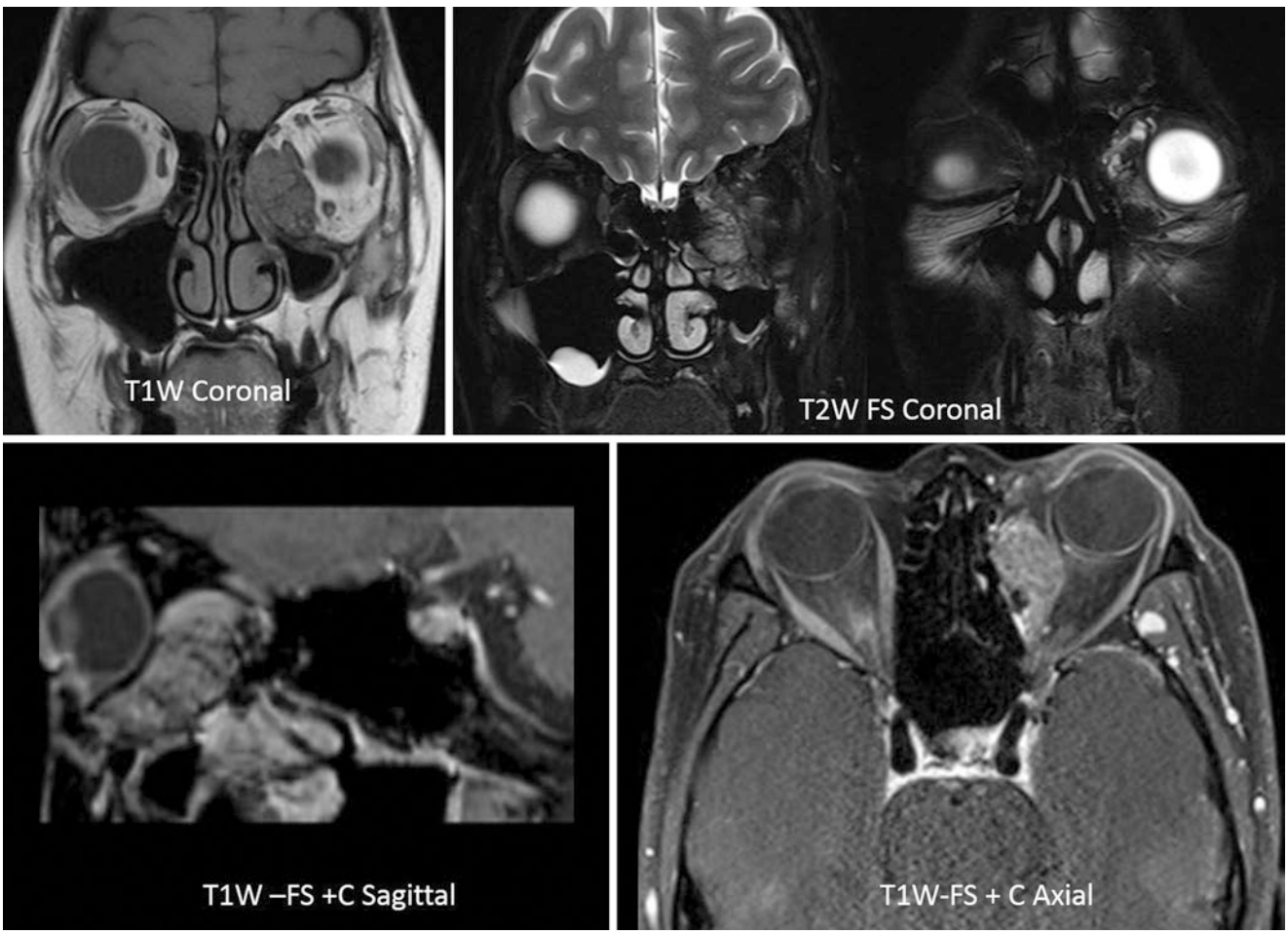

Fig. 19.4 MRI images show a multilobulated mass in the inferomedial left orbit showing a microcystic pattern with fine, enhancing septations giving a spongiform appearance

Intervention

The patient was observed for a month, and because of failure of resolution of conjunctival ecchymosis, she opted for surgical treatment. Through an anterior orbitotomy, the lesion was debulked as much as safely possible, without damage to vital structures (such as extraocular muscles and optic nerve), ensuring haemostasis along the way. There were multiple chocolate cysts, which released stale blood upon rupture.

Histopathology

The excised specimen showed haphazardly arranged, irregularly dilated lymphovascular channels surrounded by fibrous tissue. Scattered lymphoid aggregates were seen in the background (Fig. 19.5). The features were suggestive of a lymphatic-venous malformation.

Discussion

The orbit is believed to be devoid of lymphatic channels, although this concept has been challenged in recent years with some reports showing their presence in the lacrimal gland and optic nerve sheath. The venous and lymphatic vasculature in LVM are highly variable, resulting in a wide variety of clinical presentation and imaging findings. Simple LVMs are of 3 types, microcystic, macrocystic and mixed (micricystic/macrocystic) embedded in loose stroma. The combined LVM are either venous dominant (LVM-VD) or lymphatic dominant (LVM-LM). In LVM-VD, the Valsalva manoeuvre can be positive mimicking a distensible venous malformation.

Superficial lesions affect the conjunctiva. Dilated lymph channels, and/or cystic spaces, sometimes filled with blood, are visible in the conjunctiva on slit lamp examination. They do not usually cause any specific symptoms apart from cosmetic blemish; therefore, removal is optional.

The deep lesions in the orbit tend to present in childhood with episodes of spontaneous haemorrhage in previously unrecognized lesions, typically following upper respiratory infections. These lesions generally grow proportionately with the child with or without acute episodes of bleeding. Episodes of haemorrhage result in sudden proptosis, periorbital ecchymosis and swelling, and subconjunctival haemorrhage, not infrequently threatening vision. However, most exacerbations improve spontaneously. The patients need close monitoring for optic nerve compression during these episodes.

Combined lesions come to light earlier because of the more visible superficial component. Palatal lesions often corroborate the diagnosis.

On imaging, the mass lesion may be present in pre-septal, post-septal, as well as intra- and extraconal regions. Orbital expansion is obvious in most cases due to the long-standing nature of the disease. The mass has poorly defined margins and shows multiple cysts, sometimes with fluid levels. MRI shows the lesion to be heterogeneous with lymph-filled cysts appearing hypointense and haemorrhagic cysts hyperintense in T1w sequences. There is patchy contrast enhancement as some cysts do not enhance. No connection to vascular channels can be demonstrated. Pathological confirmation is not always necessary, because of the distinctive appearance on imaging.

Histopathology demonstrates dilated serous-filled channels or cysts, loose collagenous stroma, lymphorrhages, and features of old haemorrhages.

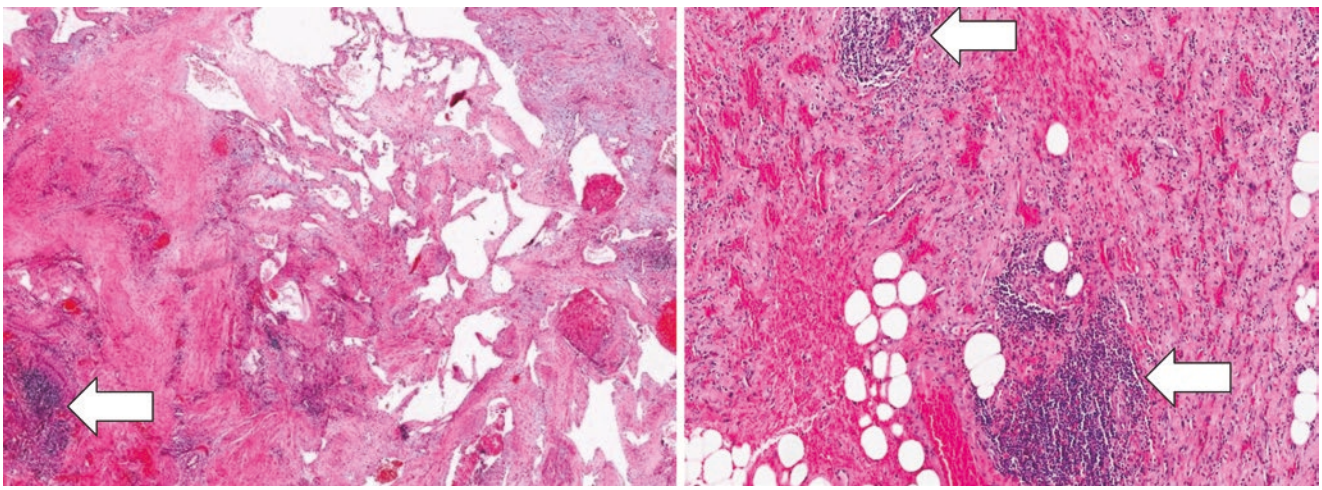

Fig. 19.5 There are haphazardly arranged, irregularly dilated, and crowded lymphatic channels. Scattered lymphoid aggregates are seen in the background (white arrows). Left: HE stain, 20× magnification. Right: HE stain, 40× magnification

Management should be conservative if the symptoms are minimal and the proptosis not severe. Surgical excision is performed only in cases with vision-threatening proptosis and unacceptable cosmetic disfigurement. During surgery, presence of multiple thin-walled chocolate cysts containing old blood is quite a characteristic of LVM. Recurrences are common after surgical excision.

Vascular interventional radiological procedures performed under image guidance, such as aspiration followed by the use of sclerosing agents, and injection of drugs that interfere with vasculogenesis (bevacizumab) have significantly changed our approaches to management of LVM. Bleomycin has been used widely in head and neck lesions, and intralesional injections of OK-432 (Picibanil) work better in macrocystic lesions within the orbit. Microcystic lesions may be managed with intralesional doxycycline. Residual mass lesions may be observed or surgically excised.

Long-term monitoring is necessary for patients with LVM. A multimodality, and multidisciplinary approach involving neuroradiologists in the hybrid operating theatre is often useful.

Learning Points

- Lymphatic-venous malformations have both lymphatic and venous elements.
- Pure lymphatic malformations are haemodynamically isolated and, therefore, do not enlarge with Valsalva.
- The combined lymphatic-venous malformations are characterized by frequent spontaneous haemorrhages and present as superficial, deep, or combined lesions in the ocular adnexa. Slow progressive growth and sudden increase due to frequent haemorrhages may cause optic nerve compression.
- Surgery is advisable for progressive lesions threatening vision or for cosmetic disfigurement. Injection of drugs that interfere with vasculogenesis, sclerotherapy or OK-432 may be tried in macrocystic lesions under image guidance.

Further Reading

1. Harris GJ. Orbital vascular malformations: a consensus statement on terminology and its clinical implications. Orbital Society. Am J Ophthalmol. 1999;127:453–5.
2. Harris GJ, Sakol PJ, Bonavolonta G, De Conciliis C. An analysis of thirty cases of orbital lymphangioma: pathophysiologic considerations and management recommendations. Ophthalmology. 1990;97:1583–92.
3. http://www.issva.org/Userfiles/file/ISSVA-Classification-2018.pdf
4. Katz SE, Rootman J, Vangveeravong S, Graeb D. Combined venous lymphatic malformations of the orbit (so-called lymphangiomas). Association with non-contiguous intracranial vascular anomalies. Ophthalmology. 1998;105:176–84.
5. Lacey B, Rootman J, Marotta TR. Distensible venous malformations of the orbit: clinical and hemodynamic features and a new technique of management. Ophthalmology. 1999;106(6):1197–209.
6. Nassiri N, Rootman J, Rootman DB, Goldberg RA. Orbital lymphaticovenous malformations: current and future treatments. Surv Ophthalmol. 2015;60(5):383–405.
7. Rootman J. Diseases of the orbit, a multidisciplinary approach. 2nd ed. Philadelphia: Wolters Kluwer Lippincott Williams & Wilkins; 2003.
8. Rootman J, Stewart B, Goldberg RA. Orbital surgery – a conceptual approach. Philadelphia: Wolters Kluwer Lippincott Williams & Wilkins; 2013. p. 381–411.
9. Shields WE, et al. Percutaneous treatment of lymphatic malformations. Otolaryngol Head Neck Surg. 2009;141:219–24.
10. Sundar G. Vascular lesions of the orbit: conceptual approach and recent advances. Indian J Ophthalmol. 2018;66(1):3.
11. Suzuki Y, Obana A, Gohto Y, Miki T, Otuka H, Inoue Y. Management of orbital lymphangioma using intralesional injection of OK-432. Br J Ophthalmol. 2000;84:614–7.

Distensible Venous Malformation

20

Shantha Amrith, Stephanie Ming Young, Poh Sun Goh, and Gangadhara Sundar

Introduction

Vascular lesions are classified into tumours and malformations, and malformations are further classified into high-flow, and low-flow lesions depending on the haemodynamic characteristics, and there can be combinations of various lesions. The classification of vascular lesions are detailed in the ISSVA (*I*nternational *S*ociety for the *S*tudy of *V*ascular *A*nomalies). Distensible venous malformation (Common venous malformation [Common, VM]), previously known as varices, is the most common type of vascular malformation in the orbit and periorbital region. It is mostly sporadic, but in about 1–2% of cases, it can be familial. It occurs at the venous end of the vascular system and communicates with the venous circulation, thereby causing an increase in size with Valsalva manoeuvre. Common VM is usually present at birth and enlarges with hormonal changes during adolescence and adulthood. Occasionally, there is sudden expansion due to bleeding.

Clinical Scenario

A 67-year-old Chinese male with a history of hyperlipidaemia was incidentally detected to have an orbital mass when he underwent a CT scan of his sinuses. He denied any symptoms, however had noticed that his left eye 'popped out' whenever he bent down.

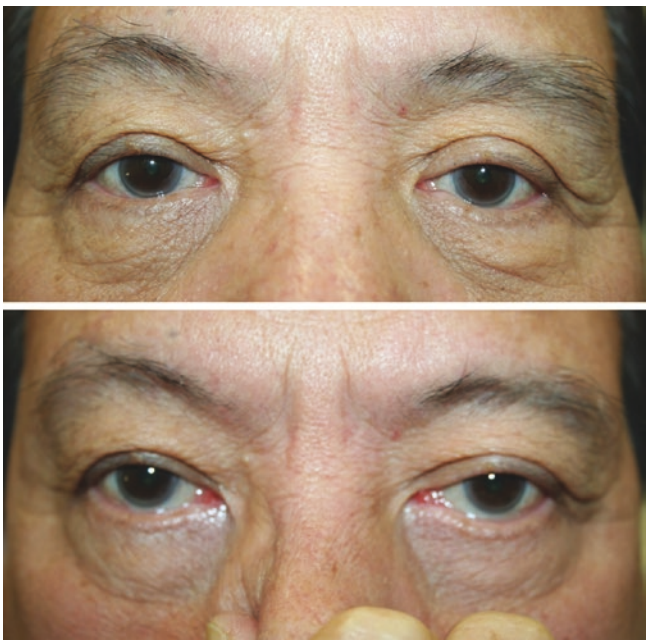

Fig. 20.1 Clinical picture of the patient at rest (top) and during Valsalva manoeuvre (bottom). Note the appearance of proptosis of the left eye in the bottom picture

Clinical examination revealed normal visual acuities, no afferent pupillary defect, normal eye movements and anterior and posterior segments. The left upper lid crease was slightly higher than that of the right. The exophthalmometry revealed 1 mm of enophthalmos in the left eye. On Valsalva manoeuvre, the left eyeball became more prominent with a proptosis of 3–4 mm (Figs. 20.1 and 20.2). The visual fields were normal.

CLOSE summary is given in Table 20.1.

S. Amrith (✉) · S. M. Young · G. Sundar
Department of Ophthalmology, National University Hospital, Singapore

Department of Ophthalmology, Yong Loo Lin School of Medicine, National University of Singapore, Singapore
e-mail: shantha_amrith@nuhs.edu.sg; gangadhara_sundar@nuhs.edu.sg

P. S. Goh
Department of Diagnostic Imaging, National University Hospital, Singapore

Department of Diagnostic Imaging, Yong Loo Lin School of Medicine, National University of Singapore, Singapore

S. Amrith et al. (eds.), *Ocular Adnexal Lesions*, https://doi.org/10.1007/978-981-13-3798-7_20

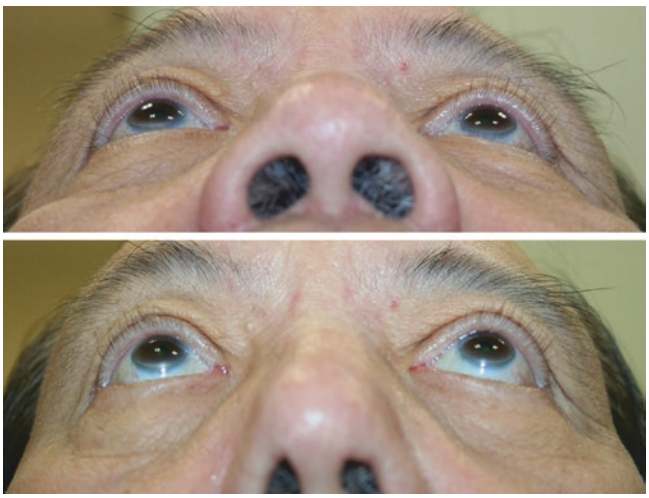

Fig. 20.2 Worm's eye view showing patient at rest (top) and proptosis of the left eye after Valsalva (bottom)

Table 20.1 CLOSE summary

*C*linical scenario: vascular lesion
*L*ocation: left orbit
*O*nset: chronic but picked up incidentally
*S*igns and symptoms: asymptomatic with higher lid crease and positive Valsalva
*E*pidemiology: 67-year-old Chinese male

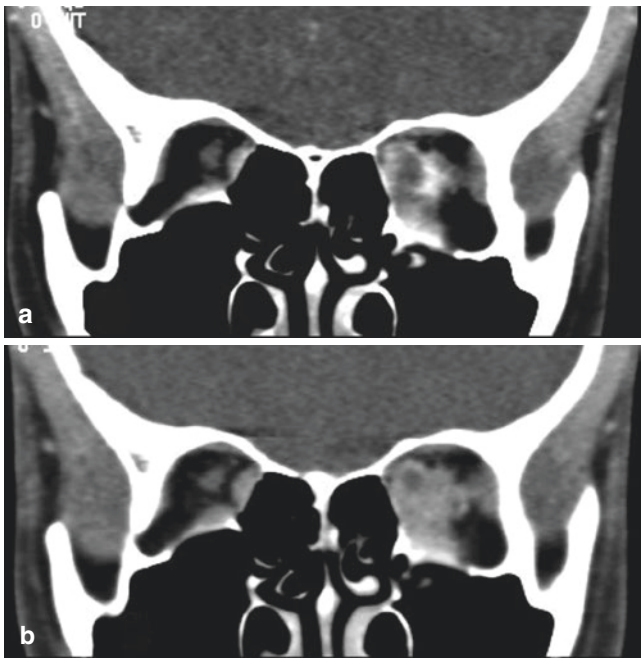

Fig. 20.3 Contrast-enhanced coronal CT showing a left intraconal lesion with irregular margins before (**a**) and increasing in size after (**b**) Valsalva manoeuvre. It is wrapped around the optic nerve and inseparable from medial and inferior rectus muscles. Note the remodeling of the orbit on the left side

Differential Diagnosis

- Distensible venous malformation
- Lymphatic-venous malformation

Imaging

Contrast-enhanced CT showed an intraconal lesion with irregular margins wrapped around the optic nerve, enhancing with contrast (Fig. 20.3a). The mass showed considerable increase in size after Valsalva manoeuvre (Fig. 20.3b). The extraocular muscles were normal and there was no calcification. This gave an impression of a common venous malformation (varices) of the orbit.

Management

As the patient was asymptomatic with normal optic nerve functions, the patient was managed conservatively and kept under observation.

Discussion

Common VM are low-flow venous malformations that communicate with the venous end of the vascular system. There are 3 types, dysmorphic, spongy and cavitary. The former two are more common in the orbit. In the ocular adnexa, they may be superficial or deep. Superficial ones occur in the eyelids and anterior orbit, and they become obvious from birth or early childhood as bluish swellings that increase in size when the child cries. They tend to enlarge during puberty due to hormonal influence. The deep lesions in the orbit may not be evident clinically, and may be completely asymptomatic. Patients present with an enophthalmos rather than proptosis. They may complain of discomfort while exercising or bending down; at the same time, they may also notice the eye getting more prominent. Some patients experience sudden pain and proptosis coinciding with an event of thrombosis, obstruction to venous flow resulting in enlargement of the malformation. With recanalization, the proptosis subsides. The thrombi get calcified over time, the evidence seen as calcification on imaging. Occasionally, there is spontaneous haemorrhage into these lesions, resulting in sudden proptosis.

Clinical examination should include the visual acuity and change in enophthalmos/proptosis at rest and on bending down to a dependent position (or on performing a Valsalva manoeuvre). The change in the eyeball position is due to increased venous pressure and expansion of the varices. D-dimer levels may be elevated, and it is considered specific for a venous malformation and may help to distinguish it from a venous dominant lymphatic-venous malformation. Lymphatic-venous malformation may also be differentiated histologically from venous malformation using the D2-40 immunostain which stains the lymphatic endothelium. Distensibility is a key feature of an orbital venous malformation. Computed tomography (CT) or MR imaging should be carried out in both supine and prone positions, alternatively with Valsalva manoeuvre. Dynamic CT angiography (CTA) with venous phase Valsalva manoeuvre is very useful to delineate the different types. If imaging is performed in children under general anaesthesia, the anaesthetists can assist in mimicking Valsalva effect by increasing the intrathoracic pressure. In long-standing cases, calcification will be evident. Establishing distensibility of these lesions is essential prior to embarking on sclerotherapy or surgery to avoid misadventures.

It is reasonable to observe asymptomatic patients. In symptomatic patients, the options include surgical excision, embolization or sclerotherapy. The indications for surgery are non-resolving episodes of thrombosis, severe disfiguring proptosis or globe displacement and optic nerve compression. For anterior lesions, surgery can be done for cosmetic reasons.

Injecting glue under fluoroscopic control may enable the surgeon to excise the tumour without the fear of haemorrhage and complications. Excising posterior lesions are extremely difficult and fraught with complications. Sclerosants are not very useful in the orbit as there is fear of drainage of these sclerosants into the eye or the cavernous sinus. Careful endovascular embolization using microballoons to block the venous outflow followed by sclerotherapy has been useful in some cases.

Learning Points

All patients with proptosis should be examined with dynamic manoeuvres to diagnose orbital varices. Documentation of increasing proptosis with exophthalmometry and photography, before and after Valsalva manoeuvre, is useful. CT scan before and after Valsalva manoeuvre or a dynamic CTA with venous phase Valsalva manoeuvre should be performed in order to confirm the diagnosis. Distensible venous malformations may be completely asymptomatic, and it is reasonable to observe patients with no symptoms. The anterior lesions often cause cosmetic concerns and therefore may be cautiously excised after injecting glue under fluoroscopic control. The posterior symptomatic ones are difficult to manage and may need a multidisciplinary approach for effective management.

Further Reading

1. Benoiton LA, Chan K, Steiner F, FitzJohn T, Tan ST. Management of orbital and periorbital venous malformation. Front Surg. 2017;4:27. https://doi.org/10.3389/fsurg.2017.00027.
2. http://www.issva.org/Userfiles/file/ISSVA-Classification-2018.pdf
3. Nassiri N, Rootman J, Rootman DB, Goldberg RA. Orbital lymphaticovenous malformations: current and future treatments. Surv Ophthalmol. 2015;60(5):383–405.
4. Rootman J. Diseases of the orbit, a multidisciplinary approach. 2nd ed. Philadelphia: Wolters Kluwer Lippincott Williams & Wilkins; 2003.
5. Rootman J, Stewart B, Goldberg RA. Orbital surgery – a conceptual approach. 2nd ed. Philadelphia: Wolters Kluwer Lippincott Williams & Wilkins; 2013. p. 381–411.
6. Rootman J, Heran MK, Graeb DA. Vascular malformations of the orbit: classification and the role of imaging in diagnosis and treatment strategies. Ophthal Plast Reconstr Surg. 2014;30:91–104.
7. Stacey AW, Gemmete JJ, Kahana A. Management of orbital and periocular vascular anomalies. Ophthal Plast Reconstr Surg. 2015;31(6):427–36.

Non-distensible Cavernous Venous Malformation (Cavernous Haemangioma)

21

Shantha Amrith, Stephanie Ming Young, Eric Ting, Bingcheng Wu, Min En Nga, and Gangadhara Sundar

Introduction

Cavernous haemangiomas, now termed as non-distensible cavernous venous malformations, are usually solitary and encapsulated. They are the most common orbital lesions in adulthood, and were once considered as benign neoplasms. But according to the current evidence (ISSVA classification) (Fig 19.1), they should more appropriately be classified as non-distensible venous malformations. They may rarely be present with other lymphatic or arteriovenous malformations in the orbit.

They occur as unilateral, intraconal (more common) or extraconal, asymptomatic and well-circumscribed mass lesions and more commonly in females (60%) in the fourth and fifth decades of life, possibly due to hormonal influence.

S. Amrith (✉) · S. M. Young · G. Sundar
Department of Ophthalmology, National University Hospital, Singapore

Department of Ophthalmology, Yong Loo Lin School of Medicine, National University of Singapore, Singapore
e-mail: shantha_amrith@nuhs.edu.sg; stephanie.young@nuhs.edu.sg; gangadhara_sundar@nuhs.edu.sg

E. Ting
Department of Diagnostic Imaging, National University Hospital, Singapore

Department of Diagnostic Imaging, Yong Loo Lin School of Medicine, National University of Singapore, Singapore

Advanced Medicine Imaging, Singapore

B. Wu
Department of Pathology, National University Hospital, Singapore

M. E. Nga
Department of Pathology, National University Hospital, Singapore

Department of Pathology, Yong Loo Lin School of Medicine, National University of Singapore, Singapore

Clinical Scenario

A healthy 50-year-old Vietnamese female noticed a difference between her two eyes for 1 year prior to presentation. She did not have any pain, blurring of vision or any double vision. On examination she had normal visual acuities, no RAPD and a normal fundus examination. However, she was noted to have a non-axial left proptosis of about 3 mm with the globe displaced downwards (Fig. 21.1). A firm non-tender, non-pulsatile mass was palpable just below the eyebrow, and it did not change with Valsalva manoeuvre. There was no overlying skin discolouration.

CLOSE summary is given in Table 21.1.

Differential Diagnosis

- Cavernous venous malformation (Cavernous haemangioma)
- Schwannoma
- Solitary fibrous tumour
- Lymphoma
- Metastasis
- Orbital inflammatory disease

The patient underwent an MRI. No serological investigations were done as clinical suspicion of inflammatory disease or thyroid eye disease was low.

Imaging

Magnetic resonance imaging (MRI) showed a well-circumscribed mass in the left orbit in the extraconal area just above the superior rectus-levator palpebrae superioris (SR-LPS) muscle complex, isointense to brain on T1-weighted sequences, hyperintense on T2-weighted sequences with patchy post-contrast enhancement in T1-weighted and fat-suppressed + contrast (T1w FS + C)

S. Amrith et al. (eds.), *Ocular Adnexal Lesions*, https://doi.org/10.1007/978-981-13-3798-7_21

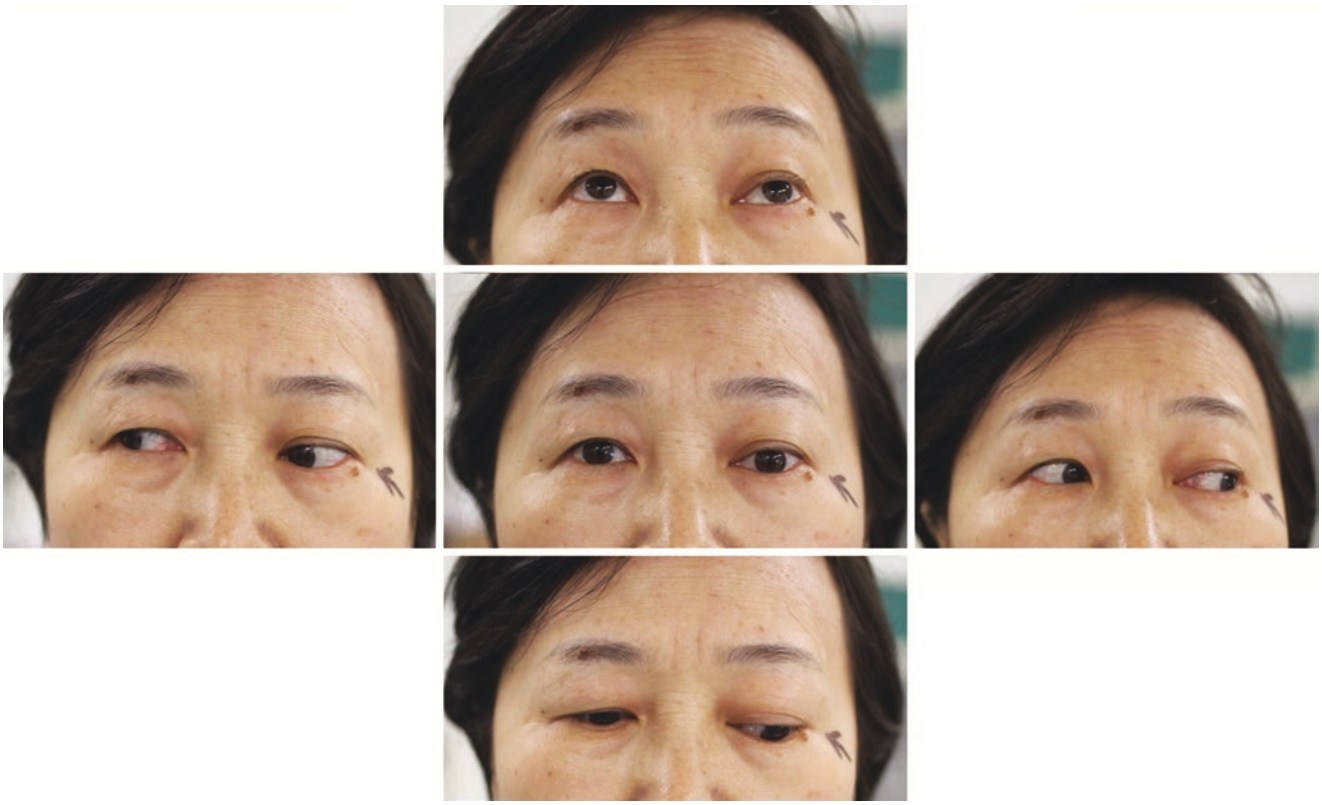

Fig. 21.1 Clinical picture of the patient showing a left non-axial proptosis with mild fullness of the upper eyelid, hypoglobus and mechanical limitation of the same eye on upgaze

Table 21.1 CLOSE summary

*C*linical process: mass effect
*L*ocation: left superior orbit
*O*nset: subacute
*S*igns and symptoms: asymmetry between two eyes
*E*pidemiology: middle-aged Asian woman

sequences. It had a lobulated appearance and seemed to indent the globe while displacing the SR-LPS complex downwards (Fig. 21.2).

Intervention

The patient underwent an anterior orbitotomy and removal of the lesion through the upper lid crease incision. The lesion was well encapsulated and purplish in colour, and after exsanguinating and decompressing it with a needle, it was delivered with blunt dissection and a cryoprobe traction (Fig. 21.3) and sent for histopathology.

Histopathology

The encapsulated, lobulated nodule, with cut section showing a spongy, reddish appearance was subjected to histopathology. Microscopic examination showed a well-circumscribed nodule composed of numerous dilated vascular channels lined by bland-appearing endothelial cells containing blood. Focal intraluminal thrombi were noted (Fig. 21.4).

The features were consistent with a diagnosis of cavernous venous malformation.

Management

The patient developed ptosis in the left eye in the immediate post-operative period but recovered completely within 3 months. She has been symptom-free since.

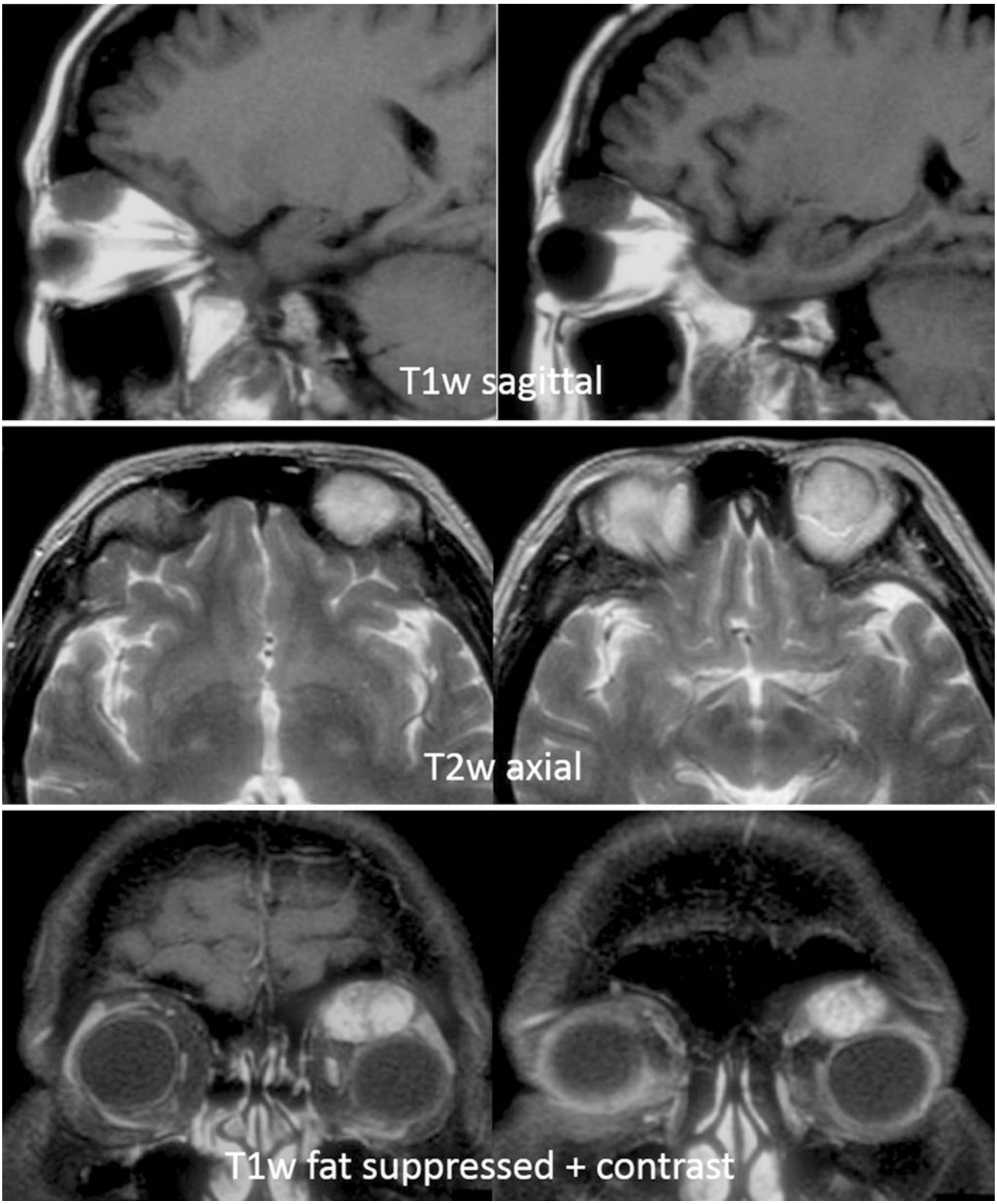

Fig. 21.2 Sagittal T1w, axial T2w and coronal T1w-FS + C sequences showing a well-circumscribed extraconal mass, isointense to brain on T1w and hyperintense on T2w with patchy post-contrast enhancement

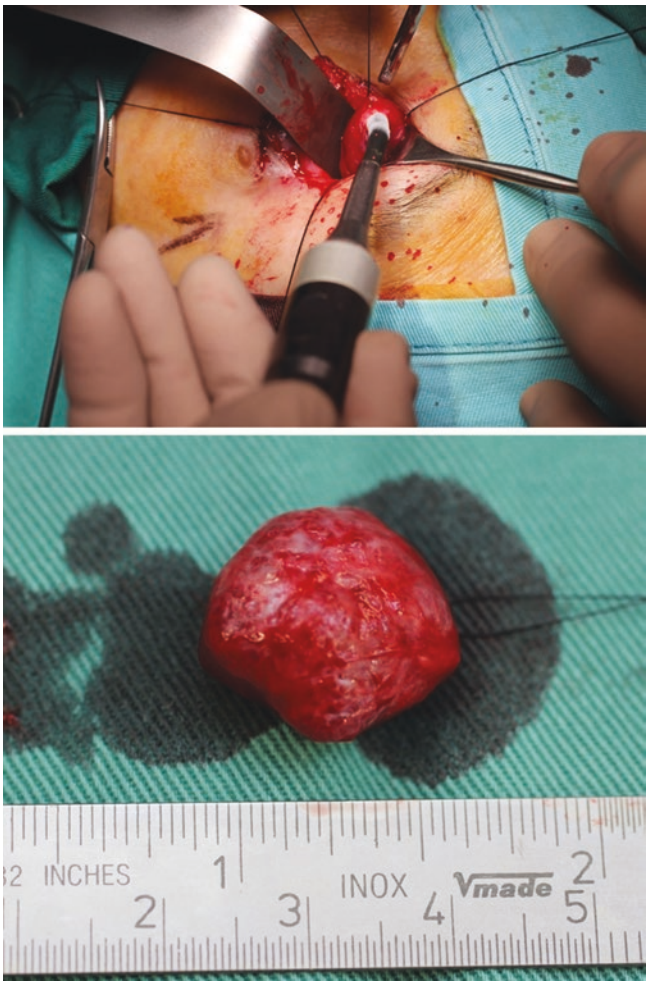

Fig. 21.3 The top picture shows the mass being removed through the upper lid crease incision using the cryoprobe with the lower picture showing the removed mass

Discussion

According to the International Society for the Study of Vascular Anomalies (ISSVA), the cavernous haemangiomas are classified as a 'low flow, non-distensible cavernous venous malformations'. This classification was arrived at by understanding of the histochemical characterisation and biological behaviour. It is believed that a neovascular impulse (vascular endothelial growth factor or VEGF) following intraluminal thrombosis is responsible for the slow growth of the lesion. Maffucci syndrome is a sporadic disease characterised by the presence of multiple enchondromas associated with multiple cavernous haemangiomas and phleboliths. In some cases, lymphangiomas may also be apparent.

Clinically, patients present with proptosis, diplopia, and visual disturbances associated with mechanical motility restriction and occasional axonal compression of the optic nerve.

Computerised tomography (CT) scan shows a well-circumscribed lesion with homogeneous soft-tissue density with bone remodeling in long-standing cases. With contrast, there is focal heterogeneous enhancement during the early phase and diffuse contrast enhancement in the late phase. On MRI, in T1-weighted images, the mass lesion appears isointense to muscle and grey matter and hypointense to fat. In T2-weighted images, it is hyperintense to fat and the brain. With contrast, the enhancement, like in CT scan, is progressive over time, being patchy and heterogeneous in the early phases to a more uniform enhancement in the later phases.

Treatment is surgical, with complete removal performed either through an anterior or a lateral orbitotomy. The main indication is a disfiguring proptosis or visual impairment. In the early asymptomatic cases, observation is a valid option.

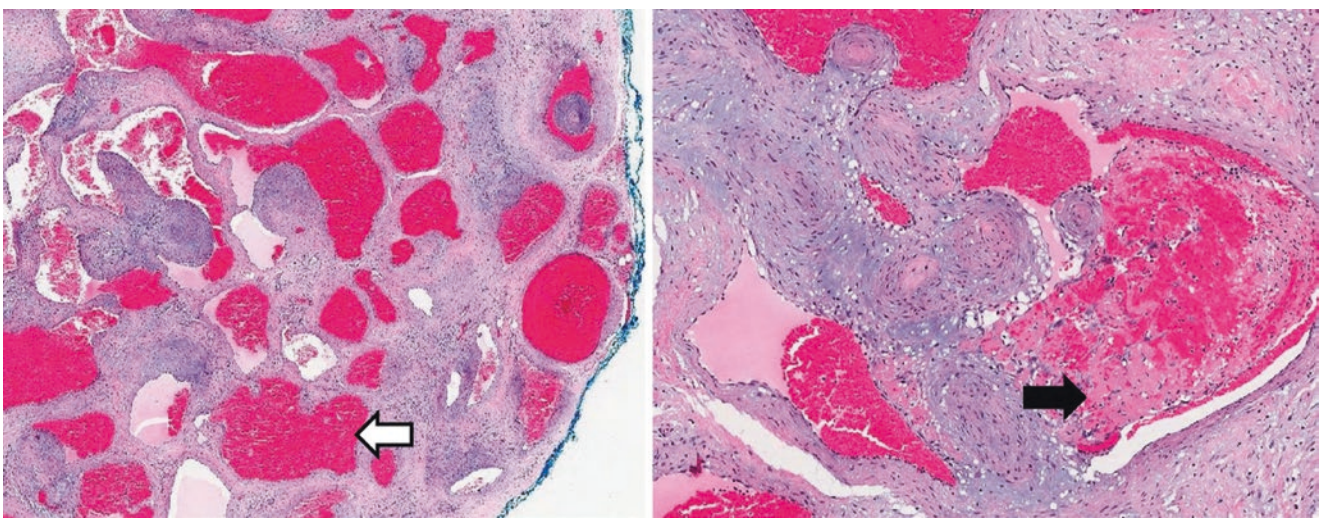

Fig. 21.4 Left – There is a well-circumscribed nodular lesion composed of irregularly shaped dilated vascular channels containing blood (white arrow). Right – Focal intraluminal thrombus, with fibrin formation (black arrow). Left: HE stain, 20× magnification. Right: HE stain, 40× magnification

Surgery is fairly easy because of its pseudo-encapsulation, loose attachment to the surrounding structures and slow venous supply.

Sclerotherapy with bleomycin or a stereotactic radiotherapy may be an option for lesions that are particularly difficult to resect because of their deep orbital position and when excision is likely to damage extraocular muscles, motor and sensory nerves and the optic nerve.

Learning Points

Non-distensible cavernous venous malformations (cavernous haemangiomas) are common vascular malformations of the orbit. Their diagnosis should be considered in all cases of slowly progressive, painless, proptosis. They may occur both intraconally and extraconally, although the former is more common. Both CT and MRI show characteristic features that make the diagnosis relatively easy. Surgical removal is the treatment of choice and curative.

Further Reading

1. Calandriello L, Grimaldi G, Petrone G, et al. Cavernous venous malformation (cavernous hemangioma) of the orbit: current concepts and a review of the literature. Surv Ophthalmol. 2017;62:393–403.
2. Jayaram A, Cohen LM, Lissner GS, Karagianis AG. A retrospective review of cases preoperatively diagnosed by radiologic imaging as cavernousvenous malformations. Orbit. 2017;36(3):128–34.
3. McNab AA, Selva D, Hardy TG, O'Donnell B. The anatomical location and laterality of orbital cavernous haemangiomas. Orbit. 2014;33(5):359–62.
4. Rootman DB, Heran MK, Rootman J, White VA, Luemsamran P, Yucel YH. Cavernous venous malformations of the orbit (so-called cavernous haemangioma): a comprehensive evaluation of their clinical, imaging and histologic nature. Br J Ophthalmol. 2014;98(7):880–8.
5. http://www.issva.org/Userfiles/file/ISSVA-Classification-2018.pdf.

Arteriovenous Malformation: Carotid-Cavernous Fistula

22

Stephanie Ming Young, Shantha Amrith, Eric Ting, and Gangadhara Sundar

Introduction

Arteriovenous anomalies are broadly divided into arteriovenous malformations and arteriovenous fistulas (Fig. 19.1). Carotid-cavernous sinus fistula (CCF) is an example of the latter, where a pathologic vascular shunt between the carotid arterial system and the cavernous sinus, or rarely, directly to an ophthalmic or orbital vein. The Barrow classification for CCF divides them into direct (type A) or indirect (types B–D). Type A, high-flow fistula, typically occurs in young adults after trauma resulting in direct communication between the internal carotid artery and the cavernous sinus. Types B and C result from shunts between the cavernous sinus and smaller branches of the internal carotid artery or the external carotid artery, respectively. Type D is a combination of fine branches of both the internal and the external carotid artery communicating with the cavernous sinus.

Case Scenario

A 58-year-old Chinese male with no significant past medical history of note presented with left eye redness and discomfort of 3 years' duration. On close questioning he admitted to a head trauma prior to developing symptoms. He was initially diagnosed with "allergic conjunctivitis" and prescribed topical eye drops. However his proptosis and swelling increased over 1 year and was subsequently diagnosed with "pseudotumour" and was managed conservatively. He suffered from worsening of proptosis and increased intraocular pressure (IOP), and at this point, he sought an opinion from our institution.

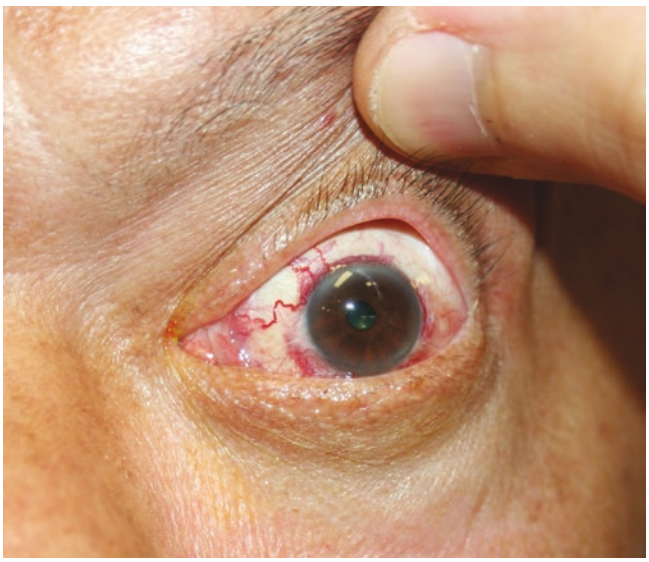

Fig. 22.1 Left conjunctival injection with 360° corkscrew vessels

On examination, his visual acuity was 6/7.5 in the affected eye with raised IOP of 26 mm Hg, but no evidence of optic nerve dysfunction. He had a left eye proptosis of 5 mm. Anterior segment examination revealed tortuous corkscrew-type blood vessels in his left eye (Fig. 22.1) associated with pulsating exophthalmos and an ocular bruit.

CLOSE summary is given in Table 22.1.

Differential Diagnosis

- Carotid-cavernous sinus fistula (CCF)
- Thyroid eye disease (TED)

S. M. Young · S. Amrith (✉) · G. Sundar
Department of Ophthalmology, National University Hospital, Singapore

Department of Ophthalmology, Yong Loo Lin School of Medicine, National University of Singapore, Singapore
e-mail: stephanie.young@nuhs.edu.sg; shantha_amrith@nuhs.edu.sg; gangadhara_sundar@nuhs.edu.sg

E. Ting
Department of Diagnostic Imaging, National University Hospital, Singapore

Department of Diagnostic Imaging, Yong Loo Lin School of Medicine, National University of Singapore, Singapore

Advanced Medicine Imaging, Singapore

S. Amrith et al. (eds.), *Ocular Adnexal Lesions*, https://doi.org/10.1007/978-981-13-3798-7_22

- Orbital inflammatory disease (OID)
- Chronic conjunctivitis
- Episcleritis/scleritis
- Distensible venous malformation

Imaging

Computerised tomography (Fig. 22.2a, b) showed a dilated left superior ophthalmic vein as well as enlargement of the extraocular muscles compared to the right. There was convex lateral border of the left cavernous sinus. Bone window CT (Fig. 22.2c) showed fracture of the left sphenoid sinus with displaced fragments. MR angiography (MRA) (Fig. 22.2d, e) demonstrated a direct carotid-cavernous sinus fistula and dilated left superior ophthalmic vein. Conventional digital subtraction angiography (Fig. 22.2f) confirmed the presence of high-flow carotid-cavernous fistula directly supplied by the left carotid artery.

Table 22.1 CLOSE summary

*C*linical process: vascular with flow abnormality
*L*ocation: left orbit
*O*nset: chronic
*S*igns and symptoms: proptosis (pulsating exophthalmos), ocular bruit, conjunctival injection and raised IOP
*E*pidemiology: Chinese male in his late 50s

Intervention

The patient underwent four-vessel angiography which revealed a left direct, high-flow CCF filling the markedly dilated superior ophthalmic vein (Fig. 22.3a). Conventional embolisation was attempted through the right femoral vein. However, the microcatheter could not be advanced into the cavernous sinus. Repeated attempts via the left common femoral vein into the left internal jugular vein to access the facial vein were also not possible as the origin of the facial vein was too tortuous. Decision for transorbital embolisation was made. The orbital septum was opened to identify the superior ophthalmic vein, which was found to be pulsatile, arterialised and dilated. A small incision was made to the vein, and a catheter was inserted in a retrograde manner towards the fistula point. After confirmation of patency by intraoperative angiography, CCF obliteration was carried out using detachable neurocoils. These platinum coils were

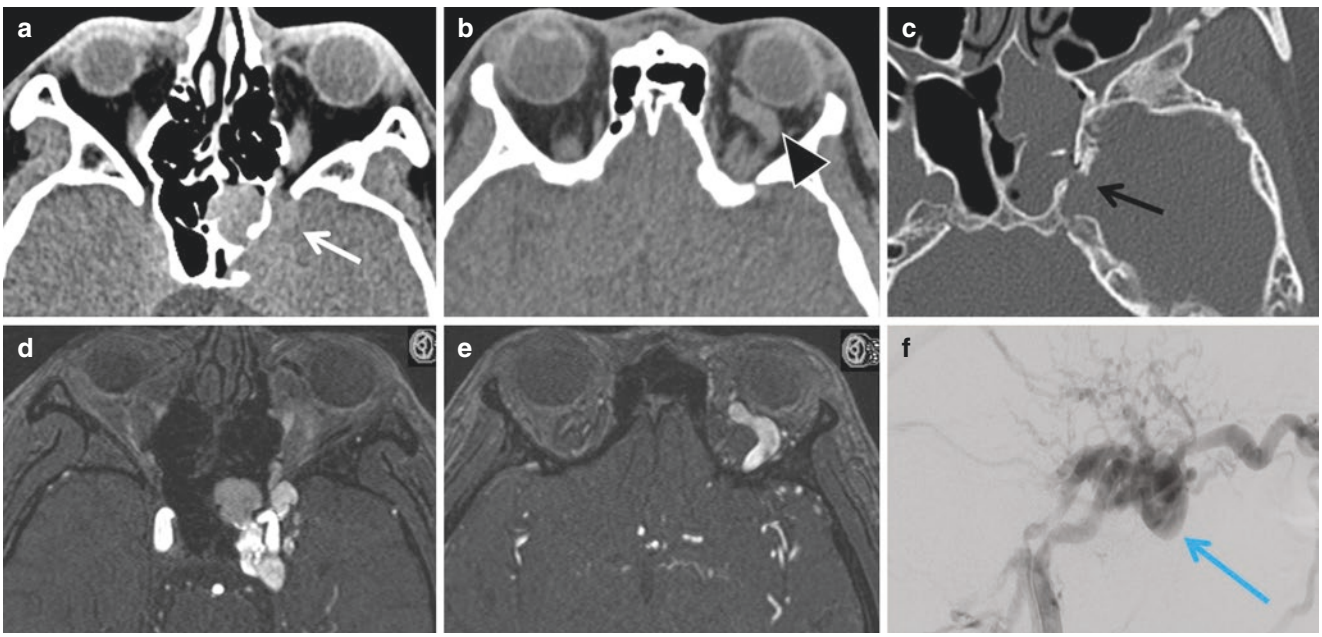

Fig. 22.2 Traumatic (direct) carotid-cavernous fistula. Axial contrast-enhanced CT (**a**, **b**) shows bulging and convex lateral border of the left cavernous sinus (white arrow) and dilatation of the left superior ophthalmic vein (black arrowhead). Bone algorithm (**c**) shows a fracture of the left sphenoid sinus lateral wall with displaced fragments in the region of the cavernous sinus (black arrow). MRA (**d**, **e**) better demonstrates the direct carotid-cavernous fistula and the dilated left superior ophthalmic vein. Conventional digital subtraction angiogram confirms the presence of a high-flow carotid-cavernous fistula (blue arrow) supplied directly by the left ICA. There is a paucity of arterial flow distally (**f**)

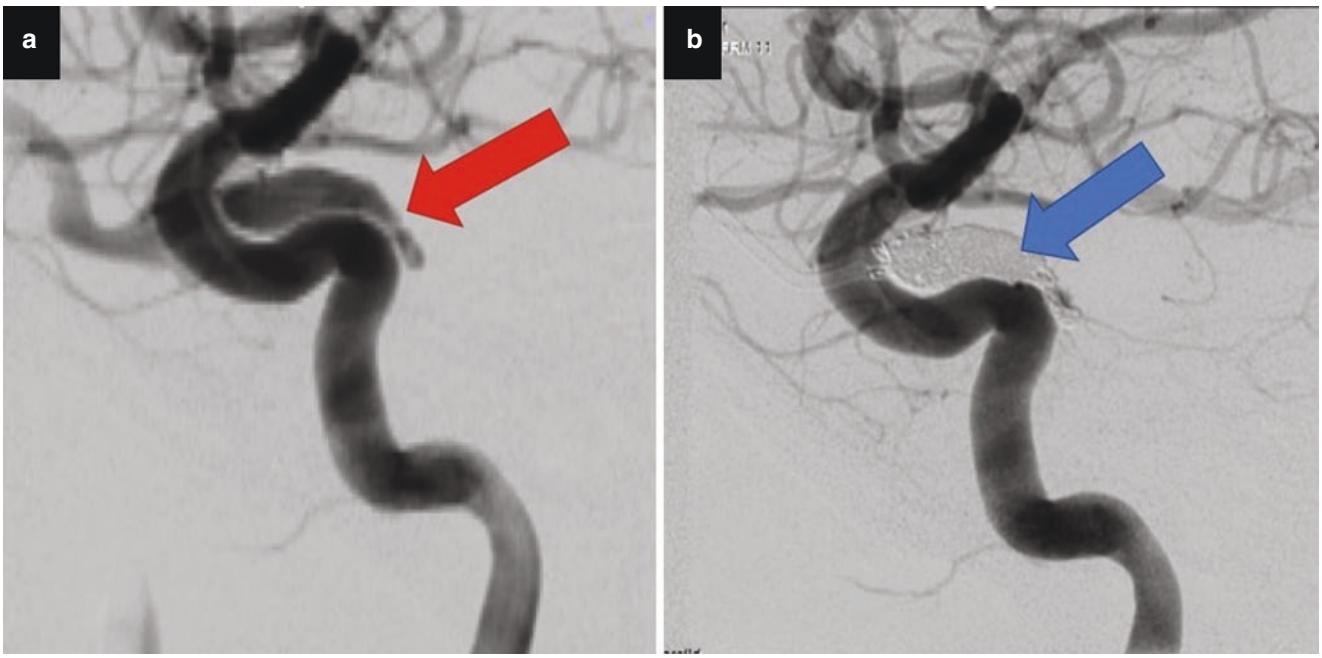

Fig. 22.3 (**a**) Conventional four-vessel angiography with digital subtraction revealed a left direct, high-flow CCF filling the markedly dilated superior ophthalmic vein (red arrow). (**b**) CCF obliteration was carried out using platinum coils (blue arrow). Adequate closure of the fistula was confirmed by angiography

deployed to occlude the fistulous point (Fig. 22.3b) and the proximal superior ophthalmic vein, from a posterior to anterior manner. Once adequate closure of the fistula was confirmed by angiography, the catheter was withdrawn and the wound closed.

Discussion

Carotid-cavernous sinus fistula (CCF) signs and symptoms are related to increased blood flow and volume in the involved cavernous sinus(es), resulting in increased venous pressures and congestion.

Ophthalmic manifestations of CCF include:

- Bruit
- Decreased visual acuity
- Increased IOP
- Diplopia
- Ophthalmalgia
- Proptosis
- Chemosis
- Headache
- Blepharoptosis
- Palsy of CN III, IV, V and VI

Funduscopic examination often demonstrates venous stasis retinopathy, dilated retinal veins and retinal haemorrhages. Severe proptosis and chemosis may result in keratopathy and corneal ulceration.

While type A presents soon after a closed head injury, typically in young adult males, indirect CCF may be insidious in onset given the reduced vascular pressures from the indirect nature of the vascular shunts. Owing to the protean manifestations of the disease, they may be commonly misdiagnosed, or there may be a delay in diagnosis.

Computerised tomography (CT) is the initial imaging modality in most institutions. Features to look out for on CT include superior ophthalmic vein and/or inferior ophthalmic vein dilatation, extraocular muscle enlargement, proptosis, cavernous sinus enlargement and early contrast opacification and skull-base fracture (in the setting of traumatic CCF). CT angiography (CTA) permits additional evaluation of the arterial and venous structures. MRI and MRA show mostly the same information as CT and CTA, respectively. However, conventional catheter angiography remains the gold standard in the diagnosis, classification and evaluation of CCF. It permits optimal evaluation of inflow and outflow vasculature, which is critical for treatment planning and deciding on possible routes for endovascular neuroradiologic therapy.

Treatment

Untreated high-flow fistulae are almost always blinding, and urgent treatment is indicated once the patient is stable. The more common low-flow fistulae were left untreated in the past era of limited interventional radiological expertise, awaiting spontaneous resolution which may take months or years with possible residual visual loss and disability. However, in the modern era of sophisticated interventional radiological techniques, and advances in liquid embolic agents and metallic coils, definitive intervention should be considered in all patients with significant symptoms. Endovascular obliteration is now the treatment of choice for closure of both direct and indirect CCFs.

The transvenous approach is recommended for CCF closure, and this is conventionally achieved transfemorally via the inferior petrosal sinus (IPS). If the IPS is inaccessible due to occlusion or lack of visualisation, the cavernous sinus may be approached via the facial vein. However, this method is often unsuccessful due to tortuosity of the facial venous system. When all venous routes have been exhausted, surgical exposure and direct cannulation of the superior ophthalmic vein (SOV) is a good alternative to access the cavernous sinus.

Learning Points

- CCF has a wide variety of clinical manifestations.
- Dural CCF can masquerade as chronic conjunctivitis, TED, OID, etc.
- Both direct and dural CCFs may potentially lead to severe visual dysfunction and should be diagnosed and treated accordingly.
- When all venous routes have been exhausted, the transorbital approach via the superior ophthalmic vein remains a viable alternative to access the fistula.

Further Reading

1. Ellis JA, Goldstein H, Connolly ES, Meyers PM. Carotid-cavernous fistulas. Neurosurg Focus. 2012;32(5):E9. https://doi.org/10.3171/2012.2.FOCUS1223.
2. Gupta AK, Purkayastha S, Krishnamoorthy T, et al. Endovascular treatment of direct carotid cavernous fistulae: a pictorial review. J Neuroradiol. 2006;48:831.
3. Korkmazer B, Kocak B, Tureci E, Islak C, Kocer N, Kizilkilic O. Endovascular treatment of carotid cavernous sinus fistula: a systematic review. World J Radiol. 2013;5(4):143–55. https://doi.org/10.4329/wjr.v5.i4.143.
4. Kupersmith MJ, Berenstein A, Flamm E, Ransohoff J. Neuroophthalmologic abnormalities and intravascular therapy of traumatic carotid cavernous fistulas. Ophthalmology. 1986;93:906.
5. Miller NR. Diagnosis and management of dural carotid–cavernous sinus fistulas. Neurosurg Focus. 2007;23(5):E13.
6. Phan K, Xu J, Leung V, et al. Orbital approaches for treatment of carotid cavernous fistulas: a systematic review. World Neurosurg. 2016;96:243–51.
7. Ringer AJ, Salud L, Tomsick TA. Carotid cavernous fistulas: anatomy, classification, and treatment. Neurosurg Clin N Am. 2005;16:279.

Part VI

Benign Neoplasms: Eyelid

Pilomatrixoma

23

Stephanie Ming Young, Shantha Amrith, Bingcheng Wu, Min En Nga, and Gangadhara Sundar

Introduction

Pilomatrixoma (pilomatricoma) is a benign skin neoplasm arising from the matrix cells at the base of the hair. It was originally described as calcified epithelioma of sebaceous glands, but later the term pilomatrixoma was suggested to denote its origin. Some authors have reported a bimodal peak during the first and sixth decades of life, with a male:female ratio of 2:3. The most frequent location is the head and neck region (>50% of cases). Involvement of the face has been reported in frontal, temporal, cheek, periorbital and preauricular areas. It must be considered in the differential diagnosis of hard masses involving the facial region.

Clinical Scenario

A 46-year-old male with no significant past medical history presented with a left eyebrow lump of 1 month's duration. The lump was progressively enlarging and associated with mild discomfort and redness, but did not cause any discharge or visual symptoms. He denied any previous history of trauma.

On examination, there was a left eyebrow mass measuring 2 × 2 cm (Fig. 23.1). It was mobile, fixed to the skin but not to underlying bone. It was pointing superiorly, but had no evidence of preseptal cellulitis. The rest of the ophthalmic examination did not reveal any abnormalities (Table 23.1).

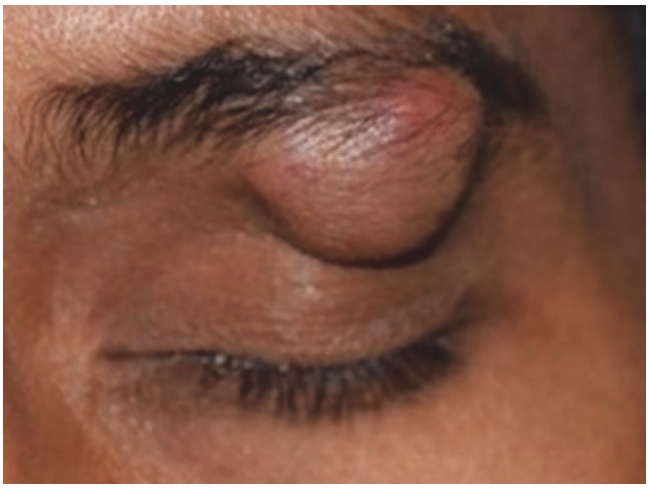

Fig. 23.1 Left sub-brow nodule, attached to overlying skin but mobile and not fixed to underlying bone

Table 23.1 CLOSE summary

*C*linical process: progressively enlarging lump
*L*ocation: sub-brow skin
*O*nset: subacute
*S*igns and symptoms: mass lesion
*E*pidemiology: adult Malay male

Differential Diagnosis

- Sebaceous cyst
- Dermal adnexal tumours

S. M. Young · S. Amrith (✉) · G. Sundar
Department of Ophthalmology, National University Hospital, Singapore

Department of Ophthalmology, Yong Loo Lin School of Medicine, National University of Singapore, Singapore
e-mail: stephanie.young@nuhs.edu.sg; shantha_amrith@nuhs.edu.sg; gangadhara_sundar@nuhs.edu.sg

B. Wu
Department of Pathology, National University Hospital, Singapore

M. E. Nga
Department of Pathology, National University Hospital, Singapore

Department of Pathology, Yong Loo Lin School of Medicine, National University of Singapore, Singapore

S. Amrith et al. (eds.), *Ocular Adnexal Lesions*, https://doi.org/10.1007/978-981-13-3798-7_23

- Sweat gland tumours: Syringoma, eccrine hidradenoma, eccrine hidrocystoma and apocrine hidrocystoma
- Hair follicle tumours: Trichoepithelioma, trichilemmoma and pilomatrixoma (pilomatricoma)

Intervention

The patient underwent excision biopsy of the cyst (Fig. 23.2).

Histopathology

There was a well circumscribed dermal nodule lined by squamous and basaloid cells with round to oval nuclei, occasional nucleoli and scant cytoplasm. Areas of the lining epithelium appeared to transit to masses of eosinophilic material containing ghost cells within the cyst. The ghost cells showed holes where nuclei once were and had more eosinophilic cytoplasm. The features are consistent with a pilomatricoma (Fig. 23.3).

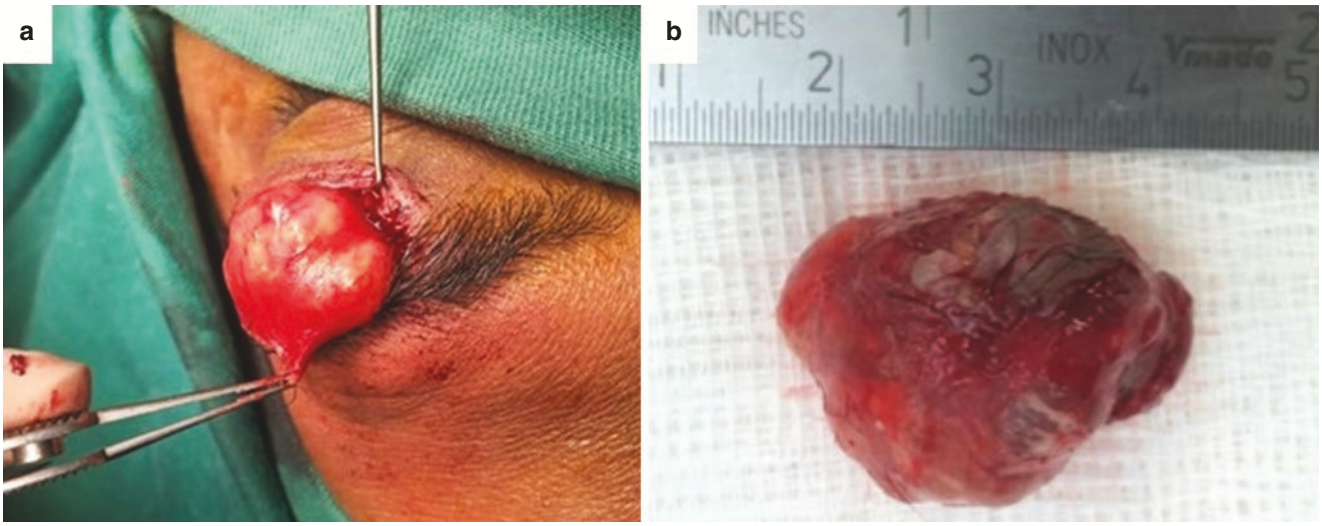

Fig. 23.2 (**a**) Excision biopsy of sub-brow lump performed through an elliptical skin excision, (**b**) well-encapsulated dermal tumour measuring approximately 2 cm in diameter

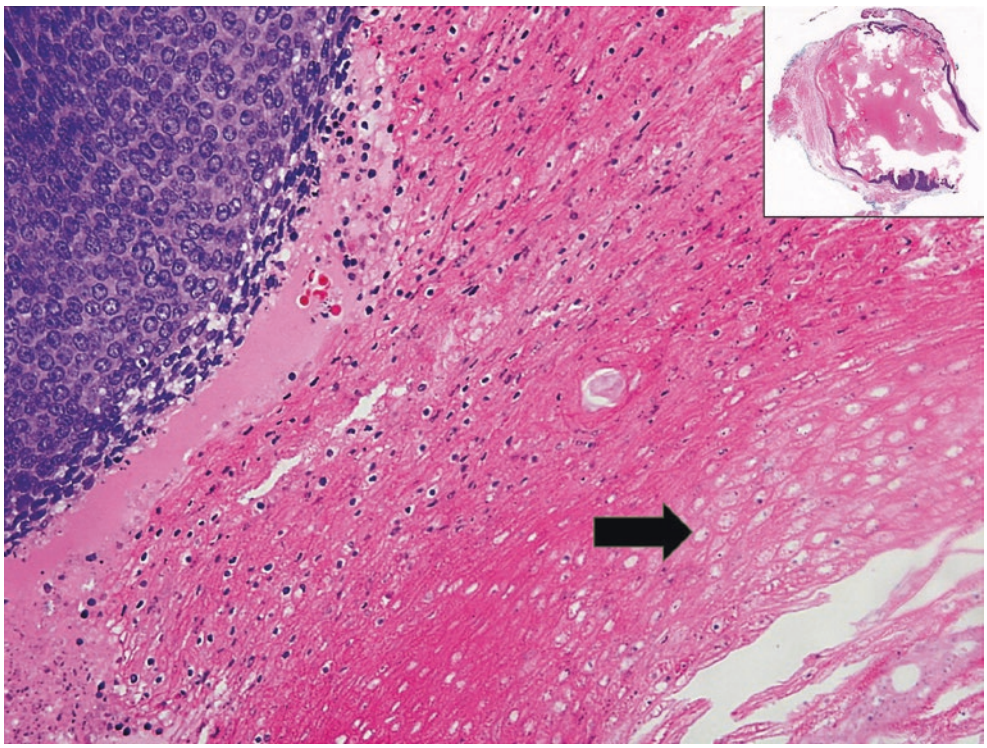

Fig. 23.3 Basaloid cells (top left corner) transitions into eosinophilic material containing "ghost cells". Some empty holes where nuclei used to be are indicated by the black arrow HE stain, 200× magnification. Inset shows a circumscribed nodule in the dermis. HE stain, 1× magnification

Discussion

The most common site for pilomatrixomas is in the head and face. In the periorbital region, pilomatrixoma usually involves the eyebrows, possibly because of high density of hair follicles. It usually presents as a solitary, slow-growing, superficial, mobile, hard mass ranging in size from 0.5 to 5 cm in diameter. It is often asymptomatic, and the overlying skin may exhibit a bluish-red discoloration or ulceration. Multiple occurrences and familial disease are associated with Gardner syndrome, sarcoidosis, and Turner syndrome.

The clinical diagnosis of a pilomatrixoma is usually difficult, and they have variably been diagnosed preoperatively as eyelid cysts (mainly sebaceous and dermoid cysts) and rarely as eyelid tumours such as papilloma, keratoacanthoma, sebaceous cell carcinoma and basal cell carcinoma. Histopathologic diagnosis is based on the presence of basophilic, as well as shadow cells, which may be associated with foreign-body giant cells, calcification, and ossification. The malignant counterpart (pilomatrix carcinoma) is extremely rare, and characterized by actively proliferating, hyperchromatic, pleomorphic basaloid cells, atypical mitosis, tumour necrosis, architectural asymmetry, and infiltrative growth pattern.

Treatment

Surgical excision is the treatment of choice. The mass is usually well encapsulated. If the margins are ill-defined or adherent to the surrounding tissues, malignancy can be suspected. Cytological sampling errors with fine-needle aspiration cytology (FNAC) may lead to misdiagnosis, especially if there are no ghost cells in the aspirate.

Learning Points

Pilomatrixoma is an uncommon, benign, cutaneous tumour with a characteristic histological appearance. Preoperative diagnosis is difficult, and thus it must be considered in the differential diagnosis of hard masses involving the facial region.

Further Reading

1. Forbis R Jr, Helwig EB. Pilomatrixoma (calcifying epithelioma). Arch Dermatol. 1961;83:606–18.
2. Kaveri H, Punnya A. Pilomatricoma: a dermal analog of calcifying odontogenic cyst. Indian J Dent Res. 2008;19:261–3.
3. Levy J, Ilsar M, Deckel Y, Maly A, Anteby I, Pe'er J. Eyelid pilomatrixoma: a description of 16 cases and a review of the literature. Surv Ophthalmol. 2008;53:526–35.

Plexiform Neurofibroma

24

Shantha Amrith, Stephanie Ming Young, Eric Ting, Bingcheng Wu, Min En Nga, and Gangadhara Sundar

Introduction

The manifestations of neurofibromatosis (NF) in the ocular adnexa consist of plexiform neurofibroma in the eyelids, often with orbital extension, and sphenoid wing hypoplasia. NF may be associated with tumours such as optic nerve gliomas, meningiomas or schwannomas. It is the most common peripheral neural tumour of the ocular adnexa causing hypertrophy of periocular tissues, resulting in mechanical ptosis with a characteristic S-shaped deformity in the upper eyelid. The criteria for diagnosis of neurofibromatosis 1 (NF-1) are given in Table 24.1.

Table 24.1 Diagnostic criteria for NF-1 (National Institute of Health Criteria)

Major criteria	Café-au-lait spots Intertriginous freckling Neurofibroma Iris hamartoma (Lisch nodules) CNS tumours Pseudoarthrosis Sphenoid dysplasia
Minor criteria	Small stature Microcephalus Scoliosis Pectus excavatum

Clinical Scenario

An 18-month-old Chinese girl presented with left upper eyelid swelling and drooping since birth. It was painless and increased in size slightly on crying.

On examination, there was fullness in the left upper lid (Fig. 24.1) with an S-shaped deformity and a mechanical ptosis (MRD 1 of −2 mm). There was ectropion of the upper lid exposing the conjunctiva that showed keratinization. There was also a left hypoglobus and non-axial proptosis. On palpation, the left upper eyelid felt soft, like a bag of worms. Ocular motility was restricted on extreme left gaze. Reliable visual acuities could not be obtained. Refraction did not show any significant astigmatism. The anterior and posterior segment examination did not show any abnormality. On systemic examination, she was noted to have multiple café-au-lait spots and axillary freckling.

CLOSE summary is in Table 24.2.

Differential Diagnosis

- Plexiform neurofibroma
- Capillary haemangioma
- Lymphatic-venous malformation

S. Amrith (✉) · S. M. Young · G. Sundar
Department of Ophthalmology, National University Hospital, Singapore

Department of Ophthalmology, Yong Loo Lin School of Medicine, National University of Singapore, Singapore
e-mail: shantha_amrith@nuhs.edu.sg; stephanie.young@nuhs.edu.sg; gangadhara_sundar@nuhs.edu.sg

E. Ting
Department of Diagnostic Imaging, National University Hospital, Singapore

Department of Diagnostic Imaging, Yong Loo Lin School of Medicine, National University of Singapore, Singapore

Advanced Medicine Imaging, Singapore

B. Wu
Department of Pathology, National University Hospital, Singapore

M. E. Nga
Department of Pathology, National University Hospital, Singapore

Department of Pathology, Yong Loo Lin School of Medicine, National University of Singapore, Singapore

S. Amrith et al. (eds.), *Ocular Adnexal Lesions*, https://doi.org/10.1007/978-981-13-3798-7_24

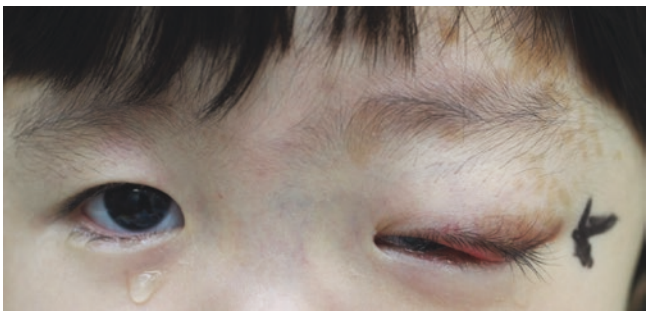

Fig. 24.1 Clinical photograph of the left upper eyelid mass, note pigmentation on the skin and ectropion of the lid margin laterally

Table 24.2 CLOSE summary

*C*linical process: benign infiltrative mass
*L*ocation: left upper eyelid and orbit
*O*nset: congenital
*S*igns and symptoms: painless upper eyelid mass with mechanical ptosis
*E*pidemiology: young Chinese girl

Imaging

Magnetic resonance imaging (MRI) of the orbits (Fig. 24.2) showed a mass in the left cavernous sinus with fingerlike extension into the superolateral orbit through the superior orbital fissure. The mass was isointense to grey matter on T1w, and T2w images, and showed avid enhancement on the post-contrast study. Numerous faint flow voids were seen in this lesion. Tortuous channels were seen in the intraconal and retrobulbar fat. The lacrimal gland was enlarged and enhanced with contrast. Eyelid lesion was seen to extend into the lateral part of the orbit along the lateral rectus muscle.

Intervention

The child underwent left upper lid ptosis correction, with resection of tumour-infiltrated levator, and horizontal shortening of the eyelid. The tissue was sent for histopathology.

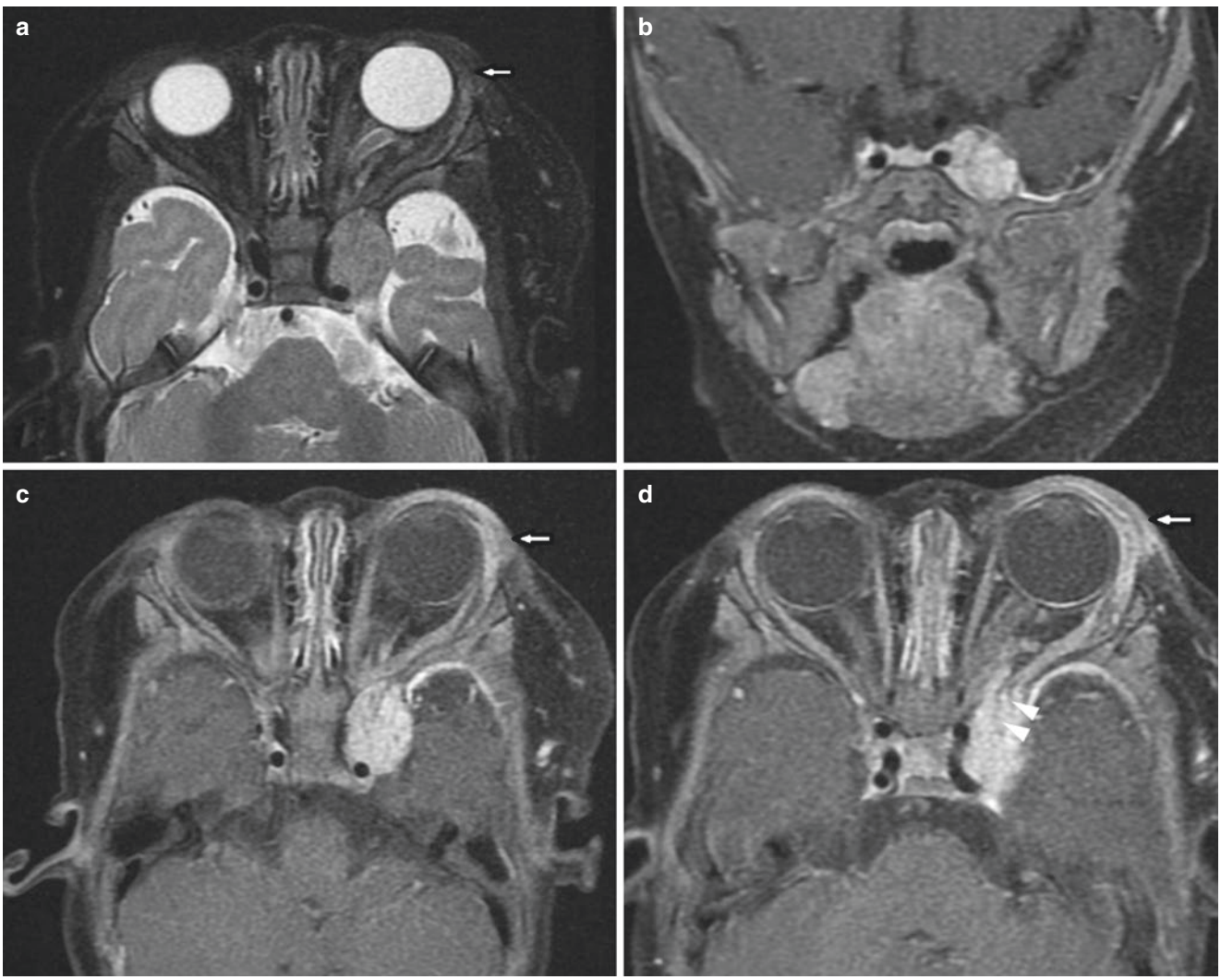

Fig. 24.2 Axial (**a**) and coronal (**b**) T2w-FS and axial (**c**, **d**) T1w-FS + contrast MRI of the orbits show avidly enhancing enlargement of the trigeminal ganglion in Meckel's cave and the lateral wall of the cavernous sinus with fingerlike extension into the superolateral orbit through the superior orbital fissure (arrowheads). White arrow shows eyelid lesion, lacrimal gland and extension into lateral orbit

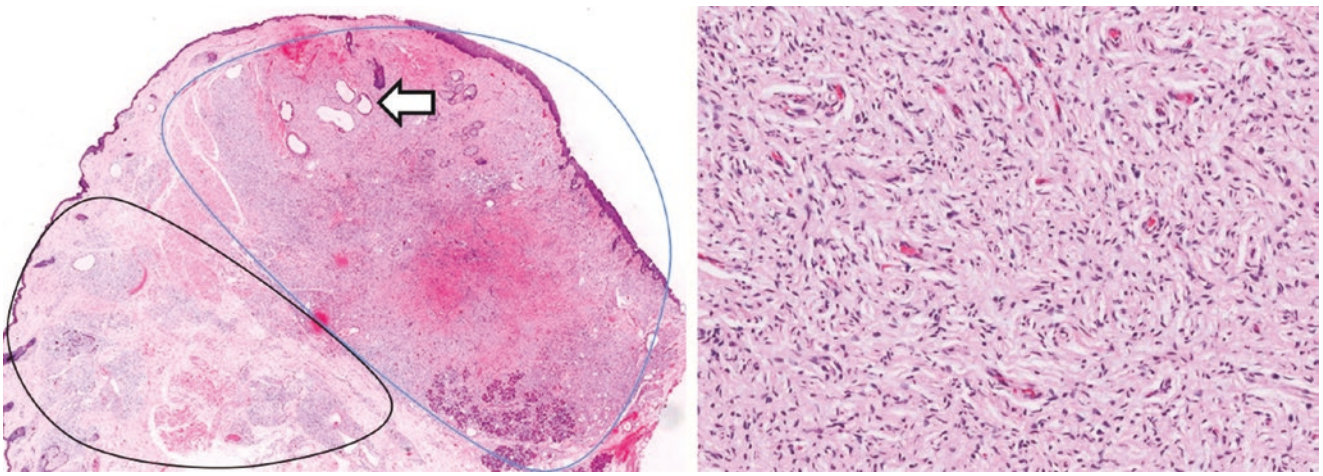

Fig. 24.3 The histopathology shows sub-epithelial spindle cell neoplasm with lobulated (outlined in blue) and plexiform (outlined in black) growth patterns. The spindle cell neoplasm grows around, but does not destroy pre-existing lacrimal glands (white arrow). The tumour is composed mainly of haphazardly arranged short spindle cells with bland-appearing, wavy nuclei. Left: HE, 20× magnification. Right: HE, 100× magnification

Histopathology

Sections showed skin with sebaceous glands and a sub-epithelial spindle cell neoplasm with lobulated and plexiform growth patterns. The spindle cell neoplasm was seen around pre-existing structures such as the lacrimal gland and was composed mainly of haphazardly arranged short spindle cells with bland-appearing, wavy nuclei (Fig. 24.3). There was also an admixture of fibroblasts, mast cells, and histiocytes. Similar features were found in the preaponeurotic tissue and levator palpebrae superioris muscle. Lesional cells were positive for S-100. The lesion extended to the base of the resection. There was no evidence of malignancy. The features were consistent with a diagnosis of plexiform neurofibroma.

Management

There was improvement in ptosis after surgery. The child was advised patching of the right eye daily. The visual acuity at 3 years was 3/3 and 3/18 by letter-matching in the right and left eyes, respectively, showing amblyopia of the left eye; therefore, the patching was continued. At the age of 4, there was recurrence of lid swelling and the ptosis. The child underwent a second procedure to debulk the tumour and correct the ptosis. At the age of 6, Snellen visual acuities were 6/6 and 6/18. Repeat MRI scans showed the cavernous sinus and the orbital masses to be stable.

Discussion

Neurofibromatosis 1 (NF-1) is an autosomal dominant condition that originates from the nerve sheath cells, and presents with variable penetrance of one in 2500–3000 live births. It is caused by a mutation in the *NF-1* tumour suppressor gene on chromosome 17q11.2.

Plexiform neurofibromas that occur in and around the eye have been termed as orbital-periorbital plexiform neurofibroma (OPPN). It may be present at birth or develop within the first year of life, grow rapidly during childhood and is fully developed by adulthood. It grows both in the subcutaneous and deep tissue planes along the distribution of the trigeminal nerve. In about 5–10% of cases, malignant transformation may occur.

Plexiform neurofibroma of the eyelid causes mass effect, and the overlying skin is thickened and often pigmented. It feels like a 'bag of worms' on palpation. It causes mechanical ptosis during the critical stage of visual development in the child. Careful evaluation of vision and correction of amblyopia are of utmost importance. Surgical treatment must be individualized, taking into consideration the disfigurement and functionality. The decision to perform early surgery for the ptosis will have to be titrated against the chances of amblyopia, and regrowth potential of the remnant tumour, which is high in childhood. The surgery may be complicated by the fact that the tumour is extensively infiltrative and highly vascularised.

Absence of sphenoidal wing causes the temporal lobe to herniate into the orbit, causing pulsatile proptosis.

Optic nerve glioma, a pilocytic astrocytoma, occurs in about 5–15% of patients with NF-1. Bilateral involvement of

the optic nerve is pathognomonic of NF-1 and causes fusiform enlargement of the optic nerve. The buckling of the nerve gives a dotted 'i' sign on imaging.

Schwannomas and meningiomas occur in neurofibromatosis 2 (NF-2), and presence of bilateral vestibular schwannoma is diagnostic of NF-2.

Learning Points

- Individualized treatment plan must be drawn after proper preoperative assessment, taking into consideration the disfigurement and functionality that a patient with NF-1 is experiencing.
- The tumour has great propensity for regrowth, and patients have to be counseled accordingly.
- The patient has to be investigated for associated lesions of NF-1 in the orbit.

Further Reading

1. Avery RA, Katowitz JA, Fisher MJ, Heidary G, Dombi E, Packer RJ, Widemann BC. Orbital/peri-orbital plexiform neurofibromas in children with neurofibromatosis type 1: multi-disciplinary recommendations for care. Ophthalmology. 2017;124(1):123–32.
2. Chaudhry IA, Morales J, Shamsi FA, Al-Rashed W, Elzaridi E, Arat YO, Jacquemin C, Oystreck DT, Bosley TM. Orbitofacial neurofibromatosis: clinical characteristics and treatment outcome. Eye (Lond). 2012;26(4):583–59.
3. National Institute of Health Consensus Development Conference. Neurofibromatosis Conference statement. Arch Neurol. 1988;45:575–8.

Part VII

Benign Neoplasms: Orbit

Schwannoma

25

Shantha Amrith, Stephanie Ming Young, Eric Ting, Bingcheng Wu, Min En Nga, and Gangadhara Sundar

Introduction

Although considered to be one of the commonest primary benign tumours of the orbit, orbital schwannomas are relatively rare. Their onset is insidious, and it grows very slowly causing minimal effect on the surrounding structures. It is a tumour that occurs typically in adults and presents as proptosis. Definitive treatment is complete surgical excision.

Clinical Scenario

A 23-year-old Indonesian female presented with progressive protrusion of her left eye of 2 years' duration, with recent onset of blurring of vision, not associated with pain or redness. On examination, her Snellen visual acuities were 6/6 and 6/9 in the right and left eyes, respectively. Examination of the left eye showed a relative afferent pupillary defect (RAPD) with red colour desaturation. Assessment of the colour vision using Ishihara isochromatic plates was normal. Fundus examination showed optic disc swelling with some striae temporal to the disc. There was some limitation of supraduction along with an axial proptosis of 3 mm (Fig. 25.1).

CLOSE summary is given in Table 25.1.

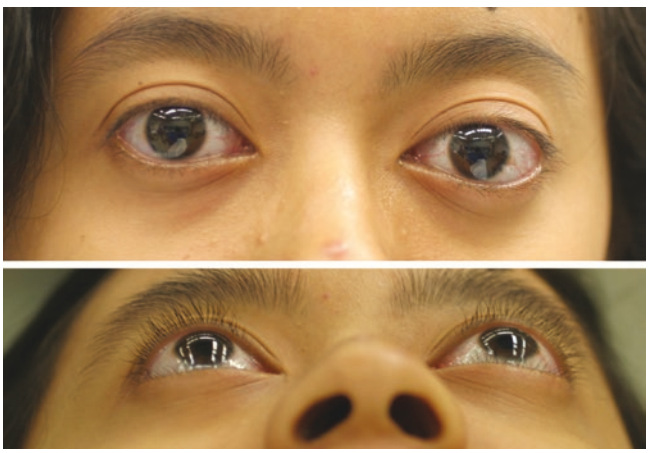

Fig. 25.1 Clinical picture showing proptosis of the left eye

Table 25.1 CLOSE summary

*C*linical process: benign mass lesion
*L*ocation: retrobulbar
*O*nset: chronic
*S*igns and symptoms: proptosis and blurring of vision
*E*pidemiology: young Indonesian female

S. Amrith (✉) · S. M. Young · G. Sundar
Department of Ophthalmology, National University Hospital, Singapore

Department of Ophthalmology, Yong Loo Lin School of Medicine, National University of Singapore, Singapore
e-mail: shantha_amrith@nuhs.edu.sg; gangadhara_sundar@nuhs.edu.sg

E. Ting
Department of Diagnostic Imaging, National University Hospital, Singapore

Department of Diagnostic Imaging, Yong Loo Lin School of Medicine, National University of Singapore, Singapore

Advanced Medicine Imaging, Singapore

B. Wu
Department of Pathology, National University Hospital, Singapore

M. E. Nga
Department of Pathology, National University Hospital, Singapore

Department of Pathology, Yong Loo Lin School of Medicine, National University of Singapore, Singapore

S. Amrith et al. (eds.), *Ocular Adnexal Lesions*, https://doi.org/10.1007/978-981-13-3798-7_25

Differential Diagnosis

- Non-distensible cavernous venous malformation (cavernous haemangioma)
- Schwannoma
- Meningioma
- Haemangiopericytoma/solitary fibrous tumour
- Thyroid eye disease

Imaging

Magnetic resonance imaging (MRI) (Fig. 25.2) showed a retrobulbar, intraconal mass in the left orbit. The mass was smooth, well defined, homogeneous, and isointense on T1w image. On T2w image, it showed cystic areas that were hyperintense. In post-contrast (T1w + C) images, the lesion was heterogeneous with peripheral rim enhancement. The mass was pushing the optic nerve and medial rectus medially. By the imaging characteristics, it appeared to be a benign lesion, raising the possibility of a schwannoma or a vascular malformation such as cavernous haemangioma.

Intervention

Through a lateral orbitotomy, the tumour was removed and sent for histopathology. The tumour appeared to arise from the frontal nerve.

Histopathology

Histopathology showed tumour tissue composed of spindle-shaped cells arranged in short fascicles (bundles). The nuclei were ovoid or elongated and showed no significant atypia. The cells had indistinct cell borders. The cellularity was variable. Nuclear palisading was seen in hypercellular areas (Fig. 25.3). Many of the blood vessels within the tumour had hyalinised (thickened, pink, and homogenous-appearing) walls. The tumour cells showed diffuse strong immunostaining for S-100 protein and were negative for epithelial membrane antigen. The features were consistent with those of a schwannoma.

Discussion

Orbital schwannoma is a benign peripheral nerve sheath tumour which can arise from cranial nerves III, IV, V, VI, and the ciliary ganglion. It comprises 1% of all the orbital tumours and may be associated with NF-1. Multiple schwannomas or schwannomatosis occurs in NF-2.

Schwannoma affects individuals in their third to sixth decade. It usually causes a slowly progressive, painless proptosis. There may be diplopia due to mechanical restriction of ocular motility. The vision is not usually affected unless it involves the orbital apex, compressing the optic nerve.

Computerised tomography (CT) scan shows a well-circumscribed round or an oval mass displacing the surrounding structures. It shows marked enhancement with

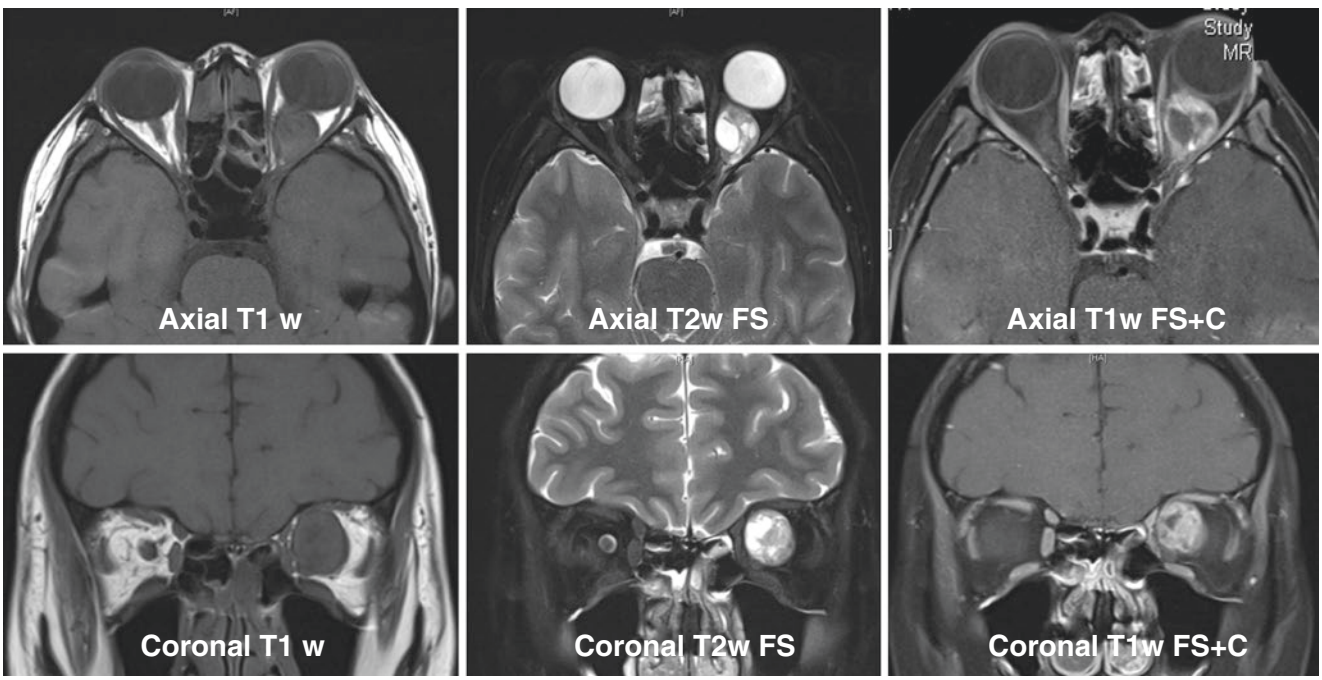

Fig. 25.2 MRI of the orbit shows a smooth well-defined intraconal mass in the superomedial aspect posterior to the left eye. The mass is homogeneous and isointense on T1w image. On T2w image, it shows hyperintense areas representing cystic changes. In post-contrast (T1w + C) images, the lesion is heterogeneous with peripheral rim enhancement. The mass is seen pushing the optic nerve and medial rectus medially

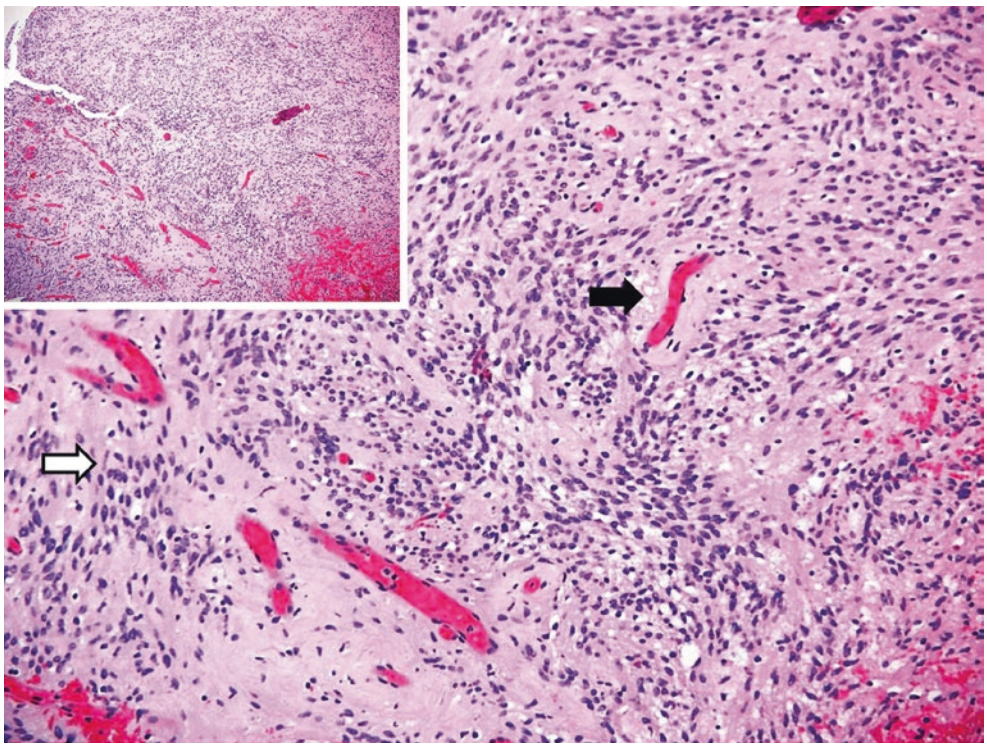

Fig. 25.3 The histopathology of the tumour shows short fascicles of bland-appearing spindle cells. Cellular areas of tumour show subtle nuclear palisading (white arrow). The blood vessel walls are hyalinised (black arrow). HE stain, 100× magnification; inset: HE stain, 40× magnification

contrast. Long-standing tumours may have cystic degeneration and calcification. It can be found both in intra- and extraconal locations. It is occasionally seen extending into the cavernous sinus.

On magnetic resonance imaging (MRI), the tumour appears as a well-circumscribed mass lesion that is isointense to extraocular muscles in T1, hyperintense in T2 weighted images, and heterogeneous due to myxoid changes. Necrosis may give a cavitary appearance and may be confused with a cystic tumour.

Histologically, the Antoni A type shows spindle-shaped cells in a palisading appearance. Occasional tangles of fibrillary processes form Verocay bodies. Antoni B type shows loose myxoid arrangement with ovoid or stellate cells. The Schwann cells show S-100 immunoreactivity.

Complete surgical excision with its capsule is the treatment of choice which is usually curative and prevents recurrence. There may be sensory deficit if the nerve of origin is a sensory nerve. Recurrence may occur where there is incomplete excision or in cases with NF-2 where there are multiple schwannomas.

Learning Points

Schwannomas may be associated with NF-1. They are slow-growing benign tumours and usually present as painless proptosis. Definitive treatment is complete surgical excision. Recurrences and malignant transformation are rare.

Further Reading

1. Kron M, Bohnsack BL, Archer SM, McHugh JB, Kahana A. Recurrent orbital schwannomas: clinical course and histopathologic correlation. BMC Ophthalmol. 2012;12:44.
2. Rootman J, Goldberg C, Robertson W. Primary orbital schwannomas. Br J Ophthalmol. 1982;66(3):194–204.

Solitary Fibrous Tumour

26

Gangadhara Sundar, Stephanie Ming Young, Eric Ting, Bingcheng Wu, Min En Nga, and Shantha Amrith

Introduction

Solitary fibrous tumours (SFT) are rare, benign mesenchymal tumours composed of CD34 strongly positive spindle cells and are part of the haemangiopericytoma spectrum. They may occur anywhere in the orbit, recur if inadequately excised and undergo malignant transformation. They rarely metastasise and hence should be excised completely.

Clinical Scenario

A 25-year-old female presented with an insidious onset of fullness of the right upper medial eyelid of a few months' duration (Fig. 26.1). She had no visual loss or double vision and she was systemically well. Ophthalmic examination revealed orthophoria with full range of ocular motility and normal pupillary reflexes with normal anterior and posterior segments. There was fullness of the right upper inner eyelid with a subcutaneous firm mass lesion that was non-tender, non-pulsatile and ballotable within the orbit.

CLOSE summary is shown in Table 26.1.

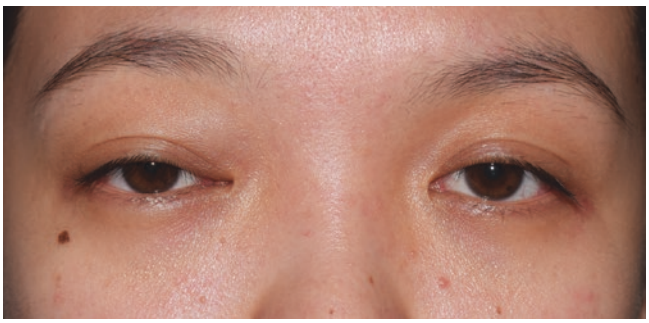

Fig. 26.1 Clinical picture showing fullness in the medial part of right upper lid with mild ptosis

Table 26.1 CLOSE summary

*C*linical process: mass lesion
*L*ocation: superomedial orbit, anteriorly
*O*nset: insidious
*S*ymptoms and signs: fullness with a palpable subcutaneous mass
*E*pidemiology: young Southeast Asian female

G. Sundar · S. M. Young · S. Amrith (✉)
Department of Ophthalmology, National University Hospital, Singapore

Department of Ophthalmology, Yong Loo Lin School of Medicine, National University of Singapore, Singapore
e-mail: gangadhara_sundar@nuhs.edu.sg; shantha_amrith@nuhs.edu.sg

E. Ting
Department of Diagnostic Imaging, National University Hospital, Singapore

Department of Diagnostic Imaging, Yong Loo Lin School of Medicine, National University of Singapore, Singapore

Advanced Medicine Imaging, Singapore

B. Wu
Department of Pathology, National University Hospital, Singapore

M. E. Nga
Department of Pathology, National University Hospital, Singapore

Department of Pathology, Yong Loo Lin School of Medicine, National University of Singapore, Singapore

S. Amrith et al. (eds.), *Ocular Adnexal Lesions*, https://doi.org/10.1007/978-981-13-3798-7_26

Differential Diagnosis

- Dermoid cyst of the orbit (second most common location)
- Epidermal inclusion cyst
- Frontal or fronto-ethmoidal mucocoele
- Lymphoproliferative disorder
- Benign soft tissue orbital mass/tumour – non-distensible cavernous venous malformation (cavernous haemangioma), schwannoma, fibrous histiocytoma, solitary fibrous tumour, etc.

Imaging

Magnetic resonance imaging (MRI) showed a well-circumscribed lesion which was hyperintense to muscle on T2w and isointense to muscle on T1w in the superomedial aspect of the right orbit (Fig. 26.2). It was just above the lacrimal sac fossa and appeared mostly pre-septal in location, possibly bulging into the post-septal orbit. There was mild mass effect with slight lateral displacement of the right globe. The mass appeared to be separate from the lacrimal sac. No deep orbital invasion was seen.

Intervention

Surgical excision biopsy was carried out. Under a frontal nerve block, a superior eyelid crease incision was used to approach the superomedial orbit. The orbital septum was opened to expose the surface of the lesion which was then dissected from the adjacent soft tissues. The lesion appeared free of the superior oblique tendon, the trochlea, the underlying bone, and the adjacent fat (Fig. 26.3). The vascular pedicle at the base was

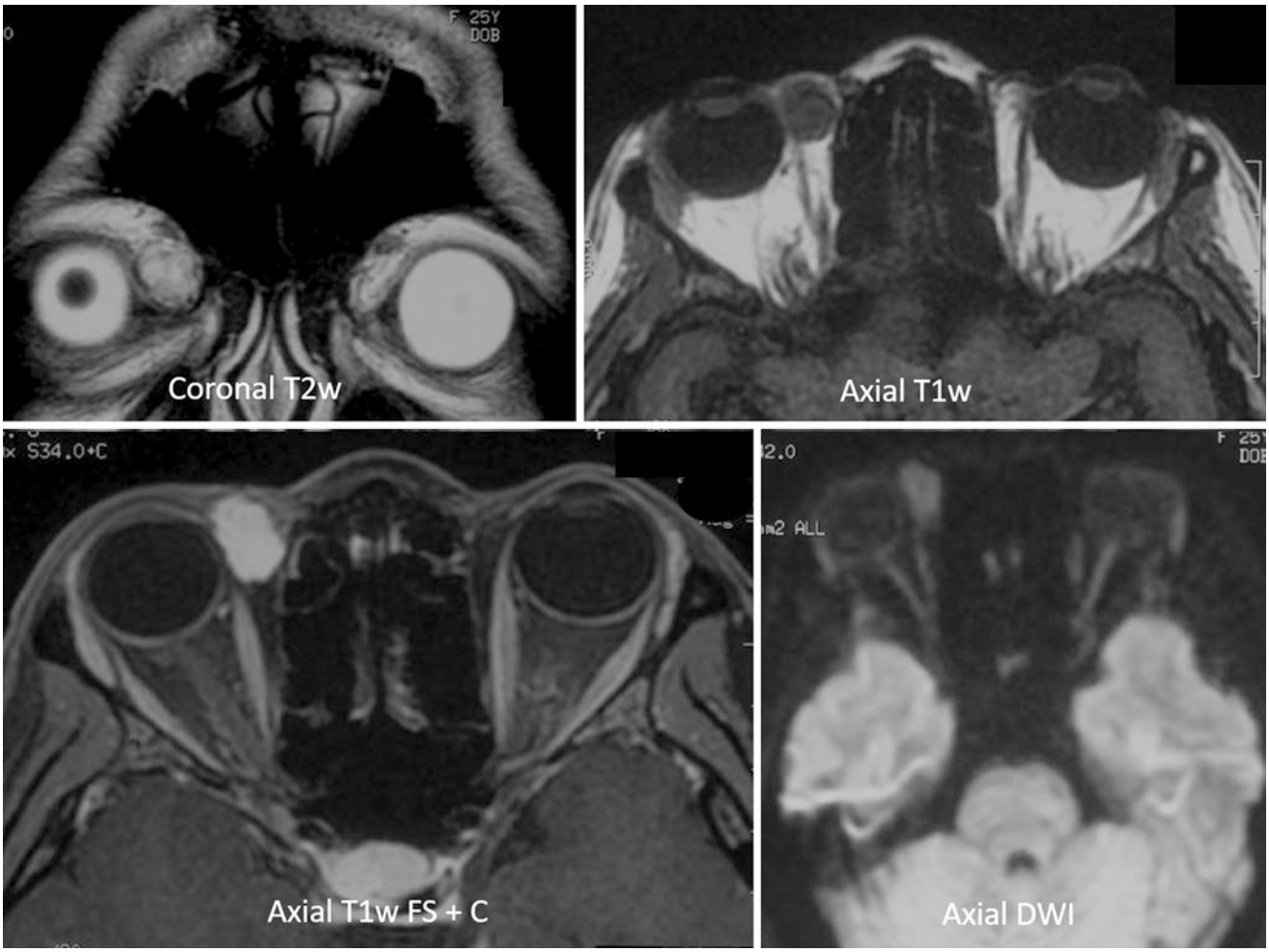

Fig. 26.2 MRI of the orbits: coronal T2w, axial T1w, axial T1w FS + C and axial DWI sequences, showing a well-circumscribed extraconal mass, hyperintense on T2w, isointense to brain on T1w images with avid and homogeneous post-contrast enhancement. DWI shows slightly restricted diffusion, which is not typical for a cavernous haemangioma

clamped, cut and cauterised. The lesion was delivered, and sent for histopathology and immunohistochemical analysis.

Histopathology

Specimen was a lobulated, circumscribed but unencapsulated tumour with variable cellularity. The tumour was composed of tightly packed cells, with ovoid to elongated nuclei, and indistinct cytoplasmic borders. A "patternless" pattern was seen. Vessels appeared open and irregular, with "staghorn"-like shapes (Fig. 26.4). Mitoses were infrequent. No evidence of malignancy was seen. Immunohistochemistry revealed the tumour cells stain positively for CD34 and BCL2 and negatively for AE1/3, SMA, desmin, H-caldesmon and S100.

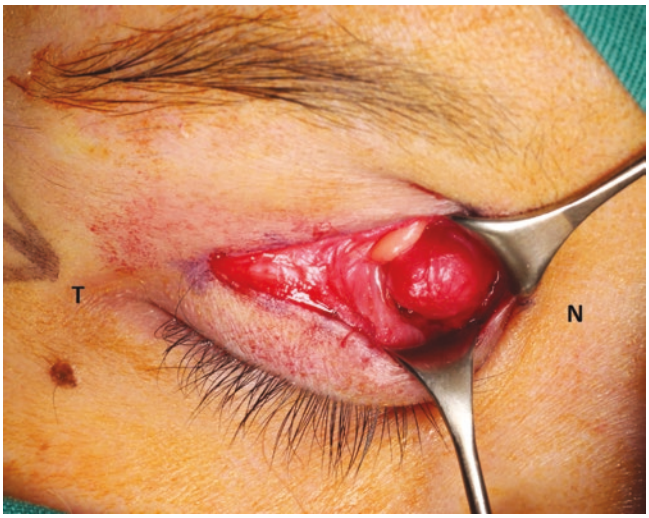

Fig. 26.3 The mass being removed by an anterior orbitotomy through a lid crease incision. N (nasal) and T (temporal) denote the orientation

Discussion

Solitary fibrous tumour (SFT) was originally described as a pleural mesothelial tumour but occurs in extra-pleural sites with the orbit being one of them. It can occur in any age group including children. Clinically, it presents as a painless, slowly growing mass, usually well circumscribed, and does not metastasise. Malignant SFT is very rare.

No serological investigations are indicated. CT or MRI shows an intensely enhancing mass with no infiltration of the muscles or the optic nerve.

Complete surgical excision forms the basis of management for most solitary fibrous tumours. Incisional biopsy and needle biopsy are sometimes inconclusive and often lead to misdiagnosis owing to the varied histopathology within the various locations of the lesion. Incomplete excision may lead to recurrent growth and the remote possibility of a malignant transformation.

Histologically, the tumour has a varied appearance. It can therefore mimic haemangiopericytoma, fibrous histiocytoma, synovial sarcoma or a neural tumour. The diagnosis is made by exclusion. Absence of a single predominant cellular feature is the

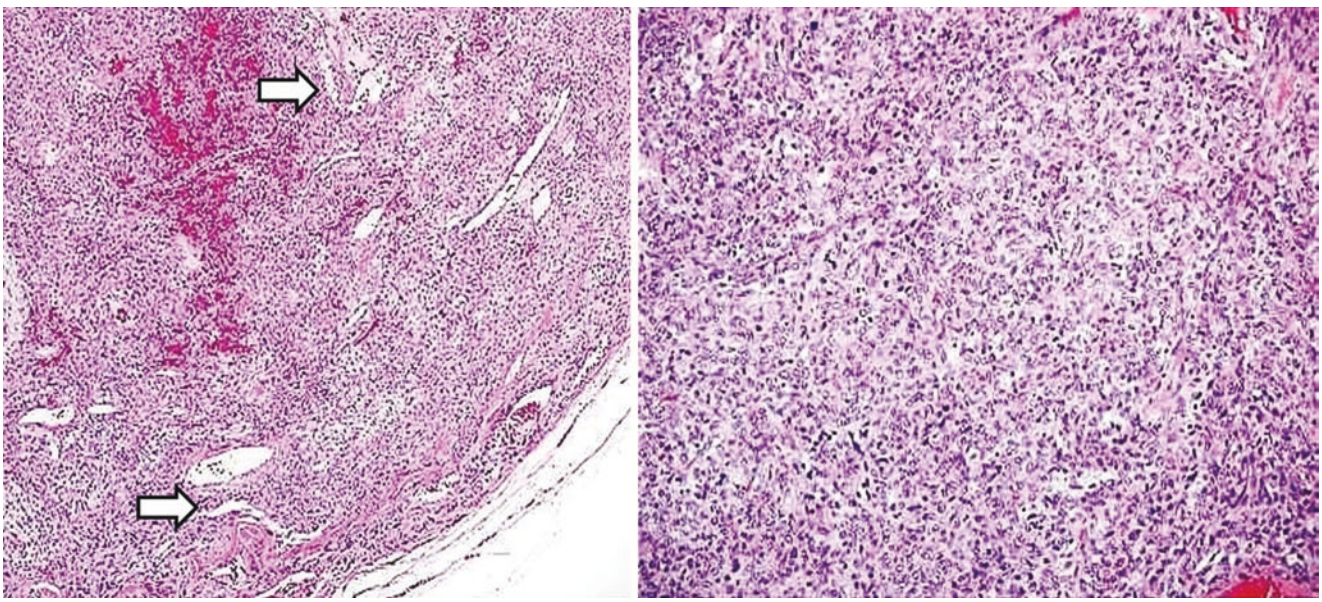

Fig. 26.4 The histopathology shows the tumour exhibiting staghorn-type vasculature (white arrows). The ovoid to spindled tumour cells are arranged in a "patternless" pattern (right image). Left: HE stain; 40× magnification. Right: HE stain; 100× magnification

main characteristic of SFT. Immunohistochemistry shows positive staining for CD34 and BCL2, typical for a solitary fibrous tumour. CD34 positivity is present in 90–100% of cases. The tumour is also positive for STAT6 and genetically harbours the NAB2-STAT6 gene fusion, which is more specific for this entity.

Learning Points

SFT should be considered in the differential diagnosis of a gradually enlarging, painless, benign tumour of the orbit. It is one of the CD34-positive mesenchymal tumours, and the management consists of complete surgical excision. A good histopathological examination is necessary for the correct diagnosis and to exclude other neoplasms that are very closely related to SFT.

Further Reading

1. Girnita L, Sahlin S, Orrego A, Seregard S. Malignant solitary fibrous tumour of the orbit. Acta Ophthalmologica. 2009;87(4):464–7.
2. Jung SK, Paik JS, Park GS, Yang SW. CD34 + tumours of the orbit including solitary fibrous tumours: a six-case series. BMC Ophthalmology. 2017 Apr 27;17(1):59. https://doi.org/10.1186/s12886-017-0455-x.
3. Krishnakumar S, Subramanian N, Mohan ER, Mahesh L, Biswas J, Rao NA. Solitary fibrous tumor of the orbit: a clinicopathologic study of six cases with review of the literature. Survey of Ophthalmology. 2003;48(5):544–54.

Meningioma

27

Hazel Anne Lin, Shantha Amrith, Clement Tan, Stephanie Ming Young, Eric Ting, Bingcheng Wu, Min En Nga, and Gangadhara Sundar

Optic Nerve Sheath Meningioma

Introduction

Optic nerve sheath meningiomas (ONSMs) are rare orbital tumours and represent 1–2% of all meningiomas. They occur more commonly in middle-aged females and can lead to slow, progressive blindness. They are known to be associated with neurofibromatosis type 2 (NF-2).

Case 1

A 50-year-old female presented with progressive blurring of vision in her right eye for about 6–7 months. She was treated at a different centre with oral steroids for a few months prior to presentation, but her vision continued to decline. On presentation, she had no perception of light in the right eye and a visual acuity of 6/6 (Snellen) in the left eye. Examination of the right eye revealed a relative afferent pupillary defect (RAPD), mild limitation of supraduction, and disc swelling with macular striae (Fig. 27.1) on fundus examination. There was 3 mm of proptosis of the right eye (Fig. 27.2). The ophthalmic examination of the left eye was normal.

The CLOSE summary is given in Table 27.1.

Differential Diagnosis

- Optic nerve sheath meningioma
- Optic nerve glioma
- Infiltrative optic neuropathy
- Thyroid eye disease

H. A. Lin
Department of Ophthalmology, National University Hospital, Singapore

S. Amrith (✉) · C. Tan · S. M. Young · G. Sundar
Department of Ophthalmology, National University Hospital, Singapore

Department of Ophthalmology, Yong Loo Lin School of Medicine, National University of Singapore, Singapore
e-mail: shantha_amrith@nuhs.edu.sg; gangadhara_sundar@nuhs.edu.sg

E. Ting
Department of Diagnostic Imaging, National University Hospital, Singapore

Department of Diagnostic Imaging, Yong Loo Lin School of Medicine, National University of Singapore, Singapore

Advanced Medicine Imaging, Singapore

B. Wu
Department of Pathology, National University Hospital, Singapore

M. E. Nga
Department of Pathology, National University Hospital, Singapore

Department of Pathology, Yong Loo Lin School of Medicine, National University of Singapore, Singapore

S. Amrith et al. (eds.), *Ocular Adnexal Lesions*, https://doi.org/10.1007/978-981-13-3798-7_27

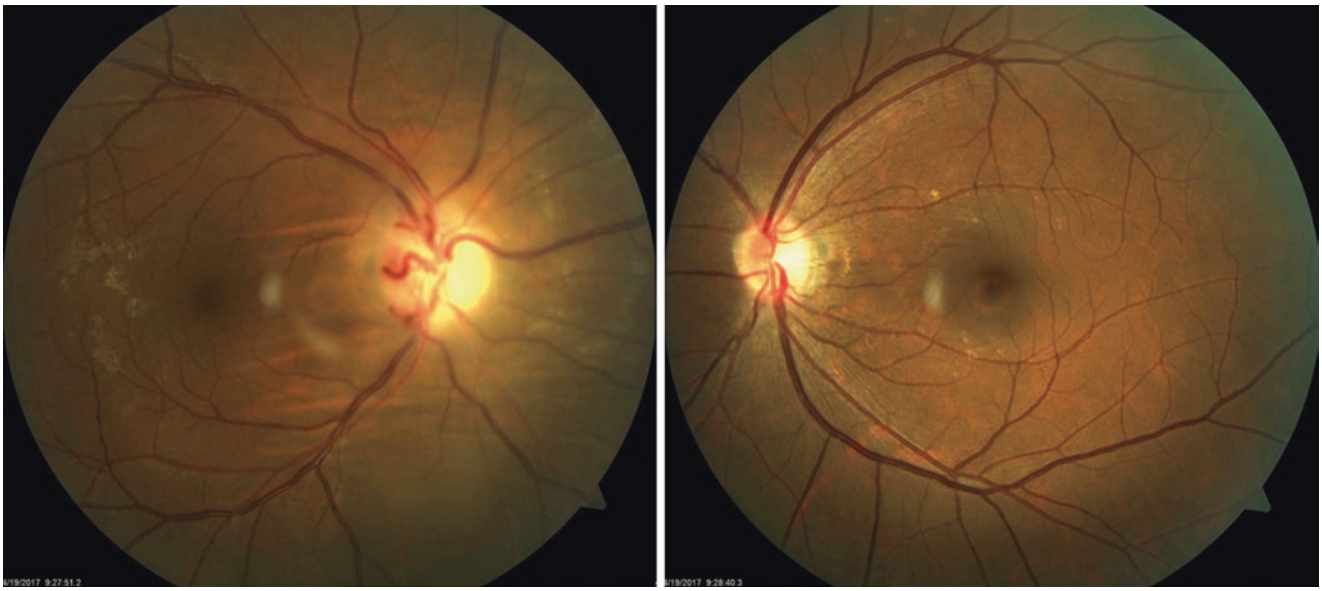

Fig. 27.1 Fundus photo showing right optic disc swelling, optociliary shunt vessels, and macular striae. Left fundus is normal

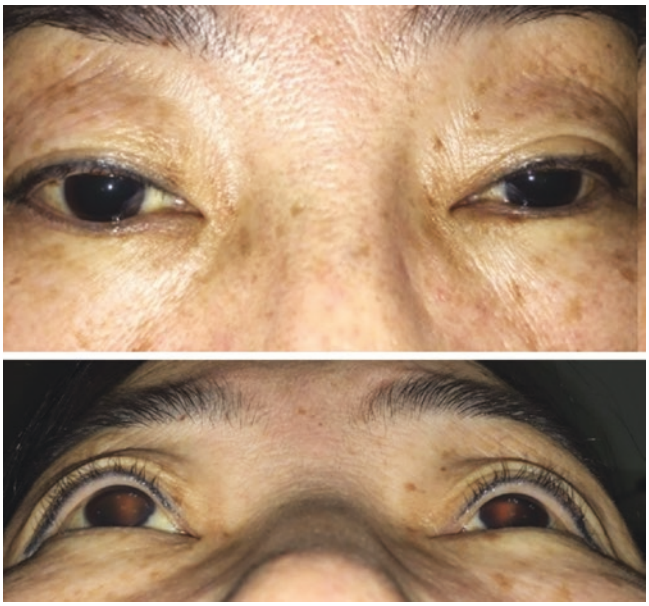

Fig. 27.2 Clinical picture of the patient with ONSM showing the right proptosis

Imaging

Magnetic resonance imaging (MRI) of the orbit showed a homogeneous lesion surrounding the right optic nerve that avidly enhanced with contrast (Fig. 27.3). The lesion extended towards the optic canal, along the pre-chiasmatic optic nerve, involving the sphenoid wing. A classic dural tail was seen. The right optic nerve looked slightly atrophic on coronal view.

Table 27.1 CLOSE summary for case 1

*C*linical Process: benign mass lesion
*L*ocation: retrobulbar, right orbit
*O*nset: chronic
*S*igns and symptoms: proptosis and blurring of vision
*E*pidemiology: 50-year-old East Asian female

Diagnosis

The above radiologic findings along with the clinical presentation and the demographics were highly suggestive of an optic nerve sheath meningioma.

Intervention

She underwent fractionated stereotactic radiotherapy of 54 Gray over 30 sessions.

Sphenoidal Wing Meningioma

Case 2

A 53-year-old female presented with a gradual onset of protrusion of her right eye for about 3 years. It was not associated with pain or blurring of vision. On examination, she had mild fullness of the right temporal region. The visual acuities were normal and there was no RAPD. The anterior and

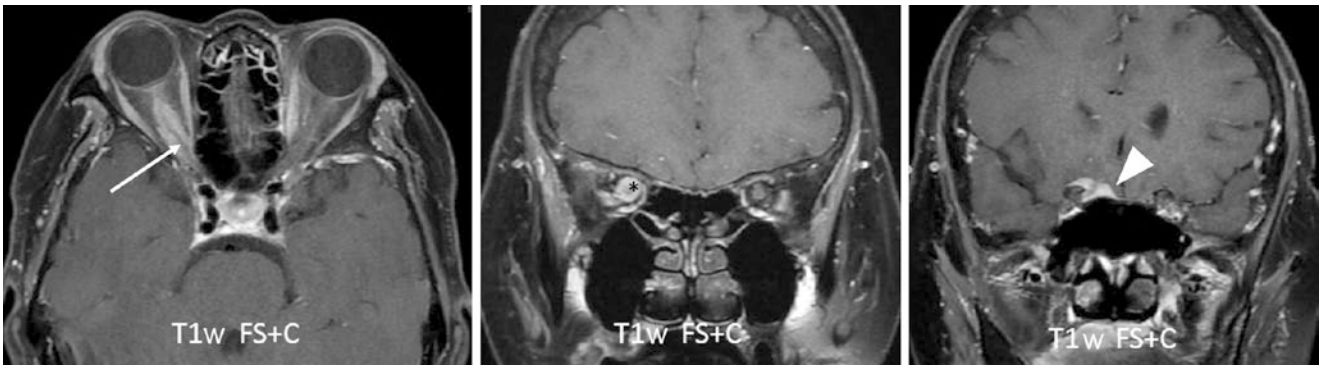

Fig. 27.3 MRI of case 1: T1w FS + C sequences show an enhancing lesion surrounding the right optic nerve (asterisk) ("tram track" sign, arrow). The lesion extends intracranially through the optic canal, involving the prechiasmal segment of the optic nerve. A dural tail is also seen (arrowhead)

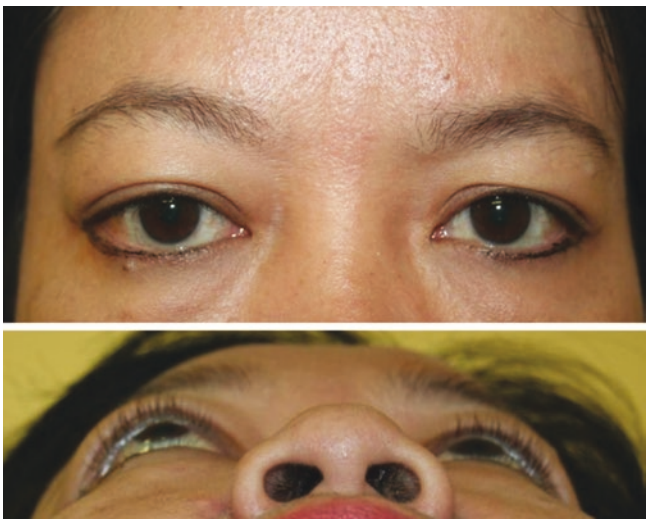

Fig. 27.4 Clinical picture of case 2, showing the right proptosis

posterior segments of both eyes were unremarkable. She had a right axial proptosis of 3 mm (Fig. 27.4) without any limitation of ocular motility. The visual field examination was unremarkable.

CLOSE summary is given in Table 27.2.

Differential Diagnosis

- Benign tumour such as schwannoma, meningioma, and solitary fibrous tumour
- Non-distensible venous malformation such as cavernous haemangioma
- Lymphoproliferative disorder including lymphoma
- Metastatic disease specifically from the breast

Table 27.2 CLOSE summary for case 2

*C*linical process: mass effect
*L*ocation: right orbit
*O*nset: chronic and gradual
*S*igns and symptoms: proptosis
*E*pidemiology: 53-year-old Malay female

Imaging

Computerised tomography (CT) scan showed a right frontal dural-based extra-axial enhancing mass lesion, indenting the frontal lobe. The underlying right frontal and right orbital roof showed increased sclerosis with focal areas of osteolysis, as well as bony expansion (Fig. 27.5). Associated bony encroachment on extraconal space of the right orbit caused mild displacement of the globe inferiorly with proptosis. There was no gross soft tissue component.

Magnetic resonance imaging (MRI) showed a well-defined extra-axial mass in the right frontal lobe with associated vasogenic oedema. It had intermediate signal on T1w and T2w sequences and demonstrated avid contrast enhancement (Fig. 27.6). It also had a large intraosseous component in the right sphenoid wing and right posterior orbital roof laterally, causing bony expansion. There was mild enhancement in the centre of this mass. There was diffuse dural thickening and enhancement in the right frontal, parietal, and temporal lobes, most marked for about 1 cm distance from the mass.

There was mild effacement of the superolateral aspect of the right orbit with subtle high signal and thickening of the right lateral rectus muscle. Periosteal enhancement was also seen along the right lateral orbital wall. There was no crowding at the orbital apex.

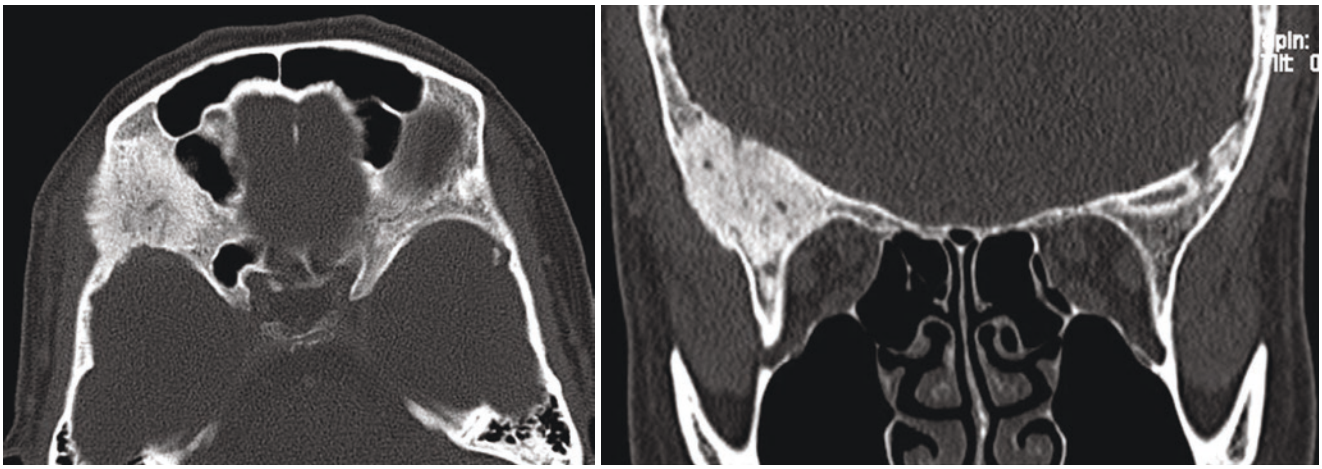

Fig. 27.5 CT scan of case 2: CT bone window images show a sclerotic, expansile lesion centred on the right sphenoid wing, causing slight narrowing of the orbital apex

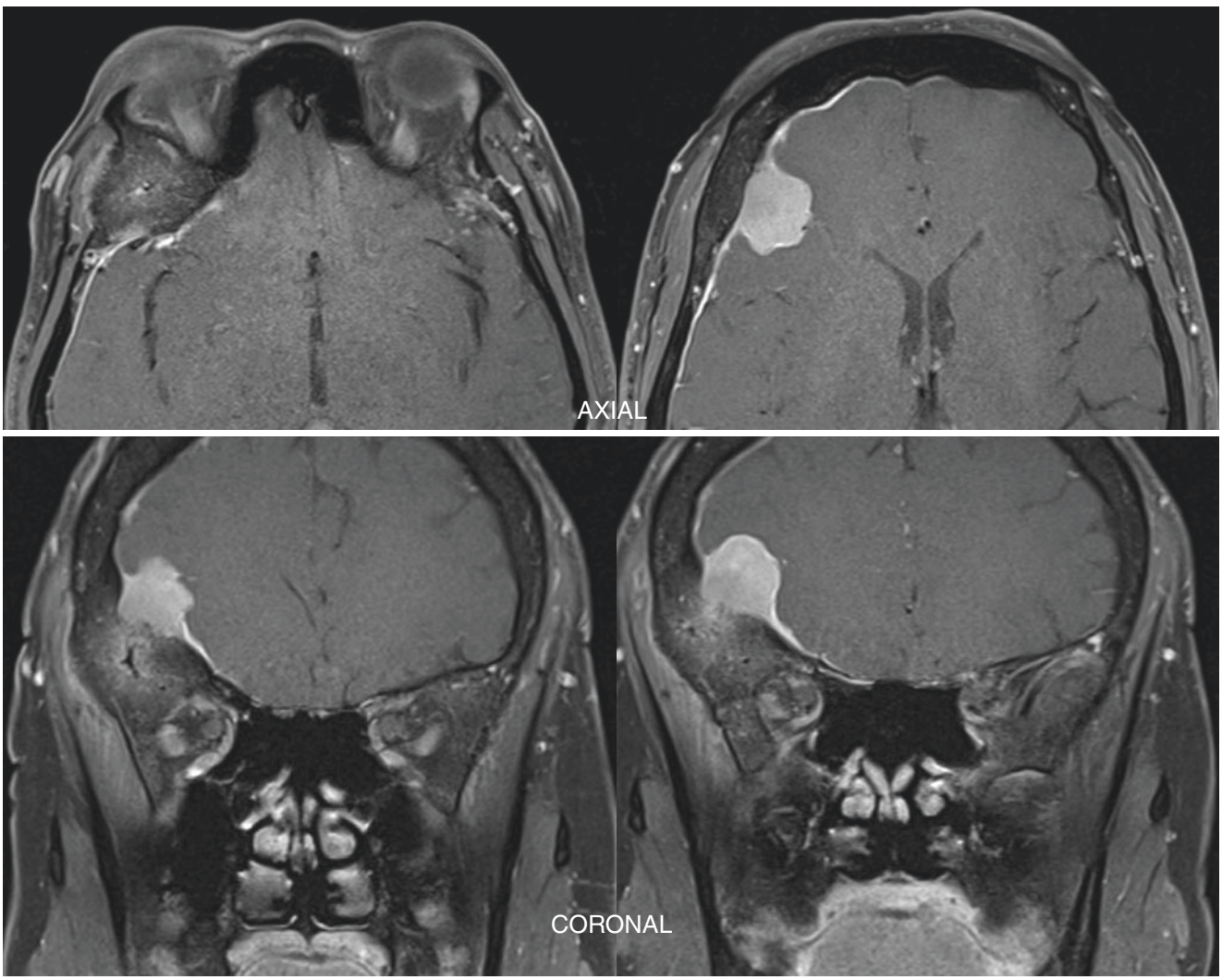

Fig. 27.6 MRI of case 2: T1w-FS + C MRI shows an associated dural based intracranial soft tissue mass with enhancing dural tail

Intervention

The patient underwent removal of the right sphenoidal wing lesion (bony part) and the intracranial soft tissue mass through a bicoronal incision, followed by reconstruction of the lateral wall and roof of the orbit by a multidisciplinary team comprising a neurosurgeon, a plastic surgeon, and an oculoplastic surgeon. The resected specimen was sent for histopathology.

Histopathology

There was a nodular tumour exhibiting nodular pattern and consisting of whorls of tumour cells with relatively uniform oval nuclei, indistinct borders, and pale eosinophilic cytoplasm (Fig. 27.7). The nuclei exhibited occasional intranuclear pseudo-inclusions. Mitotic figures were inconspicuous and tumour necrosis was absent. The stroma consisted of fibrous tissue with many blood vessels. Scattered foci of calcification were also present. No significant nuclear atypia were identified.

The histological features were those of meningothelial meningioma of WHO grade 1. The diagnosis was further confirmed by epithelial membrane antigen (EMA) and vimentin immunohistochemistry, both of which were positive.

Discussion

Optic Nerve Sheath Meningioma (ONSM)

Optic nerve sheath meningioma (ONSM) is an uncommon tumour of the orbit, arising from the intracanalicular or intraorbital portion of the nerve. It typically affects middle-aged individuals and occurs more commonly in women. The typical presentation consists of a triad of proptosis, optic disc pallor, and optociliary shunt vessels. Other symptoms include gaze-evoked amaurosis and diplopia. It is usually unilateral, but bilateral disease has been reported, especially in association with NF-2.

Computerised tomography (CT) scan typically shows tubular enlargement of the optic nerve with "tram track" calcification along the length of the nerve.

Magnetic resonance imaging (MRI) is the preferred imaging modality. On T1w with gadolinium contrast, ONSM shows characteristic diffuse tubular enlargement of the nerve, which enhances homogeneously. On coronal views, there is clear distinction of the nerve sheath tumour from the optic nerve. Other diseases such as optic perineuritis, orbital pseudotumour, and infiltrative optic neuropathy from sarcoidosis may mimic the MRI appearance of ONSM.

Histologically, the tumour arises from meningoepithelial cells in the arachnoid villi. As the tumour grows, it surrounds the optic nerve and impairs axonal transport and interferes

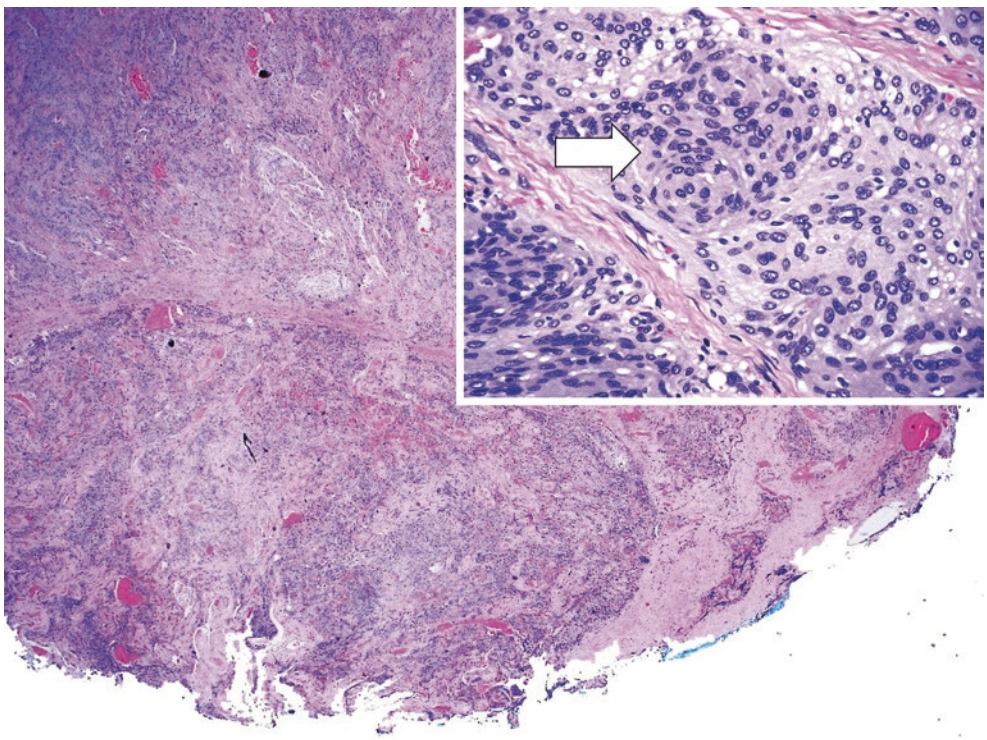

Fig. 27.7 The tumour exhibits a lobular pattern and is composed of whorls of tumour cells (white arrow) with indistinct cell borders as well as ample eosinophilic cytoplasm. No significant nuclear atypia is seen. Main: HE stain; 20× magnification. Inset: HE stain; 200× magnification

with blood supply to the optic nerve. ONSM has the potential to spread intracranially, and there is a risk of involvement of the chiasm and the fellow optic nerve.

Treatment depends on the age and health of the patient, extent of the tumour, and visual function. Options include observation, radiotherapy, and surgical excision. The main aim of treatment is to prevent disfiguring proptosis and extension of the tumour to the chiasm and fellow optic nerve. Radiotherapy has a better chance of preventing further visual loss compared with surgical excision, which has a high incidence of post-operative blindness due to disruption of pial blood supply to the optic nerve.

Sphenoidal Wing Meningiomas

The origin of sphenoidal wing meningiomas is from the meningothelial cells of arachnoid on the inner surface of the dura. They make up about 13–18% of all intracranial tumours. There are two types, an en plaque type and a globoid type with osseous involvement. Depending on their location in the sphenoidal wing, they can be further classified into medial, middle and lateral. They present with proptosis, visual impairment, and ocular motility disturbance due to the expansion and encroachment of the mass into the superior orbital fissure. Imaging shows bony expansion, an intradiploic mass, and a soft tissue component with intraorbital, temporal, and intracranial components. Dural tail, although characteristic, may be absent especially in the en plaque variant.

Asymptomatic cases may be observed, but when the vision is affected, surgery is the standard of care. Surgery entails removal of all the affected bones along with soft tissue components followed by reconstruction. If microscopic clearance is not achieved, there is a risk of recurrence. Recurrences can be treated by external beam radiotherapy or stereotactic gamma knife surgery. Hormonal treatment and chemotherapy may also be tried.

Learning Points

ONSMs are benign orbital lesions, which can cause progressive blindness. Clinical suspicion and investigations are important for diagnosis and follow up. The main aims of treatment are to prevent intracranial extension and involvement of the fellow optic nerve. Observation, radiotherapy, or surgical excision is considered depending on the visual function, proptosis, and intracranial extension.

Sphenoidal wing meningiomas, depending on the type and location, may cause proptosis, and visual and ocular motility dysfunction. Observation or surgical excision with microscopic clearance is the mainstay of treatment.

Further Reading

1. Liu G, Volpe N, Galetta S. Neuro-ophthalmology diagnosis and management. 2nd ed. Philadelphia: Saunders Elsevier; 2010. p. 167–70.
2. Saeed P, Rootman J, Nugent RA, White VA, Mackenzie IR, Koornneef L. Optic nerve sheath meningiomas. Ophthalmology. 2003;110(10):2019–30.
3. Saeed P, Blank L, Selva D, Wolbers JG, Nowak PJCM, Geskus RB, Weis E, Mourits MP, Rootman J. Primary radiotherapy in progressive optic nerve sheath meningiomas: a long-term follow-up study. Br J Ophthalmol. 2010;94(5):564–8.
4. Sughrue ME, Rutkowski MJ, Chen CJ, Shangari G, Kane AJ, Parsa AT, et al. Modern surgical outcomes following surgery for sphenoid wing meningiomas. J Neurosurg. 2013;119:86–93.
5. Walsh and Hoyt's clinical neuro-ophthalmology: the essentials. 2nd ed. Philadelphia: Lippincott Williams & Wilkins; 2008. p. 178.

Glioma

28

Hazel Anne Lin, Clement Tan, Shantha Amrith, Stephanie Ming Young, Eric Ting, Bingcheng Wu, Min En Nga, and Gangadhara Sundar

Introduction

Gliomas (pilocytic astrocytomas) are the most common primary tumours of the optic nerve. They are benign and typically present in childhood. They are not infrequently associated with neurofibromatosis type 1 (NF-1). Benign optic nerve gliomas are typically slow growing, and some individuals, especially with NF-1, may retain good visual function.

Case Scenario

A 24-year-old Chinese male presented with mild, painless, progressive blurring of left eye vision for 3–4 months prior to consultation. There was no significant past medical or family history. His Snellen visual acuities were 6/6 in the right eye and 6/9 in the left. Examination of the left eye showed a trace of relative afferent pupillary defect (RAPD), full colour vision although slower than the right, and on perimetry an inferior altitudinal defect (Fig. 28.1). Fundus examination showed a normal-looking optic disc on the right and a mildly pale disc on the left (Fig. 28.2). There was a proptosis of 2 mm on the left (Fig. 28.3). Systemic examination did not reveal any evidence of NF-1.

The CLOSE summary is given in Table 28.1.

Differential Diagnoses

- Optic nerve glioma
- Optic nerve sheath meningioma
- Schwannoma
- Thyroid eye disease
- Other benign primary orbital tumours

H. A. Lin
Department of Ophthalmology, National University Hospital, Singapore

C. Tan · S. Amrith (✉) · S. M. Young · G. Sundar
Department of Ophthalmology, National University Hospital, Singapore

Department of Ophthalmology, Yong Loo Lin School of Medicine, National University of Singapore, Singapore
e-mail: shantha_amrith@nuhs.edu.sg; gangadhara_sundar@nuhs.edu.sg

E. Ting
Department of Diagnostic Imaging, National University Hospital, Singapore

Department of Diagnostic Imaging, Yong Loo Lin School of Medicine, National University of Singapore, Singapore

Advanced Medicine Imaging, Singapore

B. Wu
Department of Pathology, National University Hospital, Singapore

M. E. Nga
Department of Pathology, National University Hospital, Singapore

Department of Pathology, Yong Loo Lin School of Medicine, National University of Singapore, Singapore

S. Amrith et al. (eds.), *Ocular Adnexal Lesions*, https://doi.org/10.1007/978-981-13-3798-7_28

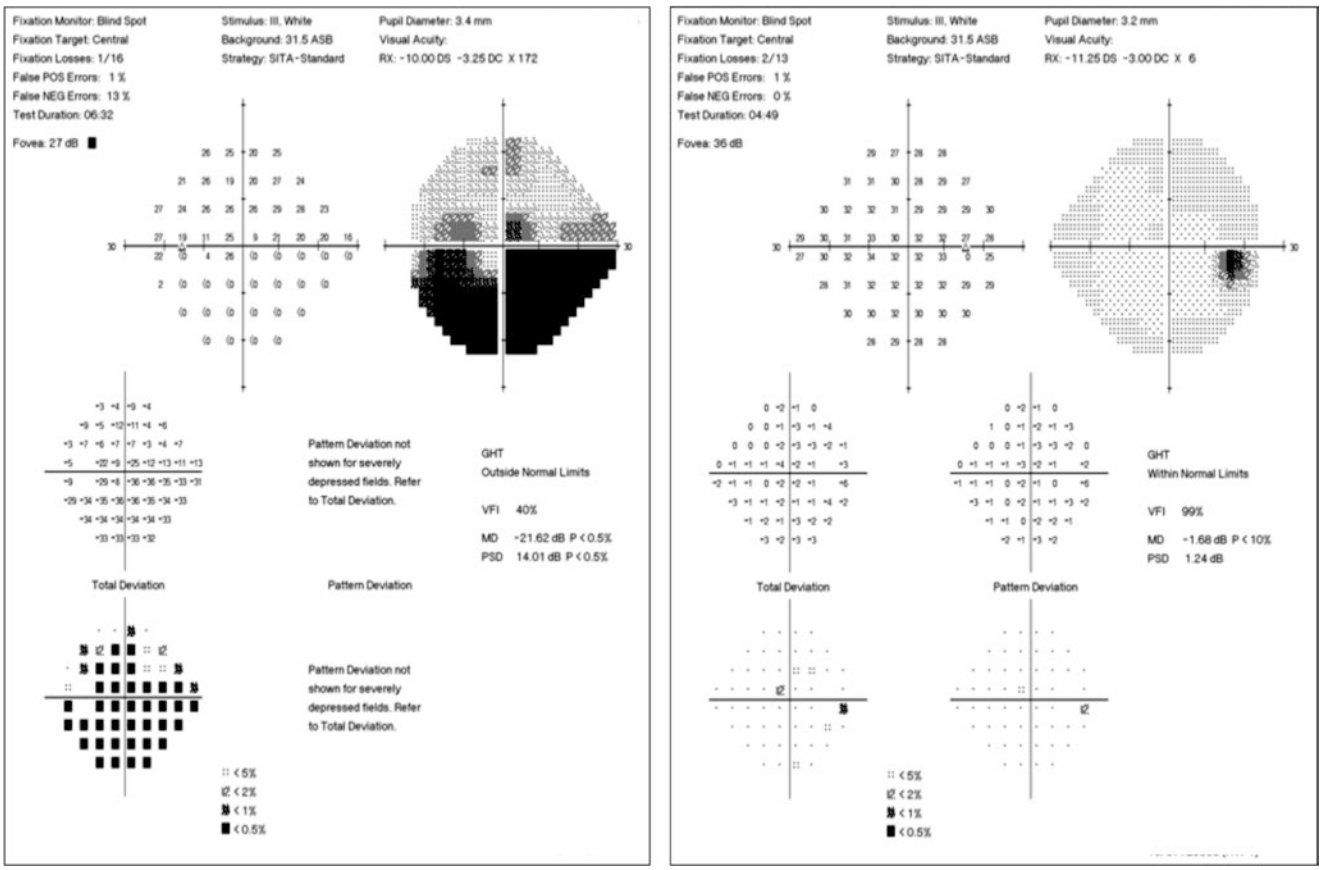

Fig. 28.1 Humphrey visual field (HVF) of the left eye (left) demonstrating an inferior altitudinal defect

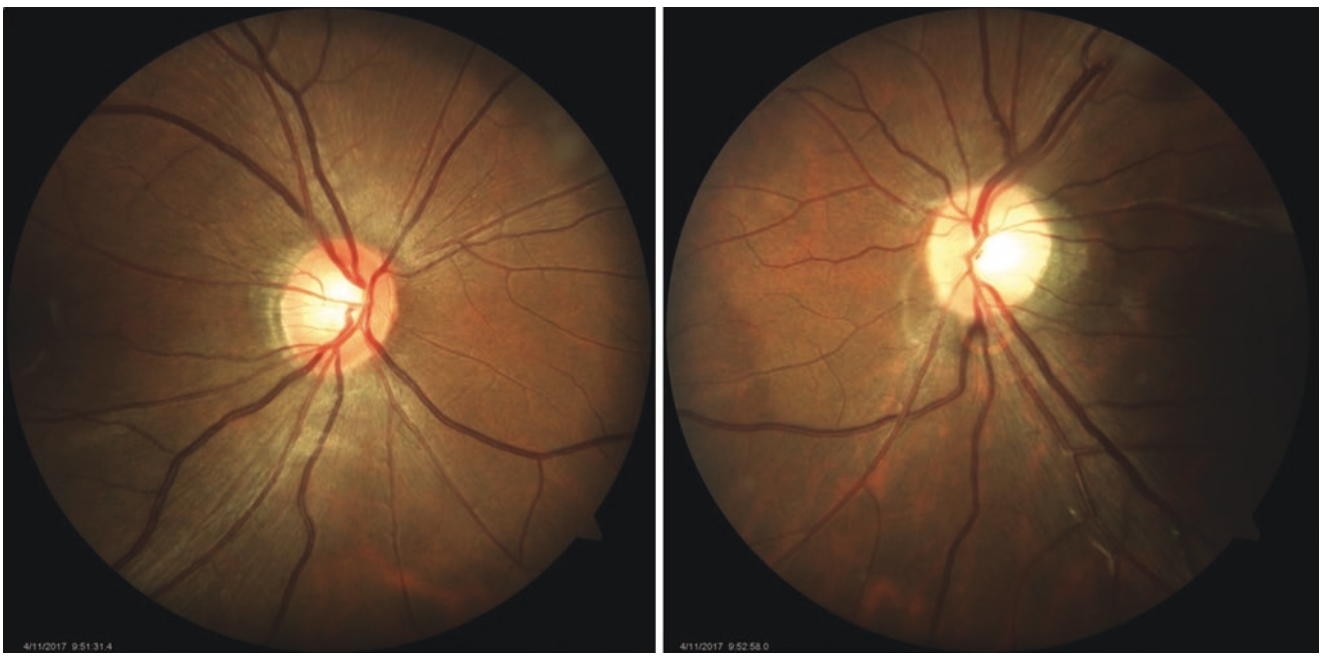

Fig. 28.2 Fundus examination showing normal right optic disc and mild left optic disc pallor

Imaging

Magnetic resonance imaging (MRI) of the orbits (Fig. 28.4) showed fusiform enlargement of the left optic nerve, involving the intraorbital and canalicular portions, extending to the left side of the optic chiasm. There was buckling of the distal nerve close to the globe, significant post-contrast enhancement, and widening of the optic canal. The coronal image showed the tumour to be arising from the optic nerve. These findings are characteristic of an optic nerve glioma.

Management

After the initial diagnosis, with the advice of a multidisciplinary team, the patient was offered observation vs chemotherapy (targeted) vs radiotherapy. The patient chose to observe. Two years later, the MRI showed tumour growth further into the chiasma with risk of involvement of the fellow eye, and a decision was made to biopsy the mass to rule out malignant transformation.

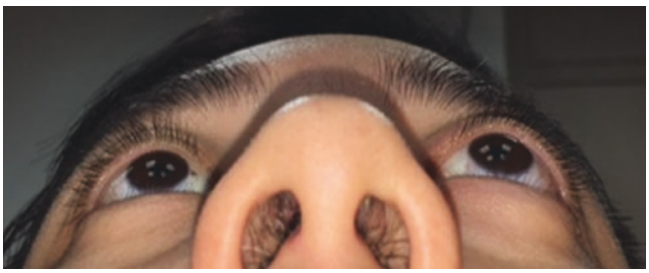

Fig. 28.3 Presence of proptosis on the left side

Table 28.1 CLOSE summary

*C*linical process: benign mass lesion
*L*ocation: retrobulbar
*O*nset: chronic
*S*igns and symptoms: painless proptosis and blurring of vision
*E*pidemiology: young Chinese male

The patient underwent a biopsy and the histopathology confirmed astrocytic pilocytoma (WHO grade 1). He was offered targeted chemotherapy vs radiotherapy vs surgery.

Histopathology

Sections showed a tumour composed of both compact fibrillar areas and looser microcystic areas, thereby giving a biphasic pattern on low-power view (Fig. 28.5). Tumour cellularity was more prominent in the compact fibrillar areas. The cells exhibited ovoid to elongated nuclei with mild nuclear atypia (Fig. 28.6) and long hairlike cytoplasmic processes, best seen on the cytology preparation (Fig. 28.7). Eosinophilic granular bodies were present within the cytoplasm, as well as Rosenthal fibres (Fig. 28.6). Mitotic activity was inconspicuous. No tumour necrosis was identified.

On immunohistochemistry, glial fibrillary acid protein (GFAP) was diffusely positive within the tumour, which confirmed its glial nature.

The features were consistent with a glial neoplasm, pilocytic astrocytoma (WHO Grade 1).

Discussion

Optic nerve gliomas are benign tumours that arise from astrocytes. They are seen more commonly in children, typically affecting individuals by the second decade of life. Thirty (30) % of patients have NF-1, and prognosis in such cases is usually good.

Clinically, optic nerve gliomas may be asymptomatic and discovered during investigation for abnormal optic discs. Sometimes, they may cause slowly progressive, painless proptosis with or without visual loss. Some of the patients may complain of diplopia due to mechanical restriction of ocular motility.

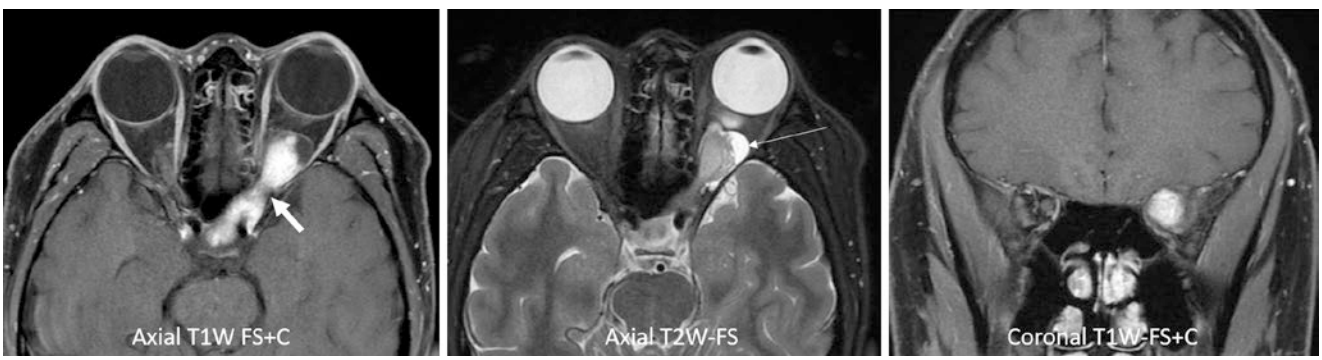

Fig. 28.4 Axial and coronal MRI of the orbits show an elongated fusiform enhancing mass involving the left optic nerve. The anterior optic nerve is kinked, and there is cyst formation at the anterior tumour margin (thin arrow). Posteriorly, there is narrowing (thick arrow) of the tumour as it traverses the widened optic canal to involve the canalicular portion and prechiasmatic optic nerve

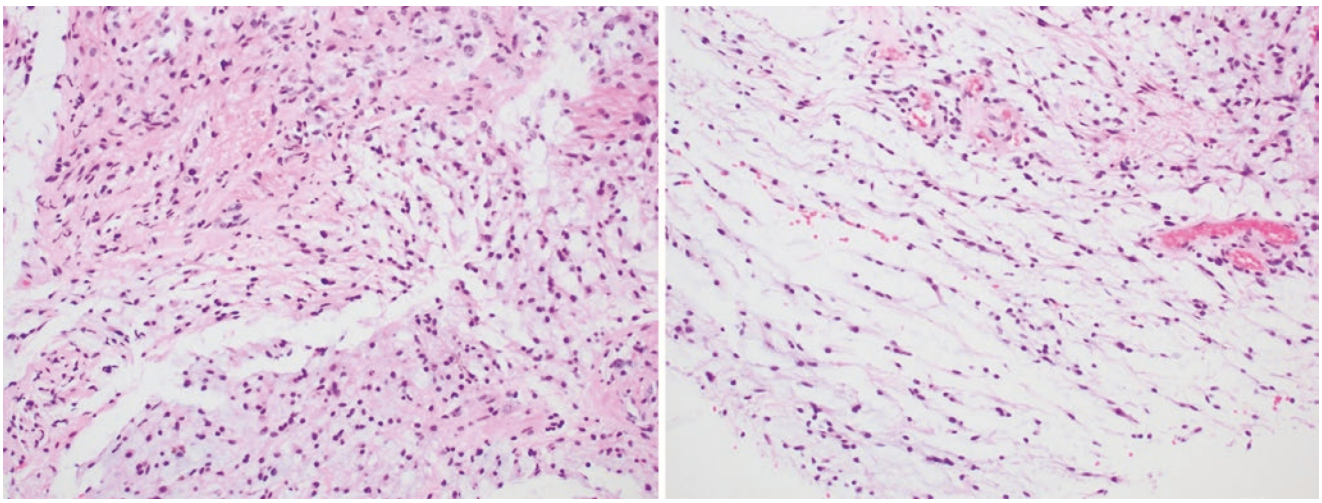

Fig. 28.5 The tumour is composed of compact fibrillar areas (left) and spongy areas with myxoid appearance (right), thereby giving a biphasic appearance. Left: HE stain; 100× magnification. Right: HE stain; 100× magnification

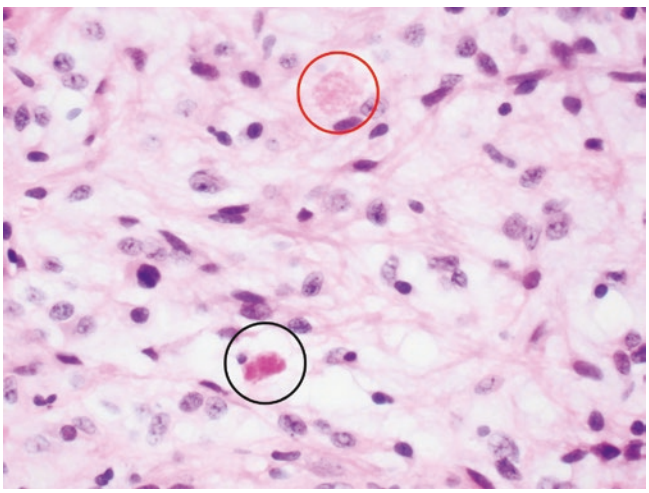

Fig. 28.6 The tumour cells exhibit ovoid to elongated nuclei with mild nuclear atypia. The tumour exhibits a fibrillary background. Eosinophilic granular body (red circle) and Rosenthal fibre (black circle) are seen. HE stain; 400× magnification

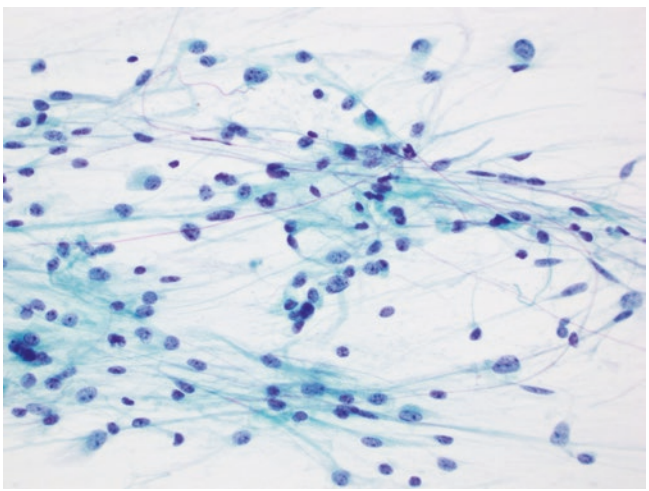

Fig. 28.7 Cytology smears (squash preparation) prepared from the fresh tumour specimen show bipolar, hairlike cells with long, narrow cytoplasmic processes and ovoid to elongated nuclei. Smear, Papanicolaou stain; 400× magnification

CT scans of these lesions show enlargement of the optic nerve, typically fusiform in shape, with kinking of the nerve.

MRI is the preferred imaging modality. Gliomas are hypointense on T1-weighted images, and the optic nerve is seen to be enlarged as compared to the other side. Contrast-enhanced scans demonstrate variable enhancement of the optic nerve and the tissue surrounding the cystic components. On T2-weighted scans, there is central hyperintensity with low signal at the periphery representing the dura.

Incisional biopsies are not typically performed as incorrect sampling can reveal meningeal hyperplasia, resulting in a false diagnosis of optic nerve sheath meningioma. In addition, biopsy of the optic nerve can worsen visual loss.

Grossly, the tumour is made up of cystic or solid components. Histologically, the fusiform intradural lesion consists of low-grade spindle-shaped pilocytic astrocytes with numerous Rosenthal's fibres and arachnoid hyperplasia.

Malignant transformation of existing benign gliomas and primary malignant gliomas (glioblastoma multiforme) are rare and typically occur in adults. They are rapidly progressive and have poor prognosis, with death occurring within a year.

Treatment depends on the age and health of the patient, extent of the tumour, and visual function. Most patients are closely observed. Treatment is indicated if there is progressive growth of the tumour towards the chiasm, deterioration

of vision, or disfiguring proptosis. Options for treatment include chemotherapy (targeted therapy), radiotherapy, and surgical excision. Chemotherapy is the preferred treatment modality in prepubertal children, in view of the side effects of radiotherapy.

Learning Points

Optic nerve glioma is the most common primary optic nerve tumour and may be associated with NF-1. They are slow-growing benign tumours and usually present as painless proptosis. Management options include observation, radiotherapy, chemotherapy, and surgical excision. Recurrences and malignant transformation are rare.

Further Reading

1. Liu G, Volpe N, Galetta S. Neuro-ophthalmology diagnosis and management. 2nd ed. Philadelphia: Saunders Elsivier. 2010. p. 166–7.
2. 2014-2015 Basic and clinical science course. Section 5: Neuro-ophthalmology. 1st Edition. American Academy of Ophthalmology. 2014. p. 138–140.

Osteoma

29

Shantha Amrith, Stephanie Ming Young, Eric Ting, Bingcheng Wu, Min En Nga, and Gangadhara Sundar

Introduction

Osteomas are common benign tumours of the paranasal sinuses. The orbit, by sharing the bony walls with the paranasal sinuses, gets affected by these tumours. The frontal bones are the most commonly affected, followed by the ethmoids, maxillary, and sphenoid bones. Primary orbital osteomas are rare, compared to sino-orbital osteomas. There is equal gender distribution, and the average age of presentation is 40–50 years.

Clinical scenario

A 20-year-old Indian male presented with a right upper lid and forehead swelling which was enlarging over a few years. He had also noticed the right eyeball protruding and pushed downwards and outwards. There was no blurring of vision, but he had noticed worsening double vision.

On examination, he had good visual acuities in both eyes. Ophthalmic examination of the right eye showed non-axial proptosis of 12 mm with hypoglobus and lateral displacement of the eyeball (Fig. 29.1). Ocular motility showed limitation of movements in all directions except infraduction. The pupils, visual fields, and fundus examination were normal. Protrusion with thickening of the superior orbital rim was evident on the right side.

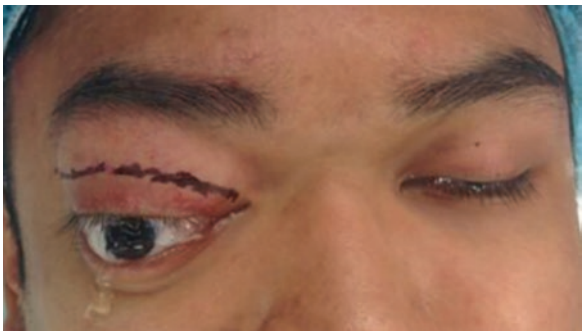

Fig. 29.1 Clinical picture showing non-axial proptosis of the right eye

Table 29.1 CLOSE summary

*C*linical process: mass effect
*L*ocation: right supero-nasal orbit
*O*nset: chronic
*S*igns and symptoms: unilateral proptosis with infero-lateral globe displacement
*E*pidemiology: young Indian male

CLOSE summary is given in Table 29.1.

S. Amrith (✉) · S. M. Young · G. Sundar
Department of Ophthalmology, National University Hospital, Singapore

Department of Ophthalmology, Yong Loo Lin School of Medicine, National University of Singapore, Singapore
e-mail: shantha_amrith@nuhs.edu.sg; gangadhara_sundar@nuhs.edu.sg

E. Ting
Department of Diagnostic Imaging, National University Hospital, Singapore

Department of Diagnostic Imaging, Yong Loo Lin School of Medicine, National University of Singapore, Singapore

Advanced Medicine Imaging, Singapore

B. Wu
Department of Pathology, National University Hospital, Singapore

M. E. Nga
Department of Pathology, National University Hospital, Singapore

Department of Pathology, Yong Loo Lin School of Medicine, National University of Singapore, Singapore

S. Amrith et al. (eds.), *Ocular Adnexal Lesions*, https://doi.org/10.1007/978-981-13-3798-7_29

Differential Diagnosis

- Osteoma
- Ossifying fibroma
- Fibrous dysplasia
- Osteoblastoma/osteosarcoma
- Osteoblastic metastasis

Imaging

Computerised tomography (CT) scan (Fig. 29.2) showed a large lobulated osseous lesion with mixed density, centred in the right fronto-ethmoidal sinuses. It also crossed the midline and affected the left frontal and ethmoid sinuses. Both frontal sinuses were completely opacified and eth-

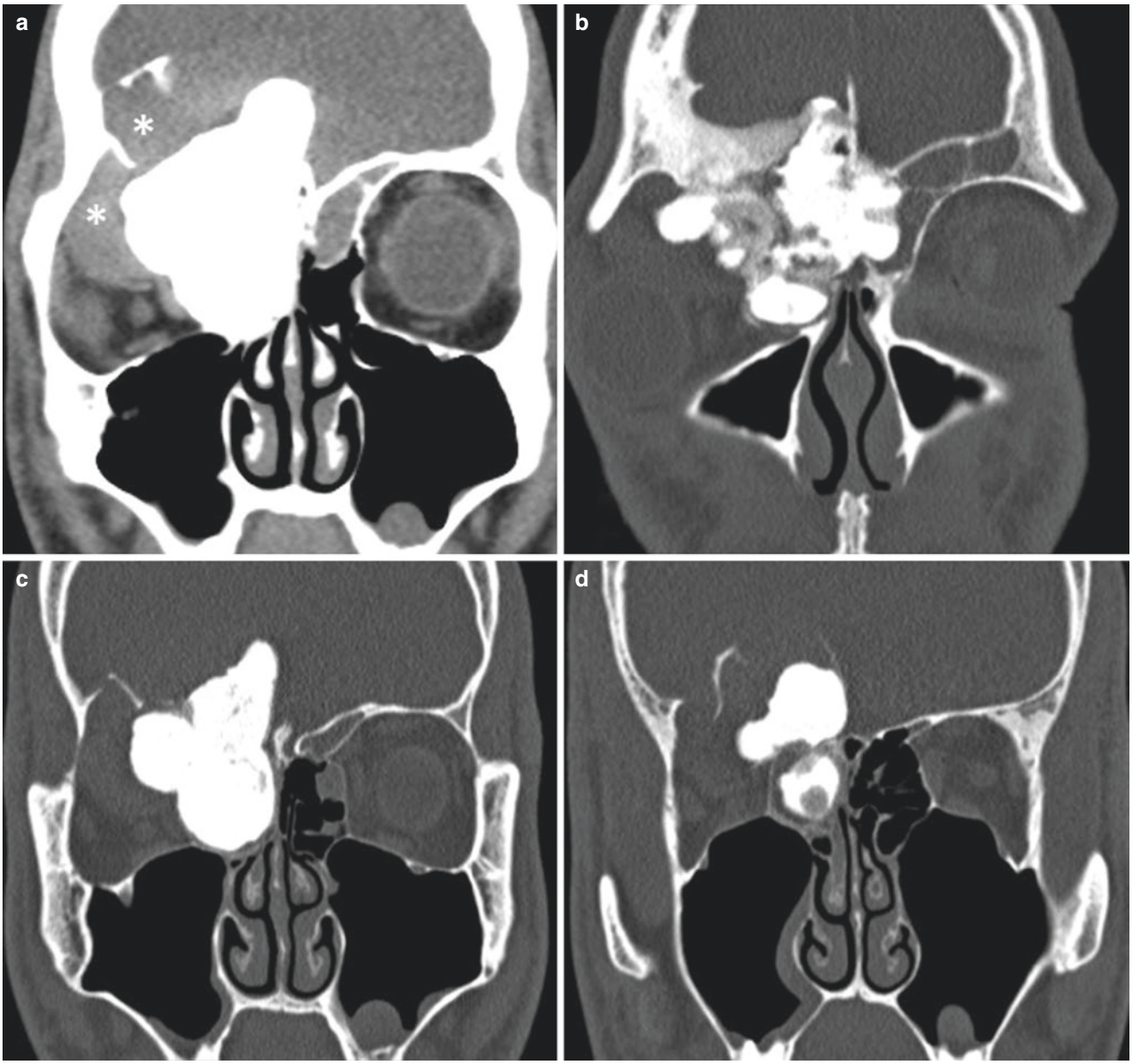

Fig. 29.2 Coronal non-contrast-enhanced soft tissue (**a**) and bone window (**b**, **c**, and **d**) CT images show a large lobulated fibro-osseous lesion with areas of dense sclerosis as well as ground-glass density. Note the presence of a mucocoele expanding superiorly into the anterior cranial fossa and inferiorly into the superolateral orbit (asterisk)

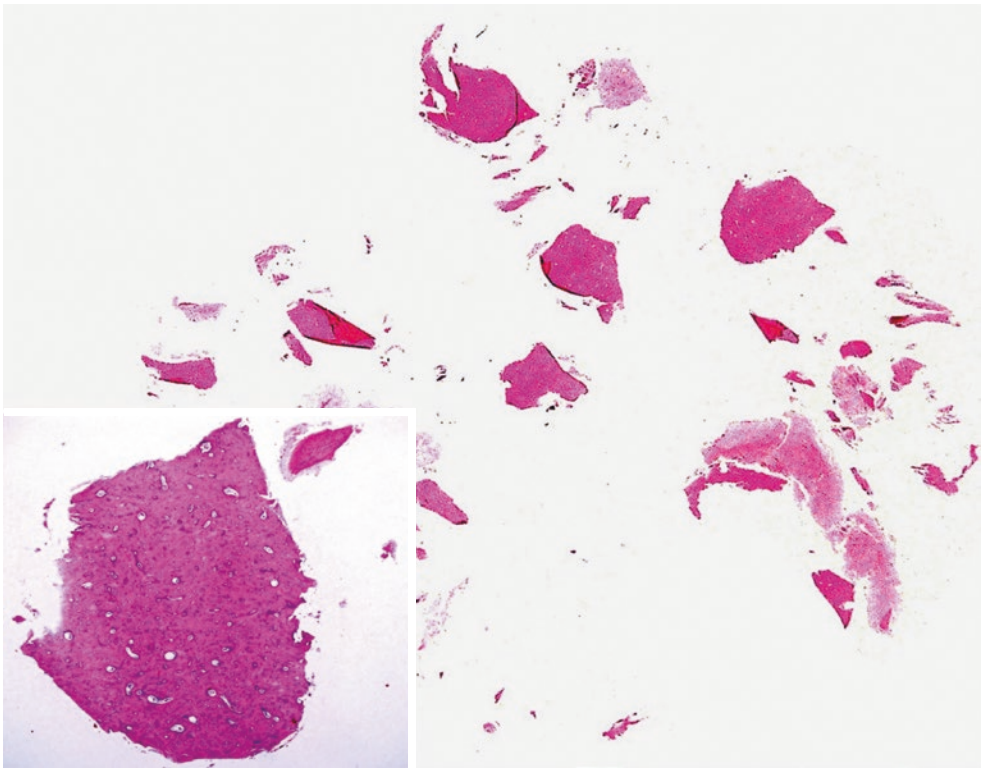

Fig. 29.3 There are multiple loose fragments of mature bone tissue. Inset: higher magnification view of bony tissue. HE stain; 20× magnification

moidal air cells partially. The mass had breached the right lamina papyracea as well as the right orbital roof to involve the right orbit. The mass was predominantly of dense osseous density with areas of ground-glass attenuation. A 21 mm thick rim of mildly hyperdense soft tissue was seen surrounding the right superolateral aspect of the mass. This had resulted in significant right proptosis with inferior and lateral displacement of the right globe and its structures. There was also breach of the right anterior cranial fossa by the soft tissue component. No definite cerebral oedema was seen. Impression was that of a fibro-osseous lesion centred around right frontal sinus with mucocoele.

Intervention

The patient underwent excision of the bony lesion with drainage of multiple pockets of mucocoele by a combined endoscopic and external approach under general anaesthesia. The orbital portion of the superomedial lesion was exposed by a lid crease incision by the oculoplastic surgeon, while the otolaryngologist performed removal of the tumour along with bilateral ethmoidectomy and middle meatal antrostomy, Lothrop procedure for frontal sinuses, and drainage of mucocoeles. The lining of frontal recess was carried out using a naso-septal flap.

Histopathology

(A) There were multiple loose fragments of mature bone tissue surrounded focally by fibrous and granulation type tissue (Fig. 29.3). The features would be consistent with an osteoma.

(B) Sections showed multiple fragments of a cystic lesion lined focally by respiratory-type epithelium and containing mucinous material. The lesion had a fibrous wall and showed non-specific acute on chronic inflammation. There was no evidence of malignancy.

The features were consistent with benign osteoma with sinus mucocoele.

Discussion

Osteomas are benign fibro-osseous lesions that occur due to proliferation of bony tissues. They commonly arise from facial bones, skull, and sinuses. Small osteomas can be asymptomatic. When they encroach upon the orbit, the patients develop progressive, painless proptosis. The bony mass may be palpable. The sinus osteomas cause obstruction to the ostia of the sinuses and cause a secondary mucocoele that may aggravate the proptosis. Besides, the patients may also develop sinusitis. Posteriorly placed osteomas, such as

those arising from sphenoid sinus, may cause optic nerve compression and affect the vision.

Computerised tomography (CT) scan is the mainstay of investigations. Osteomas appear as circumscribed, bosselated, sessile or pedunculated masses showing osteoblastic activity. Bone window settings may show trabecular pattern in the middle and thickened cortex in the periphery. Mucocoeles are hypo-intense and show expansion of the sinuses.

Sinonasal osteomas may be composed of mature dense cortical lamellar bone, or immature woven bone with features of osteoblastic rimming (plump cells that are located at the edges of bony trabeculae) and active resorption. The pattern indicates that these tumours grow from within. Histology of these lesions show compact bone, cancellous bone, and a fibrovascular stroma. There are three histological types, ivory, trabecular, and spongy, depending on the predominant presence of compact, cancellous, or fibrous tissue.

Management of asymptomatic osteomas is observation. However, if sphenoidal lesions threaten vision, they should be removed. Sinus osteomas need a combined orbital and endoscopic approach, and some may also need the help of a neurosurgeon. Surgery has very low complications, and, in rare instances, recurrence has been reported.

Learning Points

Osteomas are the most common bony tumours of paranasal sinuses, but the orbital extensions are relatively uncommon. A multidisciplinary surgical team is often required to manage these patients. The surgery is usually associated with low complication rates and recurrences.

Further Reading

1. Khong JJ, Malhotra R, Selva D, Wormald PJ. Efficacy of endoscopic sinus surgery for paranasal sinus mucocele including modified endoscopic Lothrop procedure for frontal sinus mucocele. The Journal of Laryngology and Otology. 2004;118(5):352–6.
2. Selva D, White VA, O'Connell JX, Rootman J. Primary bone tumors of the orbit. Rev Surv Ophthalmol. 2004;49(3):328–42.
3. Wei LA, Ramey NA, Durairaj VD, Ramakrishnan VR, Cruz AV, Dolman PJ, Lucarelli MJ. Orbital osteoma: clinical features and management options. Ophthalmic Plastic and Reconstructive Surgery. 2014;30(2):168–74.

Ossifying Fibromyxoid Tumour

30

Mariel Angelou Parulan, Shantha Amrith, Stephanie Ming Young, Eric Ting, Bingcheng Wu, Min En Nga, and Gangadhara Sundar

Introduction

Myxoid soft tissue neoplasms of the face and orbit may present in non-specific patterns with symptoms depending on affected structures. These are mesenchymal neoplasms characterized by the production of abundant extracellular myxoid matrix that can be categorized as benign or malignant. Among them, ossifying fibromyxoid tumour is a rare form with borderline malignant potential. Around 70% is said to arise from extremities and would occasionally involve the trunk, head and neck, oral cavity, mediastinum, and retroperitoneum. It has been reported in only 150 cases in literature, rarely in the orbit, with the first case being reported in 2006.

Case Scenario

A 9-year-old girl from Southeast Asia, with no systemic symptoms of note, presented with 1-year history of gradually progressive, painless swelling around the right eye. She had also noted gradual deterioration of vision. On examination, the visual acuity of the right eye was no light perception and that of the left eye was 6/7.5 (Snellen chart). There was a large protruding right-sided hemifacial tumour, extending from the right forehead to the nasolabial region, pushing the eyeball to the extreme medial corner (Fig. 30.1a). The lesion was non-tender, warm to touch, nonpulsatile, and nonreducible, with overlying dilated vessels. There was no regional lymphadenopathy. The right globe was phthisical with evidence of corneal perforation with iris prolapse. Examination of the left eye was unremarkable. CLOSE summary is shown in Table 30.1.

Differential Diagnosis

- Burkitt's lymphoma
- Rhabdomyosarcoma
- Retinoblastoma with orbital extension
- Primary bone tumour with secondary aneurysmal cyst
- Vascular malformation

M. A. Parulan
Department of Ophthalmology, National University Hospital, Singapore

S. Amrith (✉) · S. M. Young · G. Sundar
Department of Ophthalmology, National University Hospital, Singapore

Department of Ophthalmology, Yong Loo Lin School of Medicine, National University of Singapore, Singapore
e-mail: shantha_amrith@nuhs.edu.sg; gangadhara_sundar@nuhs.edu.sg

E. Ting
Department of Diagnostic Imaging, National University Hospital, Singapore

Department of Diagnostic Imaging, Yong Loo Lin School of Medicine, National University of Singapore, Singapore

Advanced Medicine Imaging, Singapore

B. Wu
Department of Pathology, National University Hospital, Singapore

M. E. Nga
Department of Pathology, National University Hospital, Singapore

Department of Pathology, Yong Loo Lin School of Medicine, National University of Singapore, Singapore

S. Amrith et al. (eds.), *Ocular Adnexal Lesions*, https://doi.org/10.1007/978-981-13-3798-7_30

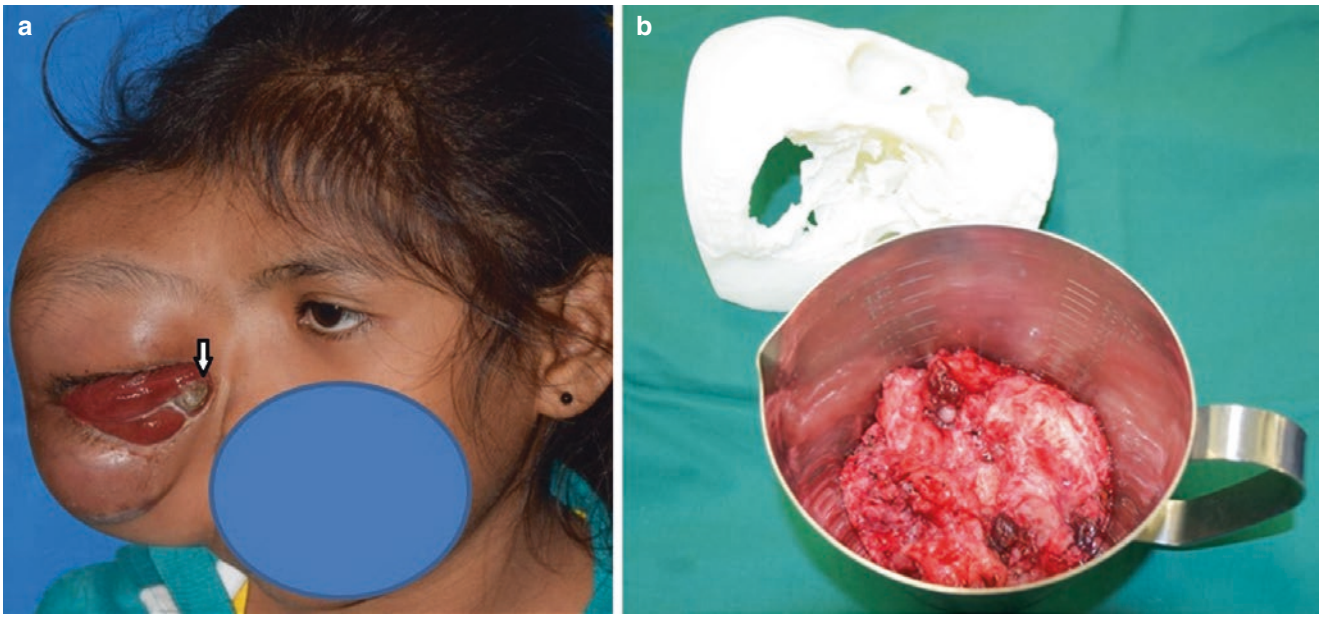

Fig. 30.1 (**a**) Clinical picture showing the presence of a large tumour on the right side of the face with orbital involvement. The tumour is seen to push the phthisical eye into the extreme right corner (arrow). (**b**) Excised tumour with prototype of the skull showing the extent of bony defect

Table 30.1 CLOSE summary

*C*linical process: infiltrative mass
*L*ocation: right orbit/face
*O*nset: chronic
*S*igns and symptoms: large expanding facial mass with blindness, and phthisis bulbi
*E*pidemiology: 9-year-old Southeast Asian female child

Imaging

Contrast-enhanced CT scan showed a large mass involving the right side of the face (Fig. 30.2). It appeared to arise from the bone, being centred on right frontal, sphenoidal and maxillary bones, with gross expansion, and deformity resulting in compression of the right orbit with inferomedial displacement of orbital contents, and extrusion and collapse/phthisis of the right globe. The lesion was predominantly lucent with a narrow zone of transition, with some areas of solid periosteal reaction and bony remodeling. The soft tissue component of this mass demonstrated multiple mildly enhancing septations with areas of hypodensity, likely to represent cystic change. The right lamina papyracea demonstrated leftward bowing. Intracranial expansion of the orbital plate of frontal bone and greater wing of sphenoid resulted in mass effect on the right frontal lobe of the brain.

Intervention

The patient underwent incisional biopsy with limited tumour debulking which showed low-grade myxoid neoplasm. A multidisciplinary meeting was conducted between paediatric oncology, ophthalmic plastic surgery, craniomaxillofacial, neurosurgery, and interventional radiology teams. A decision was made to perform complete excision, possible enucleation with implant, and primary facial/orbital socket reconstruction with a loco-regional flap.

Histopathology

Paraffin sections showed a lobulated, partially encapsulated tumour composed mainly of loose myxoid stroma with bland-appearing stellate and spindle-shaped cells. Irregular trabeculae of lamellar bone were present at the periphery of the tumour (Figs. 30.3 and 30.4). The tumour cells were diffusely positive for S100 on immunohistochemistry. Overall, the features are those of a low-grade myxoid neoplasm.

Management

Surgical debulking was carried out using a coronal flap with extension down to the preauricular region. Floor of the frontal, temporal, part of the sphenoid wing and maxilla were removed. A right frontal craniectomy was performed, and the intra- and extracranial parts of the tumour were removed piecemeal (Fig. 30.1b). Enucleation was carried out with a 22 mm acrylic implant wrapped in donor sclera.

Discussion

Ossifying fibromyxoid tumours (OFMT) are commonly seen in middle-aged adults, with median age at 50 years. It usually

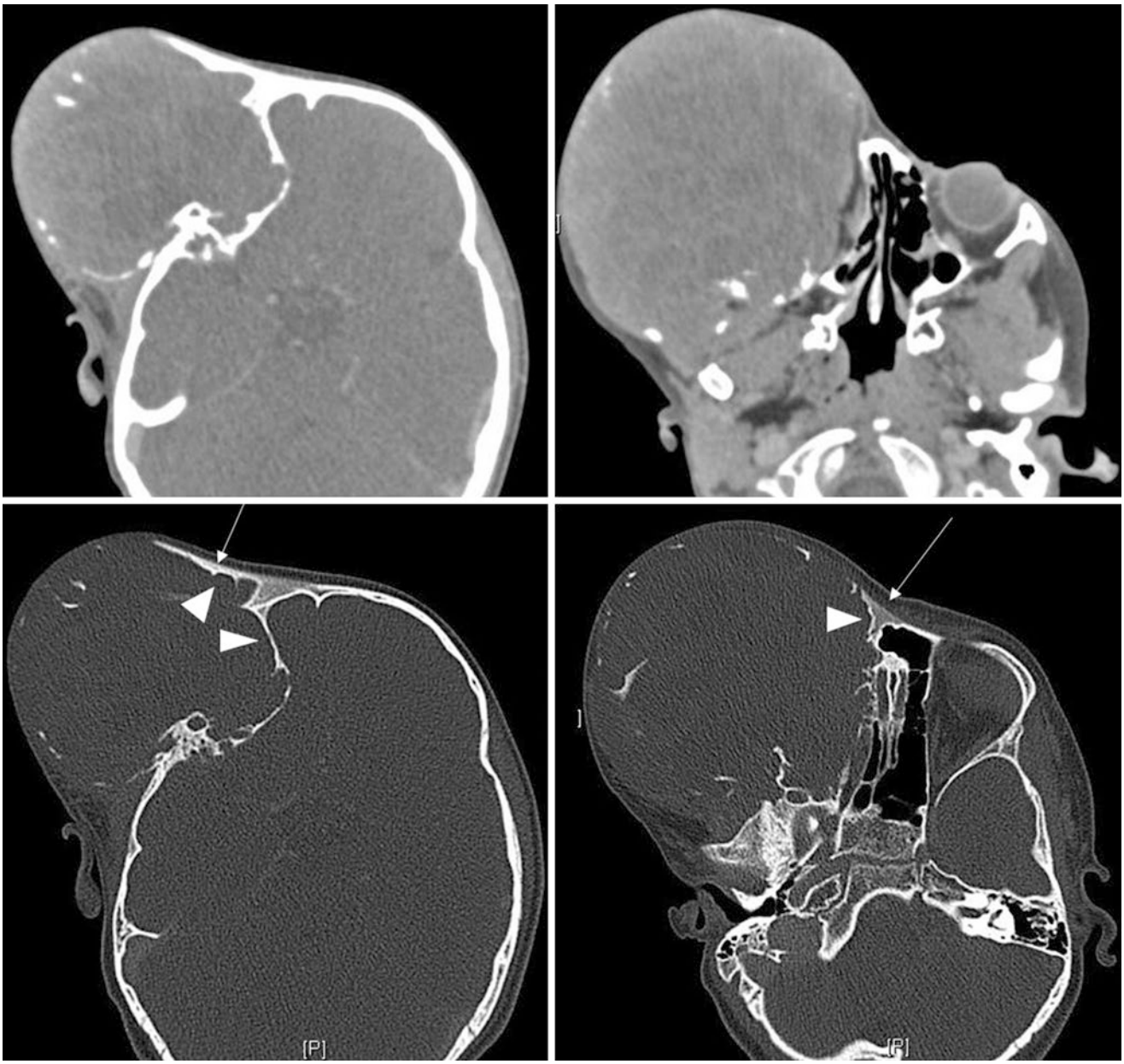

Fig. 30.2 Contrast-enhanced CT with bone and soft tissue windows showing a large, lucent, expansile mass centred on the right fronto-orbital region. There is evidence of bony remodeling with new bone formation buttressing the margins of the tumour (thin arrows) and a sclerotic rim at some of the scalloped margins (arrowhead)

presents as a tumour of the subcutaneous soft tissues or skeletal muscles of extremities, with a long-standing clinical course ranging from 1 to 20 years. Clinical features would include well-circumscribed painless, deep-seated tumour attached to underlying tendons, fascia, or skeletal muscles. Nine percent of the tumours present in the head and neck region, as painless slow-growing subcutaneous mass, typically in middle-aged men. It is rarely seen in the paediatric age group and even rarer in the orbital region.

Although the vast majority of this tumour is reported to be benign by histologic and clinical behaviour, idiosyncrasies of this lesion include occasional increased mitotic activity at 27% (>2 per 10 high power field), cytological atypia at 12%, and recurrence 6 to >10 years after surgical excision at 21%. Recurrence after excision was noted to be associated with increased mitotic activity in 93% of the cases. Some have described OFMT to have three microscopic subtypes: (1) typical, (2) atypical, and (3) malignant OFMT.

Myxoid tissues consist of a gelatinous mucopolysaccharide matrix of sulphated and nonsulphated glycosaminoglycans. Due to its high water content, the tumour presents with a hypoechoic appearance on ultrasound and low attenuation on CT scan. MRI remains the imaging modality of choice and presents with extremely low and high signal intensity on T1w and T2w imaging, respectively.

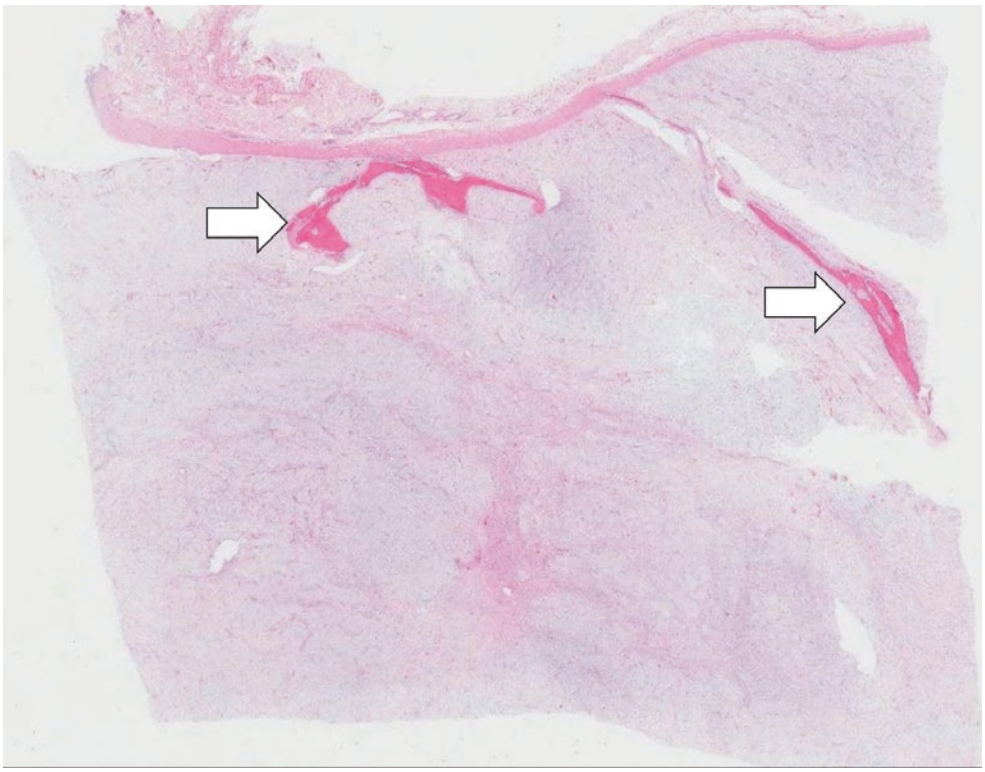

Fig. 30.3 Histology shows a lobulated, partially encapsulated tumour with abundant loose myxoid stroma. Irregular trabeculae of lamellar bone are present at the periphery of the tumour (white arrows). HE stain, 20× magnification

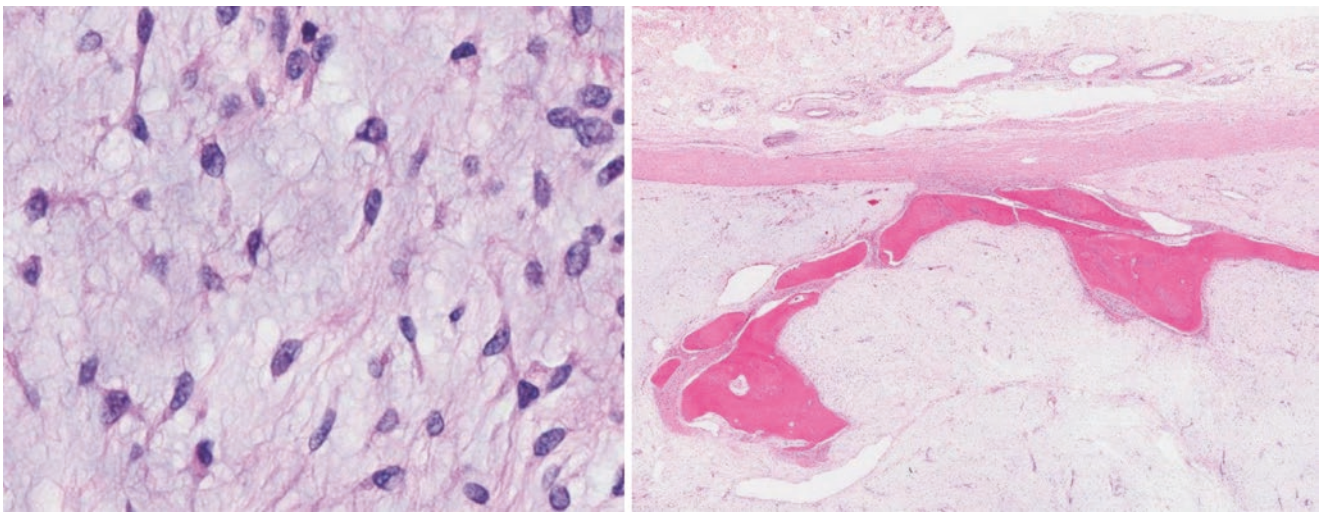

Fig. 30.4 The tumour cells within the loose myxoid stroma exhibit stellate and spindled morphology (left). Irregular trabeculae of lamellar bone are present at the periphery of the tumour (right). Left: HE stain, 400× magnification. Right: HE stain, 40× magnification

Surgical excision is the treatment of choice for these tumours. Early follow-up and close monitoring are advocated because of the tendency for tumour recurrence and metastasis. Recent advances in cytogenetic and molecular studies are well under way, and the discovery of a novel fusion gene, EP400-PHF1, may play a significant role in the diagnostic evaluation of this tumour. Currently, no studies have proven the role of adjuvant chemotherapy or targeted therapy for these tumours.

Learning Points

- Ossifying fibromyxoid tumour (OFMT), a rare adnexal neoplasm, most often has a benign clinical course, but on rare occasions, even histologically typical tumours may locally recur or metastasise several years after surgical removal.
- Because of rarity, recognition is important for appropriate management and monitoring.

Further Reading

1. Al-Mazrou KA, Mansoor A, Payne M, Richardson MA. Ossifying fibromyxoid tumor of the ethmoid sinus in a newborn: report of a case and literature review. Int J Pediatr Otorhinolaryngol. 2004;68(2):225–30.
2. Baheti AD, Tirumani SH, Rosenthal MH, Howard SA, Shinagare AB, Ramaiya NH, Jagannathan JP. Myxoid soft-tissue neoplasms: comprehensive update of the taxonomy and MRI features. Am J Roentgenol. 2015;204(2):374–85.
3. Bakiratharajan D, Rekhi B. Ossifying fibromyxoid Tumor: an update. Arch Pathol Lab Med. 2016;140(4):371–5.
4. Binesh F, Akhavan A, Navabii H. Ossifying fibromyxoid tumour: a rare soft tissue tumour of intermediate malignancy. BMJ Case Rep. 2011;2011:bcr0820103263.
5. Endo M, Kohashi K, Yamamoto H, Ishii T, Yoshida T, Matsunobu T, Iwamoto Y, Oda Y. Ossifying fibromyxoid tumor presenting EP400-PHF1 fusion gene. Hum Pathol. 2013;44(11):2603–8.
6. Folpe AL, Weiss SW. Ossifying fibromyxoid tumor of soft parts: a clinicopathologic study of 70 cases with emphasis on atypical and malignant variants. Am J Surg Pathol. 2003;27(4):421–31.
7. Kilpatrick WGW, Mozes M, Miettinen M, Fukunaga M, Fletcher CDM. Atypical and malignant variants of ossifying fibromyxoid tumor: clinicopathologic analysis of six cases. Am J Surg Pathol. 1995;19(9):1039–46.
8. Kondylidou-Sidira A, Kyrgidis A, Antoniades H, Antoniades K. Ossifying fibromyxoid tumor of head and neck region: case report and systematic review of literature. J Oral Maxillofac Surg. 2011;69(5):1355–60.
9. Nonaka CF, Pacheco DF, Nunes RP, Freitas Rde A, Miguel MC. Ossifying fibromyxoid tumor in the mandibular gingiva: case report and review of the literature. J Periodontol. 2009;80(4):687–92.
10. Park DJ, Miller NR, Green WR. Ossifying fibromyxoid tumor of the orbit. Ophthalmic Plast Reconstr Surg. 2006;22(2):87–91.
11. Sharma K, Hughes D, Harper RD. Ossifying fibromyxoid tumor (OFMT) – a rare cause of a painful thumb. Int J Surg Case Rep. 2015;7C:93–5.
12. Velasco AV, Zhang R, Li T, Wang D. Ossifying fibromyxoid tumor of soft parts in head and neck: case report and literature review. Diagn Pathol. 2018;13:21.

Part VIII

Benign Neoplasms: Lacrimal System

Lacrimal Gland: Pleomorphic Adenoma

31

Shantha Amrith, Stephanie Ming Young, Poh Sun Goh, Bingcheng Wu, Min En Nga, and Gangadhara Sundar

Introduction

Pleomorphic adenomas (also known as benign mixed tumours) of the lacrimal gland arise from epithelial and mesenchymal elements such as ducts, myoepithelial components and stroma. Up to 50% of lacrimal gland tumours are epithelial, and a good number of them are pleomorphic adenomas. They typically occur in the 2nd to 5th decades of life, with no gender predilection. Clinically, they present as mass lesions, manifesting as slowly progressive, painless proptosis.

Clinical Scenario

A 51-year-old Malay female presented with a history of progressive prominence of her right eye for a couple of years. She denied any pain, blurring of vision or double vision. On examination, the visual acuity of the right eye was slightly decreased due to the presence of a cataract. A non-axial proptosis of 6 mm with hypoglobus of the right eye was noted (Fig. 31.1). The motility of the right eye was limited on supraduction and abduction. There was no RAPD. The rest of the ophthalmic examination including the fundi were normal.

CLOSE summary is given in Table 31.1.

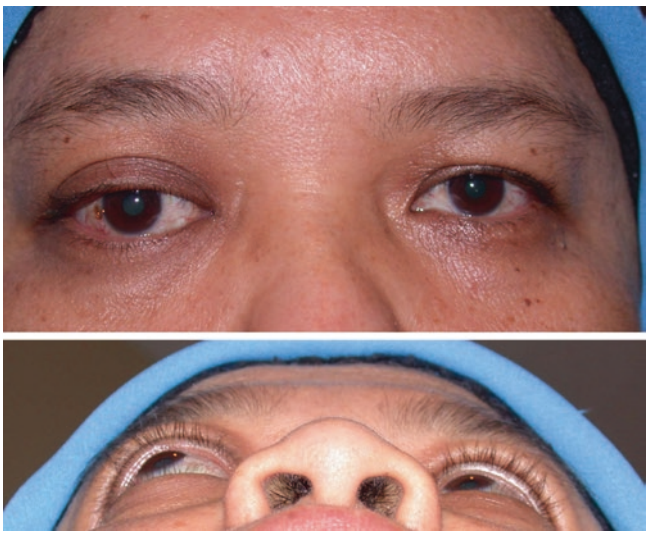

Fig. 31.1 Clinical picture showing non-axial proptosis of the right eye (note the downward displacement of the right globe)

Table 31.1 CLOSE summary

*C*linical scenario: mass lesion
*L*ocation: right superior orbit
*O*nset: chronic
*S*igns and symptoms: progressive painless proptosis
*E*pidemiology: 51-year-old Malay female

S. Amrith (✉) · S. M. Young · G. Sundar
Department of Ophthalmology, National University Hospital, Singapore

Department of Ophthalmology, Yong Loo Lin School of Medicine, National University of Singapore, Singapore
e-mail: shantha_amrith@nuhs.edu.sg; gangadhara_sundar@nuhs.edu.sg

P. S. Goh
Department of Diagnostic Imaging, National University Hospital, Singapore

Department of Diagnostic Imaging, Yong Loo Lin School of Medicine, National University of Singapore, Singapore

B. Wu
Department of Pathology, National University Hospital, Singapore

M. E. Nga
Department of Pathology, National University Hospital, Singapore

Department of Pathology, Yong Loo Lin School of Medicine, National University of Singapore, Singapore

S. Amrith et al. (eds.), *Ocular Adnexal Lesions*, https://doi.org/10.1007/978-981-13-3798-7_31

Differential Diagnosis

- Benign tumours such as schwannoma, solitary fibrous tumour, meningioma
- Non-distensible venous malformation (cavernous haemangioma)
- Benign lacrimal gland tumour such as pleomorphic adenoma
- Lymphoproliferative lesions including lymphoma
- Non-specific orbital inflammation

Radiology

Computerised tomography (CT) scan showed a 2 cm round, extraconal, enhancing soft tissue mass, arising from the upper lateral quadrant (lacrimal fossa) of the right orbit (Fig. 31.2). It was displacing the lateral rectus inferiorly and superior rectus and optic nerve medially. There was bony remodelling of the lacrimal gland fossa. From the above findings, a diagnosis of pleomorphic adenoma or dacryoadenitis due to inflammatory cause was likely.

Intervention

The patient underwent lateral orbitotomy (Fig. 31.3), and the mass was removed with intact pseudocapsule and sent for histopathology.

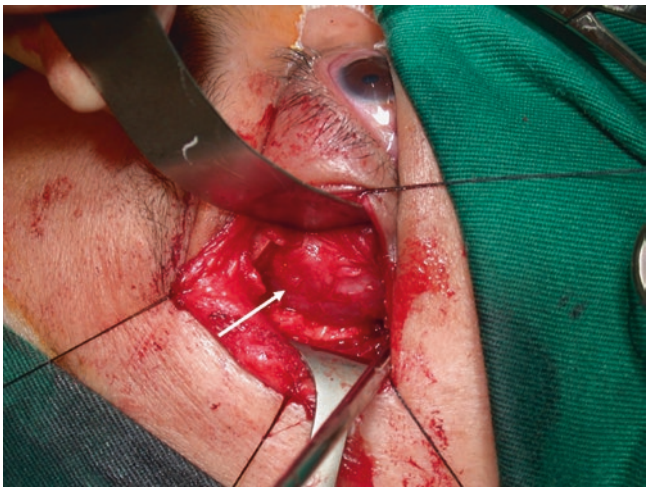

Fig. 31.3 The lacrimal gland mass exposed through a lateral orbitotomy

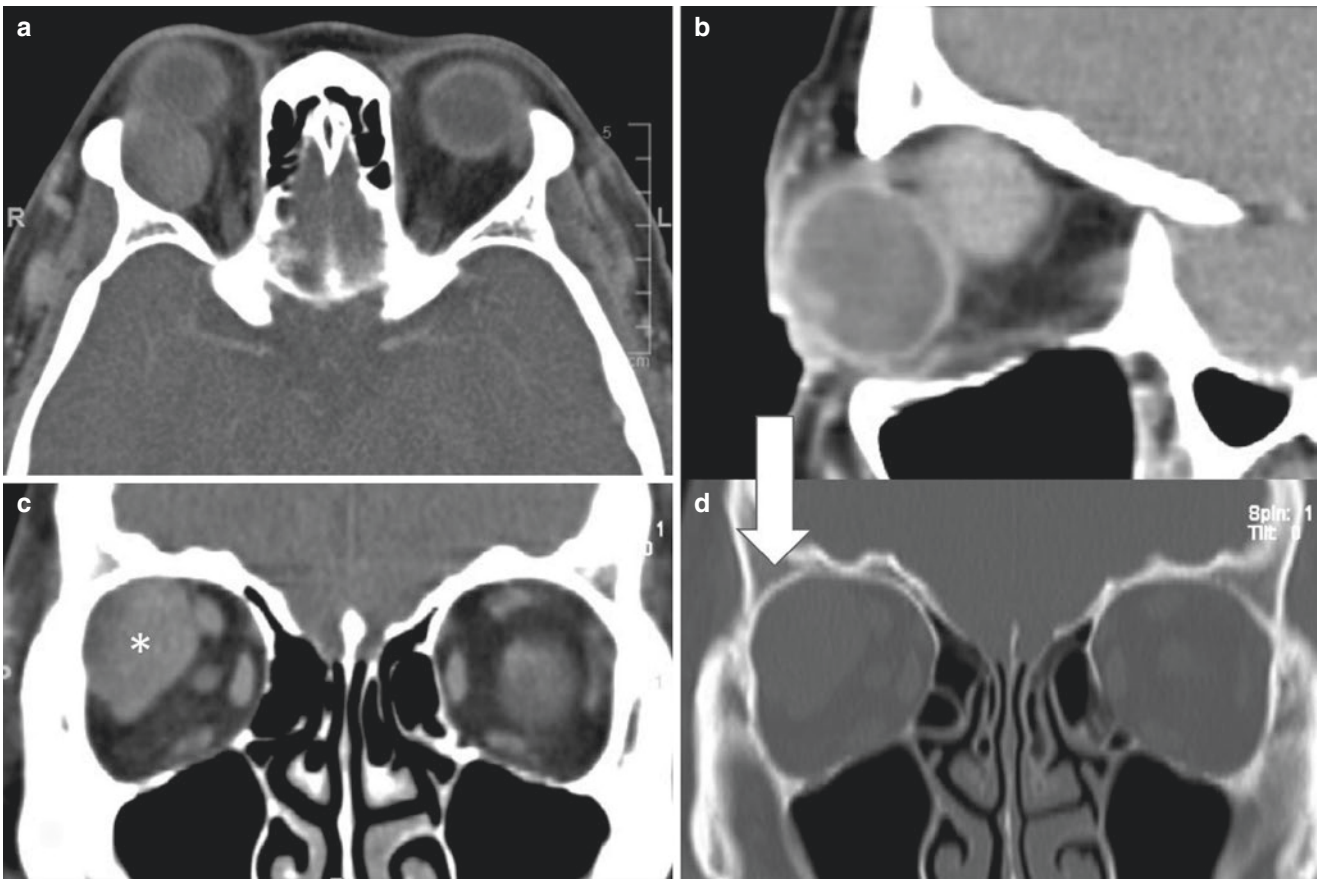

Fig. 31.2 (**a**, **b**, and **c**) Axial, sagittal and coronal CT scans showing a solid mass (*) in the right lacrimal gland fossa with uniform density and enhancement. (**d**) Coronal bone window shows remodelling of the superolateral wall of the right orbit adjacent to the mass (arrow)

Histopathology

The cut section showed a firm, whitish/yellow and partly gelatinous tumour composed of mesenchymal and epithelial elements. The epithelial elements lined several ductal and tubular structures. The myoepithelial cells appeared polygonal with clear cytoplasm. The mesenchymal elements were predominantly myxoid.

The tumour was completely surrounded by two thin fibrous capsules and was completely excised (Fig. 31.4). Sections of the lacrimal gland showed unremarkable glandular tissue with small lymphoid follicles. The histological features were consistent with the diagnosis of pleomorphic adenoma of the lacrimal gland (completely excised).

Discussion

Pleomorphic adenomas are one of the most common benign epithelial tumours of the lacrimal gland. The adenomas arising from the orbital lobe present with painless non-axial proptosis in adults, slowly progressive over a year or longer, whereas the ones arising from palpebral lobe present as eyelid lumps and present much earlier. About 10–20% of pleomorphic adenomas transform into carcinoma ex-pleomorphic adenoma in about 20 years. Pathologically, they lack a true capsule, but have a pseudocapsule, formed by the compression of the surrounding normal lacrimal gland tissues. The tumour consists of cellular cords that extend to the periphery and into the pseudocapsule; therefore, it is important to remove the entire tumour with the pseudocapsule and surrounding normal tissue. Incomplete removal may result in recurrence (10% after 20 years–20% after 30 years) and occasional malignant transformation.

Radiologically, pleomorphic adenomas of the lacrimal gland appear as well-circumscribed lesions with heterogeneous appearance representing cystic areas within the tumour. There is a smooth or scalloped bony excavation with intact cortical bone and indentation of the globe. MRI shows the heterogeneous internal architecture well on T2-weighted images and an enhancing rim on T1-weighted, fat-suppressed, contrast images. Although calcification may indicate malignancy, it may be seen in some cases of benign pleomorphic adenoma. Histologically, two-thirds are epithelial and one-third myoepithelial with myxoid and chondroid dysplasia.

An incisional biopsy may not be necessary, if clinical diagnosis of pleomorphic adenoma can be made with reasonable certainty. A history of painless lacrimal gland mass, with no sensory loss, for longer than a year, along with radiological features of a well-defined mass, bony excavation and intact cortical bone without erosion will favour a diagnosis of pleomorphic adenoma. On the other hand, a shorter history with pain, paraesthesia or loss of sensation, combined with bony erosion rather than excavation on imaging, will suggest an adenoid cystic carcinoma. When the clinical features are atypical, an open or a needle aspiration biopsy may be necessary. Where a biopsy has been per-

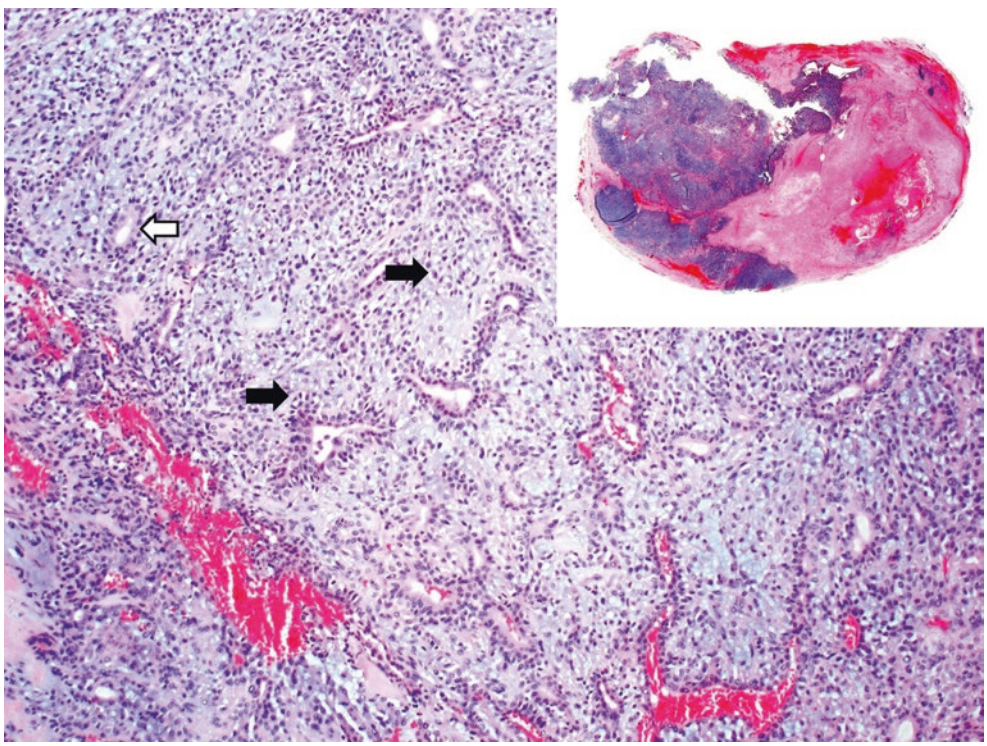

Fig. 31.4 There are haphazardly arranged tubules (white arrow) within a blue-grey myxoid stroma. Myoepithelial cells are present within the myxoid stroma and also in the outer layer of the tubules (black arrows). The tumour has very well-demarcated and smooth contours (inset). Main: HE stain, 100× magnification. Inset: HE stain, 20× magnification

formed, it may be prudent to remove the biopsy tract entirely along with the tumour, the pseudocapsule and surrounding rim of tissue to prevent recurrence. A lifelong follow-up may be necessary for these patients. Sudden painful recurrence in an incompletely removed tumour may indicate malignant transformation.

Learning Points

Pleomorphic adenoma of the orbital lobe of lacrimal gland presents as slowly progressive superotemporal mass with painless proptosis in adults. The radiological features are typical with a well-circumscribed mass in the lacrimal fossa, compressing the globe and excavating the adjacent bone. The mass should be excised completely with intact pseudocapsule and a rim of surrounding tissue in order to prevent recurrences and/or malignant transformation.

Further Reading

1. Binatli Ö, Yaman O, Özdemir N, Erdoğan IG. Pleomorphic adenoma of lacrimal gland. J Surg Case Rep. 2013;2013(10):rjt089. https://doi.org/10.1093/jscr/rjt089.
2. Gunduz K, Shiels CL, Gunalp I, Shields JA. Magnetic resonance imagining of unilateral lacrimal gland lesions. Graefes Arch Clin Exp Ophthalmol. 2003;241:907–13.
3. Jung WS, Ahn KJ, Park MR, Kim JY, Choi JJ, Kim BS, Hahn ST. The radiological spectrum of orbital pathologies that involve the lacrimal gland and the lacrimal fossa. Korean J Radiol. 2007;8(4):336–42.
4. Rootman J. Diseases of the orbit, a multidisciplinary approach. 2nd ed. Philadelphia: Wolters Kluwer Lippincott Williams & Wilkins; 2003.
5. Rose GE, Wright JE. Pleomorphic adenoma of the lacrimal gland. Br J Ophthalmol. 1992;76:395–400.
6. Watanabe A, Andrew NH, Ueda K, Kinoshita S, Katori N, Reid M, Pirbhai A, Selva D. Clinico-radiological features of primary lacrimal gland pleomorphic adenoma: an analysis of 37 cases. Jpn J Ophthalmol. 2016;60(4):286–93.
7. Weis E, Rootman J, Joly TJ et al. Epithelial Lacrimal Gland Tumors: Pathologic classification and current understanding. Arch of Ophthalmol 2009;127(8):1016–28

Lacrimal Sac Inverted Papilloma

32

Shantha Amrith, Stephanie Ming Young, Eric Ting, Bingcheng Wu, Min En Nga, and Gangadhara Sundar

Introduction

Inverted papilloma (IP), as the name suggests, is coined from the histological appearance of the epithelium inverting into the stroma. It is usually unilateral, with a male preponderance. Although it is more common in the sixth and seventh decades of life, isolated cases have been reported in the paediatric age group. Majority of the papillomas originate from the mucosal lining of the sino-nasal tract, occurring commonly in the ethmoids, lateral wall of the nasal fossa and the maxillary sinus. IP may arise primarily from the nasolacrimal duct (NLD) and the lacrimal sac, as they have similar mucosal lining. NLD and the lacrimal sac may be affected secondarily due to extension from the adjacent nasal mucosa or sinuses.

Clinical Scenario

A 19-year-old Chinese male presented with tearing in his left eye for a few months prior to consult. He had noticed some discharge which was mucoid in nature, and he denied tearing during his early childhood. On examination, he had normal visual acuity in both eyes. On the left side, he had a raised tear meniscus with swelling in the medial corner below the medial canthus, which was non-tender and cystic in nature indicative of a lacrimal sac swelling. On pressure over the sac, there was regurgitation of mucus into the conjunctival sac, confirming the presence of a lacrimal sac mucocoele.

CLOSE summary is in Table 32.1.

Table 32.1 CLOSE summary

*C*linical process: inflammatory/infiltrative
*L*ocation: left NLD/lacrimal sac
*O*nset: subacute
*S*igns and symptoms: tearing and lacrimal mucocoele
*E*pidemiology: young Chinese male

Differential Diagnosis

- Primary nasolacrimal duct obstruction
- Epidermal cyst

S. Amrith (✉) · S. M. Young · G. Sundar
Department of Ophthalmology, National University Hospital, Singapore

Department of Ophthalmology, Yong Loo Lin School of Medicine, National University of Singapore, Singapore
e-mail: shantha_amrith@nuhs.edu.sg; stephanie.young@nuhs.edu.sg; gangadhara_sundar@nuhs.edu.sg

E. Ting
Department of Diagnostic Imaging, National University Hospital, Singapore

Department of Diagnostic Imaging, Yong Loo Lin School of Medicine, National University of Singapore, Singapore

Advanced Medicine Imaging, Singapore

B. Wu
Department of Pathology, National University Hospital, Singapore

M. E. Nga
Department of Pathology, National University Hospital, Singapore

Department of Pathology, Yong Loo Lin School of Medicine, National University of Singapore, Singapore

S. Amrith et al. (eds.), *Ocular Adnexal Lesions*, https://doi.org/10.1007/978-981-13-3798-7_32

- Extrinsic tumours pressing on the lacrimal sac
- Medial angular dermoid
- Inverted papilloma of the lacrimal sac

Intervention

Under general anaesthesia, an endoscopic dacryocystorhinostomy was performed. After the osteotomy, when an attempt was made to open the lacrimal sac, the medial wall of the lacrimal sac was found to be unusually thickened and abnormal. A biopsy of the sac mucosa was performed and sent for histopathology. Dacryocystorhinostomy was completed by creating lacrimal sac flaps followed by bicanalicular intubation.

Histopathology

Paraffin sections showed a tumour (Fig. 32.1) exhibiting an inverted (inward-growing) growth pattern. A broad-pushing tumour front was appreciated. The tumour grew by dipping inwards into the underlying stroma in an endophytic pattern. The epithelium in this case was predominantly of transitional type (stratified non-squamous). The features were consistent with a lacrimal sac inverted papilloma.

Imaging

The patient underwent CT scan of the sinuses in view of the histological diagnosis. There was a soft tissue mass in the left

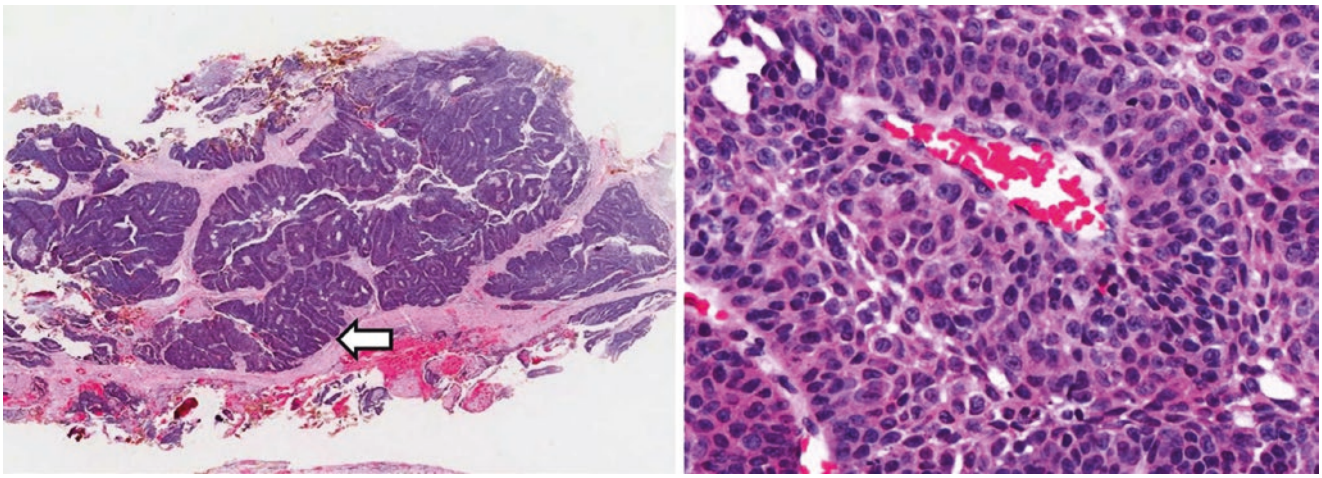

Fig. 32.1 The neoplasm shows an endophytic/inverted growth pattern. Instead of protruding outwards into the lumen, the neoplasm pushes inwards into the stroma (white arrow). The tumour epithelial cells are stratified and do not exhibit marked nuclear pleomorphism or mitotic activity. Left, HE stain (20× magnification); right, HE stain (100× magnification)

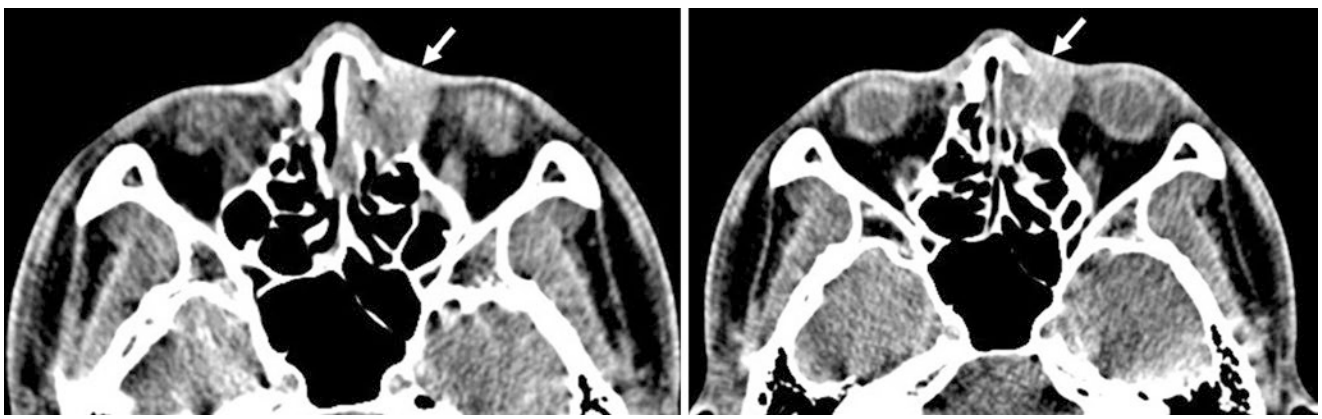

Fig. 32.2 Axial non-contrast-enhanced CT images showing a soft tissue mass (white arrows) expanding the lacrimal sac fossa. There is demineralisation and remodelling of the adjacent bones

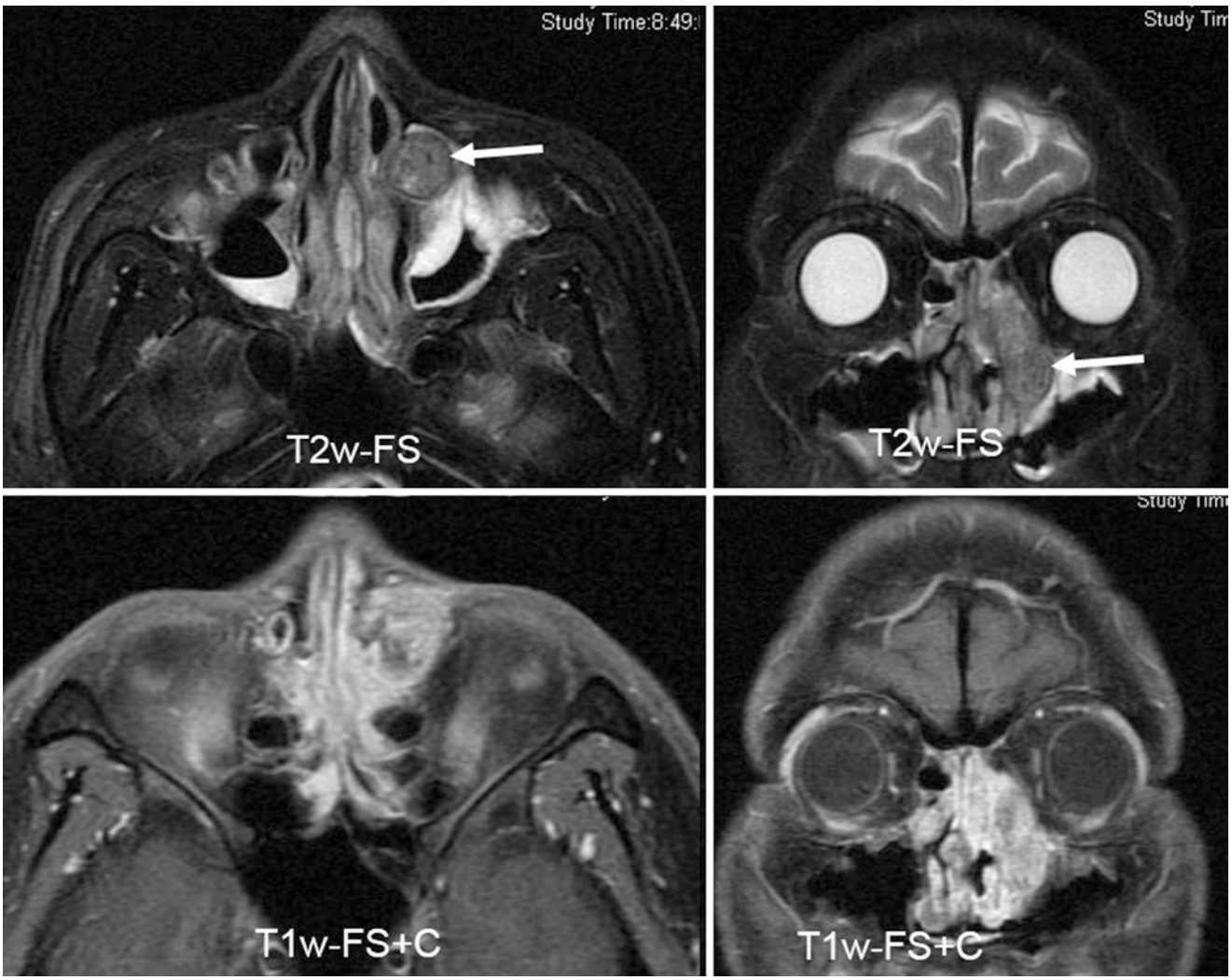

Fig. 32.3 Axial (left) and coronal (right) T2w-FS and T1w-FS + contrast images showing a soft tissue mass centred on the left lacrimal sac. The mass extends inferiorly along the nasolacrimal duct (white arrows) into the inferior meatus. Note the somewhat convoluted cerebriform pattern, seen on the axial images

lacrimal sac region. The lesion extended through the nasolacrimal duct into the inferior meatus (Fig. 32.2). The features were suggestive of a slow-growing tumour in the lacrimal sac.

Magnetic resonance imaging (MRI) showed similar results. The mass in the NLD showed lower signal intensity compared to the inflammatory changes seen in the maxillary sinus bilaterally in T2w and FLAIR images. There was also a strong contrast enhancement (Fig. 32.3).

Management

He subsequently underwent a medial maxillectomy with complete removal of the lacrimal sac and distal canaliculi by a combined endoscopic and external approach, by a team comprising a rhinologist and ophthalmic plastic surgeon.

Discussion

Inverted papilloma is also known as Schneiderian papilloma, as it arises from specialised mucosa called the Schneiderian epithelium, an ectodermal respiratory epithelium that lines the lateral nasal wall and paranasal sinuses. It is a rare benign neoplasm, is locally invasive and has great propensity for recurrence (28–74%). Occasionally, malignant transformation to transitional cell carcinoma or squamous cell carcinoma occurs. Although the aetiology remains largely unknown, human papilloma virus (HPV) types 6 and 11 and Epstein-Barr virus have been identified in the lesions. HPV's presence may indicate a higher likelihood of both malignancy and recurrence.

Primary inverted papillomas of the lacrimal sac are rare. The origin is however disputed. As IP is more common in the lateral nasal wall where the NLD opens, it is possible that the

tumour spreads along the NLD to reach the lacrimal sac. The tumour may destroy the bone and extend further into the orbit. The patients usually present with tearing, as in NLD obstruction, and often the tumour is detected unexpectedly during a routine DCR. Rarely, the patients present with serosanguinous discharge or mass lesion in the medial canthus.

On MRI, the tumour shows a typical convoluted cerebriform pattern. Histopathology shows an inward growing pattern with features of respiratory type of epithelium or squamous epithelium, the latter with scattered mucocytes interspersed within the neoplastic epithelium.

It is important to exclude malignant transformation into squamous cell carcinoma, the features of which include loss of polarity, nuclear pleomorphism, high mitotic activity, tumour necrosis and an infiltrative growth pattern. Adequate tissue sampling is important, to look for any premalignant areas (e.g. high-grade dysplasia/intraepithelial neoplasia).

The treatment of choice is complete surgical resection in the form of total sac excision with medial maxillectomy and lifelong follow-up. Early detection gives the best chance of cure. High index of suspicion can lead to diagnosis during an unsuspected DCR, when the lacrimal sac epithelium is abnormal. An endoscopic resection, in collaboration with an otolaryngologist, may be the best approach in such cases. Radiotherapy should be avoided for benign lesions. Recurrent cases should carefully be subjected to biopsy to detect early transformation to malignancy. Malignant lesion should be treated the same way as a squamous cell carcinoma.

Learning Points

Inverted papillomas are locally aggressive benign lesions with propensity for recurrence and malignant transformation.

Inverted papillomas of NLD and lacrimal sac are rare and may occur as unsuspecting lesions during a routine DCR. Proper biopsy followed by dacryocystectomy and medial maxillectomy should be performed in collaboration with an otolaryngologist.

Lifelong follow-up is necessary to detect early recurrence or malignant transformation.

Further Reading

1. Golub JS, Parikh SL, Budnick SD, Bernardino CR, DelGaudio JM. Inverted papilloma of the nasolacrimal system invading the orbit. Ophthalmic Plast Reconstr Surg. 2007;23(2):151–3.
2. Macdonald MR, Le KT, Freeman J, et al. A majority of inverted sinonasal papillomas carries Epstein-Barr virus genomes. Cancer. 1995;75:2307–12.
3. Raemdonck TYE, VanDen Broecke CM, Claerhout I, Decock CE. Inverted papilloma arising primarily from the lacrimal sac. Orbit. 2009;28(2–3):181–4.
4. Sundar G. Tumors of the lacrimal drainage system. In: Ali MJ, editor. Principles and practice of lacrimal surgery. New Delhi: Springer; 2018.
5. Walijee Z, Berry S, Quine S, Lane C, Morris DS, Bowman B. Inverted papilloma originating primarily from the nasolacrimal duct: a case report and review of the pertinent literature. Case Rep Otolaryngol. 2015;2015:123694.
6. Woodcock M, Mollan SP, Harrison D, Taylor D, Lecuona K. Mitomycin C in the treatment of a Schneiderian (inverted) papilloma of the lacrimal sac. Int Ophthalmol. 2010;30(3):303–5.

Part IX

Lymphoproliferative Disorders

Overview

33

Limei Michelle Poon

Introduction

The term lymphomas is made up of the term "lympho" (pertaining to lymph, lymphoid, or lymphatic tissues) and "oma" (indicating tumors or masses) and, as the name implies, refers to malignant neoplasms derived from monoclonal proliferation of B- or T-lymphocytes or rarely, natural killer (NK) cells. Lymphomas are divided into two large groups of neoplasms, namely, Hodgkin's lymphoma (HL) and non-Hodgkin's lymphoma (NHL). Of these, NHL is more common, constituting about 85% to 90% of all lymphomas. Ophthalmic lymphomas can be divided into (i) intraocular lymphomas (a kind of central nervous system lymphoma) or (ii) ocular adnexal lymphomas, an umbrella term encompassing the spectrum of lymphoid diseases affecting the tissues surrounding the eye. Ophthalmic lymphomas are almost always of the NHL subtypes, while HL in ophthalmic practice is extremely uncommon and will not be discussed here.

Classification of Ophthalmic Lymphomas

Primary Intraocular Lymphomas (PIOL)

Intraocular lymphomas can arise within the retina, uvea, vitreous, and optic nerve. These are usually of B-cell origin, though rarely, T-cell subtypes are also seen. Intraocular lymphoma can be divided into either primary or secondary types. Primary intraocular lymphomas (PIOL) represent a subset of primary central nervous system lymphomas (PCNSL), where the lymphoma cells occur in the eyes alone, though concomitant or subsequent intracranial involvement may be possible as well [1, 2]. Secondary intraocular lymphomas (SIOL) are lymphomas which arise outside the central nervous system and metastasize to the eyes. Both PIOL and SIOL are usually of the B-cell origin (of which diffuse large B-cell lymphoma (DLBCL) is the most common subtype) though rarely, primary T-cell intraocular lymphomas or metastatic NKT-cell lymphomas or systemic T-cell lymphomas presenting as SIOL may be seen [3–6].

Ocular Adnexal Lymphomas (OAL)

OAL are lymphomas which arise within the ocular adnexa, structures that surround and support the functioning of the eyeball. Like IOL, OAL can also be similarly divided into "primary" and "secondary" types. Primary OAL are usually associated with isolated involvement of the ocular adnexa, while in secondary OAL, lymphoma is also seen elsewhere in the body. OAL are usually of B-cell origin of which extranodal marginal zone lymphoma (ENMZL)/mucosal-associated lymphomas (MALT) is the commonest subtype, followed by follicular lymphoma (FL), diffuse large B-cell lymphoma (DLBCL), and mantle cell lymphoma (MCL).

Understanding OAL

Aetiology of OALs

There have been a number of aetiologic factors identified for primary OAL, including infective causes as well as autoimmunity. Autoimmune conditions such as Sjogren's syndrome, systemic lupus erythematosus (SLE), and rheumatoid arthritis have been shown to be in large epidemiological and clinical correlative studies to be associated with risks for development of NHL, especially mucosal-associated lymphomas (MALT) [7–10], though the exact pathogenetic

L. M. Poon (✉)
Department of Haematology-Oncology, National Cancer Institute of Singapore, Singapore

Department of Haematology-Oncology, Yong Loo Lin School of Medicine, National University of Singapore, Singapore
e-mail: michelle_poon@nuhs.edu.sg

S. Amrith et al. (eds.), *Ocular Adnexal Lesions*, https://doi.org/10.1007/978-981-13-3798-7_33

mechanisms remain unclear. Infective agents [11–13] such as *Chlamydia psittaci*, human herpes virus 6 (HHV6), and, to a lesser extent, hepatitis C have also been found to have an association with OAL MALT lymphomas, though there has been variability in the literature, possibly due to the differing geographic distributions of the organisms. Of note, the positive response of OAL to treatment with doxycycline has further supported the hypothesis of a causative association between *C. psittaci* and this lymphoma.

Clinical Features and Diagnostic Challenges for OAL

OAL generally presents in an indolent fashion with slowly progressive mass effects symptoms of the orbit, associated with minimal functional impairment. These symptoms include soft tissue swelling, proptosis, or ocular motility limitations. The diagnosis of OAL can be challenging given the lack of symptoms in the early phase of disease (leading to delayed diagnosis and treatment), as well as the overlap of these entities with other clinical and morphologic mimics. Lymphoid hyperplasia (LH) refers to lymphoid proliferations which are often polyclonal or oligoclonal. It is often difficult to differentiate LH from OAL clinically or radiologically necessitating tissue biopsy and histology for distinction. In the era where diagnosis was made based on light microscopy alone, lymphoid hyperplasia was often further classified based on histology into two main subcategories including "reactive subtypes" where the morphology and immune-phenotype was completely benign and "atypical subtypes" where histology was borderline and differentiating them from lymphoma was often difficult. With the advent of modern diagnostic techniques and molecular studies, these diagnostic challenges have significantly improved, and the majority of these previously "atypical cases" have been found to be indolent lymphomas, with few cases remaining indeterminate. In recent years, a recently characterized entity, immunoglobulin G4 (IgG4)-related systemic sclerosing disease (IgG4 disease) has also been found to be a mimic of OAL and LH.

Staging and Prognostication for OAL

Staging work-up includes imaging of the orbits, pan-body CT scans to exclude systemic disease, and possibly bone marrow studies to exclude concomitant marrow involvement. The Ann Arbor staging is the most common staging system used for NHL. Given however that most OALs are stage IE at presentation, this has limited the utility of the Ann Arbor staging for prognostication in this disease subtype. In recent years, the Ophthalmic Oncology Task Force of the American Joint Committee on Cancer has proposed a TNM staging system for OAL, aimed at overcoming the limitations of the Ann Arbor system and facilitating comparison between studies in this field. This system has been increasingly used in recent years, given its possibly better prognostication ability [14].

With regard to prognostication, patients should be evaluated using prognostic scores according to their lymphoma subtypes. These include the International Prognostic Index (IPI) in DLBCL and MALT lymphoma/EMZL, the FL International Prognostic Index (FLIPI), and the MCL International Prognostic Index [15–17].

Management

The management for IOL (both primary and secondary) involves the use of systemic chemotherapy that is able to penetrate the blood brain barrier as well as possible concomitant use of radiotherapy (RT), for local control, to prevent visual loss and CNS involvement. In addition, intravitreal injection of chemotherapy or rituximab may also be considered for disease control [18].

For OAL, treatment depends on disease stage and lymphoma subtype. RT is generally the mainstay of treatment of localized indolent subtypes of OAL, with curative intent. In contrast, for advanced stage indolent subtypes of OAL, treatment options include watchful waiting, single-agent monoclonal antibody therapy (Rituximab) or immunochemotherapy, depending on disease extent and symptoms. In contrast for patients with aggressive subtypes such as DLBCL, the mainstay of treatment remains chemoimmunotherapy ± RT.

In this section, we shall illustrate the clinical manifestations, and principles of treatment of the various subtypes of ophthalmic lymphomas, based on a series of cases discussed during ophthalmology-pathology-radiology (OPR) rounds.

References

1. Buggage RR, Chan CC, Nussenblatt RB. Ocular manifestations of central nervous system lymphoma. Curr Opin Oncol. 2001;13:137–42.
2. Chan CC, Wallace DJ. Intraocular lymphoma: update on diagnosis and management. Cancer Control. 2004;11:285–95.
3. Levy-Clarke GA, Buggage RR, Shen D, et al. Human T-cell lymphotropic virus type-1 associated t-cell leukemia/lymphoma masquerading as necrotizing retinal vasculitis. Ophthalmology. 2002;109:1717–22.
4. Goldey SH, Stern GA, Oblon DJ, et al. Immunophenotypic characterization of an unusual T-cell lymphoma presenting as anterior uveitis. A clinicopathologic case report. Arch Ophthalmol. 1989;107:1349–53.
5. Saga T, Ohno S, Matsuda H, et al. Ocular involvement by a peripheral T-cell lymphoma. Arch Ophthalmol. 1984;102:399–402.

6. Chaput F, Amer R, Baglivo E, et al. Intraocular T-cell lymphoma: clinical presentation, diagnosis, treatment, and outcome. Ocul Immunol Inflamm. 2017;25:639–48.
7. Ekstrom Smedby K, Vajdic CM, Falster M, et al. Autoimmune disorders and risk of non-Hodgkin lymphoma subtypes: a pooled analysis within the InterLymph Consortium. Blood. 2008;111:4029–38.
8. Engels EA, Cerhan JR, Linet MS, et al. Immune-related conditions and immune-modulating medications as risk factors for non-Hodgkin's lymphoma: a case-control study. Am J Epidemiol. 2005;162:1153–61.
9. Nutting CM, Shah-Desai S, Rose GE, et al. Thyroid orbitopathy possibly predisposes to late-onset of periocular lymphoma. Eye (Lond). 2006;20:645–8.
10. Wohrer S, Troch M, Streubel B, et al. MALT lymphoma in patients with autoimmune diseases: a comparative analysis of characteristics and clinical course. Leukemia. 2007;21:1812–8.
11. Carugi A, Onnis A, Antonicelli G, et al. Geographic variation and environmental conditions as cofactors in Chlamydia psittaci association with ocular adnexal lymphomas: a comparison between Italian and African samples. Hematol Oncol. 2010;28:20–6.
12. Daibata M, Komatsu T, Taguchi H. Human herpesviruses in primary ocular lymphoma. Leuk Lymphoma. 2000;37:361–5.
13. Ferreri AJ, Viale E, Guidoboni M, et al. Clinical implications of hepatitis C virus infection in MALT-type lymphoma of the ocular adnexa. Ann Oncol. 2006;17:769–72.
14. Rath S, Connors JM, Dolman PJ, et al. Comparison of American joint committee on Cancer TNM-based staging system (7th edition) and Ann Arbor classification for predicting outcome in ocular adnexal lymphoma. Orbit. 2014;33:23–8.
15. Project TIN-HsLPF. A predictive model for aggressive non-Hodgkin's lymphoma. N Engl J Med. 1993;329:987–94.
16. Solal-Celigny P, Roy P, Colombat P, et al. Follicular lymphoma international prognostic index. Blood. 2004;104:1258–65.
17. Hoster E, Dreyling M, Klapper W, et al. A new prognostic index (MIPI) for patients with advanced-stage mantle cell lymphoma. Blood. 2008;111:558–65.
18. Sagoo MS, Mehta H, Swampillai AJ, et al. Primary intraocular lymphoma. Surv Ophthalmol. 2014;59:503–16.

Reactive Lymphoid Hyperplasia

34

Mariel Angelou Parulan, Shantha Amrith, Stephanie Ming Young, Eric Ting, Bingcheng Wu, Min En Nga, and Gangadhara Sundar

Introduction

The benign form of ocular adnexal lymphoproliferative disorder (OAL) is reactive lymphoid hyperplasia (RLH). About 16% of all OAL is reactive and benign, based on immunohistopathological staining and molecular studies. All cases of RHL have to be investigated for coexistence of lymphoma elsewhere in the body and should be followed up closely for relapses and transformation to lymphoma.

Clinical Scenario

A 66-year-old Indonesian female with no past medical history presented with painless right upper lid swelling of 1–2 years' duration. She had not noticed any other lumps in the neck or axilla. Examination revealed normal visual acuities in both eyes. She was noted to have a 2 mm proptosis with a ptosis in her right eye along with fullness in the upper temporal quadrant (Fig. 34.1). A firm mass was felt in the right lacrimal fossa. She had limitation of the right eye in upgaze. The rest of the ophthalmic examination was normal.

CLOSE summary is given in Table 34.1.

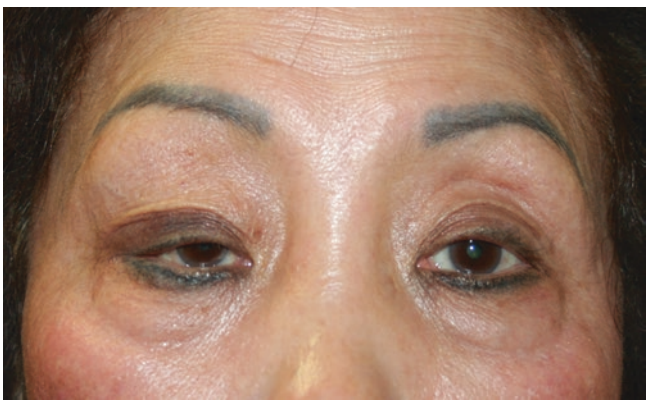

Fig. 34.1 Clinical picture showing the fullness in the temporal quadrant of the right upper lid with ptosis

Table 34.1 CLOSE summary

*C*linical process: infiltrative, mass lesion
*L*ocation: right lacrimal gland
*O*nset: chronic
*S*igns and symptoms: painless proptosis, upper lid swelling, and ptosis
*E*pidemiology: 66-year-old Indonesian female

M. A. Parulan
Department of Ophthalmology, National University Hospital, Singapore

S. Amrith (✉) · S. M. Young · G. Sundar
Department of Ophthalmology, National University Hospital, Singapore

Department of Ophthalmology, Yong Loo Lin School of Medicine, National University of Singapore, Singapore
e-mail: shantha_amrith@nuhs.edu.sg; stephanie.young@nuhs.edu.sg; gangadhara_sundar@nuhs.edu.sg

E. Ting
Department of Diagnostic Imaging, National University Hospital, Singapore

Department of Diagnostic Imaging, Yong Loo Lin School of Medicine, National University of Singapore, Singapore

Advanced Medicine Imaging, Singapore

B. Wu
Department of Pathology, National University Hospital, Singapore

M. E. Nga
Department of Pathology, National University Hospital, Singapore

Department of Pathology, Yong Loo Lin School of Medicine, National University of Singapore, Singapore

S. Amrith et al. (eds.), *Ocular Adnexal Lesions*, https://doi.org/10.1007/978-981-13-3798-7_34

Differential Diagnosis

- Lymphoproliferative disorder
- Specific orbital inflammations such as sarcoid lesion, Wegener's (GPA), Sjogren's, TB, etc.
- Non-specific orbital inflammatory disease (NSOID)
- Lacrimal gland malignancies such as adenoid cystic carcinoma, adenocarcinoma, etc.
- Pleomorphic adenoma of the lacrimal gland

Patient underwent imaging.

Radiology

CT scan of the orbits showed an enhancing lesion in the right lacrimal gland (Fig. 34.2). It seemed to wrap around the globe without indentation. There was no bony remodeling or erosion. The rest of the orbit was normal.

Intervention

An anterior orbitotomy with biopsy of the right lacrimal gland was performed through the lid crease incision. The specimen was sent fresh for histopathology.

Histopathology

Histology showed seromucinous glandular structures accompanied by heavy lymphoid infiltrate composed of small-sized lymphocytes arranged in follicles (Fig. 34.3). CD3 mainly highlighted the T-cells in the inter-follicular region, while CD20 highlighted the B-cells in the follicles (Fig. 34.4). CD21 highlighted the regular and well-demarcated follicular dendritic meshwork, which are readily seen in germinal centers in reactive follicles. Bcl-2 highlighted the marginal, mantle, and inter-follicular areas only; the germinal centers did not stain for Bcl-2, thus excluding a

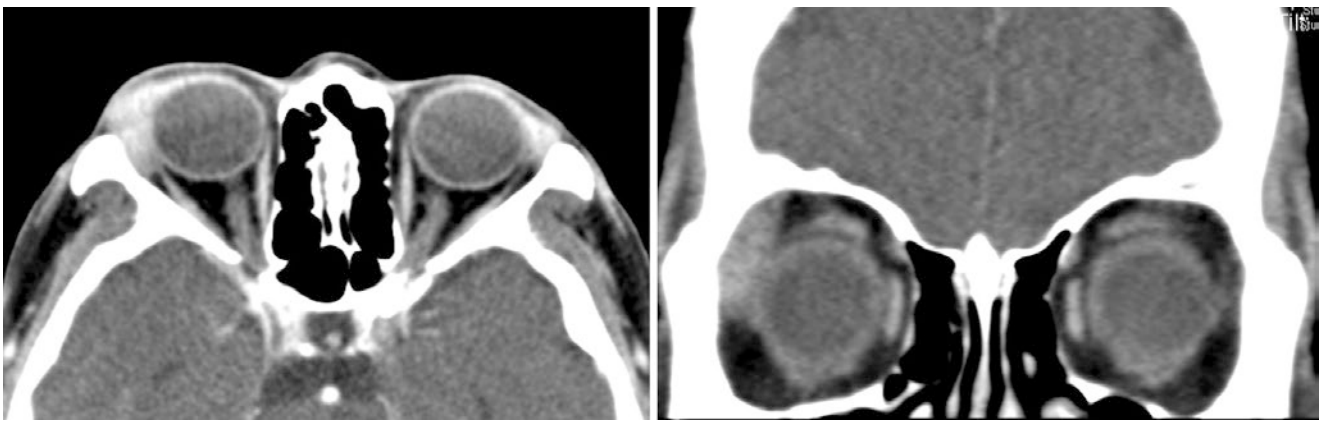

Fig. 34.2 Axial and coronal post-contrast CT images showing diffuse, homogeneous enlargement of the right lacrimal gland

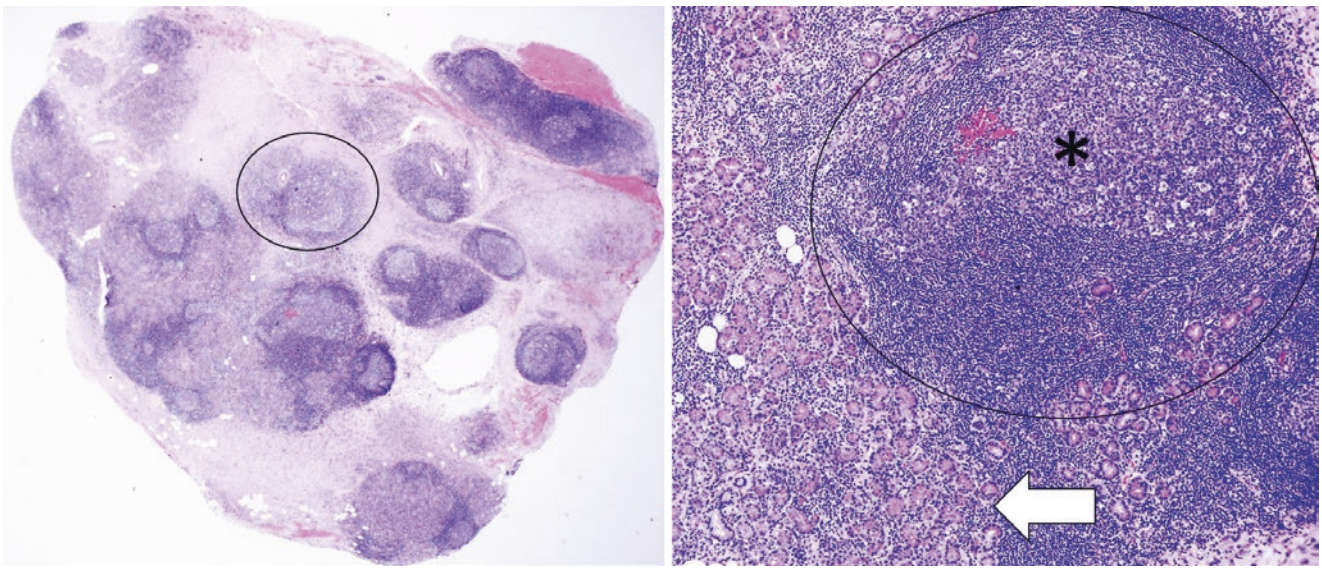

Fig. 34.3 There is a lymphoid infiltrate with follicular pattern (black circles). The lymphoid follicles exhibit germinal centers (*). Benign seromucinous glands are also present (white arrow). Left: HE stain, 20× magnification. Right: HE stain, 100× magnification

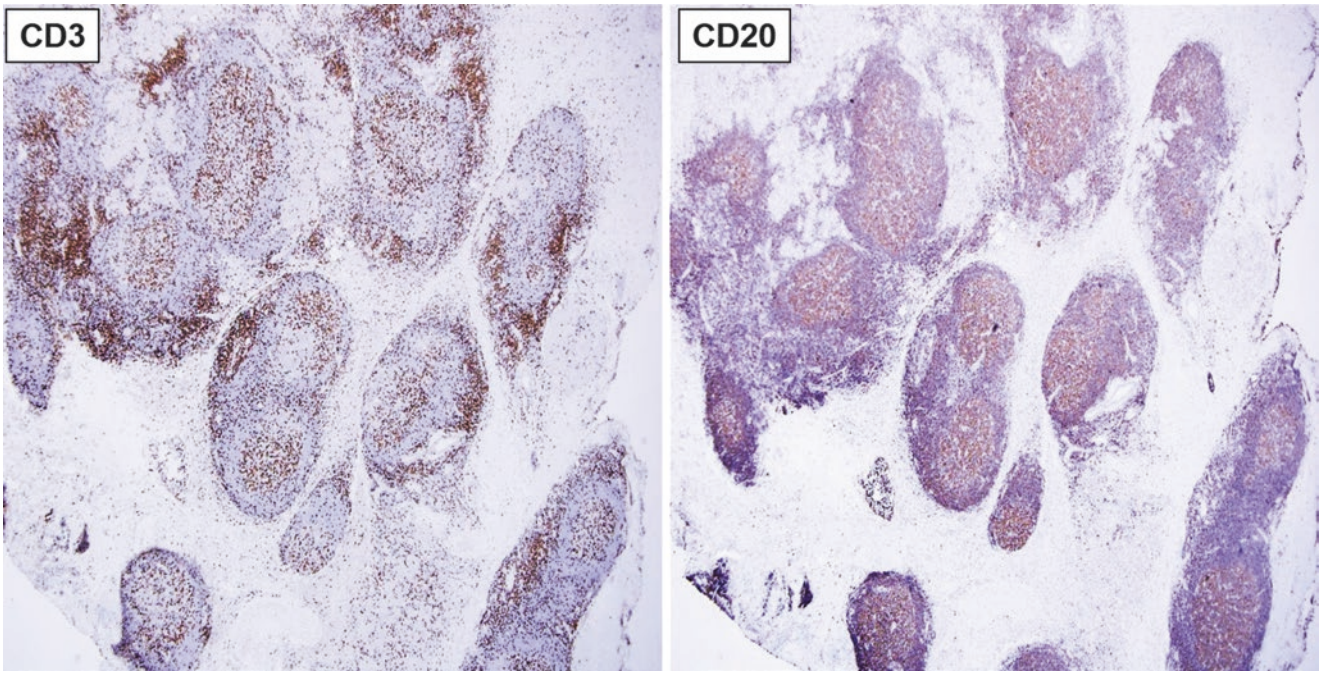

Fig. 34.4 CD3 mainly highlights the T-cells in the inter-follicular region, while CD20 mainly highlights the B-cells in the follicles. Left: Immunohistochemistry (CD3 antibody), 40× magnification. Right: Immunohistochemistry (CD20 antibody), 40× magnification

follicular lymphoma. The features were those of reactive lymphoid hyperplasia.

Management

The patient responded well to a course of oral steroids and was investigated for autoimmune disease. She was advised for close follow-up and re-biopsy should the swelling recur.

Discussion

Reactive lymphoid hyperplasia (RLH) and non-specific orbital inflammatory disorder (NSOID) are two distinct entities. RLH affects most commonly the lacrimal gland. The diagnosis is made mainly from the absence of clonal B-cell population by immunohistochemistry which can be confirmed by additional tests such as flow cytometry and/or molecular techniques. The flow cytometry requires abundant fresh tissue that may be difficult to obtain in orbital biopsies. There has been a shift in diagnostic patterns with the advent of flow cytometry and molecular testing. Some lesions that had been thought to be benign RLH have been reclassified as extranodal marginal zone lymphoma (ENMZL).

The term atypical lymphoid hyperplasia has been used for indeterminate lesions where the amount of tissue available is limited, or the combined results of flow cytometric or molecular investigations are inconclusive.

There has been an increased awareness of IgG4 inflammations in recent years. Some of the RHL can mimic IgG4 inflammation. Therefore, immunohistochemical staining for IgG and IgG4 is recommended for all cases of lymphoid hyperplasia.

A small proportion of RLH cases have been reported to transform into lymphoma at a later date. Therefore, all cases of RHL have to be investigated for coexistence of lymphoma elsewhere in the body and should be followed up closely for relapses and transformation to lymphoma.

Learning Points

Reactive lymphoid hyperplasia (RLH) is one end of the spectrum of lymphoproliferative disorders. Spread of the lesion along the planes in the absence of bony erosion in CT should raise the possibility of OAL. Immunohistochemistry, flow cytometry, and molecular techniques should be used where possible to rule out lymphomas. Thorough systemic evaluation combined with close monitoring for life is necessary in cases of RHL.

Further Reading

1. Coupland SE, Krause L, Delecluse HJ, Anagnostopoulos I, Foss HD, Hummel M, Bornfeld N, Lee WR, Stein H. Lymphoproliferative lesions of the ocular adnexa. Analysis of 112 cases. Ophthalmology. 1998;105(8):1430–41.
2. Kubota T, Moritani S, Katayama M, Terasaki H. Ocular adnexal IgG4-related lymphoplasmacytic infiltrative disorder. Arch Ophthalmol. 2010;128(5):577–84.
3. Mannami T, Yoshino T, Oshima K, et al. Clinical, histopathological, and immunogenetic analysis of ocular adnexal lymphoproliferative disorders: characterization of malt lymphoma and reactive lymphoid hyperplasia. Mod Pathol. 2001;14(7):641–9.
4. Stacy RC, Jakobiec FA, Schoenfield L, Singh AD. Unifocal and multifocal reactive lymphoid hyperplasia vs follicular lymphoma of the ocular adnexa. Am J Ophthalmol. 2010;150(3):412–26.
5. Verdijk RM. Lymphoproliferative tumors of the ocular adnexa. Asia Pac J Ophthalmol (Phila). 2017;6(2):132–42.

MALT Lymphoma

35

Shantha Amrith, Stephanie Ming Young, Poh Sun Goh, Bingcheng Wu, Min En Nga, and Gangadhara Sundar

Introduction

Among the B-cell tumours of the ocular adnexa, mucosal-associated lymphoid tissue (MALT) lymphomas are considered to be the most common and constitute about 60%. Although these are slow-growing, low-grade tumours, about 50% develop systemic disease. They are also called extranodal marginal zone lymphomas (ENMZL). MALT lymphomas were originally described in lymphoid tissue in the submucosa of the gastrointestinal system, and later research revealed *Helicobacter* infection as an aetiological factor. In the conjunctiva and the lacrimal gland, there are lymphoid follicles that may be considered mucosal-associated, whereas the orbital soft tissues do not have any lymphoid tissue; and hence, the name ENMZL, and the diagnosis is based on histopathology, immunophenotype, and molecular features. Orbital ENMZL are often painless and can be unilateral or bilateral, solitary or multicentric, with potential to disseminate to lymph nodes or to distant sites.

Case Scenario

A 53-year-old Chinese female noted swelling around her left eye for a few months. It was not associated with pain. She had a Snellen's visual acuity of 6/12 in both eyes, full motility, with normal intraocular pressures. She showed mild congestion in the conjunctiva of both eyes with a 3 mm of axial proptosis of the left eye (Fig. 35.1) on exophthalmometry. The rest of the ophthalmic examination was normal except for a mild cataract in both eyes.

CLOSE summary is given in Table 35.1.

Differential Diagnosis

- Thyroid eye disease
- Orbital inflammatory disease
- Lymphatic-venous malformation
- Benign orbital tumour
- Lymphoproliferative lesion
- Orbital metastasis

The patient underwent CT scan of the orbits.

S. Amrith (✉) · S. M. Young · G. Sundar
Department of Ophthalmology, National University Hospital, Singapore

Department of Ophthalmology, Yong Loo Lin School of Medicine, National University of Singapore, Singapore
e-mail: shantha_amrith@nuhs.edu.sg; stephanie.young@nuhs.edu.sg; gangadhara_sundar@nuhs.edu.sg

P. S. Goh
Department of Diagnostic Imaging, National University Hospital, Singapore

Department of Diagnostic Imaging, Yong Loo Lin School of Medicine, National University of Singapore, Singapore

B. Wu
Department of Pathology, National University Hospital, Singapore

M. E. Nga
Department of Pathology, National University Hospital, Singapore

Department of Pathology, Yong Loo Lin School of Medicine, National University of Singapore, Singapore

S. Amrith et al. (eds.), *Ocular Adnexal Lesions*, https://doi.org/10.1007/978-981-13-3798-7_35

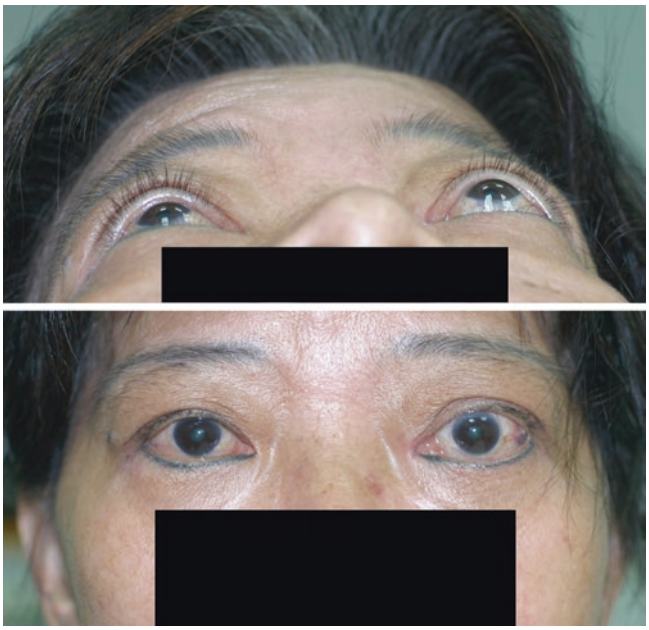

Fig. 35.1 Clinical photograph of the patient showing left proptosis

Table 35.1 CLOSE summary

*C*linical scenario: mass lesion with some inflammatory effect
*L*ocation: bilateral orbital, mainly intraconal
*O*nset: subacute to chronic
*S*igns and symptoms: proptosis/painless swelling and conjunctival injection
*E*pidemiology: 53-year-old Chinese female

Radiology

CT scan showed a hyperdense infiltrative left orbital lesion involving both the intraconal and extraconal spaces inseparable from the extraocular muscles with a similar but smaller lesion in the right orbit (Fig. 35.2). Scalloping of the medial walls of both orbits was noted, with no evidence of erosion. There was no intracranial extension. One additional differential diagnosis from the radiologist, apart from lymphoma, was Erdheim-Chester disease.

Intervention

A left anterior orbitotomy through the upper eyelid crease was performed, and the mass was debulked. Intraoperative frozen section revealed a lymphoid infiltrate. The tissue was sent fresh for histopathology.

Histopathology

H&E stain showed an atypical lymphoid population consisting predominantly of small round cells with irregular nuclei and no nucleoli. Scattered larger immunoblasts and plasma cells were also present (Fig. 35.3). Overall, the cytology appeared to be relatively bland.

On immunohistochemistry (Fig. 35.4), small cells were positive for CD20, but negative for Bcl2, CD10, CD5, cyclin

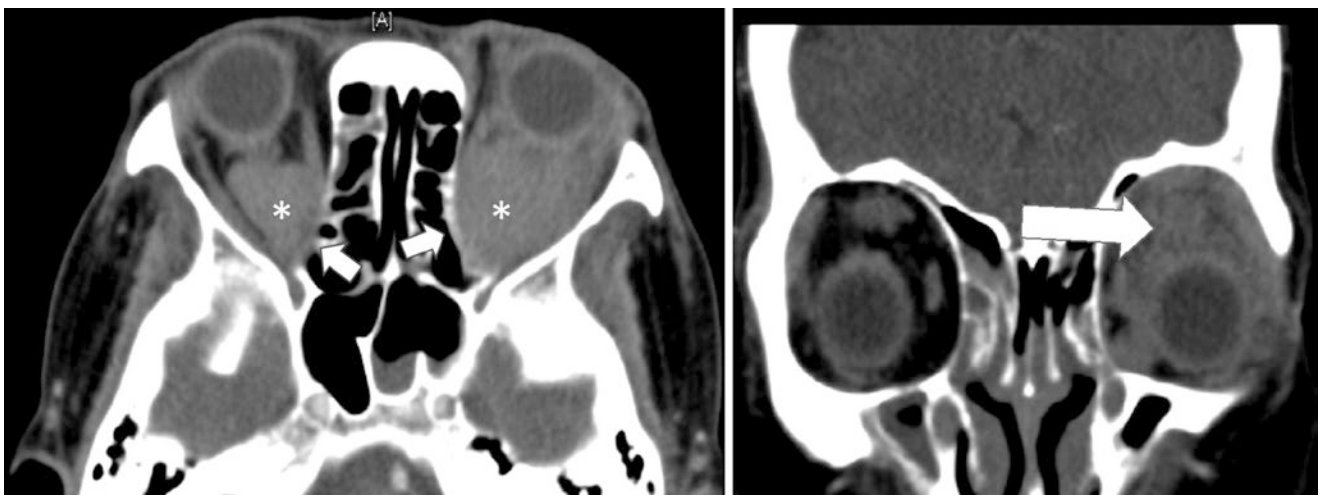

Fig. 35.2 Left: Axial contrast-enhanced CT showing bilateral intraconal mass (*) with bowing of the posterior medial wall (white arrows). Right: Coronal contrast-enhanced CT showing infiltrative tumour involving the superior muscle complex (arrow)

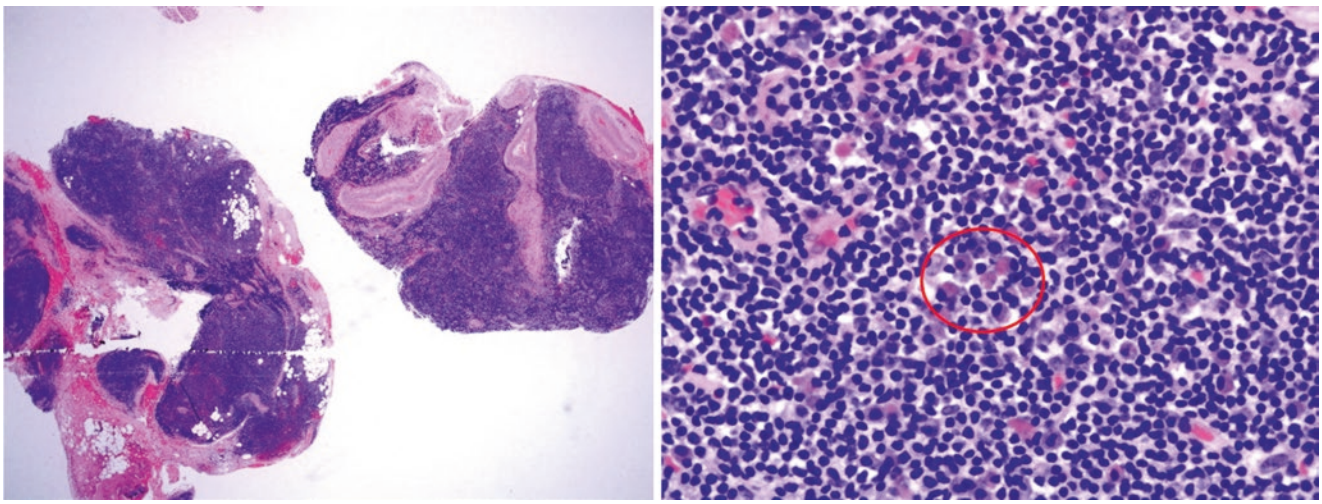

Fig. 35.3 There is an atypical population of predominantly small lymphocytes. Occasional clusters of plasma cells are seen (right, red circle) within the atypical lymphoid infiltrate. Left: HE stain, 20× magnification. Right: HE stain, 600× magnification

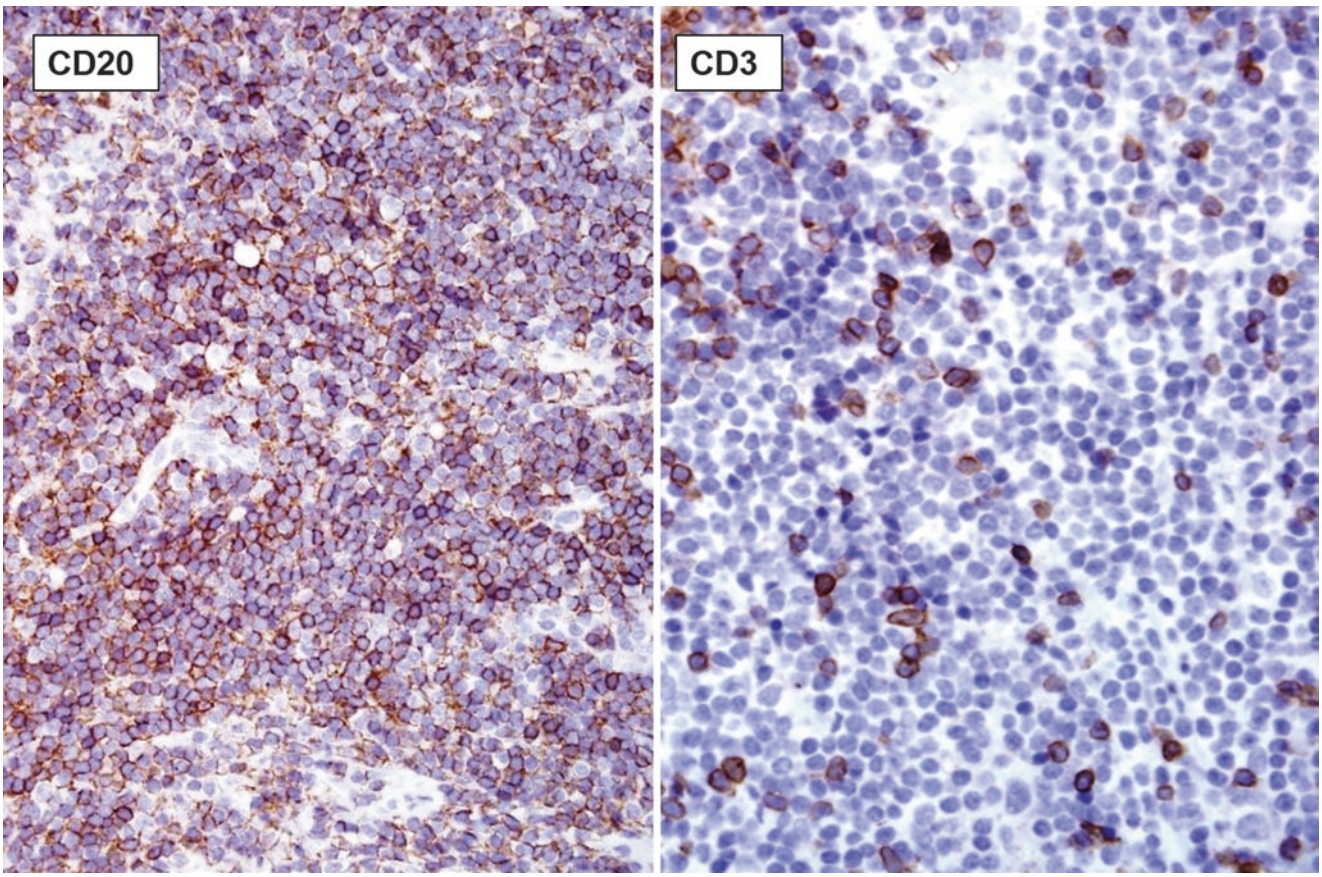

Fig. 35.4 The atypical lymphocytes show diffuse staining with CD20. In contrast, CD3 highlights only scattered reactive T-cells interspersed within the atypical lymphoid infiltrate. Left: Immunohistochemistry (CD20 antibody), 200× magnification. Right: Immunohistochemistry (CD3 antibody), 400× magnification

D1, and CD43. Ki67 was present in 10% of cells in the nodule.

Clonality studies revealed the presence of monoclonal IgH gene rearrangement, indicating that the lymphoid population was neoplastic. The findings were consistent with an extranodal marginal zone lymphoma (MALT lymphoma).

Management

Clinically, the patient was diagnosed with bilateral orbital MALT lymphoma and underwent staging work-up. CT of the neck, thorax, abdomen, and pelvis did not reveal any lymph node enlargements or any other masses in the body.

Ann Arbor staging: Stage 1E bilateral orbital lymphoma TNM: T2C, N0, M0.

The patient underwent bilateral orbital external beam radiation to the orbits at a total dose of 30.6 Gray over 17 divided sessions.

Discussion

Roughly two-thirds of ocular adnexal lymphomas (OAL) are stage 1E (localized) extranodal tumours using the Ann Arbor system. They tend to be indolent and relatively asymptomatic in most cases.

Pathophysiology

Infective agents have been implicated in the aetiology of ENMZL of the ocular adnexa based on the role of *Helicobacter pylori* in gastric MALT lymphomas. In Italy, the researchers have identified *Chlamydia psittaci* from MALT lymphomas of the ocular adnexa. The same thing could not be replicated in other geographical areas. Similarly, *H. pylori* was reported in some areas and not in others. Thus, ENMZL B-cell lymphoma of the ocular adnexa is a presumed antigen-driven neoplasm with great geographic variation. The antigenic stimulus (or stimuli) is a subject of ongoing investigation. Recently, there have been some reports of this tumour arising from an IgG4 inflammation. This again does not add much knowledge to the pathogenesis of these tumours.

Extranodal marginal zone lymphoma (ENMZL) of ocular adnexa lacks specific markers of other small-cell lymphomas and is positive for B lineage markers and Bcl2. There is a low proliferation rate. In current practice, there is no distinctive positive immunological marker for ENMZL. The immunohistochemical demonstration of light-chain restriction using formalin-fixed, paraffin-embedded tissue is challenging because detection of cytoplasmic light chains in nonplasmacytic proliferations is prone to false-negative testing. An alternative approach to demonstrating light-chain restriction is flow cytometry, which requires fresh tissue. Clonality of B-cells can be documented by polymerase chain reaction (PCR) of Ig heavy chain as demonstrated in the case above. More centres are employing combinations of immunohistochemistry, flow cytometry, and PCR to diagnose low-grade lymphoma and relying less on morphology alone.

Management

Incisional biopsy and local surgical excision, where possible, may serve as therapy for ENMZL of the ocular adnexa. Complete removal should not be attempted, especially if there is fear of severe complications to the optic nerve or orbital structures. Some of these tumours can safely be observed if they are minimally symptomatic and especially if the patient is elderly or frail. Advocating radiation therapy for localized (stage I) tumours at presentation provides excellent local control, with 4-year relapse rates of 20–25%. However, 45% of patients develop late sequelae of radiation therapy (especially cataract), and 25% of patients experience side effects such as dry eyes and keratopathy. For more advanced disease stages, chemotherapy with chlorambucil with or without prednisolone yields excellent response rates with a 5-year relapse-free survival of 60%. The use of upfront additional anthracycline-based chemotherapy does not show any clinical advantage. The use of rituximab as a single agent is associated with short-lived responses.

Learning Points

Lymphoproliferative lesions of the orbit are on the increase and must be evaluated clinically as well as with the help of radiology, histology, and molecular studies. Correct histologic typing and clinical staging is necessary to advocate appropriate therapy. Most localized ocular adnexal MALT lymphomas, either unilateral or bilateral, should be managed with radiotherapy. Chemotherapy is considered only when there is systemic involvement. Bone marrow biopsy is not indicated in localized ENMZL.

Further Reading

1. Collina F, De Chiara A, De Renzo A, et al. Chlamydia psittaci in ocular adnexa MALT lymphoma: a possible role in lymphomagenesis and a different geographical distribution. Infect Agent Cancer. 2012;7:8.
2. Ferreri AJ, Guidoboni M, Ponzoni M, et al. Evidence for an association between Chlamydia psittaci and ocular adnexal lymphomas. J Natl Cancer Inst. 2004;96:586–94.

3. Ferry JA, Fung CY, Zukerberg L, et al. Lymphoma of the ocular adnexa: a study of 353 cases. Am J Surg Pathol. 2007;31:170–84.
4. Guffey Johnson J, Terpak LA, Margo CE, Setoodeh R. Extranodal marginal zone B-cell lymphoma of the ocular adnexa. Cancer Control. 2016;23(2):140–9.
5. Nakayama R, Matsumoto Y, Horiike S, et al. Close pathogenetic relationship between ocular immunoglobulin G4-related disease (IgG4-RD) and ocular adnexal mucosa-associated lymphoid tissue (MALT) lymphoma. Leuk Lymphoma. 2014;55:1198–202.
6. Turbiner Geyer J, Knowles DM. Malignant lymphomas and lymphoid hyperplasias that occur in the ocular adnexa (orbit, conjunctiva and eyelids). In: Hematopathology N, editor. Knowles DM. Philadelphia: Lippincott Williams & Wilkins; 2013. p. 1304.
7. Uno T, Isobe K, Shikama N, et al. Radiotherapy for extranodal, marginal zone, B-cell lymphoma of mucosa-associated lymphoid tissue originating in the ocular adnexa: a multiinstitutional, retrospective review of 50 patients. Cancer. 2003;98:865–71.
8. Verdijk RM. An update of ocular adnexal lymphomas. Diagn Histopathol. 2015;21:26–33.
9. Verdijk RM. Lymphoproliferative tumors of the ocular adnexa. Asia Pac J Ophthalmol (Phila). 2017;6(2):132–42.

Follicular Lymphoma

36

Shantha Amrith, Stephanie Ming Young, Poh Sun Goh, Bingcheng Wu, Min En Nga, and Gangadhara Sundar

Introduction

About 15–20% of non-Hodgkin's lymphoma (NHL) are follicular lymphomas, and they are generally indolent and slow-growing. Ocular adnexal follicular lymphomas (OAFL) occur more commonly in males, and the 5-year-survival rate is about 72–77%. The mean age of incidence is 60–65 years.

Case 1: Eyelid

A 62-year-old Chinese female presented with a painless lump over her left upper lid which was gradual and progressive for 6 months, not associated with visual symptoms. No other lumps were noted in the body.

On examination, there was a subcutaneous mass in the left upper lid (Fig. 36.1), about 1.5 cm in diameter, which seemed to be adherent to the deeper structures. There was no change on Valsalva manoeuvre. There was a mild mechanical ptosis, but no proptosis or diplopia. The ocular motility appeared full, and the rest of the ophthalmic examination was normal.

CLOSE summary is shown in Table 36.1.

Differential Diagnosis

- Lymphoma/lymphoproliferative lesion
- Specific or non-specific inflammatory mass
- Schwannoma
- Cavernous haemangioma
- Nodular neurofibroma

Radiology

Contrast-enhanced CT scan of the orbit showed a well-defined hyperdense lesion along the preseptal compartment of the left superior orbit/eyelid bulging into the extraconal compartment along the orbital roof. The lesion was enhancing with rounded borders and seemed well circumscribed. However, a second lesion was noted more posteriorly over the superior rectus.

Intervention

An excisional biopsy of the mass was carried out under local anaesthesia. During surgery, it appeared to be well

S. Amrith (✉) · S. M. Young · G. Sundar
Department of Ophthalmology, National University Hospital, Singapore

Department of Ophthalmology, Yong Loo Lin School of Medicine, National University of Singapore, Singapore
e-mail: shantha_amrith@nuhs.edu.sg; stephanie.young@nuhs.edu.sg; gangadhara_sundar@nuhs.edu.sg

P. S. Goh
Department of Diagnostic Imaging, National University Hospital, Singapore

Department of Diagnostic Imaging, Yong Loo Lin School of Medicine, National University of Singapore, Singapore

B. Wu
Department of Pathology, National University Hospital, Singapore

M. E. Nga
Department of Pathology, National University Hospital, Singapore

Department of Pathology, Yong Loo Lin School of Medicine, National University of Singapore, Singapore

S. Amrith et al. (eds.), *Ocular Adnexal Lesions*, https://doi.org/10.1007/978-981-13-3798-7_36

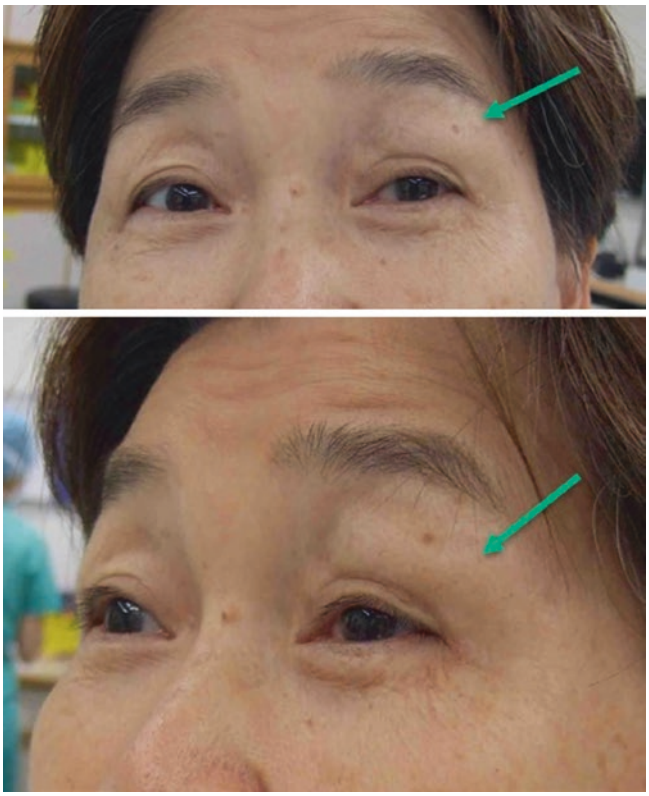

Fig. 36.1 Case 1: clinical pictures with arrows pointing to the upper lid mass

Table 36.1 CLOSE summary case 1

*C*linical process: mass lesion
*L*ocation: left upper lid
*O*nset: chronic
*S*igns and symptoms: painless lump gradually increasing in size
*E*pidemiology: 65-year-old Chinese female

circumscribed except medially where it appeared to extend posteriorly. The specimen was sent fresh for histology.

Histopathology

The sections showed fibroadipose tissue containing a dense nodular infiltrate with atypical lymphoid cells, with a vaguely follicular pattern seen best in the low power view (Fig. 36.2). Irregularly shaped follicles of varying sizes were seen. Within the follicles, there were both large and small cells with more than 15 centroblasts per high power field (Fig. 36.2), admixed with smaller centrocytes. The atypical lymphoid cells both within and in the interfollicular areas showed diffuse strong expression of CD20 and Bcl-2 on immunohistochemistry (Fig. 36.3) (benign follicles do not show any reactivity to Bcl-2). No expression of CD10 was seen. Overall, the histology indicated a high-grade follicular lymphoma consistent with follicular lymphoma of grade 3 (WHO).

Management

The patient was referred to the lymphoma specialist for systemic evaluation. CT neck, chest, abdomen, and pelvis showed splenomegaly, small volume and prominent axillary, mediastinal, and para-aortic lymph nodes. Bone marrow aspirate showed agranulocytosis with arrest of maturation with no evidence of infiltration. The lumbar puncture was also negative for tumour. The full blood count showed low RBC, WBC, and platelet counts. The renal functions were normal and LDH was raised.

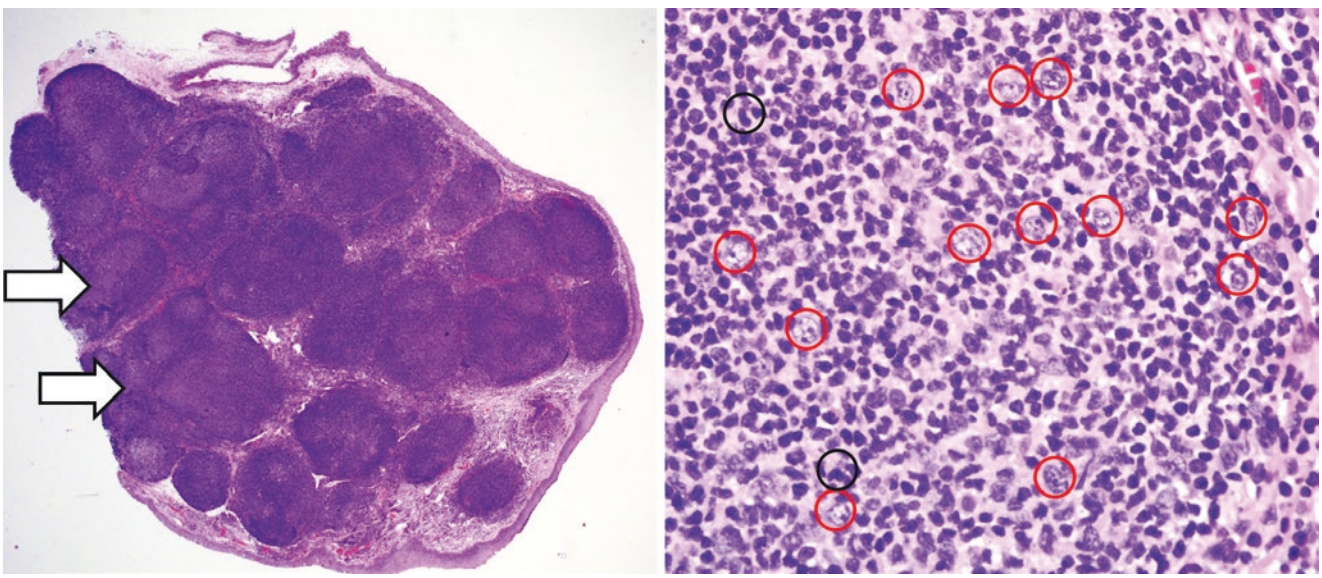

Fig. 36.2 Case 1: there is a dense nodular infiltrate of atypical lymphoid cells forming irregular follicles of varying sizes (white arrows). Within the follicles, there are many centroblasts (red circles) and admixed centrocytes (black circles). Left: HE stain, 20× magnification. Right: HE stain, 400× magnification

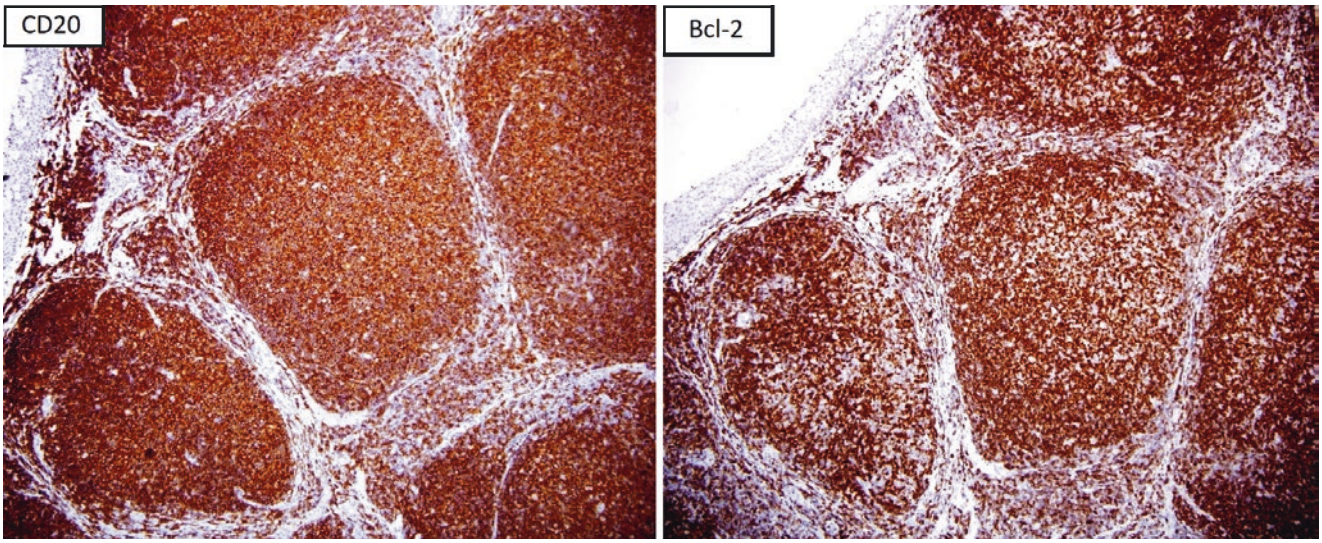

Fig. 36.3 Case 1: the atypical lymphoid cells, both within the follicles and in the inter-follicular areas, show diffuse strong expression of CD20 and Bcl-2. Left: immunohistochemistry (CD20 antibody), 100× magnification. Right: immunohistochemistry (Bcl-2 antibody), 100× magnification

Tumour staging: Ann Arbor, Stage III; TNM, T3N4M1a, histological grade 3.

The patient underwent R-CHOP (cyclophosphamide, doxorubicin, vincristine, prednisone combined with rituximab) chemotherapy due to systemic involvement.

Case 2: Conjunctiva

A 25-year-old Malay male presented with a right-sided lump in the medial aspect of the conjunctiva for about 6–12 months. He had no symptoms of pain or discharge and was not bothered by the lump. He was an ex-smoker. His ophthalmic examination was normal except for a fleshy non-tender mass in the bulbar conjunctiva at the medial canthus of the right eye (Fig. 36.4). The lump was salmon pink in colour and was seen to extend under the eyelid into the superior fornix. There was no proptosis. There were no systemic symptoms including lymph node enlargement in the body.

CLOSE summary is given in Table 36.2.

Differential Diagnosis

- Conjunctival lymphoma
- Benign lymphoid hyperplasia
- Ocular surface neoplasia including squamous cell carcinoma, amelanotic melanoma
- Pyogenic granuloma
- Amyloid deposition
- Sarcoid lesion

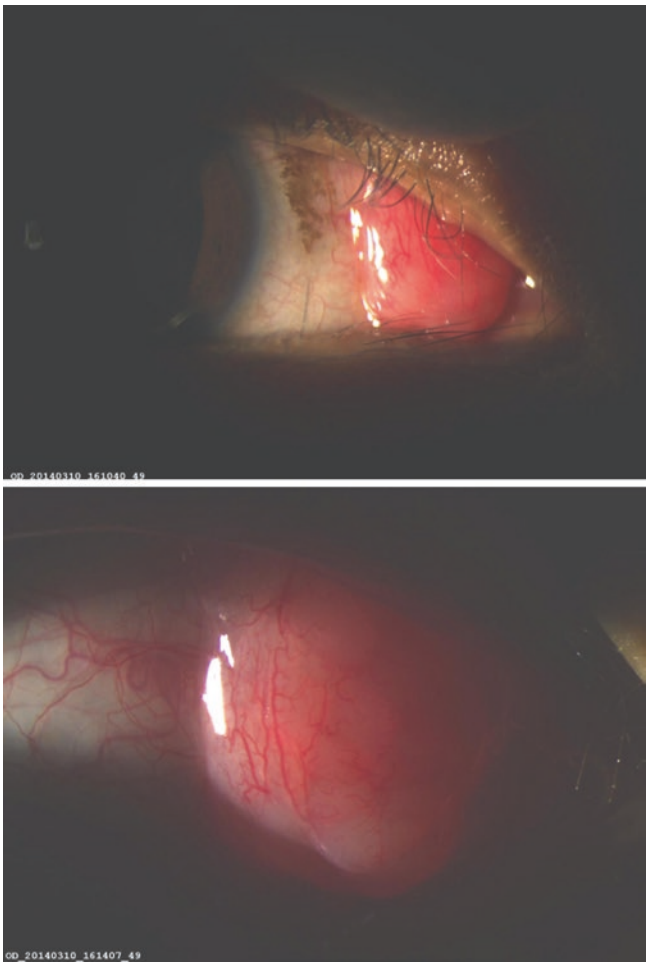

Fig. 36.4 Case 2: slit lamp photography of the fleshy bulbar conjunctival mass in the medial aspect of the right eye

Table 36.2 CLOSE summary case 2

*C*linical process: fleshy mass lesion
*L*ocation: right medial and superomedial bulbar conjunctiva
*O*nset: subacute
*S*igns and symptoms: right medial and superomedial conjunctival salmon-coloured mass, asymptomatic
*E*pidemiology: young Malay male

Radiology

CT scan of the orbits showed no posterior extension of the mass into the orbit. No other orbital mass was seen.

Intervention

An excision biopsy was performed, and the mass was dissected off the Tenon's capsule and sent fresh for histopathology.

Histopathology

Subepithelial stroma showed involvement by a neoplastic lymphoid infiltrate with nodular architecture. The nodules resembled enlarged, irregular, closely packed lymphoid follicles with attenuation of the mantle zones. The neoplastic cells in the nodules/follicles were composed of a mixture of small lymphoid cells with irregular cleaved nuclei resembling centrocytes and large centroblastic cells with vesicular nuclei and multiple membrane polarized nucleoli. The centroblastic cells in the nodules were from less than 6 to up to 15 (<6–15) per high power field.

Immunohistochemistry

The neoplastic lymphoid cells in the nodules/follicles showed positive staining for CD20, CD79A, Bcl-6, and Bcl-2 and weak positive staining for CD10. They were negative for staining for CD5 and cyclin D1. CD21 showed expanded follicular dendritic meshworks in the nodules/follicles.

A diagnosis of follicular lymphoma low grade (grade 1–2), follicular pattern (>75%) was made.

Investigations

The flow cytometry revealed abnormal B-cell population with kappa-restricted phenotypic follicular lymphoma.

PET-CT scan revealed mildly avid two cervical lymph nodes and patchy marrow signals.

Other investigations included a bone marrow biopsy which was negative for clonal population of B-cells.

Management

The patient was referred to a lymphoma specialist.

Tumour staging: Ann Arbor stage 1E, TNM, T1N0M0, histological low-grade (1–2) lymphoma of the conjunctiva.

The patient was advised radiotherapy; however, because of the fear of a second malignancy in young individuals, the patient opted for chemotherapy.

Case 3: Orbit

A 77-year-old Chinese female presented with a recent onset of visual loss in the right eye of about 10 days' duration. She had noted mild pain and swelling. On examination, the best corrected visual acuity was counting fingers at 5 metres in the right eye. She had a right RAPD, a 5 mm proptosis with chemosis, and conjunctival injection. She had a right hypotropia with limitation of ocular motility in all directions except downgaze (Fig. 36.5). Examination of the left side was unremarkable.

CLOSE summary is given in Table 36.3.

Differential Diagnosis

- Thyroid eye disease
- Non-specific orbital inflammation
- Cavernous haemangioma
- Schwannoma
- Lymphoma
- Solitary fibrous tumour
- Metastasis

Other Investigations

Thyroid functions including antibodies were normal.

CT orbits was carried out.

Radiology

CT scan: A well-delineated enhancing hyperdense intraconal mass, completely encasing and inseparable from the optic

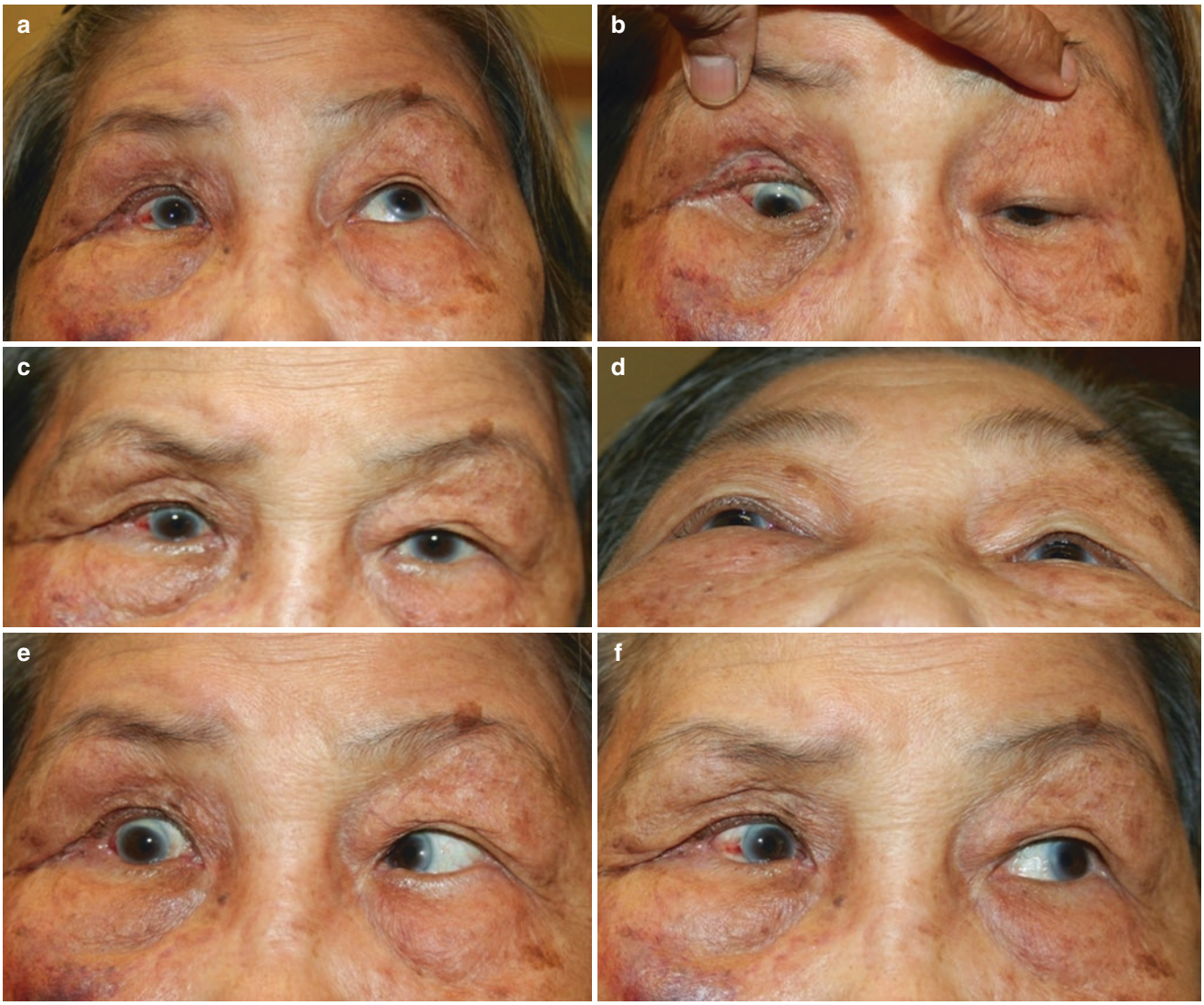

Fig. 36.5 Case 3: clinical picture showing (**a**) upgaze (note the restriction of the right eye movement) (**b**) downgaze (full movements in both eyes); (**c**) primary position showing hypotropia on the right side; (**d**) proptosis of the right eye; (**e**) right gaze (note the restriction of the right eye movement); (**f**) left gaze (note restriction of the right eye movement)

Table 36.3 CLOSE summary case 3

*C*linical process: infiltrative mass lesion
*L*ocation: right retrobulbar
*O*nset: subacute
*S*igns and symptoms: proptosis, RAPD, hypotropia, limitation of eye movements, chemosis, and conjunctival injection
*E*pidemiology: elderly Chinese female

nerve, was seen in the right orbit. It appeared to involve the medial and inferior recti. There was some remodelling of the bone, indicating the long-standing nature of the lesion (Fig. 36.6).

Intervention

An anterior orbitotomy and a biopsy of the mass were performed, and fresh tissue was sent for histology.

Histopathology

There was a dense lymphoid infiltrate with an irregular nodular configuration. The nodules were composed of rather monotonous small lymphoid cells with mildly irregular or cleaved nuclei with inconspicuous nucleoli.

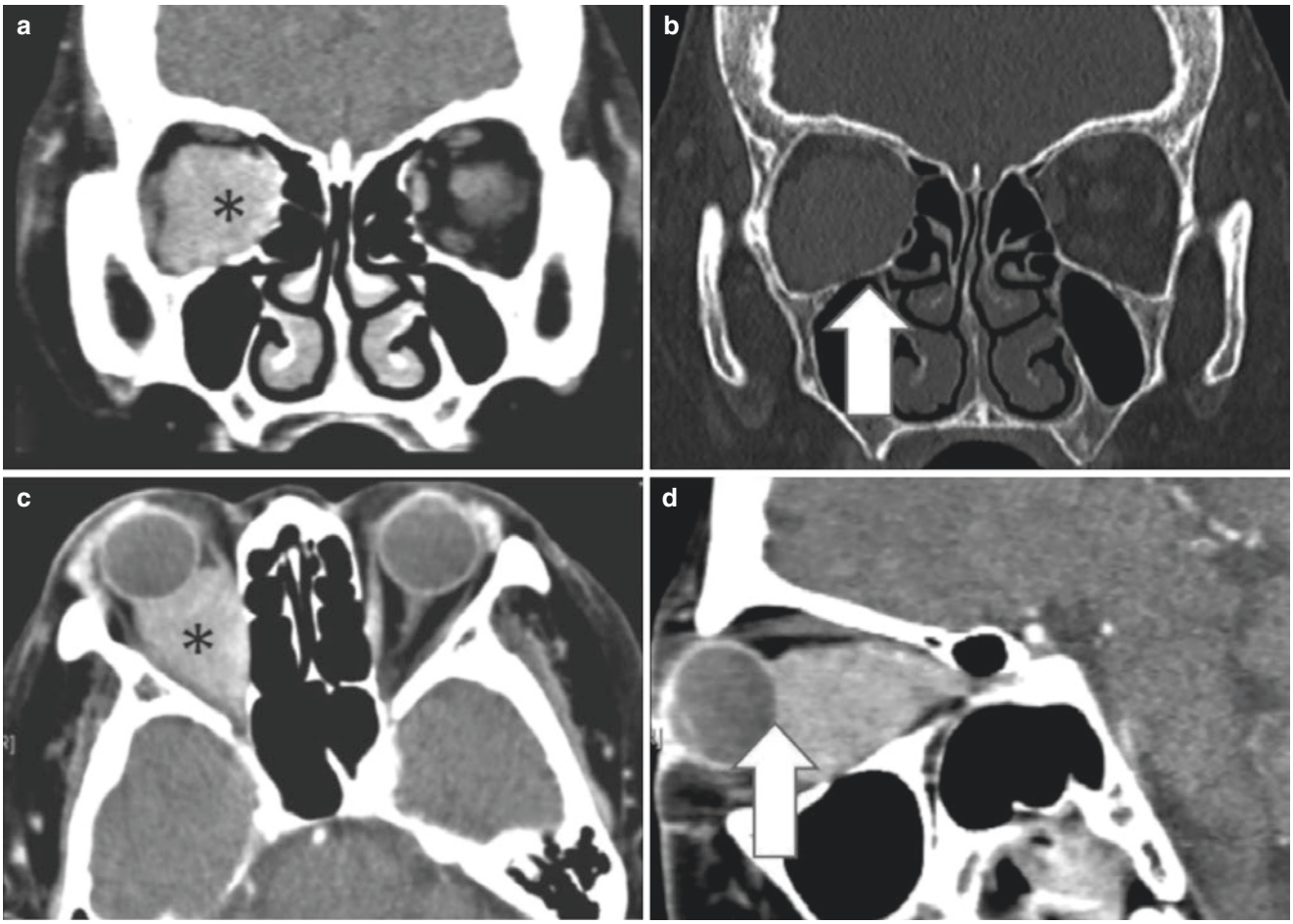

Fig. 36.6 CT scans of case 3: (**a**) and (**b**) Coronal scans with contrast and bone window showing an enhancing intraconal tumour (*), and remodelling of the medial wall of the orbit (arrow). (**c**) Axial CT scan with contrast and (**d**) sagittal CT with contrast showing enhancing intraconal mass (*) indenting the globe (arrow)

Immunohistochemistry

The small lymphoid cells in the nodules and those infiltrating the surrounding adipose tissue stained positively for CD20 and PAX5. The lymphocytes within the nodules also expressed CD10. CD21 demonstrated expanded and disrupted follicular dendritic meshworks in the nodules, confirming that they were follicular in origin.

Molecular tests: A monoclonal IgH rearrangement was detected by PCR, and t(14;18) translocation was also present.

The diagnosis was follicular lymphoma (grade 1–2).

Management

Tumour staging: Ann Arbor classification 1E, TNM T3N0M0, histological grade 1–2.

As there were no systemic findings and bone marrow examination was normal, the patient was advised external beam radiotherapy.

Discussion

The relative frequencies of ocular adnexal lymphomas (OAL) are as follows: orbit, 37%; conjunctiva, 29%; lacrimal apparatus, 20%; and eyelid, 14%. Among the B-cell lymphomas, OAFL forms about 17%, second only to mucosal-associated lymphoid tissue (MALT) lymphoma. Follicular lymphoma can present as primary ocular adnexal disease or as a secondary tumour in about one-third of cases; it may be bilateral in up to 20% of cases. The eyelids show the highest proportion of secondary lymphoma involvement. Dissemination of OAFL mainly occurs to the regional lymph nodes and the salivary glands and may involve distant lymph nodes, liver, or spleen. Splenic enlargement is present in 50% of cases.

Patients present with a space-occupying mass, growing over a period of few months to a few years. It is painful in about 20% of patients. Follicular lymphomas are composed of uniform, densely packed follicles, which may coalesce, with compression of interfollicular stroma and vessels. Small cells (centrocytes) have cleaved, indented, angulated nuclei;

large cells (centroblasts) may be cleaved or noncleaved. Follicular lymphoma grading is performed by estimating the average number of centroblasts per high power field (HPF) in ten neoplastic follicles. It is graded as follows:

- Grade 1: 0–5 centroblasts per HPF.
- Grade 2: 6–15 centroblasts per HPF.
- Grade 3A: >15 centroblasts per HPF.
- Grade 3B: contains >15 centroblasts; in addition the centroblasts form coalescent tumour areas without centrocytes.

Follicular lymphomas are Bcl-2 and CD10 antibodies positive in 85% of cases. On the genetic level, t(14;18) translocation has been recognized as a genetic hallmark of follicular lymphoma.

Suggested investigations include full blood count (FBC), blood smear (for abnormal lymphocytes), LDH, uric acid, liver function tests, creatinine, chest X-ray (if abnormal, a CT thorax), and CT of the abdomen, pelvis, kidneys, and ureters. A PET scan is recommended especially to distinguish between viable tumour and fibrosis in patients with residual lymphadenopathy after therapy. Biopsy is the mainstay in diagnosis. Bilateral post iliac crest bone marrow aspiration and biopsy will indicate if the condition is a local or systemic disease.

Treatment of OAFL is primarily radiation (30GY) if restricted to one site. If the disease is disseminated, palliative chemotherapy with rituximab or chlorambucil as monotherapy or R-CHOP is administered.

Learning Points

Follicular lymphoma is usually a systemic disease but can present as a primary tumour in the eyelid, conjunctiva, or orbit. It is usually indolent and slowly progressive. In 30% of cases, the eyelid is affected as a secondary site.

Further Reading

1. Rasmussen PK, Coupland SE, Finger PT, et al. Ocular adnexal follicular lymphoma: a multicenter international study. JAMA Ophthalmol. 2014;132:851–8.
2. Verdijk RM. Lymphoproliferative tumors of the ocular adnexa. Asia-Pac J Ophthalmol. 2017;6:132–42.

Diffuse Large B-Cell Lymphoma

37

Shantha Amrith, Stephanie Ming Young, Eric Ting, Bingcheng Wu, Min En Nga, and Gangadhara Sundar

Introduction

Among the non-Hodgkin's B-cell lymphomas, diffuse large B-cell lymphoma (DLBCL) is one of the high grade lymphoma types. It occurs less frequently compared to MALT and follicular lymphomas. High-grade lymphomas have systemic disease in addition to the ocular adnexa, relapse frequently, and exhibit poor survival rates. DLBCL is also associated with an increased risk of involvement of the central nervous system (CNS). The most common intraocular lymphoma is DLBCL, and it is usually associated with CNS involvement. It has diverse clinical presentations and outcomes, depending on genetic and phenotypic profiling.

Case Scenario

A 68-year-old Chinese lady presented with blurring of vision for 1 month and seeing clumps of hair-like strands in both eyes for 1 week not associated with any pain or redness in the eyes. Systemically, the patient had cervical and inguinal lymphadenopathy which was diagnosed to be a lymphoma (DLBCL) 1 year before the eye symptoms developed. Patient had completed a course of chemotherapy.

Examination revealed normal visual acuities, no RAPD and normal anterior segments. There was no proptosis as measured by an exophthalmometer. The fundus examination revealed clear vitreous, normal optic discs and macula. There was an indentation which appeared to be raising the retina and the choroid with choroidal folds bilaterally, left more than the right. Possibility of a choroidal or orbital lymphoma was raised.

CLOSE summary is given in Table 37.1.

The patient underwent MRI of the orbits.

Table 37.1 CLOSE summary

*C*linical process: mass lesion
*L*ocation: bilateral superolateral orbit
*O*nset: subacute
*S*igns and symptoms: blurring of vision with choroidal indentation and folds
*E*pidemiology: 68-year-old Chinese woman

S. Amrith (✉) · S. M. Young · G. Sundar
Department of Ophthalmology, National University Hospital, Singapore

Department of Ophthalmology, Yong Loo Lin School of Medicine, National University of Singapore, Singapore
e-mail: shantha_amrith@nuhs.edu.sg; stephanie.young@nuhs.edu.sg; gangadhara_sundar@nuhs.edu.sg

E. Ting
Department of Diagnostic Imaging, National University Hospital, Singapore

Department of Diagnostic Imaging, Yong Loo Lin School of Medicine, National University of Singapore, Singapore

Advanced Medicine Imaging, Singapore

B. Wu
Department of Pathology, National University Hospital, Singapore

M. E. Nga
Department of Pathology, National University Hospital, Singapore

Department of Pathology, Yong Loo Lin School of Medicine, National University of Singapore, Singapore

S. Amrith et al. (eds.), *Ocular Adnexal Lesions*, https://doi.org/10.1007/978-981-13-3798-7_37

Radiology

Bilateral diffuse lacrimal gland enlargement was seen (Fig. 37.1), demonstrating restricted diffusion, T1 intermediate and T2 intermediate signals suggestive of an orbital lymphoma. There was a smaller 0.8 mm satellite nodule along the lateral margin of the right orbit. The lacrimal gland lesions were seen to abut the insertion of the lateral recti muscles and indent the superotemporal aspects of both globes. There was no bony involvement. The optic nerves appeared normal. The other findings included bulky nodules in bilateral submandibular glands, multiple intraparotid nodules and retromaxillary, buccal as well as hard palate lesions. The brain did not reveal any abnormal lesions.

PET CT: Hypermetabolic areas were seen in multiple nodal stations from neck to inguinal regions. Multiple extranodal diseases involving multiple sites were also seen.

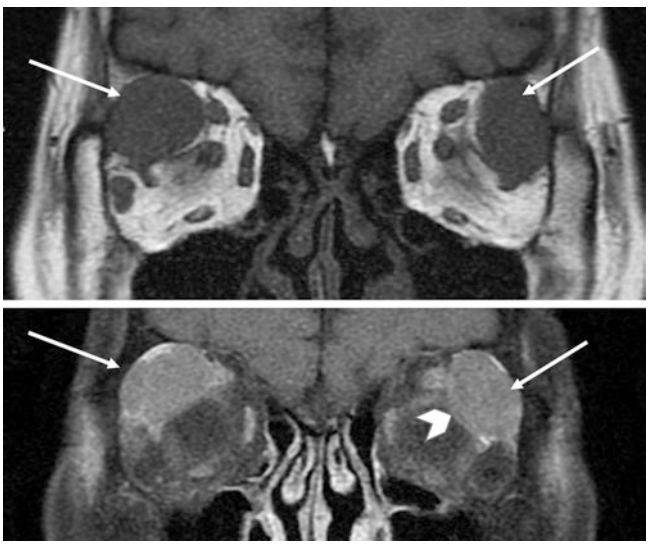

Fig. 37.1 Coronal T1w (Top) and T1w-FS + C (Bottom) images showing bilateral diffuse, smooth lacrimal gland enlargement. The tumour indents the left globe (arrow head)

Histopathology (from previous biopsy)

Histopathology showed a diffuse sheet-like infiltrate of medium- to large-sized neoplastic lymphoid cells with admixed reactive small lymphocytes. The neoplastic lymphoid cells showed some degree of nuclear pleomorphism and had single to multiple conspicuous nucleoli. There was prominent apoptotic and mitotic activity (Fig. 37.2).

Immunohistochemistry: The neoplastic lymphoid cells stained positively for CD20 and CD79A (pan B markers) (Fig. 37.3). They were negative for CD3 (pan T-cell marker). The Ki-67 proliferative index was high (approximately 80–90%) (Fig. 37.3). The neoplastic cells were negative for cyclin D1 thus excluding a pleomorphic variant of mantle cell lymphoma. A diagnosis of diffuse large B-cell lymphoma was made.

Management

Patient underwent R-EPOCH [*r*ituximab-*e*toposide, *p*rednisolone, *O*ncovin (vincristine), cyclophosphamide, *h*ydroxydaunorubicin (doxorubicin)] chemotherapy previously with intrathecal methotrexate as chemoprophylaxis for CNS relapse. In view of the PET CT showing multiple sites of relapse, a diagnosis of progressive and refractory disease

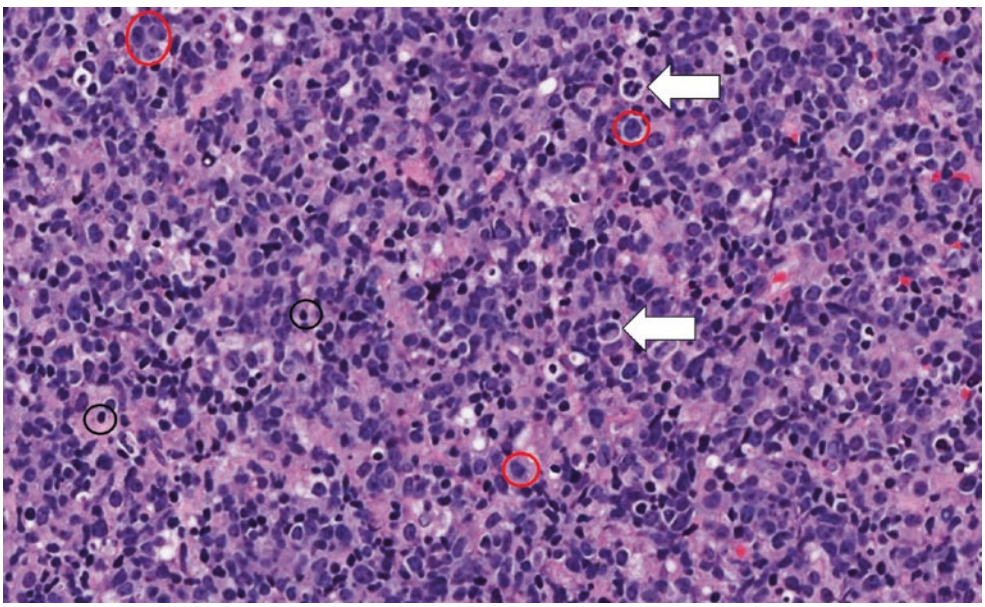

Fig. 37.2 Histology shows a diffuse sheet-like infiltrate of large neoplastic lymphoid cells (red circles) with admixed reactive small lymphocytes (black circles). The neoplastic lymphoid cells show considerable nuclear pleomorphism and possess single to multiple conspicuous nucleoli. Numerous mitoses are seen (white arrows). HE stain, 400× magnification

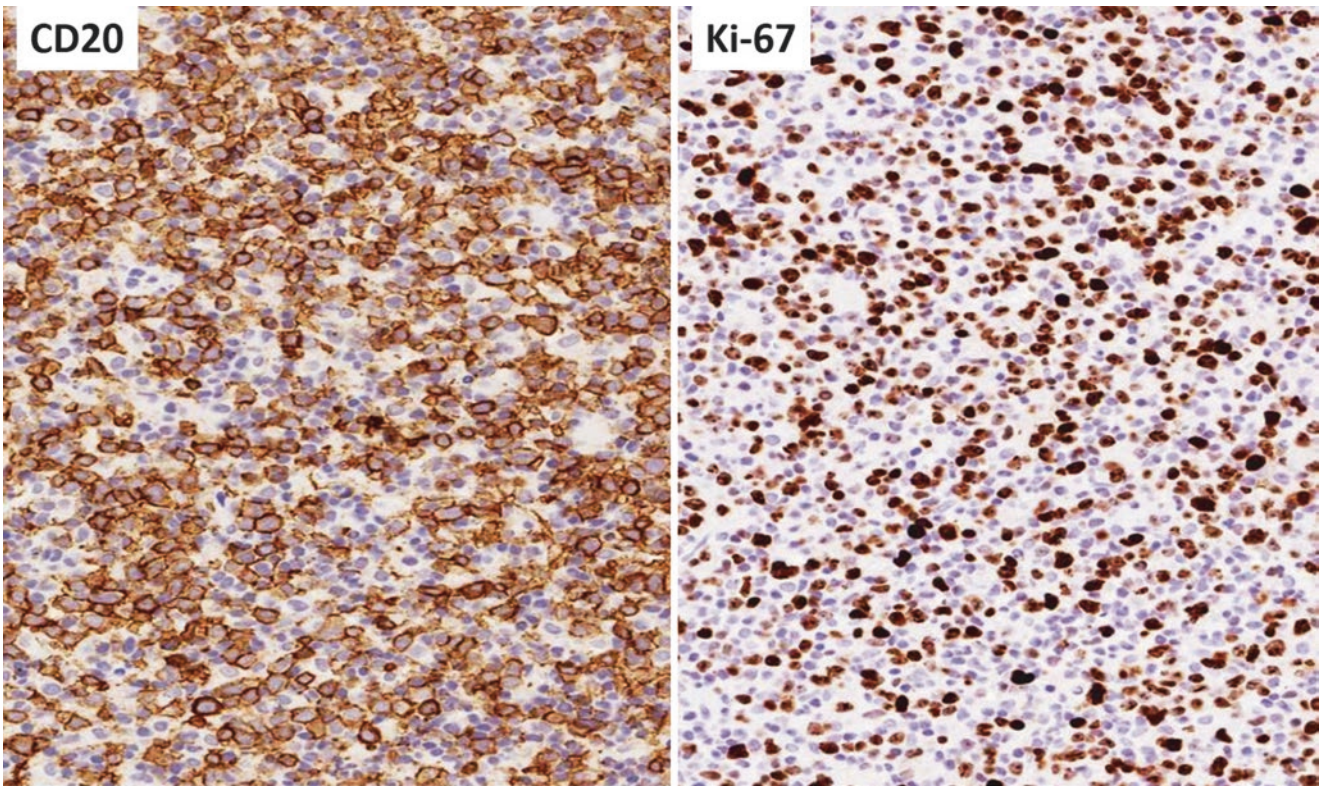

Fig. 37.3 The neoplastic lymphocytes are positive for CD20 on immunohistochemistry. Ki-67 nuclear proliferative index is approximately 80–90% (i.e. the stain is positive in 80–90% of viable malignant cell nuclei). Left, immunohistochemistry (CD20 antibody), 400× magnification. Right, immunohistochemistry (Ki-67 antibody), 400× magnification

(Ann-Arbor stage IV) was made, and the patient was started on immunotherapy with pembrolizumab.

Discussion

DLBCL generally runs an aggressive course complicated by CNS involvement, hence the need for prophylactic intrathecal methotrexate in these cases. The degree of p53 expression and Ki-67 antigen expression correlates with clinical outcome. Clinical presentation can be first in the orbit, lacrimal gland, eyelid or conjunctiva. Like all other lymphomas, CT or MRI shows a mass that infiltrates along the planes without bony erosion. Pathologically, large neoplastic lymphoid cells are seen, and with specific immunohistochemistry, the diagnosis is made. Further subtyping of large B-cell lymphomas is usually done with a panel of immunohistochemical stains and sometimes molecular tests for prognostic and treatment purposes.

The treatment is chemotherapy or radiotherapy depending on the extent of disease. Localised disease has a high (90%) 5-year survival rate, whereas advanced disease has a very poor survival (23.5%).

Learning Points

DLBCL is an aggressive form of B-cell lymphoma. Clinical presentation can be first in the orbit, lacrimal gland, eyelid or conjunctiva. It has a high propensity for CNS and intraocular lymphoma and hence the need for intrathecal methotrexate.

Further Reading

1. Cani AK, Soliman M, Hovelson DH, et al. Comprehensive genomic profiling of orbital and ocular adnexal lymphomas identifies frequent alterations in *MYD88* and chromatin modifiers: new routes to targeted therapies. Mod Pathol. 2016;29(7):685–97.
2. Coupland SE. Molecular pathology of lymphoma. Eye (Lond). 2013;27(2):180–9.
3. Ponzoni M, Govi S, Licata G, et al. A reappraisal of the diagnostic and therapeutic management of uncommon histologies of primary ocular adnexal lymphoma. Oncologist. 2013;18(7):876–84.
4. Zarrabi K, Desai V, Yim B, Gabig TG. Primary diffuse large B-cell lymphoma localized to the lacrimal sac: a case presentation and review of the literature. Case Rep Hematol. 2016;2016:5612749.

Mantle Cell Lymphoma

38

Shantha Amrith, Stephanie Ming Young, Eric Ting, Bingcheng Wu, Min En Nga, and Gangadhara Sundar

Introduction

Mantle cell lymphoma (MCL) of the ocular adnexa does not differ from systemic mantle cell lymphoma in its biological and clinical behaviour. As the name suggests, it arises from the mantle zone of the lymphoid follicles. It is a mature B-cell lymphoma, which is much less common than the other subtypes of B-cell lymphomas, and has an aggressive clinical course. It commonly affects men with a mean age of 74, and more than two thirds of the patients have disseminated disease or bilateral disease at presentation.

Clinical Scenario

A 74-year-old Southeast Asian male presented with the history of stage IV A mantle cell lymphoma for which he had received treatment in the form of chemotherapy. He was also previously treated with antiviral drug for hepatitis C.

He presented with irritation in both eyes of 1 month duration, and had noted swelling and redness of both eyes and double vision just prior to consultation. On examination, his visual acuities were normal. There was a salmon patch on the lateral aspect of bulbar conjunctiva of the left eye (Fig. 38.1). Apart from a diffuse keratopathy, the anterior and posterior segment examination was normal. There was mild proptosis and fullness in the lateral aspects of both eyes, indicating bilateral lacrimal gland enlargement (Fig. 38.1). There was limitation of abduction in the left eye with resultant diplopia on extremes of left gaze.

CLOSE summary is given in Table 38.1.

Differential Diagnosis

- Orbital lymphoid tumour relapse of mantle cell lymphoma
- Second primary lymphoma of the orbit
- Specific and non-specific orbital inflammation/dacryoadenitis

Patient underwent MRI.

S. Amrith (✉) · S. M. Young · G. Sundar
Department of Ophthalmology, National University Hospital, Singapore

Department of Ophthalmology, Yong Loo Lin School of Medicine, National University of Singapore, Singapore
e-mail: shantha_amrith@nuhs.edu.sg; stephanie.young@nuhs.edu.sg; gangadhara_sundar@nuhs.edu.sg

E. Ting
Department of Diagnostic Imaging, National University Hospital, Singapore

Department of Diagnostic Imaging, Yong Loo Lin School of Medicine, National University of Singapore, Singapore

Advanced Medicine Imaging, Singapore

B. Wu
Department of Pathology, National University Hospital, Singapore

M. E. Nga
Department of Pathology, National University Hospital, Singapore

Department of Pathology, Yong Loo Lin School of Medicine, National University of Singapore, Singapore

S. Amrith et al. (eds.), *Ocular Adnexal Lesions*, https://doi.org/10.1007/978-981-13-3798-7_38

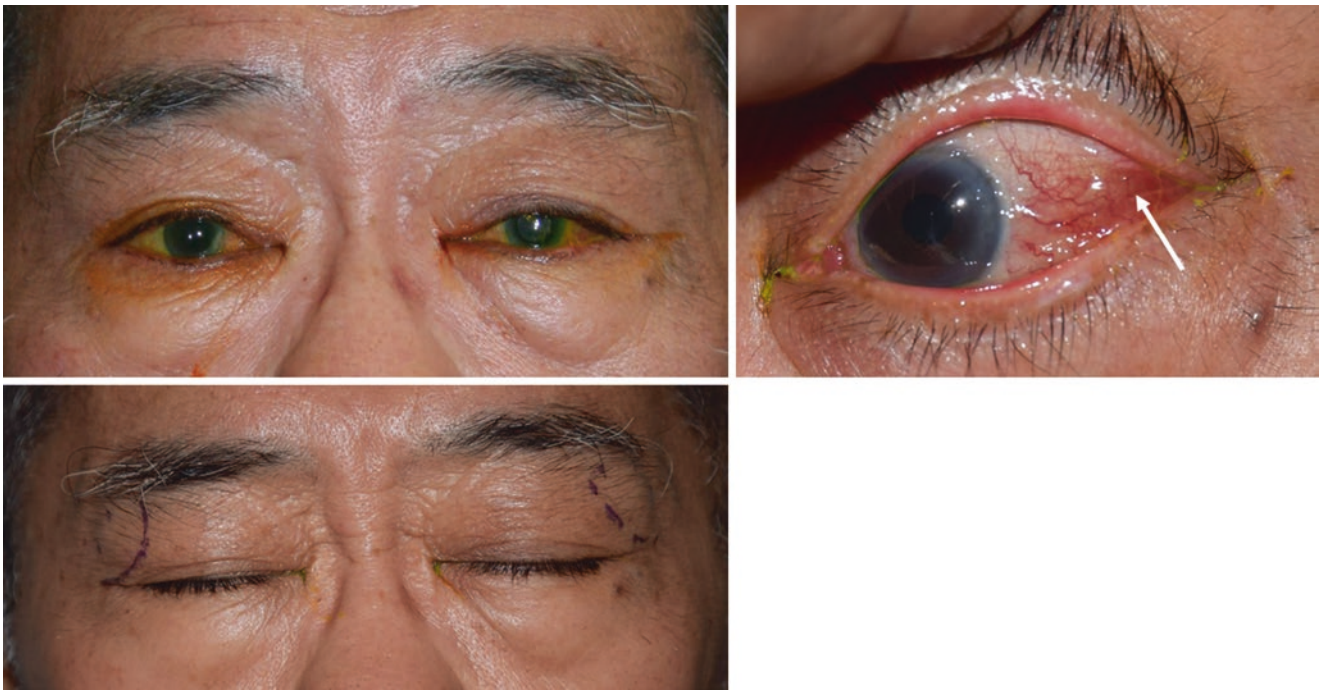

Fig. 38.1 Clinical picture showing swelling, redness, salmon patch (white arrow and lacrimal gland swelling (black circles)

Table 38.1 CLOSE summary

*C*linical process: mass effect with infiltration
*L*ocation: lacrimal glands and conjunctiva
*O*nset: subacute
*S*igns and symptoms: swelling and red eyes with bilateral lacrimal gland enlargement
*E*pidemiology: 74-year-old Southeast Asian male

Imaging

Diffuse enlargement and homogeneous enhancement of both lacrimal glands were seen, more prominently on the left. There was posterior extension of the glands into the superolateral extra-conal space, demonstrating mass effect on the superior and lateral rectus muscles bilaterally (Fig. 38.2). There was no infiltration of the optic nerve. The globes appeared normal. The findings were suspicious for lymphomatous infiltration.

Intervention

An anterior orbitotomy (Fig. 38.3) with biopsy of the left lacrimal gland was carried out under local anaesthesia. Specimen was sent fresh for histology.

Histopathology

Sections showed tumour composed of a diffuse and vaguely nodular proliferation of lymphoid cells. In some areas, the neoplastic lymphoid cells showed mildly irregular nuclei without distinct nucleoli, while in other areas, they appeared larger with paler chromatin and distinct nucleoli (Fig. 38.4). The latter type of morphology was indicative of aggressive variant of mantle cell lymphoma.

Immunohistochemistry

The neoplastic lymphoid cells were positive for CD20 and CD79A (pan B-cell markers). They were also positive for CD5, cyclinD1 (Fig. 38.5), SOX11, and Bcl-2. CD23 highlighted the disrupted meshwork, likely representing disrupted follicular dendritic meshwork; Ki-67 proliferation index in some areas showed higher proliferation (up to 40–50).

Features were consistent with mantle cell lymphoma of pleomorphic or blastoid variety.

Management

A diagnosis of recurrent lymphoma was made. The patient was seen by the lymphoma specialist. PET scan showed only orbital disease without systemic involvement. The options of

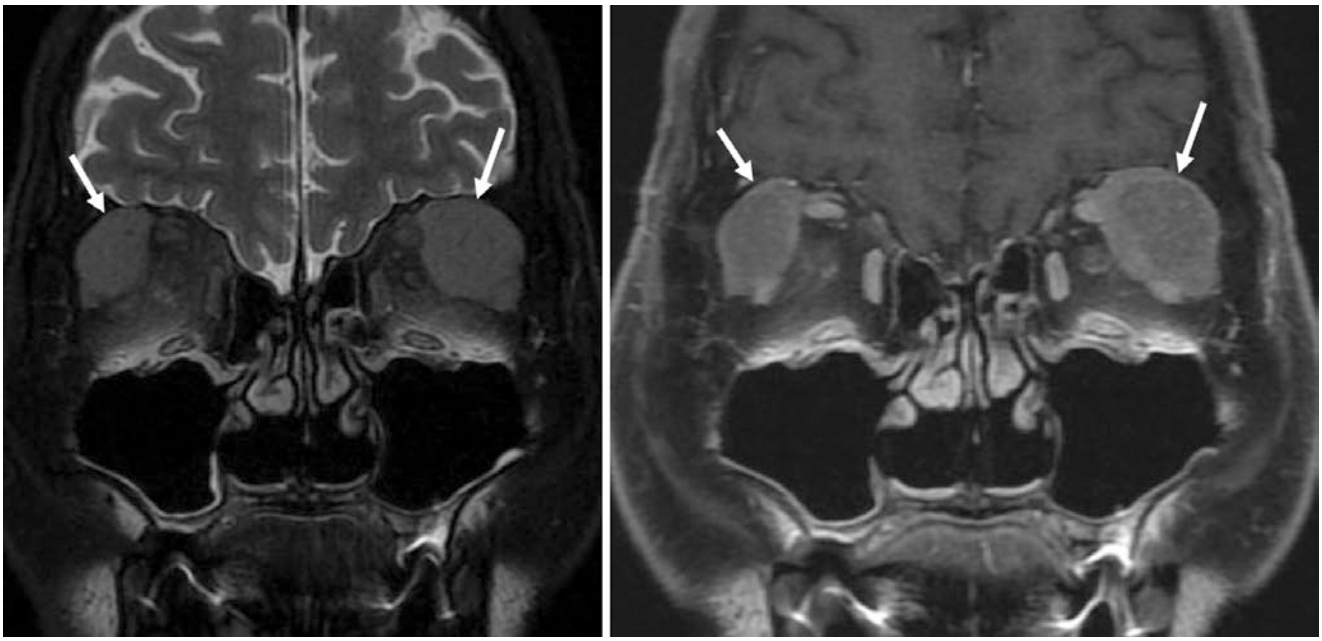

Fig. 38.2 Coronal T1w (Left) and T1w-FS + C (Right) images showing bilateral diffuse, smooth lacrimal gland enlargement (white arrows) with homogeneous enhancement

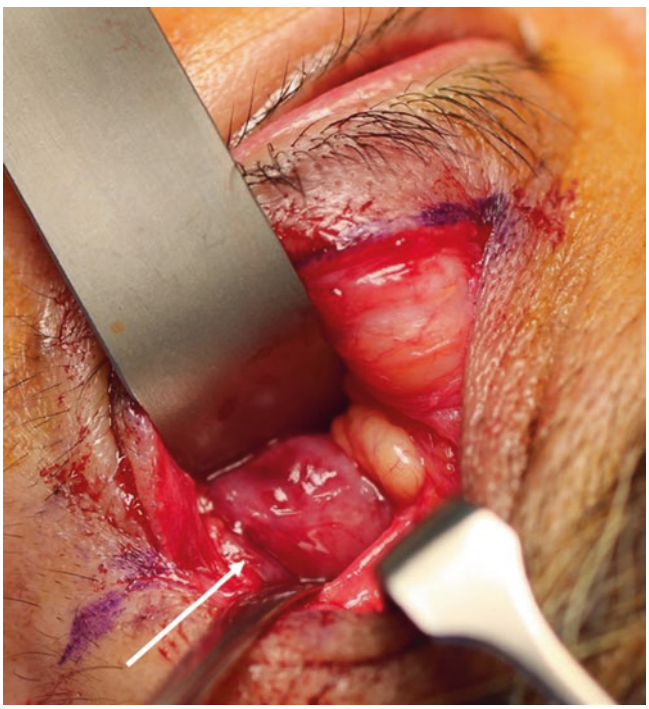

Fig. 38.3 Picture shows lacrimal gland (white arrow) exposed by anterior orbitotomy

treatment were between radiotherapy and systemic targeted therapy. Given his severe dry eyes, patient underwent systemic chemotherapy with VR CAP (bortezomib, rituximab, cyclophosphamide, doxorubicin, and prednisolone).

Discussion

Mantle cell lymphoma is an uncommon type of B-cell lymphoma that shows aggressive behaviour with a male to female ratio of about 2:1. Bilateral disease is more common with primary than with secondary ocular adnexal mantle cell lymphomas. Among the ocular adnexal tissues, the orbit and eyelids are commonly involved. Clinically, the patients present with varying degrees of proptosis, diplopia, conjunctival (salmon-pink) swelling, conjunctival redness and irritation, and ptosis.

There are four cellular variants known, small cell, marginal zone-like, pleomorphic, and blastoid. The latter two are more aggressive and have poorer prognosis.

Genetically, t(11;14)(q13; q32) and cyclin D1 are overexpressed. Cyclin D1 immunoreactivity allows for the correct identification of MCL. Before the availability of cyclin D1 immunostaining, it is probable that some cases of ENMZL with adverse prognosis were actually unrecognized cases of MCL. Rarely, some cases of MCL of ocular adnexa may be negative for cyclin D1; in such instances, SOX11 immunoreactivity is a reliable diagnostic marker.

Treatment is by chemotherapy as most patients are at an advanced stage of the disease by the time the ocular adnexal lesions occur. A few cases of MCL limited to the ocular adnexa can be treated with radiotherapy. Bortezomib-based chemotherapy (VR CAP) seems to give better survival compared to R-CHOP therapy in cases of mantle cell lymphoma.

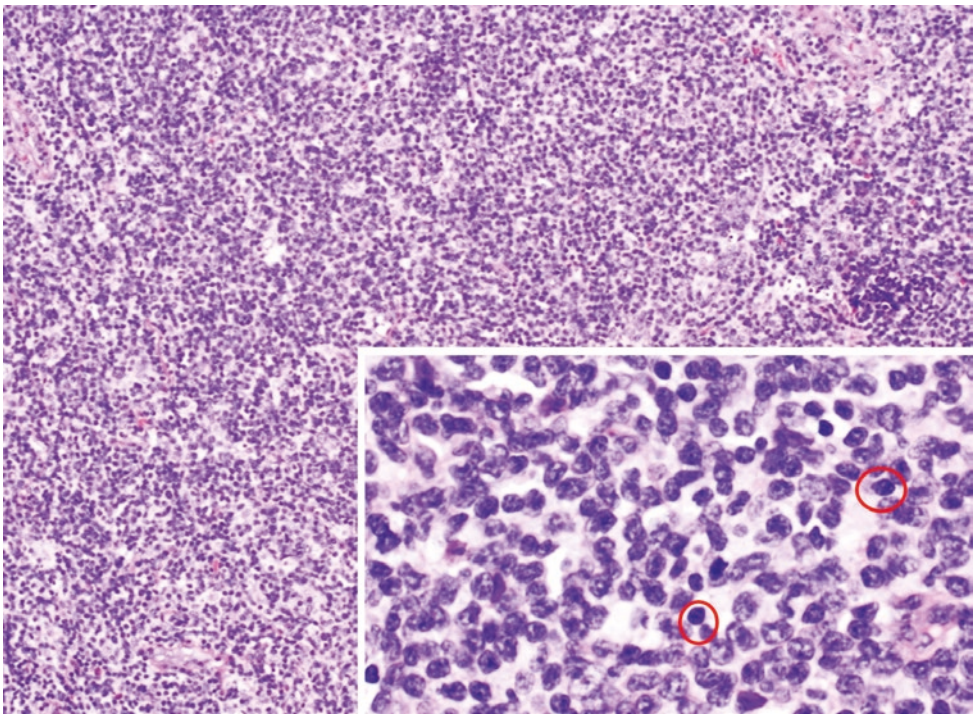

Fig. 38.4 There is a diffuse infiltrate of neoplastic lymphoid cells with medium- to large-sized nuclei, open chromatin, and irregular nuclear membranes. In contrast, the non-neoplastic lymphoid cells are smaller in size, with rounded and darker nuclei, as well as smooth nuclear membranes (red circles). Main: HE stain, 40× magnification. Inset: HE stain, 400× magnification

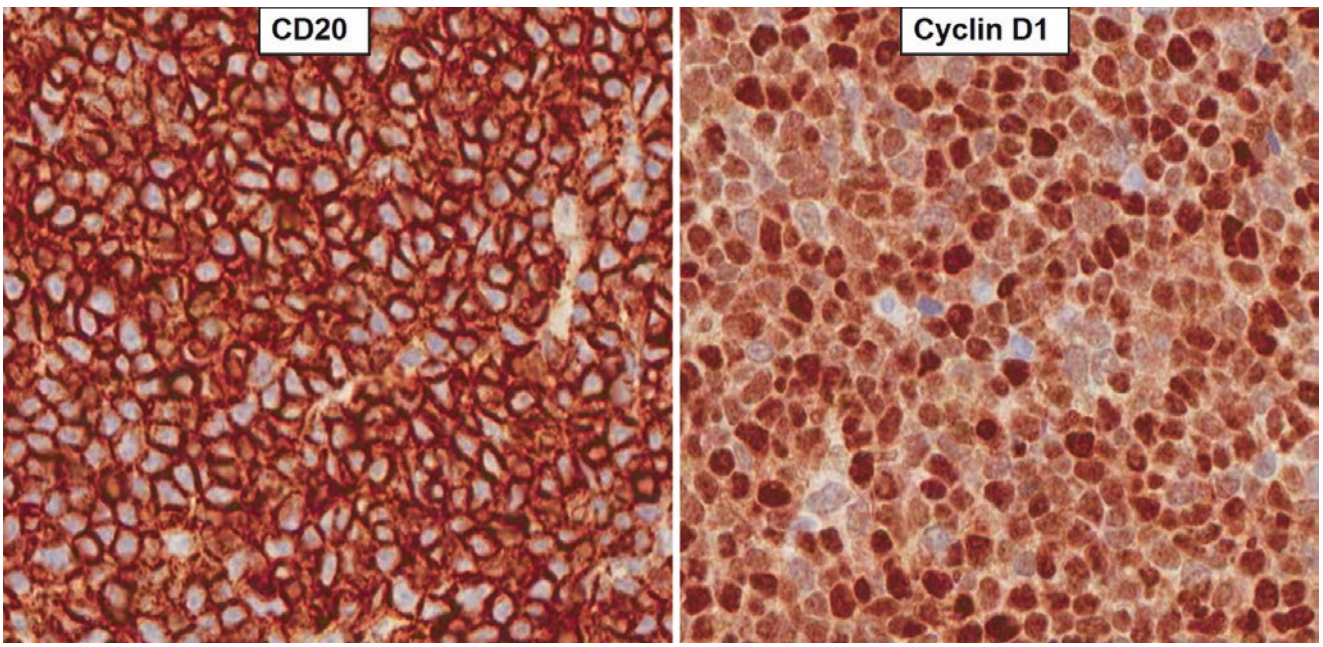

Fig. 38.5 The tumour cells are diffusely positive for CD20 and cyclin D1 immunohistochemistry. Left: Immunohistochemistry (CD20 antibody), 400× magnification. Right: Immunohistochemistry (cyclin D1 antibody), 400× magnification

Learning Points

If a patient with a previous history of lymphoma, presents with a red eye, the index of suspicion of recurrence should be high. A subconjunctival salmon-pink patch must prompt an investigation for a lymphoid tumour. Mantle cell lymphoma is a rare variant of B-cell lymphoma, and it tends to be more aggressive compared to other forms.

Further Reading

1. Looi A, Gascoyne RD, Chhanabhai M, Connors JM, Rootman J, White VA. Mantle cell lymphoma in the ocular adnexal region. Ophthalmology. 2005;112(1):114–9.
2. Ponzoni M, Govi S, Licata G, et al. A reappraisal of the diagnostic and therapeutic management of uncommon histologies of primary ocular adnexal lymphoma. Oncologist. 2013 Jul;18(7):876–84.
3. Rasmussen P, Sjö LD, Prause JU, Ralfkiaer E, Heegaard S. Mantle cell lymphoma in the orbital and adnexal region. Br J Ophthalmol. 2009;93(8):1047–51.
4. Vose JM. Mantle cell lymphoma: 2012 update on diagnosis, risk-stratification, and clinical management. Am J Hematol. 2012;87:604–9.

T-Cell Lymphoma

39

Gangadhara Sundar, Stephanie Ming Young, Poh Sun Goh, Bingcheng Wu, Min En Nga, and Shantha Amrith

Introduction

Orbital neoplasms are not uncommon. The vast majority are benign lesions that may present either in children or adults. The most common primary malignant neoplasms of the orbit are lymphomas. Most lymphomas of the orbit and adnexal region are B-cell lymphomas with mucosa-associated lymphoid tissue (MALT) being the most common. T-cell lymphomas are extremely rare and when present may be a manifestation of known preexisting systemic disease. They arise primarily from the paranasal sinuses, more commonly in East Asians. While B-cell lymphomas are usually well recognized and more easily treated, T-cell lymphomas often carry a guarded prognosis.

Clinical Scenario

A 55-year-old East Asian male presented with a lump in the inner corner of the right eye of a few months' duration. He did recall generalized weakness and weight loss over the past several months, but without fever, night sweats, nasal obstruction, epistaxis or any visual symptoms. He had no known previous systemic disease. Ophthalmic examination at presentation revealed normal visual acuity in both eyes. Examination of the left eye and adnexa were within normal limits. On the right, while the globe and intraocular examination were unremarkable, there was a firm injected subconjunctival lesion of the medial canthus, without tenderness, reducibility or compressibility (Fig. 39.1). There was no proptosis. Evaluation of the lacrimal drainage system and a transnasal endoscopic exami-

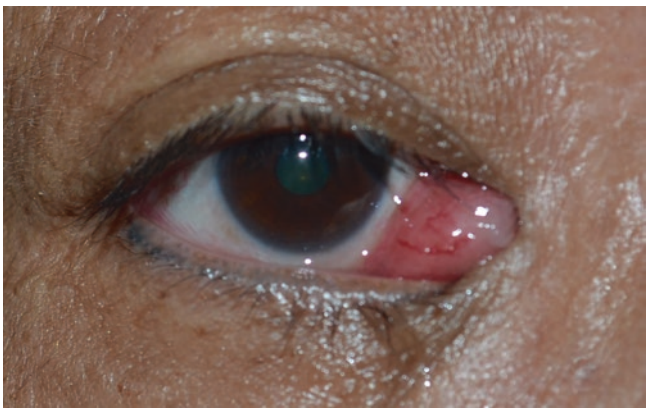

Fig. 39.1 Clinical picture showing the medial conjunctival mass in the right eye

G. Sundar · S. M. Young · S. Amrith (✉)
Department of Ophthalmology, National University Hospital, Singapore

Department of Ophthalmology, Yong Loo Lin School of Medicine, National University of Singapore, Singapore
e-mail: gangadhara_sundar@nuhs.edu.sg; stephanie.young@nuhs.edu.sg; shantha_amrith@nuhs.edu.sg

P. S. Goh
Department of Diagnostic Imaging, National University Hospital, Singapore

Department of Diagnostic Imaging, Yong Loo Lin School of Medicine, National University of Singapore, Singapore

B. Wu
Department of Pathology, National University Hospital, Singapore

M. E. Nga
Department of Pathology, National University Hospital, Singapore

Department of Pathology, Yong Loo Lin School of Medicine, National University of Singapore, Singapore

S. Amrith et al. (eds.), *Ocular Adnexal Lesions*, https://doi.org/10.1007/978-981-13-3798-7_39

Table 39.1 CLOSE summary

*C*linical process: mass, infiltrative lesion
*L*ocation: right medial canthus/anterior orbit
*O*nset: chronic
*S*ymptoms and signs: fullness with palpable mass
*E*pidemiology: middle-aged East Asian male

nation were within normal limits. There was no regional or generalized clinical lymphadenopathy.

CLOSE Summary is given in Table 39.1.

Differential Diagnosis

- Inflammatory
  - Infective: chronic dacryocystitis, lacrimal sac mucocoele (atypical)
  - Non-infective
    - Specific orbital inflammatory syndromes: Granulomatosis with polyangiitis (GPA/Wegener's granulomatosis), sarcoidal lesion, other specific orbital inflammatory syndromes
    - Non-specific orbital inflammatory syndrome (NSOID)
- Neoplastic
  - Benign: soft tissue tumours (fibroma, nodular fasciitis, fibrous histiocytic tumours, myxoma, non-distensible cavernous venous malformation (cavernous haemangioma))
  - Malignant: lymphoma, paranasal sinus tumour with orbital invasion, carcinoma arising from the caruncle, metastasis

Radiology

CT scan showed an enhancing medial canthal mass abutting but not arising from the lacrimal sac (Fig. 39.2). Extraocular muscles and rest of the orbits were normal. Underlying paranasal sinuses and rest of the orbital cavity were clear.

Several rim-enhancing enlarged right 1B neck lymph nodes were noted. These were separate from the right submandibular gland, but some were contacting the gland. Several enhancing sub-centimetre nodes were also seen in both parotids. The rest of the imaged cervical lymph nodes were not enlarged by size criteria.

Intervention

Patient underwent a transconjunctival anterior orbitotomy with excision biopsy (Fig. 39.3) of the lesion. The lesion appeared to be free from the globe, the medial rectus, the lacrimal sac and the underlying bone.

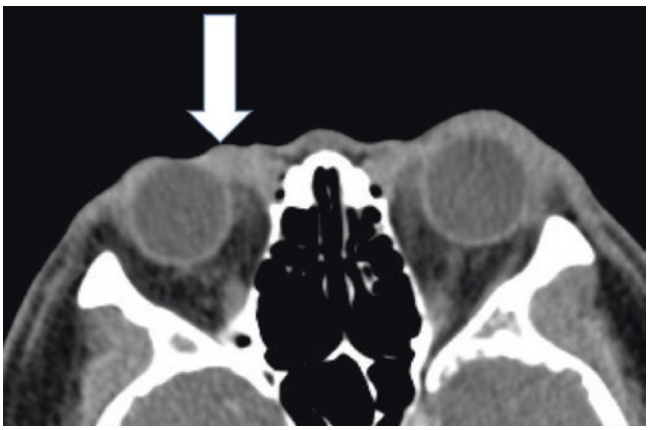

Fig. 39.2 Axial CT scan showing a diffuse bilateral preseptal mass involving the lacrimal sac fossa area (arrow showing the right sided mass) with mild enhancement with contrast

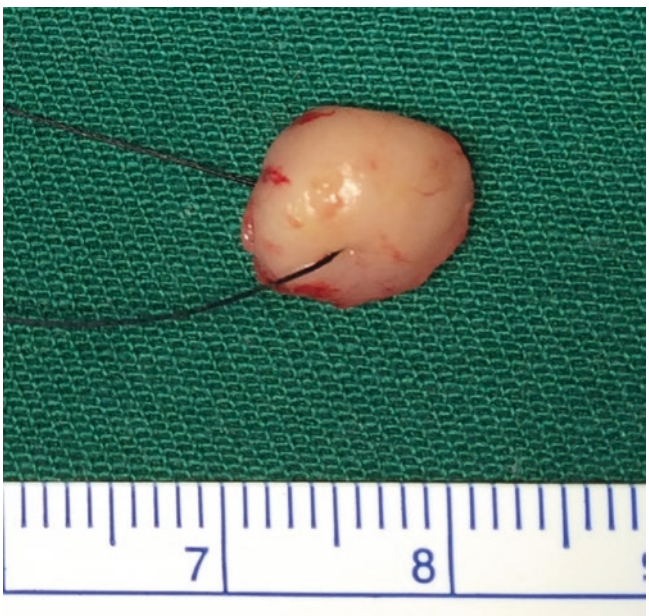

Fig. 39.3 Well-circumscribed lesion excised from the medial canthal area of the right eye

Histopathology

Section showed a piece of tissue with extensive infiltration by atypical lymphoid cells composed of large-sized neoplastic lymphoid cells with irregular nuclear membranes and ample cytoplasm. Mitotic activity was brisk (Fig. 39.4). Some neoplastic lymphoid cells displayed horseshoe or kidney-shaped nuclei resembling hallmark cells.

Immunohistochemistry showed the neoplastic lymphoid cells to be diffusely positive for CD3 (Fig. 39.5) and negative for CD20.The lymphoid cells were positive for CD30 immunohistochemistry (Fig. 39.5), which together with their pleomorphic appearance and large-size cells supported the diagnosis of anaplastic large cell lymphoma (ALCL). TCR

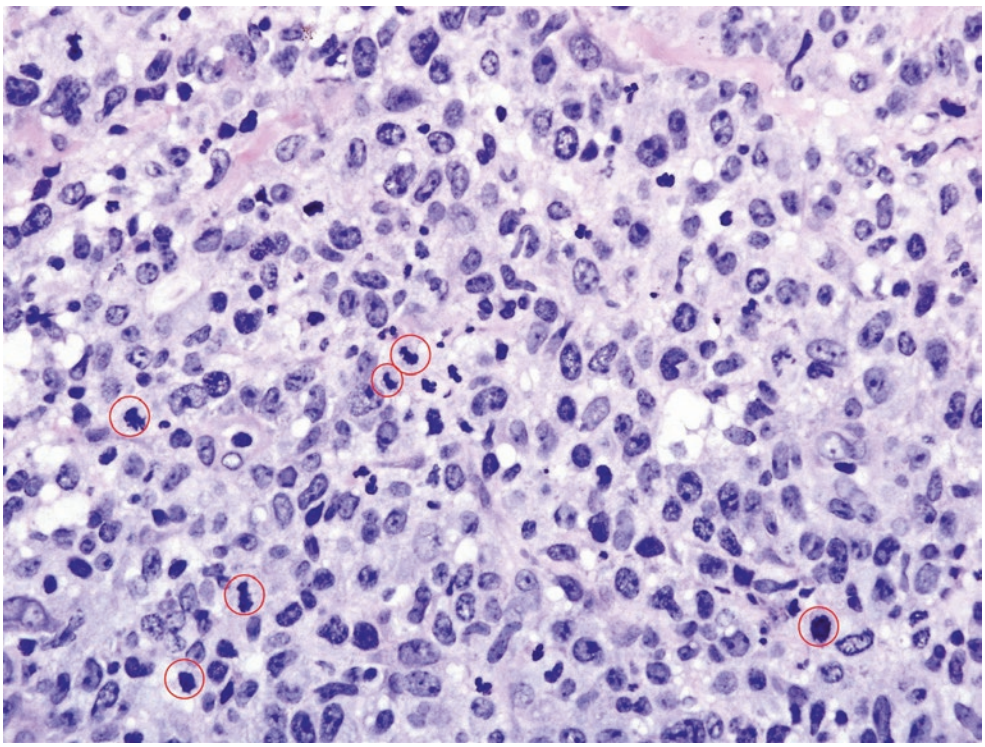

Fig. 39.4 There is a pleomorphic lymphoid cell population composed of large lymphoid cells with irregular nuclear membranes and ample cytoplasm. Mitotic activity is brisk (red circles)

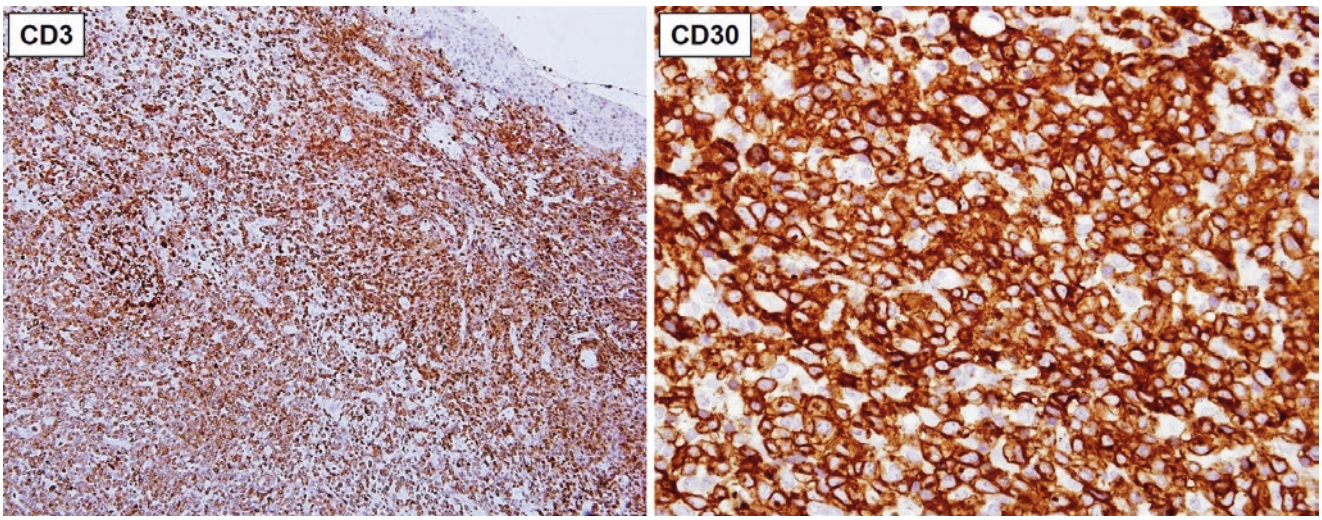

Fig. 39.5 The neoplastic lymphoid cells are diffusely positive for CD3 and CD30 immunohistochemistry Left: Immunohistochemistry (CD3 antibody), 100× magnification. Right: Immunohistochemistry (CD30 antibody), 400× magnification

Beta was positive. The Ki-67 proliferative index was approximately 70%.

Final diagnosis: Anaplastic large cell lymphoma (ALCL) of the primary T-cell type of the orbit.

Systemic Investigations

PET-CT scan showed systemic lymphadenopathy with sparing of the mediastinum.

Bone marrow biopsy was negative.

Management

With an Ann Arbor stage IIIE and TNM T1bN3M0, the patient was referred to the lymphoma specialist for systemic chemotherapy (R-CHOP) followed by bone marrow transplantation with autologous stem cell rescue.

Discussion

T-cell lymphoma affecting the orbit and ocular adnexa is extremely rare. There are many types of T-cell lymphomas, some examples being cutaneous T-cell lymphoma (such as mycosis fungoides), the natural killer (null cell) T-cell lymphoma (NKTL), angioimmunoblastic T-cell lymphoma (AITL), peripheral T-cell lymphoma not otherwise specified (PTCL-NOS), and nodal T-cell lymphoma, including anaplastic large cell lymphoma (ALCL). The cutaneous T-cell lymphomas may be present as a primary manifestation or as part of a systemic disease and rarely affect the orbit with visual significance. NKT lymphomas, more commonly seen as sinonasal lesions, have a variable prognosis. AITL is a rare form of mature peripheral T-cell lymphoma, whereas PTCL-NOS is the most common type of peripheral T-cell lymphoma.

Anaplastic large cell lymphoma (ALCL) is generally an aggressive type of T-cell lymphoma and may be ALK (anaplastic lymphoma kinase) positive or negative on immunohistochemistry. It is often positive for cytotoxic molecules such as granzyme B, as well as epithelial membrane antigen (EMA). ALK positivity appears to give a better prognosis. Sometimes ALCLs may resemble poorly differentiated carcinomas, owing to the large cell size and nuclear pleomorphism. The diagnosis is usually made from both morphology and immunophenotype. They are often treated by a combination of chemotherapy (CHOP regimen), radiation and even autologous bone marrow transplantation.

Learning Points

Orbital tumours and infiltrations have varied aetiology. A tissue diagnosis with systemic workup guides not only management but also long-term follow-up and prognostication. T-cell lymphomas are rare but should still be kept in the differential diagnosis of orbital lesions especially in adults and the elderly and in high-risk groups (East Asians, immunosuppressed patients).

Further Reading

1. Allen CE, Kent CJ, Rubin PAD, Jakobiec FA. Other lymphatic disease processes. In: Albert MA, editor. Albert & Jakobiec's principles and practice of ophthalmology. 3rd ed. Blodi: Saunders Elsevier; 2008.
2. Jimenez-Perez JC, Yoon MK. Natural killer T-cell lymphoma of the orbit. An evidence based approach. Semin Ophthalmol. 2017;32(1):116–24.
3. Kuwabara H, et al. Nasal-type NK/T-cell lymphoma of the orbit with distant metastasis. Hum Pathol. 2003;34:290–2.
4. Montes-Mojarro IA, Steinhilber J, Bonzheim I, Quintanilla-Martinez L, Fend F. The pathological spectrum of systemic anaplastic large cell lymphoma (ALCL). Cancers (Basel). 2018;10(4) https://doi.org/10.3390/cancers10040107.

Plasmacytoma/Multiple Myeloma

40

Shantha Amrith, Stephanie Ming Young, Eric Ting, Bingcheng Wu, Min En Nga, and Gangadhara Sundar

Introduction

Plasmacytoma is a descriptive term applied to tumours consisting of plasma cells. International Myeloma Working Group has described three types, solitary, extramedullary and multiple plasmacytoma. Solitary is involvement of a single bone, extramedullary a localized collection of plasma cells in the soft tissue at an extraskeletal site such as the orbit, whereas multiple involves many bones. They all lack systemic involvement. When there is a systemic plasma cell disorder, it is called multiple myeloma. The incidence of plasmacytoma in the orbits is very rare, and rarer still is an orbital mass as a presenting feature in multiple myeloma.

Clinical Scenario

A 34-year-old healthy Malay male presented with left periorbital pain and bulging of his left eye with double vision. On examination, the right eye was normal. The left ophthalmic examination revealed Snellen visual acuity of 6/6, with a non-axial proptosis of 2 mm, hypoglobus, fullness in the left upper eyelid and a mild ptosis (Fig. 40.1). A firm ill-defined tender mass was palpable in the superotemporal quadrant, and the ocular motility was restricted in upgaze with a resultant diplopia. There was no afferent pupillary defect, and the anterior segment examination was normal. The fundus examination revealed choroidal striae in the superotemporal quadrant. Systemic examination did not reveal any lymphadenopathy or hepatosplenomegaly.

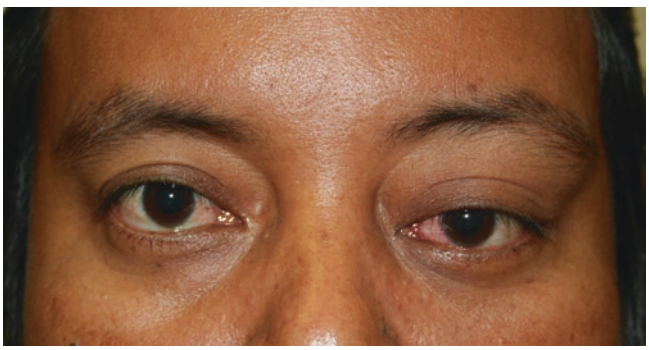

Fig. 40.1 Clinical picture showing a left proptosis, downward displacement, fullness in the left upper lid with ptosis

CLOSE summary is given in Table 40.1.

S. Amrith (✉) · S. M. Young · G. Sundar
Department of Ophthalmology, National University Hospital, Singapore

Department of Ophthalmology, Yong Loo Lin School of Medicine, National University of Singapore, Singapore
e-mail: shantha_amrith@nuhs.edu.sg; stephanie.young@nuhs.edu.sg; gangadhara_sundar@nuhs.edu.sg

E. Ting
Department of Diagnostic Imaging, National University Hospital, Singapore

Department of Diagnostic Imaging, Yong Loo Lin School of Medicine, National University of Singapore, Singapore

Advanced Medicine Imaging, Singapore

B. Wu
Department of Pathology, National University Hospital, Singapore

M. E. Nga
Department of Pathology, National University Hospital, Singapore

Department of Pathology, Yong Loo Lin School of Medicine, National University of Singapore, Singapore

S. Amrith et al. (eds.), *Ocular Adnexal Lesions*, https://doi.org/10.1007/978-981-13-3798-7_40

Differential Diagnosis

- Inflammatory lesions:
  - Dacryoadenitis
  - Non-specific orbital inflammation
  - Specific inflammation such as sarcoidal lesion, granulomatous polyangiitis (Wegener's), Sjogren's, IgG4 ROD, etc.
- Lymphoproliferative lesions such as reactive lymphoid hyperplasia and lymphoma
- Malignant tumours such as adenoid cystic carcinoma of lacrimal gland, haematological malignancies
- Metastatic lesions

Imaging

Axial and coronal T1w images (Fig. 40.2) showed an enhancing extraconal mass arising from the zygomatic process of the frontal bone in the superotemporal quadrant of the left orbit with bony involvement and adjacent dural thickening. It was displacing the superior and lateral recti medially. The optic nerve and the globe were normal. There was an additional enhancing lesion noted in the medulla of the greater wing of the sphenoid on the right side.

MRI and CT scan of the lumbar spine (Fig. 40.3) showed an osteolytic lesion in lumbar 1 vertebra.

Table 40.1 CLOSE summary

*C*linical scenario: infiltrative mass lesion
*O*nset: subacute (2 weeks)
*L*ocation: left superotemporal orbit
*S*igns and symptoms: left upper eyelid swelling, proptosis, pain and diplopia
*E*pidemiology: young Malay adult male

Intervention

The patient underwent an incision biopsy with debulking of the tumour through an anterior orbitotomy using a left lid crease incision. Fresh tissue was sent for histopathological examination.

Histopathology

Paraffin sections showed a tumour with sheets of atypical plasma cells with enlarged hyperchromatic nuclei with a clumped chromatin eccentric nuclei and modest amounts of basophilic cytoplasm. Some nuclei showed prominent nucleoli (Fig. 40.4). Immunohistochemistry for CD138 (Fig. 40.4 inset), CD79a and CD56 were positive. Lambda light chain restriction was demonstrated on in situ hybridization, suggesting a clonal cell population. The features were those of plasmacytoma.

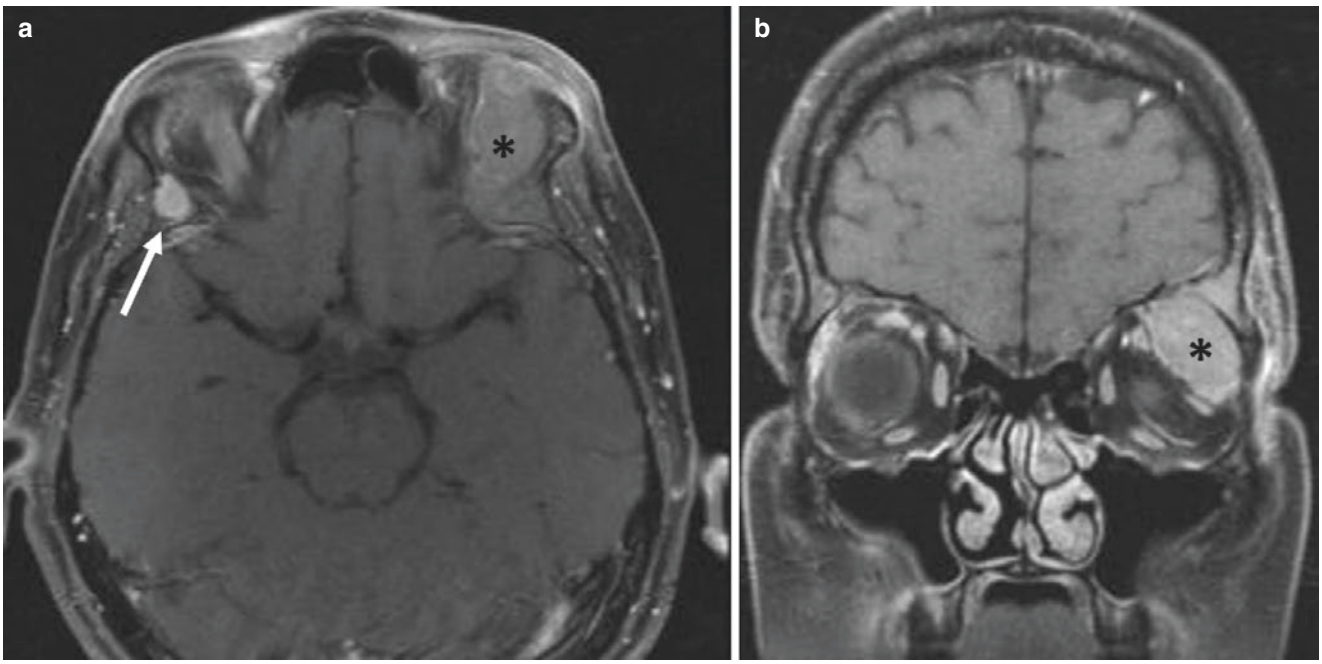

Fig. 40.2 Magnetic resonance imaging: (**a**) axial, (**b**) coronal: T1w+C images show an enhancing extraconal mass in the left superomedial orbit (*) with involvement of the adjacent bone, as well as a clinically undetected lesion in the marrow space of the right greater wing of sphenoid (white arrow)

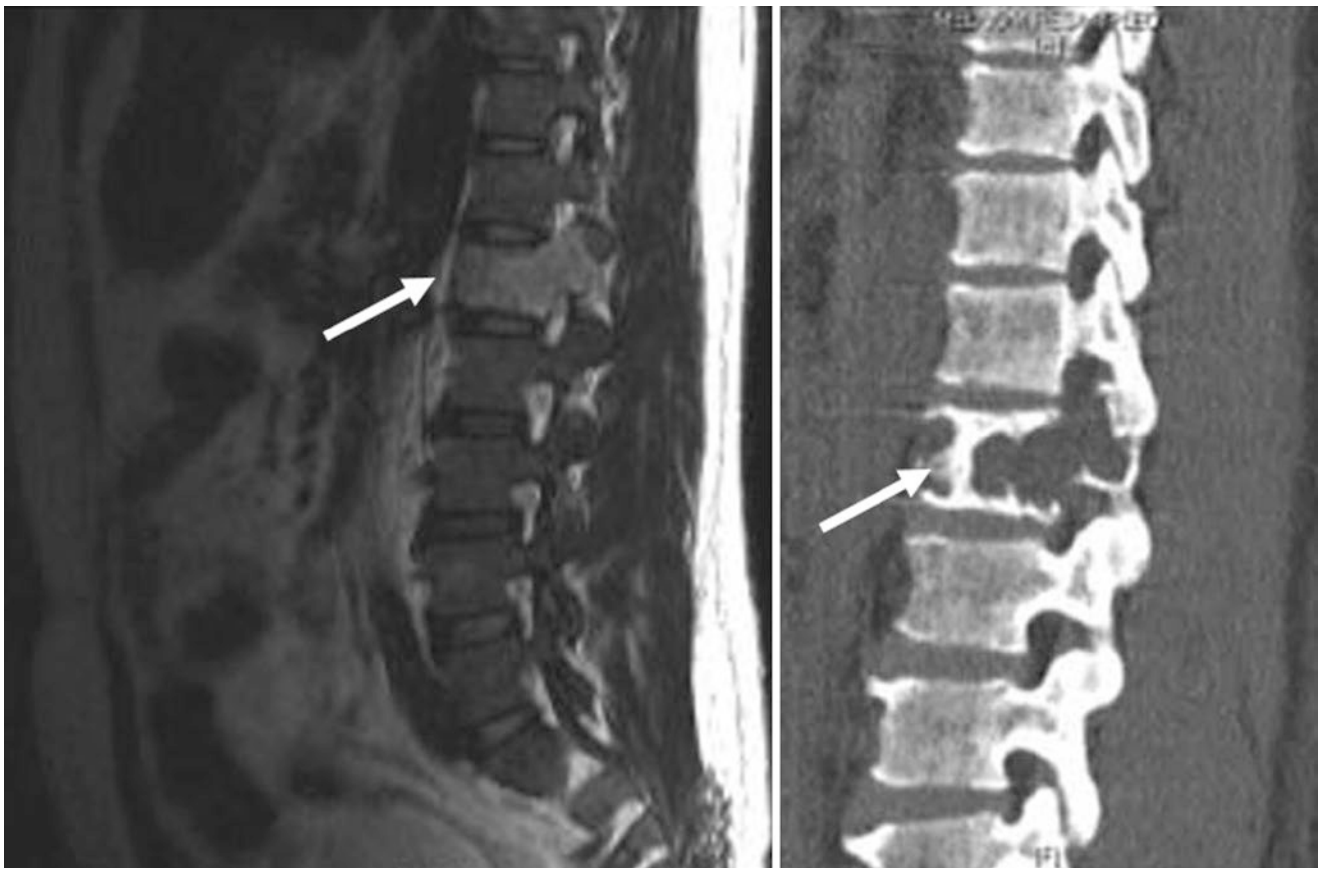

Fig. 40.3 Sagittal T2w MRI scan of the lumbar spine (left) and sagittal CT scan of the lumbar spine (right) showing a lytic lesion in the first lumbar vertebra (white arrow)

Further Investigation

Bone marrow biopsy showed atypical plasmacytic infiltrate consistent with multiple myeloma. Serum immunoglobulin showed Ig myeloma positivity. Other serological tests showed renal impairment and hypercalcaemia.

Management

In view of the systemic involvement, a diagnosis of multiple myeloma was made, and the patient underwent systemic chemotherapy with bortezomib, lenalidomide and prednisolone. In addition, bisphosphonates were given to prevent fractures.

Discussion

About 80% of the plasma cell neoplasms are multiple myeloma. For a diagnosis of solitary or extramedullary plasmacytoma to be made, there should be no bone marrow lesions or systemic involvement.

About 70% of patients with multiple myeloma present with bone pain. Patients presenting as an orbital mass as a first presentation of multiple myeloma are very rare. Orbit can be secondarily involved in patients with known multiple myeloma. The orbital lesions usually present as proptosis, pain and diplopia. Systemic symptoms consist of bone pain; pathological fractures and spinal cord compression are common. Anaemia and thrombocytopenia can cause weakness and bleeding tendencies.

The diagnosis is usually made by a combination of laboratory tests, imaging and tissue biopsy, where available. Bone marrow biopsy should show more than 30% of plasma cells. Presence of myeloma immunoglobulin in the blood and presence of anaemia, hypercalcaemia and renal impairment are some of the laboratory changes seen in multiple myeloma. Imaging shows osteoclastic lesions in flat bones.

Management is in the form of radiotherapy for the non-systemic types. Chemotherapy induction with thalidomide derivative, bortezomib and prednisolone followed by maintenance with thalidomide or bortezomib gives a disease-free survival of longer periods compared to older regimes. Bisphosphonates should always be used for fracture preven-

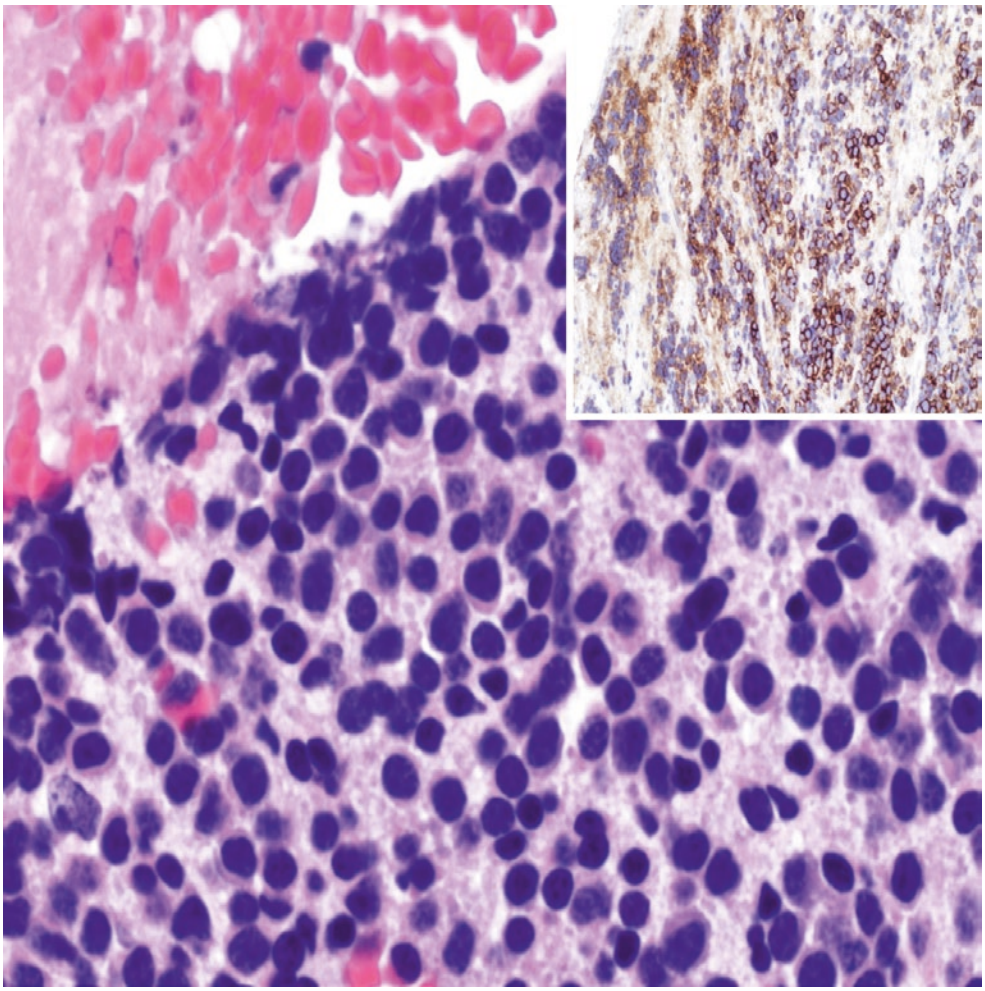

Fig. 40.4 Histological examination of the orbital mass showing sheets of atypical plasma cells with enlarged hyperchromatic nuclei, clumped chromatin pattern and eccentric nuclei with modest amounts of basophilic cytoplasm. The tumour cells are diffusely positive for CD138 on immunohistochemistry (inset). Main: HE stain; 600× magnification. Inset: Immunohistochemistry (CD138 antibody); 400× magnification

tion and erythropoietin for anaemia. Bone marrow transplantation can be considered in suitable cases.

Learning Points

Orbital presentation as a first sign of multiple myeloma is very rare. The radiological appearance combined with histopathology and laboratory tests should alert the ophthalmologist about the diagnosis. Management and close monitoring should be done by a haemato-oncology team.

Further Reading

1. Adkins JW, Shields JA, Shields CL, Eagle RC Jr, Flanagan JC, Campanella PC. Plasmacytoma of the eye and orbit. Int Ophthalmol. 1997;20:339–43.
2. Lazaridou MN, Micallef-Eynaud P, Hanna IT. Soft tissue plasmacytoma of the orbit as part of the spectrum of multiple myeloma. Orbit. 2007;26:315–8.
3. Sharma A, Kaushal M, Chaturvedi NK, Yadav R. Cytodiagnosis of multiple myeloma presenting as orbital involvement: a case report. Cyto J. 2006;10:3–19.

Part X

Primary Malignant Neoplasms: Eyelid

Basal Cell Carcinoma

41

Stephanie Ming Young, Shantha Amrith, Bingcheng Wu, Min En Nga, and Gangadhara Sundar

Introduction

Basal cell carcinoma (BCC) is the most common human malignancy, with major risk factors being ultraviolet (UV) light exposure and Caucasian race. Other risk factors include immunosuppression, genetic disorders such as basal cell nevus syndrome (BCNS, Gorlin syndrome), and xeroderma pigmentosum. They typically appear on sun-exposed skin (e.g. face). In the periocular region, BCC most commonly occurs on the lower eyelid, followed by the medial canthus, upper lid, and lateral canthus. While they are slow-growing, they can be locally destructive, often presenting as slowly enlarging, non-healing lesions that bleed when traumatised. They rarely metastasise.

Case Scenario

A 77-year-old Chinese female, with no past medical history of note, presented with a slow-growing, painless right lower lid lesion of 12 years' duration. The patient reported previous ulceration with abscess formation that "dropped off" and reformed again.

On examination, there was a non-tender, ulcerated, and pigmented lesion with rolled edges occupying a third of the right lower eyelid (Fig. 41.1). It involved the lid margin causing distortion, destruction, as well as loss of eyelashes.

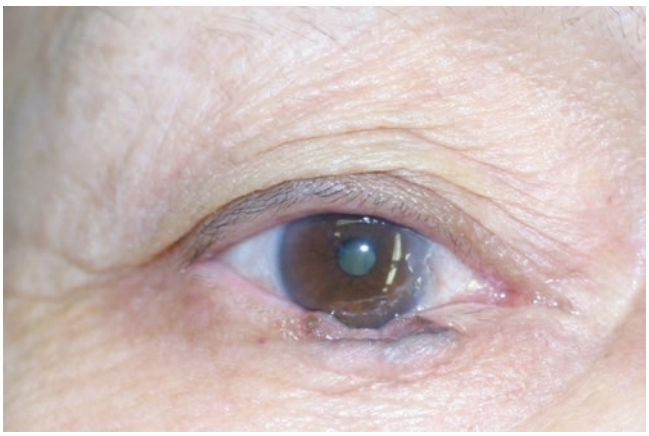

Fig. 41.1 Pigmented ulcerated lesion with rolled edges in the right lower lid

CLOSE summary is shown in Table 41.1.

Differential Diagnosis

- Basal cell carcinoma
- Other malignant skin tumours

S. M. Young · S. Amrith (✉) · G. Sundar
Department of Ophthalmology, National University Hospital, Singapore

Department of Ophthalmology, Yong Loo Lin School of Medicine, National University of Singapore, Singapore
e-mail: stephanie.young@nuhs.edu.sg; shantha_amrith@nuhs.edu.sg; gangadhara_sundar@nuhs.edu.sg

B. Wu
Department of Pathology, National University Hospital, Singapore

M. E. Nga
Department of Pathology, National University Hospital, Singapore

Department of Pathology, Yong Loo Lin School of Medicine, National University of Singapore, Singapore

S. Amrith et al. (eds.), *Ocular Adnexal Lesions*, https://doi.org/10.1007/978-981-13-3798-7_41

Management

The patient underwent an excision of the right eyelid tumour and reconstruction with Hughes flap and free skin graft under frozen section control. Excision of the lower lid lesion was performed with 3 mm free margin from lateral, medial, and inferior margins (Fig. 41.2a, b). After ensuring margin clearance, a Hughes flap was constructed from the upper lid (Fig. 41.2c). A horizontal tarsal incision was made 4 mm from the lid margin, followed by two vertical incisions to form the flap. The tarsal flap was slid inferiorly and sutured to the lower lid (Fig. 41.2d). A free skin graft was harvested from the preauricular area to form the anterior lamella (Fig. 41.2e, f).

Table 41.1 CLOSE summary

*C*linical process: infiltrative mass causing distortion of normal anatomy
*L*ocation: lid margin of the right lower lid
*O*nset: chronic
*S*igns and symptoms: painless ulcerated lesion
*E*pidemiology: elderly Chinese female

Histopathology

There was a basaloid tumour centred in the superficial dermis, with a connection to the overlying basal layer of the epidermis. The tumour was composed of interconnected islands and trabeculae (broad elongated islands) of basaloid cells with prominent peripheral palisading. There was a fairly loose, myxoid stroma with peripheral clefting between the edges of tumour islands and the stroma (Fig. 41.3).

The features were consistent with a basal cell carcinoma.

Discussion

Basal cell carcinoma (BCC) may have the following clinical presentations:

- Nodular: A pearly papule or nodule with surface telangiectasia and a rolled edge. It gradually enlarges to form a dome-shaped lesion, which may develop central ulceration.
- Superficial: A slow-growing, scaly, erythematous patch or plaque which may resemble dermatitis.
- Morphoeic (sclerosing): An indurated, poorly defined, white to pink, scar-like plaque. This appearance is also sometimes termed as "infiltrative" BCC.

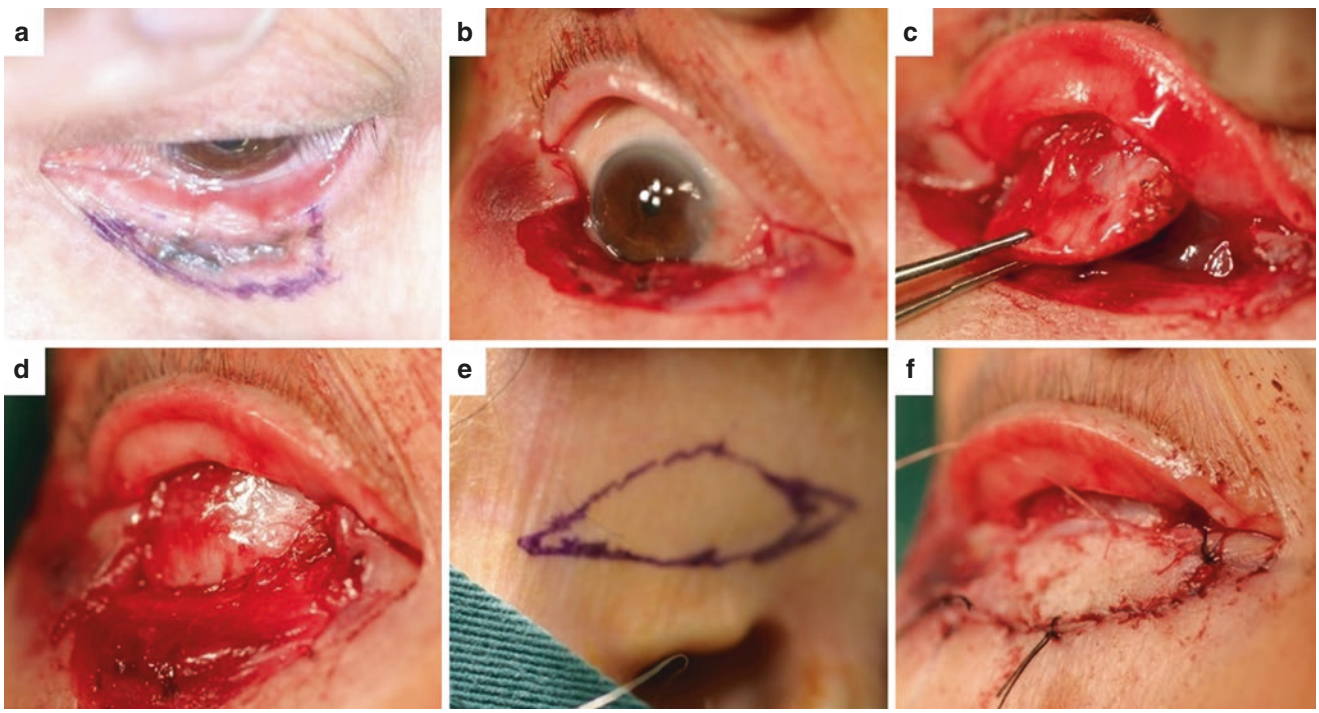

Fig. 41.2 (**a** and **b**) Excision of the lower lid lesion with 3 mm free margin from lateral, medial, and inferior margins. (**c**) Hughes flap being constructed from the upper tarsoconjunctiva. (**d**) The tarsal flap is sutured to the posterior lamellar defect in the lower lid. (**e** and **f**) Free skin graft being harvested from the preauricular area to form the anterior lamella. Right eyelid tumour excision and reconstruction with Hughes flap and free skin graft

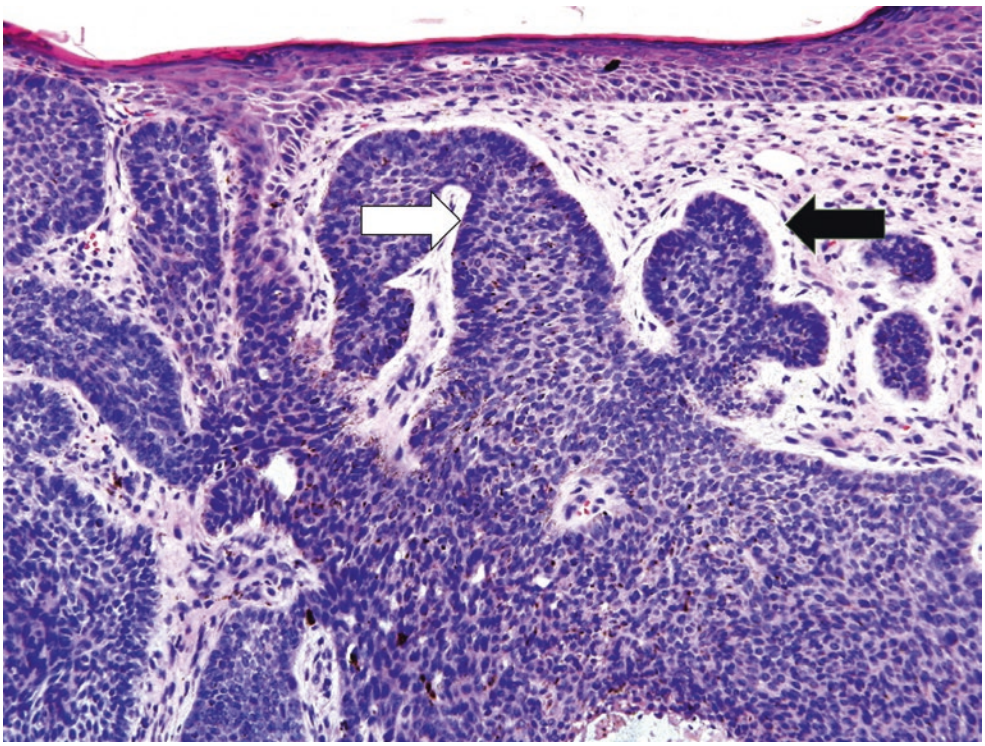

Fig. 41.3 The tumour is composed of interconnected islands and trabeculae of uniform basaloid cells with prominent peripheral palisading (white arrow). There is a fairly loose, myxoid stroma with peripheral clefting of the tumour islands (black arrow). HE stain; 200× magnification

- Pigmented: BCC can have uniform or variegated brown, grey-blue, or black pigmentation and may mimic nevi or melanoma. This type is most common among pigmented races and is uncommon in Whites.

A skin biopsy is often required to confirm the diagnosis and determine the histologic subtype. On histopathology, the tumour cells form dermal nests, cords, and islands. The cells forming nests are small and round and resemble basal keratinocytes. At the periphery of the nests, these cells elongate in parallel array, forming a palisading pattern. Tumour cells have little pleomorphism, and mitosis are infrequent. Cracking artefacts may be present and represent artificial separations between the tumour and the stroma.

Treatment

Excision with confirmation of clear margins by histopathologic examination is the mainstay of treatment. If available, some form of intraoperative margin control such as Mohs micrographic surgery (MMS) is preferable for periocular BCC to minimize recurrence risks and conserve tissue. However, depending on resources, intraoperative margin control may be reserved for higher-risk tumours or used in an attempt to conserve functional structures such as the lacrimal drainage system.

Other treatment options include destructive treatments such as radiotherapy and cryotherapy. However, these treatments have the disadvantages of lacking histologic confirmation of clearance, higher recurrence rates than surgery, and difficulty in detection of recurrence in treated areas. Hence, apart from radiotherapy in patients who are not candidates for surgery, or as adjunctive treatment in high-risk lesions, these destructive treatments are not widely used in the periocular region.

Although surgery remains the treatment of choice for most BCCs, chemotherapy has shown promising results in patients with extensive tumours and patients with basal cell nevus syndrome. This includes topical therapy with imiquimod and systemic therapy with vismodegib, a hedgehog signalling pathway antagonist.

Learning Points

Basal cell carcinoma is a common skin malignancy and may have various clinical presentations. Any suspicious lesion should be confirmed histopathologically, and excision biopsy with clear margins should be performed.

Further Reading

1. Avril MF, Auperin A, Margulis A, et al. Basal cell carcinoma of the face: surgery or radiotherapy? Results of a randomized study. Br J Cancer. 1997;76(1):100–6.
2. Prabhakaran VC, Gupta A, Huilgol SC, et al. Basal cell carcinoma of the eyelids. Compr Ophthalmol Updat. 2007;8(1):1–14.
3. Smeets NW, Krekels GA, Ostertag JU, et al. Surgical excision vs Mohs' micrographic surgery for basal-cell carcinoma of the face: randomised controlled trial. Lancet. 2004;364(9447):1766–72.
4. Malhotra R, Huilgol SC, Huynh NT, Selva D. The Australian Mohs database, part II: Periocular basal cell carcinoma outcome at 5-year follow-up. Ophthalmology. 2004;111(4):631–36.

Squamous Cell Carcinoma

42

Shantha Amrith, Stephanie Ming Young, Bingcheng Wu, Min En Nga, and Gangadhara Sundar

Introduction

Malignant tumours of the eyelid have certain clinical characteristics. There may be distortion of the eyelid margin with loss of eyelashes, ulceration, telangiectasia, or induration. There may also be cicatrization with secondary ectropion or retraction. The most common malignant tumour of the eyelid is basal cell carcinoma (BCC). Squamous cell carcinoma (SCC) is less common (5–10% of all eyelid malignancies) but has the same risk factors as BCC, such as Fitzpatrick skin types I and II and ultraviolet light exposure. It is more common in males over 60 years of age, in the lower than upper lids, and biologically more aggressive than BCC.

Case Scenario

A 95-year-old Chinese female, a poor historian, presented with redness and poor vision in her right eye when admitted to the hospital for a fall and a left neck of femur fracture. On examination, she was found to have a near vision of N48 with severe blepharitis and keratitis in the right eye but milder signs in the left eye (Fig. 42.1a, b). The anterior chamber and the fundus examinations were normal. She was treated with lid scrubs and antibiotic eye drops. On subsequent review, she was found to have a central epithelial defect associated with more severe blepharoconjunctivitis in the right eye. The non-healing of the epithelial defect was considered to be due to the presence of a spastic entropion which was present in both eyes. To help in the corneal healing, a Quickert everting suture was advised. While applying the sutures, it was noted that the right lower lid had cicatricial changes in the conjunctiva. Four months later, the patient returned with a nodular lesion in the right lower palpebral conjunctiva (Fig. 42.1c) with submandibular lymph node enlargement. The rest of the systemic examination was normal.

CLOSE summary is shown in Table 42.1.

Differential Diagnosis

- Chronic blepharitis
- Pyogenic granuloma
- Sebaceous gland carcinoma
- Squamous cell carcinoma
- Basal cell carcinoma

S. Amrith (✉) · S. M. Young · G. Sundar
Department of Ophthalmology, National University Hospital, Singapore

Department of Ophthalmology, Yong Loo Lin School of Medicine, National University of Singapore, Singapore
e-mail: shantha_amrith@nuhs.edu.sg; stephanie.young@nuhs.edu.sg; gangadhara_sundar@nuhs.edu.sg

B. Wu
Department of Pathology, National University Hospital, Singapore

M. E. Nga
Department of Pathology, National University Hospital, Singapore

Department of Pathology, Yong Loo Lin School of Medicine, National University of Singapore, Singapore

S. Amrith et al. (eds.), *Ocular Adnexal Lesions*, https://doi.org/10.1007/978-981-13-3798-7_42

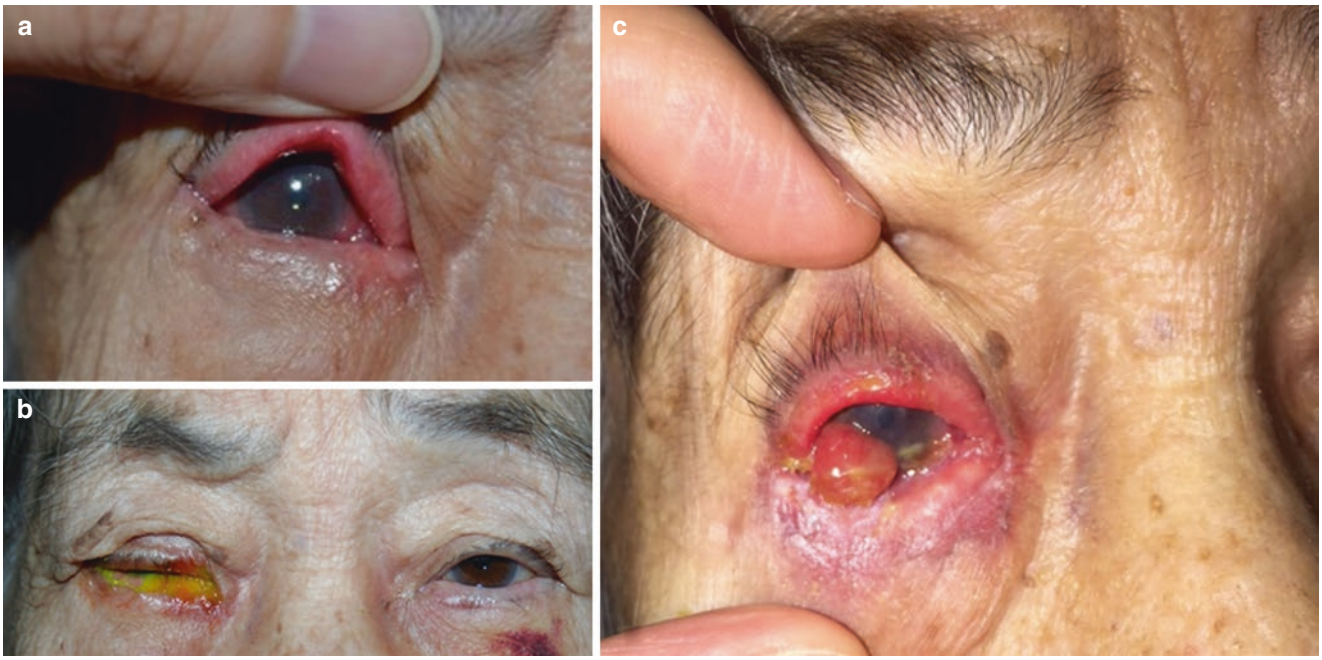

Fig. 42.1 (**a**) Ocular surface disease with erythema of lid margin and lower lid entropion of the right eye. (**b**) Three weeks after the everting sutures. (**c**) Nodular mass in the lateral aspect of the right lower lid with destruction of lid margin architecture

Table 42.1 CLOSE summary

*C*linical process: mass lesion with inflammatory effect
*L*ocation: right lower lid
*O*nset: chronic
*S*ymptoms and signs: conjunctival injection, lid erythema, ocular surface disease, cicatrization of conjunctiva, discharge, and mass lesion
*E*pidemiology: elderly Chinese female

Intervention

The mass as well as a full thickness lid margin tissue was excised and sent for histology which showed squamous cell carcinoma. The patient was advised a CT scan to rule out globe and orbital involvement, but declined.

Diagnosis: Squamous cell carcinoma with TNM staging: T3b,N1,M0

Histopathology

The tumour was poorly differentiated; hence, keratinization was not evident. It was composed of sheets of large pleomorphic cells with hyperchromatic nuclei, coarse nuclear chromatin, and dense eosinophilic cytoplasm, surrounded by a desmoplastic stroma. Intercellular bridges were seen. Many mitoses were seen (Fig. 42.2). The features were those of a poorly differentiated squamous cell carcinoma.

Management

The patient declined further investigations and wanted palliative treatment. She also declined palliative radiotherapy. Imiquimod 5% cream every night along with steroid eye drops was prescribed. An option of interferon alpha-2b (IFN α-2b) eye drops or mitomycin C (MMC) eye drops was also considered, but rejected by the patient. Over a period of 6 months, there was progressive infiltration of the globe and anterior orbit. The patient declined all forms of treatment.

Discussion

SCC can arise de novo or from areas of premalignant lesions such as actinic keratosis, Bowen's disease, keratoacanthoma, or radiation dermatosis. It is also more common than BCC in renal transplant patients. Clinical diagnosis is challenging due to its varied presentations, and it may masquerade as an ocular surface disease or lid malposition as in the case above.

Histologically, the main features suggesting squamous differentiation in a malignant tumour include keratinization (keratin pearls), ample dense eosinophilic cytoplasm, and intercellular bridges. Immunohistochemical stains that could be used to confirm squamous differentiation include p40 and high molecular weight cytokeratins such as cytokeratin 5/6 (both expected to be positive in tumours with squamous differentiation).

It spreads locally through direct extension or perineural infiltration, and regionally via the lymphatics, and to distant organs by haematogenous route. Perineural infiltration along

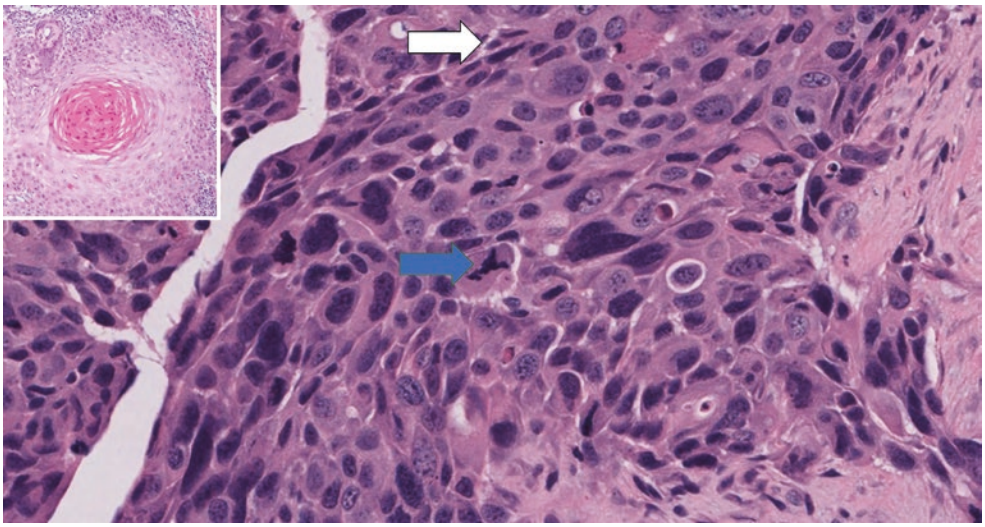

Fig. 42.2 Sheets of malignant cells with hyperchromatic nuclei, coarse nuclear chromatin, and dense eosinophilic cytoplasm. Intercellular bridges are also seen (white arrow). An atypical mitosis with tripolar configuration is seen in the centre of the field (blue arrow). The inset shows a typical keratin pearl that would be seen in a case of keratinizing squamous cell carcinoma. HE stain; 600× magnification

the trigeminal and motor nerves of the orbit facilitates spread of the tumour into the orbit and intracranial cavity. Poor prognostic factors include poorly differentiated tumour, large size, and perineural invasion. There is usually a 1–24% chance of a lymph node spread and distant metastasis. Orbital invasion occurs in about 6% of cases.

The gold standard treatment for SCC is wide surgical excision with clear margins under frozen section control, followed by reconstruction. Mohs micrographic excision helps to get clearance of the tumour with preservation of normal tissues for reconstruction. Less aggressive alternative treatments may be indicated if the patient is unfit for surgery, refuses surgery, or has multiple lesions.

Radiotherapy is given in fractionated doses, and the dosage depends on the size and depth of the lesion. It gives comparable cure rates for small lesions, does not require hospitalization, and is useful for palliative treatment or incomplete tumour excision. However, with radiotherapy, there is no evidence for histological clearance of the tumour. Post-operative radiotherapy is advised for perineural infiltration. The recurrence after radiotherapy is higher than that for surgery, and there is also the risk of a second malignancy. The other complications of radiotherapy include radiation dermatitis, skin necrosis, depigmentation, madarosis, dry eyes, cataract formation, conjunctival keratinization, and canalicular occlusion.

Cryotherapy can be considered for small tumours where the tumour is frozen to −30 °C while protecting the globe, using a double freeze-thaw technique. Permanent changes such as skin atrophy, notching of lid margin, loss of eyelashes, and scarring can occur with cryotherapy.

Topical imiquimod, an immunomodulatory agent, as a 5% cream is under study to treat superficial and recurrent BCC and SCC. The clearance rates are low compared to surgery. Adverse events such as burning sensation, erythema, blistering, excoriation, and conjunctival hyperaemia are common. Clinical trials with targeted systemic therapy with vismodegib, a hedgehog signalling pathway antagonist, seem to be promising.

Learning Points

Differentiating benign and malignant periocular skin lesions can be challenging because malignant lesions occasionally masquerade as benign pathology, and therefore any suspicious lesion in the eyelid should be biopsied for early detection. Mohs micrographic excision or wide excision under frozen section control is the standard of care for SCC. If detected early and treated adequately, the prognosis is excellent. Perineural spread is a poor prognostic sign. Understanding what is in the best interest of patients, the most aggressive treatment modality may not necessarily be the best.

Further Reading

1. Cottel WI. Perineural invasion by squamous cell carcinoma. J Dermatol Surg Oncol. 1982;8:589–600.
2. Faustina M, Diba R, Ahmadi MA, et al. Patterns of regional and distant metastasis in patients with eyelid and periocular squamous cell carcinoma. Ophthalmology. 2004;111:1930–2.
3. Leatherbarrow B. Oculoplastic Surgery. 2nd ed. London: Informa Healthcare; 2011.
4. Limawararut V, Leibovitch I, Sullivan T, Selva D. Periocular squamous cell carcinoma. Clin Exp Ophthalmol. 2007;35(2):174–85.
5. Love WE, Bernhard JD, Bordeaux JS. Topical imiquimod or fluorouracil therapy for basal and squamous cell carcinoma: a systematic review. Arch Dermatol. 2009;145(12):1431–8.
6. Murchison AP, Walrath JD, Washington CV. Non-surgical treatments of primary, non-melanoma eyelid malignancies: a review. Clin Exp Ophthalmol. 2011;39(1):65–83.
7. Reifler DM, Hornblass A. Squamous cell carcinoma of the eyelid. Surv Ophthalmol. 1986;30:349–65.
8. Rene C. Oculoplastic aspects of ocular oncology. Eye (Lond). 2013;27(2):199–207.
9. Thosani MK, Schneck G, Jones EC. Periocular Squamous Cell Carcinoma. Dermatol Surg. 2008;34(5):585–99.
10. Yin VT, Pfeiffer ML, Esmaeli B. Targeted therapy for orbital and periocular basal cell carcinoma and squamous cell carcinoma. Ophthal Plast Reconstr Surg. 2013;29(2):87–92.

Sebaceous Gland Carcinoma

43

Shantha Amrith, Stephanie Ming Young, Poh Sun Goh, Bingcheng Wu, Min En Nga, and Gangadhara Sundar

Introduction

Sebaceous gland carcinoma (SGC) is usually considered a rare eyelid tumour (1–5% of all cutaneous malignancies in the USA), but higher incidence rates have been seen in Asia (28–60%). It has a tendency for intraepithelial spread, as well as regional and distant metastases. Early diagnosis and timely management can help reduce morbidity and mortality.

In the eyelids, it may arise from meibomian glands (most common), glands of Zeis or sebaceous glands associated with the caruncle. It is two to three times more common in the upper lids due to the higher number of meibomian glands. It usually affects people in their sixth–eighth decade and females more than males.

Clinical Scenarios

Case 1

A 37-year-old Chinese female presented with a painless lump in the lower lid, of 3 weeks' duration. There was some discharge, but no redness.

On examination, she was found to have normal visual acuity and a firm, non-tender lump in the right lower lid. The lid margin seemed a little thickened with telangiectasia, but the margin architecture was well preserved (Fig. 43.1). There was no regional lymphadenopathy.

CLOSE summary is given in Table 43.1.

Case 2

An 84-year-old male noticed a right upper eyelid lump progressively increasing in size over 6 months. Examination revealed a nodular mass involving the eyelid margin with variable pigmentation (Fig. 43.2). Regional examination did not reveal any lymph node enlargement.

CLOSE summary is shown in Table 43.2.

Differential Diagnosis

- Benign: chalazion, sebaceous cyst, lipoma, pyogenic granuloma (Case 2)

S. Amrith (✉) · S. M. Young · G. Sundar
Department of Ophthalmology, National University Hospital, Singapore

Department of Ophthalmology, Yong Loo Lin School of Medicine, National University of Singapore, Singapore
e-mail: shantha_amrith@nuhs.edu.sg; stephanie.young@nuhs.edu.sg; gangadhara_sundar@nuhs.edu.sg

P. S. Goh
Department of Diagnostic Radiology, National University Hospital, Singapore

Department of Diagnostic Imaging, Yong Loo Lin School of Medicine, National University of Singapore, Singapore

B. Wu
Department of Pathology, National University Hospital, Singapore

M. E. Nga
Department of Pathology, National University Hospital, Singapore

Department of Pathology, Yong Loo Lin School of Medicine, National University of Singapore, Singapore

S. Amrith et al. (eds.), *Ocular Adnexal Lesions*, https://doi.org/10.1007/978-981-13-3798-7_43

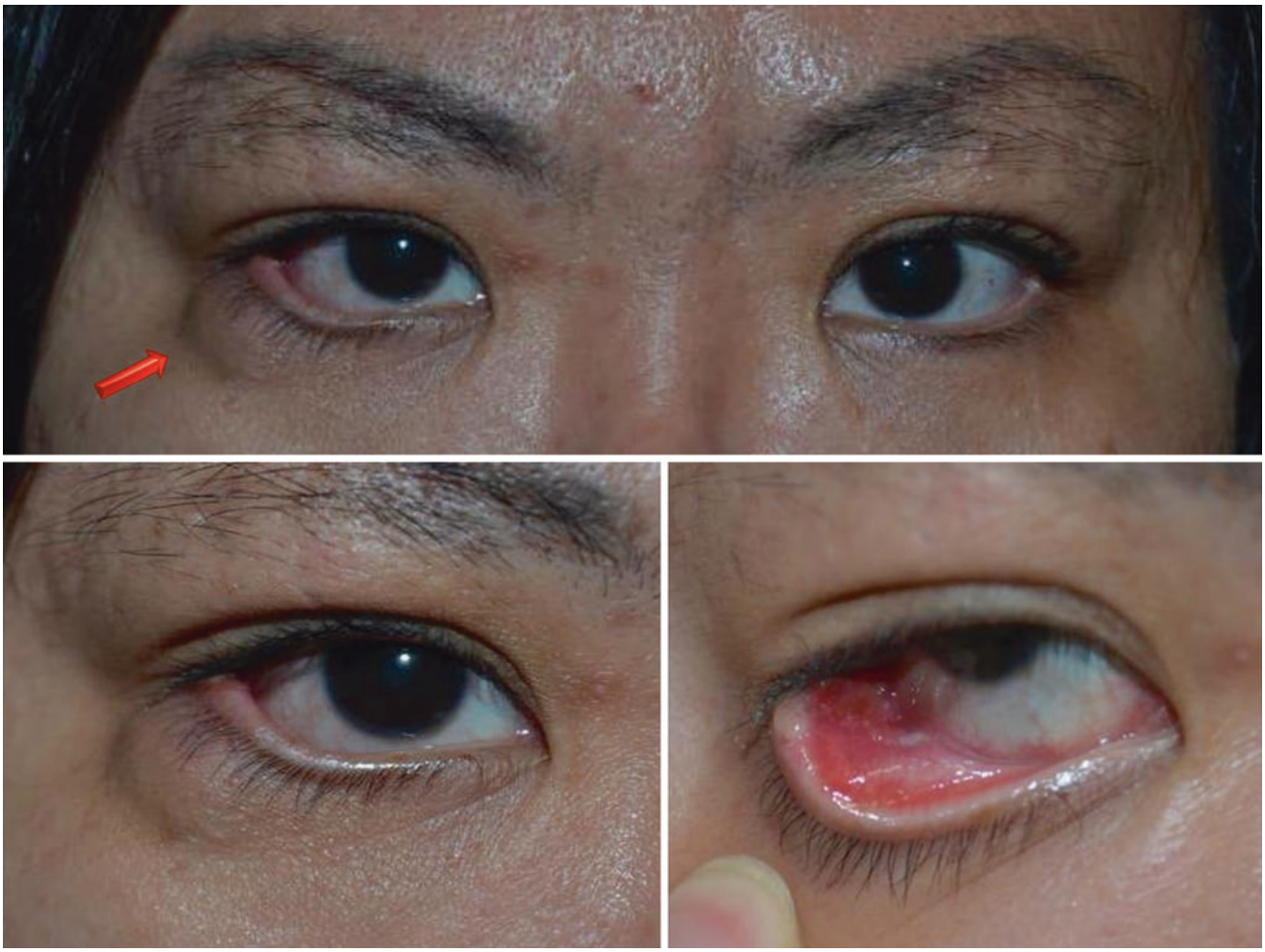

Fig. 43.1 Clinical photograph showing the right lower lid mass with slight thickening of the eyelid margin in case 1

Table 43.1 CLOSE summary for case 1

*C*linical process: well circumscribed mass lesion
*L*ocation: right lateral lower lid
*O*nset: subacute
*S*igns and symptoms: swelling and discharge
*E*pidemiology: young Asian female

- Malignant: sebaceous gland carcinoma, squamous cell carcinoma, basal cell carcinoma, mucinous carcinoma, and Merkel cell carcinoma

Intervention

In case 1, incision and curettage was attempted, but an incisional biopsy was performed instead, as the lesion appeared solid unlike a typical chalazion. The histopathology was reported as sebaceous gland carcinoma. CT scan ruled out orbital involvement. In Case 2, an excision biopsy under frozen section control was performed, followed by primary reconstruction. The frozen section of the tumour was reported as sebaceous gland carcinoma.

TNM staging for both patients: T2b, N0, M0.

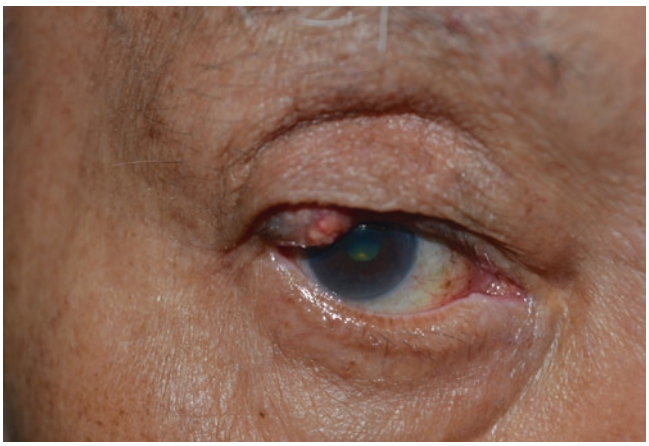

Fig. 43.2 The clinical picture shows a tumefactive lesion in the right upper lid margin in Case 2

Table 43.2 CLOSE summary for case 2

*C*linical process: nodular lesion
*L*ocation: right upper lid margin
*O*nset: subacute
*S*igns and symptoms: progressively enlarging painless eyelid lump
*E*pidemiology: elderly Chinese male

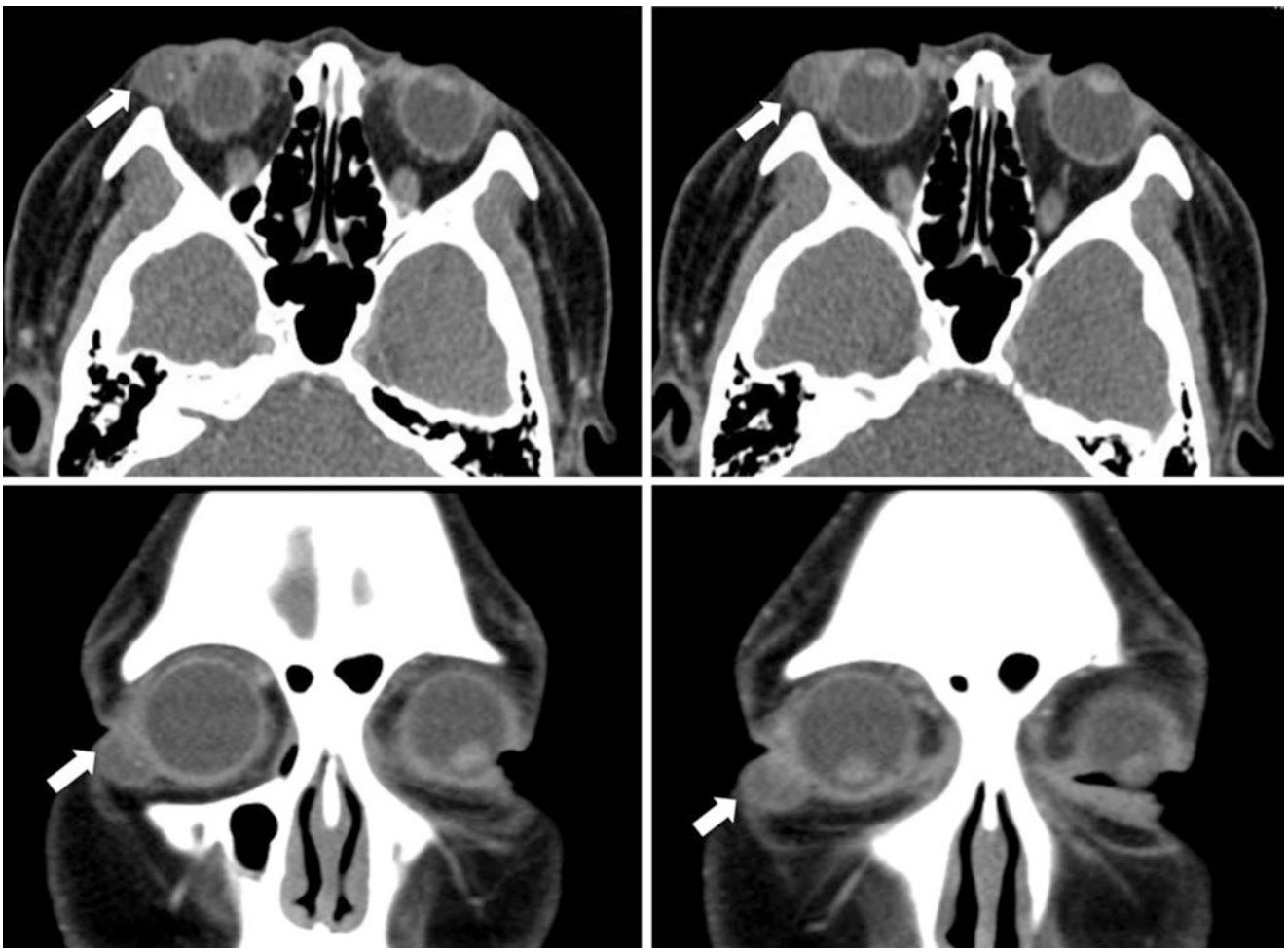

Fig. 43.3 Axial (above) and coronal (below) contrast-enhanced CT scans of the orbits showing the mass (arrows) in the anterolateral preseptal/eyelid region abutting the globe. It is centrally hypodense, indicating a cystic component

Imaging

Contrast-enhanced CT (case 1) showed a focal, heterogeneous, soft tissue mass with a focus of calcification and cystic component in the right lower eyelid. The mass was seen abutting the right globe, and no involvement of adjacent bone or muscle was noted (Fig. 43.3).

Management

Case 1 was evaluated by an oncologist for systemic metastasis, and a subsequent colonoscopy revealed no abnormality, ruling out the possibility of Muir-Torre syndrome.

A wide surgical excision of the right lower lid was performed under frozen section control, along with conjunctival map biopsy and reconstruction. Tissues were sent fresh for histopathology. The posterior lamellar reconstruction was carried out using Hughes tarsoconjunctival flap from the upper lid and a periosteal flap from lateral orbital rim. The skin was advanced to cover the flaps anteriorly. The postoperative period was uneventful and the Hughes flap was divided after 4 weeks.

Case 2: Map biopsies of the conjunctiva were performed. The margins and the conjunctival map biopsies were free of tumour. The posterior lamella was reconstructed with a free tarsoconjunctival graft from the contralateral upper eyelid and the anterior lamella reconstructed with a sliding skin flap.

Histology

Histology of both specimens showed similar findings. A lobulated, well-defined solid cystic tumour was seen within the eyelid. Several areas exhibited cells with pale eosinophilic cytoplasm and prominent intracytoplasmic vacuoles (Fig. 43.4). Frozen sections of the tumour showed positive staining of these intracytoplasmic vacuoles with Oil Red O (Fig. 43.5). The tumour cells featured pleomorphic nuclei with increased nuclear-cytoplasmic ratios. Frequent mitoses with atypical forms were seen.

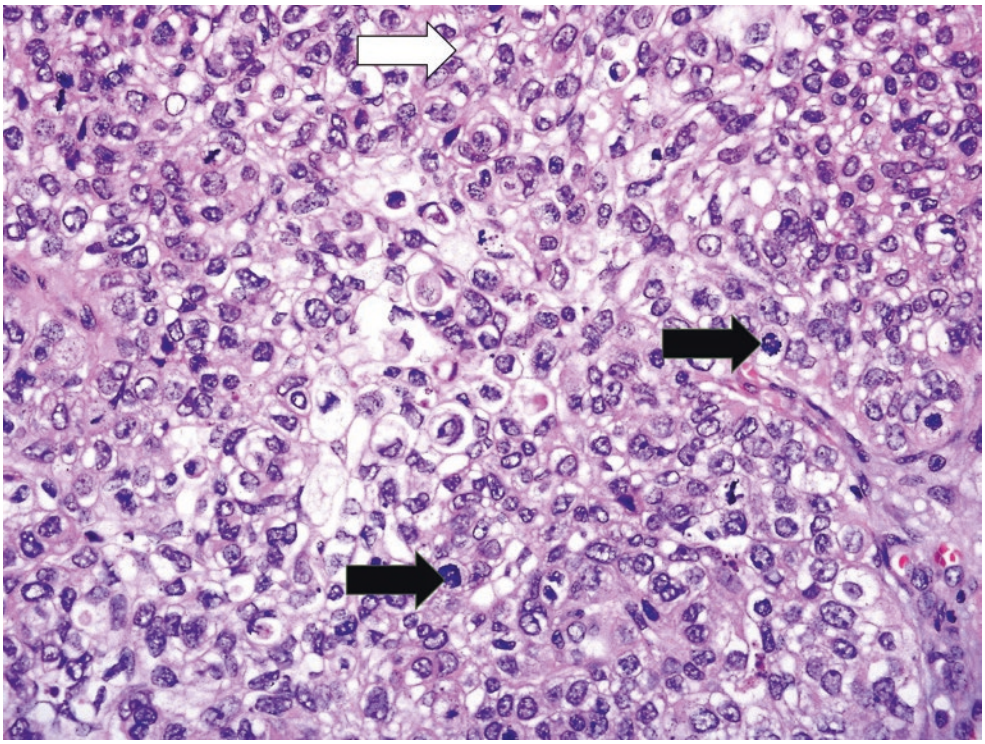

Fig. 43.4 The tumour cells exhibit pale eosinophilic cytoplasm and prominent intracytoplasmic vacuoles (white arrow). The tumour cells also display pleomorphic nuclei with increased nuclear-cytoplasmic ratios and frequent mitoses (black arrow). HE stain; 400× magnification

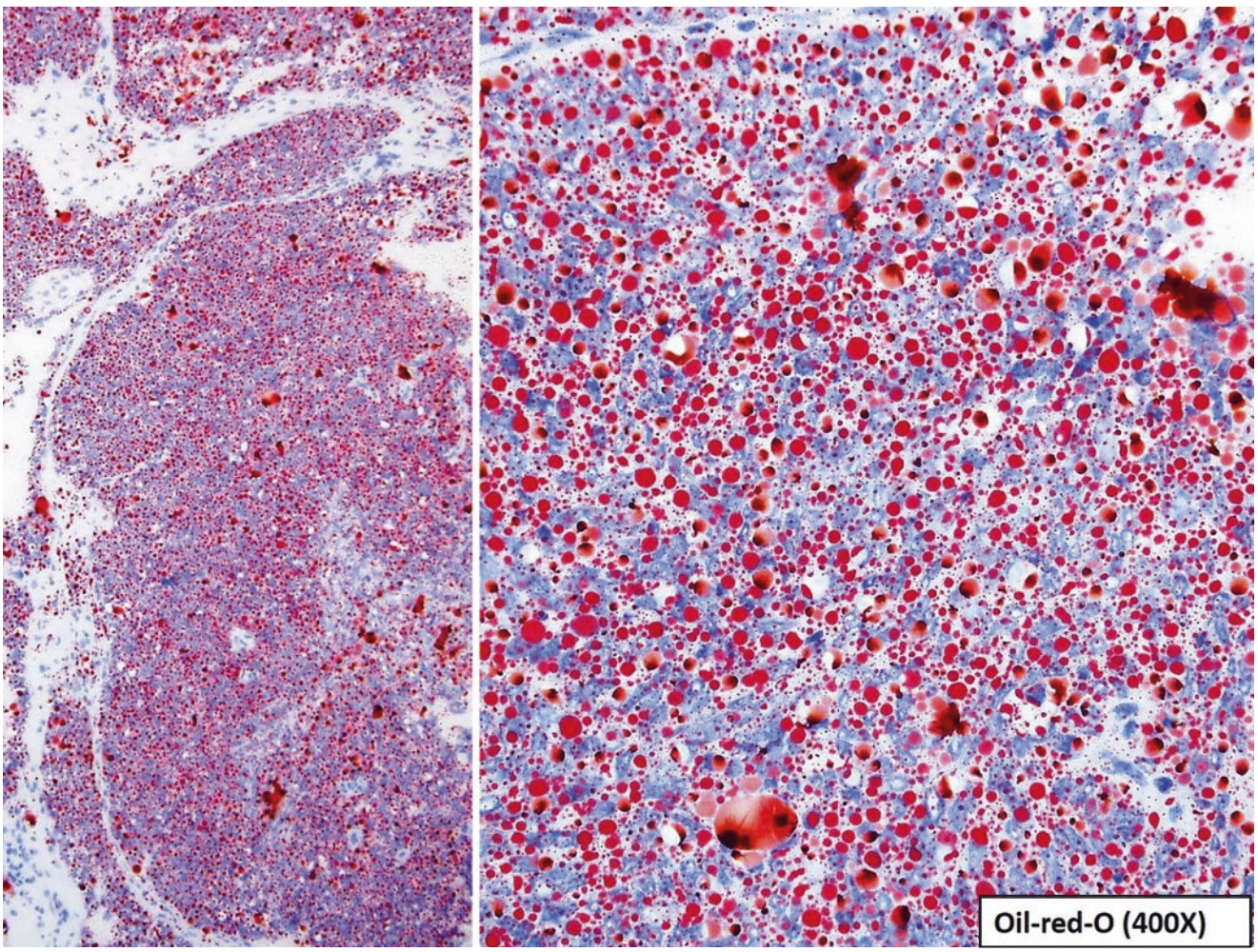

Fig. 43.5 Frozen section of the tumour demonstrates lipid material showing Oil Red O positivity within the cytoplasmic vacuoles. Oil Red O stain; 100× magnification (left) and 400× magnification (right)

Discussion

Sebaceous gland carcinoma (SGC) is called meibomian gland carcinoma when it arises from the tarsal glands of the eyelid. It is sometimes associated with Muir-Torre syndrome, a rare autosomal dominant non-polyposis colorectal carcinoma, sebaceous gland tumours and other visceral carcinomas.

Pathophysiology: The tumour can have multifocal origin and tends to spread in a pagetoid fashion unlike basal cell and squamous cell carcinomas which spread in a radial fashion. It can also present as epithelial dysplasia or carcinoma in situ. Occasionally, there are bizarre and atypical tripolar mitotic cells. No expression of p53 suggests dysplasia; on the other hand over-expression of p53 suggests invasiveness.

Immunohistopathology: Cells occur in irregular lobular masses with distinctive pale foamy vacuolated cytoplasm and hyperchromatic nuclei. Cells stain positive with lipid stain such as Oil Red O. Adipophilin immunohistochemical stain is a relatively new ancillary test that helps to confirm the presence of sebaceous differentiation. It can be performed on formalin fixed tissue, unlike the Oil Red O stain, which can only be performed on fresh tissue. Hence, if Adipophilin is available, there is no need to send fresh tissue samples for histology in suspected cases of sebaceous carcinoma. A discussion with the pathologist prior to biopsy or surgical excision is advisable.

Clinically, there are two forms, nodular and pagetoid types.

Nodular form is a discrete, hard, immobile nodule with yellowish appearance due to lipid content. Any chalazion of unusual consistency or with recurrence after incision and curettage >3 times should undergo full-thickness resection and histological examination to rule out SGC.

The pagetoid form presents with diffuse intraepithelial infiltration of the eyelid skin with thickening of the lid margin and madarosis. It may resemble chronic blepharoconjunctivitis and may spread to involve both eyelids and conjunctival epithelium.

Apart from local spread to the conjunctiva, the tumour may infiltrate into the globe, extraocular muscles, orbit, ethmoidal sinuses, the base of skull, and the brain. The lymphatic spread involves the preauricular, submandibular and cervical nodes, and haematologic spread occurs to the lungs and liver.

Treatment depends on tumour stage at the time of presentation. When the disease is localised, wide local excision with adequate margins and map biopsy for multicentric tumour or conjunctival spread are necessary. Cryotherapy by double freeze-thaw technique to the residual bed may be indicated. Additional brachytherapy may also be indicated for residual local disease. Orbital exenteration with radical neck resection followed by radiation and chemotherapy are necessary in extensive local disease with lymph node involvement. Moh's micrographic technique may be employed to conserve maximum tissue for reconstruction.

Poor prognostic factors are:

- Involvement of upper eyelid or both eyelids
- Tumour size ≥10 mm
- Duration of symptoms >6 months
- Poorly differentiated tumours
- Vascular/lymphatic infiltration
- Orbital extension
- Multicentric origin
- Pagetoid spread

Overall mortality rate is 5–10%. Metastatic disease occurs in about 14–25% of cases. Five-year mortality in metastatic disease is 50–60%.

Learning Points

SGC presents a challenging diagnosis for both clinicians and pathologists. It is an aggressive tumour with a high rate of recurrence and metastasis. The diagnosis is often missed due to masquerades such as recurrent chalazion and blepharoconjunctivitis. Any unilateral blepharoconjunctivitis with loss of eyelashes and thickening of lid margin that fails to respond to treatment should be biopsied, and so should an atypical or recurrent chalazion. Early diagnosis and timely management can help reduce morbidity and mortality. Map biopsies are necessary as the tumour is notorious for pagetoid spread.

Further Reading

1. Buitrago W, Review JAK. Sebaceous carcinoma: the great masquerader: emerging concepts in diagnosis and treatment. Dermatol Ther. 2008;21(6):459–66.
2. Condon GP, Brownstein S, Codere F. Sebaceous carcinoma of the eyelid masquerading as superior limbic keratoconjunctivitis. Arch Ophthalmol. 1985;103(10):1525–9.
3. Foster CS, Allansmith MR. Chronic unilateral belpharoconjunctivitis caused by sebaceous carcinoma. Am J Ophthalmol. 1978;86:218–20.
4. Levitt SH, Bogardus CR, Brandt EN. Complications and late changes following radiation therapy for carcinoma of the eyelid and canthi. Radiology. 1966;87:340–7.
5. Mashburn MA, Chonkich GD, Chase DR. Meibomian gland adenocarcinoma of the eyelid with preauricular lymph node metastasis. Laryngoscope. 1985;95:1441–3.
6. Rao NA, Hidayat AA, Mclean IW, et al. Sebaceous carcinomas of the ocular adnexa: A clinico-pathological study of 104 cases, with five year follow up date. Hum Pathol. 1982;13:113–22.
7. Russell WG, Page DL, Hough AJ, et al. Sebaceous carcinoma of the eyelid. Errors in clinical and pathological diagnosis. Am J Surg Pathol. 1984;8:597–606.
8. Shields JA, Demirci H, Marr BP, et al. Sebaceous carcinoma of the eyelids: personal experience with 60 cases. Ophthalmology. 2004;111(12):2151–7.
9. Shields JA, Demirci H, Marr BP, Eagle RC Jr, Shields CL. Sebaceous carcinoma of the ocular region: a review. Surv Ophthalmol. 2005;50:103–22.
10. Upender KW, Abdullah A. Sebaceous gland carcinoma of the eyelid. Oman J Ophthalmol. 2010;3(3):117–21.

Merkel Cell Carcinoma

44

Gangadhara Sundar, Stephanie Ming Young, Eric Ting, Bingcheng Wu, Min En Nga, and Shantha Amrith

Introduction

Merkel cell tumours are rare neoplasms of the skin with about half of them presenting in the head and neck region. They were once thought to arise from the dendritic (neuroendocrine) cells of the skin which serve as mechanoreceptors. They often present as painless, erythematous nodules with less than 10% arising in the ocular adnexa, especially in the upper eyelid, and are frequently missed. With local recurrences and regional and systemic spread, they have an estimated 5-year survival of less than 40%.

Case Scenario

A 60-year-old Southeast Asian male presented with a recurrent lump of the left lower eyelid of more than 6 months' duration. He reported having undergone multiple surgeries for 'chalazion' with recurrences. While he was healthy otherwise, he had noted a recent onset fullness of the left cheek area prior to presentation. There were no other skin lesions in the face or the rest of the body. Ophthalmic examination was unremarkable on the right side. On the left, he had multiple erythematous nodules of the inferior tarsal and palpebral conjunctiva with bulbar conjunctival injection (Fig. 44.1). The lid margin appeared intact without loss of eyelashes.

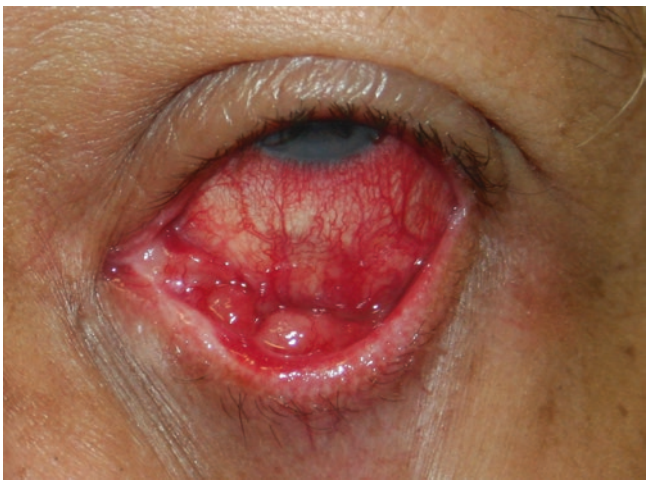

Fig. 44.1 Clinical picture showing multiple inferior palpebral conjunctival nodules and conjunctival injection in the left eye

G. Sundar · S. M. Young · S. Amrith (✉)
Department of Ophthalmology, National University Hospital, Singapore

Department of Ophthalmology, Yong Loo Lin School of Medicine, National University of Singapore, Singapore
e-mail: gangadhara_sundar@nuhs.edu.sg; stephanie.young@nuhs.edu.sg; shantha_amrith@nuhs.edu.sg

E. Ting
Department of Diagnostic Imaging, National University Hospital, Singapore

Department of Diagnostic Imaging, Yong Loo Lin School of Medicine, National University of Singapore, Singapore

Advanced Medicine Imaging, Singapore

B. Wu
Department of Pathology, National University Hospital, Singapore

M. E. Nga
Department of Pathology, National University Hospital, Singapore

Department of Pathology, Yong Loo Lin School of Medicine, National University of Singapore, Singapore

S. Amrith et al. (eds.), *Ocular Adnexal Lesions*, https://doi.org/10.1007/978-981-13-3798-7_44

There was no proptosis, and he had a full range of ocular motility. The rest of the anterior segment and fundus examination were unremarkable. Regional examination revealed ipsilateral non-tender preauricular and cervical lymphadenopathy. Systemic examination was unremarkable.

CLOSE summary is given in Table 44.1.

Differential Diagnosis

- Recurrent chalazia
- Conjunctival granuloma
- Sebaceous gland carcinoma
- Squamous cell carcinoma
- Lymphoma – less likely
- Metastasis

Table 44.1 CLOSE summary

*C*linical process: infiltrative, inflammatory mass lesion
*L*ocation: left Inferior tarsal and palpebral conjunctiva
*O*nset: chronic
*S*ymptoms and signs: painless mass lesion with injection of the conjunctiva with regional lymphadenopathy
*E*pidemiology: elderly Southeast Asian male

Intervention

The patient underwent an outpatient incisional biopsy of the left lower conjunctival lesions under local anaesthesia. Specimens were sent fresh for histopathology and additional tests as indicated.

Histopathology

Sections showed infiltrative nests and cords of malignant cells with high nuclear/cytoplasmic ratios, scant cytoplasm and stippled chromatin (Fig. 44.2). Mitotic activity and apoptotic bodies were prominent. Immunohistochemistry showed the tumour cells to be positive for cytokeratin AE1/AE3 pan cytokeratin, as well as NSE, and CD56.

Additional Investigations

The patient underwent MRI of the head and neck region with gadolinium which revealed minor increased soft tissue and hazy enhancement in the region of the left medial canthus. There was no extension to the post-septal orbit. The lacrimal glands were unremarkable.

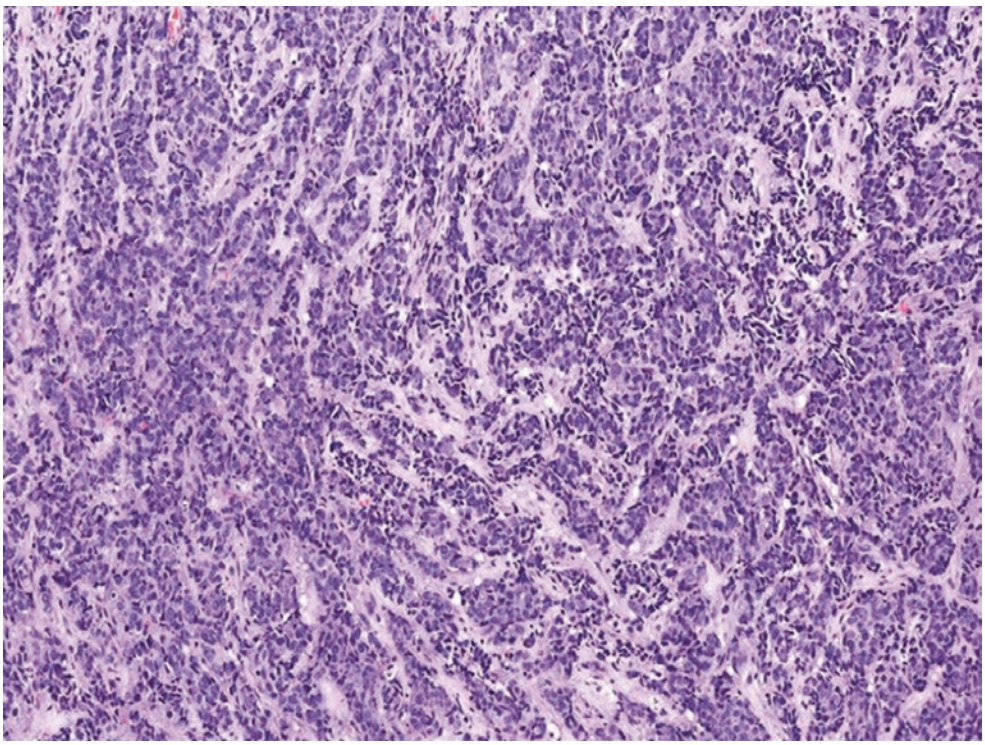

Fig. 44.2 Section showing infiltrative nests and cords of malignant cells with high nuclear/cytoplasmic ratios and scant cytoplasm. HE stain, 200× magnification

The left parotid and submandibular glands appeared bulky, with enlarged intra-parotid lymph nodes seen inferiorly. Heterogeneously enhancing, conglomerate left-sided nodal mass involving level II, III, IV and V lymph nodes (Fig. 44.3) was also seen.

He subsequently underwent a PET-CT scan which revealed FDG-avid skin thickening of the left inferior eyelid and multiple FDG-avid nodes in the neck, thorax and abdomen suspicious of widespread nodal metastasis. Multiple FDG-avid lesions in liver and bones were also suspicious of metastasis (Fig. 44.4).

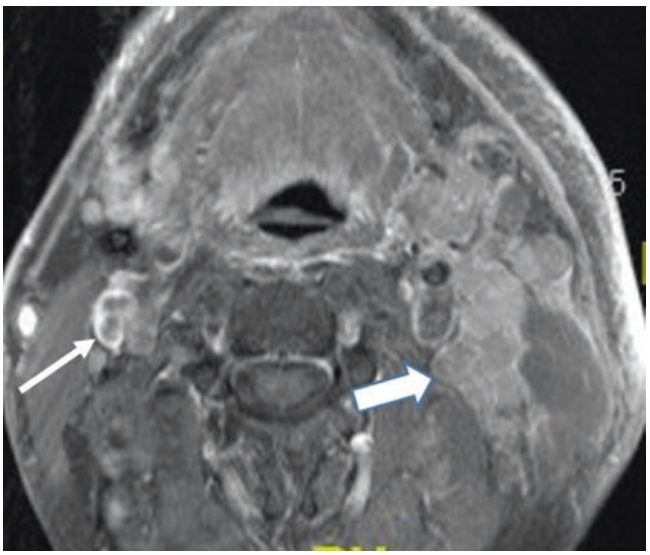

Fig. 44.3 T1w FS + C image showing enlarged, matted cervical lymph nodes (block arrow) on the left associated with thickening of the overlying skin and subcutaneous tissues. There are also abnormal necrotic lymph nodes on the right (arrow)

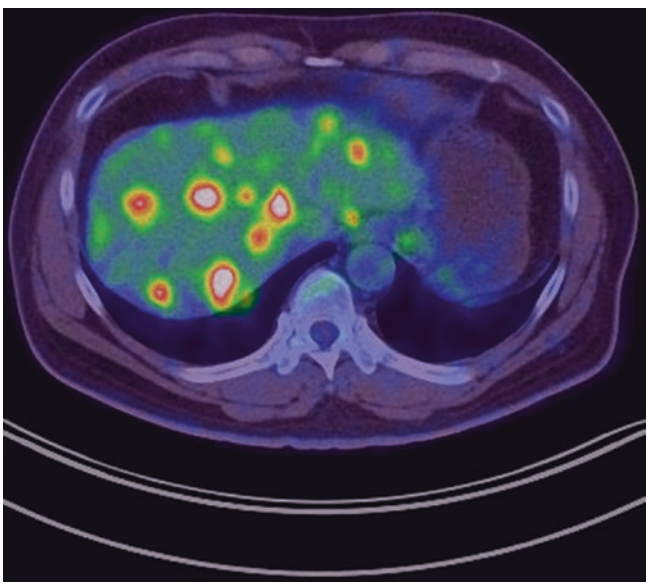

Fig. 44.4 FDG PET-CT fused image shows diffuse liver metastases

Final Diagnosis

Merkel cell carcinoma – poorly differentiated, Stage IV, T1 N3 M1.

Management

Given the late stage of the disease, he underwent palliative systemic chemotherapy with radiation to the cervical region and succumbed to the disease 9 months later.

Discussion

Although Merkel cell carcinoma was initially thought to arise from mechanoreceptors, it is now thought to arise from proliferation of dermal pluripotent stem cells of neural crest origin without mechanoreceptor function but with similar characteristics as Merkel cells. It is also strongly associated with the polyoma virus with higher risk in patients with ultraviolet exposure and immunocompromised status. Atypical findings in this patient include appearance in the conjunctiva, sparing the anterior eyelid and preserved eyelashes. Typical histopathological findings include poorly defined groupings of small cells in the dermis and subcutaneous tissue with scant cytoplasm, finely dispersed chromatin (salt and pepper appearance), and characteristic cytoplasmic granules on electron microscopy. Positive immunohistochemical staining for neurofilament protein, cytokeratin 20 and neuron-specific enolase with the absence of leukocyte common antigen, and S-100 is highly suggestive of the disease.

A high degree of suspicion for atypical pathology and atypical presentation of chalazia including location and recurrence of conjunctival nodules should be present in all patients with this rare malignancy. Ideal management includes early and accurate diagnosis, complete local excision and sentinel lymph node biopsy wherever possible, with close monitoring for regional spread. Regional lymph node dissection and parotidectomy, with and without radiation, should be considered in selected patients.

Learning Points

High suspicion of atypical conjunctival and eyelid lesions for malignancy should be maintained, especially when lesions are recurrent. All such recurrent and atypical lesions should be routinely sent for histopathological examination. Merkel cell carcinoma is a highly aggressive ocular adnexal and cutaneous neoplasm and when inadequately and poorly managed often develops regional and systemic spread with guarded prognosis for life.

Further Reading

1. Merritt H, Sniegowski MC, Esmaeli B. Merkel cell carcinoma of the eyelid and periocular region. Cancers. 2014;6:1128–37.
2. Peters GB III, Meyer DR, Shields JA, et al. Management and prognosis of Merkel cell carcinoma of the eyelid. Ophthalmology. 2001;108(9):1575–9.
3. Shah JM, Sundar G, Tan KB, Zee YK. Unusual Merkel cell carcinoma of the eyelid. Orbit. 2012;31(6):425–7. https://doi.org/10.3109/01676830.2012.689084.

Mucinous Carcinoma

45

Shantha Amrith, Stephanie Ming Young, Poh Sun Goh, Bingcheng Wu, Min En Nga, and Gangadhara Sundar

Introduction

Mucinous carcinoma of the eyelid is a rare neoplasm and most often occurs as a secondary tumour. It is a cutaneous carcinoma arising from the sweat gland and has a predilection for periocular skin. It has a striking morphological and immunophenotypical similarity to ductal carcinoma in situ (DCIS) of the breast. It may rarely occur in patients with colon cancer.

Case Scenario

A 65-year-old Malay male noted a small lump in the right lower eyelid which gradually and slowly enlarged over 2 years. There was no pain or bleeding associated with the mass. He had been examined elsewhere 6 months earlier and advised conservative management.

On examination, there was a lump in the lateral third of his right lower lid which showed ulceration on the surface, loss of eyelashes and lid margin architecture, and a mechanical ectropion (Fig. 45.1). There was no tethering of the eyelid to the globe or the orbital rim. No regional lymphadenopathy was noted. The rest of the ophthalmic examination was within normal limits. There was no palpable regional or systemic lymphadenopathy.

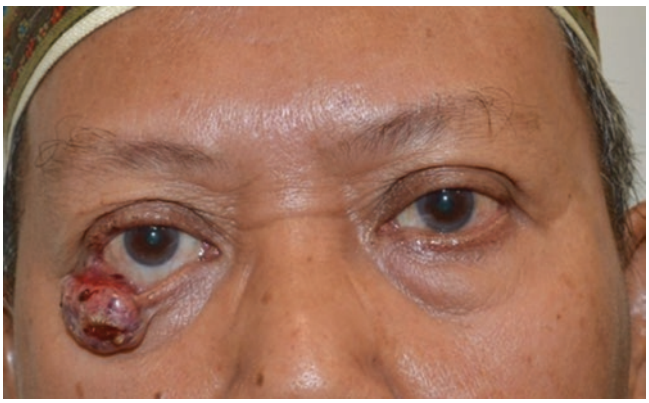

Fig. 45.1 Clinical picture showing the right lower lid lump with mechanical ectropion

CLOSE summary is given in Table 45.1.

S. Amrith (✉) · S. M. Young · G. Sundar
Department of Ophthalmology, National University Hospital, Singapore

Department of Ophthalmology, Yong Loo Lin School of Medicine, National University of Singapore, Singapore
e-mail: shantha_amrith@nuhs.edu.sg; stephanie.young@nuhs.edu.sg; gangadhara_sundar@nuhs.edu.sg

P. S. Goh
Department of Diagnostic Imaging, National University Hospital, Singapore

Department of Diagnostic Imaging, Yong Loo Lin School of Medicine, National University of Singapore, Singapore

B. Wu
Department of Pathology, National University Hospital, Singapore

M. E. Nga
Department of Pathology, National University Hospital, Singapore

Department of Pathology, Yong Loo Lin School of Medicine, National University of Singapore, Singapore

S. Amrith et al. (eds.), *Ocular Adnexal Lesions*, https://doi.org/10.1007/978-981-13-3798-7_45

Differential Diagnosis

- Chalazion/pyogenic granuloma
- Sebaceous gland carcinoma
- Basal cell carcinoma
- Squamous cell carcinoma
- Merkel cell carcinoma
- Sweat gland apocrine or eccrine tumours

Imaging

A uniformly T1 hypointense, T2 hyperintense, avidly enhancing, lobulated, exophytic mass was noted centred at the right lower eyelid (Fig. 45.2). The mass involved pre-septal region with no gross post-septal extension. The right globe, extraocular muscles, orbital fat, and right optic nerve appeared normal.

Intervention

An outpatient incisional biopsy of the lid margin was performed. Histology revealed a diagnosis of mucinous carcinoma of the right lower lid.

Table 45.1 CLOSE summary

*C*linical process: mass effect, infiltrative
*L*ocation: right lower eyelid
*O*nset: chronic
*S*igns and symptoms: right lower lid lump with ulceration on the surface, and ectropion
*E*pidemiology: elderly Malay male

Further investigations: PET-CT scan was carried out which showed FDG avid right lower lid lesion and no other significant regional or systemic involvement. TNM staging: T2bN0M0.

Management

Patient underwent excision of the tumour under frozen section control under local anaesthesia. The posterior lamella was reconstructed with a periosteal flap from the lateral orbital rim and the anterior flap with Tenzel advancement flap. The specimen was sent for histopathology, and the patient was referred to the oncologist for further screening and follow-up.

Histopathology

Gross examination of the specimen revealed a nodular lesion with gelatinous/mucoid cut surface. The lobulated tumour was composed of pools of mucin containing free-lying clusters of tumour cells with focal glandular differentiation (Fig. 45.3). The tumour cells had mildly pleomorphic vesicular nuclei and eosinophilic cytoplasm. Scattered mitotic figures, as well as occasional psammomatous type of calcifications, were seen without any dysplastic changes in the overlying stratified squamous epithelium. The tumour was seen invading the underlying fibroadipose tissue and skeletal muscle. The features were consistent with the diagnosis of mucinous carcinoma.

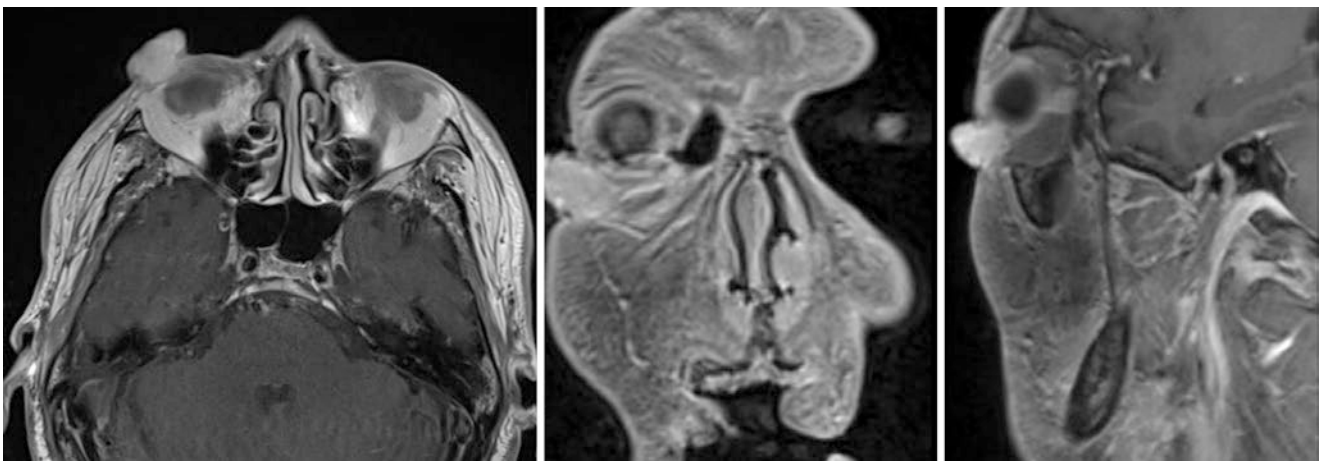

Fig. 45.2 Contrast-enhanced T1w (fat suppressed) images (from the left – axial, coronal, and sagittal) showing exophytic-enhancing bulky lid mass, abutting the anterior globe

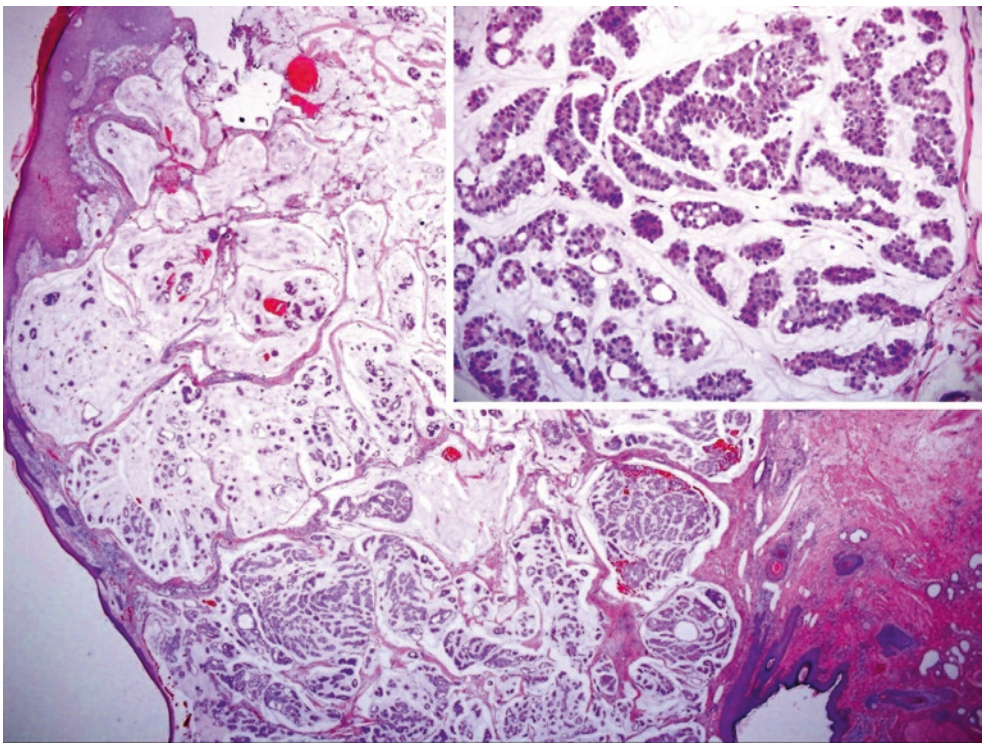

Fig. 45.3 Histopathology shows a lobulated tumour composed of pools of mucin containing free-lying clusters of tumour cells. Gland formation is seen within the clusters of tumour cells. Main: HE stain; 20× magnification. Inset: HE stain; 100× magnification

Discussion

Mucinous carcinomas or eccrine sweat gland carcinomas affect people in their fifth to eighth decades. There is no race predilection, but genetics may play a role in the development of these tumours (TP53 alterations). The rate of metastasis tends to be high in these tumours.

The classification of eccrine carcinomas is complex. They can broadly be classified as those arising de novo from the normal skin and those arising from pre-existing benign sweat gland tumours. Precise diagnosis with histology is important for therapy and prognosis. Malignant eccrine tumours can present both as slow-growing tumours as well as rapidly growing ones. No specific guidelines exist for investigations due to rarity of these tumours.

Histologically, the distinction between benign and malignant eccrine lesions is made based on the extent of invasion and nuclear atypia. Sometimes, they appear as a poorly differentiated adenocarcinoma.

Recurrences after surgical excision are quite common. Mohs micrographic surgery appears to be the choice for removal of eccrine carcinomas as it seems to have the lowest recurrence rates. Radiation therapy has been used in selected cases. Chemotherapy has not been used, presumably due to lack of response.

Further Reading

1. Dhaliwal CA, Torgersen A, Ross JJ, Ironside JW, Biswas A. Endocrine mucin-producing sweat gland carcinoma: report of two cases of an under-recognized malignant neoplasm and review of the literature. Am J Dermatopathol. 2013;35(1):117–24.
2. Hoguet A, Warrow D, Milite J, McCormick SA, Maher E, Della Rocca R, Della Rocca D, Goldbaum A, Milman T. Mucin-producing sweat gland carcinoma of the eyelid: diagnostic and prognostic considerations. Am J Ophthalmol. 2013;155(3):585–92.
3. Koike T, Mikami T, Maegawa J, Iwai T, Wada H, Yamanaka S. Recurrent endocrine mucin producing sweat gland carcinoma in the eyelid. Aust J Dermatol. 2013;54(2):e46–9.

Liposarcoma

46

Shantha Amrith, Stephanie Ming Young, Eric Ting, Bingcheng Wu, Min En Nga, and Gangadhara Sundar

Introduction

The development of a liposarcoma from a preexisting benign lipoma is rare. Liposarcoma of the ocular adnexa frequently arises from deep-seated stroma rather than the submucosal or subcutaneous fat. Worldwide annual incidence of this tumour is 2.5 cases per million population. This accounts for approximately 17% of all soft tissue sarcomas and 3% of all tumours in the head and neck region. Liposarcomas are slightly more common in males than females. Mean patient age at onset is 50 years. The lungs and the liver are the most common sites of metastases. Primary cutaneous liposarcoma has an indolent course. These tumours very rarely occur in the eyelids.

Case Scenario

A 68-year-old Chinese man with a blind left eye from advanced diabetic retinopathy, presented with a left lower eyelid mass (Fig. 46.1) of 5 years' duration. The mass which had been growing gradually, showed a rapid growth in the last 2 months. The mass was not associated with pain and redness, and there was no increase in size on straining.

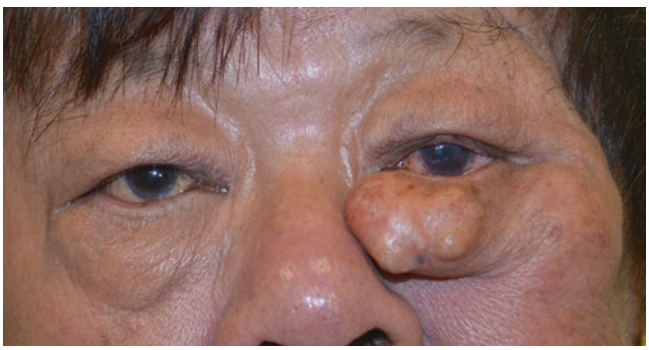

Fig. 46.1 Shows the left lower lid mass with yellowish discolouration on the skin

On examination, he had no perception of light in the left eye. There was corneal neovascularisation and opacification precluding visualisation of the anterior chamber or fundus. There was a large soft boggy multilobulated lesion in the left lower eyelid with yellowish discolouration of the overlying skin (Fig. 46.1). On palpation, the medial part of the mass was soft, but temporal part was firm to hard in consistency. The lesion was mobile, not tethered to the underlying bone, and not involving the lid margin. It was

S. Amrith (✉) · S. M. Young · G. Sundar
Department of Ophthalmology, National University Hospital, Singapore

Department of Ophthalmology, Yong Loo Lin School of Medicine, National University of Singapore, Singapore
e-mail: shantha_amrith@nuhs.edu.sg; stephanie.young@nuhs.edu.sg; gangadhara_sundar@nuhs.edu.sg

E. Ting
Department of Diagnostic Imaging, National University Hospital, Singapore

Department of Diagnostic Imaging, Yong Loo Lin School of Medicine, National University of Singapore, Singapore

Advanced Medicine Imaging, Singapore

B. Wu
Department of Pathology, National University Hospital, Singapore

M. E. Nga
Department of Pathology, National University Hospital, Singapore

Department of Pathology, Yong Loo Lin School of Medicine, National University of Singapore, Singapore

S. Amrith et al. (eds.), *Ocular Adnexal Lesions*, https://doi.org/10.1007/978-981-13-3798-7_46

Table 46.1 CLOSE summary

*C*linical process: mass effect
*L*ocation: left lower eyelid
*O*nset: chronic
*S*igns and Symptoms: left lower eyelid mass with mechanical ectropion
*E*pidemiology: elderly Chinese male

non-tender, non-reducible, non-pulsatile and Valsalva-negative and causing a left lower eyelid mechanical ectropion.

There were no café-au-lait spots or other nodular masses in the body.

CLOSE summary is described in Table 46.1.

Differential Diagnosis

- Neurofibroma
- Lipoma
- Pleomorphic adenoma
- Liposarcoma

Intervention

As the lesion was superficial, the patient underwent an excision biopsy. Intraoperatively, there were no clear demarcating planes, and the major part of the soft medial mass was removed along with overlying discoloured skin. The mass was noted to have lateral extensions over the cheek and temple, some of which were removed piecemeal (Fig. 46.2). Lower lid reconstruction was carried out with a Tenzel skin flap and a lateral tarsal strip.

Histopathology

The tumour was composed of lobules of adipocytes separated by thin fibrovascular septa. The adipocytes showed moderate variation in cell size. Scattered adipocyte nuclei showed atypia, consisting of nuclear enlargement and hyperchromasia, some with irregular outlines. Focally, there were areas composed of more spindle-shaped cells with nuclear atypia (Fig. 46.3). No necrosis was seen. No high-grade sarcomatous change or heterologous elements were identified.

Fluorescence in situ hybridization (FISH) test showed the tumour to be positive for MDM2 (murine double minute-2) amplification, which in this context is diagnostic of atypical lipomatous tumour/well-differentiated liposarcoma.

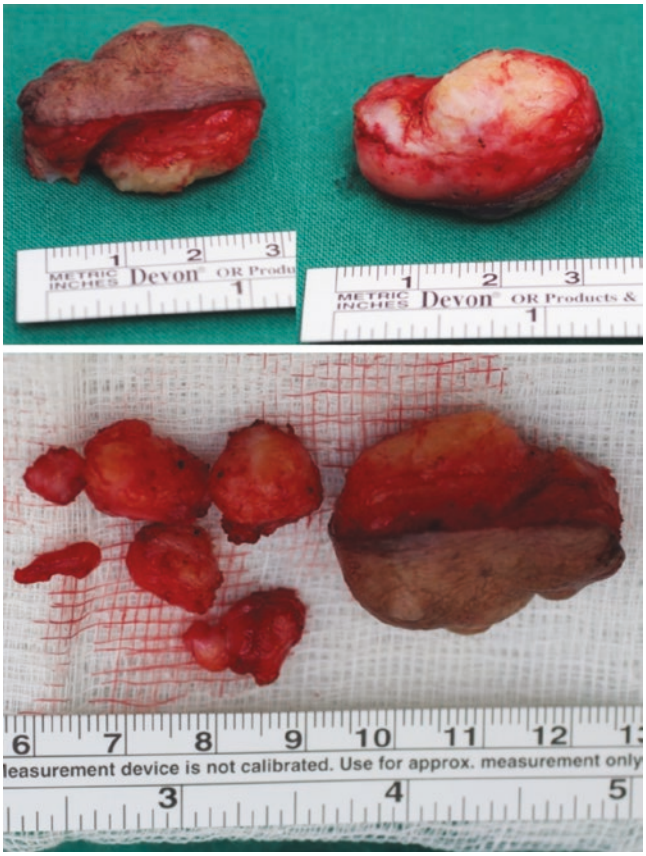

Fig. 46.2 Main mass with skin attached. Multiple subcutaneous pieces from the temporal aspect of the left lower lid

Management

The patient was referred to oncology service for further management of the residual tumour. Although the sarcoma tumour board recommended extended and wide resection, the patient was unwilling initially but underwent conservative tumour removal a year later. Repeat MRI (Fig. 46.4) showed a small residual tumour in the outer aspect of the left lateral canthus which was closely monitored.

Discussion

Liposarcomas arise de novo and appear as slowly enlarging, painless, deep-seated masses in middle-aged persons. Dermal/subcutaneous lesions are rare, and exophytic, and therefore, appear polypoidal, resembling pleomorphic fibroma. As they have minimal tendency to grow deeper into the underlying subcutaneous tissue, they have a better prognosis compared to their deeper counterparts.

They appear as hyperintense lobular lesions in T1- and T2-weighted MRI and show no contrast enhancement.

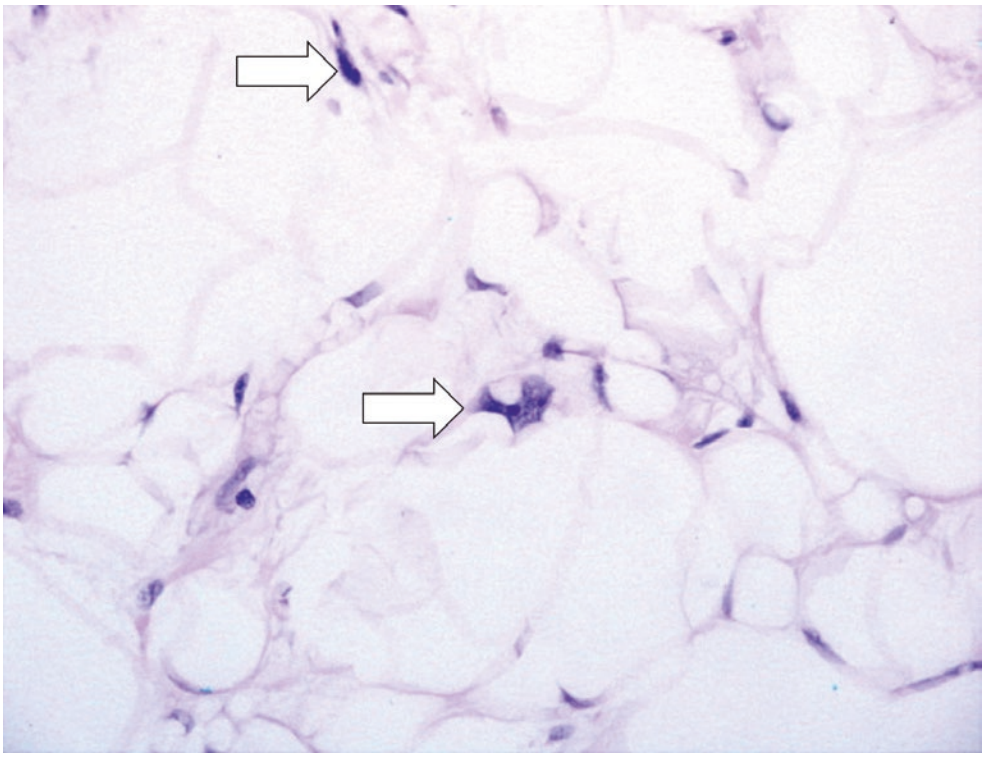

Fig. 46.3 The adipocytic tumour exhibits scattered enlarged, indented and hyperchromatic nuclei with irregular outlines (white arrows). This degree of nuclear atypia is worrisome for atypical lipomatous tumour/well-differentiated liposarcoma. Note the differing sizes of the adipocytes. HE stain; 400× magnification

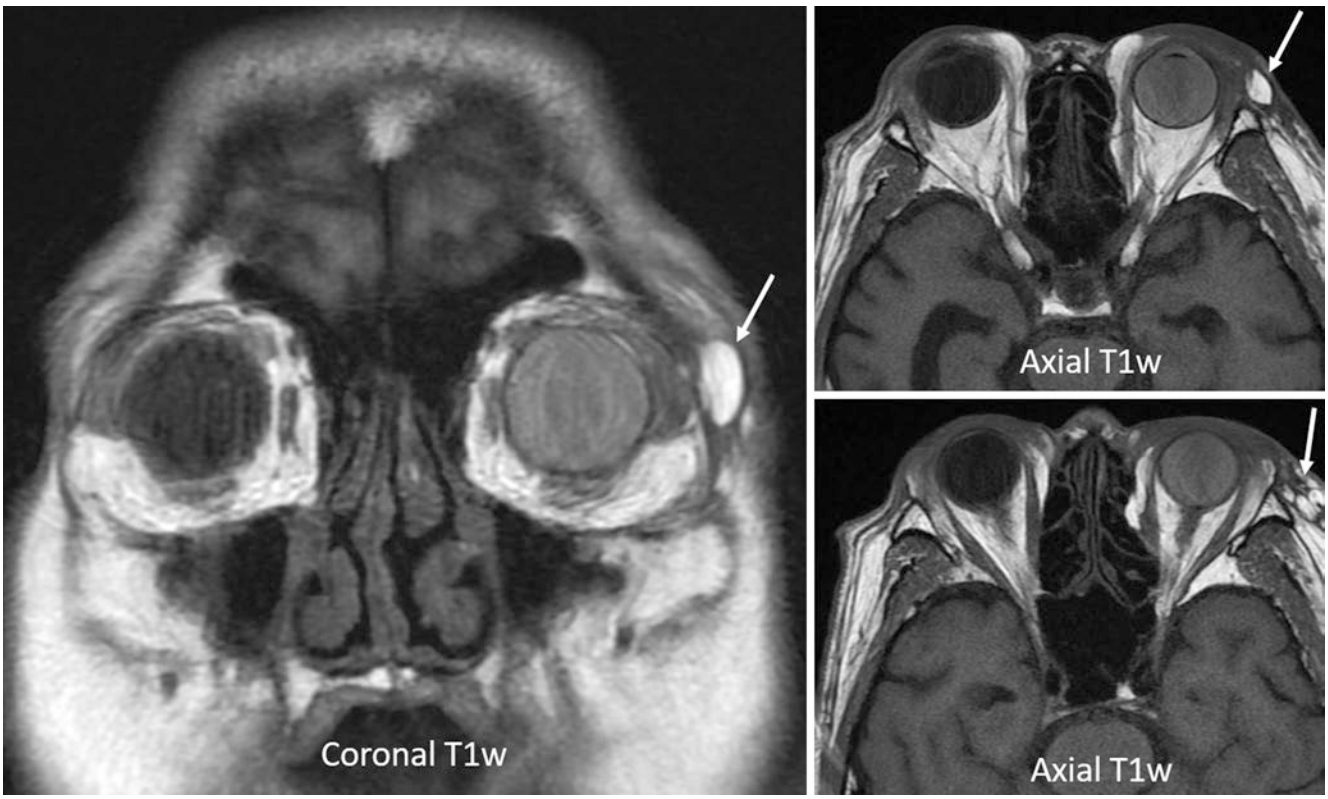

Fig. 46.4 Coronal and axial T1w images showing a multilobulated fat-signal intensity lesion (white arrow). High T1w signal in the left globe is consistent with intraocular haemorrhage related to diabetic retinopathy

MDM2 gene amplification by FISH test seems to be specific for distinguishing a well-differentiated liposarcoma from benign lipoma and is used in genetic studies to classify tumours and determine prognosis.

Mainstay of treatment is surgery. Principal determinant of survival is the histological type, with 100% survival in well-differentiated tumours. It has been found that survival is better in patients who had surgery alone, compared to surgery and radiotherapy. The tumours are usually not chemosensitive. Local recurrences are common after surgical removal. Adjuvant radiotherapy is advised only in high-grade tumours.

Learning Points

Liposarcoma has a very nondramatic presentation and can easily be assumed to be benign on presentation. Cytogenetics helps in distinguishing well-differentiated liposarcoma from a lipoma and may help to determine the prognosis. Surgery is the mainstay of treatment, and liposarcomas are generally chemoresistant and only mildly radiosensitive.

Cutaneous and subcutaneous liposarcomas have a more favourable outcome compared with their deep-seated counterparts.

Further Reading

1. Dantey K, Schoedel K, Yergiyev O, Bartlett D, Rao UNM. Correlation of histological grade of dedifferentiation with clinical outcome in 55 patients with dedifferentiated liposarcomas. Hum Pathol. 2017;66:86–92.
2. de Bree E, Karatzanis A, Hunt JL, Strojan P, Rinaldo A, Takes RP, Ferlito A, de Bree R. Lipomatous tumours of the head and neck: a spectrum of biological behaviour. Eur Arch Otorhinolaryngol. 2015;272(5):1061–77.
3. Gerry D, Fox NF, Spruill LS, Lentsch EJ. Liposarcoma of the head and neck: analysis of 318 cases with comparison to non-head and neck sites. Head Neck. 2014;36(3):393–400.
4. Gritli S, Khamassi K, Lachkhem A, Touati S, Chorfa A, Ben Makhlouf T, El May A, Gammoudi A. Head and neck liposarcomas: a 32 years experience. Auris Nasus Larynx. 2010;37(3):347–51.
5. Hailu Y, Schneider J, AT T/G, Bayu S, Adamu Y. Liposarcoma presenting as a recurrent eyelid tumour. Ethiop Med J. 2008;46(3):281–5.
6. Pattani KM, Lian TS. A unique case of infraorbital myxoid liposarcoma. Ear Nose Throat J. 2010;89(9):466–7.

Melanoma of Ocular Adnexa

47

Gangadhara Sundar, Stephanie Ming Young, Bingcheng Wu, Min En Nga, and Shantha Amrith

Introduction

Tumours of the medial canthus may arise from the skin, subcutaneous tissues, and lacrimal drainage system or rarely as secondary extension from the underlying nasal cavity and paranasal sinuses. Rarely, pigmented neoplasms like melanoma may arise from the conjunctiva, lacrimal sac ocular surface or eyelid and propagate through deep layers of epithelium or via tear film.

Clinical Scenario

A 32-year-old Southeast Asian male, otherwise healthy, presented with a blackish lump over the inner corner of the left eye of a few months duration. He recalled developing a pigmented lesion on the ocular surface a few years earlier for which he had been advised excision but declined. Ophthalmic evaluation revealed good visual acuity in both eyes. Examination of the right eye and adnexa was within normal limits. On the left, he had a pigmented firm mass of the medial canthus abutting the upper and lower eyelids (Fig. 47.1). Examination of the conjunctiva and eyelid margins revealed a pigmented lesion involving the perilimbal bulbar conjunctiva, caruncle, and the forniceal conjunctiva (Fig. 47.2). The rest of the anterior segment and fundus

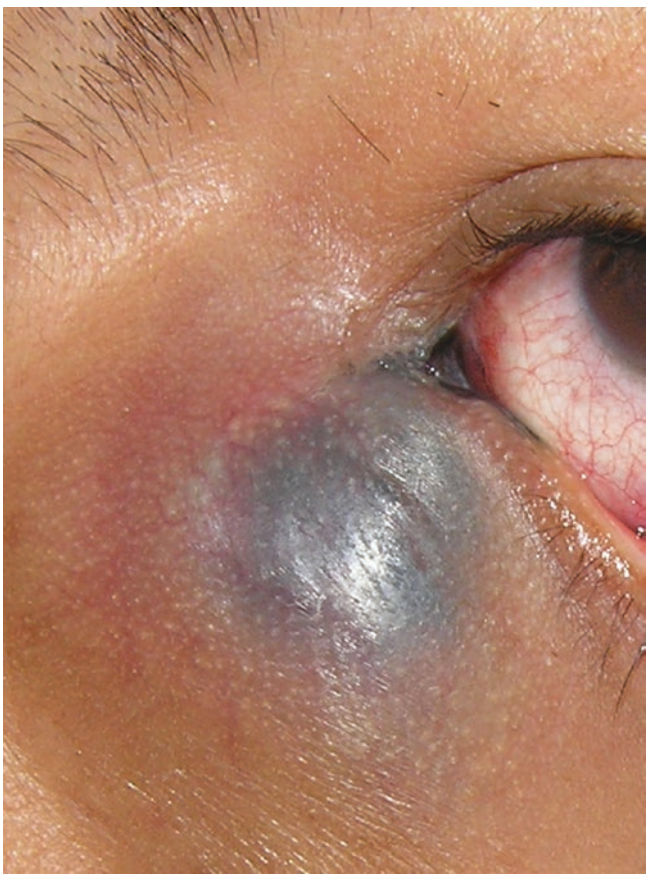

Fig. 47.1 Clinical picture showing the left lacrimal sac mass with blackish discolouration of the overlying skin

G. Sundar · S. M. Young · S. Amrith (✉)
Department of Ophthalmology, National University Hospital, Singapore

Department of Ophthalmology, Yong Loo Lin School of Medicine, National University of Singapore, Singapore
e-mail: gangadhara_sundar@nuhs.edu.sg; stephanie.young@nuhs.edu.sg; shantha_amrith@nuhs.edu.sg

B. Wu
Department of Pathology, National University Hospital, Singapore

M. E. Nga
Department of Pathology, National University Hospital, Singapore

Department of Pathology, Yong Loo Lin School of Medicine, National University of Singapore, Singapore

S. Amrith et al. (eds.), *Ocular Adnexal Lesions*, https://doi.org/10.1007/978-981-13-3798-7_47

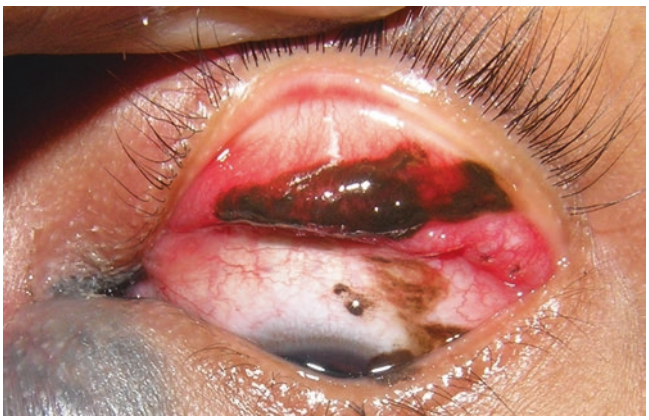

Fig. 47.2 Note the presence of extensive melanotic lesions in the superior palpebral conjunctiva as well as the limbus, bulbar conjunctiva, and caruncle of the left eye

Table 47.1 CLOSE summary

*C*linical process: mass, infiltrative lesion
*L*ocation: left lacrimal sac/drainage system, eyelid, and conjunctival surface
*O*nset: Subacute – chronic
*S*ymptoms and signs: pigmented mass lesion with infiltration, extensive conjunctival pigmentation
*E*pidemiology: young Southeast Asian male

examination was unremarkable. Regional examination revealed no preauricular or cervical lymphadenopathy.

CLOSE summary is given in Table 47.1.

Differential Diagnosis

- Conjunctival melanoma with spread to the lacrimal sac
- Primary lacrimal sac melanoma
- Pigmented carcinoma of the lacrimal sac
- Sinonasal malignancy with lacrimal sac and conjunctival extension

Imaging

Computerised tomography (CT) scan revealed an enhancing mass lesion of the left lacrimal sac fossa involving the lacrimal sac and nasolacrimal duct with erosion of the lacrimal sac fossa (Fig. 47.3). An additional lesion was seen in the bulbar/palpebral conjunctiva abutting the globe.

On MRI, the mass involving the left lacrimal sac, nasolacrimal duct, and roof of the maxilla showed high signal intensity on T1w images and low signal on T2w images with homogeneous enhancement with gadolinium. There was no regional or cervical lymphadenopathy.

Intervention

An incisional biopsy of the conjunctival lesion was performed under local anaesthesia.

Histopathology

There were sheets of tumour cells with enlarged pleomorphic nuclei, prominent nucleoli, and occasional intracytoplasmic brown melanin pigment. Mitotic activity was brisk. Fontana-Masson stain highlighted the intracytoplasmic melanin pigment (Fig. 47.4). The tumour cells were positive for Melan A and SOX10 on immunohistochemistry.

The features were those of a melanoma.

Diagnosis

Presumptive clinical diagnosis was melanoma of the ocular surface and eyelids, with involvement of the left lacrimal drainage system and the maxilla.

Management

Patient underwent systemic screening, including abdominal imaging, which was unremarkable. Liver function tests were within normal limits. The tumour was staged at T4aN0M0.

He underwent a left orbital exenteration with total maxillectomy under frozen section control until margins were clear (Fig. 47.2). Reconstruction was performed using a free latissimus dorsi flap anastomosed to the facial artery.

Discussion

Mucosal melanomas are very rare and comprise less than 10% of head and neck melanomas. Conjunctival melanomas, in particular are 360–900 times less common than skin melanomas. Risk factors for melanomas include dysplastic nevi and predisposing conditions such as xeroderma pigmentosum and oculodermal melanocytosis, family history, and light skin with sun exposure. Conjunctival melanomas can arise de novo (more common) or from pre-existing nevi.

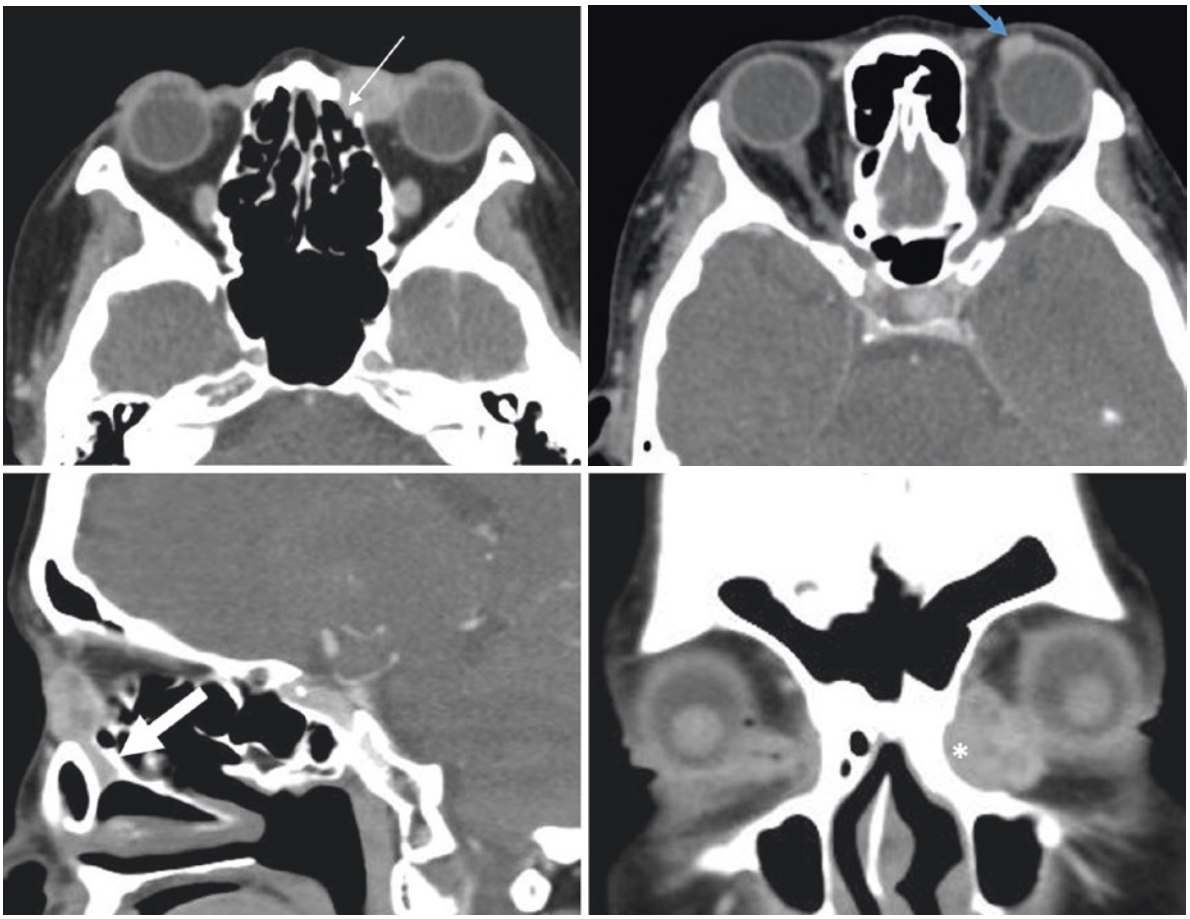

Fig. 47.3 Contrast-enhanced axial CT scan (Top) shows an enhancing mass lesion in the lacrimal sac fossa with bony erosion (thin arrow) and a conjunctival lesion (blue arrow). Sagittal scan (bottom left) shows spread into the NLD (thick arrow). Coronal scan (bottom right) shows the mass in the lacrimal fossa (*)

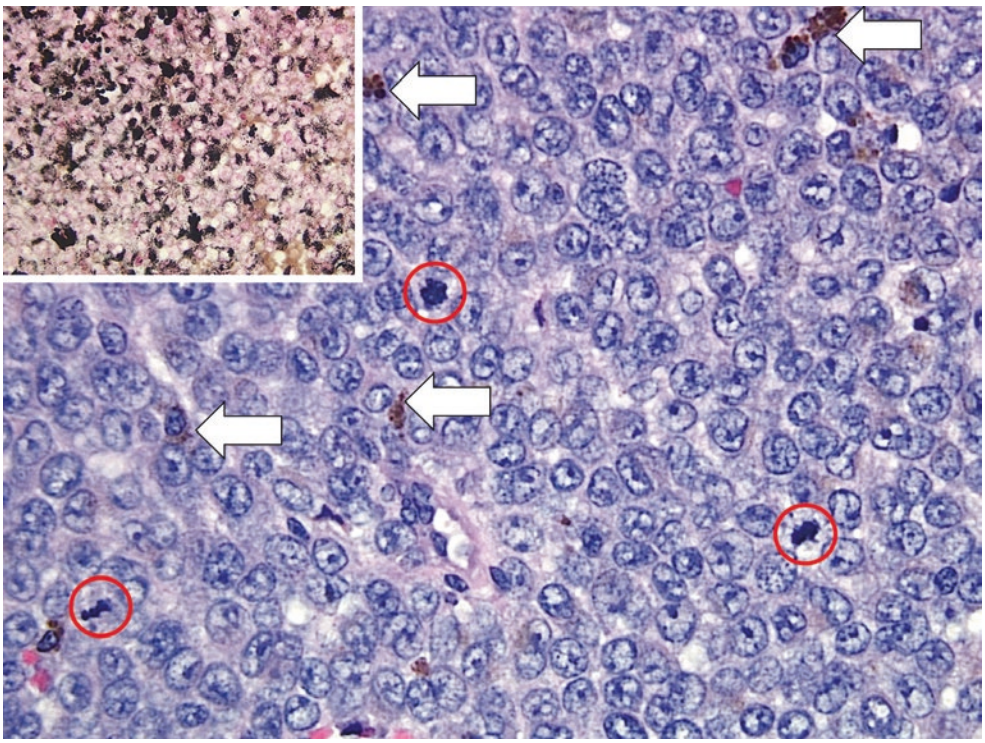

Fig. 47.4 The tumour cells exhibit large pleomorphic nuclei, prominent nucleoli, and occasional intra-cytoplasmic melanin pigment (white arrows). Frequent mitotic figures are seen (red circles). Fontana-Masson stain highlights the intra-cytoplasmic melanin pigment (inset). Main: HE stain; 400× magnification. Inset: Fontana-Masson stain; 200× magnification

In addition, primary acquired melanosis (PAM) with severe atypia can transform into a melanoma. Conjunctival melanomas are potentially life-threatening due to local invasion and systemic spread via lymphatics and vascular channels. The spread to the lacrimal sac from a conjunctival melanoma may be due to malignant cells being propagated via deeper layers of epithelium or the tears.

In this patient with a combined non-contiguous melanoma of the conjunctiva and lacrimal sac, it is debatable which the primary site is. Amongst malignant neoplasms of the lacrimal drainage system, carcinomas are the most common. Pigmented lesions, especially melanomas of the lacrimal sac per se are rare. The most common cause of pigmentation in the lacrimal sac mucosa is pigment spread from ocular surface (eyelid cosmetics), not an uncommon finding during routine external or endonasal dacryocystorhinostomy. In such situations, a routine intraoperative specimen for histopathology may be indicated.

Management Principles of management of melanoma of the head and neck region in the absence of regional or systemic spread include a wide resection under frozen and permanent section control with clear margins, with or without regional lymph node dissection/sentinel node biopsy, with reconstruction. This may be followed by evidence-supported regional radiation, chemotherapy, immunotherapy, or targeted therapy. Regardless, the prognosis is usually guarded for these conditions.

Learning points Melanoma of ocular adnexa is very rare especially in Asians. Conjunctival melanomas can arise de novo (more common) or from pre-existing nevi. In addition, primary acquired melanosis (PAM) with severe atypia can transform into a melanoma. Rarely, pigmented neoplasms like melanoma may either arise from the lacrimal sac. Principles of management of melanoma of the head and neck region in the absence of regional or systemic spread include a wide resection under frozen and permanent section control with clear margins. The prognosis however remains poor.

Further Reading

1. Collin JRO, Allen LH, Garner A, Hungerford JL. Malignant melanoma of the eyelid and conjunctiva. Aust N Z J Ophthalmol. 1986;14(1):29–34.
2. Gleizal A, Kodjikian L, Lebreton F, Beziat JL. Early CT-scan for chronic lacrimal duct symptoms: case report of a malignant melanoma of the lacrimal sac and review of the literature. J Craniomaxillofac Surg. 2005;33:201–4.
3. Hoyt DJ, Jordan T, Fisher SR. Mucosal melanoma of the head and neck. Arch Otolaryngol Head Neck Surg. 1989;115:1096–9.
4. Nam JH, Kim SM, Choi JH, Lee YK, Baek JH, Jang TJ, Park KU. Primary malignant melanoma of the lacrimal sac: a case report. Korean J Intern Med. 2006;21(4):248–51.
5. Owens RM, Wax MK, Kostik D, Linberg JV, Hogg J. Malignant melanoma of the lacrimal sac. Otolaryngol Head Neck Surg. 1995;113:634–40.
6. Sendra Tello J, Galindo Campillo N, Rodriguez-Peralto JL, Alvarez-Linera J, Garabito Cocina I. Malignant melanoma of the lacrimal sac. Otolaryngol Head Neck Surg. 2004;131:334–6.
7. Stefanyszyn MA, Hidayat AA, Pe'er JJ, Flanagan JC. Lacrimal sac tumours. Ophthal Plast Reconstr Surg. 1994;10:169–84.
8. Wong JR, Nanji AA, Gator A, Karp CL. Management of conjunctival malignant melanoma: a review and update. Expert Rev Ophthalmol. 2014;9(3):185–204.

Part XI

Primary Malignant Neoplasms: Orbit

Rhabdomyosarcoma

48

Gangadhara Sundar, Stephanie Ming Young, Eric Ting, Bingcheng Wu, Min En Nga, and Shantha Amrith

Introduction

Rhabdomyosarcoma is the most common primary orbital neoplasm in children, typically in the 5–10-year age group. It may present either as a rapidly progressive or, less commonly, a slowly progressive proptosis in a healthy child and may mimic an orbital cellulitis with the absence of constitutional signs or symptoms. It is an ocular adnexal emergency, requiring urgent imaging followed by an incisional biopsy with debulking. A workup for systemic staging and referral to a paediatric oncologist is mandatory for treatment. The general principles of management include safe debulking of the tumour (reduce total tumour burden to improve local treatment response) followed by chemotherapy and external beam radiation (Intergroup Rhabdomyosarcoma Studies I–IV). The prognosis nowadays is good with multimodal therapy, especially for certain histological subtypes.

Case Scenario

A 7-year-old boy initially presented to the ophthalmologist for swelling and redness of the right upper eyelid. He was treated elsewhere for preseptal cellulitis with systemic antibiotics without response. He was subsequently seen by his primary care physician who advised CT imaging followed by a biopsy. Initial histopathology report elsewhere labelled it as an 'undifferentiated tumour – indeterminate' before referral to our institution for specific diagnosis and management.

On examination, the child was afebrile with discomfort from the prominence and swelling of the right eye. Ophthalmic examination was normal on the left side. On the right, he had severe non-pulsatile proptosis, and a tense, non-tender upper eyelid swelling, and vascular dilatation. Palpation of the upper eyelid revealed a firm mass. There was a downward displacement of the eyeball with pronounced chemosis (Fig. 48.1a, b) and global limitation of ocular motility. A right grade I RAPD and a congested optic nerve head were noted. There was no regional lymphadenopathy. Systemic examination was unremarkable (Table 48.1).

G. Sundar · S. M. Young · S. Amrith (✉)
Department of Ophthalmology, National University Hospital, Singapore

Department of Ophthalmology, Yong Loo Lin School of Medicine, National University of Singapore, Singapore
e-mail: gangadhara_sundar@nuhs.edu.sg; stephanie.young@nuhs.edu.sg; shantha_amrith@nuhs.edu.sg

E. Ting
Department of Diagnostic Imaging, National University Hospital, Singapore

Department of Diagnostic Imaging, Yong Loo Lin School of Medicine, National University of Singapore, Singapore

Advanced Medicine Imaging, Singapore

B. Wu
Department of Pathology, National University Hospital, Singapore

M. E. Nga
Department of Pathology, National University Hospital, Singapore

Department of Pathology, Yong Loo Lin School of Medicine, National University of Singapore, Singapore

S. Amrith et al. (eds.), *Ocular Adnexal Lesions*, https://doi.org/10.1007/978-981-13-3798-7_48

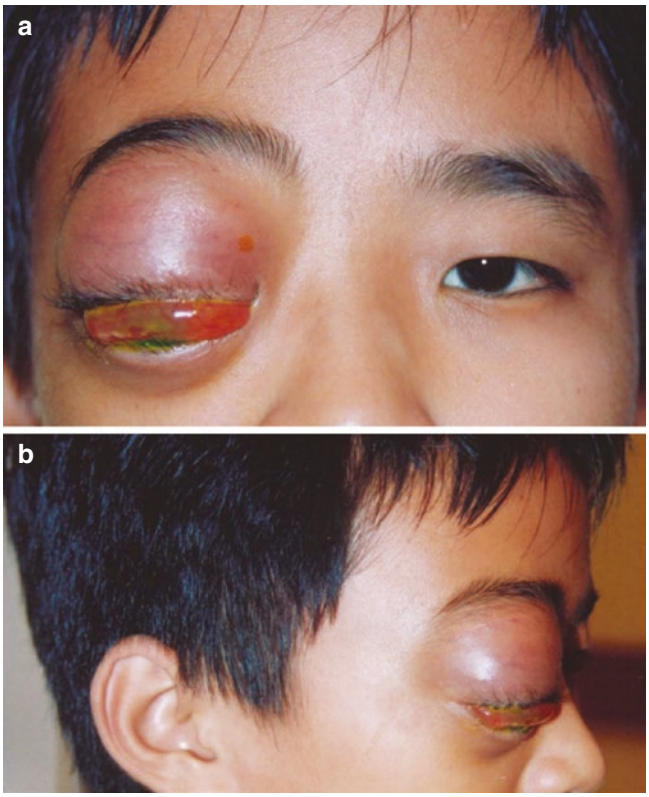

Fig. 48.1 (**a** and **b**) Clinical picture of the child showing tense non-axial proptosis and lid swelling

Table 48.1 CLOSE summary

*C*linical process: mass effect, less likely inflammatory or infectious
*L*ocation: right superior and posterior orbit
*O*nset: subacute
*S*ymptoms and signs: swelling, prominence/proptosis, discomfort
*E*pidemiology: East Asian male child

Differential Diagnosis

- Orbital cellulitis
- Rhabdomyosarcoma
- Leukaemic infiltrate of the orbit (myeloid sarcoma)
- Orbital inflammatory disorder (specific or nonspecific)
- Other mesenchymal neoplasms

Investigations

Full blood count: normal (no leucocytosis or suggestion of leukaemia)

Renal panel: unremarkable

CT scan of orbits or MRI orbits with contrast

Bone scan

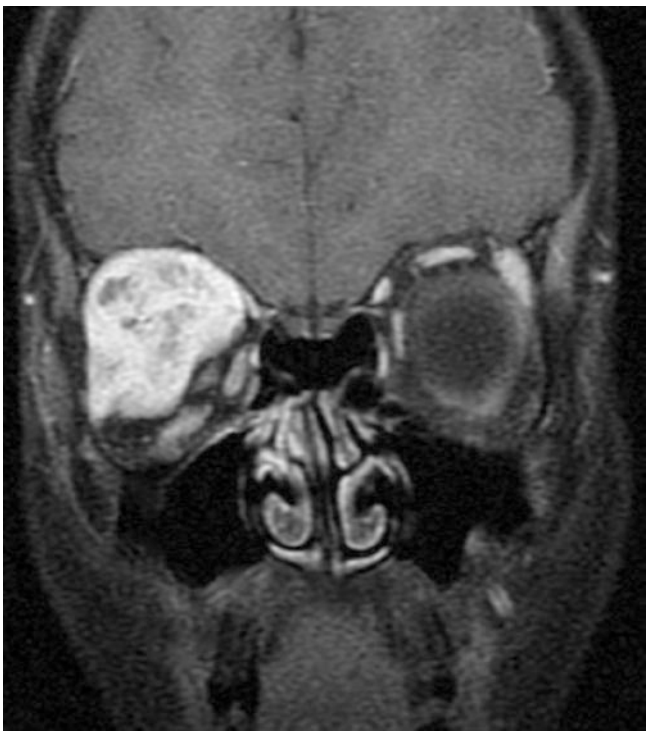

Fig. 48.2 MRI of the orbits: Coronal T1w FS + C showing a large, enhancing extraconal mass displacing the optic nerve inferomedially. There is infiltration of the extraocular muscles and remodelling of the orbit

Imaging

On MRI of the orbits, there was a large intraorbital mass in the superior and lateral aspect of the right orbit extending to the apex. It was isointense on T1-weighted, intermediate to hyperintense on T2-weighted sequences and demonstrated fairly homogeneous and intense enhancement (Fig. 48.2). There was involvement of the preseptal and orbital compartments, causing right proptosis and downward displacement of the right globe. Some indentation of the superior aspect of the right globe was noted, with displacement of the optic nerve inferomedially. The right lacrimal gland, lateral rectus, superior rectus, and superior oblique extraocular muscles could not be identified presumably due to infiltration by the tumour mass.

Intervention

An incisional biopsy with debulking of the right orbital mass was performed through a lid crease approach, avoiding damage to the extraocular muscles, globe, and the optic nerve.

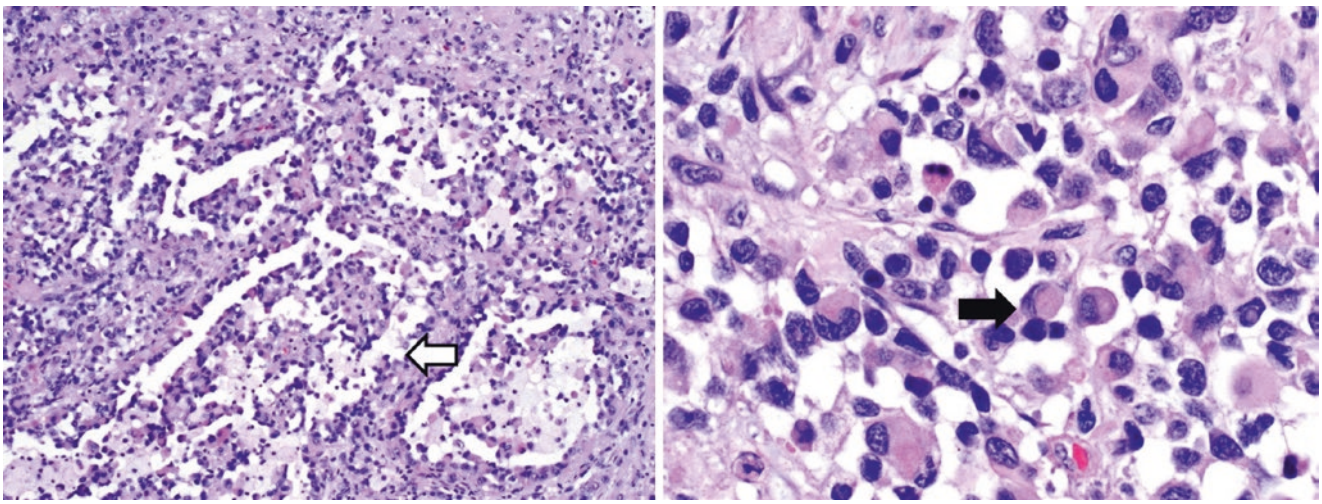

Fig. 48.3 The tumour showed an alveolar growth pattern with central discohesion (white arrow). The tumour cells exhibited rhabdoid morphology [round cells with eccentric nuclei and densely eosinophilic cytoplasm (black arrow)]. Left: HE stain; 100× magnification. Right: HE stain; 400× magnification

Histopathology

Histopathology showed a tumour with an alveolar growth pattern, composed of nests of tumour cells arranged in alveolar spaces with central discohesion. The tumour cells adhered to the periphery of the alveolar spaces and exhibited rhabdoid morphology (round cells with eccentric nuclei and densely eosinophilic cytoplasm) (Fig. 48.3).

The features were consistent with the diagnosis of alveolar rhabdomyosarcoma.

Management

The patient was subsequently referred to the paediatric oncologist. Systemic workup including bone scan and bone marrow biopsy was performed, both of which were normal. Based on the IRSG protocol, he was started on the VAC (vincristine, actinomycin-D, and cyclophosphamide) regimen, followed by external beam radiation to the right orbit.

The patient has been under follow-up for 14 years. Posttreatment, the patient developed radiation-induced cataract in the right eye for which he has had phacoemulsification with intraocular lens implant. He developed madarosis of the right eyebrow with a mild superior sulcus deformity. He has remained disease-free and maintains annual follow-up.

Discussion

Orbital rhabdomyosarcoma, a common type of head and neck rhabdomyosarcoma, has one of the best outcomes with timely and optimal management, and most often without significant residual functional deficit. Prior to the 1960s, orbital exenteration was the standard treatment option, with poor aesthetic and functional outcome and poor prognosis for life. Since then, radiotherapy and chemotherapy have transformed outcomes.

There are four different histological subtypes, namely, embryonal, pleomorphic, alveolar, and botryoid. Embryonal rhabdomyosarcoma is the most common histopathological type (80%) with very good clinical prognosis and has a 10-year survival rate of around 95%. Pleomorphic rhabdomyosarcoma is the least common, and the most differentiated, and has the highest survival rate of around 97%. Alveolar rhabdomyosarcoma, which has a predilection for the inferior orbit, is the most malignant form and has a reported 10-year survival rate of only 10%. Botryoid is a rare variant, arising either from the conjunctiva or more commonly from adjacent paranasal sinuses.

With immunohistochemistry, the tumour cells show nuclear positivity for myogenin and myoD1, which are markers for skeletal muscle differentiation. They would also be positive for either t(2;13) PAX3-FKHR or t(1;13) PAX7-FKHR translocations.

Principles of management include clinical suspicion, complete evaluation with early diagnosis, systemic workup, and aggressive evidence-based multimodal treatment of the tumour with surgical debulking, chemo-radiotherapy, and long-term follow-up. Local radiation dose varies between 4500 and 6000 cGY over 6 weeks as a fractionated stereotactic treatment.

Learning Points

Orbital rhabdomyosarcoma should be ruled out in all children presenting with an 'orbital cellulitis' like picture and is the prime indication for orbital imaging. There should be no delay in histopathological diagnosis and initiation of treatment. Multidisciplinary multimodality treatment is essential in delivering the best possible outcome.

Further Reading

1. Kodet R, jr NWA, Hamoudi AB, Asmar L, Wharam MD, Maurer HM. Orbital rhabdomyosarcomas and related tumours in childhood: relationship of morphology to prognosis – an Intergroup Rhabdomyosarcoma Study. Med Pediatr Oncol. 1997;29(1):51–60.
2. Malempati S, Hawkins DS. Rhabdomyosarcoma: review of the Children's Oncology Group (COG) Soft-Tissue Sarcoma Committee experience and rationale for current COG studies. Pediatr Blood Cancer. 2012;59(1):5–10.
3. Shields CL, Shields JA, Honavar SG. Demirci. Clinical spectrum of primary ophthalmic rhabdomyosarcoma. Ophthalmology. 2001;108(12):2284–92.

EBV Smooth Muscle Tumour

49

Stephanie Ming Young, Shantha Amrith, Eric Ting, Bingcheng Wu, Min En Nga, and Gangadhara Sundar

Introduction

Epstein-Barr virus-associated smooth muscle cell tumour (EBV-SMT) is a rare entity that may be encountered in immunocompromised patients. The association of EBV and SMT in immunocompromised patients was first reported in the early 1990s by Chadwick et al.

Case Scenario

A 31-year-old Chinese female, who underwent a living donor renal transplant at 18 years of age for idiopathic chronic glomerulonephritis, first presented with a painless right eye prominence of 2 months' duration. She did not have any visual symptoms. She had a history of right knee and left hand swellings 8 and 5 years after the transplant, respectively.

On examination, she had a right proptosis of 5 mm (Fig. 49.1), with resistance to retropulsion. There was no palpable mass, the orbit was non-inflamed and non-tender and

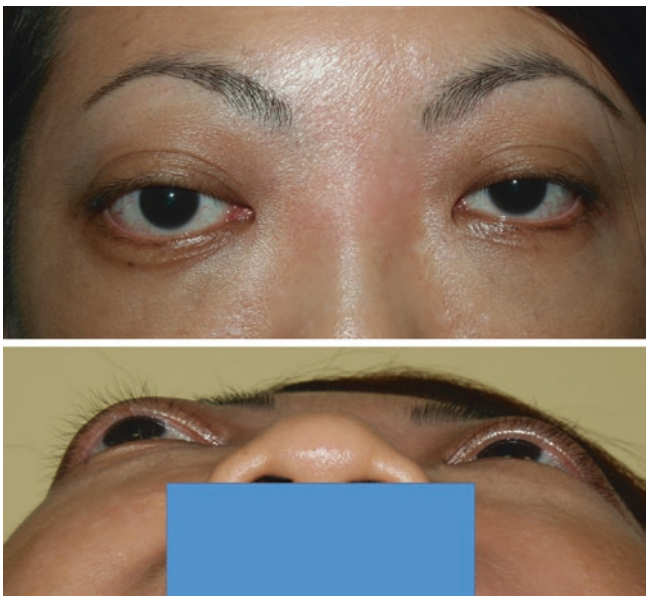

Fig. 49.1 Clinical picture showing a right proptosis

S. M. Young · S. Amrith (✉) · G. Sundar
Department of Ophthalmology, National University Hospital, Singapore

Department of Ophthalmology, Yong Loo Lin School of Medicine, National University of Singapore, Singapore
e-mail: stephanie.young@nuhs.edu.sg; shantha_amrith@nuhs.edu.sg; gangadhara_sundar@nuhs.edu.sg

E. Ting
Department of Diagnostic Imaging, National University Hospital, Singapore

Department of Diagnostic Imaging, Yong Loo Lin School of Medicine, National University of Singapore, Singapore

Advanced Medicine Imaging, Singapore

B. Wu
Department of Pathology, National University Hospital, Singapore

M. E. Nga
Department of Pathology, National University Hospital, Singapore

Department of Pathology, Yong Loo Lin School of Medicine, National University of Singapore, Singapore

S. Amrith et al. (eds.), *Ocular Adnexal Lesions*, https://doi.org/10.1007/978-981-13-3798-7_49

the globe was ballotable. Snellen visual acuity in her right eye was 6/7·5 and left eye 6/6. She had no relative afferent pupillary defect. Colour vision, intraocular pressures and ocular motility were normal in both eyes. Apart from bilateral 'steroid-induced' posterior subcapsular cataracts, the rest of the anterior segment and fundus examination were normal in both eyes.

Computed tomography (CT) of her orbits showed a well-circumscribed, heterogeneous right extraconal lesion in the superomedial orbital space. The patient was advised to undergo surgical resection, but she elected to be observed instead.

Five months later, she presented with decreased visual acuity of the right eye (6/12), with grade 2 relative afferent pupillary defect, and decreased colour vision (1/13 of the Ishihara test plates), with further increase in proptosis by 6 mm. Ocular motility was restricted in abduction.

Systemic investigations revealed similar lesions in the long bones and liver.

CLOSE summary is given in Table 49.1.

Differential Diagnosis

- Inflammatory disorder:
  - Specific orbital inflammation
  - Non-specific orbital inflammatory syndrome
- Vascular lesion, e.g. cavernous haemangioma
- Orbital schwannoma
- Solitary fibrous tumour
- Orbital metastasis
- Lymphoproliferative disorder, e.g. lymphoma

Table 49.1 CLOSE summary

*C*linical process: mass lesion
*L*ocation: right superomedial extraconal orbital space
*O*nset: subacute to chronic (months)
*S*igns and symptoms: proptosis
*E*pidemiology: 30-year-old Chinese female with past history of renal transplant

Imaging

Orbital CT showed a well-circumscribed mass in the superomedial aspect of the right orbit with smooth remodelling of the medial orbital wall (Fig. 49.2). Magnetic resonance imaging (MRI), which was performed at a later date, showed the large, well-circumscribed mass in the right orbit had slightly increased in size. The lesion was slightly hyperintense in T2-weighted and hypointense in T1-weighted images with central cystic necrosis, and it enhanced on post contrast examination. The lesion appeared to be extraconal but bulged laterally into and deformed the conus, distorting the medial rectus, which was displaced into an inferior plane. The optic nerve was also displaced laterally, abutting the tumour (Fig. 49.3). There was associated proptosis.

Contrast-enhanced CT scan of the abdomen revealed a transplanted kidney in the right iliac fossa and a soft tissue mass in the liver (Fig. 49.4).

Intervention

At this point, she agreed to undergo surgical excision. She underwent a right anterior orbitotomy, via a vertical lid split incision extending above the lid crease. The tumour appeared bosselated and measured 12 millilitres in volume.

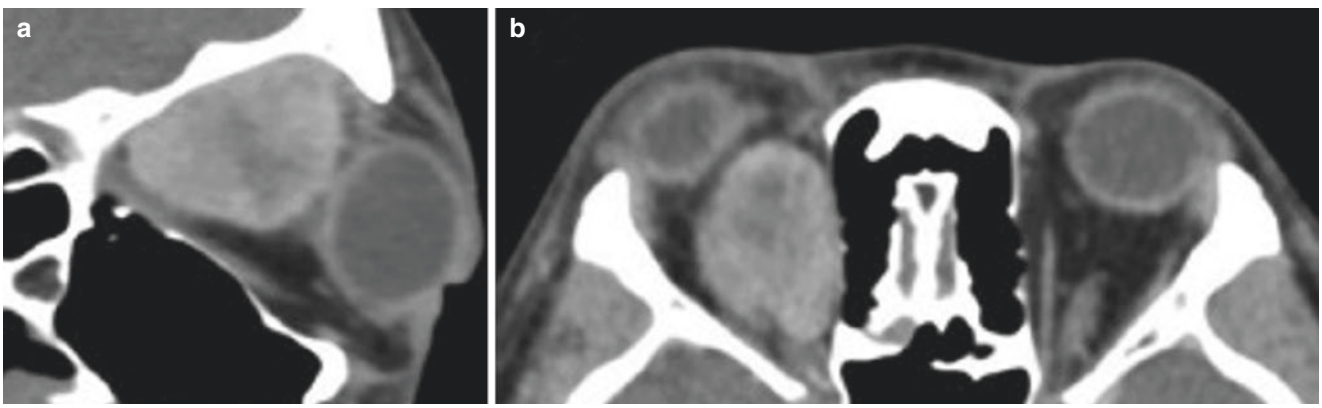

Fig. 49.2 Sagittal (**a**) and Axial (**b**) CT orbits show a right heterogeneous, predominantly extraconal mass in superomedial orbital space with remodelling of the medial orbital wall

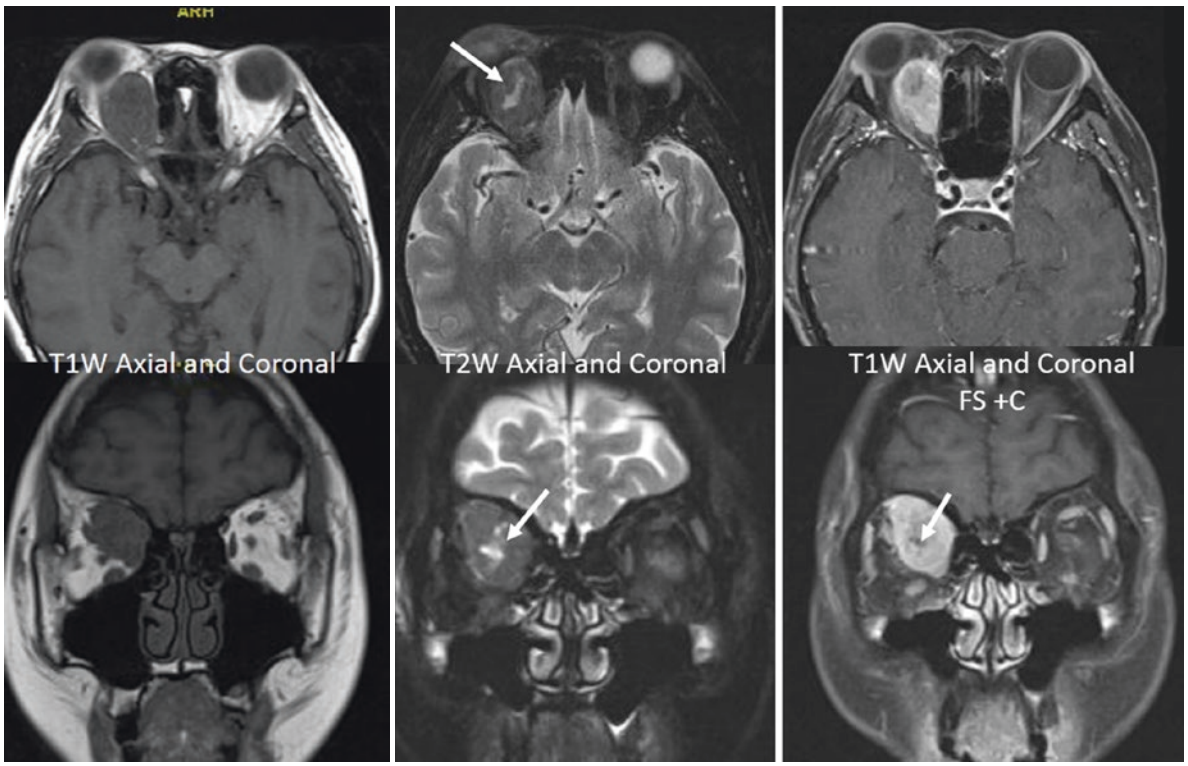

Fig. 49.3 T1w, T2w and T1w-FS + C sequences show a large, fairly well-circumscribed extraconal mass in the superomedial aspect of the right orbit. The lesion is isointense to grey matter on T1w images, slightly hypointense on T2w images with central T2w hyperintense scar (arrows) and show slightly heterogeneous enhancement with contrast. Note the lateral displacement of the medial and superior rectus muscles as well as the optic nerve

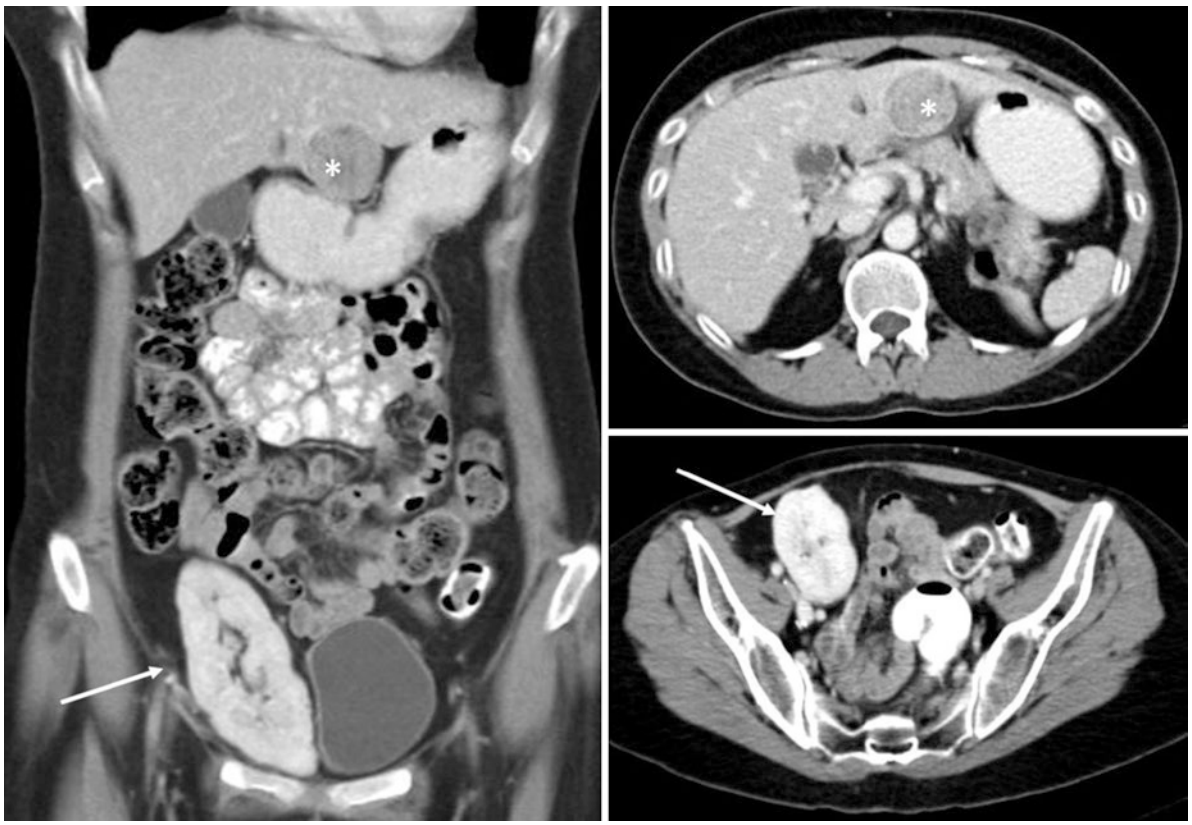

Fig. 49.4 Contrast-enhanced CT abdomen shows evidence of soft tissue mass in the liver (*). Note the transplant kidney in the right iliac fossa (white arrow)

Histopathology

Sections showed that the tumour was partially circumscribed with occasional tongues protruding into the surrounding tissue (Fig. 49.5). It was composed of spindle cells with elongated blunt-ended nuclei and ample eosinophilic cytoplasm. In most areas, the tumour cells were disposed in vague fascicles, while in some areas, the tumour cells were arranged somewhat more haphazardly (Fig. 49.6). Scattered irregularly, dilated thin-walled blood vessels were seen throughout the tumour.

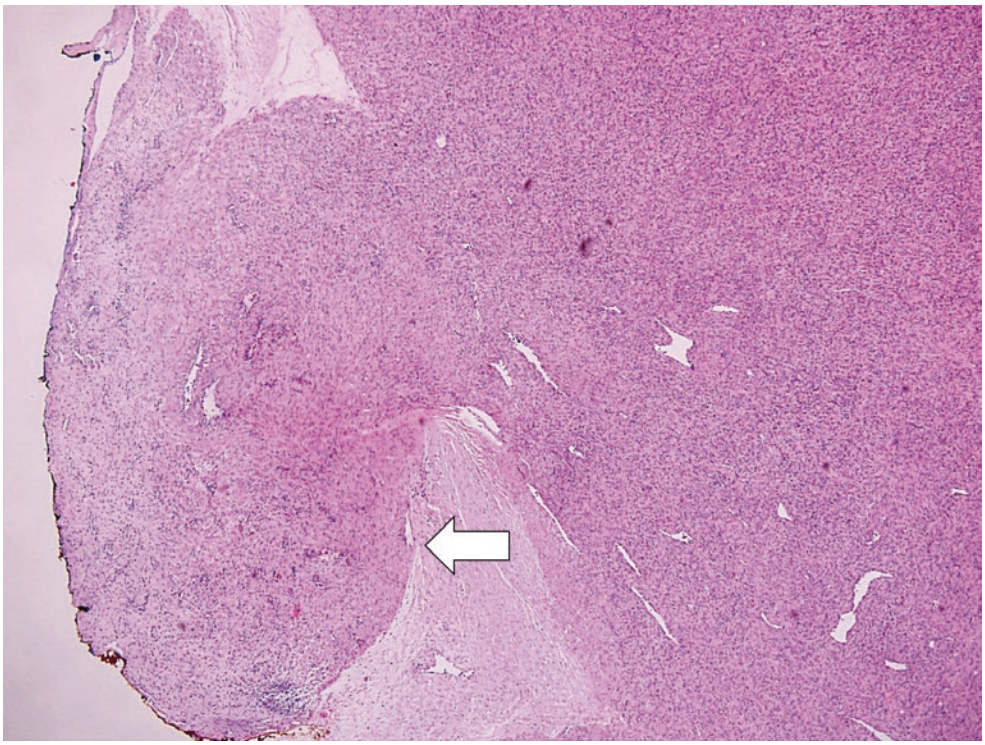

Fig. 49.5 The figure shows the tumour to be partially circumscribed with a tongue of tumour protruding into the surrounding tissue (white arrow). A vaguely fascicular pattern is appreciated. Irregularly dilated thin-walled blood vessels are seen. HE stain, 20× magnification

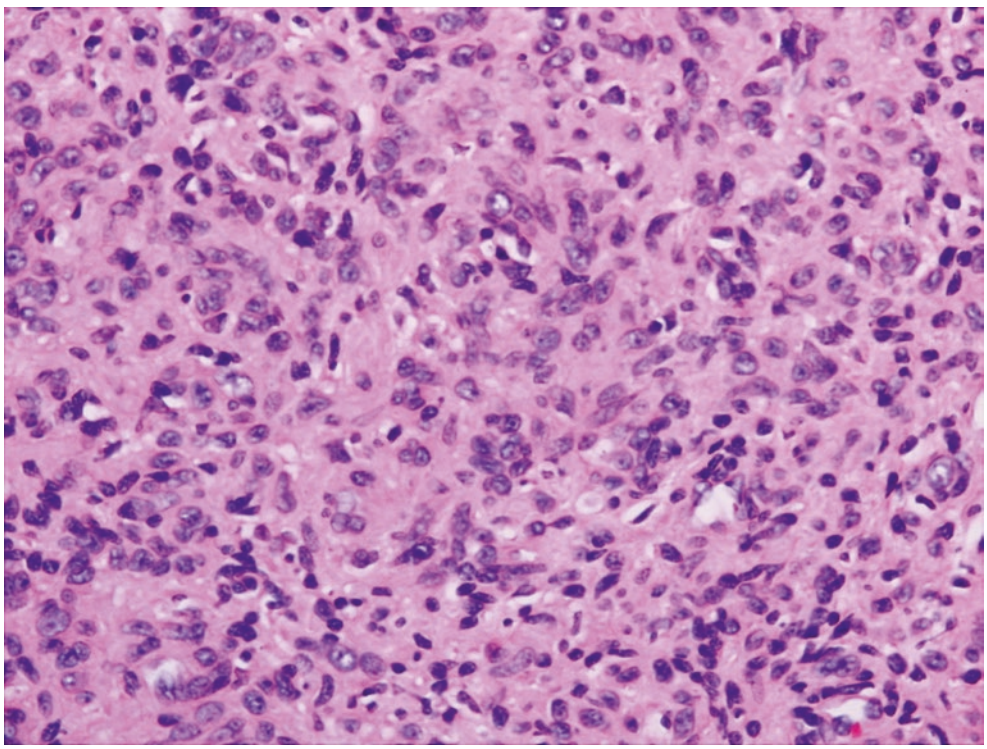

Fig. 49.6 The tumour cells exhibit spindled morphology, elongated blunt-ended nuclei and ample eosinophilic cytoplasm. In this field, the tumour cells are disposed in a somewhat haphazard manner. HE stain, 400× magnification

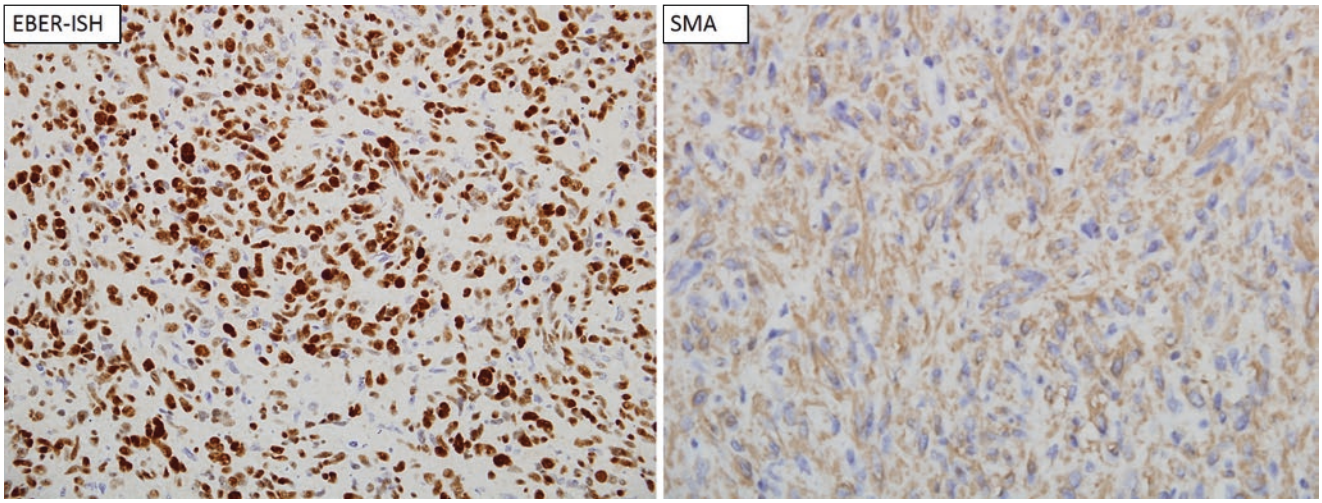

Fig. 49.7 The tumour cells are positive for EBER-ISH and SMA immunohistochemistry

The tumour cells were positive for Epstein-Barr virus encoding region in situ hybridization (EBER-ISH), as well as smooth muscle antigen (SMA) (Fig. 49.7), and H-caldesmon on immunohistochemistry. The features were consistent with Epstein-Barr virus smooth muscle tumour.

Discussion

EBV-SMT usually presents as multiple lesions (59%), with the commonly involved organs being the central nervous system (20%) and soft tissues (18.5%). Orbital involvement is rare and occurs mostly in HIV-related patients. The presence of lesions in multiple locations is more likely to represent multifocal origin rather than spread from a single site.

Treatment

The only reliable treatment for the tumour is reduction of immunosuppression, but there is a fine balance between controlling tumour growth and the underlying disease. Death in EBV-SMT patients is usually due to other causes, rather than by the tumour itself.

Learning Points

EBV-SMT should be considered as one of the differential diagnosis of well-circumscribed soft tissue tumours of the orbit, especially in immunocompromised and post-solid organ transplant patients. Greater awareness is needed as the incidence of such soft tissue tumours increases with more organ transplantations and more aggressive immunosuppression.

Further Reading

1. Chadwick EG, Connor EJ, Hanson ICG, et al. Tumours of smooth-muscle origin in HIV-infected children. JAMA. 1990;263:3182–4.
2. Yu L, Aldave AJ, Glasgow BJ. Epstein-Barr virus-associated smooth muscle tumour of the iris in a patient with transplant: a case report and review of the literature. Arch Pathol Lab Med. 2009;133(8):1238–41.
3. Purgina B, Rao U, Miettinen M, Pantanowitz L. AIDS-related EBV-associated smooth muscle tumours: a review of 64 published cases. Pathol Res Int. 2011;2011:1–10.
4. Gallien S, Zuber B, Polivka M, et al. Multifocal Epstein-Barr virus–associated smooth muscle tumour in adults with AIDS: case report and review of the literature. Oncology. 2008;74:167–76.
5. Kim JW, Lee DK, Fishman M. Orbital smoothmuscletumour associated with Epstein-Barr virus in a human immunodeficiencyvirus-positive patient. Arch Ophthalmol. 2010;128:1084–5.

Alveolar Soft Part Sarcoma

50

Mariel Angelou Parulan, Shantha Amrith, Stephanie Ming Young, Eric Ting, Bingcheng Wu, Min En Nga, and Gangadhara Sundar

Introduction

In 1952, the term alveolar soft part sarcoma (ASPS) was coined by Christopherson when he reported 12 cases of lesions that had an appearance similar to granular cell myoblastoma but were arranged in an alveolar pattern around a central space. It is considered a rare malignancy that accounts for less than 1% of all soft tissue tumours. In a localized disease, it has a reported 5-year disease-free survival of 71% and decreases to 20% in patients who present with metastases. Although it has been more than half a decade since this condition has been reported, there is still limited knowledge available regarding this condition.

Clinical Scenario

A 16-month-old South Asian boy was referred following a biopsy elsewhere, with a history of a left lower lid redness of 3 months' duration for which he was initially treated as conjunctivitis. A month later, the parents noted swelling of the left lower eyelid. Examination showed a left lower lid swelling with mild conjunctival injection. There was a left hyperglobus with mild limitation of motility in the vertical direction. Forced duction test was positive with vertical restriction, more on upward than downward movement. Examination of the globe was unremarkable (Fig. 50.1).

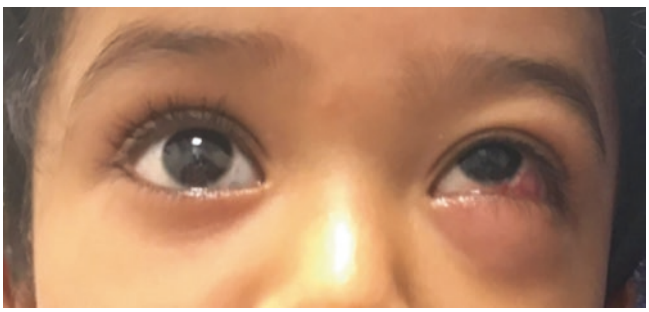

Fig. 50.1 Clinical picture showing left lower lid swelling with a left hyperglobus

CLOSE summary is given in Table 50.1.

M. A. Parulan
Department of Ophthalmology, National University Hospital, Singapore

S. Amrith (✉) · S. M. Young · G. Sundar
Department of Ophthalmology, National University Hospital, Singapore

Department of Ophthalmology, Yong Loo Lin School of Medicine, National University of Singapore, Singapore
e-mail: shantha_amrith@nuhs.edu.sg; stephanie.young@nuhs.edu.sg; gangadhara_sundar@nuhs.edu.sg

E. Ting
Department of Diagnostic Imaging, National University Hospital, Singapore

Department of Diagnostic Imaging, Yong Loo Lin School of Medicine, National University of Singapore, Singapore

Advanced Medicine Imaging, Singapore

B. Wu
Department of Pathology, National University Hospital, Singapore

M. E. Nga
Department of Pathology, National University Hospital, Singapore

Department of Pathology, Yong Loo Lin School of Medicine, National University of Singapore, Singapore

S. Amrith et al. (eds.), *Ocular Adnexal Lesions*, https://doi.org/10.1007/978-981-13-3798-7_50

Differential Diagnosis

- Rabdomyosarcoma
- Vascular tumour and malformation such as infantile haemangioma and venous or lymphatic-venous malformation
- Orbital inflammatory disease
- Langerhan cell histiocytosis
- Haematological malignancy such as chloroma
- Metastasis such as neuroblastoma

Table 50.1 CLOSE summary

*C*linical scenario	Space-occupying lesion
*L*ocation	Left inferior orbit
*O*nset	Subacute
*S*ymptom	Left lower lid swelling
*E*pidemiology	16-month-old South Asian boy

Imaging

MRI showed a low to isointense T2w and T1w lesion at the left inferior orbit involving the inferior rectus muscle and tendon with extension close to the orbital apex (Fig. 50.2). Some small internal flow voids were seen. The lesion was relatively well circumscribed and likely contained within the inferior rectus muscle. There was adjacent mass effect on the inferior globe but no gross extension through the sclera. The left globe was displaced anterosuperiorly. No gross mass effect on the optic nerve was seen.

There was also bony remodelling and mild bowing of the left orbital floor.

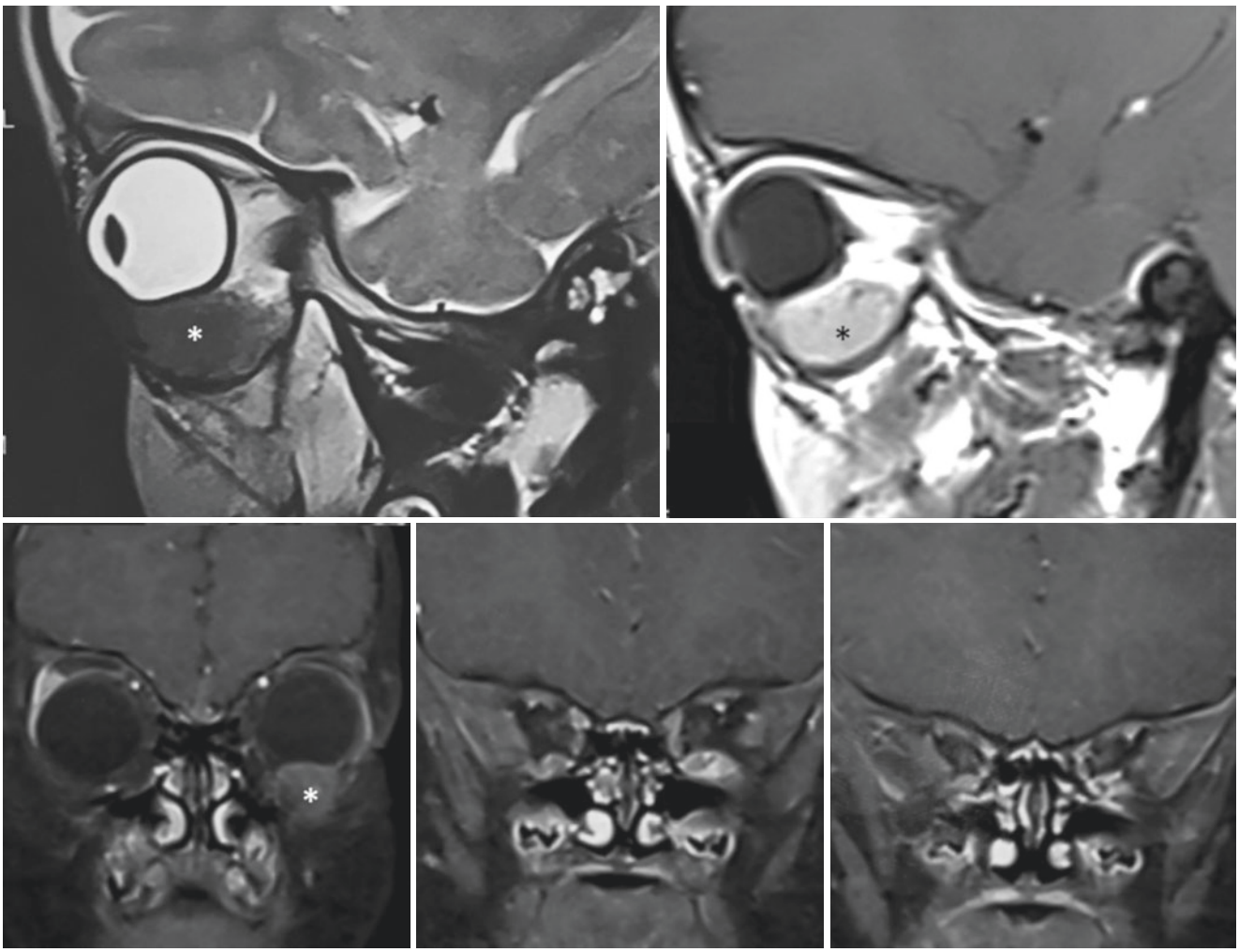

Fig. 50.2 Top: Sagittal T2w and contrast-enhanced T1w MRI scans show a mass (*) in the left inferior orbit involving the inferior rectus muscle and tendon. Bottom: Coronal T1w FS + C images showing extension of the mass posteriorly towards the orbital apex

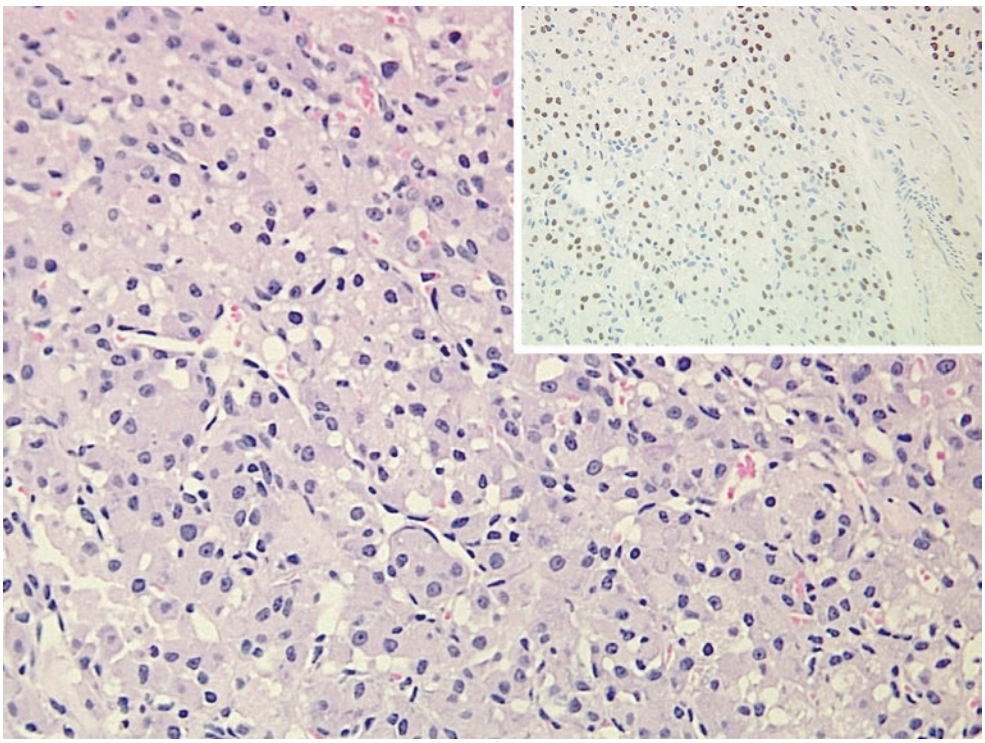

Fig. 50.3 The tumour has a nested appearance with delicate sinusoidal vessels between the nests of tumour cells. The tumour cells exhibit ample amphophilic (pink-purplish) granular cytoplasm and round nuclei with prominent nucleoli. TFE3 positivity on immunohistochemistry (inset) is consistent with the diagnosis of ASPS. Main: HE stain; 400× magnification. Inset: Immunohistochemistry (TFE3 antibody); 100× magnification

Histopathology

Review of histopathology from the previous biopsy showed a lobulated tumour with fibrous septa comprising mostly solid nests of epithelioid cells with abundant eosinophilic/granular cytoplasm and prominent nucleoli. Delicate sinusoidal vessels were seen between nests of tumour cells (Fig. 50.3). In some areas, there was discohesion of the tumour cells imparting a pseudo-alveolar growth pattern. Intracytoplasmic granules were noted on the DPAS stain, but definite crystals were not seen. There was mild to moderate atypia but no evidence of marked pleomorphism. Mitotic activity was low. The tumour cells were diffusely positive for TFE3 (nuclear stain) (Fig. 50.3 inset). The features were compatible with an alveolar soft part sarcoma.

Management

Surgical excision followed by radiation was advised, but the patient defaulted follow-up.

Discussion

Although there is debate as to the origin of this tumour, the predominant theory is that it is a muscle-derived tumour. It is a slow-growing, rare malignancy that is commonly seen in the extremities of young patients, occasionally in the head and neck area and rarely in the orbital region. It has been reportedly seen in a wide age group (1–31), and features may be variable. The most common presentation is proptosis which may be accompanied by lid swelling, conjunctival congestion, pain and lastly diplopia.

Since this may present similar to other types of soft tissue tumours in the orbit, histologic evaluation becomes vital. Some features on histologic studies include an organoid to pseudo-alveolar arrangement of epithelioid-appearing tumour cells, separated by fibrovascular septae. It is reported that approximately 80% of ASPS will have PAS-positive and diastase-resistant crystalline structures, and this seems to be quite characteristic of this tumour. Besides, ASPS is characterized by der(17)t(X;17)(p11.2;q25) translocation resulting in fusion of ASPSCR1 and TFE3 genes. A molecular assay for this translocation will help to confirm the diagnosis.

Although noted to be slow-growing, these lesions are known to recur despite surgical excision which is the first line of management. Postoperative radiotherapy has been advocated with reported local control rate of up to 90%. Because of its indolent nature, symptoms do not always present early in the tumour development and are often diagnosed at a more advanced stage. Metastasis may rarely be the first manifestation of the disease. Commonly, the metastases occur in the lungs, bones, CNS and liver, and may occur up to 15 years after initial presentation. Survival rates reported to be 77% at 2 years, 60% at 5 years, 38% at 10 years, and 15% at 20 years.

Due to its rarity and lack of large randomized controlled trials, no validated treatment protocol is available. For recurrent cases, some still advocate exenteration, followed by radiation therapy. However, with the advent of new medications such as targeted therapy, and other chemotherapeutic agents, this morbidly debilitating treatment strategy could be avoided in future management approaches.

Learning Points

- Alveolar soft part sarcoma (ASPS) is a rare malignancy with poor long-term survival prognosis.
- In children, ASPS may arise in the head and neck, particularly the orbit and tongue.
- Local surgical excision appears to provide the best chance of controlling the disease involving the orbit.

Further Reading

1. Chung EM, Smirniotopoulos JG, Specht CS, Schroeder JW, Cube R. From the archives of the AFIP: pediatric orbit tumours and tumour like lesions: non-osseous lesions of the extraocular orbit. Radiographics. 2007;27(6):1777–99.
2. Fay A, Dolman PJ. Diseases and disorders of the orbit and ocular adnexa. Edinburgh: Elsevier; 2017.
3. Folpe AL, Deyrup AT. Alveolar soft-part sarcoma: a review and update. J Clin Pathol. 2006;59(11):1127–32.
4. Honavar S, Reddy VA, Mulay K, Ali M. Orbital alveolar soft-part sarcoma: clinico-pathological profiles, management and outcomes. J Cancer Res Ther. 2014;10(2):294.
5. Rose AM, Kabiru J, Rose GE. Alveolar soft-part sarcoma of the orbit. Afr J Paediatr Surg. 2011;8(1):82–4.

Part XII

Primary Malignant Neoplasms: Lacrimal System

Lacrimal Gland: Adenoid Cystic Carcinoma

51

Shantha Amrith, Stephanie Ming Young, Eric Ting, Bingcheng Wu, Min En Nga, and Gangadhara Sundar

Introduction

Lacrimal gland lesions make up approximately 10% of all the space-occupying lesions of the orbit and are broadly classified into non-epithelial and epithelial (Fig. 51.1). Both salivary glands and lacrimal glands have similar morphological features and thus similar tumour types. Salivary gland tumours, however, are more common, and a lot of the information about the genetics and management are applicable to lacrimal gland tumours.

Among the malignant epithelial neoplasms, adenoid cystic carcinoma (ACC) is the most common, making up to 60% of all the malignant tumours of the lacrimal gland. ACC affects patients in their 40s, although bimodal distribution is well known with another peak at the first or second decade of life. In young individuals these tumours tend to behave less aggressively.

Clinical Scenario

A 44-year-old Chinese female noticed swelling and droopiness of the left upper lid, with painless proptosis of 1 month duration. She had noticed numbness over her left forehead and some blurring of vision on up gaze.

On examination, the visual acuity was normal in both eyes. The examination of the right globe and orbit was unremarkable. On the left, there was mild conjunctival injection, mild ptosis and a non-axial proptosis of 2 mm with downward displacement of the eyeball (Fig. 51.2). There was limitation of ocular motility on supraduction and abduction. There was no RAPD and the anterior and posterior segments were normal. There was loss of sensation over the lateral aspect of the left forehead. There was no regional or systemic lymphadenopathy.

CLOSE summary is given in Table 51.1.

S. Amrith (✉) · S. M. Young · G. Sundar
Department of Ophthalmology, National University Hospital, Singapore

Department of Ophthalmology, Yong Loo Lin School of Medicine, National University of Singapore, Singapore
e-mail: shantha_amrith@nuhs.edu.sg; stephanie.young@nuhs.edu.sg; gangadhara_sundar@nuhs.edu.sg

E. Ting
Department of Diagnostic Imaging, National University Hospital, Singapore

Department of Diagnostic Imaging, Yong Loo Lin School of Medicine, National University of Singapore, Singapore

Advanced Medicine Imaging, Singapore

B. Wu
Department of Pathology, National University Hospital, Singapore

M. E. Nga
Department of Pathology, National University Hospital, Singapore

Department of Pathology, Yong Loo Lin School of Medicine, National University of Singapore, Singapore

S. Amrith et al. (eds.), *Ocular Adnexal Lesions*, https://doi.org/10.1007/978-981-13-3798-7_51

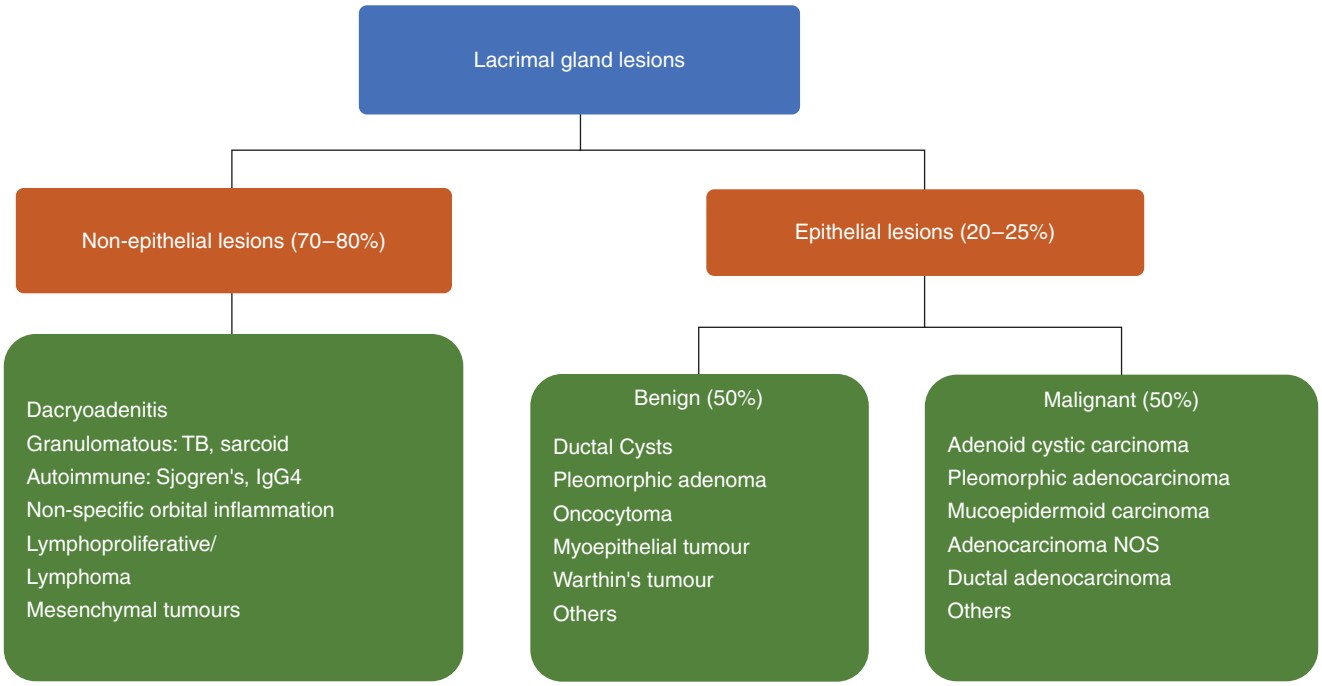

Fig. 51.1 Classification of lacrimal gland lesions

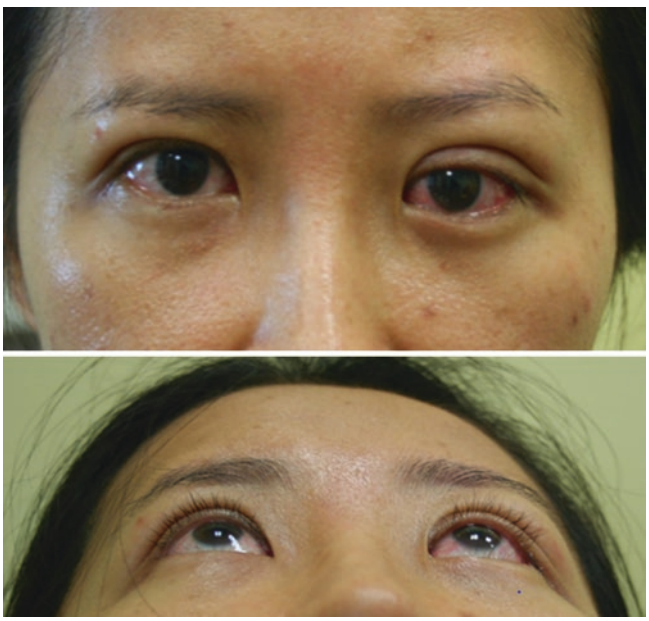

Fig. 51.2 Clinical picture showing left proptosis, hypoglobus with upper lid swelling, ptosis and mild conjunctival injection

Table 51.1 CLOSE summary

*C*linical process: infiltrative, mass lesion
*L*ocation: left orbit, involving the lacrimal gland
*O*nset: subacute
*S*igns and symptoms: left eye proptosis and eyelid swelling and loss of forehead sensation
*E*pidemiology: 44-year-old Chinese female

Differential Diagnosis

- Lacrimal gland malignant tumour such as ACC, pleomorphic adenocarcinoma, mucoepidermoid carcinoma, etc.
- Lymphoma and reactive lymphoid hyperplasia
- Dacryoadenitis specific and non-specific
- Metastasis

Imaging

On MRI, a lobular extraconal mass with irregular margins was seen in the left lacrimal gland fossa with proptosis. It was isointense to muscle in T1w, heterogeneously hyperintense in T2w sequences with intense contrast enhancement (Fig. 51.3). Low T2w signal foci within the mass were suggestive of blood products or calcification.

Laterally, the mass was seen to invade the lateral wall of the left orbit (Figs. 51.3 and 51.4). There was also extension into the periorbital soft tissues. The mass was abutting left lateral aspect of the globe but the scleral margins remained well-defined (Fig. 51.4). Superiorly, there was also suggestion of erosion of orbital roof, but no definite intracranial extension was noted. There was retrobulbar extension of the mass inseparable from the superior rectus-levator muscle complex and the lateral rectus muscle.

The impression was of an aggressive left lacrimal gland mass with osseous invasion into the lateral wall and possibly roof of the left orbit. No definite intracranial or perineural extension was noted.

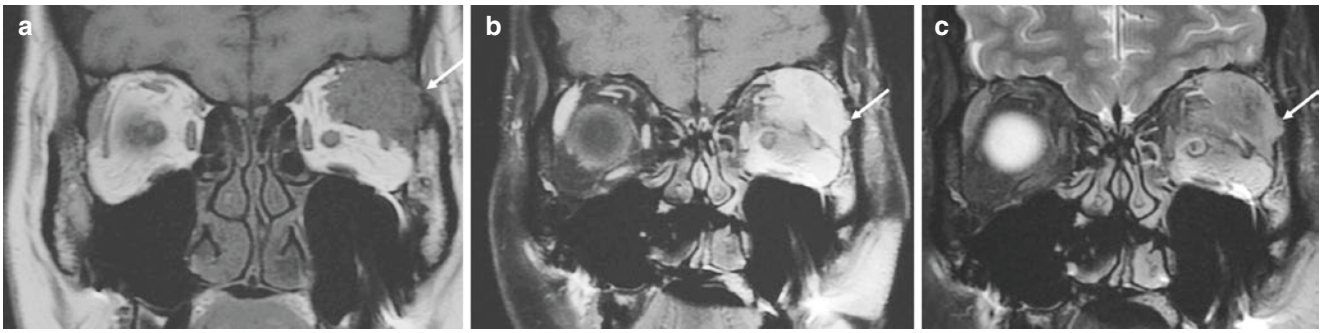

Fig. 51.3 (**a**) T1w pre-contrast, (**b**) T1w post-contrast and (**c**) T2w-FS coronal MRI sections of the orbits showing a lobulated soft tissue mass with irregular borders in the supero-lateral aspect of left orbit, inseparable from the lacrimal gland, superior muscle complex and lateral rectus with invasion of the lateral orbital wall (white arrow)

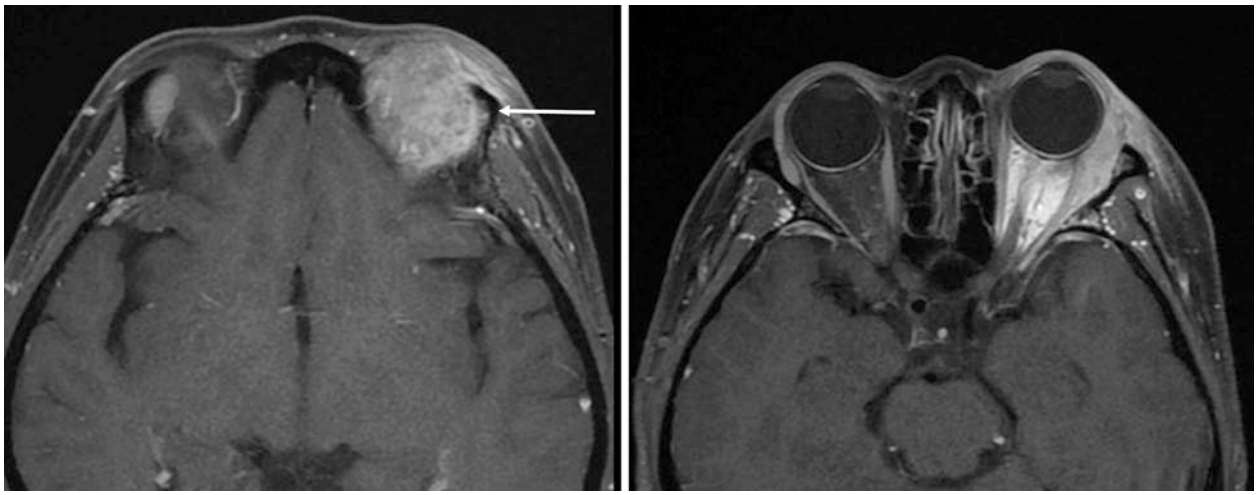

Fig. 51.4 T1w post-contrast axial MR images. Left: showing soft tissue mass occupying the superior aspect of the left orbit with invasion of the mass into the lateral orbital wall (white arrow). Right: showing the mass abutting the globe and the lateral rectus. Note the left proptosis

Intervention

Following an incisional biopsy of the mass through a lid crease approach, the patient subsequently underwent a lateral orbitotomy with removal of the tumour and overlying bone.

Histopathology

The tumour predominantly exhibited infiltrative nests of cells with cribriform and tubular pattern (Fig. 51.5). Cribriform pattern is one where there are multiple rounded lumina within a sheet of cells. The pattern is classically seen in adenoid cystic carcinoma. The tumour cells were small with dark angulated hyperchromatic nuclei and scant amounts of cytoplasm. They surround pseudo-glandular spaces containing basement membrane material, as well as true glandular spaces containing mucin (Fig. 51.6). Mitotic activity was 3/10 HPFs. The stroma showed hyalinization, focal myxoid change and calcifications. Perineural invasion

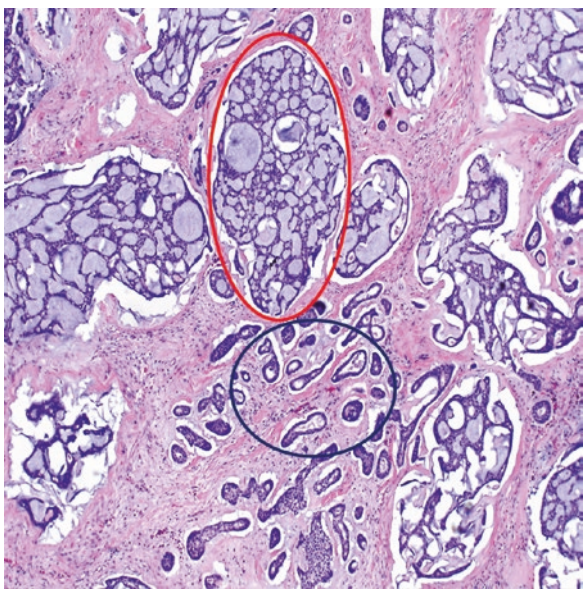

Fig. 51.5 The tumour exhibits both cribriform (red circle) and tubular (black circle) areas. Within the cribriform areas, some greyish mucoid material is seen within the lumina. This appearance is very classical in adenoid cystic carcinoma. HE stain, 40× magnification

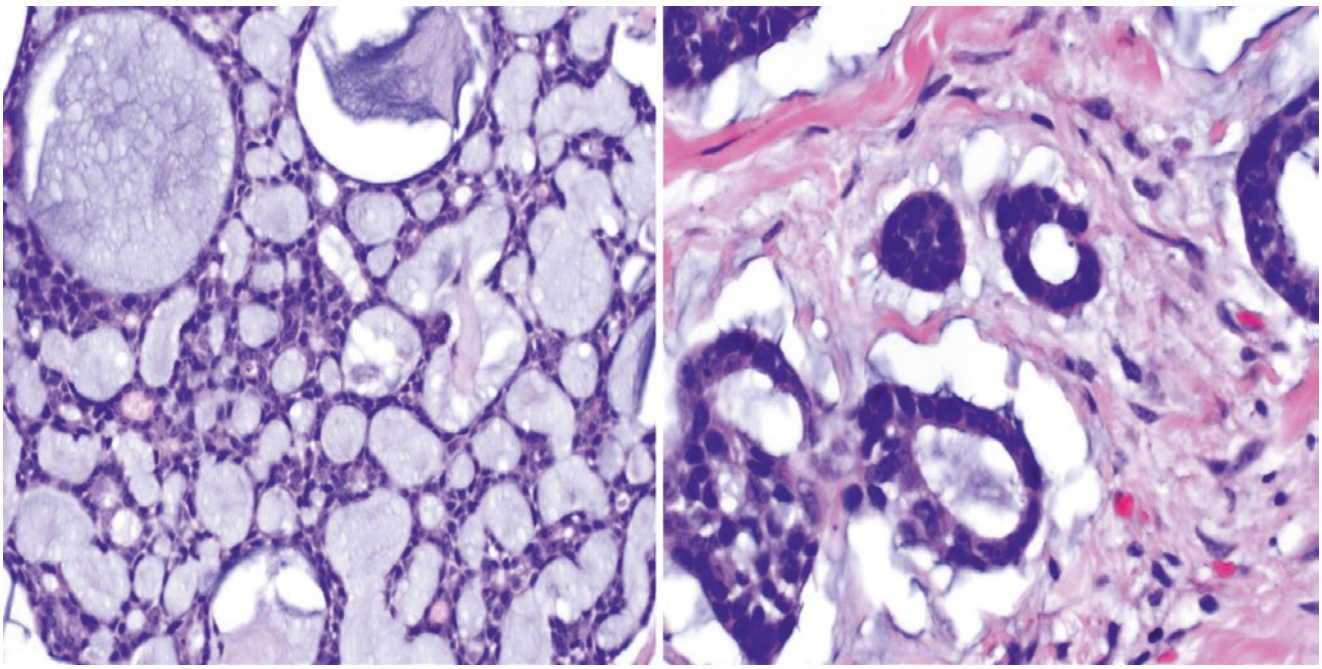

Fig. 51.6 The tumour cells are small with dark angulated hyperchromatic nuclei and scant amounts of cytoplasm. They surround pseudoglandular spaces containing myxoid basophilic material (left), as well as true glandular spaces containing mucin (right). Left: HE stain; 200× magnification. Right: HE stain; 400× magnification

(common in adenoid cystic carcinoma) and infiltration and destruction of smooth muscle fibre bundles were seen. Normal lacrimal gland parenchyma was not identified.

Immunohistochemistry: Tumour cells exhibited strong CD117 and CK7 positivity which confirmed the diagnosis of adenoid cystic carcinoma. p53 showed nuclear positivity in abluminal tumour cells around the tubules and scattered cells at the periphery of solid cell nests. Ki67 proliferation index was about 15–20%.

A diagnosis of basaloid neoplasm, most consistent with adenoid cystic carcinoma (grade 3), was made.

Management

Systemic workup including PET scan was negative for regional and distant tumour metastasis. Final staging: TNM classification, T3N0M0.

She was subjected to concurrent adjuvant chemo (with cisplatin) and fractionated stereotactic radiotherapy surgical excision. The patient has been on regular follow-up and after 3 years of disease free interval, she presented with recurrence of the disease in cavernous sinus and multiple distant metastasis.

Discussion

Malignant lacrimal gland tumours present with shorter duration of history, usually less than a year of clinical symptoms compared to benign tumours. The proptosis is usually in a down- and inward direction. Malignant epithelial lesions typically present as pain or paraesthesia over V1 distribution due to perineural invasion. A hard lump in the lacrimal gland fossa may be palpable. An incisional biopsy is appropriate, especially if the imaging findings also suggest an infiltrative lesion or bone erosion. The imaging characteristics are irregular margins, nodularity, infiltration of adjacent tissues, calcification and bone destruction. If there is any suspicion of a benign tumour, complete removal of the tumour is advised. Tumour staging (TNM) for malignant lacrimal gland tumour has been worked out in detail by the American Joint Committee on Cancer (AJCC).

A t(6;9) chromosomal translocation resulting in MYB-NFIB gene fusion is present in adenoid cystic carcinomas. A molecular assay can be used to test for the presence of MYB-NFIB gene fusion in the tumour, and this opens the avenue for research into targeted therapy in future.

Histologically, there are five types recognized, namely, cribriform, sclerosing, basaloid, comedogenic and ductal.

ACC is notorious for slow growth and local recurrences despite treatment. The estimated 5-year survival is about 50%, regardless of treatment. The prognosis depends on age (less aggressive in children and adolescents), AJCC T category (worse in cases with T3 with 2.5–5 cm in greatest diameter), histological type (basaloid pattern carrying the worst prognosis), perineural invasion and bone invasion. About 93% of patients with local recurrence had perineural invasion at diagnosis. The tumour disseminated faster if the bone invasion was evident.

Management although controversial, has evolved significantly over the decades. Exenteration followed by orbitectomy and adjuvant radiotherapy was the standard of treatment in the past with no survival benefits. Currently, the recommended regimen is to resect the tumour fully, followed by adjuvant platinum-based chemotherapy and external beam radiation. The other alternatives to external beam radiation are proton beam therapy and brachytherapy with I-125, which have only been used in small number of patients. Neoadjuvant intra-arterial chemotherapy followed by exenteration and radiotherapy and further adjuvant chemotherapy improved survival in a study with small number of patients. The intra-arterial chemotherapy needs additional case-controlled studies to substantiate its effectiveness without serious side effects.

Learning Points

ACC is a difficult tumour to treat and should be suspected in cases where there is painful mass lesion in the lacrimal gland with a shorter duration of history. It is important to know the clinical signs and imaging characteristics so as to diagnose the tumour early. Current consensus on management regimen includes tumour resection followed by either radiotherapy or chemo-radiotherapy.

Further Reading

1. Andreason S, Esmaeli B, von Holstein SL, et al. An update on tumours of the lacrimal gland- a review. Asia Pac J Ophthalmol. 2017;6:159–72.
2. Ahmad SM, Esmaeli B, Williams M, et al. American joint committee on Cancer classification predicts outcome of patients with lacrimal gland adenoid cystic carcinoma. Ophthalmology. 2009;116:1210–5.
3. Gamel JW, Font RL. Adenoid cystic carcinoma of the lacrimal gland: the clinical significance of a basaloid histologic pattern. Hum Pathol. 1982;13:219–25.
4. Rootman J. Diseases of the orbit, a multidisciplinary approach. 2nd ed. Philadelphia: Wolters Kluwer Lippincott Williams & Wilkins; 2003.
5. Shields JA, Sheilds CL, Freire JE, et al. Plaque radiotherapy for selected orbital malignancies: preliminary observations. Ophthal Plast Reconstr Surg. 2003;19:91–5.
6. Tellado MV, McLean IW, Specht CS, et al. Adenoid cystic carcinomas of the lacrimal gland in childhood and adolescence. Ophthalmology. 1997;104:1622–5.
7. Tse DT, Kossler AL, Feuer WJ, et al. Long-term outcomes of neoadjuvant intra-arterial cytoreductive chemotherapy for lacrimal gland adenoid cystic carcinoma. Ophthalmology. 2013;120:1313–23.
8. von Holstein SL, Coupland SE, Briscoe D, et al. Epithelial tumours of the lacrimal gland: a clinical, histopathological, surgical and oncological survey. Acta Ophthalmol. 2013;91(3):193–293, e169–e252
9. Williams MD, Al-Zubidi N, Debnam JM, et al. Bone invasion by adenoid cystic carcinoma of the lacrimal gland: preoperative imaging assessment and surgical considerations. Ophthal Plast Reconstr Surg. 2010;26:403–8.
10. Woo KI, Yeom A, Esmaeli B. Management of Lacrimal Gland Carcinoma: lessons from the literature in the past 40 years. Ophthal Plast Reconstr Surg. 2016;32:1–10.
11. Wright JE, Rose GE, Garner A. Primary malignant neoplasms of the lacrimal gland. Br J Ophthalmol. 1992;76:401–7.

Lacrimal Gland: Ductal Adenocarcinoma

52

Gangadhara Sundar, Stephanie Ming Young, Eric Ting, Bingcheng Wu, Min En Nga, and Shantha Amrith

Introduction

Lacrimal gland fossa lesions account for 10–15% of all orbital neoplasms. Pathologic entities of the lacrimal gland generally follow the rule of 'half and half, and yet another half'. Depending on how it is classified, about half of the pathology are inflammatory lesions, and half of the remainder are malignant neoplasms. These include the sinister spectrum of carcinomas. It is for this reason a high degree of suspicion should be had for significant pathology in all lacrimal gland lesions, especially in the adults and elderly, with a low threshold for tissue diagnosis following imaging.

Clinical Scenario

A 48-year-old Southeast Asian male presented with a 2-month history of redness, pain, and blurred vision of the left eye. He was reportedly well prior to this illness and had been treated as a viral conjunctivitis without response. He was subsequently suspected to have an orbital lymphoma prior to referral to our institution. Ophthalmic examination revealed a normal right globe and adnexa. On the left, he had a subnormal visual acuity, conjunctival injection, grade I RAPD, and 6 mm of proptosis with global restriction of ocular motility especially in down gaze (Fig. 52.1). There was a firm palpable mass in

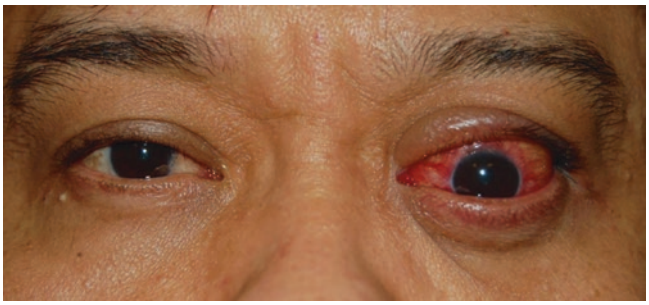

Fig. 52.1 Clinical picture of the patient showing a left proptosis with downward displacement of the eye and conjunctival injection

Table 52.1 CLOSE summary

*C*linical process – mass, infiltrative lesion
*L*ocation – left superotemporal quadrant of the orbit
*O*nset – subacute to chronic
*S*ymptoms and signs – pain, redness and fullness of the upper lid with palpable mass, and limitation of ocular motility
*E*pidemiology – young Southeast Asian male

G. Sundar · S. M. Young · S. Amrith (✉)
Department of Ophthalmology, National University Hospital, Singapore

Department of Ophthalmology, Yong Loo Lin School of Medicine, National University of Singapore, Singapore
e-mail: gangadhara_sundar@nuhs.edu.sg; stephanie.young@nuhs.edu.sg; shantha_amrith@nuhs.edu.sg

E. Ting
Department of Diagnostic Imaging, National University Hospital, Singapore

Department of Diagnostic Imaging, Yong Loo Lin School of Medicine, National University of Singapore, Singapore

Advanced Medicine Imaging, Singapore

B. Wu
Department of Pathology, National University Hospital, Singapore

M. E. Nga
Department of Pathology, National University Hospital, Singapore

Department of Pathology, Yong Loo Lin School of Medicine, National University of Singapore, Singapore

S. Amrith et al. (eds.), *Ocular Adnexal Lesions*, https://doi.org/10.1007/978-981-13-3798-7_52

the superotemporal quadrant with paraesthesia of the left supraorbital and lacrimal region. The corneal epithelium was irregular, and anterior chamber was quiet but with an irregular pupil. Fundus examination was normal. Regional and systemic examinations were unremarkable (Table 52.1).

Differential Diagnosis

- Inflammatory
  - Infective dacryoadenitis: e.g. tuberculosis, viral dacryoadenitis
  - Non-infective: ruptured dermoid cyst, specific orbital inflammatory syndromes: granulomatosis with polyangiitis (GPA/Wegener's), sarcoidal lesion, other specific orbital inflammatory syndromes, NSOID
- Neoplastic
  - Malignant: lymphoma (high grade), primary malignant neoplasm of the lacrimal gland (adenoid cystic carcinoma, adenocarcinoma, mucoepidermoid carcinoma, etc.), lacrimal gland invasion from overlying ocular surface malignancy, e.g. sebaceous gland carcinoma, and metastasis

Imaging

MRI with gadolinium showed a poorly marginated, infiltrative, enhancing mass centred on the left lacrimal gland, with extensive intra- and extraconal extensions in the superior and lateral orbit (Fig. 52.2). Posteriorly, it extended to the orbital apex, with infiltration of the lateral rectus and superior muscle complex. The supraorbital nerve was encased within the mass and showed abnormal enhancement. There was infiltration of the preseptal soft tissues spilling out over the lateral orbital rim. There was suspicion of bony erosion at the level of the frontozygomatic suture, with loss of the normal marrow signal in the zygoma, and part of the greater wing of the sphenoid. The left globe was displaced inferiorly and left-sided proptosis was observed.

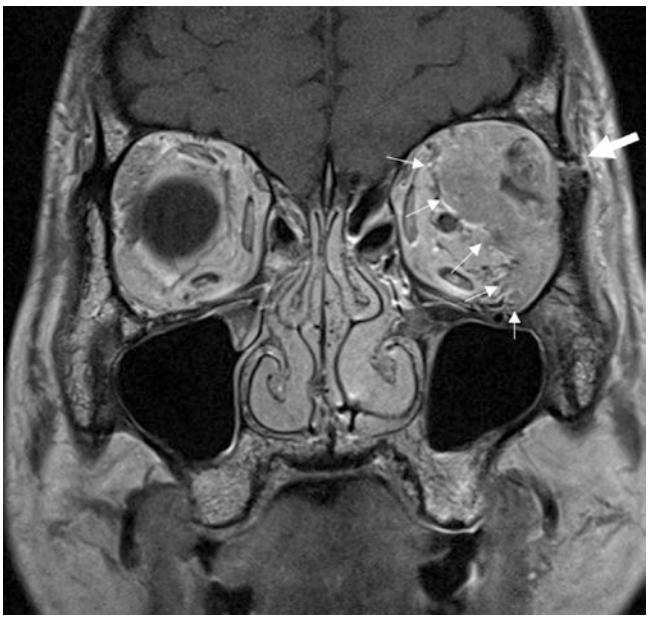

Fig. 52.2 Coronal T1w + C image showing a poorly marginated, infiltrative mass centred on the left lacrimal gland, with extensive intra- and extraconal extensions (thin white arrows). There is infiltration of the lateral rectus and superior muscle complex. Bony involvement of the left lateral orbital rim and wall is present (thick white arrow)

Intervention

As the suspicion for primary malignancy was high, an incisional biopsy was performed. The lacrimal gland appeared inflamed and felt gritty on dissection. Specimen was sent for imprint cytology and formal histopathology.

Histopathology

There was effacement of the lacrimal gland by a malignant tumour composed of infiltrative clusters and variably sized rounded nests of malignant cells (Fig. 52.3). Comedonecrosis (central areas of necrosis) was conspicuous within the rounded nests (Fig. 52.3-inset). The polygonal neoplastic cells exhibited moderate to marked and ample amounts of eosinophilic cytoplasm. Mitotic figures were frequently seen.

No normal lacrimal gland or epithelial-lined structure was evident.

Immunohistochemistry: The tumour cells were positive for CK7 and CerbB2 (Fig. 52.4).

The morphological and immunohistochemical features were consistent with a primary poorly differentiated ductal adenocarcinoma. Further molecular testing for HER-2/neu gene amplification showed positive results.

Final diagnosis of ductal type of adenocarcinoma of the left lacrimal gland with HER-2/neu positivity was made.

Systemic Investigation

PET–CT scan revealed the absence of regional or distant systemic metastasis.

Management

The patient underwent three cycles of neoadjuvant therapy (chemoreduction) with targeted therapy against Herceptin receptor (cisplatin, docetaxel, and Herceptin) following which he underwent a complete lacrimal gland excision with

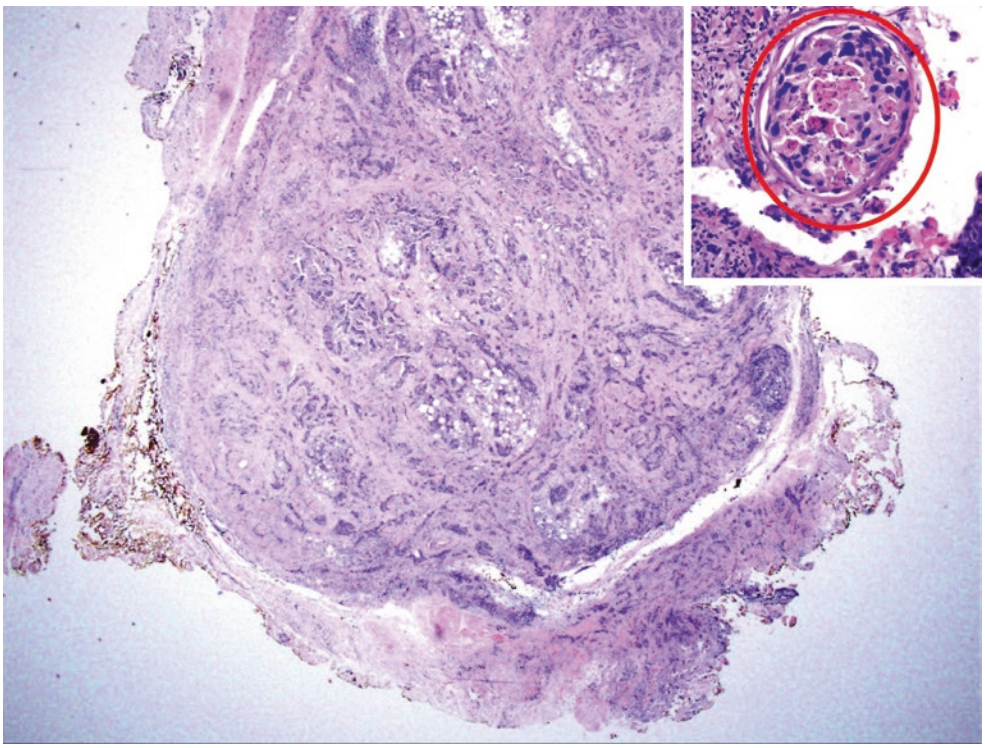

Fig. 52.3 There is effacement of lacrimal gland by a malignant tumour composed of infiltrative clusters and rounded nests of malignant cells. Comedonecrosis is conspicuous within these tumour cell nests (inset; red circle). The polygonal neoplastic cells exhibit moderate to marked nuclear atypia and ample amounts of eosinophilic cytoplasm. Main: HE stain; 40× magnification. Inset: HE stain; 200× magnification

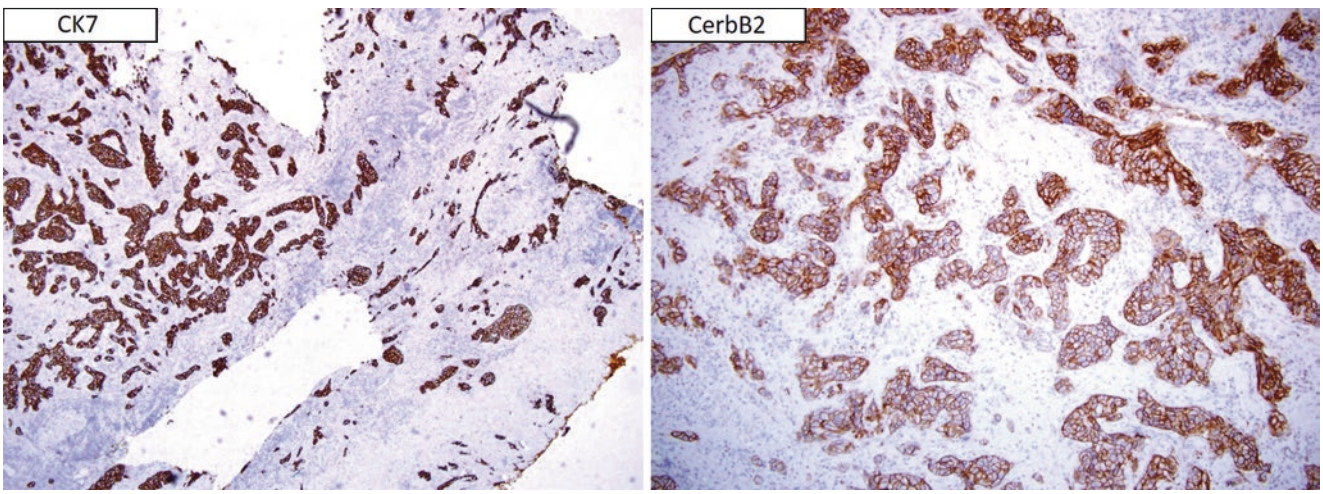

Fig. 52.4 The tumour cells are positive for CK7 (left) and CerbB2 (right). Left: Immunohistochemistry (CK7 antibody), 40× magnification. Right: Immunohistochemistry (CerbB2 antibody), 100× magnification

overlying orbitectomy under frozen section control. Both tissues showed extensive fibrosis without obvious evidence of viable tumour. He continued six more cycles of chemotherapy followed by radiation of the left orbit, overlying bone, and the cavernous sinus.

Discussion

Ductal adenocarcinoma, first described in the lacrimal gland by Katz et al., is a rare tumour and affects men (4:1 male to female ratio) typically in their seventh decade. It is similar to the salivary ductal carcinoma and that of the breast. The more common types of malignant neoplasms of the lacrimal gland include adenoid cystic carcinoma, including its various histopathological types, adenocarcinoma, mucoepidermoid carcinoma, and carcinoma ex pleomorphic adenoma (malignant mixed cell tumour).

Primary malignant epithelial neoplasms of the lacrimal gland are frequently misdiagnosed in their early stages and often carry a poor prognosis even when aggressively managed. Factors associated with poor prognosis include late detection with extensive orbital invasion, overlying bone invasion, preexisting undetected cavernous sinus or skull base extension, poor differentiation, regional or systemic spread at presentation, and inadequate and incomplete treat-

ment. Drawing from the experience of the salivary gland ductal carcinomas, the poor prognosis of patients with lacrimal duct carcinomas could be associated with the overexpression of androgen receptor (in 83%), HER-2/neu protein positivity (in 66.6%), and Ki-67 and p53 expressions. Principles of management include high degree of suspicion with early detection by tissue diagnosis and systemic or local chemoreduction followed by either globe-sparing surgical removal or orbital exenteration. Regional lymph node dissection when tumour spread is detected preoperatively followed by postoperative radiation should be considered. Long-term monitoring for local recurrence (facial, intracranial) and regional (cervical lymph nodes) and systemic metastasis should be performed. Overexpression of androgen receptor and HER-2/neu protein positivity raises the possibility of targeted therapy in these patients. The mortality is about 40%.

Learning Points

Malignant tumours of the lacrimal gland should be considered in the differential diagnosis of persistent 'inflammatory, painful' lesions of the lacrimal gland in adults especially if not responding to conservative management. An earlier stage at diagnosis followed by appropriate management by a multimodal multidisciplinary approach with long-term monitoring often benefits the patients. Despite early and aggressive intervention, the prognosis remains guarded. Patients need regular follow-up and close monitoring.

Further Reading

1. Katz SE, Rootman J, Dolman PJ, White VA, Berean KW. Primary ductal adenocarcinoma of the lacrimal gland. Ophthalmology. 1996;103(1):157–62.
2. Kubota T, Moritani S, Ichihara S. Clinicopathologic and immunohistochemical features of primary ductal adenocarcinoma of lacrimal gland: five new cases and review of literature. Graefes Arch Clin Exp Ophthalmol. 2013;251(8):2071–6.
3. Tse DT, Hui JI. Epithelial tumours of the lacrimal gland. In: Albert DM, Miller JW, Azar DT, et al., editors. Albert & Jakobiec's principles and practice of ophthalmology. 3rd ed. Philadelphia: Saunders Elsevier; 2008.

Lacrimal Sac: Epithelial Tumours

53

Shantha Amrith, Stephanie Ming Young, Eric Ting, Bingcheng Wu, Min En Nga, and Gangadhara Sundar

Introduction

Since the 1930s, only 775 cases of lacrimal sac tumours have been reported worldwide. Among these, more than 55% are malignant, of which more than 66% are of epithelial origin, the most common being squamous cell carcinoma (58%). Other sac tumours include epithelial tumours such as adenocarcinoma, mucoepidermoid carcinoma, adenoid cystic carcinoma, and occasionally non-epithelial tumours such as lymphoma and rarely melanoma. Due to rarity of these tumours, most of the data is extrapolated from studies on sinonasal malignancies with orbital and lacrimal system involvement. The sinister nature of these tumours has been well recognized, and the lack of a consensus continues to make the management of these tumours a challenge.

Case Scenario 1

A 62-year-old Chinese male presented with tearing from the left eye of 2 months' duration. This was associated with pain and swelling on the inner corner. On examination, there was a left non-axial globe displacement superolaterally, with a firm noncompressible medial canthal mass, fixed to deeper structures. There was ulceration on the overlying skin (Fig. 53.1). The mass involved the lower lid, inferior punctum and lower canaliculus, with normal-appearing superior punctum. The patient was orthophoric, with full ocular motility, and the rest of the ophthalmic examination was normal.

Regional examination did not reveal any palpable preauricular and submandibular nodes. On nasal endoscopy, there was crowding of the left nasal cavity, with fullness of the lateral nasal wall involving the inferior/middle turbinate.

CLOSE summary is given in Table 53.1.

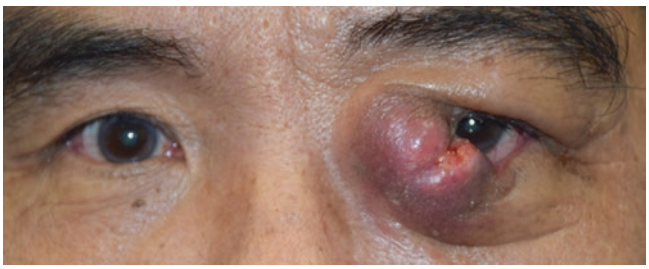

Fig. 53.1 Clinical picture of case 1 showing an ulcerated mass in the left medial canthal area

S. Amrith (✉) · S. M. Young · G. Sundar
Department of Ophthalmology, National University Hospital, Singapore

Department of Ophthalmology, Yong Loo Lin School of Medicine, National University of Singapore, Singapore
e-mail: shantha_amrith@nuhs.edu.sg; stephanie.young@nuhs.edu.sg; gangadhara_sundar@nuhs.edu.sg

E. Ting
Department of Diagnostic Imaging, National University Hospital, Singapore

Department of Diagnostic Imaging, Yong Loo Lin School of Medicine, National University of Singapore, Singapore

Advanced Medicine Imaging, Singapore

B. Wu
Department of Pathology, National University Hospital, Singapore

M. E. Nga
Department of Pathology, National University Hospital, Singapore

Department of Pathology, Yong Loo Lin School of Medicine, National University of Singapore, Singapore

S. Amrith et al. (eds.), *Ocular Adnexal Lesions*, https://doi.org/10.1007/978-981-13-3798-7_53

Differential Diagnosis

- Inflammatory: chronic dacryocystitis, sarcoidal lesion, and granulomatosis with polyangiitis (GPA or Wegener's granulomatosis)
- Malignant lesions of the lacrimal sac: squamous cell carcinoma, transitional cell carcinoma, mucoepidermoid carcinoma and adenocarcinoma, lymphoma and melanoma
- Nasopharyngeal carcinoma
- Benign lesions: inverted papilloma and oncocytoma

Imaging

Computerized tomography (CT) with contrast showed an enhancing radiodense mass centred on the left lacrimal sac with extension to the NLD, the nose and the sinuses. There was bony erosion in the medial orbital wall. MRI showed moderate enhancement and relatively low T2 signal intensity, suggestive of a cellular tumour. The lesion extended anteriorly to the skin and laterally into the orbit compressing the left globe. The mass had also extended into the ethmoids, nasolacrimal duct and left nasal cavity/maxillary sinus which had resulted in obstruction to the drainage (Fig. 53.2). Mucosal thickening and fluid retention were noted in the left maxillary and frontal sinuses.

Table 53.1 CLOSE summary case 1

*C*linical process: infiltrative
*L*ocation: left orbit and lacrimal outflow system
*O*nset: chronic
*S*igns and symptoms: tearing with ulcerated medial canthal mass
*E*pidemiology: elderly Chinese male

Intervention

A transnasal incisional biopsy confirmed the initial impression of malignant tumour of the lacrimal sac. Following a multidisciplinary tumour board discussion, a decision was made to perform wide resection of the tumour, with the possibility of an orbital exenteration.

Histopathology

Nasal mucosal biopsy sections showed multiple fragments of tissue lined by respiratory epithelium admixed with mostly detached nests/strips of squamous epithelium. An

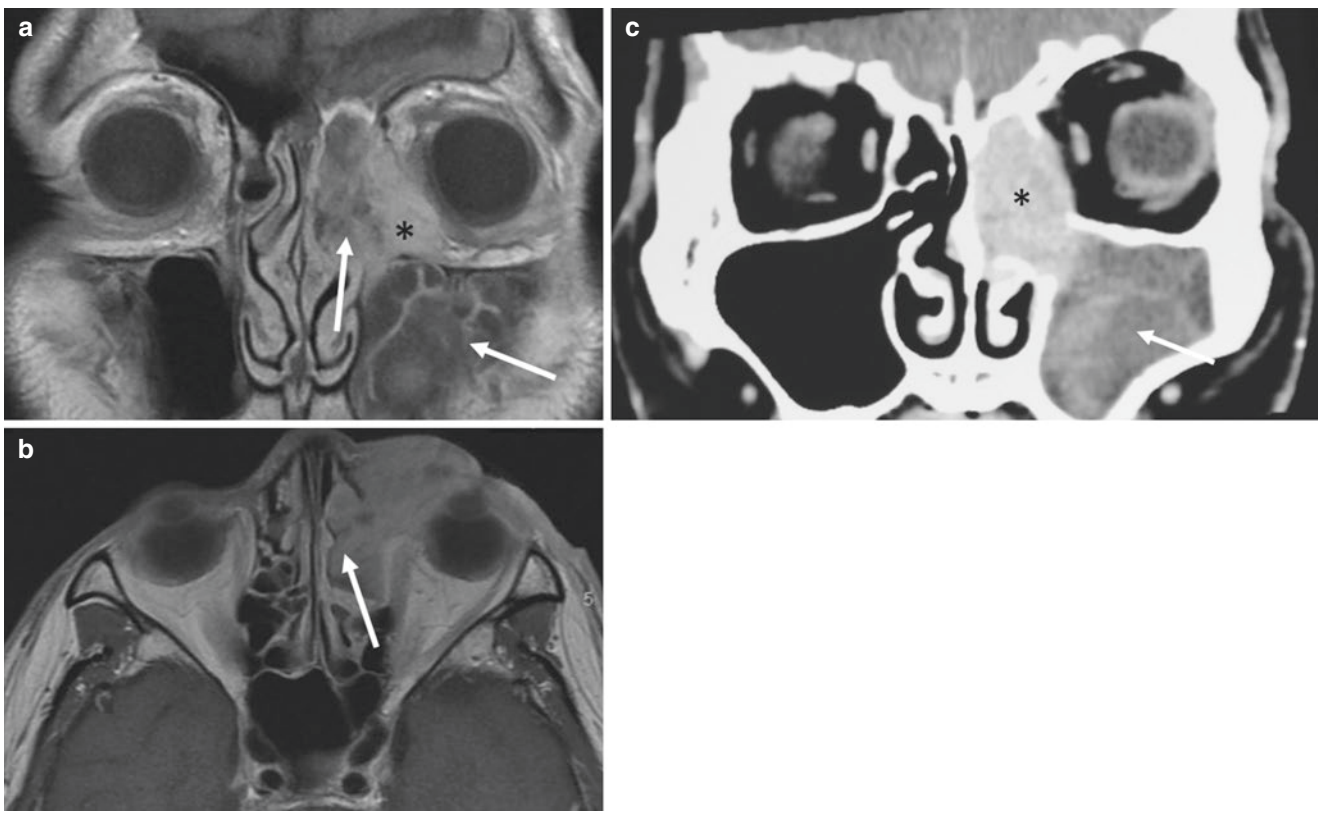

Fig. 53.2 Coronal (**a**) and axial (**b**) contrast-enhanced T1w MRI and coronal CT (**c**) showing enhancing tumour extending from the left lacrimal fossa (*) involving also adjacent ethmoid sinus and medial maxillary sinus with retained secretions (white arrow), and mucosal thickening. Note the thinning/erosion of the medial orbital wall in coronal contrast CT

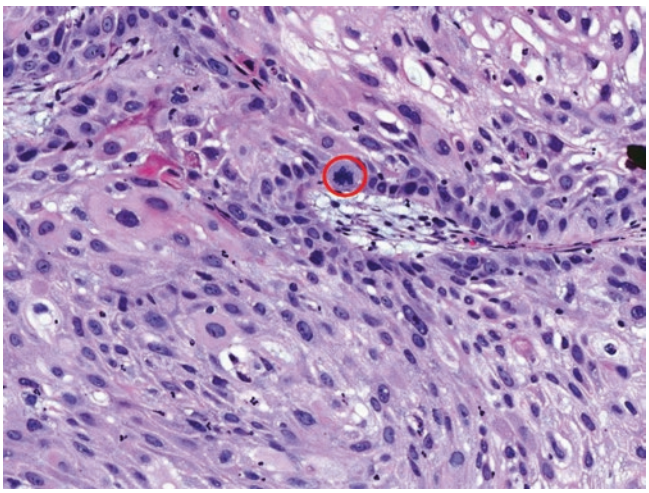

Fig. 53.3 The tumour showing squamous differentiation and nuclear atypia. A mitotic figure seen (red circle). HE stain, 400× magnification

infiltrative tumour composed of invasive nests and sheets of malignant squamous epithelium with nuclear atypia and brisk mitotic activity (Fig. 53.3) was seen. The features were consistent with invasive squamous cell carcinoma.

Management

Staging with TNM classification, the tumour was T4N0M0.

After three cycles of TPF (docetaxel, cisplatin and fluorouracil) induction therapy, the patient had significant regression of mass. He subsequently underwent a left medial maxillectomy with orbitectomy followed by orbital reconstruction.

Case Scenario 2

A 61-year-old Chinese male presented with tearing in his right eye for 2 years. On examination, he was noted to have fullness of the right lacrimal sac area, and a right hyperglobus with no obvious proptosis (Fig. 53.4). The visual acuities, colour vision, pupils and ocular motility were normal. The fundus examination was unremarkable. Syringing on the right side showed regurgitation of clear fluid through the opposite punctum indicating a common canalicular obstruction.

On systemic examination, there was some fullness noted on the right side of the neck.

CLOSE summary is given in Table 53.2.

Differential Diagnosis

Same as case 1

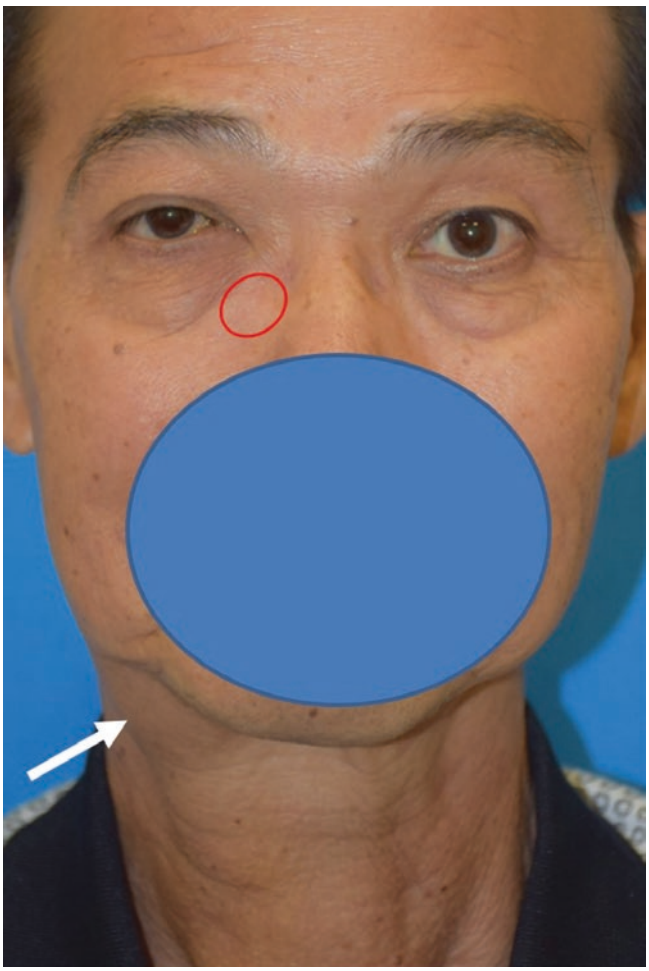

Fig. 53.4 Clinical picture of case 2 showing hyperglobus, reduced palpebral aperture of the right eye and fullness in the lacrimal sac area (red circle). Note the fullness in the neck indicating lymph node enlargement (white arrow)

Imaging

The MRI showed a lobulated heterogeneously enhancing soft tissue mass seen centred in the right lacrimal sac. Anteriorly, the lesion had eroded through the anterior and medial walls of the maxillary sinus, involving the right nasolacrimal duct. The mass was seen extending into the anterior right nasal cavity abutting the middle nasal turbinate (Fig. 53.5). Superiorly, the lesion extended into the floor of the right orbit where it was closely related to the inferior rectus muscle and inferior globe (mildly indented). No intraconal extension was noted.

Intervention

A biopsy from the inferior meatus was obtained and sent for histopathological examination.

Histopathology

Paraffin sections showed fragments of tissue lined by respiratory epithelium and subepithelial stroma containing seromucinous glands. The tumour was composed of infiltrative nests and complex glandular structures within a desmoplastic stroma (Fig. 53.6). The cells exhibited vesicular nuclei and prominent nucleoli. Immunohistochemical stains: the atypical cells were positive for cytokeratin 7. The histological features were consistent with adenocarcinoma. The tumour showed invasion of the maxillary bone and orbital soft tissue.

Table 53.2 CLOSE summary case 2

*C*linical process: mass effect
*L*ocation: right orbit and lacrimal outflow system and neck
*O*nset: subacute
*S*igns and symptoms: tearing with complete lacrimal outflow obstruction and a neck swelling
*E*pidemiology: elderly Asian male

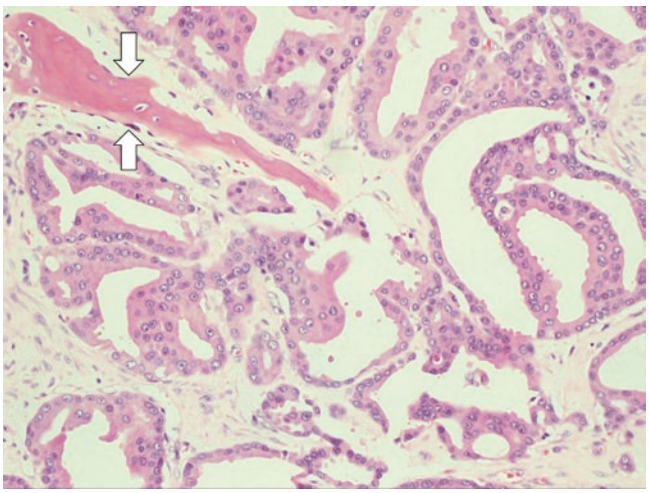

Fig. 53.6 The tumour is composed of infiltrative nests and complex glandular structures within a desmoplastic stroma. The tumour cells possess vesicular nuclei and prominent nucleoli. The tumour invades into the bone (white arrows indicate a bony trabeculum, which is surrounded by tumour). HE stain, 400× magnification

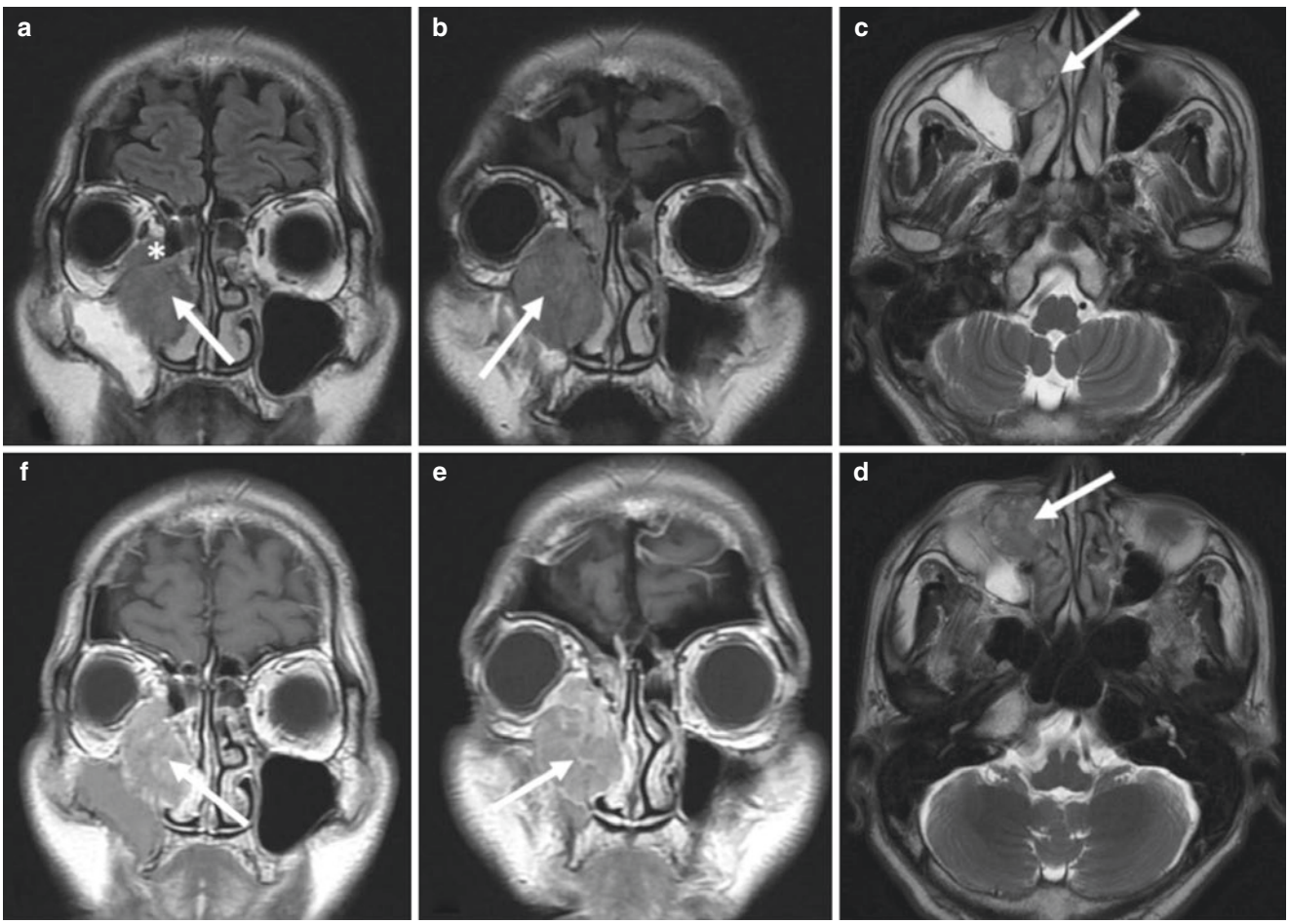

Fig. 53.5 MRI scans: coronal T1w pre- (**a** and **b**) and post-contrast (**e** and **f**) and axial T2w scans (**c** and **d**) showing heterogeneous, contrast-enhancing tumour occupying the nasolacrimal fossa (*), extending into the nasolacrimal duct (white arrow) and involving both the medial right maxillary antrum and floor and medial wall of the right orbit abutting inferomedial surface of the right globe

Management

Staging with TNM classification, the tumour was T4N1M0.

Following a multidisciplinary tumour board discussion, the patient underwent resection of right nasolacrimal tumour with maxillectomy and exenteration with regional lymph node dissection. Frozen sections during surgery revealed tumour-free margins. A primary reconstruction with free flap was performed followed by postoperative radiotherapy.

Discussion

The diagnosis of lacrimal sac tumours is often missed because it usually presents like a dacryocystitis from the nasolacrimal duct obstruction. Initial findings include palpable medial canthal mass that is differentiated from a dacryocoele by its firm and incompressible features as well as its extension above the medial canthal tendon. Other symptoms include epiphora, bloodstained tears, epistaxis, skin telangiectasia over the lacrimal sac and ulceration in late stages of the tumour. Some of the features that may be indicative of a possible lacrimal sac tumour include the presence of a tumefaction in the lacrimal sac fossa with extension above the medial canthal tendon, rapid rate of progression, invasion of neighbouring anatomical structures and resistance to antibiotic treatment.

Typical findings on CT imaging include an enhancing lacrimal sac mass with bony erosion and invasion of tumour into surrounding structures such as the orbit and the paranasal sinuses. T1- and T2-weighted MRI with gadolinium contrast can differentiate between a cystic, inflammatory and solid mass and is able to provide better delineation of neighbouring soft tissue structures such as orbital fatty tissues and extraocular muscles.

Lacrimal sac carcinomas spread mainly by direct invasion of the orbit, paranasal sinuses and the base of the skull. Metastases to preauricular, submandibular, jugulodigastric and cervical lymph nodes are usually late occurrences.

The recommended treatment strategy for lacrimal sac malignancies includes wide surgical resection to include the superior and inferior canaliculi, lacrimal sac, nasolacrimal duct, lacrimal sac fossa and the adjacent ethmoid cells followed by radiation and chemotherapy. Treatment guidelines are veering away from traditional orbital exenteration, and newer methods of intervention are being explored such as intraarterial chemotherapy. Although premature, and lacking long-term follow-up results, initial data shows that this may be a feasible treatment for advanced lacrimal sac carcinoma.

Learning Points

- Symptoms of tearing should not be trivialized. Early diagnosis of lacrimal sac carcinoma is key to the management of this condition.
- Although traditionally orbital exenteration has been considered as “standard of care” for advanced orbital malignancy, new trends are gaining popularity for orbit-sparing approaches (i.e. chemoreduction, radiotherapy, intraarterial chemotherapy).

Further Reading

1. Ali-Farid S, Behn L, Rothamel D, et al. Therapy of sinonasal malignancies invading the orbit-orbital exenteration versus preservation of the orbit plus radiotherapy. *J Craniomaxillofac Surg*. 2017;45(2):258–61.
2. Hibiya R, Ohba S, Fujimaki M, Kojima M, Yokoyama J, Ikeda K. Successful application of intra-arterial chemotherapy for advanced lacrimal sac carcinoma: a report of two cases. Otolaryngol Head Neck Surg. 2016;2(1):128–30.
3. Krishna Y, Coupland S. Lacrimal sac Tumours. Asia-Pac J Ophthalmol. 2017;6:173–8.
4. Montalban A, Liétin B, Louvrier C, Russier M, Kemeny JL, Mom T, Gilain L. Malignant lacrimal sac tumours. Eur Ann Otorhinolaryngol Head Neck Dis. 2010;127(5):165–72.
5. Parmar DN, Rose GE. Management of lacrimal sac tumours. Eye (Lond). 2003;17(5):599–606.
6. Rahangdale SR, Castillo M, Shockley W. MR in squamous cell carcinoma of the lacrimal sac. Am J Neuroradiol. 1995;16(6):1262–4.

Part XIII

Metastatic Tumours

Overview

54

Shantha Amrith and Gangadhara Sundar

Orbital metastatic disease is rare. But with increasing longevity, there has been an increase in the incidence of metastatic disease involving the ocular adnexa in recent years. Carcinomas are more common than melanomas and sarcomas; and adults, aged 40 years and above, are more commonly affected than children. Bilateral orbital metastasis is rare, except in breast carcinoma in adults, and neuroblastoma in children. Common locations of origin include the breast, lung, prostate, gastrointestinal system, and, in Caucasians, cutaneous melanomas. Melanoma and breast cancer have a strong tendency to localize in the orbital fat and muscles, while prostate cancer is well known to metastasize to the bone (hyperostotic lesions).

The metastatic lesions (such as those from breast cancer) may appear months or years after the diagnosis and management of systemic disease. They appear well before the discovery of the primary lesion in a quarter of cases, especially with lung, gastrointestinal, thyroid, and renal carcinomas. When metastasis occurs before the discovery of the primary lesion, exhaustive medical investigations would be necessary to find the primary site including a thorough history taking, a high index of suspicion, and a multidisciplinary approach.

In recent years, there have been advances that make it easier to find the primary tumor. An increase in carcinoembryonic antigen (CEA) is non-specific but, nevertheless, can alert one to the presence of metastasis. Similarly, an increase in prostate-specific antigen in a patient with prostate cancer can suggest metastasis. Some of the other tests include human chorionic gonadotropin (HCG) in seminoma and 5-hydroxyindoleacetic acid (5-HIAA) in urine in carcinoid tumors.

S. Amrith (✉) · G. Sundar
Department of Ophthalmology, National University Hospital, Singapore

Department of Ophthalmology, Yong Loo Lin School of Medicine, National University of Singapore, Singapore
e-mail: shantha_amrith@nuhs.edu.sg; gangadhara_sundar@nuhs.edu.sg

Advanced imaging techniques, fine-needle aspiration biopsies (FNAB), as well as advanced serological and molecular studies may further aid in the identification of the primary tumor. Despite these advances, the primary site remains unknown in about 2% of oncological referrals. Identification of primary site does not alter the management or the prognosis in a majority of cases except lymphomas.

Patients with orbital metastases usually present with rapid onset of diplopia, mild proptosis, displacement of the globe, ptosis of the eyelid, eyelid swelling, pain and redness of the eye with chemosis, and more importantly a decrease in vision. Rarely, the patients develop enophthalmos rather than proptosis. Misdiagnosis and lengthy delay in diagnosis are common in metastatic cancer to the orbit. The signs are often confused with orbital cellulitis, myositis, and idiopathic orbital inflammatory syndrome (pseudotumor). The other differential diagnoses that need to be considered are acute active thyroid orbitopathy, carotico-cavernous fistula, orbital apex (Tolosa-Hunt) syndrome, primary lacrimal gland tumors, and lymphoproliferative disorders. The ophthalmologist, the general physician, and the oncologist should therefore maintain a high level of suspicion in patients with a known history of malignancy, presenting with an acute or subacute ocular, orbital, or adnexal "inflammatory mass" lesion.

Radiological features include diffuse intraconal infiltration, enlargement of a single extraocular muscle, extraconal infiltrative mass, or bony destruction with adjacent soft tissue involvement. Orbital metastasis from breast cancer tends to be diffuse and irregular, often growing along the rectus muscles and fascial planes. On the other hand, orbital metastasis from carcinoid tumor, renal cell carcinoma, and melanoma tends to be more circumscribed in the early stages, before they spread inside the orbit.

Majority of cases (90%) can be diagnosed with a needle aspiration biopsy. Some cases of scirrhous carcinomas (from the lung or breast) or small apical lesions may not yield sufficient tissue for diagnosis. Where a metastasis is sus-

S. Amrith et al. (eds.), *Ocular Adnexal Lesions*, https://doi.org/10.1007/978-981-13-3798-7_54

pected, an open biopsy with debulking of the tumor may be carried out especially if there is optic neuropathy. FNAB can be performed with the tumor exposed by open surgery. The advantage of doing FNAB is less damaging to normal structures especially when there is no clear demarcation between abnormal and normal tissues. The other advantage of needle biopsy is that it not only helps in cytological diagnosis, but also provides a "cell block" for a reasonable histological diagnosis.

Patients with widespread metastasis are treated with chemotherapy. In carcinoma of the breast and prostate, hormone therapy may be considered. Radioiodine in thyroid carcinoma and immunotherapy in melanoma may be helpful.

Isolated orbital metastasis or progression of orbital disease despite chemotherapy can be treated with radiotherapy or proton beam therapy in cases of melanoma. The mean survival of patients with orbital metastasis is about 1.3–2 years, and the survival is not different in patients with and without a known primary. There is slightly a better prognosis in patients with orbital metastasis from breast carcinoma. In some metastatic tumors, such as renal carcinoma, long-term survival after removal of a solitary orbital metastasis has been reported.

In conclusion, although the prognosis is poor, orbital metastases can be treated to give patients a better quality of life.

Further Reading

1. Ahmad SM, Esmaeli B. Metastatic tumors of the orbit and ocular adnexa. Curr Opin Ophthalmol. 2007;18(5):405–13.
2. Char DH, Miller T, Kroll S. Orbital metastasis: diagnosis and course. Br J Ophthalmol. 1997;81(5):386–90.
3. Goldberg RA, Rootman J, Cline RA. Tumors metastatic to the orbit: a changing picture. Surv Ophthalmol. 1990;35(1):1–24.
4. Goldberg R, Rootman J. Clinical characteristics of metastatic orbital tumors. Ophthalmology. 1990;97(5):620–4.
5. Holland D, Maune S, Kovács G, et al. Metastatic tumors of the orbit: a retrospective study. Orbit. 2003;22(1):15–24.
6. Shields JA, Shields CL, Brotman HK, Carvalho C, Perez N, Eagle RC Jr. Cancer metastatic to the orbit: the 2000 Robert M. Curts Lecture. Ophthal Plast Reconstr Surg. 2001;5:346–54.
7. Tijl J, Koornneef L, Eijpe A, Thomas L, Gonzalez DG, Veenhof C. Metastatic tumors to the orbit – management and prognosis. Graefes Arch Clin Exp Ophthalmol. 1992;230(6):527–30.
8. Valenzuela AA, Archibald CW, Fleming B, et al. Orbital metastasis: clinical features, management and outcome. Orbit. 2009;28(2–3):153–9.
9. Volpe NJ, Albert DM. Metastatic and secondary orbital tumors. In: Principles and practice of ophthalmology. 2nd ed. Philadelphia: Saunders; 2003.

Neuroblastoma

55

Mariel Angelou Parulan, Shantha Amrith, Stephanie Ming Young, Eric Ting, Bingcheng Wu, Min En Nga, and Gangadhara Sundar

Introduction

Neuroblastoma, a primary tumour of the adrenal glands, is the most frequent extracranial solid tumour of childhood that arises from the neural crest. The median age of incidence is 1 year. Metastasis from neuroblastoma should be suspected in a child less than 2 years old, presenting with unilateral or bilateral periorbital ecchymosis (raccoon eye), periorbital swelling, haemorrhage, strabismus with restricted eye motility, ptosis or opsoclonus. The most common site of orbital metastasis is the posterolateral orbital wall.

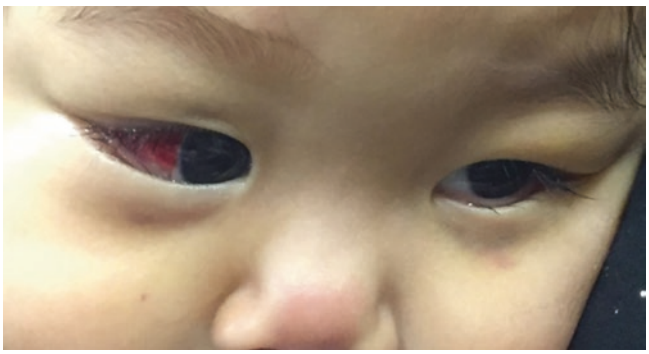

Fig. 55.1 Clinical picture showing right proptosis and fullness in the upper lids with subconjunctival haemorrhage

Case Scenario

A 14-month-old Chinese boy presented with bilateral recurrent bruising which the parents noticed for 2 months prior to presentation. The child was tested for coagulation profile and was found to be normal. There was no history of trauma or fever or any constitutional symptoms. On examination, the child had a gross right proptosis, bilateral ecchymosis and a left hypertropia (Fig. 55.1) with slight fullness in the superotemporal quadrant of both eyes. There was no RAPD.

CLOSE summary is given in Table 55.1.

M. A. Parulan
Department of Ophthalmology, National University Hospital, Singapore

S. Amrith (✉) · S. M. Young · G. Sundar
Department of Ophthalmology, National University Hospital, Singapore

Department of Ophthalmology, Yong Loo Lin School of Medicine, National University of Singapore, Singapore
e-mail: shantha_amrith@nuhs.edu.sg; stephanie.young@nuhs.edu.sg; gangadhara_sundar@nuhs.edu.sg

E. Ting
Department of Diagnostic Imaging, National University Hospital, Singapore

Department of Diagnostic Imaging, Yong Loo Lin School of Medicine, National University of Singapore, Singapore

Advanced Medicine Imaging, Singapore

B. Wu
Department of Pathology, National University Hospital, Singapore

M. E. Nga
Department of Pathology, National University Hospital, Singapore

Department of Pathology, Yong Loo Lin School of Medicine, National University of Singapore, Singapore

S. Amrith et al. (eds.), *Ocular Adnexal Lesions*, https://doi.org/10.1007/978-981-13-3798-7_55

Table 55.1 CLOSE summary

*C*linical process: infiltrative neoplasia/inflammatory
*L*ocation: bilateral orbit
*O*nset: subacute
*S*igns and symptoms: recurrent ecchymosis and bilateral proptosis
*E*pidemiology: 14-month-old Chinese male child

Differential Diagnosis

- Benign:
  - Dermoid cyst (rupture from trauma)
- Malignant:
  - Langerhans cell histiocytosis
  - Rhabdomyosarcoma
  - Neuroblastoma
  - Chloroma

Radiology

The coronal view of CT scan of the orbits and brain showed an expansile destructive bony lesion involving the superolateral wall of the right orbit associated with a large soft tissue component. The right eyeball was displaced medially and anteriorly. The destructive lesion involved the right sphenoid wing (Fig. 55.2).

There was also a large soft tissue component present, just posterior to the right zygomatic arch. Similar bony and soft tissue mass was present involving the lateral wall of the left orbit. There was also involvement of the anterior wall of the left middle cranial fossa (Fig. 55.2). Soft tissue densities were seen in the maxillary antra, and these were associated with soft tissue extension beyond the lateral wall of the left maxillary antrum. These were also similar to lesions described above.

There was no intra-axial mass seen in the brain. The ventricles were not dilated and there was no midline shift.

Intervention

The child underwent right anterior orbitotomy and biopsy, and debulking was carried out. Haemostasis was achieved with bone wax.

Histopathology

Sections showed a small round blue cell tumour composed of sheets of malignant cells with relatively small nuclei, scant cytoplasm, brisk mitotic activity (Fig. 55.3) and frequent apoptotic bodies. No neuropil was seen. The tumour cells were positive for chromogranin (Fig. 55.3) and neuron-specific enolase (NSE), which would be consistent with the diagnosis of neuroblastoma.

Immunohistochemistry: GD2, CD56, CD81 and CD90 were expressed in 30–40% of cells. The cells did not show any staining on CD45, CD34 and CD1a.

Possibility of metastasis from neuroblastoma was considered.

Management

Referral to paediatric oncology service was made.

Bilateral bone marrow aspiration and PET-CT were carried out. The bone marrow showed large and small clusters of round blue non-haemopoietic mononuclear cells with high nuclear cytoplasmic ratio and basophilic cytoplasm with occasional vacuoles. They expressed neuroblastoma-associated immunophenotype.

PET-CT showed increased uptake of radiotracer in both orbits and maxillary sinus, right suprarenal mass, pancreatic head and multiple bones and bone marrow (Fig. 55.4).

Cytogenetics revealed massive MYCN gene amplification and 1p deletion in 26% of cells. 11q deletion was absent.

Tumour staging: International neuroblastoma staging system (INSS): Stage 4.

The child was started on alternating cycles of chemotherapy with vincristine, cyclophosphamide, cisplatin and etoposide and the above regimen except cisplatin which was substituted with carboplatin.

Discussion

Neuroblastoma is a tumour of the sympathoadrenal lineage of the neural crest and the sympathetic nervous system. Presentation is usually with the metastatic disease. Skin metastasis appears bluish, and is sometimes confused with bruising in child abuse. It can be associated with fever, anaemia or weight loss.

Imaging with CT shows aggressive destruction of orbital walls with enhancing soft tissue masses in the orbit and extradural region. MRI shows low signal on T1w image with heterogeneous enhancement and heterogeneous signal in T2w image due to haemorrhage and necrosis. PET-CT helps in staging of the disease and to monitor disease progression.

Histologically round blue cells, uniform in size, with hyperchromatic nuclei and minimal cytoplasm are characteristic. The list of differential diagnoses for paediatric small round blue cell tumours is long: neuroblastoma, rhabdomyosarcoma, Ewing sarcoma and lymphoma to name a few. Correlation with clinical findings and ancillary tests is necessary to ascertain a definitive diagnosis. A novel immunohistochemical marker that has been shown to be sensitive and specific for neuroblastoma is PHOX2B. Amplification of

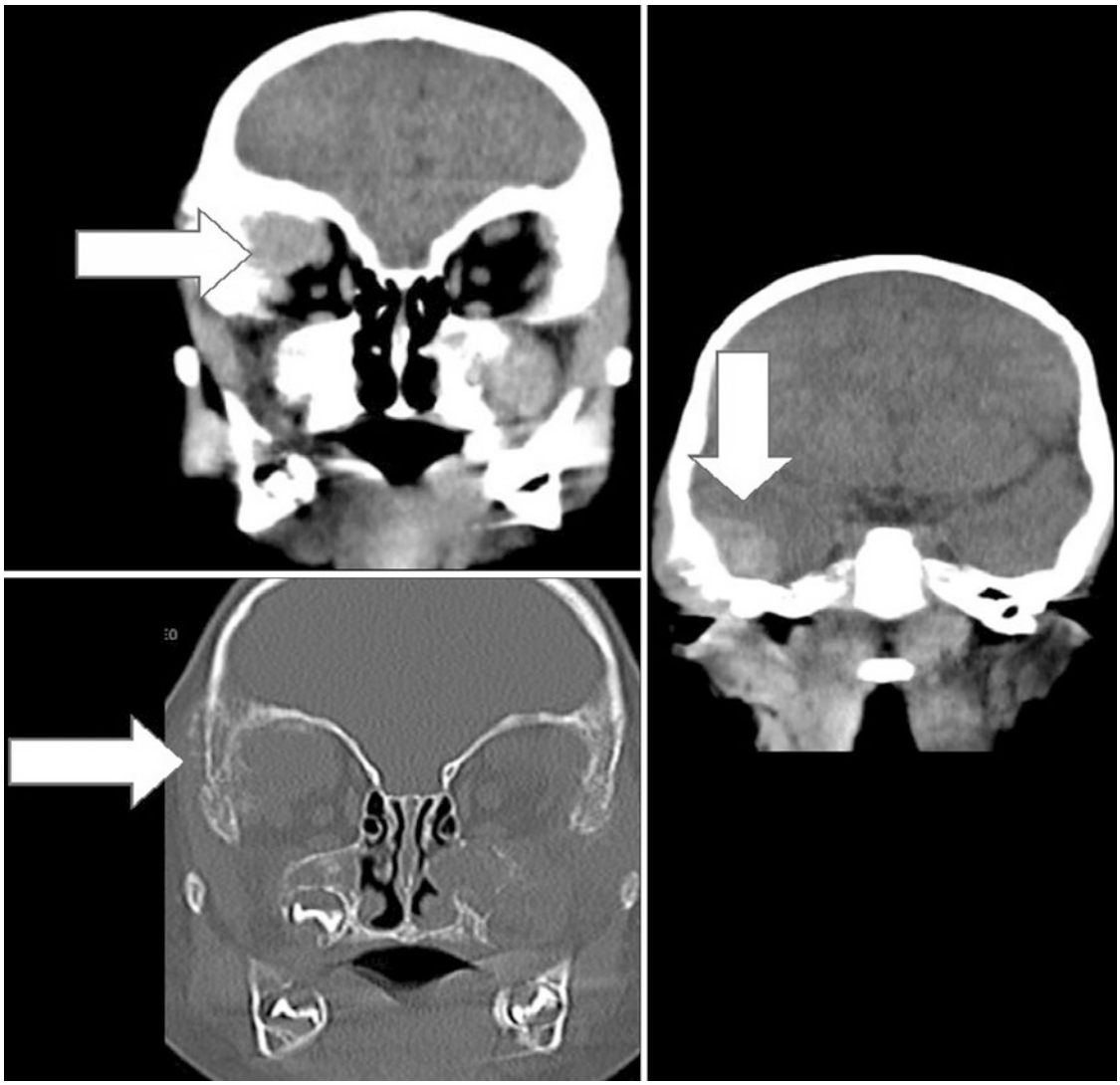

Fig. 55.2 Clockwise from the top left: coronal CT scan showing extraconal tumour (arrow) in the right orbit displacing the superior muscle complex medially and inferiorly (and note an infratemporal mass on the left side), coronal CT scan through the temporal lobe of the brain showing an extra-axial tumour indenting the temporal lobe (arrow), coronal CT scan-bone window showing osseous involvement of the roof and the lateral wall of the right orbit

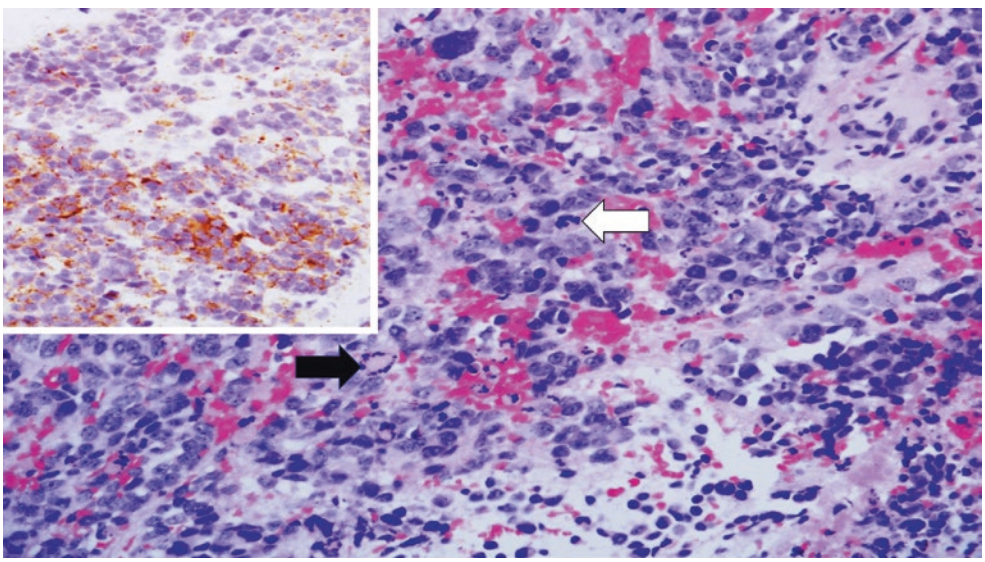

Fig. 55.3 This shows a small round blue cell tumour composed of sheets of malignant cells with hyperchromatic nuclei, high nuclear/cytoplasmic ratios and scant cytoplasm. Mitoses (white arrow) and apoptotic figures (black arrow) are frequently seen. The tumour cells are positive for chromogranin immunohistochemistry (inset). Main: HE stain, 600× magnification. Inset: immunohistochemistry, chromogranin antibody, 400× magnification

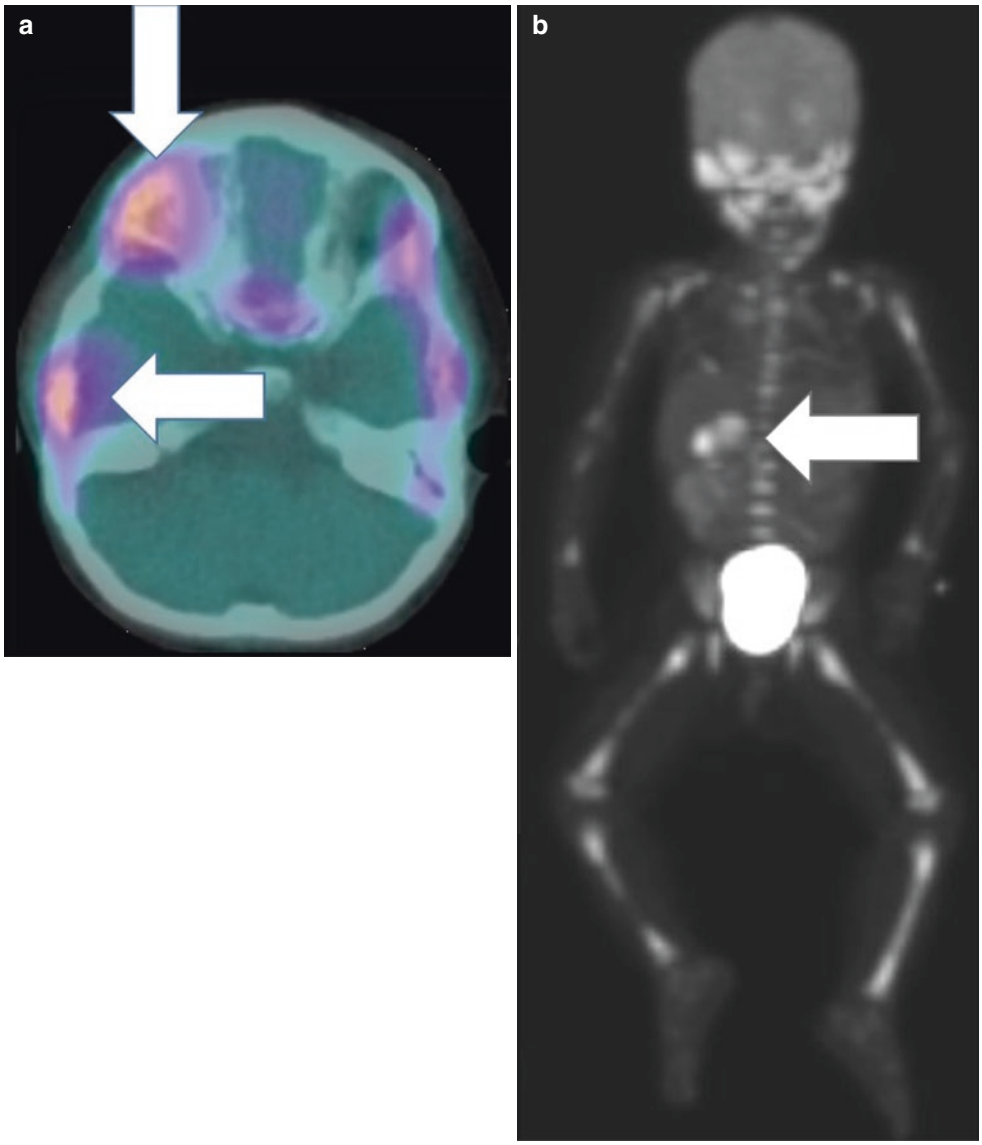

Fig. 55.4 (**a**) Axial PET-CT scan shows abnormal bone activity in the roof of the orbit and temporal bone (arrows). (**b**) Coronal PET scan shows the primary suprarenal tumour (arrow) and multiple osseous deposits

MCY-N oncogene of more than ten copies in metastatic disease indicates poor prognosis, and so does the presence of deletion in 1p36.3 and 11q23.

Treatment depends on stage, size and location of the tumour. Treatment modalities such as observation, surgery, chemotherapy, radiotherapy, stem cell transplant/bone marrow transplant, retinoid therapy and immunotherapy are considered.

Disseminated neuroblastoma has a better prognosis in infants, with a 5-year survival of 80.5%, compared to when they present at more than 1 year of age, where the 5-year survival drops to 45%.

Learning Points

Diagnosis of neuroblastoma should be considered in paediatric patients presenting with proptosis, ecchymosis, ptosis (Horner's syndrome) or opsoclonus. Superotemporal lytic lesions in CT in children with proptosis are almost diagnostic. Multidisciplinary approach in identifying primary tumour, staging, and molecular risk factors is important in the management of patients with neuroblastoma.

Further Reading

1. Kaneko M, Tsuchida Y, Mugishima H, et al. OPEC/OJEC is a well-tolerated therapy for stage 4 neuroblastoma over 1 year of age. Stage 4 neuroblastoma with MYCN amplification. J Pediatr Hematol Oncol. 2002;24(8):613–21.
2. Rao AA, Naheedy JH, Chen JY-Y, Robbins SL, Ramkumar HL. A clinical update and radiologic review of pediatric orbital and ocular tumors. J Oncol. 2013. Article ID 975908, 22 pages. https://doi.org/10.1155/2013/975908.

Carcinoma of Breast

56

Gangadhara Sundar, Stephanie Ming Young, Eric Ting, Bingcheng Wu, Min En Nga, and Shantha Amrith

Introduction

Breast carcinoma accounts for 20–75% of ocular adnexal metastatic tumours. The most common variant is the lobular rather than ductal type. Metastasis to the orbit may occur many years after the primary tumour has been treated, and occasionally bilateral metastasis occurs.

Case Scenario

A 60-year-old South Asian female, presented with a recent onset of pain, pressure sensation and blurring of vision in the left eye for a few weeks before consultation. Prior to referral, she was treated with antibiotics for orbital cellulitis without any response and subsequently with oral steroids with partial improvement. She gave a history of 'lumpectomy' of the left breast a few years earlier without additional treatment.

Ophthalmic examination revealed a Snellen visual acuity of 6/6 and 6/12 in the right and left eyes, respectively. There was a mild left proptosis with redness and brawny induration of the left lower eyelid (Fig. 56.1), a left RAPD and a normal fundus examination. There was global limitation of ocular motility.

CLOSE summary is given in Table 56.1.

Differential Diagnosis

- Inflammatory disorder:
  - Specific orbital inflammation
  - Non-specific orbital inflammatory syndrome
- Neoplastic lesion:
  - Metastatic lesion
  - Hematogenous malignancies (multiple myeloma, leukaemia, etc.)
  - Primary: lymphoproliferative disorders

Imaging

Magnetic resonance imaging (MRI) scan: There was diffuse thickening and enhancement of the left extraocular muscles and retrobulbar fat around the globe indicative of an infiltrative tumour (Fig. 56.2). An irregular soft tissue infiltration was also noted in the pre- and post-septal tissues of the lower eyelid (Fig. 56.2) possibly involving the inferior rectus muscle.

G. Sundar · S. M. Young · S. Amrith (✉)
Department of Ophthalmology, National University Hospital, Singapore

Department of Ophthalmology, Yong Loo Lin School of Medicine, National University of Singapore, Singapore
e-mail: gangadhara_sundar@nuhs.edu.sg; stephanie.young@nuhs.edu.sg; shantha_amrith@nuhs.edu.sg

E. Ting
Department of Diagnostic Imaging, National University Hospital, Singapore

Department of Diagnostic Imaging, Yong Loo Lin School of Medicine, National University of Singapore, Singapore

Advanced Medicine Imaging, Singapore

B. Wu
Department of Pathology, National University Hospital, Singapore

M. E. Nga
Department of Pathology, National University Hospital, Singapore

Department of Pathology, Yong Loo Lin School of Medicine, National University of Singapore, Singapore

S. Amrith et al. (eds.), *Ocular Adnexal Lesions*, https://doi.org/10.1007/978-981-13-3798-7_56

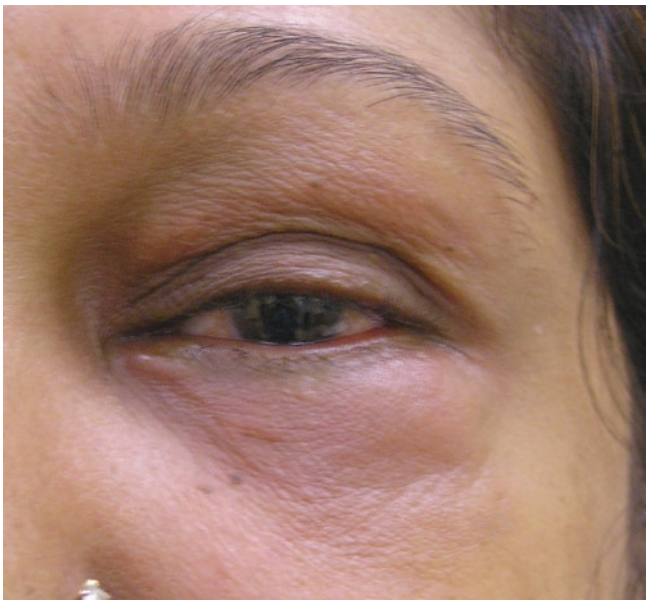

Fig. 56.1 Left periorbital fullness with induration

Table 56.1 CLOSE summary

*C*linical process: inflammatory, infiltrative lesion
*L*ocation: diffuse orbital fat and extraocular muscles, retrobulbar, peribulbar soft tissues
*O*nset: subacute
*S*ymptoms and signs: fullness and induration in the eyelid, proptosis, ocular motility restriction with blurred vision
*E*pidemiology: 60-year-old South Asian female

Intervention

Incisional biopsy of the left inferior rectus and inferior orbital intraconal fat was performed under local anaesthesia through a transconjunctival approach.

Histopathology

There were infiltrative nests of tumour cells within a desmoplastic stroma. Glandular differentiation was seen. The tumour cells exhibited moderate nuclear pleomorphism and strong diffuse nuclear positivity with oestrogen receptor (ER) on immunohistochemistry (Fig. 56.3). The features were those of a metastatic adenocarcinoma. Given the positivity for ER immunohistochemistry, a breast primary was likely and would be consistent with the given clinical history of known left breast carcinoma.

Final Diagnosis

Metastatic carcinoma from the breast to the left orbit

Management

The patient underwent systemic work-up including a PET-CT which revealed multiple bony and lung metastases. She underwent palliative chemotherapy with radiotherapy to the left orbit.

Discussion

There are two phenotypic presentations of metastatic breast carcinoma to the orbit. First is a mass lesion as evidenced by proptosis and imaging features of a distinct mass in the orbit. The second type is where the patient presents with enophthalmos or without proptosis with an ill-defined infiltrative lesion on imaging. Sometimes a small volume mass causes disproportionate symptoms due to its infiltrative nature.

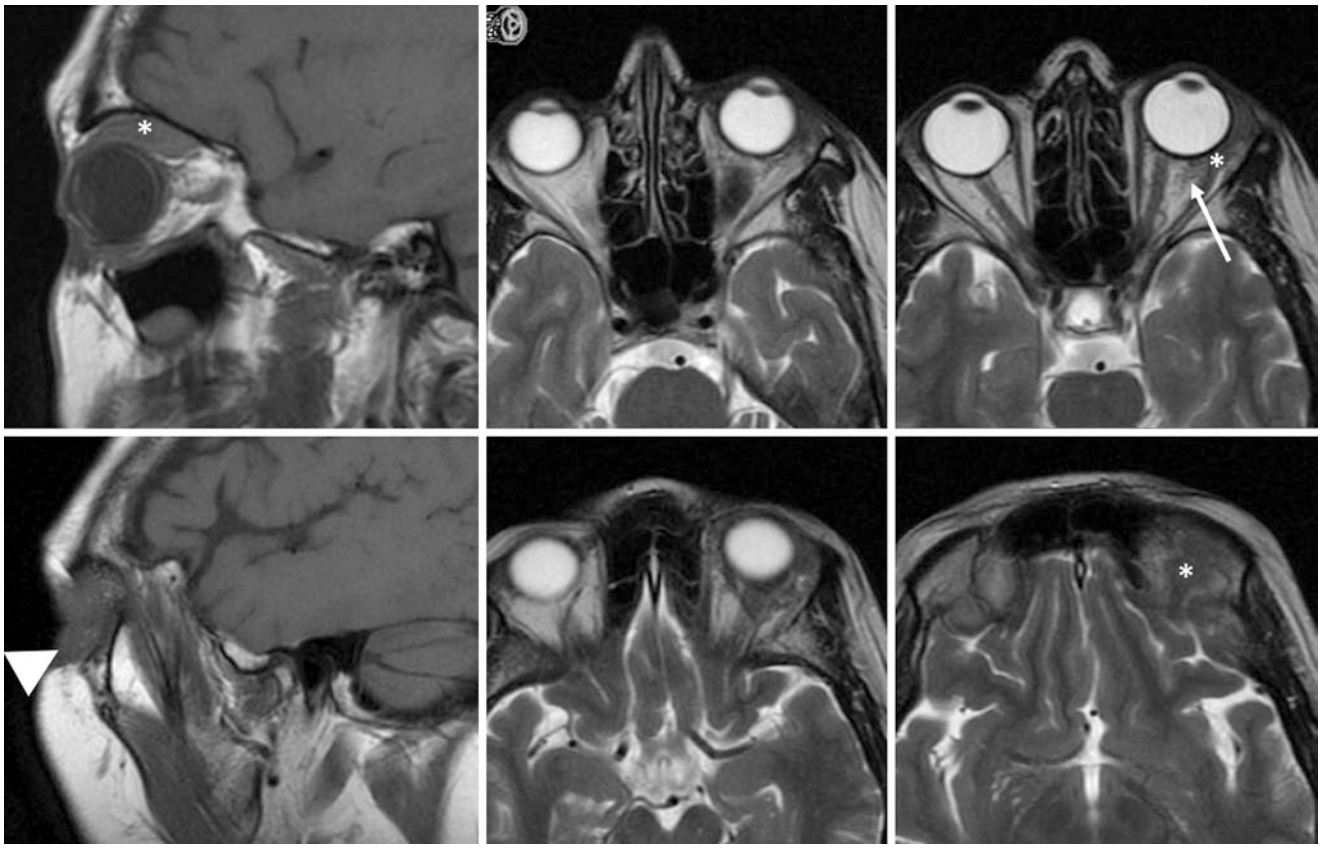

Fig. 56.2 Sagittal T1w and axial T2w sequences showing irregular soft tissue infiltration of the left orbit, involving the pre-septal (arrow head) and post-septal tissues, extraocular muscles (*) and retrobulbar fat (white arrow)

Common presentations include diplopia due to infiltration of muscles and fat, proptosis or enophthalmos, eyelid swelling, ptosis and pain. There may be an associated increase in serum tumour markers.

A biopsy or needle aspiration is not usually necessary as the diagnosis can be made from the history, clinical presentation, imaging characteristics and serological findings. A somewhat more specific immunohistochemical test is GATA3, a nuclear stain which is often positive in breast carcinomas. It should be noted, however, that neither ER nor GATA3 are fully specific, as they might be seen in some other types of tumours as well.

Treatment is palliative, in the form of stereotactic radiotherapy. However, if there is concomitant systemic progressive disease, patients may need additional treatment such as chemotherapy and hormonal therapy in hormone-sensitive cases.

Prognosis of cases with orbital metastasis is rather poor with a median survival of 22–31 months.

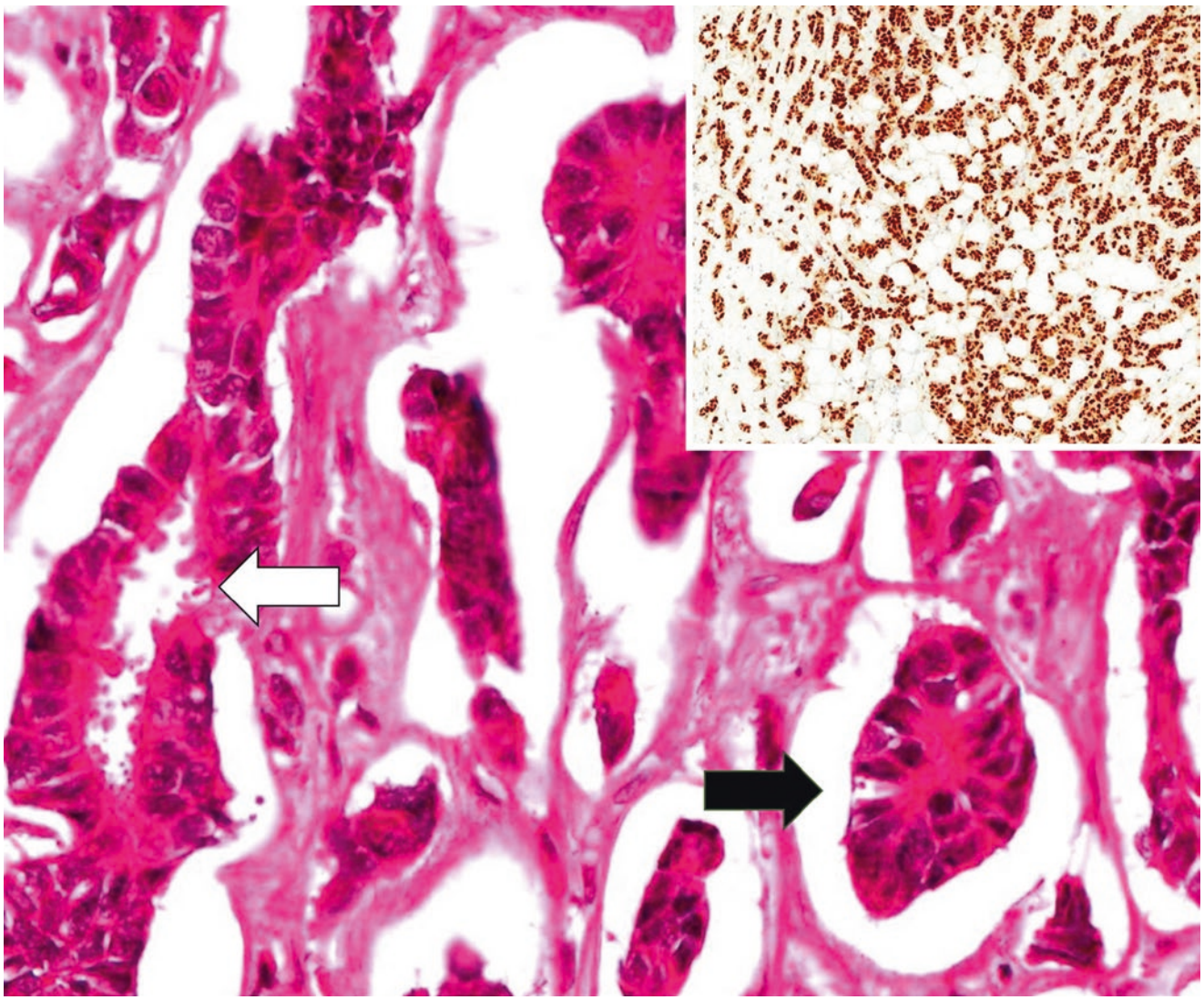

Fig. 56.3 There are infiltrative nests of tumour cells with occasional gland formation (white arrow). Moderate nuclear pleomorphism is appreciated. Artefactual retraction spaces are seen around the tumour nests (black arrow). Main: HE stain, 400× magnification, Inset: Immunohistochemistry, ER antibody, 100× magnification

Learning Points

Obtaining a good history goes a long way in quick diagnosis and management of cases with orbital metastasis from breast carcinoma. Awareness of the clinical presentation and imaging features also help in the diagnosis.

Further Reading

1. Chang BY, Cunniffe G, Hutchinson C. Enophthalmos associated with primary breast carcinoma. Orbit. 2002;21:307–10.
2. Kuzma BB, Goodman JM. Slowly progressive bilateral enophthalmos from metastatic breast carcinoma. Surg Neurol. 1998;50:600–2.
3. Panagiotis JV, Voutsadakis IA, Papandreou CN. Orbital metastasis of breast carcinoma. Breast Cancer (Auckl). 2009;3:91–7.
4. Raap M, Antonopoulos W, Dammrich M, et al. High frequency of lobular breast cancer in distant metastases to the orbit. Cancer Med. 2015;4:104–11.

Prostate Adenocarcinoma

57

Gangadhara Sundar, Stephanie Ming Young, Eric Ting, Bingcheng Wu, Min En Nga, and Shantha Amrith

Introduction

Prostate accounts for the third most common primary site for metastasis to the orbit. The majority of cancers arising from the prostate are adenocarcinomas. The mean age at diagnosis is 70 years. The degree of tumour differentiation measured by Gleason score correlates directly with distant metastasis and death. The metastasis occurs by two methods, haematological route through ophthalmic artery and venous route through Bateson's venous plexus and cranial venous sinuses (ophthalmic vein).

Case Scenario

An 81-year-old South Asian male, a past smoker with a history of hypertension, ischemic heart disease and treatment for prostate carcinoma 5 years earlier, presented with a subacute visual loss, pain and redness of the left eye for about 4 weeks. There was no history of diabetes or trauma. Ophthalmic examination revealed normal findings on the right eye. On the left, there was no light perception with a down-and-in proptosis, grade IV RAPD, conjunctival injection with chemosis, and global limitation of ocular motility (Fig. 57.1). Fundus examination was unremarkable. Significant fullness of the left temporal area was noted.

CLOSE summary is given in Table 57.1.

Differential Diagnosis

- Orbital inflammatory disorder: specific vs nonspecific
- Neoplastic:
  - Primary:
    - Lymphoproliferative disorder
    - Primary lacrimal gland malignancies such as adenoid cystic carcinoma, adenocarcinoma, mucoepidermoid carcinoma, ductal carcinoma, etc.
  - Secondary metastatic lesion

G. Sundar · S. M. Young · S. Amrith (✉)
Department of Ophthalmology, National University Hospital, Singapore

Department of Ophthalmology, Yong Loo Lin School of Medicine, National University of Singapore, Singapore
e-mail: gangadhara_sundar@nuhs.edu.sg; stephanie.young@nuhs.edu.sg; shantha_amrith@nuhs.edu.sg

E. Ting
Department of Diagnostic Imaging, National University Hospital, Singapore

Department of Diagnostic Imaging, Yong Loo Lin School of Medicine, National University of Singapore, Singapore

Advanced Medicine Imaging, Singapore

B. Wu
Department of Pathology, National University Hospital, Singapore

M. E. Nga
Department of Pathology, National University Hospital, Singapore

Department of Pathology, Yong Loo Lin School of Medicine, National University of Singapore, Singapore

S. Amrith et al. (eds.), *Ocular Adnexal Lesions*, https://doi.org/10.1007/978-981-13-3798-7_57

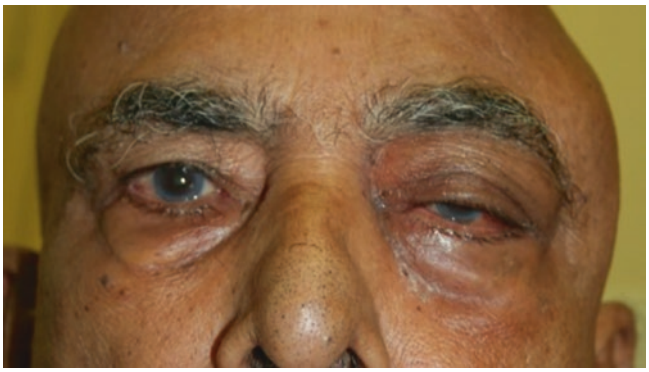

Fig. 57.1 Left proptosis and temporal fullness

Table 57.1 CLOSE summary

*C*linical process: infiltrative, mass effect
*L*ocation: left superotemporal orbit and temporal fossa
*O*nset: subacute
*S*ymptoms and signs: pain, injection, proptosis, and visual loss
*E*pidemiology: elderly South Asian male

Further Investigations

Systemic workup: Full blood count, ESR, CRP, renal function tests and liver function tests were normal. Prostate-specific antigen (PSA) was raised (436.5 µg/L; normal 4–10 µg/L).

Imaging

B-scan ultrasound orbits showed a heterogeneous high reflective retrobulbar mass with globe indentation. (Fig. 57.2a).

Contrast-enhanced CT scan showed destruction of the superotemporal orbit with a combination of soft tissue mass and multiple lytic bony lesions encroaching onto the posterior orbit, middle cranial fossa, and the temporal region. The anatomical location was the trigone of the greater wing of sphenoid. The location and findings were characteristic of metastatic prostate cancer (Fig. 57.2b, c and d).

A follow-up bone scan revealed multiple metastases involving the spine and bone.

Histopathology

A review of previous pathology from 5 years ago showed a poorly differentiated tumour with haphazard groups of cells infiltrating the stroma. No evidence of glandular differentiation was seen. The tumour cells exhibited hyperchromatic nuclei with scant cytoplasm (Fig. 57.3). Based on tumour morphology, the considerations would include poorly differentiated carcinoma and lymphoma. Given the past history of prostatic carcinoma with Gleason grade 5 component, the patient's presenting features would be consistent with metastatic prostatic carcinoma.

Note that the usual morphology of prostatic carcinoma is that of well-formed glandular/acinar structures, formed by cells with fairly small nuclei and prominent nucleoli and fairly abundant cytoplasm. This case showed a poorly differentiated tumour with no appreciable gland formation.

Management

On the advice of the oncologist, he underwent external beam radiation therapy with significant symptomatic improvement. He had undergone bilateral orchidectomy and thus did not require hormonal therapy.

Discussion

Most common metastatic sites for prostate carcinoma are pelvic nodal chains and axial skeleton. In the orbits, prostate metastases tend to present in an osteoblastic pattern. Although they are less frequent, osteolytic lesions are also possible in advanced cases of prostate carcinomas. Orbital involvement as a primary presentation and involvement of soft tissue, extraocular muscle, and bilateral occurrence have all been reported as single cases.

Confirmatory immunohistochemical tests would include AE1/AE3 (a pan-cytokeratin cocktail that would confirm the epithelial lineage of the tumour cells) and, for site of origin, PSA (prostate-specific antigen), PSMA (prostate-specific membrane antigen) or PSAP (prostatic acid phosphatase). However, poorly differentiated and/or metastatic prostate cancer can be negative for PSA and PSAP.

Hormonal therapy, namely, anti-androgen therapy, is the treatment of choice in disseminated disease. The metastasis often regresses, needing no further treatment until resistance to hormonal therapy develops, when chemotherapy may be considered. In isolated orbital involvement, radiotherapy or even surgical resection may give good results. The survival, once orbital metastasis occurs, has been reported as 4–26 months.

Learning Points

Orbital metastases from prostate carcinoma may occur as an osteoblastic or osteoclastic lesion. Whether isolated or in the context of disseminated disease, they have a bad prognosis. Orbital symptoms must be correlated with clinical history; however, radiologic findings and histopathologic analysis

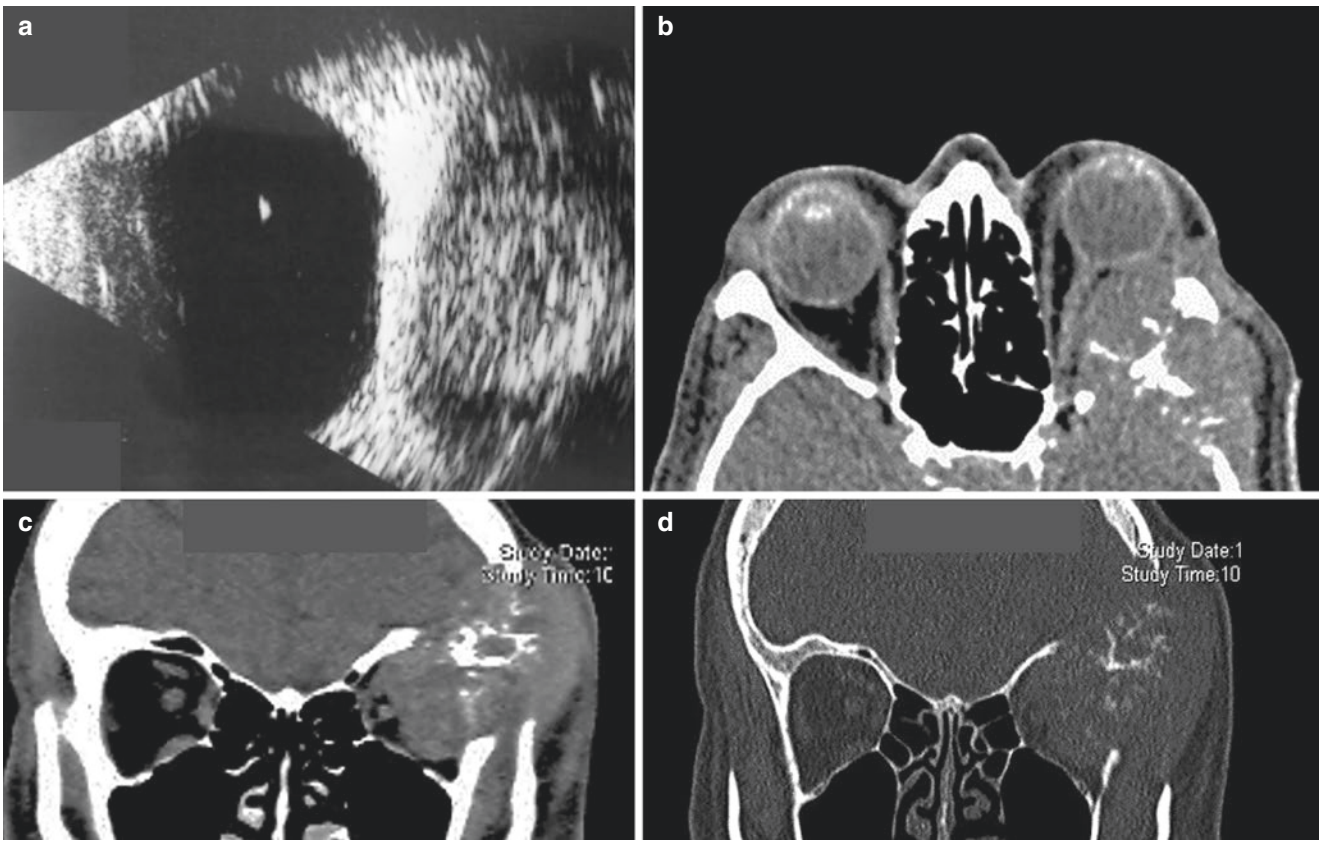

Fig. 57.2 (**a**): Ultrasound B-scan showing heterogeneous high reflective retrobulbar mass with globe indentation. Axial (**b**) coronal (**c**) contrast-enhanced CT scan shows a large mass centred on the left sphenoid wing, expanding into the orbit, middle cranial fossa and temporal fossa. (**d**): Coronal bone window shows an aggressive pattern of bony destruction with a 'sunburst' pattern of periosteal new bone radiating out from the centre of the lesion

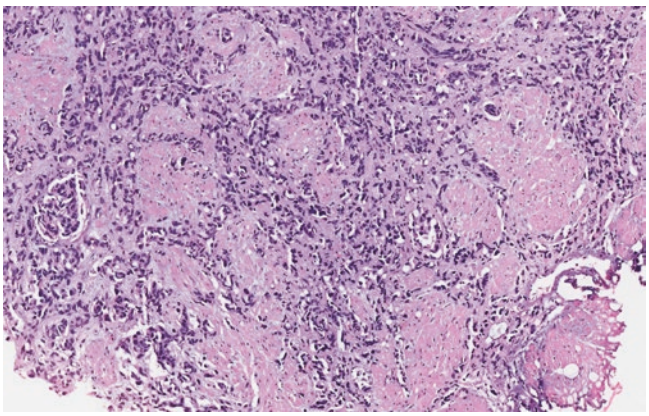

Fig. 57.3 This is a poorly differentiated tumour with haphazardly infiltrating cells. No gland formation is seen. The features would be consistent with a Gleason grade 5 metastatic prostatic carcinoma. HE stain, 100× magnification

are essential for definitive diagnosis. The choice of therapy should be individualized to the patient depending on the aggressiveness of disease, number of metastases and emergency of the situation to prevent vision loss.

Further Reading

1. Boldt HC, Nerad JA. Orbital metastases from prostate carcinoma. Arch Ophthalmol. 1988;106:1403–8.
2. Nayyar R, Singh P, Panda S, Kashyap S, Gupta NP. Proptosis due to "isolated" soft tissue orbital metastasis of prostate carcinoma. Indian J Cancer 2010;47:74–6.
3. Rosado P, de Vicente JC, Vivanco B, et al. Clinical and immunohistochemical analysis of orbital metastasis from prostate carcinoma. J Craniofac Surg. 2011;22(6):2141–3.

Gastric Carcinoma

58

Gangadhara Sundar, Stephanie Ming Young, Eric Ting, Bingcheng Wu, Min En Nga, and Shantha Amrith

Introduction

Discrete involvement of extraocular muscle in metastatic disease is a very rare event. In adults, metastases to extraocular muscles occur mostly from cutaneous melanomas and breast and lung carcinomas. Rarely, they may originate from a carcinoma of the gastrointestinal tract. The majority of patients with metastases to extraocular muscles already have a known primary malignancy at presentation. The most frequently affected extraocular muscle is the medial rectus, followed by lateral rectus, superior rectus, and inferior rectus. Bilateral extraocular muscle involvement is rare but has been reported.

Case Scenario

A 62-year-old Chinese male presented with a 1-month history of pain, redness, tearing, and blurred vision in his left eye. One week prior to consult, he had noted double vision and a left-sided weakness of the face with palpable lumps in his neck. He was a known hypertensive, with a family history of lung cancer (father). He had reportedly undergone surgery followed by chemotherapy for a gastrointestinal malignancy a year earlier.

Ophthalmic examination revealed normal findings in the right eye. On the left, his best corrected visual acuity with a hyperopic correction was 20/40. There was a 3 mm left proptosis with significant global limitation of ocular motility (Fig. 58.1). There was significant resistance to retropulsion and no RAPD. Anterior segment was unremarkable except for severe conjunctival injection, and fundus examination revealed temporal choroidal folds. Cranial nerve examination revealed a left lower motor neuron facial palsy. Other cranial nerves were normal. Regional examination revealed multiple ipsilateral cervical lymphadenopathy.

CLOSE summary is given in Table 58.1.

Differential Diagnosis

- Neoplastic lesion
  - Secondary
    - Metastatic lesion from primary gastrointestinal malignancy

G. Sundar · S. M. Young · S. Amrith (✉)
Department of Ophthalmology, National University Hospital, Singapore

Department of Ophthalmology, Yong Loo Lin School of Medicine, National University of Singapore, Singapore
e-mail: gangadhara_sundar@nuhs.edu.sg; stephanie.young@nuhs.edu.sg; shantha_amrith@nuhs.edu.sg

E. Ting
Department of Diagnostic Imaging, National University Hospital, Singapore

Department of Diagnostic Imaging, Yong Loo Lin School of Medicine, National University of Singapore, Singapore

Advanced Medicine Imaging, Singapore

B. Wu
Department of Pathology, National University Hospital, Singapore

M. E. Nga
Department of Pathology, National University Hospital, Singapore

Department of Pathology, Yong Loo Lin School of Medicine, National University of Singapore, Singapore

S. Amrith et al. (eds.), *Ocular Adnexal Lesions*, https://doi.org/10.1007/978-981-13-3798-7_58

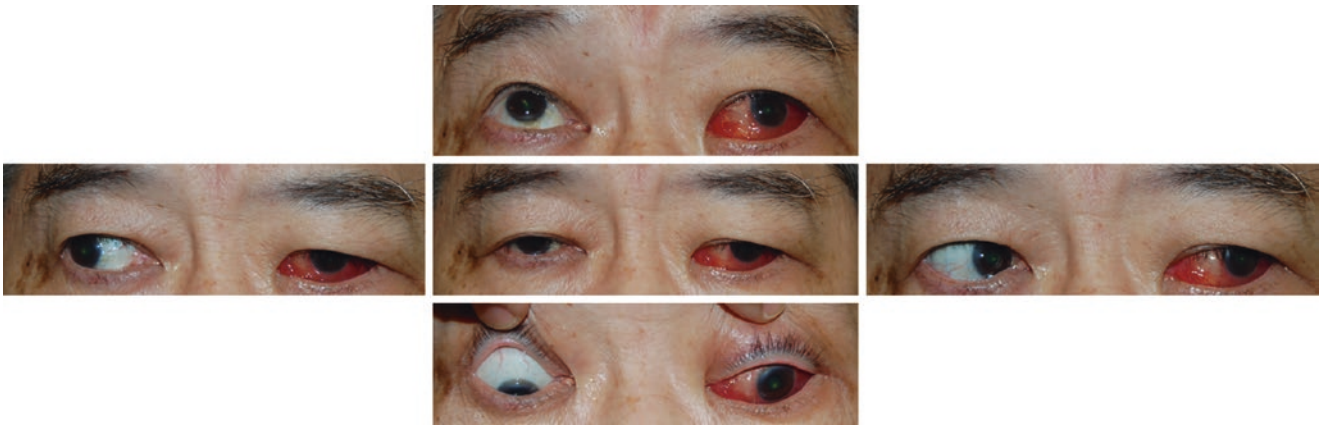

Fig. 58.1 Clinical picture showing left proptosis, limitation of ocular motility, and conjunctival injection

Table 58.1 CLOSE summary

*C*linical process: inflammatory, infiltrative, mass effect
*L*ocation: left retrobulbar, parabulbar
*O*nset: subacute
*S*ymptoms and signs: conjunctival injection, blurred vision, ocular motility disorder, facial weakness, regional lymphadenopathy
*E*pidemiology: 62-year-old Chinese male

  - Hematogenous malignancies (multiple myeloma, leukemia, etc.)
- Primary: lacrimal gland neoplasms (adenoid cystic carcinoma, adenocarcinoma, mucoepidermoid carcinoma, etc.)
- Lymphoproliferative disorders
- Inflammatory disorder, e.g., Tolosa hunt syndrome

Imaging

Computed tomography (CT) scan (Fig. 58.2) showed enhancing mass lesion at the anterior half of left lateral rectus abutting, indenting, and displacing the globe. The overlying bone appeared intact.

Gadolinium-enhanced MRI (Fig. 58.3) revealed a soft tissue lesion involving the left lateral rectus with a soft tissue intraconal component displacing the optic nerve medially. The intraocular and intracranial cavities appeared normal. In addition there was a parotid nodule and infiltration of the temporalis, masseter, and prevertebral muscles with cervical lymphadenopathy.

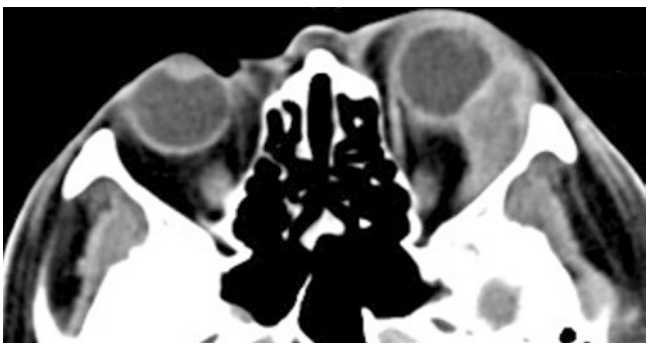

Fig. 58.2 Axial contrast-enhanced CT showing a left lateral rectus mass indenting the globe

Intervention

The patient underwent a transconjunctival core needle biopsy (CNB) with cytology and cell block.

Histopathology

Cellular smears showed crowded groups of atypical epithelial cells with overlapping nuclei and modest amounts of cytoplasm. Acinar (gland-like arrangements) formation was prominent. Cell block showed complex glandular structures. Mucin was seen within the glandular lumina [the mucin is highlighted by the periodic acid-Schiff stain with digestion by diastase (DPAS stain)] (Fig. 58.4). The findings were

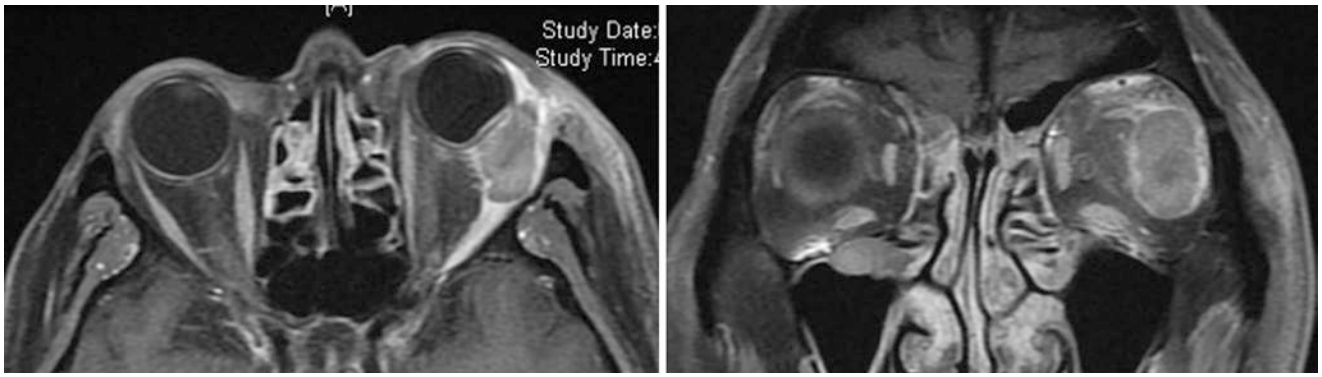

Fig. 58.3 Axial (Left) and coronal (Right) T1w FS + C images showing left lateral rectus infiltration with indentation of the globe and intraconal involvement

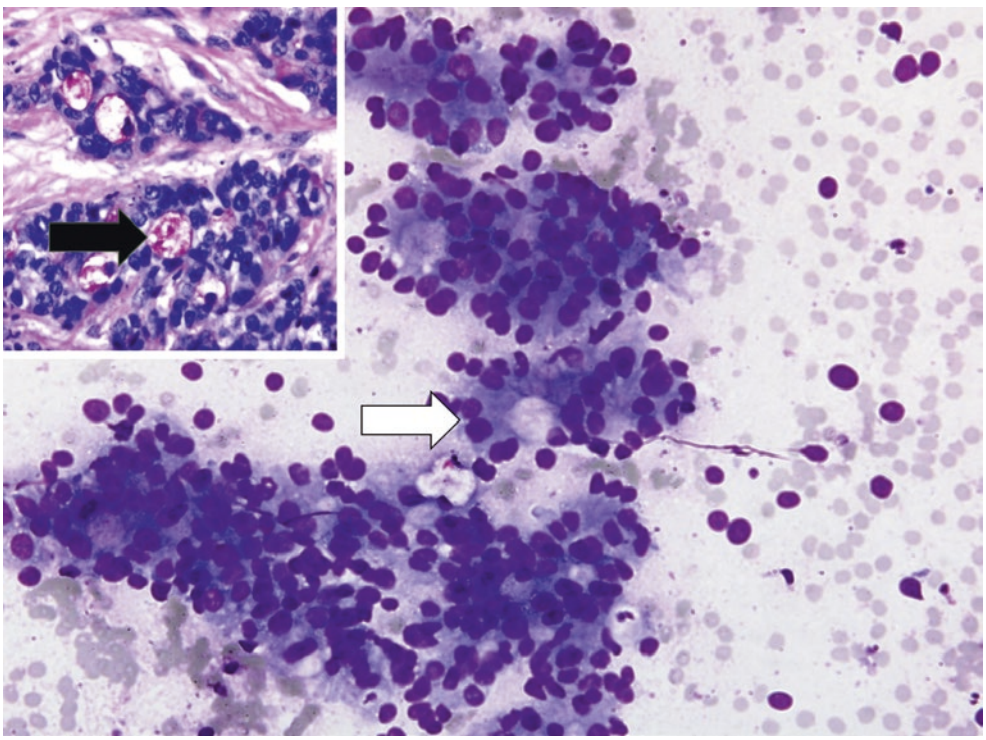

Fig. 58.4 Cellular smears show crowded groups of atypical epithelial cells with overlapping nuclei and modest amounts of cytoplasm. Acinar formation is prominent (white arrow). The cell block shows atypical glands containing luminal mucin (inset, black arrow). Main: Air-dried smear, Hemacolor stain, 200× magnification. Inset: Cell block, DPAS stain, 400× magnification

those of a malignant gland-forming carcinoma, hence adenocarcinoma, most likely metastatic.

The malignant epithelial cells were positive for cytokeratin 7 (CK7) on immunohistochemistry (Fig. 58.5).

Management

Given the CK7 positivity, some possible primary sites are the stomach, pancreato-biliary system, lung, and breast. Clinical and radiological correlation is required to determine the site of origin of the adenocarcinoma. Staging workup with CT scan of the neck, chest, abdomen, and pelvis revealed multiple heterogeneously enhancing nodules of the chest and abdominal walls and cavities (lung, adrenals).

A final diagnosis of metastatic gastric carcinoma, stage IV was made after review of gastrointestinal pathology combined with staging workup.

As per the advice of the oncology team, he underwent palliative chemotherapy with orbital and parotid radiotherapy but passed away in 3 months.

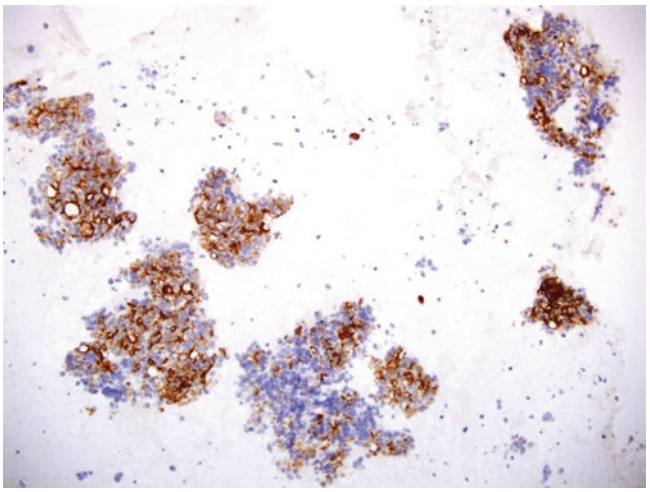

Fig. 58.5 The tumor cells are positive for CK7 immunohistochemistry. Cell block, immunohistochemistry (CK7 antibody), 100× magnification

Discussion

Extraocular muscle shows segmental widening rather than diffuse enlargement in a metastasis from gastric carcinoma. There may be associated soft-tissue involvement. Multiple muscle enlargement has been described, but bilateral involvement is very rare.

Learning Points

Isolated lateral rectus enlargement should always be considered as metastatic as it is very unusual in Grave's orbitopathy. The other differential diagnosis will include an orbital myositis or a non-specific orbital inflammatory syndrome and lymphoma.

Further Reading

1. Souayah N, Krivitskaya N, Lee HJ. Lateral rectus muscle metastasis as the initial manifestation of gastric cancer. J Neuroophthalmol. 2008;28(3):240–1.
2. Van Gelderen WF. Gastric carcinoma metastases to extraocular muscles. J Comput Assist Tomogr. 1993;17:499–500.

Ewing Sarcoma

59

Shantha Amrith, Stephanie Ming Young, Eric Ting, Bingcheng Wu, Min En Nga, and Gangadhara Sundar

Introduction

Ewing sarcoma is a bone tumour that is named after James Ewing. It is the second most common malignant tumour of the bone affecting children and young adults (10–20 years of age). It is more common in Caucasians and affects males more than females; the male to female ratio is 1.5:1. It arises from the primitive neuroectoderm and is very rare in the orbit. Quite often, it appears in the orbit as a metastatic lesion from elsewhere. There have been reports of extraskeletal Ewing sarcoma in the soft tissues of the orbit.

Clinical Scenario

A 21-year-old Chinese male with a past history of chest wall mass that was diagnosed and treated for Ewing sarcoma 6 years previously developed a scalp lump with intracranial extension, and it was successfully resected. A diagnosis of recurrent Ewing sarcoma was made. Around the same time, he developed bulging of the left eye with decrease in vision. Ophthalmic examination of the right eye was normal, whereas the left revealed 6 mm of proptosis with hypoglobus (Fig. 59.1a and b), and limitation on supraduction. The Snellen visual acuity was 6/9, and on fundus examination (Fig. 59.1c and d), there were striations in the macula.

CLOSE summary is given in Table 59.1.

Differential Diagnosis

- Rhabdomyosarcoma
- Inflammatory mass specific and non-specific
- Lymphoma
- Ewing sarcoma
- Chronic osteomyelitis
- Eosinophilic granuloma

Imaging

Computed tomography (CT) scan showed a well-defined mass located over the superolateral aspect of the left orbit. This extraconal mass was seen to displace the superior and

S. Amrith (✉) · S. M. Young · G. Sundar
Department of Ophthalmology, National University Hospital, Singapore

Department of Ophthalmology, Yong Loo Lin School of Medicine, National University of Singapore, Singapore
e-mail: shantha_amrith@nuhs.edu.sg; stephanie.young@nuhs.edu.sg; gangadhara_sundar@nuhs.edu.sg

E. Ting
Department of Diagnostic Imaging, National University Hospital, Singapore

Department of Diagnostic Imaging, Yong Loo Lin School of Medicine, National University of Singapore, Singapore

Advanced Medicine Imaging, Singapore

B. Wu
Department of Pathology, National University Hospital, Singapore

M. E. Nga
Department of Pathology, National University Hospital, Singapore

Department of Pathology, Yong Loo Lin School of Medicine, National University of Singapore, Singapore

S. Amrith et al. (eds.), *Ocular Adnexal Lesions*, https://doi.org/10.1007/978-981-13-3798-7_59

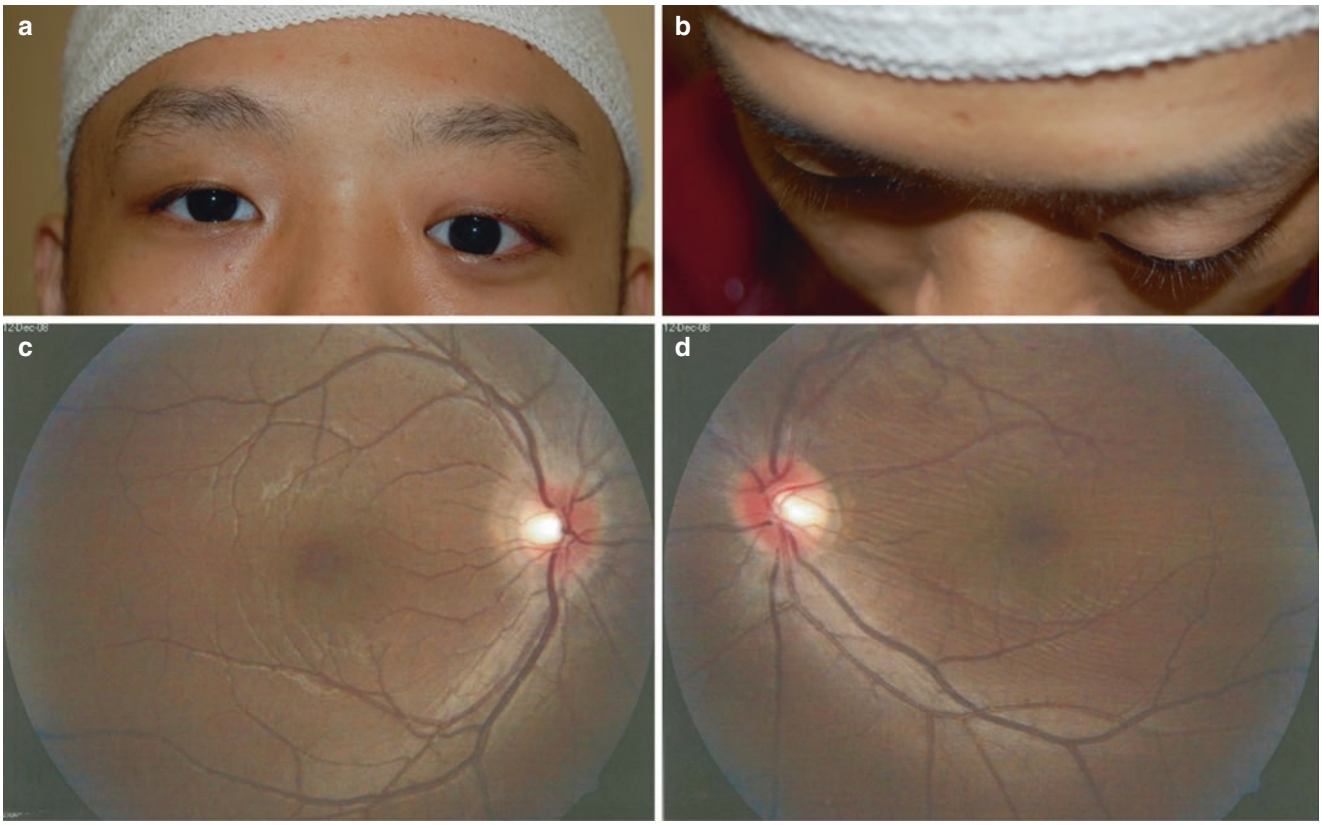

Fig. 59.1 Clinical picture showing left hypoglobus (**a**) and proptosis (**b**). The fundus photo shows a normal right fundus (**c**) and choroidal striae at the macula of the left eye (**d**)

Table 59.1 CLOSE summary

*C*linical scenario: mass effect
*L*ocation: left superior orbit
*O*nset: subacute
*S*igns and symptoms: left proptosis with hypoglobus
*E*pidemiology: 21-year-old Chinese male

lateral recti muscles as well as the globe inferiorly. There was erosion of the adjacent bone (Fig. 59.2).

Multiplanar MRI of the brain showed a lesion at the parietal vault. It was broad-based with an extra-osseous component extending from both the inner and outer table causing some local mass effect. The lesion was minimally enhancing. A similar lesion was seen in the left superolateral orbit with osseous and extra-osseous components (Fig. 59.3) confirming the CT scan findings.

Intervention

As the patient underwent a recent resection of the scalp and intracranial mass, no biopsy of the orbital mass was performed. The diagnosis was extrapolated from the scalp biopsy.

Histopathology

Paraffin sections revealed a cellular tumour composed of round cells with stippled chromatin, enlarged nuclei and scant cytoplasm (Fig. 59.4). The tumour cells were disposed in sheets and associated with mitotic activity as well as tumour necrosis.

On immunohistochemistry, the tumour was diffusely positive for CD99 but negative for chromogranin, desmin and leucocyte common antigen (LCA). The morphological and immunohistochemical features were highly suggestive of Ewing sarcoma.

Fluorescent in situ hybridization (FISH) test for EWS (22q12) gene rearrangement was positive, which in the context of morphological and immunohistochemical features confirmed the diagnosis of Ewing sarcoma.

Management

The patient underwent chemotherapy. Initially he was treated with VAC (vincristine, doxorubicin and prednisolone) with chest wall resection. Recurrence in the scalp and brain was again treated with surgical resection followed by ifosfamide and etoposide.

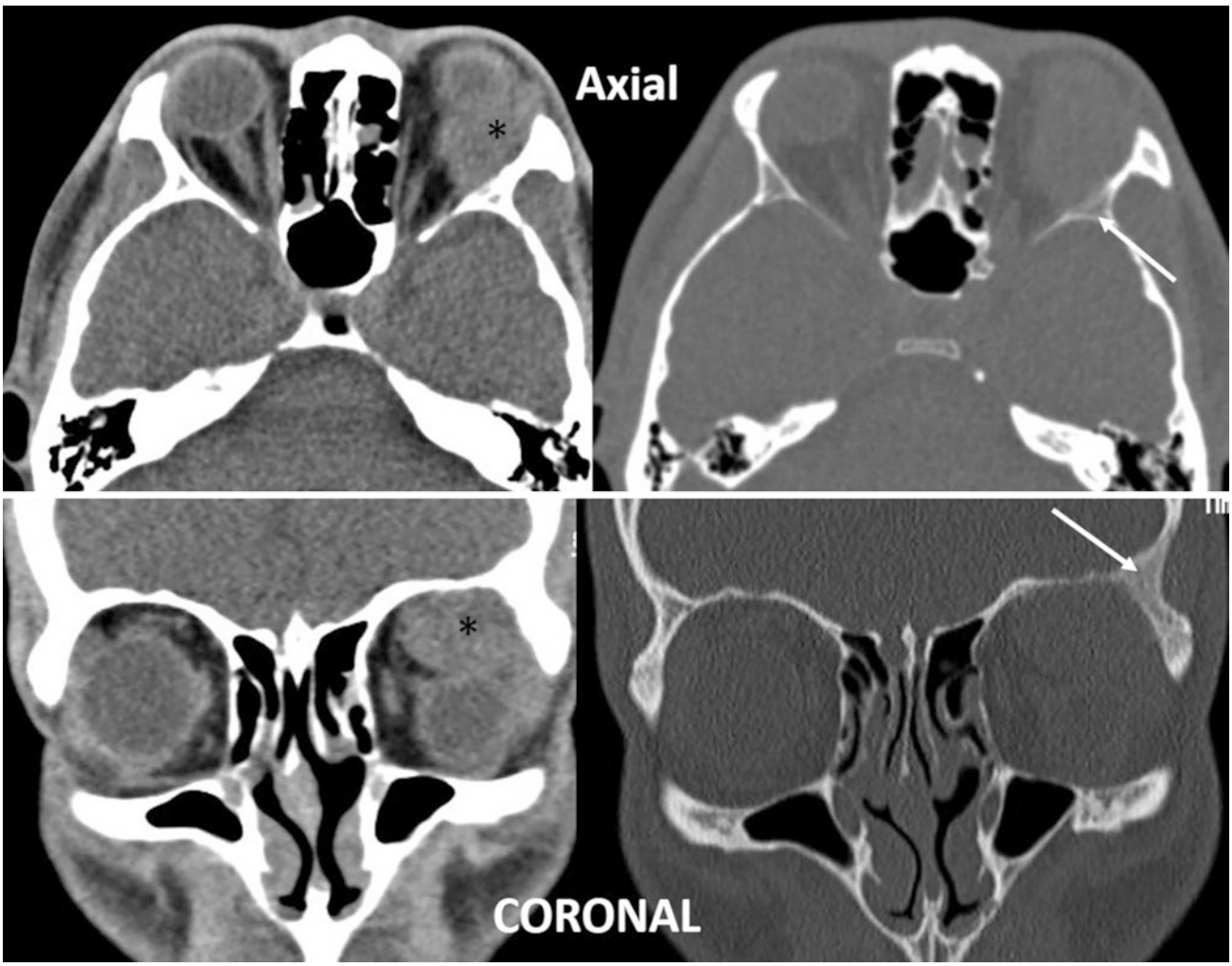

Fig. 59.2 CT scan of the orbits (soft-tissue imges -left and bone window images- right) showing a left extraconal mass (*) with erosion of the adjacent bone (white arrows)

Discussion

Ewing sarcoma is a highly malignant primary tumour of the bone. It is derived from the red bone marrow. It is a round cell tumour associated with primitive peripheral neuroectodermal tumours (PNET); however, the origin of these tumours is controversial. They can have very different presentations. At one end of the spectrum there is a poorly differentiated tumour showing no evidence of its cellular origin, and at the other end there is a very well-differentiated peripheral neuroectodermal tumour.

It is most common in the lower extremities, pelvis, trunk and the upper limbs. Head and neck tumours are quite rare, and only 2–3% of primary cases involve the skull. Metastasis is mostly to the lungs and other bones.

Orbit is usually involved in metastatic disease, and very few cases of tumours have been reported to arise primarily from the orbit. Patients may present with proptosis, large palpable mass, pain, tender swelling, and diplopia. The mass may mimic chronic osteomyelitis, and is usually seen in the superolateral quadrant. There may be constitutional symptoms such as fever, loss of weight, and anaemia, with increased ESR, WBC count, and raised LDH.

The expanding bony lesion with destruction, enhancing with contrast, is well seen on CT scan. Periosteal reaction with an onion skin appearance may suggest Ewing sarcoma. Extraskeletal soft tissue mass is sometimes seen in young adults, and it erodes the adjacent bone.

Histologically, the tumour is characterized by small basophilic round cells, and electron microscopy shows cytoplasmic glycogen pooling, and poorly developed cell junctions, typical of Ewing sarcoma. Cytologic evaluation reveals a fine nuclear chromatin pattern with basophilic cytoplasm and prominent vacuolization.

Factors associated with poor prognosis are male gender, age more than 12 years, anaemia, raised LDH, and poor chemotherapeutic response.

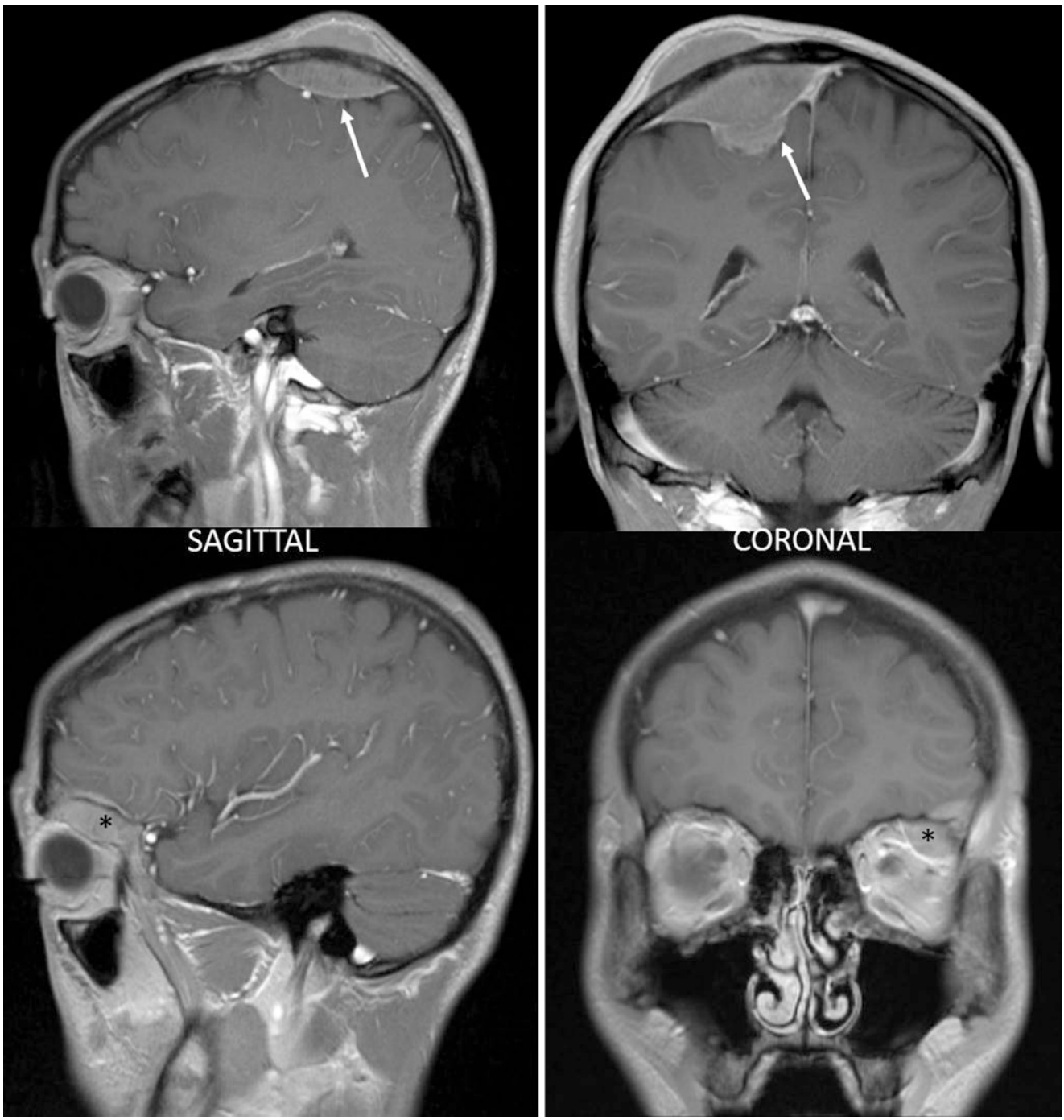

Fig. 59.3 MRI T1w + C showing metastases to the skull (white arrow) and left orbital roof (*) with large extra-osseous soft tissue components

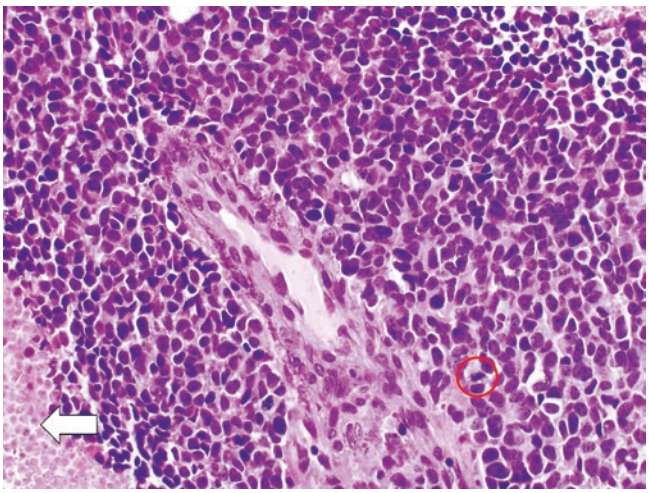

Fig. 59.4 Histopathology showing sheets of round tumour cells with stippled chromatin and scant cytoplasm. A mitotic figure (red circle) and tumour necrosis (white arrow) are seen. HE stain; 100× magnification

Management of local disease is surgery and radiotherapy. For systemic disease, the first line of chemotherapy is VIDE (vincristine, ifosfamide, doxorubicin, etoposide). Despite the multimodality treatment, the prognosis of Ewing sarcoma metastatic to orbit remains poor.

Learning Points

Ewing sarcoma is a rare neoplasm that arises from neuroectodermal tissue. It affects bones of extremities, pelvis and trunk. When it affects the orbit, it has a predilection for the superotemporal quadrant and tends to infiltrate the soft tissue and bone. Despite treatment, prognosis of Ewing sarcoma metastatic to the orbit is poor.

Further Reading

1. Alfaar AS, Zamzam M, Abdalla B, et al. Childhood Ewing sarcoma of the orbit. J Pediatr Hematol Oncol. 2015;37(6):433–7.
2. Chokthaweesak W, Annunziata CC, Alsheikh O, et al. Primitive neuroectodermal tumor of the orbit in adults: a case series. Ophthalmic Plast Reconstr Surg. 2011;27(3):173–9.
3. Dutton JJ, Rose JG Jr, DeBacker CM, Gayre G. Orbital Ewing's sarcoma of the orbit. Ophthalmic Plast Reconstr Surg. 2000;16(4):292–300.
4. Kaliki S, Rathi SG, Palkonda VAR. Primary orbital Ewing sarcoma family of tumors: a study of 12 cases. Eye (Lond). 2018;32(3):615–21.
5. Li T, Goldberg RA, Becker B, McCann J. Primary orbital extraskeletal Ewing sarcoma. Arch Ophthalmol. 2003;121(7):1049–52.

Renal Cell Carcinoma

60

Shantha Amrith, Stephanie Ming Young, Eric Ting, Bingcheng Wu, Min En Nga, and Gangadhara Sundar

Introduction

Renal cell carcinoma commonly metastasises to the lung, liver, and bone and only rarely to the orbit, eyelid, or choroid. Similar to other metastatic tumours, most cases of renal cell carcinoma metastatic to the orbit have a known primary neoplasm that may have been diagnosed many years earlier. The metastatic lesion may rarely be the first presentation.

Clinical Scenario

A healthy 48-year-old Malay male presented with a history of painless protrusion of his right eye for 3 weeks. He had no history of trauma or any constitutional symptoms such as weight loss. His Snellen visual acuities were 6/9 and 6/7.5 in the right and left eyes, respectively. The pupils were normal and there was no RAPD. The left ophthalmic examination revealed a complete ptosis (Fig. 60.1), limitation of up-gaze, and a 7 mm proptosis with downward displacement of the globe. The rest of the ophthalmic examination was normal.

CLOSE summary is given in Table 60.1.

Differential Diagnosis

- Orbital inflammation: specific or non-specific
- Primary neoplastic process such as lymphoma
- Secondary neoplastic process: from adjacent sinus and nasopharynx
- Distant metastasis

Imaging

Magnetic resonance imaging (MRI) of the left orbit (Fig. 60.2) showed a well-defined heterogeneous mass with rim enhancement that appeared to be in the superior muscle complex. Centrally, the mass was hypointense giving an appearance of a cyst. No scolex was identified. It was seen abutting and displacing the left optic nerve inferiorly.

Impression: Mass lesion in superior rectus muscle. To rule out primary tumour or metastasis.

The patient was advised biopsy but did not want it immediately.

S. Amrith (✉) · S. M. Young · G. Sundar
Department of Ophthalmology, National University Hospital, Singapore

Department of Ophthalmology, Yong Loo Lin School of Medicine, National University of Singapore, Singapore
e-mail: shantha_amrith@nuhs.edu.sg; stephanie.young@nuhs.edu.sg; gangadhara_sundar@nuhs.edu.sg

E. Ting
Department of Diagnostic Imaging, National University Hospital, Singapore

Department of Diagnostic Imaging, Yong Loo Lin School of Medicine, National University of Singapore, Singapore

Advanced Medicine Imaging, Singapore

B. Wu
Department of Pathology, National University Hospital, Singapore

M. E. Nga
Department of Pathology, National University Hospital, Singapore

Department of Pathology, Yong Loo Lin School of Medicine, National University of Singapore, Singapore

S. Amrith et al. (eds.), *Ocular Adnexal Lesions*, https://doi.org/10.1007/978-981-13-3798-7_60

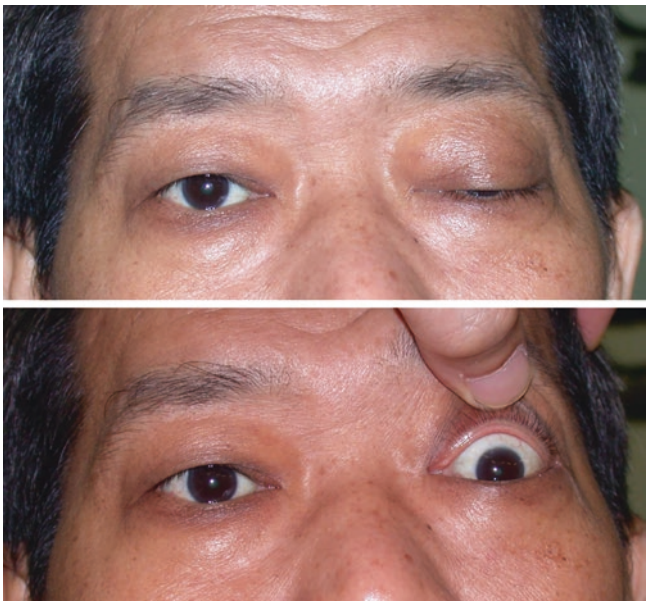

Fig. 60.1 Clinical picture showing left complete ptosis and proptosis with downward displacement

Table 60.1 CLOSE summary

*C*linical scenario: infiltrative mass
*L*ocation: left orbit
*O*nset: subacute
*S*igns and symptoms: painless proptosis with complete ptosis
*E*pidemiology: 48-year-old Malay male

A repeat CT scan 6 weeks later (Fig. 60.3) showed an increase in the size of the mass.

Intervention

Patient underwent a biopsy of the superior rectus mass through a lid crease incision 6 weeks after the initial presentation. The mass was red in colour (Fig. 60.4), and stale blood oozed out from what appeared to be a cystic lesion.

Histopathology

Paraffin sections showed closely packed nests of epithelial cells with central round nuclei and ample amounts of optically clear cytoplasm (Fig. 60.5). The nests of tumour cells were separated by thin fibrovascular septations. Focal areas showed higher grades of the tumour exhibiting nuclear enlargement, prominent nucleoli, and more ample eosinophilic cytoplasm.

The tumour cells were positive for pan-cytokeratin AE1/AE3 (Fig. 60.6), confirming the epithelial nature of the tumour, and for PAX8, pointing to renal origin. The tumour cells were also positive for CD10 (Fig. 60.5) and renal cell carcinoma (RCC) marker, both of which are often expressed in clear cell renal cell carcinoma.

Overall features were consistent with metastatic clear cell renal carcinoma.

Management

The patient lost 20 kg of weight over 3 months preceding the biopsy. He also complained of backache. MRI of the thoracolumbar area showed extensive vertebral metastasis involving the thoracic and lumbosacral vertebrae as well as the iliac bones. CT scan of the abdomen (Fig. 60.7) showed the presence of a large mass arising from the lateral aspect of the right kidney associated with abdominal lymph nodes and peritoneal deposits. Unfortunately, the patient succumbed to the disease before any definitive therapy could be started.

Discussion

Renal cell carcinoma arises from the renal cortex and affects males of 30–60 years of age. Most orbital metastases involve orbital fat, muscles, bone, and rarely the lacrimal gland. The clinical presentation can masquerade as a benign lesion delaying diagnosis. A good clinical history of the treatment of primary tumour can arouse the physician's suspicion of metastasis.

Radiologically, the mass presents as a round to ovoid well-circumscribed lesion mimicking a cavernous hemangioma or a benign-appearing lesion. Pseudo-encapsulation shows an enhancing rim. It is well known that there can be extensive haemorrhage in the primary as well as the metastatic renal cell carcinoma. The extensive vascularity may be evident during imaging and the red colour seen during surgery.

Optimal therapeutic option is in the form of surgery, i.e. resection of primary renal tumour and solitary metastasis or multiple resectable lung metastases when present. Radiotherapy, immunotherapy, and chemotherapy are the main reported treatments for extensive metastasis. The tumour is not very radio-sensitive; however, radiotherapy may help to stabilize metastatic tumour especially in the orbit.

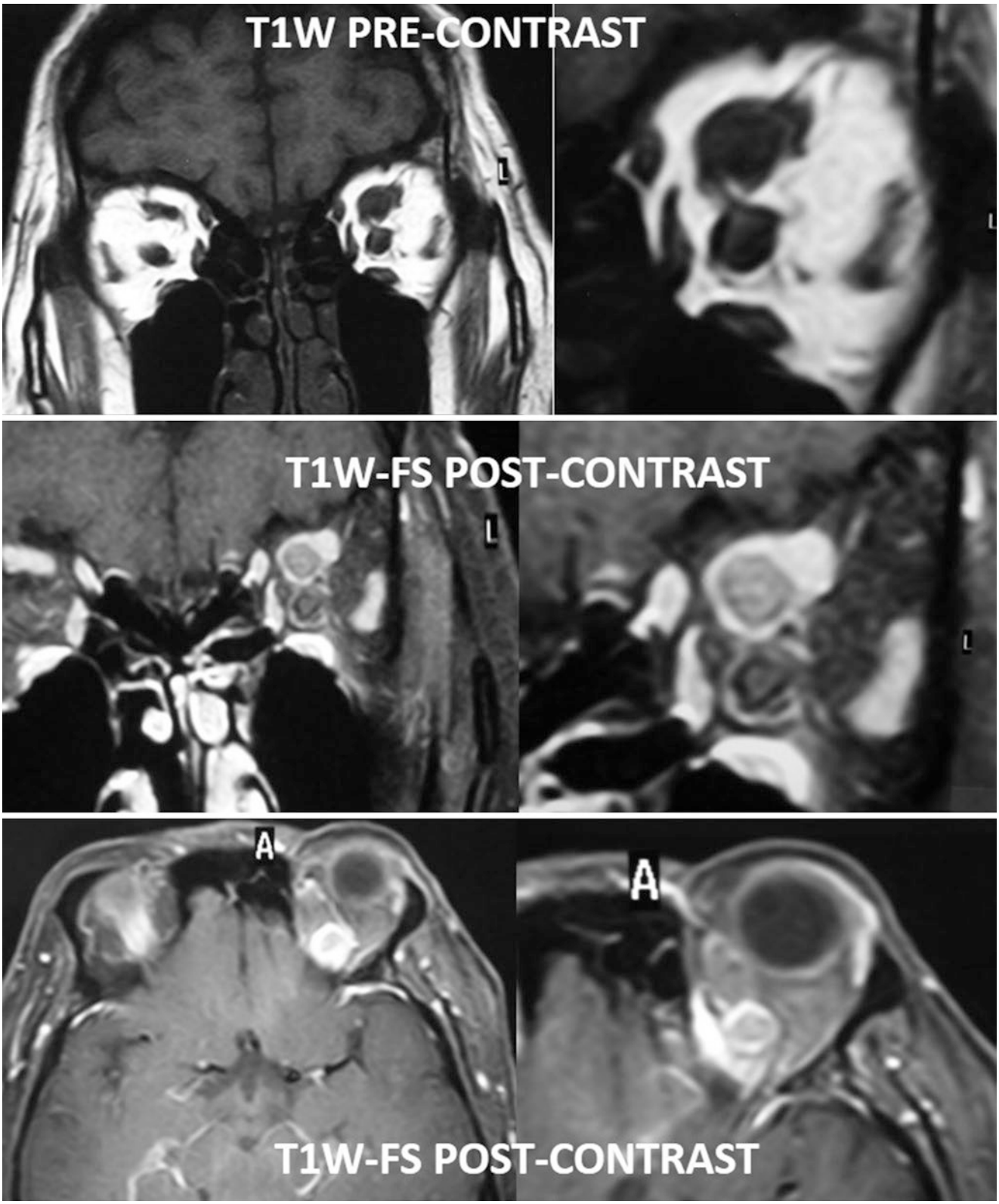

Fig. 60.2 MRI sequences (coronal, top and middle; axial, bottom) showing a well-defined heterogeneous mass with rim enhancement that appears to be in the superior muscle complex. Centrally the mass is poorly enhancing giving an appearance of central necrosis or cystic change

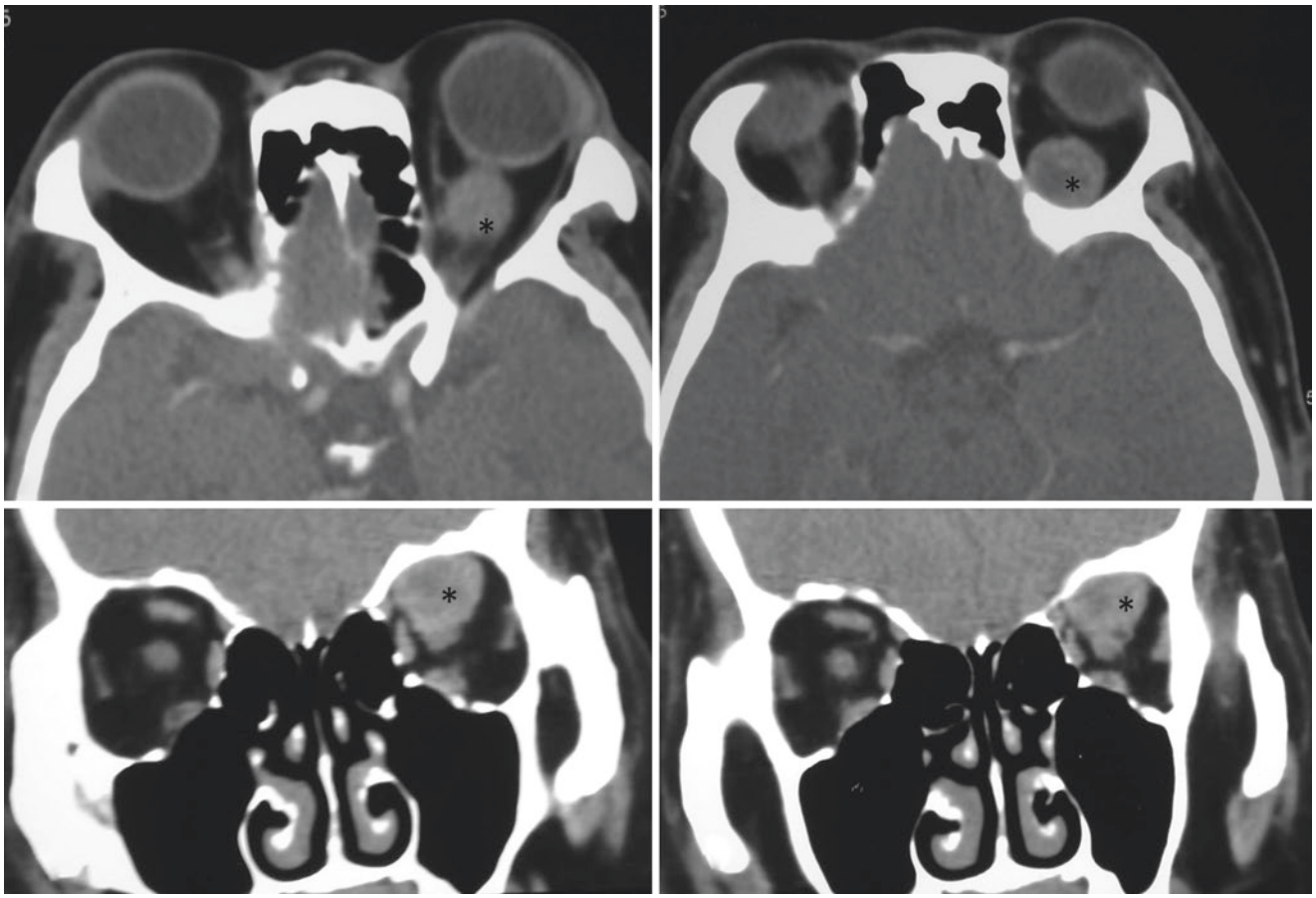

Fig. 60.3 Axial and coronal CT scans (6 weeks after initial presentation) show enlargement of the mass in the superior muscle complex on the left side (asterisk)

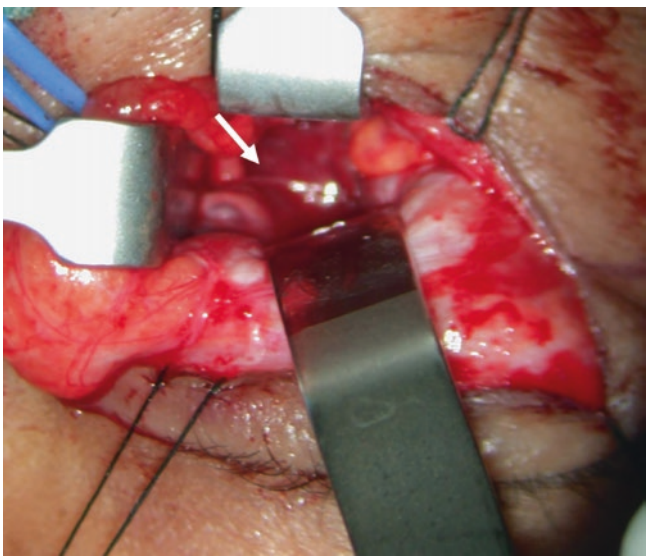

Fig. 60.4 Intraoperative appearance, note the reddish colour of the mass typical of a metastasis from a renal cell carcinoma

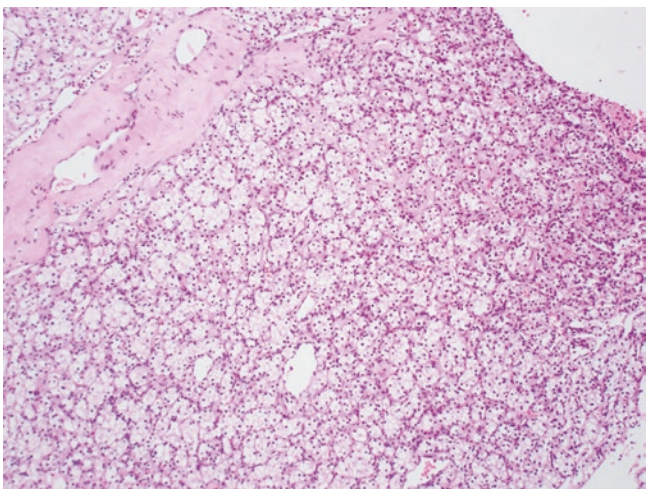

Fig. 60.5 The tumour is composed of closely packed nests of cells with central round nuclei and ample clear cytoplasm. The nests of tumour cells are separated by thin fibrovascular septae. HE stain, 100× magnification

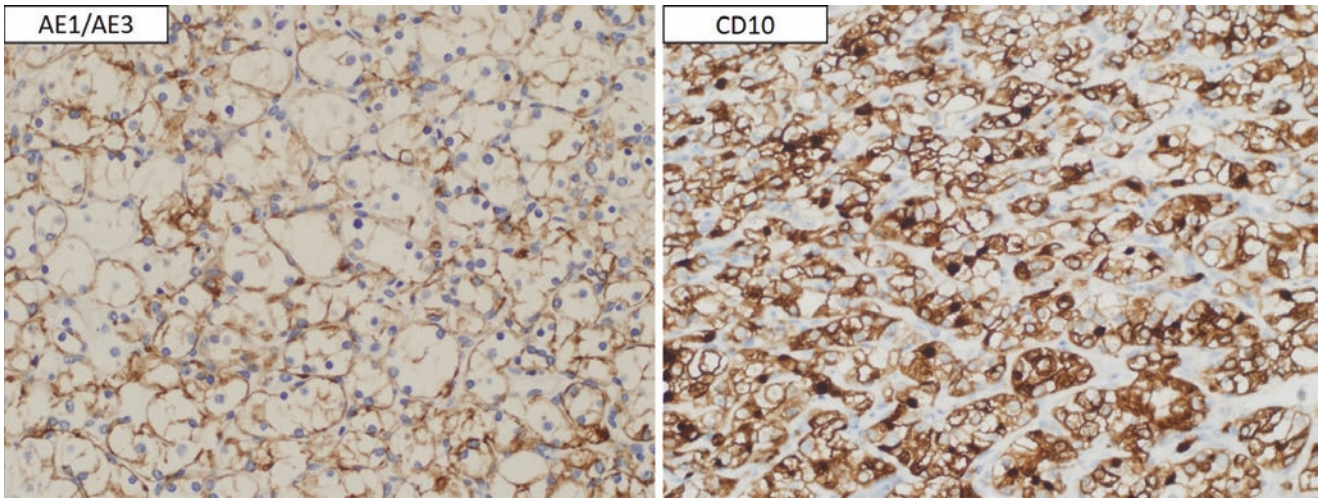

Fig. 60.6 Immunohistochemistry shows the tumour cells to be positive for AE1/AE3 pan-cytokeratin and CD10. Left: Immunohistochemistry (AE1/AE3 antibodies), 400× magnification. Right: Immunohistochemistry (CD10 antibody), 400× magnification

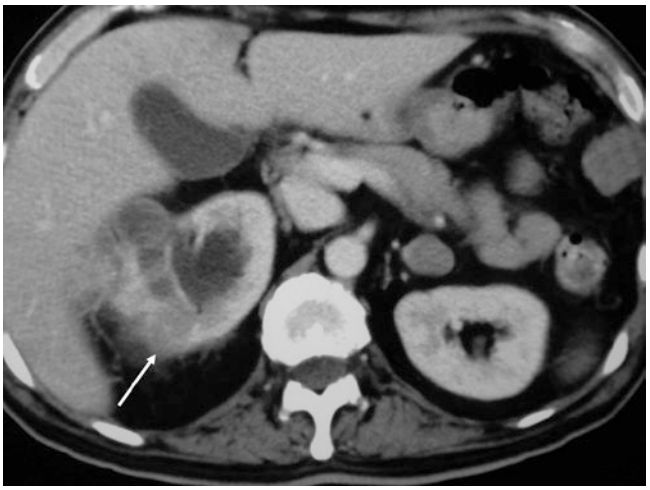

Fig. 60.7 Axial post contrast CT of the abdomen showing the primary tumour in the right kidney (white arrow)

Prognosis of patients with orbital metastasis is not considered good despite appropriate treatment.

Learning Points

Renal cell carcinoma may metastasise to the orbit many years after the treatment of the primary tumour and may rarely present with orbital metastasis. It tends to mimic a benign tumour or a cystic lesion. It is highly vascular and enhances with contrast during imaging. Surgical excision is recommended for resectable metastatic tumours.

Further Reading

1. Antonelli A, Zani D, Cozzoli A, Cunico SC. Surgical treatment of metastases from renal cell carcinoma. Arch Ital Urol Androl. 2005;77:125–8.
2. Bersani TA, Costello JJ Jr, Mango CA, et al. Benign approach to a malignant orbital tumor: metastatic renal cell carcinoma. Ophthal Plast Reconstr Surg. 1994;10:42–4.
3. Kindermann WR, Shields JA, Eiferman RA, Stephens RF, Hirsch SE. Metastatic renal cell carcinoma to the eye and adnexa: a report of three cases and review of the literature. Ophthalmology. 1981;88:1347–50.
4. Mezer E, Gdal-On M, Miller B. Orbital metastasis of renal cell carcinoma masquerading as Amaurosis fugax. Eur J Ophthalmol. 1997;7:301–4.
5. Parnes RE, Goldberg SH, Sassani JW. Renal cell carcinoma metastatic to the orbit: a clinicopathologic report. Ann Ophthalmol. 1993;25:100–2.
6. Preechawai P, Amrith S, Yip CC, Goh KY. Orbital metastasis of renal cell carcinoma masquerading as cysticercosis. Orbit. 2008;27:370–3.
7. Shome D, Honavar SG, Gupta P, Vemuganti GK, Reddy PV. Metastasis to the eye and orbit from renal cell carcinoma--a report of three cases and review of literature. Surv Ophthalmol. 2007;52(2):213–23.

Part XIV

Tumours from the Globe

Retinoblastoma

61

Gangadhara Sundar, Stephanie Ming Young, Eric Ting, Bingcheng Wu, Min En Nga, and Shantha Amrith

Introduction

Retinoblastoma is the most common primary intraocular tumour in children globally, with an average incidence of 1 in 12–15,000 live births. While most sporadic retinoblastomas arise beyond 2 years of age and are unilateral, those from germline mutations are often multifocal and bilateral with much earlier onset. Despite numerous advances of globe-sparing treatment, enucleation with primary orbital implantation is still practised worldwide when indicated, with good prognosis for life. However, extraocular spread to the orbit and brain is associated with high mortality. Likewise, pathologic high-risk characteristics even if confined within the globe are associated with a significantly high risk of systemic metastasis.

Clinical Scenario

A 2-year-old child with no significant family history presented with discoloration, discomfort, photophobia, and tearing from the left eye of over 6 months duration. The mother had noted abnormal light reflex in that eye more than a year ago. Ophthalmic examination revealed a normal visual acuity in the right eye and light perception in the left. While the right eye was unremarkable, the left eye was injected with hazy cornea, poor visualization of details of the anterior chamber and no visualization of the fundus (Fig. 61.1). Intraocular pressures were 18 and 44 mmHg in the right and left eyes, respectively. Review of systems was unremarkable. CLOSE summary is given in Table 61.1.

Differential Diagnosis

- Traumatic hyphaema with secondary glaucoma
- Benign intraocular tumours, e.g. xanthogranuloma
- Malignant intraocular tumours, e.g. retinoblastoma and medulloepithelioma
- Masquerade syndromes

G. Sundar · S. M. Young · S. Amrith (✉)
Department of Ophthalmology, National University Hospital, Singapore

Department of Ophthalmology, Yong Loo Lin School of Medicine, National University of Singapore, Singapore
e-mail: gangadhara_sundar@nuhs.edu.sg; stephanie.young@nuhs.edu.sg; shantha_amrith@nuhs.edu.sg

E. Ting
Department of Diagnostic Imaging, National University Hospital, Singapore

Department of Diagnostic Imaging, Yong Loo Lin School of Medicine, National University of Singapore, Singapore

Advanced Medicine Imaging, Singapore

B. Wu
Department of Pathology, National University Hospital, Singapore

M. E. Nga
Department of Pathology, National University Hospital, Singapore

Department of Pathology, Yong Loo Lin School of Medicine, National University of Singapore, Singapore

S. Amrith et al. (eds.), *Ocular Adnexal Lesions*, https://doi.org/10.1007/978-981-13-3798-7_61

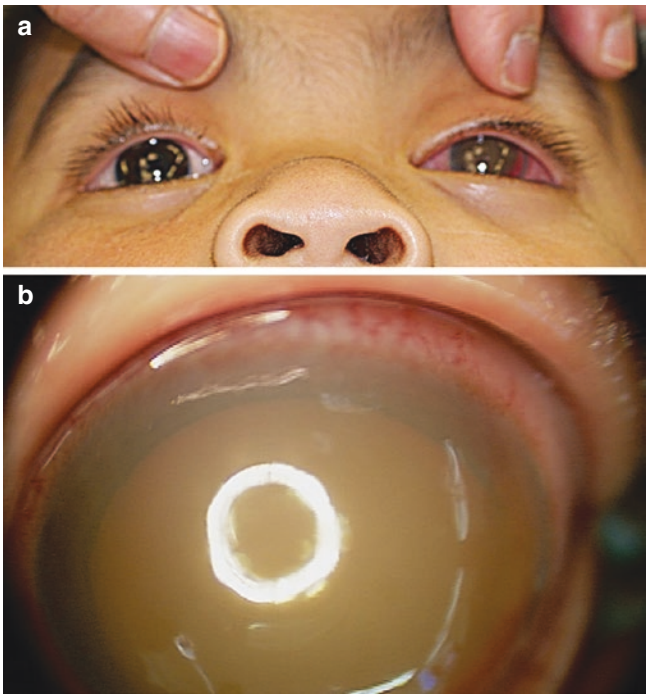

Fig. 61.1 Injected left eye with hazy cornea (**a**). Hazy cornea, secondary glaucoma, poor visualization of anterior chamber details and fundus (**b**)

Table 61.1 CLOSE summary

*C*linical scenario: intraocular tumour
*L*ocation: left eye
*O*nset: subacute
*S*igns and symptoms: red eye with hazy cornea, raised intraocular pressure, and hyphaema
*E*pidemiology: 2-year-old male child

Imaging

Ultrasound B-scan of the left eye revealed a shallow anterior chamber with hyperechogenicity of the posterior segment with focal high reflective spikes suggestive of calcification. There was increased axial length, but without disruption of the scleral coats (Fig. 61.2).

Contrast-enhanced multiplanar MRI images showed a faintly enhancing intraocular mass contrasted against the vitreous, which was hyperintense due to haemorrhage. The mass was seen to infiltrate the optic nerve inside the orbit, as evidenced by the enlargement of the optic nerve and enhancement of the optic nerve sheath (Fig. 61.3).

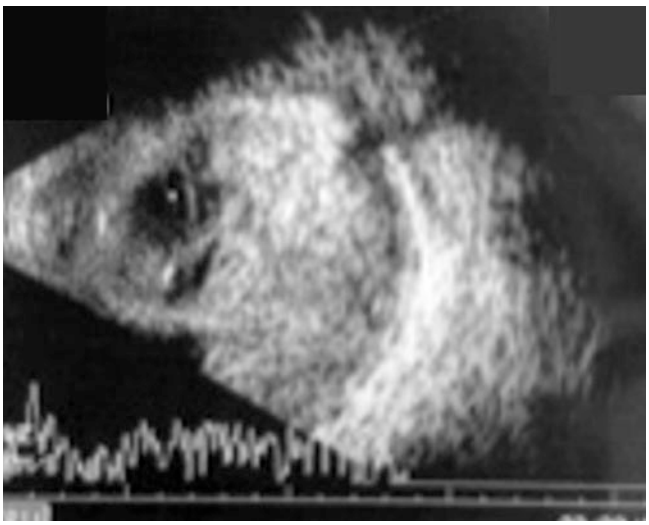

Fig. 61.2 Ultrasound B-scan showing posterior segment mass with high reflective echoes and calcification with intact scleral coat

Other Investigations

Systemic workup including lumbar puncture and bone marrow biopsy were negative.

Diagnosis

Retinoblastoma – unilateral, probable sporadic germline mutation, group E, stage IIIa

Management

Following a negative systemic workup and a normal right eye, he underwent an enucleation of the left eye with a long segment of the optic nerve.

Histopathology

Examination of the globe revealed the tumour to arise from the retina and was mainly centred in the vitreous chamber of the eye (Fig. 61.4). The tumour was composed of confluent islands of malignant cells with angulated nuclei, stippled chromatin pattern, minimal cytoplasm and high nuclear/cytoplasmic ratios. Extensive tumour necrosis is seen. The tumour

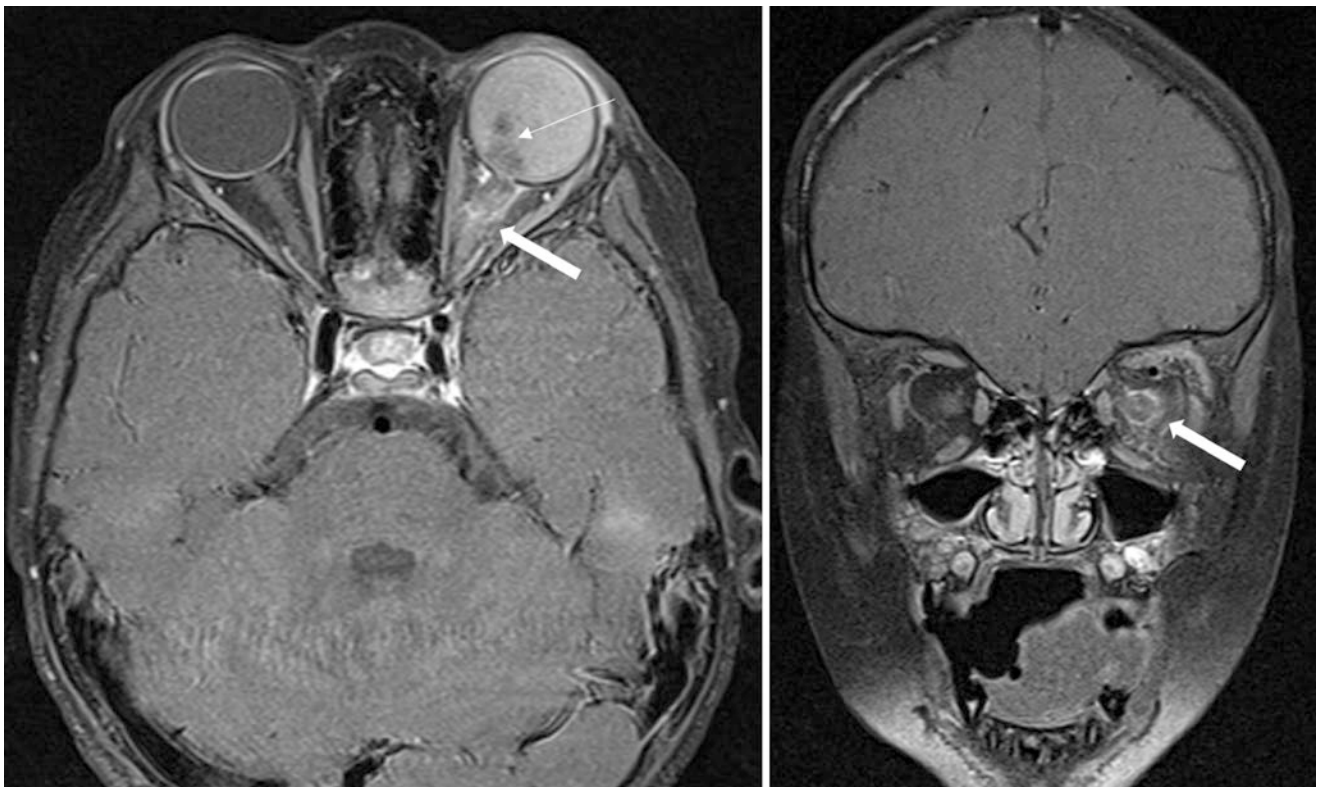

Fig. 61.3 Axial and coronal T1w-FS + C MRI images show a faintly enhancing intraocular mass (thin arrow) contrasted against the vitreous, which is hyperintense due to haemorrhage. Note the enlargement of the optic nerve and enhancement of the optic nerve sheath due to optic nerve invasion (thick arrow)

cells were seen to form Homer-Wright type pseudo-rosettes (radial arrangement of cells around a central tangle of fibrils) as well as Flexner-Wintersteiner type rosettes (clusters of short columnar cells arranged around a central lumen, with nuclei displaced away from lumen) (Fig. 61.4 inset).

There was evidence of massive choroidal invasion and post-laminar invasion of the optic nerve. The distal cut end of the optic nerve was also positive for tumour.

Further Management

Postoperatively, the patient underwent six cycles of adjuvant chemotherapy (vincristine, etoposide, carboplatin) along with orbital irradiation. He has since been followed up regularly without local, regional or systemic spread of the disease.

Discussion

Retinoblastoma is a lethal disease if untreated or poorly treated especially if there is orbital, intracranial or systemic spread. However, if diagnosed early, globe salvaging options may be considered including systemic chemoreduction along with local treatment modalities such as transpupillary thermotherapy (TTT), cryotherapy and, for residual vitreous seeding, intravitreal chemotherapy (IViC). Late-stage disease, for example, group E disease or with a suspicion of extraocular spread, is usually managed by ocular enucleation with histopathologic examination for extraocular spread or pathologic high-risk characteristics. Anterior segment invasion, massive choroidal invasion or post-laminar spread warrant systemic adjuvant chemotherapy, combined with orbital irradiation when the cut end of the optic nerve is positive or

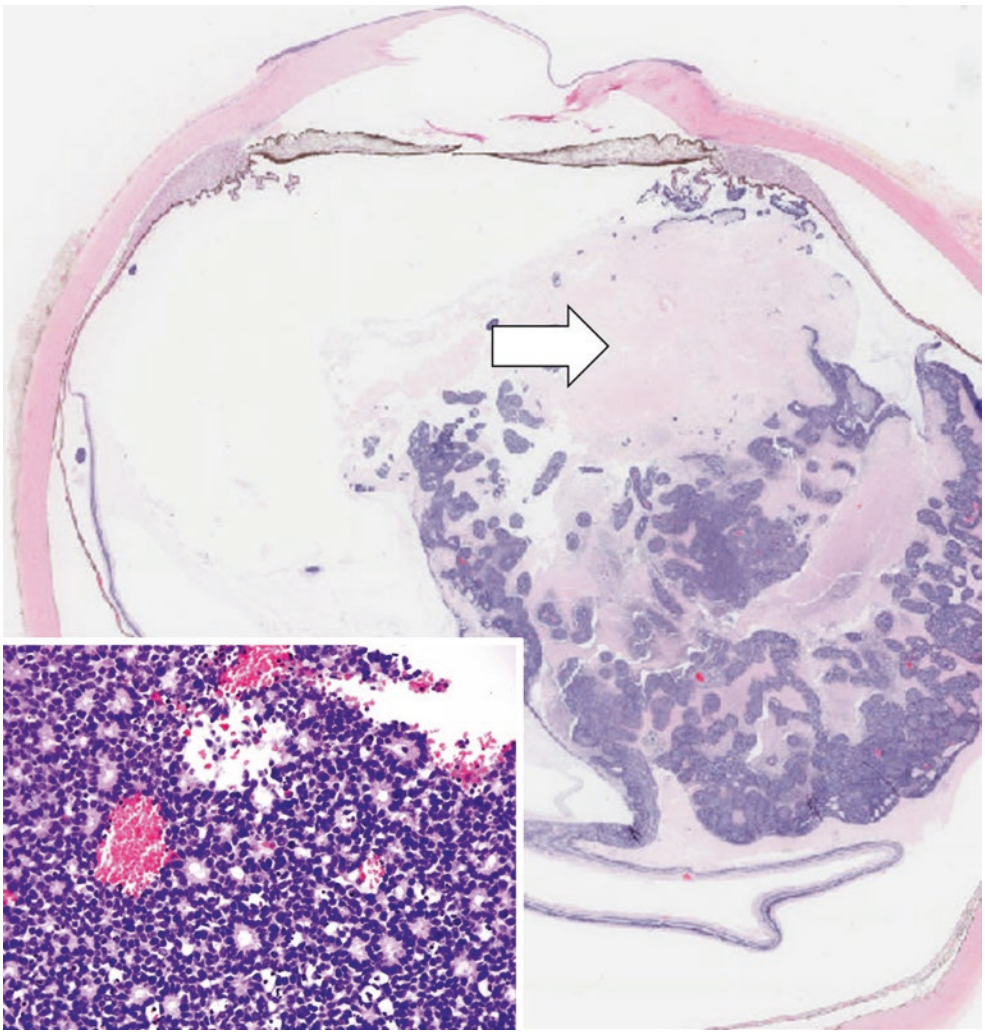

Fig. 61.4 The tumour is seen to arise from the retina and is mainly centred in the vitreous chamber of the eye. Extensive tumour necrosis is seen (white arrow). The tumour cells exhibit angulated nuclei with stippled chromatin and scant cytoplasm. Flexner-Wintersteiner rosettes, composed of clusters of short columnar cells arranged around a central lumen, with nuclei displaced away from the lumen, are seen in the inset. Main: HE stain; whole mount magnification. Inset: HE stain; 200× magnification

when there is overt orbital involvement. Close monitoring of the contralateral eye (germline mutation retinoblastoma) and systemic examination for advanced disease until 5–10 years of age, coupled with genetic testing, and counselling are recommended.

Learning Points

Retinoblastoma, although primarily an intraocular disease, may develop extraocular extension with secondary orbital and/or optic nerve invasion with intracranial extension or systemic spread. Early diagnosis with a combination of chemoreduction followed by consolidation are the basis of management. Principles of management include life salvage followed by globe salvage wherever possible, with vision salvage in patients with macular preservation.

Further Reading

1. Al Ali A, Kletke S, Gallie B, Lam WC. Retinoblastoma for pediatric ophthalmologists. Asia Pac J Ophthalmol (Phila). 2018;7(3):160–8. https://doi.org/10.22608/APO.201870. Epub 2018 May 8
2. Honavar SG. Retinoblastoma. They live and they see. www.Aios.org/cme/cmeseries 25.pdf
3. Pérez V, Sampor C, Rey G, et al. Treatment of nonmetastatic unilateral retinoblastoma in children. JAMA Ophthalmol. 2018;136(7):747–52.

Uveal Melanoma

62

Mariel Angelou Parulan, Shantha Amrith, Stephanie Ming Young, Eric Ting, Bingcheng Wu, Min En Nga, and Gangadhara Sundar

Introduction

Melanoma is a relatively rare, highly aggressive tumour that arises from melanocytes located in different parts of the body, and among them, 5% have been reported to arise from the eye and adnexa. Intraocular tumours may initially be missed because they masquerade as another ocular pathology. They can easily mimic the presentation of either a vascular or an inflammatory condition and present with vascular occlusive changes in the eye, elevated intraocular pressure, cataracts, and retinal detachment.

Case Scenario

A 46-year-old Malay male presented with a red painful left eye of a few days' duration. Eight months prior to consult, the patient had noted blurring of vision in that eye which gradually progressed to a total loss of vision. He had earlier been diagnosed and managed as a case of neovascular glaucoma, for which no cause could be identified. On examination, the Snellen visual acuity was 6/6 in the right eye, and no perception of light (NPL) in the left eye. The intraocular pressures were 14 and 50 mm Hg in the right and left eye, respectively. Examination of the right eye was normal, whereas the left eye showed conjunctival injection, corkscrew vessels along nasal conjunctiva with subconjunctival haemorrhage. There were areas of thinning and discolouration of the sclera (Fig. 62.1). Seidel's test was negative. There were peripheral anterior synechiae with oedematous cornea, a few cells in the anterior chamber, ectropion uveae, and nuclear sclerotic cataract. There was no visualization of the posterior segment due to media opacities. Dynamic B-scan was suggestive of a massive subretinal bleed. A CT scan suggested the possibility of an intraocular tumour. Given the poor vision, high intraocular pressure with discomfort, and suggestion of an intraocular tumour, he was advised an enucleation of the left eye.

CLOSE summary is given in Table 62.1.

M. A. Parulan
Department of Ophthalmology, National University Hospital, Singapore

S. Amrith (✉) · S. M. Young · G. Sundar
Department of Ophthalmology, National University Hospital, Singapore

Department of Ophthalmology, Yong Loo Lin School of Medicine, National University of Singapore, Singapore
e-mail: shantha_amrith@nuhs.edu.sg; stephanie.young@nuhs.edu.sg; gangadhara_sundar@nuhs.edu.sg

E. Ting
Department of Diagnostic Imaging, National University Hospital, Singapore

Department of Diagnostic Imaging, Yong Loo Lin School of Medicine, National University of Singapore, Singapore

Advanced Medicine Imaging, Singapore

B. Wu
Department of Pathology, National University Hospital, Singapore

M. E. Nga
Department of Pathology, National University Hospital, Singapore

Department of Pathology, Yong Loo Lin School of Medicine, National University of Singapore, Singapore

S. Amrith et al. (eds.), *Ocular Adnexal Lesions*, https://doi.org/10.1007/978-981-13-3798-7_62

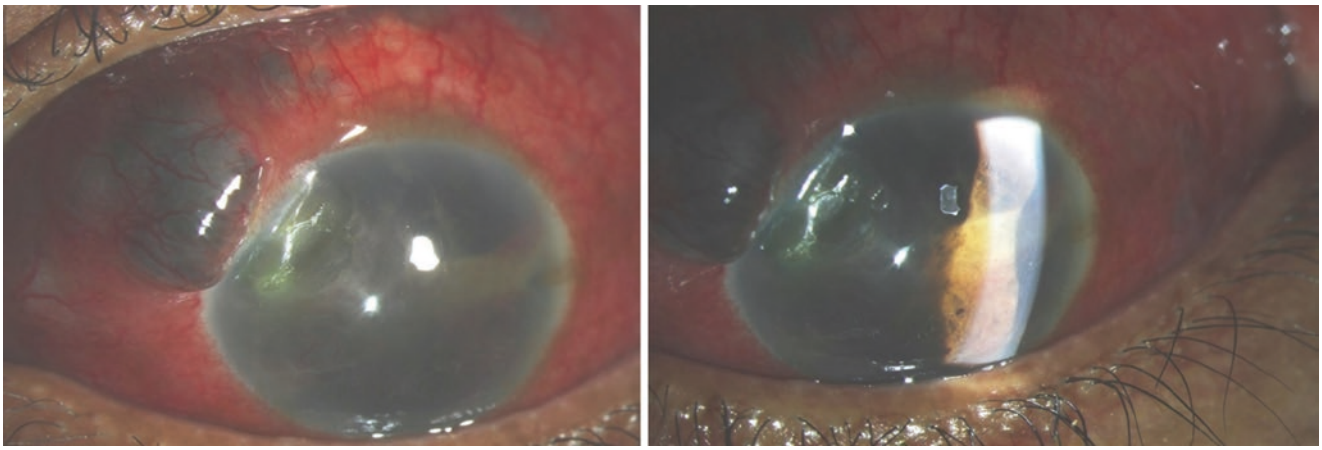

Fig. 62.1 Showing hazy cornea, ectasia of sclera in the superonasal aspect of the left eye with extrascleral extension of the melanoma

Table 62.1 CLOSE summary

*C*linical process	Inflammatory/infiltrative, neovascular glaucoma
*L*ocation	Left eye/orbit
*O*nset	Chronic over 8 months
*S*ymptoms and signs	Left eye pain, redness, and scleral ectasia
*E*pidemiology	46-year-old Malay male

Differential Diagnosis

- Occult neoplasm of the eye
- Carotid cavernous fistula
- Ocular ischaemia
- Scleritis

Imaging

Computerised tomography (CT) of the orbits (Fig. 62.2) showed marked uveoscleral thickening and enhancement of the left globe; there was a note of a hyperdense soft tissue mass along the nasal aspect. The vitreous was generally increased in density, and the left lens was not well visualized. There was also increased soft tissue stranding with thickening and enhancement of soft tissues surrounding the globe, including tendinous insertions of the extraocular muscles (particularly the superior rectus/levator complex) and the lacrimal gland, as well as the left optic nerve sheath. Possibility of an intraocular tumour with extrascleral extension was considered.

Intervention

Systemic workup showed thrombocytosis; hence, a referral to haematology was made. The ultrasound of the abdomen showed numerous heterogeneous, hypoechoic nodules in the liver. CT scan of the abdomen revealed the presence of hepatomegaly secondary to multiple isodense to hypodense hepatic lesions with target sign appearance. A liver core biopsy was performed for a more definitive diagnosis. He subsequently underwent enucleation of the left eye with acrylic implant under general anaesthesia.

Histopathology

Liver biopsy showed multiple tissue cores with nests and cords of tumour cells containing melanin. The features were consistent with a diagnosis of metastatic melanoma.

Enucleated globe showed a tumour occupying the entire posterior and anterior chambers (Fig. 62.3). No residual non-neoplastic uveal tissue was identified. The lens was dislocated and was entirely surrounded by tumour. There were sheets of tumour cells with enlarged pleomorphic nuclei, prominent nucleoli, and intracytoplasmic melanin pigment (Fig. 62.4) with extensive tumour necrosis. Mitotic activity was brisk. There was a note of extrascleral extension, present in the region of the three nodules seen grossly. The tumour extended into the adjacent extraocular fibroadipose and skeletal muscle tissues. The tumour invaded the optic nerve head and through the full thickness of the cornea. The cut end of the optic nerve was free of tumour. The features were consistent with malignant melanoma involving posterior and anterior chambers with extrascleral extension.

Management

The patient was diagnosed with stage 4 (AJCC: T4e, N0, M1c) malignant melanoma and was co-managed with the oncology team. He was started on targeted immune therapy with pembrolizumab. However, the patient died due to liver failure which he had developed before starting immunotherapy.

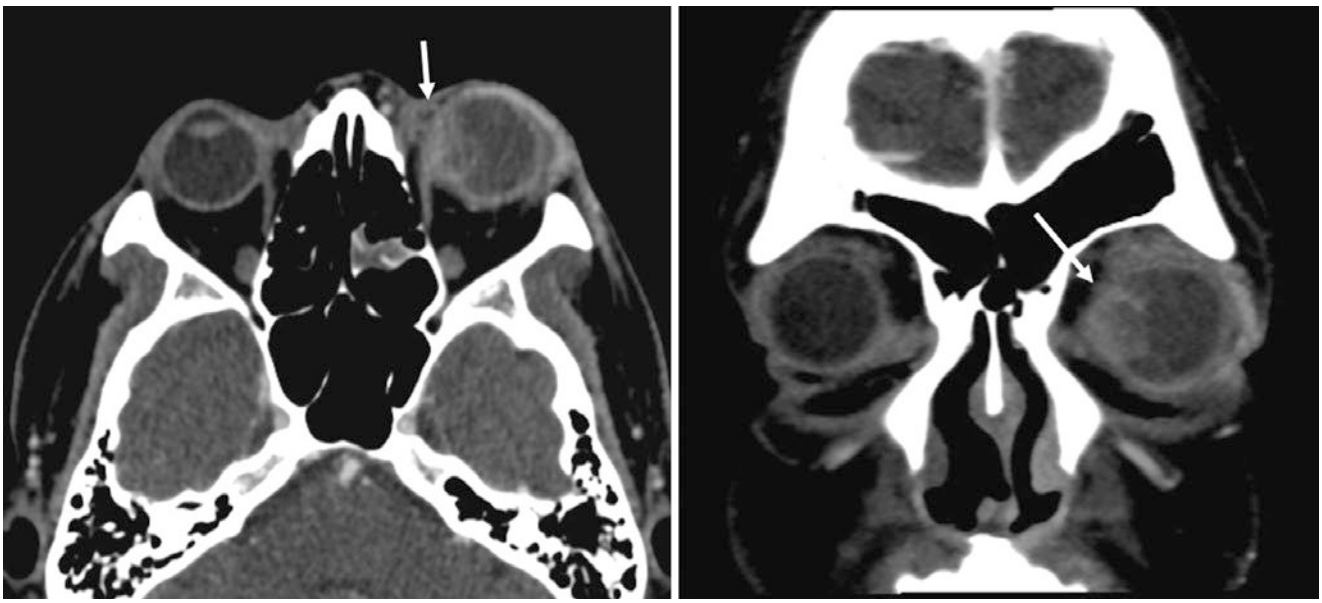

Fig. 62.2 Axial and coronal CT images showing an enhancing choroidal mass (white arrow) in the nasal aspect of the left globe, with distortion of the sclera suggestive of extraocular extension. Note enlargement of the entire left globe with increased density of the vitreous due to haemorrhage

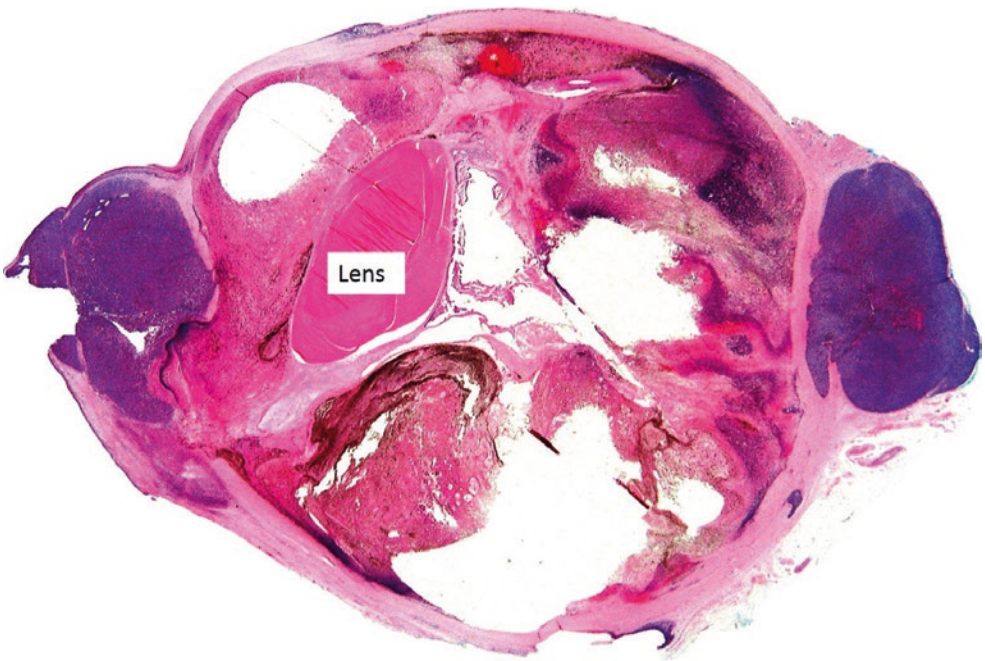

Fig. 62.3 Tumour fills the entire anterior and posterior chambers, with extra-scleral extension. HE stain; whole-mount (1× magnification)

Discussion

Uveal melanoma has a mean age-adjusted incidence of 5.1 cases per million per year among Caucasians and a lower incidence of 0.38 per million per year for Asians. Although uncommon, 79–81% of malignant tumours of the eye are of this type in Caucasians. They are known to be aggressive malignant tumours with early metastasis and poor prognosis. Metastasis occurs haematogenously in 50% of the patients, with the most common site being the liver (60.5–89%), lung (24.4%), skin/soft tissue (10.9%), and bone (8.4%). Approximately 50% of patients with this condition develop metastasis in 10 years, irrespective of treatment type, indicating the presence of clinically undetectable micrometastasis even before the treatment of the primary lesion. Risk factors for tumour dissemination are large size of the uveal melanoma, involvement of the ciliary body, and extraocular extension.

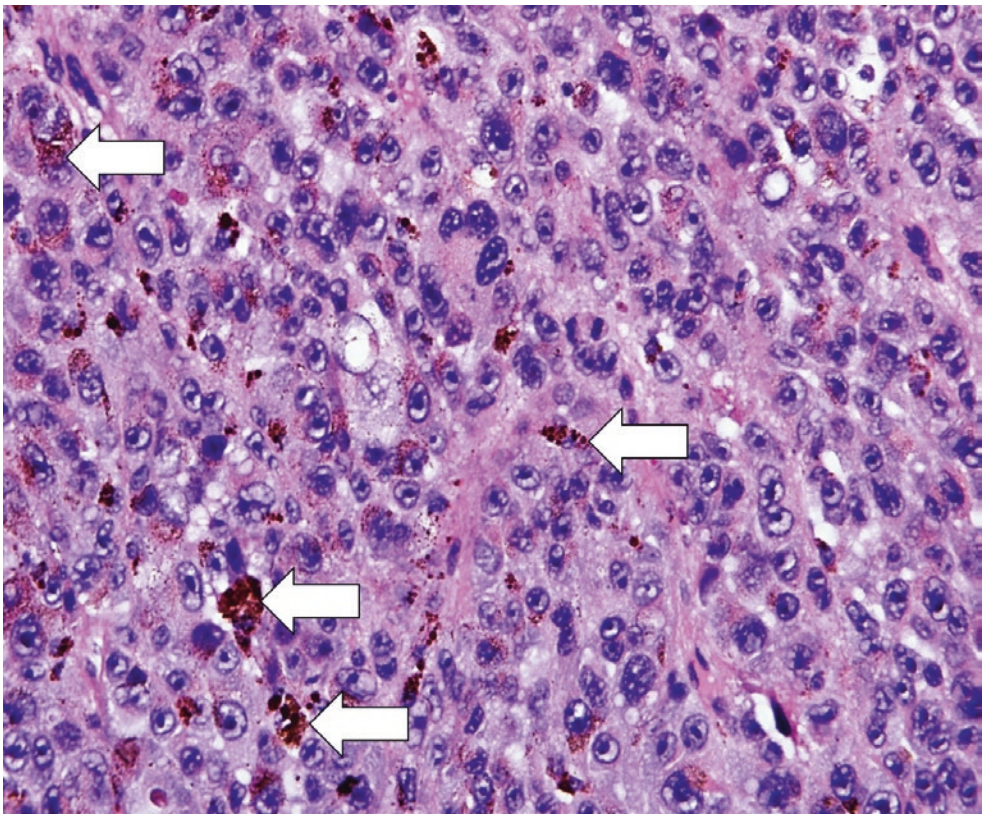

Fig. 62.4 The tumour cells exhibit enlarged pleomorphic nuclei, prominent nucleoli, and intracytoplasmic melanin pigment (white arrows). HE stain; 200× magnification

Presenting symptoms may be variable, which include blurring of vision (37.8%), photopsia (8.6%), floaters (7%), visual field loss (6.1%), visible tumour (3.1%), pain (2.4%), and metamorphopsia (2.2%), and 30% may be asymptomatic at the time of diagnosis. Mechanisms by which tumour induces elevated IOP include local tumour effects causing compression of surrounding structures, direct invasion of ocular structures, associated exudative retinal detachment, tumour necrosis, and haemorrhage. Long-standing exudative retinal detachment with the development of ischaemia possibly results in neovascular glaucoma.

Predisposing factors identified for uveal melanoma include Caucasian race, light skin and eye colour, oculodermal melanocytosis, cutaneous iris and choroidal nevus, and environmental factors (i.e. sunlight exposure and intermittent exposure to artificial ultraviolet light). Chromosome 3 monosomy/BAP1 mutation is associated with higher risk of metastatic disease.

When patients present with painful blind eye, it is important to rule out intraocular tumours such as malignant melanoma. Despite the rarity of this condition in Asians, it is prudent to always consider it in the differential diagnosis due to the aggressive and masquerading nature of this tumour.

Learning Points

- Uveal melanoma is a rare condition especially in Asians, but a high index of suspicion should be present for eye conditions whose underlying cause cannot be completely ascertained. It may present variably but should be considered as a differential diagnosis in painful blind eyes, vascular occlusive, inflammatory, and chronic refractory eye conditions such as neovascular glaucoma.
- Prognosis remains poor especially for advanced stages, and early diagnosis becomes crucial in optimizing management of these patients.

Further Reading

1. Hu DN, Yu GP, McCormick SA, Schneider S, Finger PT. Population-based incidence of uveal melanoma in various races and ethnic groups. Am J Ophthalmol. 2005;140(4):612–7.
2. Kaliki S, Shields CL, Shields JA. Uveal melanoma: estimating prognosis. Indian J Ophthalmol. 2015;63(2):93–102.

3. Kaliki S, Shields CL. Uveal melanoma: relatively rare but deadly cancer. Eye (Lond). 2017;31(2):241–57.
4. Krantz BA, Dave N, Komatsubara KM, Marr BP, Carvajal RD. Uveal melanoma: epidemiology, etiology, and treatment of primary disease. Clin Ophthalmol (Auckland, NZ). 2017;11:279–89.
5. Othman IS, Assem M, Zaki IMA. Secondary glaucoma as initial manifestation of uveal melanoma. Saudi J Ophthalmol. 2013;27(3):203–8.
6. Radcliffe NM, Finger PT. Eye cancer related glaucoma: current concepts. Surv Ophthalmol. 2009;54(1):47–73.
7. Rietschel P, Panageas KS, Hanlon C, Patel A, Abramson DH, Chapman PB. Variates of survival in metastatic uveal melanoma. J Clin Oncol. 2005;23(31):8076–80.
8. Zhao M, Mu Y, Dang Y, Zhu Y. Secondary glaucoma as initial manifestation of ring melanoma: a case report and review of literature. Int J Clin Exp Pathol. 2014;7(11):8163–9.

Part XV

Tumours from Paranasal Sinuses and Nasopharynx

Paranasal Sinus Mucocoele

63

Shantha Amrith, Stephanie Ming Young, Poh Sun Goh, Bingcheng Wu, Min En Nga, and Gangadhara Sundar

Introduction

A mucocoele is a chronic, cystic lesion of the paranasal sinuses, lined by pseudostratified or low columnar epithelium. There is background inflammation, with the cyst filled with mucus, exerting pressure on the boundaries of the sinus due to obstruction of the sinus ostium. The obstruction is caused by congenital anomalies, allergy, infection, trauma, neoplasms and sinus surgery.

Clinical Scenario

A 50-year-old Malay male presented with a history of gradually increasing eyelid swelling over 2 weeks. He felt that his left eye was protruding. It was associated with painless blurring of vision and diplopia in horizontal and vertical gazes. There was no history of fever, previous trauma or surgery.

The right ophthalmic examination was completely normal. Examination of the left eye showed a normal visual acuity, no RAPD and normal anterior and posterior segments. There was fullness of the upper eyelid along with a non-axial proptosis with inferolateral globe displacement (Fig. 63.1). Left supraduction and adduction were limited.

CLOSE summary is given in Table 63.1.

Differential Diagnosis

- Frontoethmoidal sinus mucocoele
- Primary malignancy such as lymphoma
- Secondary malignancy such as nasopharyngeal carcinoma, epithelial malignancy and other tumours arising from the sinuses
- Thyroid eye disease

Imaging

Magnetic resonance imaging (MRI) showed an expanded left frontal sinus due to the presence of a large T2w (Fig. 63.2a) and T1w hyperintense, non-enhancing cystic lesion (mucocoele), which had herniated through the roof of the left orbit. The intraorbital portion displaced the

S. Amrith (✉) · S. M. Young · G. Sundar
Department of Ophthalmology, National University Hospital, Singapore

Department of Ophthalmology, Yong Loo Lin School of Medicine, National University of Singapore, Singapore
e-mail: shantha_amrith@nuhs.edu.sg; stephanie.young@nuhs.edu.sg; gangadhara_sundar@nuhs.edu.sg

P. S. Goh
Department of Diagnostic Imaging, National University Hospital, Singapore

Department of Diagnostic Imaging, Yong Loo Lin School of Medicine, National University of Singapore, Singapore

B. Wu
Department of Pathology, National University Hospital, Singapore

M. E. Nga
Department of Pathology, National University Hospital, Singapore

Department of Ophthalmology, Yong Loo Lin School of Medicine, National University of Singapore, Singapore

S. Amrith et al. (eds.), *Ocular Adnexal Lesions*, https://doi.org/10.1007/978-981-13-3798-7_63

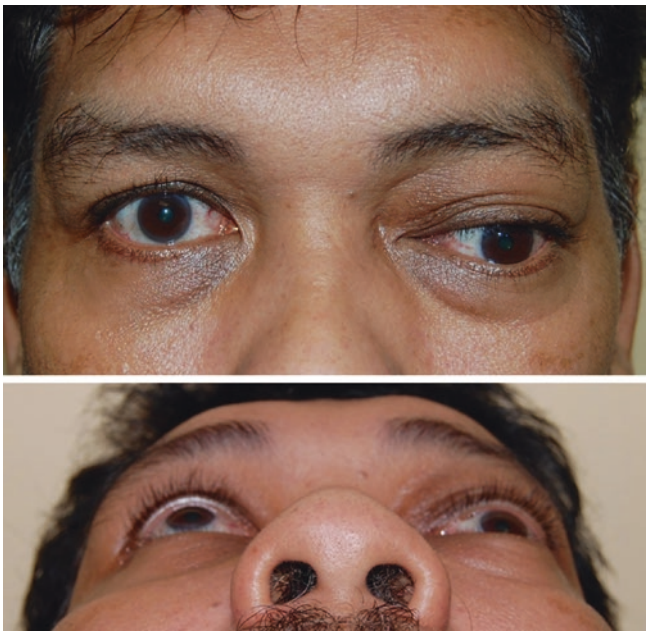

Fig. 63.1 Clinical picture showing left proptosis with the eyeball pushed down and out indicating a mass lesion in the superomedial orbit

Table 63.1 CLOSE summary

*C*linical scenario: mass lesion
*L*ocation: superomedial, extraconal orbit (paranasal sinuses)
*O*nset: subacute
*S*igns and symptoms: left non-axial proptosis with fullness of upper lid and blurring of vision
*E*pidemiology: 50-year-old-Malay male

levator-superior rectus muscle complex inferiorly and was causing proptosis and inferior displacement of the left globe.

There was also expansion of the left spheno-ethmoidal (Onodi) cell by a T2w hypointense and T1w hyperintense, non-enhancing mucocoele. No signal change or enhancement was seen within the optic nerve.

CT scan (Fig. 63.2b and c) showed bony details such as dehiscence of the left orbital roof, body of the sphenoid, anterior clinoid, as well as the medial wall of the optic canal and other soft tissue changes seen on MRI.

A diagnosis of left fronto-spheno-ethmoidal mucocoele was made.

Intervention

The patient was referred to a rhinologist. The patient underwent a functional endoscopic sinus surgery (FESS) with image guidance under general anaesthesia. Complete drainage of the mucocoele was carried out (Fig. 63.3).

Histopathology

Sections showed polypoid looking fragments of respiratory mucosa with cystically dilated subepithelial mucinous glands and extravasated mucin pools within an inflamed, oedematous stroma (Figs. 63.4 and 63.5).

Discussion

Mucocoeles can affect any age group but are most commonly seen between the fourth and seventh decade. There is no gender predilection. The common sites for sinus mucocoele are the frontal, anterior ethmoidal and maxillary sinuses. The posterior ethmoids and the sphenoid sinuses are rarely affected. These lesions expand slowly over the years before they become symptomatic.

The patients may not have any nasal symptoms and may present first with ophthalmic symptoms. Nasal symptoms include blocked nose and headache.

Ophthalmic symptoms appear as the mucocoele increases in size and causes bony erosion extending into the orbit. It causes proptosis which is usually non-axial. There may be associated pain, swelling and diplopia. Loss of vision is unusual but can happen in an expanding lesion in the sphenoid sinus. Occasionally, a mass can be visible on the forehead or the cheek. Intracranial expansion may cause meningitis or brain abscess.

Surgery is necessary for a complete cure. The ultimate goal of surgical intervention involves in re-establishing the sinus drainage and obliteration of the cavity with complete resection of the sinus mucosal lining. It can be carried out endoscopically, externally or by a combined approach. If there is intracranial extension, a craniotomy via an eyelid or a coronal approach along with an endoscopic approach may be necessary for complete resection.

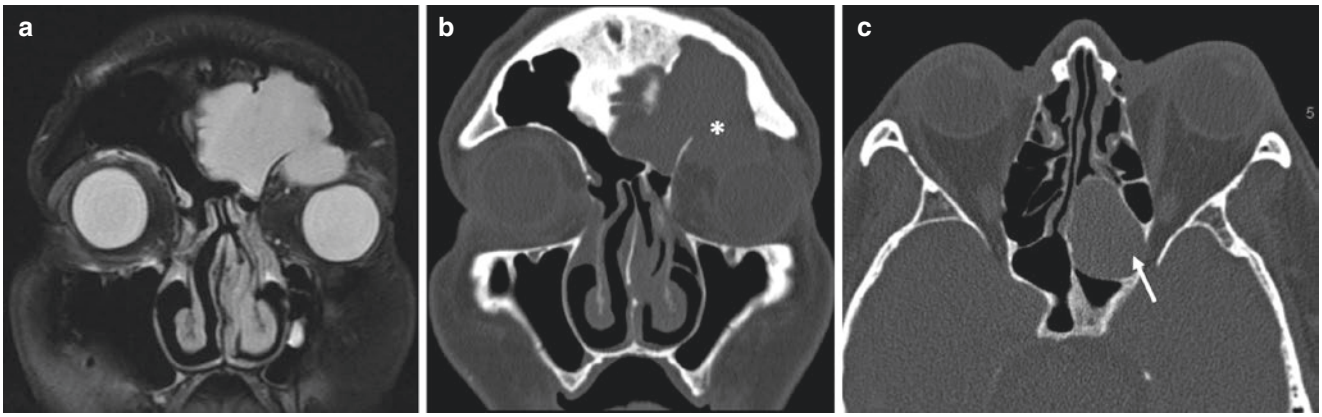

Fig. 63.2 Fronto-ethmoidal sinus mucocoele filling the sinuses on T2w coronal MRI (**a**) and extending into superior left orbit eroding through the roof of the orbit (*) as shown on coronal bone window CT (**b**) and ethmoidal component (white arrow) expanding the sinus and narrowing left orbital apex on axial bone window CT (**c**)

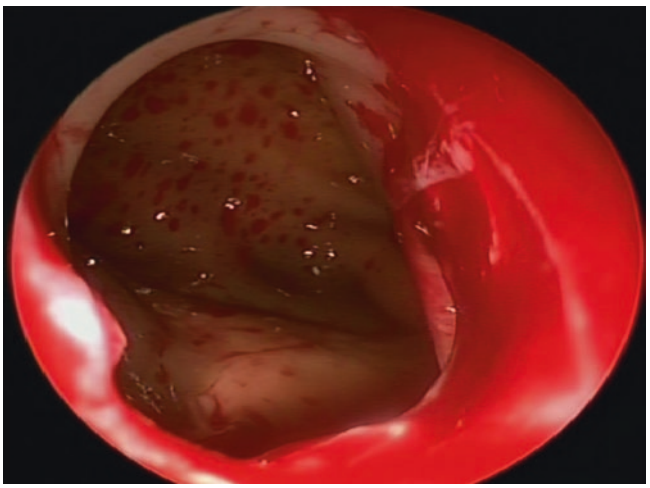

Fig. 63.3 Intraoperative picture of fronto-ethmoidal sinus cavity after the drainage of the mucocoele

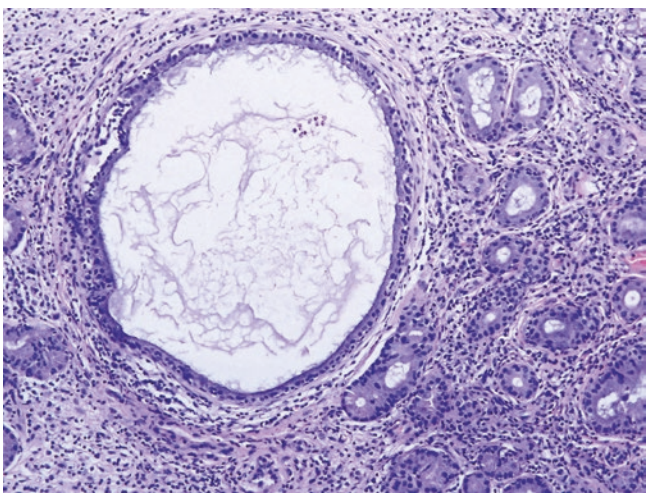

Fig. 63.4 A cystically dilated mucinous gland is seen with chronic inflammatory cells in the surrounding stroma. HE stain; 200× magnification

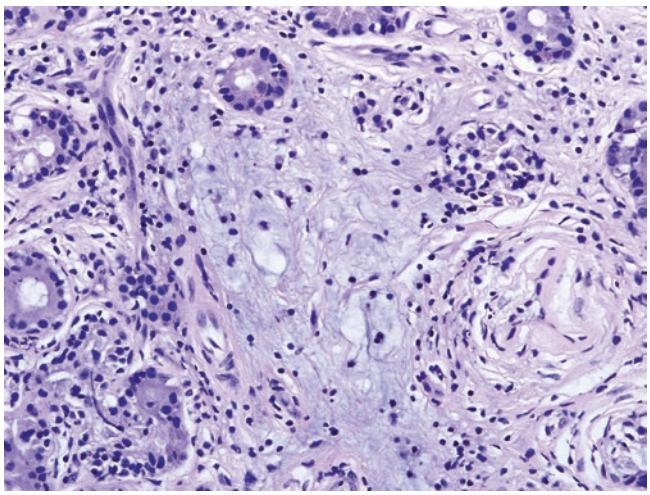

Fig. 63.5 A pool of extravasated mucin is seen within the inflamed stroma. HE stain; 300× magnification

Learning Points

Paranasal sinus mucocoeles affect the orbit as they expand and erode the bone. The patients may first present to an ophthalmologist with symptoms such as non-axial proptosis, pain and diplopia. It is important to recognize the symptoms and make appropriate referral to the rhinologist. Management is surgical and involves complete removal and re-establishing drainage of the affected sinuses.

Further Reading

1. Amrith S, Lin KK, Sundar JKG, Shuen CS. A review of orbital involvement in patients with primary paranasal sinus space occupying lesions in a south-east Asian Tertiary Centre. J Otol Rhinol. 4:3.

2. Hayasaka S, Shibasaki H, Sekimoto M, Setogawa T, Wakutani T. Ophthalmic complications in patients with paranasal sinus mucopyoceles. Ophthalmologica. 1991;203:57–63.
3. Khong JJ, Malhotra R, Wormald PJ, Selva D. Endoscopic sinus surgery for paranasal sinus mucocele with orbital involvement. Eye. 2004;18:877–81.
4. Lai PC, Liao SL, Jou JR, Hou PK. Transcaruncular approach for the management of frontoethmoida mucoceles. Br J Ophthalmol. 2003;87:699–703.
5. Rao VM, Sharma D, Madan A. Imaging of frontal sinus disease: concepts, interpretation, and technology. Otolaryngol Clin N Am. 2001;34:23–39.
6. Tan CSH, Yong VKY, Yip LW, Amrith S. An unusual presentation of a giant frontal sinus mucocele manifesting with a subcutaneous forehead mass. Ann Acad Med Singap. 2005;34(5):397–8.

Malignant Epithelial Tumours of Paranasal Sinuses

64

Shantha Amrith, Stephanie Ming Young, Eric Ting, Bingcheng Wu, Min En Nga, and Gangadhara Sundar

Introduction

The orbits share two walls with the nasal cavity and paranasal sinuses, the medial wall with the ethmoids and the floor with the maxillary sinus. In addition, the medial part of the roof of the orbit shares a common wall with the frontal sinus. The spread of sinonasal tumours into the orbit is facilitated by the preformed channels (neurovascular bundles) and thin bones like the lamina papyracea. The periorbita forms a barrier to the spread of the tumour into the orbit. Once the tumour transgresses the periorbita, it spreads into a space which has no barriers.

Malignant epithelial tumours of the sinuses are more common (65%) than lymphomas or sarcomas. The maxillary sinus is the most affected followed by ethmoids. Malignant tumours arising from the frontal sinus are very rare. As the sinuses are air-filled cavities, carcinomas of the sinuses tend to be confined locally until late stages. They become locally invasive with tumour expansion and involve the adjacent structures such as the orbit, brain and oral cavity.

Case Scenarios

Case 1

A 68-year-old Chinese female complained of progressive left eye swelling, redness and pain over 1 month. She also complained of a nasal block in the left nostril, without epistaxis. On examination, the visual acuity, the anterior and posterior segments of both eyes, were within normal limits. There was a left hyperglobus of 7 mm with proptosis. The palpebral aperture was grossly reduced, and the conjunctiva showed injection and chemosis. Ocular motility was severely limited on infraduction. There was fullness and erythema with a non-tender mass lesion on the left cheek with no paraesthesia. Left endoscopic nasal examination revealed a bluish gelatinous lesion with uneven surface between the nasal septum and middle turbinate (Fig. 64.1).

CLOSE summary is given in Table 64.1.

S. Amrith (✉) · S. M. Young · G. Sundar
Department of Ophthalmology, National University Hospital, Singapore

Department of Ophthalmology, Yong Loo Lin School of Medicine, National University of Singapore, Singapore
e-mail: shantha_amrith@nuhs.edu.sg; stephanie.young@nuhs.edu.sg; gangadhara_sundar@nuhs.edu.sg

E. Ting
Department of Diagnostic Imaging, National University Hospital, Singapore

Department of Diagnostic Imaging, Yong Loo Lin School of Medicine, National University of Singapore, Singapore

Advanced Medicine Imaging, Singapore

B. Wu
Department of Pathology, National University Hospital, Singapore

M. E. Nga
Department of Pathology, National University Hospital, Singapore

Department of Pathology, Yong Loo Lin School of Medicine, National University of Singapore, Singapore

S. Amrith et al. (eds.), *Ocular Adnexal Lesions*, https://doi.org/10.1007/978-981-13-3798-7_64

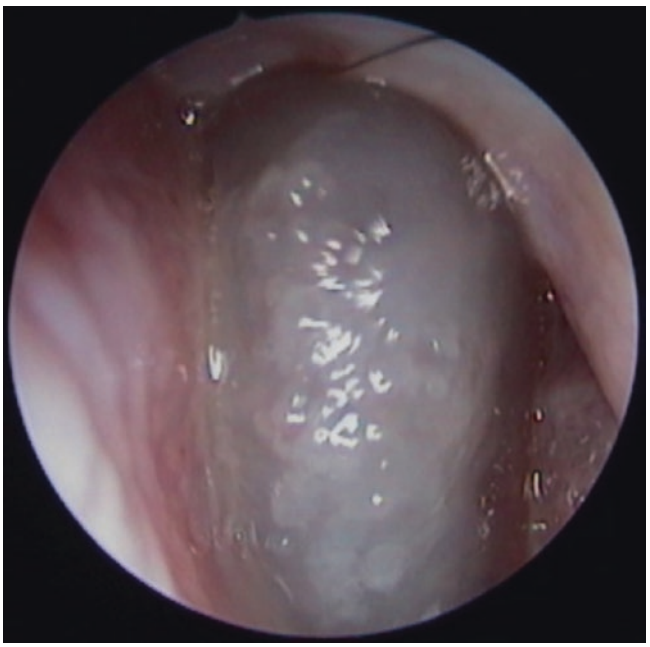

Fig. 64.1 Endoscopic nasal examination of Case 1 showing a bluish, gelatinous looking mass in the nasal cavity

Table 64.1 CLOSE summary for Case 1

*C*linical process: infiltrative mass
*L*ocation: left inferior orbit and cheek
*O*nset: subacute
*S*ign and symptoms: erythematous conjunctiva, hyperglobus and mass in the cheek with nasal obstruction
*E*pidemiology: elderly Chinese female

Differential Diagnosis

- Infective: Fungal most likely
- Inflammatory: Granulomatosis with polyangiitis (GPA or Wegener's)
- Epithelial malignant tumour of the maxillary sinus with orbital extension
- Lymphoma
- Nasopharyngeal carcinoma
- Inverted papilloma
- Sarcoma

Imaging

On contrast-enhanced CT images, a heterogeneously enhancing sinonasal mass, occupying the left maxillary sinus and nasal cavities with invasion into the left orbit, was seen (Fig. 64.2). There were bony erosions of the lamina papyracea and orbital floor with infiltration of the inferior rectus muscle. Superiorly, the mass invaded the intracranial cavity through the ethmoidal roof and cribriform plate. Posterolaterally there was extension into the infratemporal fossa and pterygopalatine fossa. Anteriorly, there was extension into the premaxillary soft tissues.

Intervention

Under local anaesthesia, a transnasal incisional biopsy was obtained by the rhinologist through an endoscopic approach, and tissue was sent for histopathology.

Histopathology

Fragments of sinus mucosa showed infiltrative nests of malignant squamous epithelium with prominent nuclear atypia, surrounded by desmoplastic stroma (Fig. 64.3). The features were consistent with squamous cell carcinoma.

Management

The patient was co-managed with the oncologist. Systemic evaluation showed no nodal or distant metastasis.

Tumour was staged at T4N0M0 (moderately differentiated SCC).

The patient was advised chemoradiotherapy followed by surgery.

Case 2

A 63-year-old Chinese female presented with pain and progressive deterioration of vision in the left eye for 2 months. On examination of the left eye, the visual acuity was counting fingers at ½ metre associated with a relative afferent pupillary defect (RAPD). The anterior and posterior segments were unremarkable. There was a non-axial proptosis of 2 mm with hyperglobus (Fig. 64.4). The ocular motility was full in all directions of gaze. The left infraorbital area was swollen, giving an impression of a mass lesion. The right ophthalmic examination was completely normal.

CLOSE summary is given in Table 64.2.

Differential Diagnosis

Same as the ones listed for Case 1.

Imaging

Computerised tomography (CT) scan showed similar findings as Case 1.

Intervention

A transnasal incisional biopsy was performed by the rhinologist.

Histopathology

Maxillary sinus tissue showed infiltrative nests of tumour cells arranged in a cribriform architecture (smaller lumina within a single sheet/nest). The surrounding stroma was desmoplastic (Fig. 64.5). The cells were

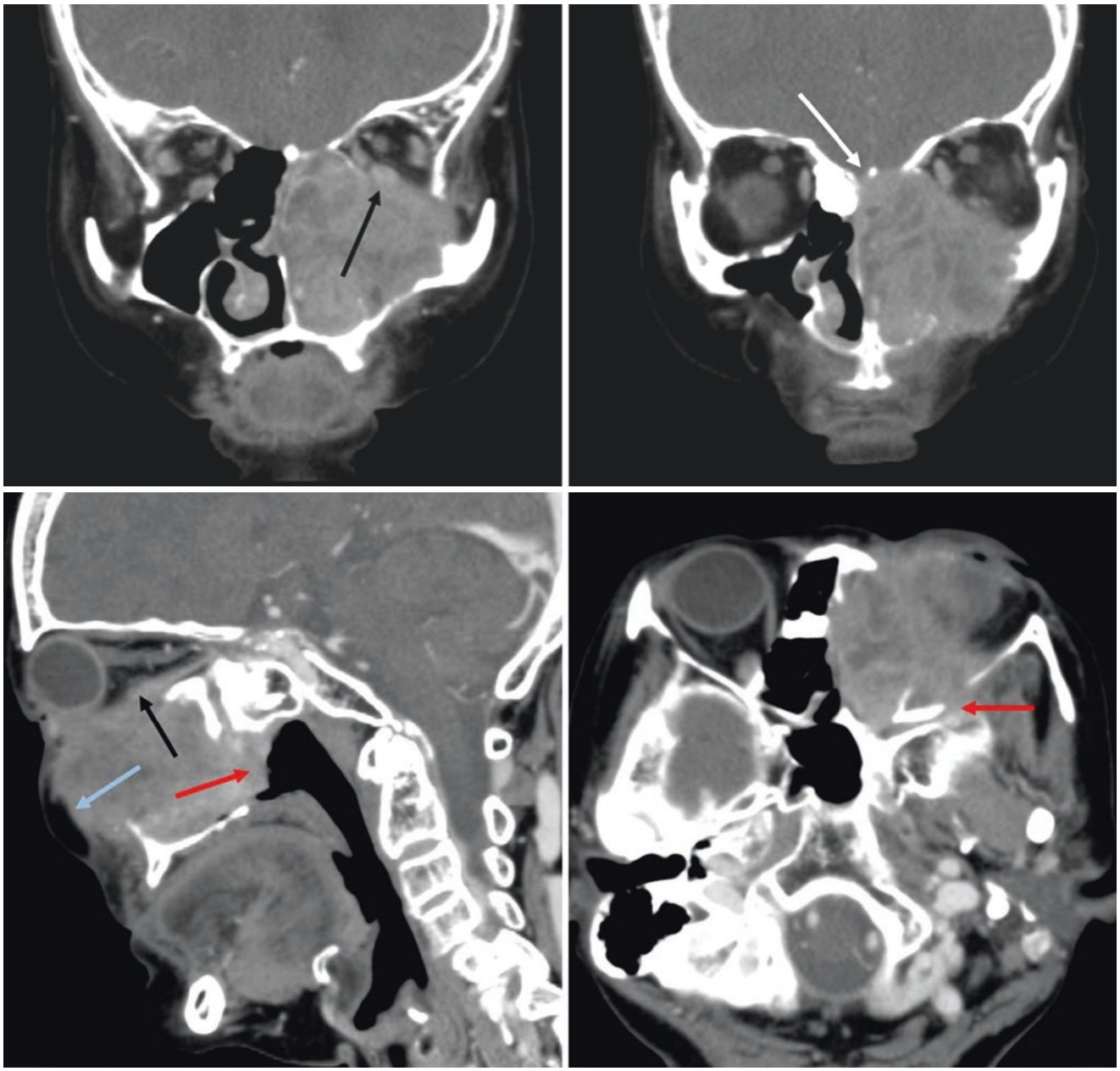

Fig. 64.2 Contrast-enhanced CT images (top, coronal, and bottom, axial) showing an aggressive, heterogeneously enhancing sinonasal mass invading the left orbit. There is aggressive bony erosion of the lamina papyracea and orbital floor, with infiltration of the inferior rectus muscle (black arrow). Superiorly, the mass has invaded the intracranial cavity through the ethmoid roof and cribriform plate (white arrow). Posterolaterally, there is extension into the infratemporal fossa and pterygopalatine fossa (red arrows). Anteriorly, there is extension into the premaxillary soft tissues (blue arrow)

basaloid with rather angulated nuclei and high nuclear/cytoplasmic ratio (Fig. 64.6). Tumour was also seen within a vascular space (Fig. 64.5). Many of the tumour cells were positive for CD117 on immunohistochemistry. The features were consistent with a sinonasal adenoid cystic carcinoma.

Management

After systemic investigations, the tumour was staged at T4N0M0. The patient underwent external beam radiotherapy (33 sessions). She was well for about 1 year, but developed metastasis in the vertebrae, and died of metastatic disease within 3 years of diagnosis.

Discussion

Carcinomas of the paranasal sinuses form about 2–3% of all the head and neck carcinomas. Males are more commonly affected with male to female ratio of 2:1. They generally

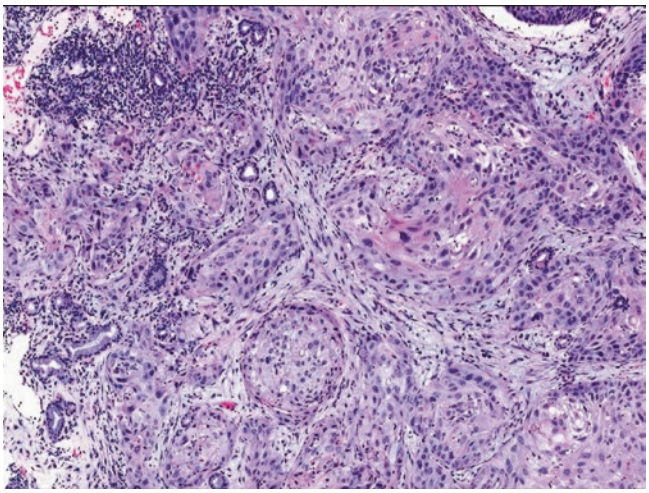

Fig. 64.3 There are infiltrative nests of malignant squamous epithelium with prominent nuclear atypia, surrounded by desmoplastic stroma. HE stain; 200× magnification

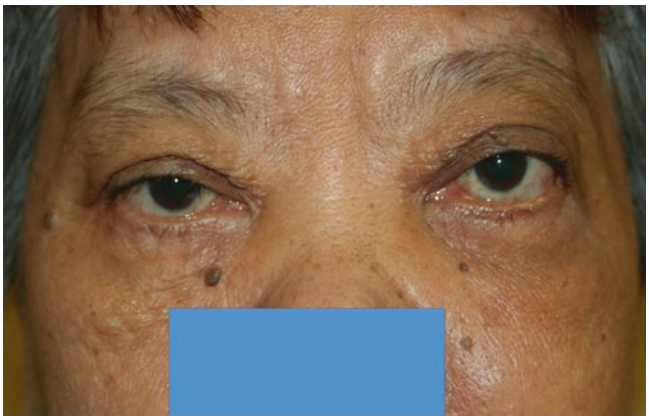

Fig. 64.4 Clinical picture of Case 2 showing hyperglobus and prominence in the left infraorbital area

Table 64.2 CLOSE summary of Case 2

*C*linical process: mass effect
*L*ocation: left orbit
*O*nset: subacute
*S*igns and symptoms: painful loss of vision with proptosis
*E*pidemiology: elderly Chinese female

affect people who are 50–70 years old. The common aetiological factors include inhaled carcinogens and human papilloma virus. The most common is squamous cell carcinoma (73%), followed by adenocarcinoma and adenoid cystic carcinoma (10% each).

Patients present with facial swelling, pain and paraesthesia over the cheek. As the tumour spreads to the nasal cavity, they develop epistaxis, nasal obstruction and nasal discharge. Orbital invasion causes proptosis, diplopia, impaired vision and orbital pain.

Imaging plays an important role in determining the origin and extent of local invasion. Factors indicative of poor prognosis are advanced T-stage, nodal stage (N1-3), as well as recurrence due to incomplete local tumour clearance. Distant metastasis is only seen in 12%. Some authors report a 5-year survival of 17% with orbital involvement, as opposed to 49% without.

The treatment in early stages is surgical removal (an endoscopic approach is feasible in most cases) and sometimes combined with external beam radiotherapy. In advanced stages, the patients should be managed by a multidisciplinary team because of the proximity of the sinuses to the orbits and brain. An aggressive local removal including orbital exenteration and craniofacial resection should be combined with concomitant chemo-radiation to prevent local recurrence. Orbital exenteration is indicated when the orbital apex, extraocular muscles, conjunctiva and the periorbita are involved. The craniofacial resection carries with it high morbidity, and it involves further surgeries for reconstruction of the surgical defect. The eye function may be adversely affected in orbit-sparing procedures especially if it involves the maxillary sinus. The dystopia due to the removal of orbital floor results in troublesome diplopia and limitation of eye movements. Therefore, large defects resulting from complete removal of the orbital floor and medial wall, as well as large portions of orbital periosteum, should undergo reconstruction in order to preserve the eye function.

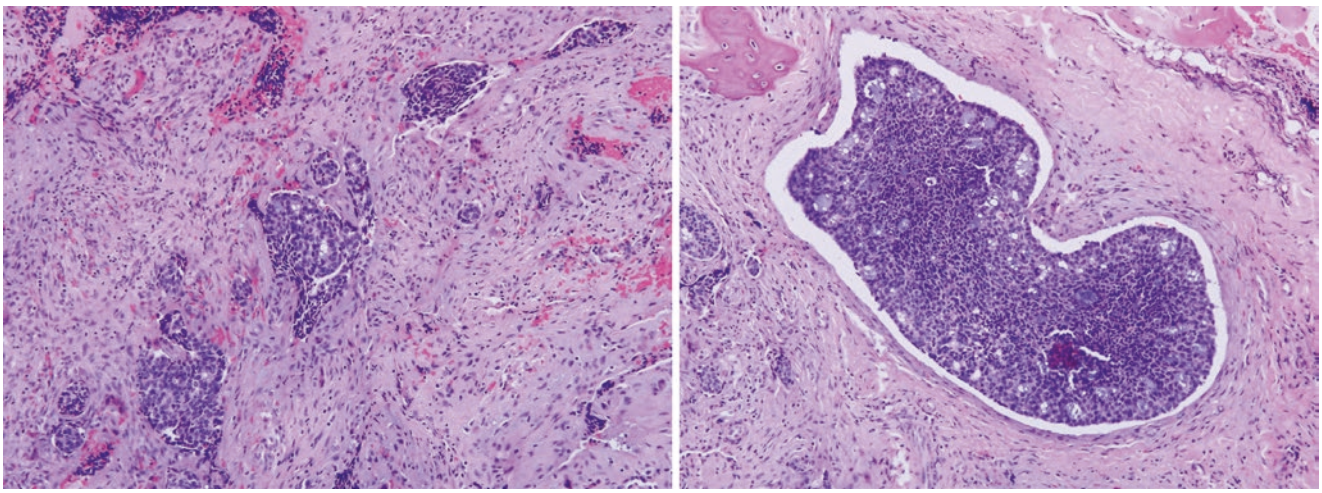

Fig. 64.5 Histopathology shows infiltrative nests of tumour cells surrounded by desmoplastic stroma (left). Tumour is also seen within a vascular space (right). Left: HE stain; 40× magnification. Right: HE stain; 40× magnification

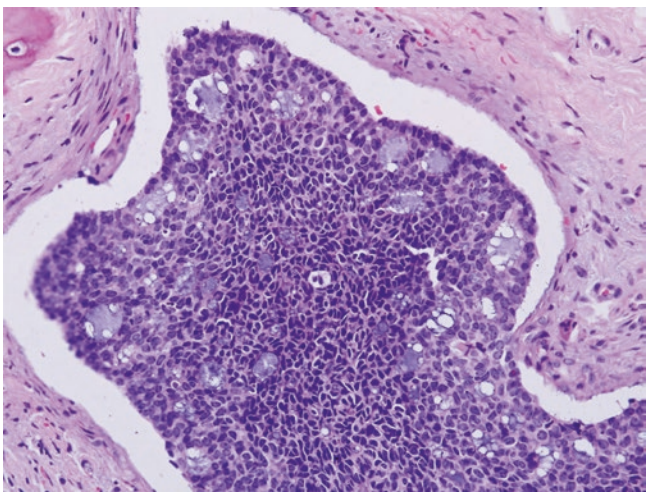

Fig. 64.6 Cribriform architecture is discerned. The tumour cells feature angulated hyperchromatic nuclei and high nuclear/cytoplasmic ratios. HE stain; 200× magnification

Learning Points

Sinonasal carcinomas are locally invasive and affect the orbits and brain. Eye-sparing surgery should be tried where possible, but orbital exenteration is inevitable if orbital apex, extraocular muscles, conjunctiva and periorbita are involved. Radical surgery should be followed by chemo-radiation in advanced cases. The prognosis is poor with than without orbital involvement.

Further Reading

1. Kawaguchi M, Kato H, Tomita H, et al. Imaging characteristics of malignant sinonasal tumors. J Clin Med. 2017;6(12):116.
2. Lewis JS. Sinonasal squamous cell carcinoma: a review with emphasis on emerging histologic subtypes and the role of human papillomavirus. Head Neck Pathol. 2016;10(1):60–7.
3. Nishino H, Ichimura K, Tanaka H, Ishikawa K, Abe K, et al. Results of orbital preservation for advanced malignant maxillary sinus tumors. Laryangoscope. 2003;113:1064–9.
4. Resto VA, Chan AW, Deschler DG, Lin DT. Extent of surgery in the management of locally advanced sinonasal malignancies. Head Neck. 2008;30(2):222–9.
5. Suárez C, Ferlito A, Lund VJ, et al. Management of the orbit in malignant sinonasal tumours. Head Neck. 2008;30:242–50.
6. Tiwari R, et al. Squamous cell Ca of maxillary sinus. Head Neck. 2000;22:164–9.

Sino-nasal Lymphomas

65

Shantha Amrith, Stephanie Ming Young, Eric Ting, Bingcheng Wu, Min En Nga, and Gangadhara Sundar

Introduction

Primary nasal lymphoma is more common among Asians compared to Westerners. Significant differences exist in the incidence and immunophenotypic characteristics among different geographic areas and ethnic groups. Nasal lymphoma of natural killer (NK) T-cell phenotype is more common in Far East Asian countries (Japan, Korea, Taiwan, and China) and B-cell lymphoma in the West. NK T-cell lymphomas tend to be nasal and are usually Epstein-Barr virus (EBV) positive, whereas B-cell lymphomas tend to be sino-nasal and are negative for EBV. The orbits are more commonly involved in the latter. The most common subtype of sino-nasal lymphoma is the diffuse large B-cell lymphoma (DLBCL). The prognosis for this tumour is generally poor.

Case Scenario

A 65-year-old otherwise healthy Chinese male presented with redness and swelling in the inner corner of the left eye of 2 weeks' duration, not associated with visual symptoms or pain. Examination of the left eye showed conjunctival injection, swelling in the medial part of the upper lid, and a non-axial proptosis of 5 mm with displacement of the eyeball laterally (Fig. 65.1). Ocular motility was full except for a mild adduction deficit. Rest of the eye examination including the vision, pupil, and anterior and posterior segments were normal. The right eye examination was unremarkable.

CLOSE summary is given in Table 65.1.

Differential Diagnosis

- Fronto-ethmoidal mucocoele
- Sino-nasal malignant epithelial tumour
- Lymphoproliferative lesion of the orbit or sinus
- Medial orbital inflammatory mass
- Metastatic lesion
- Dermoid – unlikely due to age
- Thyroid eye disease

Imaging

Contrast-enhanced CT of the orbits and sinuses showed a smooth, lobulated, expansile mass centred on the left frontal, ethmoidal and sphenoidal sinuses, with intranasal and

S. Amrith (✉) · S. M. Young · G. Sundar
Department of Ophthalmology, National University Hospital, Singapore

Department of Ophthalmology, Yong Loo Lin School of Medicine, National University of Singapore, Singapore
e-mail: shantha_amrith@nuhs.edu.sg; stephanie.young@nuhs.edu.sg; gangadhara_sundar@nuhs.edu.sg

E. Ting
Department of Diagnostic Imaging, National University Hospital, Singapore

Department of Diagnostic Imaging, Yong Loo Lin School of Medicine, National University of Singapore, Singapore

Advanced Medicine Imaging, Singapore

B. Wu
Department of Pathology, National University Hospital, Singapore

M. E. Nga
Department of Pathology, National University Hospital, Singapore

Department of Pathology, Yong Loo Lin School of Medicine, National University of Singapore, Singapore

S. Amrith et al. (eds.), *Ocular Adnexal Lesions*, https://doi.org/10.1007/978-981-13-3798-7_65

extraconal orbital extension encroaching on the orbital apex. There was accompanying bony erosion (Fig. 65.2). The appearances were compatible with a rapidly growing mucocoele; however, an MRI was advised in view of fairly extensive bony destruction to rule out a soft tissue tumour.

Contrast-enhanced MRI of the nasal cavity and neck showed moderately enhancing smooth, lobulated, expansile mass of soft tissue intensity filling the left ethmoid, frontal, sphenoid sinuses, and superior nasal cavity. The mass was encroaching onto the left orbital extraconal space, pushing the medial rectus and the eyeball laterally (Fig. 65.3). The appearance in MRI was consistent with an infiltrative soft tissue tumour.

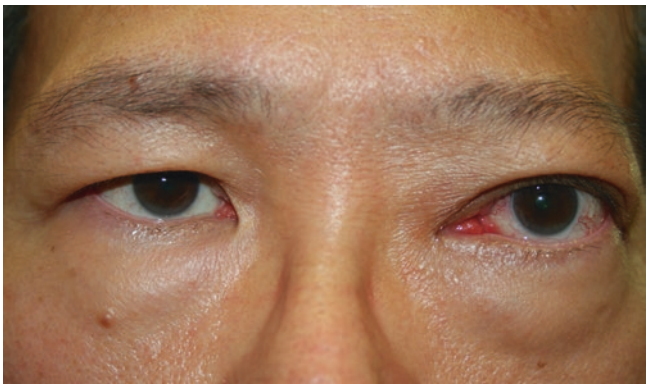

Fig. 65.1 Clinical picture showing redness, swelling of the eyelid and non-axial proptosis with lateral displacement of the globe

Table 65.1 CLOSE summary

*C*linical process: mass lesion
*L*ocation: left orbit
*O*nset: acute
*S*igns/symptoms: swelling in the inner corner of the upper lid with redness of the left eye
*E*pidemiology: 65-year-old Chinese male

Intervention

The patient was referred to a rhinologist, who performed a transnasal, endoscopic incisional biopsy of the nasal mass. The tissue was sent fresh for histopathological analysis.

Histopathology

The microscopic sections showed a diffuse sheetlike infiltrate of medium- to large-sized neoplastic lymphoid cells with admixed reactive small lymphocytes. The neoplastic lymphoid cells showed considerable nuclear pleomorphism and multiple conspicuous nucleoli. There was prominent apoptotic and mitotic activity.

Immunohistochemistry The neoplastic lymphoid cells stained positively for CD20, CD79A, BCL2, and MUM-1. No follicular dendritic meshworks were seen on CD21 immunostain. In situ hybridization for EBER (EBER-ISH) was negative in the neoplastic lymphoid cells. The Ki-67 proliferative index was approximately 80–90%. The features were consistent with a diagnosis of diffuse large B cell lymphoma (DLBCL).

(For histopathological figures, please refer to Fig. 37.2 and 37.3 on DLBCL).

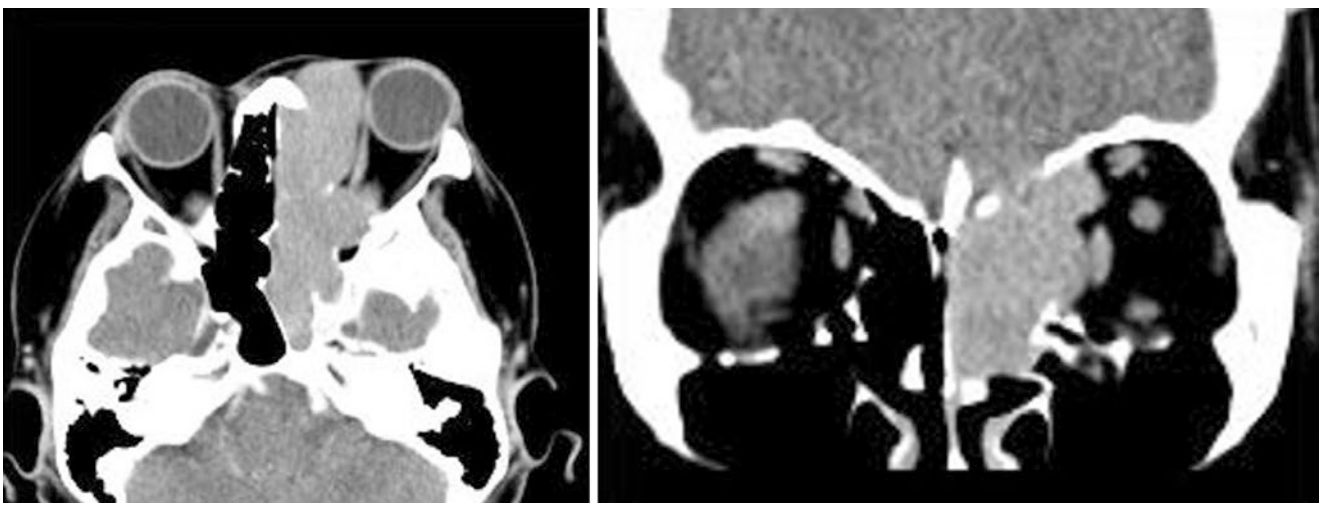

Fig. 65.2 Contrast-enhanced axial and coronal CT scans showing smooth, lobulated, expansile mass centred on the left frontal, ethmoid and sphenoid sinuses, with intracranial, nasal cavity and extraconal orbital extension where it encroaches on the orbital apex. Note the accompanying bony erosion

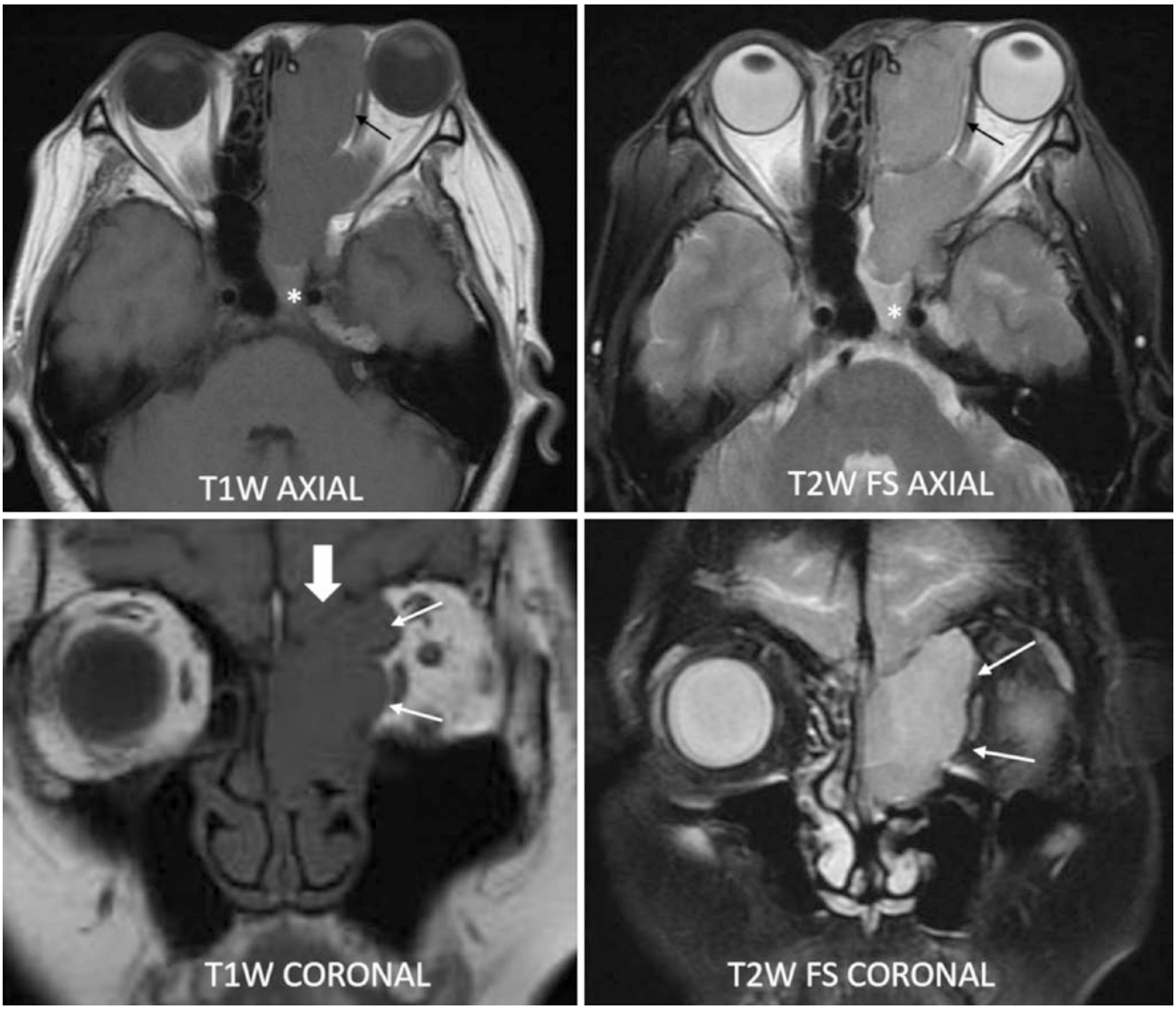

Fig. 65.3 MRI scan of the sinuses shows a smooth, lobulated, expansile mass, almost isointense to grey matter on T1 and T2w sequences, filling the left ethmoidal, frontal and sphenoidal sinuses, and nasal cavity. Note the expansion into the left orbit pushing the medial rectus and eye ball (thin arrows) and intracranial space (block arrow). Note the difference in signal intensity between the mass and the obstructed, protein-rich secretions in the sphenoid sinus (*)

Management

The patient was referred to a lymphoma specialist, who carried out a systemic workup including PET CT, bone marrow biopsy, and lumbar puncture, all of which were negative.

The tumour was staged as Ann Arbor stage 2e. The patient underwent six cycles of R-CHOP therapy along with four cycles of intrathecal methotrexate. The patient has remained free of tumour recurrence for 7 years.

Discussion

Patients with nasal lymphoma may present with ophthalmic symptoms secondary to orbital invasion. Symptoms include painless swelling, mass lesions in the medial part of the eyelids with minimal inflammatory symptoms, and proptosis.

The most common lymphoma to arise in the sino-nasal area is DLBCL, followed by nasal NK/T-cell lymphoma. DLBCL usually affects sinuses without nasal involvement,

whereas NK/T-cell type lymphomas affect the nasal cavity without sinus involvement. Patients with DLBCL are older with a higher male-to-female ratio compared to patients with nasal NK/T-cell lymphomas. Lymphomas of B-cell lineage are more likely to be associated with extension to the orbit, thereby giving rise to ophthalmic symptoms than lymphomas of T- or NK-cell lineage. Asian studies show that the nasal NK/T-cell lymphoma has a very poor prognosis, unlike the West, where both nasal NK/T-cell lymphomas and DLBCL have a similar outcome.

It may be challenging to distinguish these lesions from sinus mucocoele based on CT scan alone. An MRI is preferable to arrive at the proper diagnosis.

(Refer to chapter 37 on DLBCL for more details on this tumour).

Learning Points

Non-axial proptosis in a lateral direction should always raise the suspicion of a lesion in the paranasal sinuses. Both CT and MRI may be necessary as CT helps to evaluate bony erosion, while MRI gives a better soft tissue definition and helps to distinguish tumour from mucocoele. DLBCL (B-cell tumour) and NK-T-cell lymphomas are more common in the sino-nasal area.

Sino-nasal DLBCL is more common in Westerners compared to NK-T cell lymphoma (more common in Asians). DLBCL tends to affect the paranasal sinuses, and hence the orbits, whereas NK T-cell lymphoma affects the nasal cavity. The prognosis is generally poor for both types of lymphoma.

Further Readings

1. Cuadra-Garcia I, Proulx GM, Wu CL, Wang CC, Pilch BZ, Harris NL, Ferry JA. Sinonasal lymphoma: a clinicopathologic analysis of 58 cases from the Massachusetts General Hospital. Am J Surg Pathol. 1999;23(11):1356–69.
2. Azarpira N, Monabati A, Makarempour A, et al. Primary lymphoma of nasal cavity and paranasal sinuses. Lab Med. 2012;43(6):294–9.

Nasopharynx: Nasopharyngeal Carcinoma

66

Shantha Amrith, Stephanie Ming Young, Eric Ting, Bingcheng Wu, Min En Nga, and Gangadhara Sundar

Introduction

Nasopharyngeal carcinoma (NPC), a specific variant of squamous cell carcinoma of the nasopharynx, is a common malignancy in Southeast Asia and Southern China. The incidence of NPC is reported to be 30 times higher among the Chinese, compared to Caucasians. Ophthalmic manifestations of NPC usually occur due to an intracranial extension of the tumour, and they include isolated or multiple cranial nerve palsies, orbital apex or cavernous sinus syndromes and papilloedema or unilateral optic disc swelling. Orbital involvement in NPC occurs in about 3% of patients, which may present as proptosis, diplopia, blurring of vision, eyelid swelling, orbital pain, and epiphora.

Case Scenario

A 34-year-old Chinese male with no significant medical history of note presented with facial numbness over the right infraorbital area of 1 year duration. Subsequently, he noticed double vision and progressive protrusion of the right eye with disappearance of his double eyelid crease. MRI of the orbits performed elsewhere showed a mass lesion in the right orbit, for which an incisional biopsy through a lateral orbitotomy was performed. It was reported as squamous cell carcinoma.

The ocular examination revealed normal visual acuities, colour vision, and pupils. The anterior and posterior segment examinations were normal. He was noted to have a surgical scar at the lateral canthal area of the right eye from his previous orbitotomy. Right ophthalmic examination further revealed a non-axial proptosis of 6 mm with hyperglobus (Fig. 66.1), and global restriction of ocular motility with resultant double vision in all directions. A mass was palpable in the deep inferior orbit with resistance to retropulsion. Regional examination did not reveal any lymphadenopathy, but there was hypoaesthesia over the distribution of the cranial nerves V2 and V3.

CLOSE summary is given in Table 66.1.

S. Amrith (✉) · S. M. Young · G. Sundar
Department of Ophthalmology, National University Hospital, Singapore

Department of Ophthalmology, Yong Loo Lin School of Medicine, National University of Singapore, Singapore
e-mail: shantha_amrith@nuhs.edu.sg; stephanie.young@nuhs.edu.sg; gangadhara_sundar@nuhs.edu.sg

E. Ting
Department of Diagnostic Imaging, National University Hospital, Singapore

Department of Diagnostic Imaging, Yong Loo Lin School of Medicine, National University of Singapore, Singapore

Advanced Medicine Imaging, Singapore

B. Wu
Department of Pathology, National University Hospital, Singapore

M. E. Nga
Department of Pathology, National University Hospital, Singapore

Department of Pathology, Yong Loo Lin School of Medicine, National University of Singapore, Singapore

S. Amrith et al. (eds.), *Ocular Adnexal Lesions*, https://doi.org/10.1007/978-981-13-3798-7_66

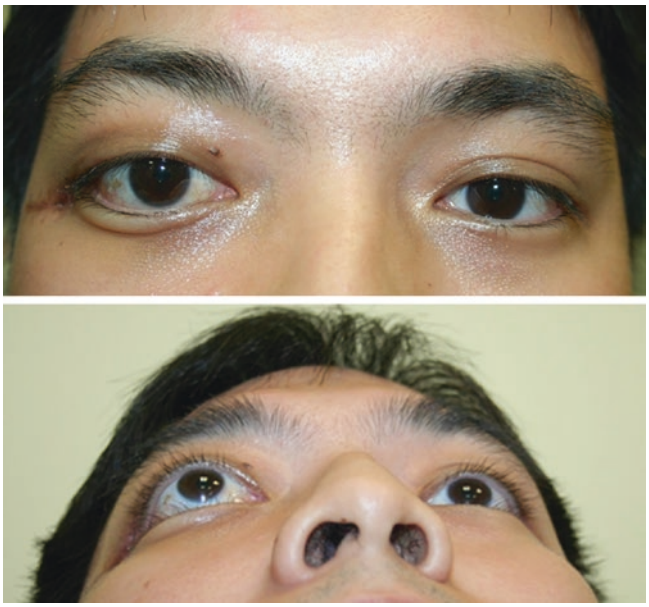

Fig. 66.1 Clinical picture showing the right proptosis with absence of lid crease

Table 66.1 CLOSE summary

*C*linical process: infiltrative mass
*L*ocation: right inferior orbit
*O*nset: chronic
*S*igns and symptoms: right proptosis, dry eye, middle and lower face numbness and limitation of ocular movements
*E*pidemiology: young Chinese male

Differential Diagnosis

- Orbital granuloma – infective or inflammatory
- Orbital lymphoma
- Secondary from another source – sinus nasopharynx, etc.
- Metastasis from a distant site

Imaging

Multiplanar multisequence contrast-enhanced MRI of the head and neck showed a focal T1- and T2-weighted isointense lesion at the inferior aspect of the right orbit, surrounding and displacing the inferior rectus muscle and inseparable from the medial and lateral recti (Fig. 66.2). The right optic nerve appeared uninvolved, although it appeared to be in close proximity to the mass. The lesion was seen to extend posteriorly to the orbital apex and inferior orbital fissure with involvement of the pterygopalatine fossa, sphenopalatine foramen and roof of the nasopharynx (Fig. 66.2). The lesion was seen to extend laterally via the pterygomaxillary fissure with mild extension along the retromaxillary fat pad of the infratemporal fossa.

There was abnormal enhancement of the right infraorbital nerve, maxillary and mandibular divisions of the trigeminal nerve, the trigeminal ganglion as well as the vidian nerve, suspicious of perineural involvement.

The patient underwent a PET-CT scan which showed hypermetabolic focus at the roof of the right posterior nasopharynx. There was concomitant FDG-avid right orbital mass (Fig. 66.3), with no regional or systemic involvement.

Intervention

In view of the radiological suspicion of involvement of the roof of the nasopharynx, an incisional biopsy was obtained from the corresponding area by the rhinologist, although there were no visible changes seen on endoscopy.

Histopathology

Sections showed syncytial sheets of malignant cells with enlarged nuclei, prominent nucleoli and ill-defined cytoplasm. Scattered lymphocytes were also present in close association with the tumour (Fig. 66.4). Scattered mitoses were present.

Immunohistochemistry The epithelial islands were strongly positive for cytokeratin (AE1/AE3) and Epstein-Barr virus encoding region in situ hybridization (EBER-ISH) (Fig. 66.4 inset).

The histological features in conjunction with immunohistochemistry of nasopharyngeal biopsy were compatible with a non-keratinising, differentiated nasopharyngeal carcinoma.

Management

The patient was referred to the oncology service, and he was treated with radical chemotherapy with cisplatin and gemcitabine with concurrent radiotherapy (70 Gy in 33 factions).

Discussion

Nasopharyngeal carcinoma is a rare tumour arising from the epithelium of the nasopharynx and seldom comes to medical attention before it has spread to regional lymph nodes. It usually presents with nasal symptoms such as bleeding, obstruction, and discharge and ear symptoms such as infection,

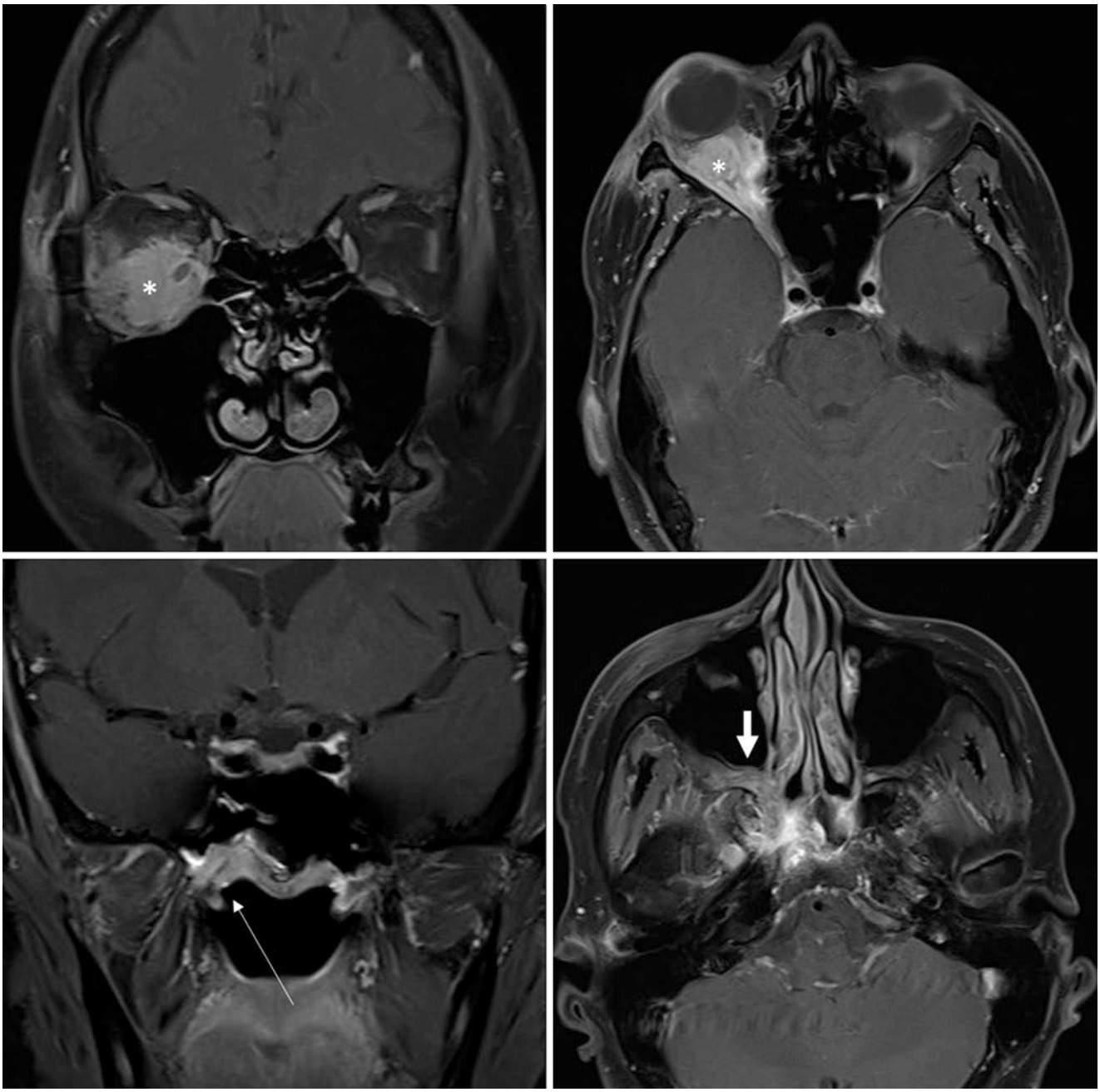

Fig. 66.2 Top: T1w FS + C coronal and axial images showing the bulk of the mass centred within the right inferior orbit (asterisk). Bottom: T1w FS + C coronal and axial images showing the tumour extending through the inferior orbital fissure to the pterygopalatine fossa (thick arrow) leading to its origin from the roof of the nasopharynx (thin arrow)

deafness or tinnitus. Patients may complain of headaches or neck swellings. Twenty-five percent of patients present with cranial nerve palsies. The most frequent site of origin is the fossa of Rosenmüller.

Orbital involvement is reported in 2.6% of patients. The pterygopalatine and infratemporal fossa are the most common routes for invasion of NPC, followed by invasion via the paranasal sinuses. The inferior orbital fissure is a direct communication channel between the apex of the orbit and pterygopalatine and infratemporal fossae. Another common route for spread to the orbit is via base of skull and cavernous sinus.

Pathophysiology Copies of Epstein-Barr virus (EBV) genome have been identified in the preinvasive lesions, suggesting a causal effect. Certain ethnic groups, patients with first-degree relatives with the disease and patients with A2 HLA haplotype are more prone, suggesting a genetic aetiol-

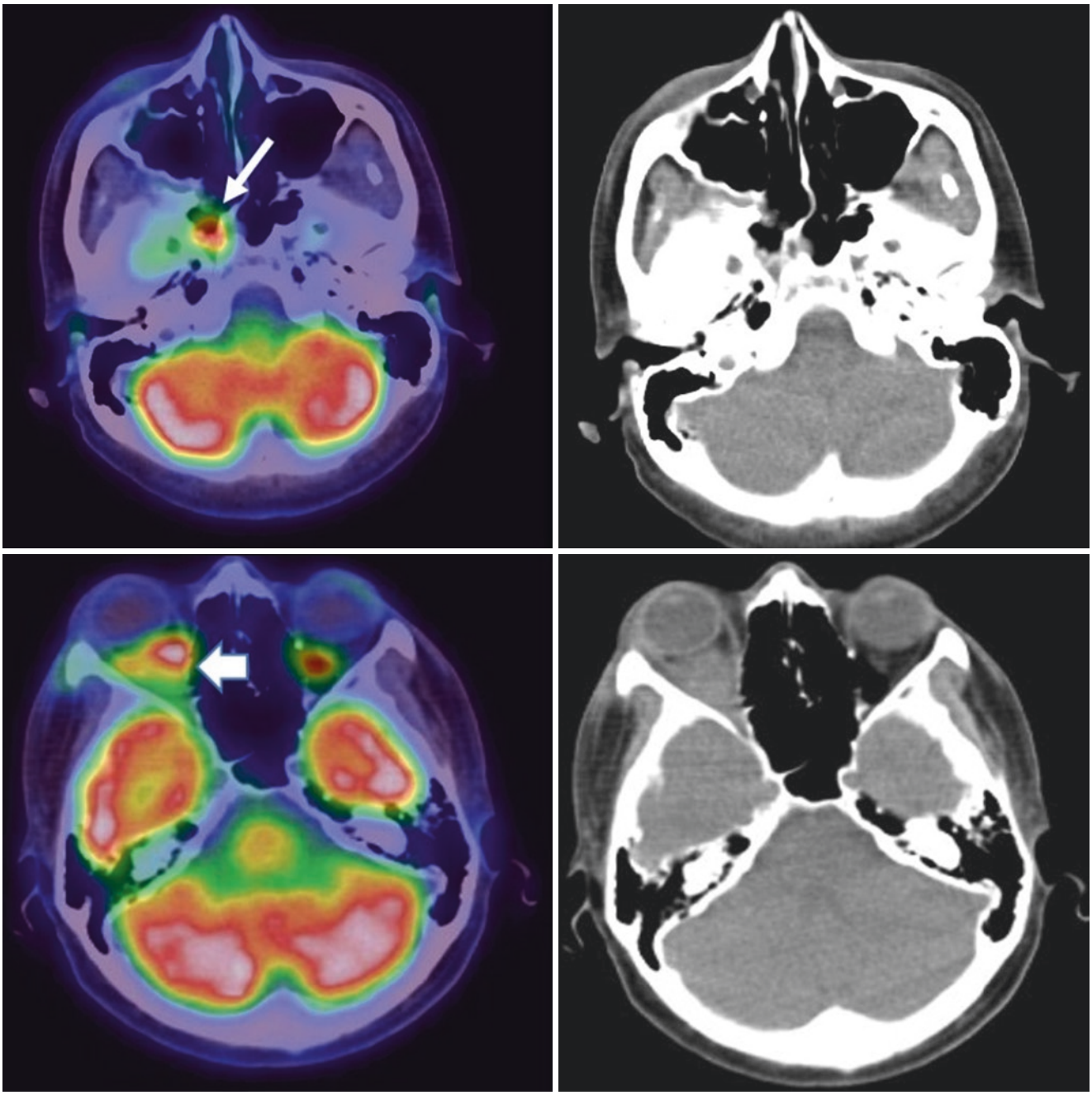

Fig. 66.3 Fused PET-CT and CT images showing the FDG-avid tumour in the roof of the nasopharynx (white arrow) and in the orbit (block arrow)

ogy. Geographic distribution, bimodal age incidence and association seen in patients consuming large amounts of preserved food or salted fish may point to some of the environmental causes.

Male to female ratio is roughly 2:1. Teenage children and late middle-aged adults (bimodal distribution) and people of Asian, Middle-Eastern and North African descent are more commonly affected.

The World Health Organization (WHO) has classified nasopharyngeal carcinoma into three categories:

- WHO-1 is defined as well to moderately differentiated squamous or transitional cell carcinoma with keratin production.
- WHO-2 is a non-keratinising carcinoma.
- WHO-3 is an undifferentiated carcinoma, including lymphoepithelioma. This entity consists of malignant epithelial cells with lymphocytic infiltration.

Management is by chemo-radiation. When radiotherapy is used alone, the survival is only 40–50%, whereas use of chemotherapy with concomitant radiation therapy allows for long-term survival rates of 55–80%.

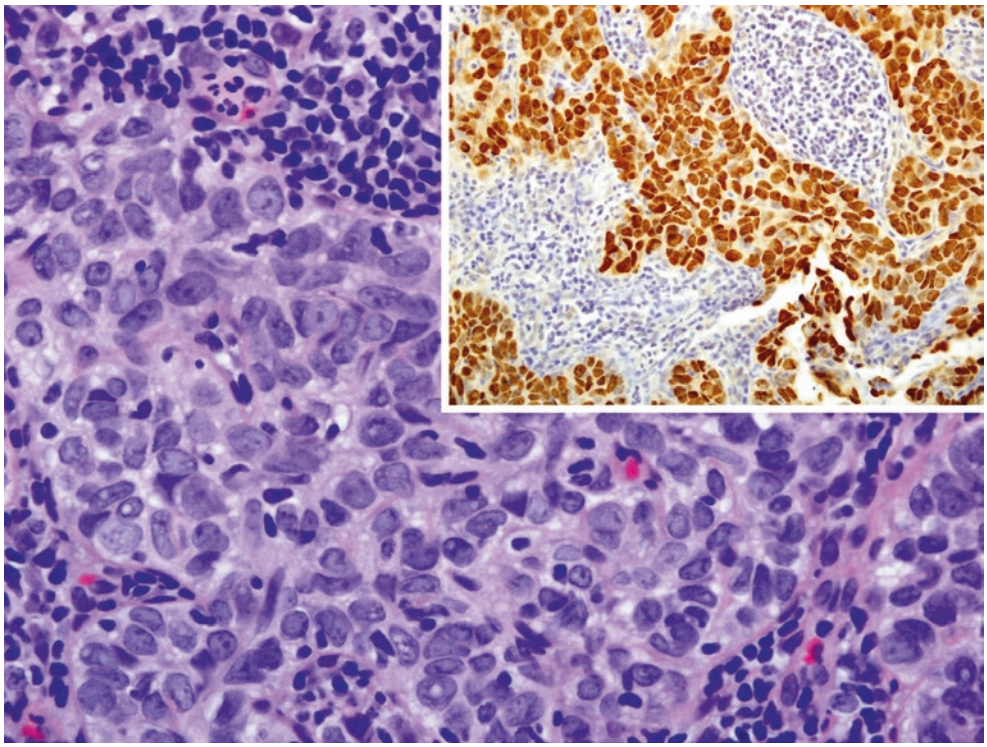

Fig. 66.4 Section shows syncytial sheets of tumour cells with enlarged nuclei, prominent nucleoli and ill-defined cytoplasm. Scattered lymphocytes are also present within the sheets of tumour cells. The tumour cells are positive for Epstein-Barr virus encoding region in situ hybridization (inset). Main: HE stain; 600× magnification. Inset: in situ hybridization (Epstein-Barr virus encoding region RNA probe); 200× magnification

Learning Points

- Ophthalmic symptoms may be a presenting feature of NPC.
- Primary tumour can be extremely small, while the secondary spread may be extensive.
- High index of suspicion for NPC especially in those of Southern Chinese descent is necessary when patients present with numbness, double vision or proptosis.
- Referral should be made to the rhinologists and medical and radiation oncologists for prompt management.
- Ethnicity has a strong correlation with NPC.

Further Reading

1. Chen MS, Lin FJ, Tang SG, Leung WM, Leung W. Clinical significance of cranial nerve deficit in the therapy of nasopharyngeal carcinoma. Brit J Radiol. 1989;62(740):739–43.
2. Heng DMK, Wee J, Fong KW, et al. Prognostic factors in 677 patients in Singapore with non-disseminated nasopharyngeal carcinoma. Cancer. 1999;86:1912–20.
3. Hsu MM, Tu SM. Nasopharyngeal carcinoma in Taiwan, clinical manifestation and results of therapy. Cancer. 1983;52:362–8.
4. Hsu WM, Wang AG. Nasopharyngeal carcinoma with orbital invasion. Eye (Lond). 2004;18(8):833–8.
5. Lee KY, Seah LL, Tow S, Cullen JF, Fong KS. Nasopharyngeal carcinoma with orbital involvement. Ophthal Plast Reconstr Surg. 2008;24(3):185–9.
6. Li JC, Mayr NA, Yuh WTC, Wang JZ, Jiang GL. Cranial nerve involvement in nasopharyngeal carcinoma: response to radiotherapy and its clinical impact. Ann Otol Rhinol Laryngol. 2006;115(5):340–5.
7. Luo CB, Teng MMH, Chen SS, Liring JF, Guo WY, Chang T. Orbital invasion in nasopharyngeal carcinoma: evaluation with computed tomography and magnetic resonance imaging. Chin Med J. 1998;61:382–8.
8. Matz R. Principles of medicine. NY State J Med. 1977;77:99–101.
9. Singapore Cancer Registry, Interim Report (Trends In Cancer Incidence In Singapore 2009-2013).
10. Witte MC, Neel HB III. Nasopharyngeal cancer. In: Byron JB, editor. Head and neck surgery—otolaryngology. Philadelphia: Lippincott-Raven; 1998. p. 1637–52.
11. Wong MW, Young SM, Amrith S. Ophthalmic involvement in nasopharyngeal carcinoma. Orbit. 2017;36(2):84–90.

Correction to: Ocular Adnexal Lesions: A Clinical, Radiological and Pathological Correlation

Shantha Amrith, Gangadhara Sundar, and Stephanie Ming Young

Correction to:
S. Amrith et al. (eds.), *Ocular Adnexal Lesions*, https://doi.org/10.1007/978-981-13-3798-7

The book was inadvertently published with error and the same has been updated later. A reference has been added "Rootman J, Stewart B, Goldberg RA. Orbital surgery: a conceptual approach. 2nd ed. Philadelphia: Wolters Kluwer Lippincott Williams & Wilkins; 2014." in the preface in front matter.

The updated online version of this book can be found at
https://doi.org/10.1007/978-981-13-3798-7

S. Amrith et al. (eds.), *Ocular Adnexal Lesions*, https://doi.org/10.1007/978-981-13-3798-7_67

Index

S. Amrith et al. (eds.), *Ocular Adnexal Lesions*, https://doi.org/10.1007/978-981-13-3798-7